KU LEUVEN

ARENBERG DOCTORAL SCHOOL
Faculty of Science

Energy problems and quadratic differentials in random matrix theory

Guilherme L. F. Silva

Supervisor:
Prof. dr. ir. A. B. J. Kuijlaars

Dissertation presented in partial fulfillment of the requirements for the degree of Doctor in Science: Mathematics

April 2016

Energy problems and quadratic differentials in random matrix theory

Guilherme L. F. SILVA

Examination committee:
Prof. dr. J. Quaegebeur, chair
Prof. dr. ir. A. B. J. Kuijlaars, supervisor
Prof. dr. ir. D. Huybrechs
Prof. dr. W. Van Assche
Prof. dr. T. Grava
(University of Bristol, United Kingdom, and SISSA, Italy)
Prof. dr. A. Martínez-Finkelshtein
(Universidad de Almería, Spain)

Dissertation presented in partial fulfillment of the requirements for the degree of Doctor in Science: Mathematics

April 2016

© 2016 KU Leuven – Faculty of Science
Uitgegeven in eigen beheer, Guilherme L. F. Silva, Celestijnenlaan 200B, B-3001 Leuven (Belgium)

Alle rechten voorbehouden. Niets uit deze uitgave mag worden vermenigvuldigd en/of openbaar gemaakt worden door middel van druk, fotokopie, microfilm, elektronisch of op welke andere wijze ook zonder voorafgaande schriftelijke toestemming van de uitgever.

All rights reserved. No part of the publication may be reproduced in any form by print, photoprint, microfilm, electronic or any other means without written permission from the publisher.

To my little brothers Muzinho and Digão.

Aos meus irmãozinhos Muzinho e Digão, dedico.

Acknowledgements

These pages are the final outcome of an intense period of four years I have spent in Leuven. They contain concrete and (hopefully) valuable mathematics I produced during this period, but nothing of it would have been possible without the help, support and friendship of many whom have crossed my path, and it is a pleasure to thank these special people.

My first thanks go to Arno Kuijlaars, my supervisor. During my Ph.D he has given support for my development as a scientist, providing a great research environment and encouraging me to meet and discuss with many other great mathematicians.

Special thanks also go to Andrei Martínez-Finkelshtein, member of my jury, coauthor and friend. His support as a mentor and the time we spent together discussing math for leisure cannot be measured only from our joint collaboration, and he definitely influences me as a mathematician.

Nothing of this would have been possible without the support and trust of Dimitar Dimitrov. I am honored to have given my first steps in research under his guidance. I am also thankful for

I would like to thank the members of my examination committee: Johan Quaegebeur, Daan Huybrechs, Walter Van Assche and Tamara Grava, for accepting my invitation and giving feedback on my work.

During my Ph.D. I was pleased to talk to many talented minds. Special thanks to Abey López, Adrien Hardy, Alexander Tovbis, Alfredo Deaño, Bernd Beckermann, Ferenc Balogh, Jesper Ipsen, Lun Zhang, Marco Bertola, Maurice Duits, Maxim Derevyagin, Maxim Yatsselev, Pavel Bleher, Roman Riser, Thomas Bothner, Thorsten Neuschel, Tom Claeys and Walter Van Assche. I am grateful for the, sometimes short, but always enlightening, discussions I have had with you all.

The long cloudy days in Leuven were made much easier with the great company

of amazing colleagues. It is a great pleasure to thank Alfredo Deaño, Anna Krogager, Arnaud Brothier, Benjamin Fahs, Dries Stivigny, Hugo Sobreira, Jonas Wahl, Julio Landim, Leslie Molag, Marco Stevens, Mihai Berbec, Niels Meerschaert, Pablo Román, Philip Dowerk, Silvia Menchón, Stijn Toth, Sven Raum, Tim de Laat and Yuki Arano. The time (and beers) spent together have been truly delightful.

I am sincerely grateful for the true friends I have back in Brazil: Eliel dos Santos, Ericson Orsi, Heron Félix, Leandro Tavares, Rodrigo Euzébio, Rony Borsato and Ricardo Hideaki. Although we haven't met recently as much as I wish, every time when we hang out together it feels like time never passed by.

Everything would be in vain without the love, support and care of my father João, my second mother Irani and my partner Andressa. And the constant renewal of energies and dreams through my little brothers Murilo and Rodrigo keeps me moving forward. I cannot imagine my life without you!

Tudo seria vazio se não fosse pelo suporte, amor e carinho do meu pai João, minha segunda mãe Irani e minha companheira Andressa. E o renovar de energias e sonhos através dos meus irmãozinhos Murilo e Rodrigo me mantém seguindo em frente. Eu não consigo imaginar minha vida sem vocês!

My final thanks go to my family back in Brazil, in particular my mother Josi and my cousin Beatriz, who have been following my days in Leuven closely.

Meus agradecimentos finais são para minha família, em particular minha mãe Josi e minha prima Beatriz, que têm acompanhado meu dia a dia de perto.

Abstract

This thesis concerns the potential-theoretic problems underlying three random matrix models: (a) the hermitian matrix model with complex potential, (b) the hermitian matrix model with external source, and (c) the normal matrix model with a cubic potential. Their common feature is that the limit of the sequence of zero counting measures for their average characteristic polynomials can be characterized in terms of free-boundary problems in logarithmic potential theory: (a) a max-min equilibrium problem, (b) critical vector-valued measures, and (c) the mother body problem. We study in depth these free boundary problems, unrevealing their deep connection with quadratic differentials on compact Riemann surfaces.

Beknopte samenvatting

Deze thesis behandelt de potentiaaltheoretische problemen die horen bij een van volgende drie random matrix modellen: (a) het hermitische matrixmodel met een complexe potentiaal, (b) het hermitische matrixmodel met een externe bron, en (c) het normale matrix model met een kubische potentiaal. Deze drie modellen hebben gemeen dat de limiet van de rij van nulpunttellende maten horende bij de karakteristieke veeltermen uitgedrukt kan worden in logaritmische potentiaaltheorie als een probleem met vrije grenzen. Bij (a) betreft het een max-min evenwichtsprobleem, bij (b) kritieke vectorwaardige maten, en bij (c) het zogenaamde "mother body" probleem. We bestuderen in detail deze problemen met vrije grenzen en we tonen hun verband met kwadratische differentialen op compacte Riemann oppervlakken.

Contents

Chapter 1

Summary of the thesis

It was already known in the 1950's that eigenvalues statistics of some random matrix models can be expressed in terms of orthogonal polynomials. But this relation was fully exploited for the first time only in the late 90's, when Deift, Kriecherbauer, McLaughlin, Venakides and Zhou [54], and about the same time Bleher and Its [34], successfully applied the Deift-Zhou steepest descent method [56] to compute asymptotics for orthogonal polynomials, solving several long-standing problems in random matrix theory. These techniques have been extended in several directions, and proven to be extremely powerful in many other models of mathematical physics, for instance in non-intersecting Brownian paths [57], the six-vertex model [39], Painlevé equations [46] and the Ising model [52], to mention only a few.

However, little is known when the orthogonality involved does not display symmetries, and this thesis contributes to a better understanding of asymptotics in those situations. More specifically, the central aspect of this thesis is on developing and employing techniques in (vector) logarithmic potential theory and deformation of quadratic differentials to perform asymptotics for (non-hermitian) orthogonal polynomials arising in different matrix models.

In this introductory chapter, we motivate our studies with a discussion of the random matrix models that are underlying the potential-theoretic problems studied in the subsequent chapters. This chapter also summarizes some of the main results obtained in this thesis.

Asymptotic analysis of large random matrices

The investigation in this thesis is motivated towards understanding certain random matrix models in the large size limit. A *random matrix model* consists of a space of matrices equipped with a probability distribution. For an $n \times n$ random matrix M with eigenvalues $\lambda_1, \ldots, \lambda_n$, there are three objects of great interest for us: the *empirical measure*

$$\nu_n = \frac{1}{n} \sum_{j=1}^{n} \delta_{\lambda_j},$$

the *average characteristic polynomial*

$$p_n(z) = \mathbb{E}\,(zI - M) = \mathbb{E}\left(\prod_{j=1}^{n} (z - \lambda_j)\right)$$

and its associated (normalized) *zero counting measure* $\mu(p_n)$, where for any polynomial p

$$\mu(p) = \frac{1}{\deg p} \sum_{p(w)=0} \delta_w.$$

It is the main focus of this thesis to analyze the large n behavior of ν_n, p_n and $\mu(p_n)$ for certain random matrix models.

1.1 Hermitian matrix model

To leverage our discussion with a concrete example, in this section we discuss the hermitian matrix model, which is among the most classical and better understood matrix models.

The *hermitian random matrix model* consists of the space $\mathcal{H}_n$ of $n \times n$ hermitian matrices M equipped with the probability distribution

$$\frac{1}{\mathcal{Z}_n} e^{-n \operatorname{Tr} V(M)} dM, \tag{1.1}$$

where $\mathcal{Z}_N$ is a normalization constant and V is a real-valued function, commonly called the *external potential*, for which $V(M)$ is given by the spectral calculus. Although very general potentials V can be considered, for simplicity we assume for the rest of this section that V is a polynomial of even degree and positive leading coefficient.

Eigenvalue distribution

Any matrix $H \in \mathcal{H}_n$ can be diagonalized as $H = U\Lambda U^*$, where U is unitary and Λ is a diagonal matrix containing the eigenvalues $\lambda_1, \ldots, \lambda_n$ of H. The diagonalization process can be seen as a change of coordinates

$$\mathcal{H}_n \ni H \mapsto (\lambda, U) \in \mathbb{R}^n \times \mathcal{U}_n,$$

where $\lambda = (\lambda_1, \ldots, \lambda_n) \in \mathbb{R}^n$ is the vector of eigenvalues of M and $\mathcal{U}_n$ is the group of $n \times n$ unitary matrices. This change of coordinates induces the *eigenvalue distribution* [50,51]

$$\mathcal{P}_n(\lambda)d\lambda = \frac{1}{Z_n} \prod_{j<k} (\lambda_k - \lambda_j)^2 \prod_j e^{-nV(\lambda_j)} d\lambda \tag{1.2}$$

on $\mathbb{R}^n$, where

$$Z_n = \int_{\mathbb{R}^n} \prod_{j<k} (\lambda_k - \lambda_j)^2 \prod_j e^{-nV(\lambda_j)} d\lambda \tag{1.3}$$

is the normalization constant, called the *partition function* of (1.2).

Orthogonal polynomials in the hermitian matrix model

For $n \in \mathbb{N}$, associated to the weight $e^{-nV(x)}$ on the real line are the sequence $(p_{j,n})$ of *orthogonal polynomials*, defined by the condition that $p_{j,n}$ is a monic polynomial of degree j satisfying

$$\int_{\mathbb{R}} p_{j,n}(x) p_{k,n}(x) e^{-nV(x)} dx = \delta_{k,j} h_{j,n}^2, \quad h_{j,n} > 0, \quad j,k = 0,1,2,\ldots, \tag{1.4}$$

and the *correlation kernels*

$$K_n(x,y) = e^{-\frac{n}{2}(V(x)+V(y))} \sum_{j=0}^{n-1} \frac{p_{j,n}(x) p_{j,n}(y)}{h_{j,n}^2}.$$

It turns out that many quantities of interest for the model (1.1) (or, equivalently, for (1.2)) can be expressed in terms of the orthogonal polynomials and correlation kernels. For instance, the average characteristic polynomial for the hermitian matrix model (1.1) coincides with the orthogonal polynomial $p_{n,n}$, the eigenvalue distribution (1.2) admits the determinantal representation with correlation kernel K_n,

$$\mathcal{P}_n(\lambda_1, \ldots, \lambda_n) = \frac{1}{n!} \det\left(K_n(\lambda_j, \lambda_k)\right)_{j,k=1}^n$$

and the partition function Z_n in (1.3) is expressed in terms of these quantities as

$$Z_n = n! \prod_{j=1}^{n} h_{j,n}^2. \tag{1.5}$$

Thus, in some sense the sequence of orthogonal polynomials encodes all the information on the model (1.2), and questions about the large n behavior of (1.2) can be translated into questions on the large n behavior of the functions $p_{n,n}$ and K_n.

The associated equilibrium problem

It is natural to expect that the sequences of empirical measures (ν_n) and zero counting measures $(\mu(p_{n,n}))$ have the same large n behavior. For V a polynomial potential as we are assuming here, this is indeed the case: the random sequence (ν_n) converges almost surely to a probability measure μ_V, which is also the limit of $(\mu(p_{n,n}))$.

The measure μ_V is characterized as the *equilibrium measure in the external field* V [50]: it is the (unique) measure minimizing the energy functional

$$I^V(\mu) := I(\mu) + \int V(x) d\mu(x) \tag{1.6}$$

over all probability measures supported on $\mathbb{R}$. Here and in what follows, we denote by

$$I(\mu, \nu) = \iint \log \frac{1}{|x-y|} d\mu(x) d\nu(y)$$

the logarithmic energy between two measures μ and ν and set $I(\mu) = I(\mu, \mu)$, and by

$$U^\mu(z) = \int \log \frac{1}{|x-z|} d\mu(x)$$

we denote the logarithmic potential of the measure μ.

Because $\operatorname{supp} \mu_V$ has zero planar Lebesgue measure and connected complement, the convergences of (ν_n) and $(\mu(p_{n,n}))$ to μ_V can be alternatively characterized through the limits

$$\lim_{n\to\infty} U^{\mu(p_{n,n})}(z) = U^{\mu_V}(z) = \lim_{n\to\infty} U^{\nu_n}(z), \quad z \in \mathbb{C} \setminus \operatorname{supp} \mu_V. \tag{1.7}$$

1.2 Non-hermitian orthogonality in polynomial external field

When V is a real polynomial of odd degree, the expressions (1.1) and (1.2) are not integrable, and thus it is meaningless to talk about the associated random matrix model. Nevertheless, at the formal level the associated partition function (1.3) is still of interest, as its (formal) asymptotic expansion in powers of n gives rise to generating functions of counting graphs on compact Riemann surfaces. This fact was probably first observed by Brézin, Itzykson, Parisi and Zuber [43] in the late 1970's, building on an original idea of 't Hooft [83], and since then it has been fruitfully exploited in other contexts as well [29, 58, 66, 78, 80]. To make these formal computations rigorous, one has to move from the standard orthogonality on the real line (1.4) to *non-hermitian orthogonality*, as explained next.

For an arbitrary complex polynomial V of degree at least 2, denote by $\mathcal{T}$ the set of rectifiable contours that extend to ∞ within two given sectors on the complex plane along which $\operatorname{Re} V(z) \to +\infty$ as $z \to \infty$. The associated family of non-hermitian orthogonal polynomials $(p_{j,n})$ is defined by the relations

$$\int_\Gamma p_{j,n}(z) p_{k,n}(z) e^{-nV(z)} dz = \delta_{j,k} h_{j,n}^2, \quad j,k = 0,1,2,\dots, \tag{1.8}$$

where $p_{j,n}$ is a monic polynomial of degree j, and Γ is any contour in the class $\mathcal{T}$ - in virtue of the analyticity of the integrand, the integrals above do not depend on the choice of $\Gamma \in \mathcal{T}$. The term *non-hermitian* comes from the fact that the integral in (1.8) can be expressed as $\langle p_{j,n}, p_{k,n} \rangle$, where $\langle \cdot, \cdot \rangle$ is the non-hermitian bilinear form defined for monomials as

$$\langle z^j, z^k \rangle = \int_\Gamma z^{j+k} e^{-nV(z)} dz \quad j,k = 0,1,2,\dots,$$

and extended to the whole space of polynomials by linearity. In particular, due to this non-hermitian nature, typically one can only be sure that $h_{n,n} \neq 0$ for sufficiently large n, and only after an asymptotic analysis.

Although its probabilistic meaning is now lost, the partition function Z_n is still well defined in terms of the n-fold contour integral

$$Z_n = \int_{\Gamma^n} \prod_{j<k} (z_k - z_j)^2 \prod_j e^{-nV(z_j)} dz_1 \cdots dz_n.$$

Using the Deift-Zhou nonlinear steepest descent method, Bleher and Deaño [31, 32] computed the large n asymptotics of the polynomials $p_{n,n}$ and also of

the partition function Z_n for a cubic polynomial V, rigorously establishing the results predicted by Bessis, Itzykson and Zuber [29]. In a similar spirit, Bertola and Tovbis [28] studied the asymptotics of $p_{n,n}$ when V is a quartic polynomial. The first source of problems to extend their analysis to general polynomial V is regarding the determination of the limit of the sequence $(\mu(p_{n,n}))$, which plays a crucial role in the construction of the so-called g-function. In virtue of the low degree of the potential in [28, 31, 32], the authors could compute this limit in a somewhat explicit manner, as in their cases there were only few free parameters involved.

The Gonchar-Rakhmanov-Stahl (GRS) theory

To gain a better understanding on the asymptotic behavior of the zeros of the orthogonal polynomials in (1.8), we make a digression for a moment. Suppose f is an algebraic function that is analytic in a neighborhood of ∞. Denote by $\mathcal{F}$ the class of bounded rectifiable contours Γ for which $\mathbb{C}\setminus\Gamma$ is connected and f admits a single-valued analytic extension to $\mathbb{C}\setminus\Gamma$. The associated sequence (q_n) of non-hermitian orthogonal polynomials is thus defined through the condition that q_n is monic, has degree n and satisfies

$$\oint_\Gamma q_n(z) z^k f(z) dz = 0, \quad k = 0, \dots, n-1. \tag{1.9}$$

Thanks to the analyticity of the integrand the sequence (q_n) does not depend on the precise choice of Γ. In the seminal works [128, 129, 130], Stahl gave a complete characterization of the limit of the sequence of zero counting measures $(\mu(q_n))$, as we explain next.

The *Robin measure* ω_Γ of $\Gamma \in \mathcal{F}$ is the unique measure minimizing the log energy $I(\cdot)$ among all probability measures supported on Γ. The log energy of $\Gamma \in \mathcal{F}$ is then defined by $I(\Gamma) = I(\omega_\Gamma)$.

The associated *max-min energy problem* asks for finding a contour $\Gamma_0 \in \mathcal{F}$ for which the energy $I(\cdot)$ attains its maximum over all contours in $\mathcal{F}$; in other words, Γ_0 should satisfy

$$I(\Gamma_0) = \max_{\Gamma\in\mathcal{F}} I(\Gamma) = \max_{\Gamma\in\mathcal{F}} \min_{\substack{|\mu|=1 \\ \operatorname{supp}\mu\subset\Gamma}} I(\mu). \tag{1.10}$$

In [128], Stahl showed that there exists a (essentially unique) contour $\Gamma_0 \in \mathcal{F}$ solving the max-min energy problem (1.10). In addition, in [129] he characterized

the set Γ_0 as an *S-contour*: its equilibrium measure ω_{Γ_0} satisfies the *S-property*

$$\frac{\partial U^{\omega_{\Gamma_0}}}{\partial n_+}(z) = \frac{\partial U^{\omega_{\Gamma_0}}}{\partial n_-}(z), \quad z \in \operatorname{supp}\omega_{\Gamma_0}, \tag{1.11}$$

where $n_\pm$ are the unit normal vectors to Γ_0 at z. Finally, in [130] he also proved that the convergence of $(\mu(q_n))$ to μ_{Γ_0} follows from the S-property (1.11).

Inspired by the works of Stahl, Gonchar and Rakhmanov [71] studied the limiting behavior of the sequence of zero counting measures $(\mu(p_{n,n}))$ for the orthogonal polynomials in (1.8). For a contour $\Gamma \in \mathcal{T}$, the associated *equilibrium measure in the external field* $\operatorname{Re} V$ is the unique probability measure μ_Γ supported on Γ that minimizes the energy

$$I^V(\mu) = I(\mu) + \int \operatorname{Re} V(x) d\mu(x),$$

over all probability measures supported on Γ. A contour $\Gamma_0 \in \mathcal{T}$ is said to have the *S-property in the external field* $\operatorname{Re} V$, or is simply an *S-contour*, if its equilibrium measure μ_{Γ_0} satisfies

$$\frac{\partial}{\partial n_+}\left(U^{\mu_{\Gamma_0}} + \frac{\operatorname{Re} V}{2}\right)(z) = \frac{\partial}{\partial n_-}\left(U^{\mu_{\Gamma_0}} + \frac{\operatorname{Re} V}{2}\right)(z), \quad z \in \operatorname{supp}\mu_{\Gamma_0}. \tag{1.12}$$

The main result of Gonchar and Rakhmanov says that the sequence of zero counting measures $(\mu(p_{n,n}))$ for the orthogonal polynomials in (1.8) converges weakly to the equilibrium measure μ_{Γ_0} of the S-contour $\Gamma_0 \in \mathcal{T}$, provided it exists. However, they were not able to address the existence of the S-contour.

It is worth mentioning that the notion of the S-property also found a natural interpretation in the light of the Deift-Zhou's non-linear steepest descent method for Riemann-Hilbert problems [50]. One of the key steps in this asymptotic analysis is the deformation of the contours, which transforms oscillatory behavior into a non-oscillatory plus exponentially decaying one. This deformation consists in "opening of lenses" along the level sets of certain functions (known as *g-functions*). It is precisely the S-property (1.12) which guarantees the exponential decay on all non-relevant contours.

The existence result on the S-property

Recently, Rakhmanov returned to the problem of settling down the existence of the S-contour from a general perspective [116]. His main ideas, a generalization of Stahl's approach previously explained, allow to formulate the existence problem of the S-contours in terms of max-min problems in a fairly general

setting. According to his work, any set maximizing the minimal energy should also be an S-contour. However, due to severe technical restrictions, his results in [116] do not cover the case of polynomial external fields as in (1.12).

In Chapter 2 we adapt Rakhmanov's techniques to the setup of the orthogonality (1.8), hence establishing the existence of the S-contour $\Gamma_0 \in \mathcal{T}$ as in (1.12). We prove

Theorem 1.2.1 (see Theorem 2.2.3)**.** *For any complex polynomial V of degree at least 2, there exists a contour $\Gamma_0 \in \mathcal{T}$ with the S-property in the external field $\operatorname{Re} V$. This contour satisfies the max-min property*

$$I^V(\mu_{\Gamma_0}) = \max_{\Gamma \in \mathcal{T}} \min_{\substack{\mu(\mathbb{C})=1 \\ \operatorname{supp}\mu \subset \Gamma}} I^V(\mu).$$

Furthermore, there exists a polynomial R such that the Cauchy transform $C^{\mu_{\Gamma_0}}$ satisfies the algebraic equation

$$\left(C^{\mu_{\Gamma_0}}(z) + \frac{V'(z)}{2}\right)^2 = R(z) \tag{1.13}$$

for $z \in \mathbb{C} \setminus \operatorname{supp}\mu_{\Gamma_0}$, and μ_{Γ_0} is supported on critical trajectories of the quadratic differential $-R(z)dz^2$ defined on $\overline{\mathbb{C}}$. Finally, the S-property (1.12) holds true for Γ_0.

The connection between measures with algebraic Cauchy transform and quadratic differentials, exemplified by Theorem 1.2.1, is central in this thesis. As it was mentioned above, the Riemann-Hilbert asymptotic analysis for 2×2 matrix-valued functions characterizing the non-hermitian orthogonality provides another natural connection with quadratic differentials: the "right" level curves for the g-functions, that usually have a quite complicated structure, are trajectories of a suitable quadratic differential. Thus, the problem of existence of the appropriate curves can be reduced to the question about the global structure of such trajectories. This is not a simplification (the description of the global structure can be a formidable task), but it opens the gate to other techniques from the geometric function theory. In the same spirit and in a much more explicit form, quadratic differentials also appeared in similar asymptotic problems in [15, 16, 82, 92, 93, 102]. We emphasize that in all these problems, as well as in Theorem 1.2.1, the underlying quadratic differentials are defined on the complex plane.

Still under the light of the Riemann-Hilbert approach, Bertola [24] developed deformation techniques that ultimately lead to the existence of the S-contour. He does not rely on any equilibrium problem, thus does not solve the max-min

problem as in Theorem 1.2.1. Instead, he writes down certain transcendental conditions - the Boutroux conditions - that should be satisfied by the underlying algebraic equation in order to be able to apply the steepest descent method for the non-hermitian orthogonal polynomials (1.8). Using deformation techniques, he then shows that the Boutroux conditions can always be achieved under certain regularity assumptions. The downside is that these regularity assumptions do not always hold true, and consequently his approach does not cover every choice of polynomial potential V.

Chapter 2 is dedicated to the proof of Theorem 1.2.1 (in the slightly more general form of Theorem 2.2.3). The main aspects in this proof are summarized in Section 2.2.5, but we stress here the importance of the notion of *critical measures*. A measure μ is called (scalar) critical if for any continuous family of perturbations (μ^t) of μ, $\mu^0 = \mu$, the limit

$$\lim_{t\to 0} \frac{I^V(\mu^t) - I^V(\mu)}{t} = 0 \tag{1.14}$$

holds true (we refer to Definition 2.3.2 in Chapter 2 for details). The fact of the matter, already observed by Rakhmanov and rigorously established in our context by Corollary 2.4.4, is that the equilibrium measure of any local maximum of $I^V(\Gamma)$ is a critical measure, so that we can translate considerations for sets maximizing the energy to considerations for critical measures. Adapting the techniques developed by Martínez-Finkelshtein and Rakhmanov [104], we thus are able to give the complete characterization of μ_{Γ_0} (including the S-property (1.12)) after a systematic study of critical measures.

1.3 The hermitian matrix model with external source

The *hermitian matrix model with external source* is the space of $n \times n$ hermitian matrices M equipped with the probability distribution

$$\frac{1}{\mathcal{Z}_n} e^{-n \operatorname{Tr}(V(M) - AM)} dM, \tag{1.15}$$

where $\mathcal{Z}_n$ is a normalization constant, V is a real-valued function and A is a given $n \times n$ deterministic hermitian matrix. When $A = 0$, this model reduces to (1.1). As before, we assume that V is a real polynomial of even degree and positive leading coefficient, although some of the aspects in the following discussion could be suitably adapted to cover more general potentials as well.

We denote by $a_1, \ldots, a_m$ the m distinct eigenvalues of A, with multiplicities $n_1, \ldots, n_m$, respectively. If $m = n$, that is, A has no eigenvalues with multiplicity,

the induced eigenvalue distribution for the hermitian matrix model with external source takes the form

$$\mathcal{P}_n(\lambda)d\lambda = \frac{1}{Z_n}\prod_{j<k}(\lambda_k-\lambda_j)\det\left(e^{-n(V(\lambda_j)-a_k\lambda_j)}\right)_{j,k=1}^{n} d\lambda. \tag{1.16}$$

where Z_n is the associated partition function. When A has eigenvalues with multiplicity, an expression for $\mathcal{P}_n$ can be obtained from the formula (1.16) with appropriate confluent limits.

Multiple orthogonal polynomials in the external source model

We keep denoting by $n_1,\dots,n_m$ the multiplicities of the eigenvalues $a_1,\dots,a_m$ of the external source A. The monic polynomial $p_{j,n}$ of degree j that satisfies

$$\int_{\mathbb{R}} p_{j,n}(x)x^l e^{-n(V(x)-a_k x)}dx = 0, \quad l=0,\dots,n_k-1, \quad k=1,\dots,m, \tag{1.17}$$

is called the *multiple orthogonal polynomial* of degree j with respect to the weights $e^{-n(V(x)-a_1x)},\dots,e^{-n(V(x)-a_mx)}$.

Closely related is the dual function $q_{j-1,n}$, which is defined by the conditions to be in the linear span of

$$\{x^l e^{na_kx} \mid l=0,\dots,n_k-1,\ k=1,\dots,m\}$$

and to satisfy

$$\int_{\mathbb{R}} x^l q_{j-1,n}(x)e^{-nV(x)}dx = \delta_{j-1,l}, \quad l=0,1,\dots,j-1.$$

Consequently, the functions p's and q's form a biorthogonal system, that is,

$$\int_{\mathbb{R}} p_{j,n}(x)q_{k,n}(x)e^{-nV(x)}dx = \delta_{j,k}, \quad j,k=0,\dots,n-1.$$

Zinn-Justin [138] showed that $\mathcal{P}_n$ in (1.16) admits the determinantal representation

$$\mathcal{P}_n(\lambda) = \frac{1}{n!}\det\left(K_n(\lambda_j,\lambda_k)\right)_{j,k=1}^{n}$$

for a certain kernel K_n. Bleher and Kuijlaars [36] showed that K_n can be chosen to be

$$K_n(x,y) = e^{-\frac{n}{2}(V(x)+V(y))}\sum_{j=0}^{n-1} p_{j,n}(x)q_{j,n}(y), \tag{1.18}$$

thus expressing K_n in terms of the multiple orthogonal polynomials and the dual functions. Furthermore, they also proved that the average characteristic polynomial for (1.15) is the multiple orthogonal polynomial $p_{n,n}$. In the particular case when $m = 2$, $n_1 = n_2$ and $a_1 = -a_2 = a$, these connections have successfully led to the asymptotic analysis of the model (1.15) under certain symmetry conditions, as we explain next.

Vector equilibrium problems for the limiting eigenvalue distribution

For a vector of measures (ν_1, ν_2), define the energy functional

$$E_c(\nu_1, \nu_2) = I(\nu_1) + I(\nu_2) - I(\nu_1, \nu_2) + \int (V(x) - a|x|)\, d\nu_1(x). \tag{1.19}$$

Bleher, Delvaux and Kuijlaars [33] considered the following *constrained vector equilibrium problem*: minimize E_c among all vectors (ν_1, ν_2) that satisfy the conditions

$$\operatorname{supp}\nu_1 \subset \mathbb{R}, \quad \operatorname{supp}\nu_2 \subset i\mathbb{R}, \quad |\nu_1| = 2|\nu_2| = 1, \quad \nu_2 \leq \sigma, \tag{1.20}$$

where σ is the measure on $i\mathbb{R}$ with constant density

$$\frac{d\sigma}{|ds|} = \frac{a}{\pi}, \quad s \in i\mathbb{R}. \tag{1.21}$$

In the symmetric situation that V is an even polynomial and the external source has exactly two distinct eigenvalues a and $-a$ with equal multiplicity, they proved that the vector equilibrium problem above has a unique solution $(\mu_{1,c}, \mu_{2,c})$ which relates to the model (1.15) through the weak limits

$$\lim_{n\to\infty} \mu(p_{n,n}) = \mu_{1,c} = \lim_{n\to\infty} \nu_n \tag{1.22}$$

where we recall that $\mu(p_{n,n})$ is the zero counting measure for $p_{n,n}$ and ν_n is the empirical measure for (1.15) (for which the convergence should be understood in the almost surely sense).

Their proof consists of obtaining asymptotic formulas for the polynomials p's in (1.17), and consequently for the kernel (1.18). However, their analysis heavily relied on the symmetry $V(-z) = V(z)$ assumed for the potential, and also on the condition that A has exactly two eigenvalues with equal multiplicities. These assumptions are reflected in the conditions (1.20)–(1.21) for the second

measure ν_2, and it is not clear how to extend this equilibrium problem to cover non-symmetric situations as well.

Aptekarev, Lysov and Tulyakov [12,13] brought new light to this problem from the perspective of the GRS theory. For a contour Γ that is invariant under complex conjugation, intersects $\mathbb{R}$ at a unique point x_* and extends to ∞ along the right half plane, they replaced the energy E_c by the energy

$$E_s(\nu_1,\nu_2,\nu_3) = I(\nu_1) + I(\nu_2) + I(\nu_3) + I(\nu_1,\nu_2) + I(\nu_1,\nu_3) - I(\nu_2,\nu_3)$$
$$+ \int (V(z) + az)\, d\nu_1(z) + \int (V(z) - az)\, d\nu_2(z) + 2a \int \operatorname{Re} z \; d\nu_3(z) \quad (1.23)$$

on the class $\mathcal{M}(\Gamma)$ of vectors of measures $\vec{\nu} = (\nu_1,\nu_2,\nu_3)$ satisfying

$$\operatorname{supp}\nu_1 \subset (-\infty, x_*], \quad \operatorname{supp}\nu_2 \subset [x_*, +\infty), \quad \operatorname{supp}\nu_3 \subset \Gamma, \quad (1.24)$$

$$|\nu_1| + |\nu_2| = 1, \quad |\nu_2| - |\nu_3| = \frac{1}{2}. \quad (1.25)$$

According to the general potential theory [79,111], for each contour Γ as above there exists a unique vector $\vec{\mu}_\Gamma$ minimizing E_s on $\mathcal{M}(\Gamma)$. Following the GRS theory, Aptekarev, Lysov and Tulyakov suggested that there should be a contour Γ_0 solving the associated max-min problem: its vector equilibrium measure $\vec{\mu}_{\Gamma_0} = (\mu_{1,s},\mu_{2,s},\mu_{3,s})$ should satisfy

$$E_s(\vec{\mu}_{\Gamma_0}) = \sup_\Gamma E_s(\vec{\mu}_\Gamma) = \sup_\Gamma \inf_{\vec{\nu}\in\mathcal{M}(\Gamma)} E_s(\vec{\nu}). \quad (1.26)$$

Once one has at hand the contour Γ_0, they claimed (without proof!) that the S-property

$$\frac{\partial}{\partial n_+}\Big(2U^{\mu_{3,s}}(z) + U^{\mu_{1,s}}(z) - U^{\mu_{2,s}}(z) + 2a\operatorname{Re} z\Big)$$
$$= \frac{\partial}{\partial n_-}\Big(2U^{\mu_{3,s}}(z) + U^{\mu_{1,s}}(z) - U^{\mu_{2,s}}(z) + 2a\operatorname{Re} z\Big), \quad z \in \operatorname{supp}\mu_3 \quad (1.27)$$

should hold. In other words, Γ_0 should be an S-contour in the sense above. When V is the (symmetric) quartic plus quadratic polynomial, they were able to make an educated guess for the S-contour Γ_0, and explicitly computing its vector equilibrium measure $\vec{\mu}_{\Gamma_0}$ they could verify the S-property (1.27). Using the S-contour, they applied the Deift-Zhou Steepest Descent method for the multiple orthogonal polynomials (1.17), concluding at the end that

$$\mu_{1,c} = \mu_{1,s} + \mu_{2,s},$$

that is, the limiting eigenvalue distribution in (1.22) decomposes as the sum of the first two components of the vector equilibrium measure for the S-contour Γ_0.

Comparing to the vector equilibrium problem (1.19)–(1.21), the constraint is traded by the allowance of charges to "flow" between different measures, as expressed in (1.25). The price to pay is that we now have the "free boundary" Γ_0 to be determined. As the reader might have already realized, this approach is a natural generalization of the GRS theory to the setting of multiple orthogonal polynomials. It is also promising, as in principle it does not require any symmetry assumption on the potential V. But as we already mentioned, Aptekarev, Lysov and Tulyakov could only make it work for the quartic plus quadratic potential and in a somewhat ad hoc manner, and new tools from potential theory have to be developed in order to deal with more general polynomial weights.

Critical measures for vector energy

For polynomials Φ_1, Φ_2 and Φ_3 satisfying the compatibility condition

$$\Phi_1'(z) - \Phi_2'(z) = \Phi_3'(z),$$

and the positive semi-definite symmetric matrix

$$A = (a_{j,k})_{j,k=1}^3 = \begin{pmatrix} 1 & \frac{1}{2} & \frac{1}{2} \\ \frac{1}{2} & 1 & -\frac{1}{2} \\ \frac{1}{2} & -\frac{1}{2} & 1 \end{pmatrix},$$

we define the external fields $\phi_j = \operatorname{Re} \Phi_j$, $j = 1, 2, 3$, and consider the energy functional

$$E(\mu_1, \mu_2, \mu_3) = \sum_{j,k=1}^{3} a_{j,k} I(\mu_j, \mu_k) + \sum_{j=1}^{3} \int \phi_j(z) d\mu_j(z), \tag{1.28}$$

defined over the set $\mathcal{M}_\alpha$ of vectors of measures $\vec{\mu} = (\mu_1, \mu_2, \mu_3)$ satisfying

(a) For the given parameter $\alpha \in [0, 1]$, the total masses of the components of $\vec{\mu} \in \mathcal{M}_\alpha$ satisfy

$$|\mu_1| + |\mu_2| = 1, \quad |\mu_1| + |\mu_3| = \alpha, \quad |\mu_2| - |\mu_3| = 1 - \alpha. \tag{1.29}$$

(b) Each μ_j is a compactly supported Borel measure on $\mathbb{C}$, and its support has zero planar Lebesgue measure.

(c) Any pairwise intersection $\operatorname{supp}\mu_j \cap \operatorname{supp}\mu_k$, $j \neq k$, is finite.

Observe that the energy (1.28) and the conditions on the masses (1.29) generalize (1.23) and (1.25). In contrast to the vector equilibrium problem (1.23)–(1.25), where one seeks to minimize E_c over the *prescribed* sets (1.24), we instead are interested in the *saddle points*, or *critical vector-valued measures* for the energy (1.28).

A vector of measures $\vec{\mu} \in \mathcal{M}_\alpha$ is said to be *critical* if any one-parameter continuous deformation $\vec{\mu}^t \in \mathcal{M}_\alpha$ of $\vec{\mu}$, $\vec{\mu}^0 = \vec{\mu}$, satisfies

$$\lim_{t\to 0} \frac{E(\vec{\mu}^t) - E(\vec{\mu})}{t} = 0. \tag{1.30}$$

We refer the reader to Definition 3.2.1 for a precise meaning of the class of deformations $\vec{\mu}^t$. Equation (1.30) is the natural extension of (1.14) to the vector energy setting, and the systematic study of critical vector-valued measures is amongst the fundamental steps to be performed for the extension of the GRS theory to the context of the multiple orthogonality (1.17).

Some instances of critical vector-valued measures have appeared in the literature, basically in the study of the limiting zero distribution of some multiple orthogonal polynomials satisfying non-hermitian orthogonality conditions. The most studied cases are those presenting strong symmetries, so that the support of these measures can be easily derived. Other works, such as [11,14], consider non-symmetric situations. Their basic approach is to start from a general form expected for a cubic equation that should govern the system, and then make a genus ansatz, hence reducing the free parameters of the equation to a minimum. Although a vector equilibrium is present, due to the explicit form of the deduced algebraic equation its detailed study is not needed and usually bypassed. Moreover, in such situations there is no external field involved, which is a considerable simplification, even in the scalar case.

In Chapter 3 we study in depth the critical vector-valued measures, obtaining several structural results about them. We summarize some of them in the following result.

Theorem 1.3.1 (see Theorems 3.2.2–3.2.3 and 3.2.8)**.** *A vector of measures $\vec{\mu} = (\mu_1, \mu_2, \mu_3) \in \mathcal{M}_\alpha$ is critical if, and only if, there exists a polynomial R and a rational function D with poles of order at most* 2 *such that their shifted*

Cauchy transforms

$$\xi_1(z) = \frac{\Phi_1'(z)}{3} + \frac{\Phi_2'(z)}{3} + C^{\mu_1}(z) + C^{\mu_2}(z),$$

$$\xi_2(z) = -\frac{\Phi_1'(z)}{3} - \frac{\Phi_3'(z)}{3} - C^{\mu_1}(z) - C^{\mu_3}(z),$$

$$\xi_3(z) = -\frac{\Phi_2'(z)}{3} + \frac{\Phi_3'(z)}{3} - C^{\mu_2}(z) + C^{\mu_3}(z)$$

satisfy the algebraic equation

$$\xi^3 - R(z)\xi + D(z) = 0 \tag{1.31}$$

for almost every $z \in \mathbb{C}$.

Each of the measures μ_1, μ_2, μ_3 *is supported on a union of analytic arcs. They satisfy the Euler-Lagrange type equilibrium conditions, namely*

$$\sum_{k=1}^{3} a_{j,k} U^{\mu_k}(z) + \frac{\phi_j(z)}{2} = l, \quad z \in \operatorname{supp}\mu_j,$$

for some constant l *(that depends on the connected component of* $\operatorname{supp}\mu_j$*). Furthermore, for* z *on the open arcs of* $\operatorname{supp}\mu_j$*, the S-property*

$$\frac{\partial}{\partial n_+}\left(\sum_{k=1}^{3} a_{jk} U^{\mu_k}(z) + \frac{\phi_j(z)}{2}\right) = \frac{\partial}{\partial n_-}\left(\sum_{k=1}^{3} a_{jk} U^{\mu_k}(z) + \frac{\phi_j(z)}{2}\right)$$

holds true.

Equation (1.31) is the higher order analogue of (1.13) and it is known in the context of random matrix theory as the *spectral curve*.

For each $z \in \mathbb{C}$, (1.31) admits three solutions ξ_1, ξ_2 and ξ_3. As it is explained in Chapter 3, (1.31) defines a three-sheeted Riemann surface $\mathcal{R} = \mathcal{R}_1 \cup \mathcal{R}_2 \cup \mathcal{R}_3$ on which the function $\xi : \mathcal{R} \to \overline{\mathbb{C}}$ defined as $\xi\big|_{\mathcal{R}_j} \equiv \xi_j$ is meromorphic.

The next result, which is actually a simple observation, lies at the technical core of this thesis.

Theorem 1.3.2 (see Theorem 3.2.9)**.** *For a critical measure* $\vec{\mu} \in \mathcal{M}_\alpha$*, let* $\mathcal{R} = \mathcal{R}_1 \cup \mathcal{R}_2 \cup \mathcal{R}_3$ *be the Riemann surface associated to* (1.31)*. The expression*

$$\varpi = \begin{cases} -(\xi_2(z) - \xi_3(z))^2 dz^2, & z \in \mathcal{R}_1 \\ -(\xi_1(z) - \xi_3(z))^2 dz^2, & z \in \mathcal{R}_2 \\ -(\xi_1(z) - \xi_2(z))^2 dz^2, & z \in \mathcal{R}_3. \end{cases}$$

defines a meromorphic quadratic differential on $\mathcal{R}$ *for which* $\operatorname{supp}\mu_j$ *is an arc of trajectory of* ϖ.

As it was already mentioned, the relation between measures with algebraic Cauchy transforms and quadratic differentials is not new. For quadratic equations this connection was already indicated in Theorem 1.2.1, and in fact it has been exploited before, as in the aforementioned GRS theory for non-hermitian orthogonality [127, 129], and also in the context of the Deift-Zhou steepest descent analysis for Riemann-Hilbert problems in several models of mathematical physics, such as Painlevé equations [18, 25], in theoretical physics [2,3,31,32] and in numerical analysis [49]. However, apart from degree 2 algebraic equations as in Theorem 1.2.1, this connection has only been exploited *locally* but not *globally* on a compact Riemann surface, as it is stated in Theorem 1.3.2. The idea of defining the quadratic differential as in Theorem 1.3.2 also plays a fundamental role in Chapter 4, as will be explained in the next section.

Theorem 1.3.2 provides a tool to construct critical measures and study the dynamics of their supports. In Chapter 3 we explore this connection for (1.31) with the choice of coefficients

$$R(z) = 3z^4 - 3z - c, \quad D(z) = -2z^6 + 3z^3 + cz - 3\alpha(1-\alpha), \tag{1.32}$$

where

$$c = -\left(\frac{243}{64}(1 - 4\alpha(1-\alpha))^2\right)^{1/3}. \tag{1.33}$$

We prove

Theorem 1.3.3 (see Theorems 3.2.12 and 3.2.14)**.** *For every value of* $\alpha \in [0, 1/2)$*, there exists a critical vector-valued measure* $\vec{\mu}_\alpha \in \mathcal{M}_\alpha$ *for the choice of potentials*

$$\Phi_1(z) = \Phi_2(z) = z^3, \quad \Phi_3(z) = 0,$$

for which the corresponding algebraic equation has coefficients (1.32)–(1.33)*. Moreover, there exists a critical value* $\alpha_c \in (0, 1/2)$ *such that*

- *if* $0 < \alpha < \alpha_c$*, then* $\mu_3 = 0$ *and* $\operatorname{supp}\mu_1, \operatorname{supp}\mu_2$ *are disjoint connected arcs;*
- *if* $\alpha > \alpha_c$*, then none of the measures is zero and* $\operatorname{supp}\mu_1, \operatorname{supp}\mu_2$ *and* $\operatorname{supp}\mu_3$ *are connected arcs intersecting at one common point.*

The construction of $\vec{\mu}_\alpha$ and the dynamics of the supports of its components heavily rely on Theorem 1.3.2. For $\alpha = 0$, the trajectories of ϖ can be described

in an explicit way, and $\vec{\mu}_\alpha$ can be embedded on its trajectories. For general α, the structure of trajectories can be quite complicated, but we are able to control them by analyzing certain parameters - the so-called width parameters - for ϖ. Once we control these parameters, we can keep track of the deformation of $\vec{\mu}_\alpha$, thus obtaining Theorem 1.3.3.

1.4 Normal matrix model

The last model we consider is the *normal matrix model*, which consists of the space of $n \times n$ normal matrices M equipped with the probability distribution

$$\frac{1}{\mathcal{Z}_n} e^{-n \operatorname{Tr} \mathcal{V}(M)} dM. \tag{1.34}$$

Here $\mathcal{V} : \mathbb{C} \to \mathbb{R}$ is a given real-valued function for which $\mathcal{V}(M)$ is defined by the spectral calculus and $\mathcal{Z}_n$ is the normalization constant.

In a similar manner as for the hermitian matrix model (1.1)–(1.2), diagonalizing M the distribution (1.34) induces the eigenvalue distribution

$$\mathcal{P}_n(\lambda) d\lambda = \frac{1}{Z_n} \prod_{j<k} |\lambda_j - \lambda_k|^2 \prod_j e^{-n\mathcal{V}(\lambda_j)} d\lambda, \tag{1.35}$$

on the vector of *complex* eigenvalues $\lambda = (\lambda_1, \ldots, \lambda_n) \in \mathbb{C}^n$.

Planar orthogonality in the normal matrix model

The sequence $(p_{j,n})$, where each $p_{j,n}$ is a monic polynomial of degree j satisfying

$$\int_{\mathbb{C}} p_{j,n}(z) \overline{p_{k,n}(z)} e^{-n\mathcal{V}(z)} dA(z) = \delta_{j,k} h_{j,n}^2, \quad h_{j,n} > 0, \quad j,k = 0, 1, \ldots, \tag{1.36}$$

and dA is the Lebesgue measure on $\mathbb{C}$, is called the sequence of *planar orthogonal polynomials* for the weight $e^{-n\mathcal{V}(z)}$. Again, the relevance of the sequence $(p_{j,n})$ is that $p_{n,n}$ coincides with the average characteristic polynomial of (1.35), and the eigenvalue distribution (1.35) admits the determinantal representation

$$\mathcal{P}_n(\lambda_1, \ldots, \lambda_n) = \frac{1}{n!} \det \left(K_n(\lambda_j, \lambda_k) \right)_{1 \le j,k \le n}, \tag{1.37}$$

where the correlation kernel K_n takes the form

$$K_n(z,w) = e^{-n(\mathcal{V}(z)+\mathcal{V}(w))} \sum_{j=0}^{n-1} \frac{\overline{p_{j,n}(w)} p_{j,n}(z)}{h_{j,n}^2}. \tag{1.38}$$

Equilibrium problem for the limiting eigenvalue distribution and the associated mother body problem

Under the assumptions that $\mathcal{V}$ is continuous and satisfies the growth condition

$$\lim_{z\to\infty} \frac{\mathcal{V}(z)}{\log(1+|z|^2)} = +\infty,$$

there exists a unique probability measure $\mu_{\mathcal{V}}$ minimizing the energy functional

$$E^{\mathcal{V}}(\mu) = I(\mu) + \int \mathcal{V}(z)d\mu(z) \tag{1.39}$$

over all probability measures on $\mathbb{C}$ [120]. In contrast to the previous sections, where the minimization problems were posed over sets of zero Lebesgue measure (real line or, more generally, contours), note that now we are minimizing over the set $\mathbb{C}$. Consequently, if we know that the interior of $\operatorname{supp}\mu_{\mathcal{V}}$, say Ω, has positive Lebesgue measure and $\mu_{\mathcal{V}}$ is absolutely continuous with respect to dA on Ω, then its density assumes the form

$$d\mu_{\mathcal{V}}(z) = \frac{1}{4\pi}\Delta\mathcal{V}(z)dA(z), \quad z\in\Omega,$$

where Δ is the usual Laplacian. In particular, if $\Delta\mathcal{V}$ is constant, then $\mu_{\mathcal{V}}$ is the uniform measure on the closure of its support, and the determination of $\mu_{\mathcal{V}}$ is completely solved once $\operatorname{supp}\mu_{\mathcal{V}}$ is found.

Given a probability measure μ, the associated *weak mother body problem* asks for finding another probability measure μ_* with the following properties.

(M1) $\operatorname{supp}\mu_*$ has null area measure;

(M2) $\operatorname{supp}\mu_* \subset \operatorname{supp}\mu$;

(M3) $U^{\mu}(z) \le U^{\mu_*}(z),\ z\in\mathbb{C}$;

(M4) $U^{\mu}(z) = U^{\mu_*}(z),\ z\in\mathbb{C}\setminus\operatorname{supp}\mu$.

Such a measure μ_*, if it exists, is called a *weak mother body* for μ. Furthermore, μ_* is a (strong) *mother body* for μ if it additionally satisfies the condition

(M5) $\mathbb{C}\setminus\operatorname{supp}\mu_*$ is connected.

If μ is the uniform measure of the closure of a domain $\Omega\subset\mathbb{C}$, μ_* is also called a mother body for Ω. Conditions (M1)–(M5) are, generally speaking, quite

demanding, and consequently (weak) mother bodies for a given measure are somewhat rare and found on a case-by-case basis. In contrast, (M1)–(M5) do not guarantee that the mother body of a given measure μ is unique.

Let us go back to our discussion on the normal matrix model (1.35). Contrary to the hermitian models discussed in Sections 1.1–1.3, the sequences of empirical measures (ν_n) and of zero counting measures $(\mu(p_{n,n}))$ associated to the average characteristic polynomials of (1.35) do not have the same limit. Hedenmalm and Makarov [81] showed that the convergence of the sequence (ν_n) of empirical measures

$$\nu_n \xrightarrow{*} \mu_{\mathcal{V}} \tag{1.40}$$

holds true almost surely. On the other hand, there is no general results concerning the limit of $(\mu(p_{n,n}))$, but in several cases the convergence

$$\mu(p_{n,n}) \xrightarrow{*} \mu_*, \tag{1.41}$$

where μ_* is a (weak) mother body for $\mu_{\mathcal{V}}$, has been verified [19, 20, 119]. Taking into account (M2) and (M4), the limits (1.40)–(1.41) express that

$$\lim_{n\to\infty} U^{\mu(p_{n,n})}(z) = U^{\mu_*}(z) = U^{\mu_{\mathcal{V}}}(z) = \lim_{n\to\infty} U^{\nu_n}(z), \quad z \in \mathbb{C} \setminus \operatorname{supp} \mu_{\mathcal{V}},$$

which is a generalization of (1.7).

The cut-off approach for algebraic potentials

Following Lee and Makarov [98], a potential $\mathcal{V}$ is called *algebraic* if it is of the form

$$\mathcal{V}(z) = \frac{1}{t_0}(|z|^2 - 2\operatorname{Re} V(z)), \quad t_0 > 0, \tag{1.42}$$

for some analytic function V with rational derivative. At the formal level, the normal matrix model with algebraic potentials is intimately connected with the Laplacian growth problem and quadrature domains [88, 98]. In virtue of this connection, the constant t_0 can also be regarded as time or area parameter.

At the rigorous level, the densities in (1.34)–(1.35) for algebraic potentials are divergent, unless V assumes the form

$$V(z) = az^2 + 2bz + \sum_j c_j \log(z - z_j), \quad |a| < \frac{1}{2},\ c_j > 0.$$

Thus for other choices of V, the normal matrix model is ill-defined. In order to regularize it, Elbau and Felder [65] introduced the *cut-off* approach. For the

algebraic potential (1.42) with the choice

$$V(z) = \sum_{k=1}^{d+1} \frac{t_k}{k} z^k, \qquad d \geq 2, \quad t_k \in \mathbb{C}, \quad t_{d+1} \neq 0,$$

instead of considering (1.34) on the whole set of normal matrices, they consider it on the set of matrices whose eigenvalues are restricted to lie within a fixed compact set $D \subset \mathbb{C}$. In this setup, the eigenvalue distribution (1.35) assumes the form

$$\mathcal{P}_n(\lambda)d\lambda = \frac{1}{Z_n} \prod_{j<k} |\lambda_j - \lambda_k|^2 \prod_j \chi_D(\lambda_j) e^{-n\mathcal{V}(\lambda_j)} d\lambda, \tag{1.43}$$

where χ_D is the characteristic function of D, the orthogonality (1.36) has to be replaced by

$$\int_D q_{j,n}(z)\overline{z}^k e^{-n\mathcal{V}(z)} dA(z) = 0, \quad k = 0, 1, \ldots, j-1 \tag{1.44}$$

$q_{n,n}$ is the average characteristic polynomial of (1.43) and the identity (1.38) still holds true if one replaces the polynomials p's by the q's therein. Furthermore, Elbau and Felder also proved the convergence of the empirical measure (μ_n) to the measure μ_0 minimizing the energy (1.39) over all probability measures supported on the cut-off D.

Under the extra conditions that

(a) the boundary ∂D of the cut-off is sufficiently smooth,

(b) the potential $\mathcal{V}$ has exactly one minimum on D, and

(c) the parameter t_0 is sufficiently small,

they also showed that the equilibrium measure μ_0 assumes the form

$$d\mu_0(z) = \frac{1}{\pi t_0} \chi_\Omega(z) dA(z),$$

where χ_Ω is the characteristic function of a simply connected domain Ω whose closure is contained on the interior of D, and whose boundary is given by $\partial\Omega = h(\partial\mathbb{D})$ for some rational function h of the form

$$h(w) = rw + \sum_{j=0}^{d} \frac{a_j}{w^d}, \quad r > 0, \ a_j \in \mathbb{C}, \ a_d \neq 0. \tag{1.45}$$

In addition, they determined a system of algebraic equations that should relate the parameters $t_0, t_1, \ldots t_{d+1}$ with the parameters $r, a_0, \ldots, a_d$.

Still for polynomial V, Elbau [64] investigated the behavior of the sequence of zero counting measures $(\mu(q_{n,n}))$ in the large n limit, showing that any accumulation point of $(\mu(q_{n,n}))$ (in the weak topology) should satisfy (M4), and he conjectured that at least one of the accumulation points of $(\mu(q_{n,n}))$ should be a mother body for $\mu_{\mathcal{V}}$.

Algebraic potentials with discrete symmetry

Still in the context of algebraic potentials, the choice

$$V(z) = \frac{1}{d+1} z^{d+1}, \quad d \geq 2, \tag{1.46}$$

for t_0 smaller than a certain (explicit) critical value $t_{0,c}$ was studied in details by Bleher and Kuijlaars [38] (see also [95] for $t_0 > t_{0,c}$) for $d = 2$, and their analysis was further extended by Kuijlaars and López [90] for general $d \geq 2$, as we explain next.

Their starting point is to replace the planar orthogonality by an orthogonality over contours. For a given cut-off D, assumed to be invariant over rotations by $2\pi/(d+1)$, consider the star-like set

$$\Sigma = \{z \in D \ \mid \ z^{d+1} \in [0, +\infty)\}.$$

For any polynomial Q, Kuijlaars and López use Green's Theorem to write

$$2i \iint_D Q(z) \bar{z}^k e^{-n\mathcal{V}(z)} dA(z) = \int_\Sigma Q(s) w_{k,n}(s) ds + \oint_{\partial D} Q(s) \widetilde{w}_{k,n}(s) ds$$

where $w_{k,n}$ and $\widetilde{w}_{k,n}$ are (explicit) holomorphic and anti-holomorphic functions, respectively (see Section 4.2.7 for more details when $d = 2$). This formula means that (1.44) is equivalent to

$$\int_\Sigma q_{j,n}(s) w_{k,n}(s) ds + \oint_{\partial D} q_{j,n}(s) \widetilde{w}_{k,n}(s) ds = 0, \quad k = 0, 1, \ldots, j-1. \tag{1.47}$$

Guided by the fact that the contributions coming from ∂D should be exponentially small in the large n limit, Kuijlaars and López [90] neglected the integral over ∂D on (1.47), and considered the monic polynomial $P_{n,n}$ of degree n determined through the conditions

$$\int_\Sigma P_{n,n}(s) w_{k,n}(s) ds = 0, \quad k = 0, 1, \ldots, n-1.$$

It turns out that this polynomial $P_{n,n}$ satisfies the multiple orthogonality conditions

$$\int_{\Sigma} P_{n,n}(s) z^k w_{j,n}(s) ds = 0, \quad k = 0, \dots, \left\lceil \frac{n-j}{d} \right\rceil - 1, \ j = 0, \dots, d-1. \tag{1.48}$$

Thus, at the heuristic level, the approach taken in [90] is to replace the sequence of planar orthogonal polynomials $(q_{n,n})$ in (1.44) by the sequence of (non-hermitian) multiple orthogonal polynomials $(P_{n,n})$ in (1.48), for which there is no complex conjugation involved in the integrand. The main advantage is that $P_{n,n}$ can be characterized in terms of the solution to a $(d+1) \times (d+1)$ Riemann-Hilbert problem, and using this representation the authors in [90] (and in a similar spirit in [38, 95]) were able to obtain asymptotic results for $(P_{n,n})$. One of these outcomes is the convergence

$$\mu(P_{n,n}) \to \mu_*,$$

where μ_* is a mother body for μ_0, thus showing that the sequence $(P_{n,n})$ indeed captures one of the main aspects expected to hold for the orthogonal polynomials in (1.44).

The cubic plus linear potential

One of the essential technical feature in the works [38, 90, 95] is the underlying $(d+1)$-fold symmetry present in their whole analysis, which is induced by potentials of the form (1.46).

Motivated towards gaining a better understanding of models without symmetries, in Chapter 4 we study the normal matrix model (1.43) with algebraic potential (1.42) for

$$V(z) = \frac{1}{3} z^3 + t_1 z, \quad -\frac{3}{4} < t_1 < \frac{1}{4}.$$

To state some of our results, we introduce some terminology. One of the main objects in Chapter 4 is the rational function (1.45), which in the present case reduces to the form

$$h(w) = rw + a_0 + \frac{2a_0 r}{w} + \frac{r^2}{w^2}, \tag{1.49}$$

where $r = r(t_0, t_1)$ and $a_0 = a_0(t_0, t_1)$ relate to (t_0, t_1) through the system

$$\begin{cases} 2r^4 - r^2(1 - 4a_0^2) = -t_0, \\ a_0^2 - (1 - 4r^2)a_0 = -t_1. \end{cases} \tag{1.50}$$

The rational function h gives rise to a Riemann surface $\mathcal{R}$ via

$$\mathcal{R} = \{(\xi, z) \in \overline{\mathbb{C}}^2 \ \mid \ (\xi, z) = (h(w^{-1}), h(w)),\ w \in \overline{\mathbb{C}}\}.$$

$\mathcal{R}$ is known as the *spectral curve* of the normal matrix model. As it is shown in Chapter 4, $\mathcal{R}$ can be alternatively described as the pairs (ξ, z) satisfying the algebraic equation

$$\xi^3 + z^3 - z^2\xi^2 - t_1(\xi^2 + z^2) - (1 + t_0)z\xi + (B + t_1)(\xi + z) + A = 0 \quad (1.51)$$

for certain explicit coefficients $A = A(t_0, t_1)$ and $B = B(t_0, t_1)$.

The algebraic equation (1.51) admits three solutions $\xi_1(z), \xi_2(z)$ and $\xi_3(z)$, which we label in such a way that

$$\begin{aligned}
\xi_1(z) &= z^2 + t_1 + \frac{t_0}{z} + \mathcal{O}(z^{-2}), \\
\xi_2(z) &= -z^{1/2} + \frac{t_1}{2z^{1/2}} - \frac{t_0}{2z} + \mathcal{O}(z^{-3/2}), \qquad \text{as } z \to \infty, \qquad (1.52) \\
\xi_3(z) &= z^{1/2} - \frac{t_1}{2z^{1/2}} - \frac{t_0}{2z} + \mathcal{O}(z^{-3/2}).
\end{aligned}$$

We prove

Theorem 1.4.1 (see Theorems 4.2.2–4.2.5 and Proposition 4.2.7)**.** *Given $t_1 \in (-3/4, 1/4)$, there exists $t_{0,crit} = t_{0,crit}(t_1) > 0$ such that if $t_0 < t_{0,crit}$, then the system (1.50) admits a solution (r, a_0) for which the function h in (1.49) is a conformal map from $\mathbb{C} \setminus \mathbb{D}$ to the complement of a simply connected domain Ω.*

Furthermore, under certain conditions on D, the sequence of empirical measures (ν_n) for (1.43) converges almost surely to the uniform measure on $\overline{\Omega}$.

Finally, the solution ξ_1 to (1.51) is the Schwarz function of $\partial\Omega$, that is, it admits a meromorphic continuation to a neighborhood of $\mathbb{C} \setminus \Omega$, and satisfies

$$\xi_1(z) = \overline{z}, \quad z \in \partial\Omega.$$

The mother body phase transition

We also study in detail the mother body problem for the domain Ω. We prove

Theorem 1.4.2 (see Theorems 4.2.9 and 4.2.10)**.** *There exists an oriented contour $\Sigma_* \subset \Omega$ for which ξ_1 is analytic on $\mathbb{C} \setminus \Sigma_*$, and the measure*

$$d\mu_*(s) = \frac{1}{2\pi i t_0}(\xi_{1-}(s) - \xi_{1+}(s))ds, \quad s \in \Sigma_*,$$

is a mother body for Ω.

Furthermore, there exists a value $\tilde{t}_{0,crit} = \tilde{t}_{0,crit}(t_1) < t_{0,crit}$ *such that*

- *if* $t_1 > 0$ *and* $t_0 \leq \tilde{t}_{0,crit}$, *then* $\operatorname{supp}\mu_*$ *is an interval of the real line;*
- *if* $t_1 < 0$ *and* $t_0 \leq \tilde{t}_{0,crit}$, *then* $\operatorname{supp}\mu_*$ *is a single analytic arc connecting two (non real) points;*
- *if* $t_0 > \tilde{t}_{0,crit}$, *then* $\operatorname{supp}\mu_*$ *consists of three analytic arcs intersecting at a common point.*

A combination of Theorems 1.4.1 and 1.4.2 thus says that $\tilde{t}_{0,crit}$ determines a *phase transition* for μ_* which is not reflected on Ω, in the sense that $\partial\Omega$ depends analytically on t_0 in a neighborhood of $\tilde{t}_{0,crit}$, whereas the topology of $\Sigma_* = \operatorname{supp}\mu_*$ changes from "one-cut" to "three-cuts" when t_0 moves beyond $\tilde{t}_{0,crit}$. This is what we call the *mother body phase transition*, and to our knowledge it is the first time such a phase transition is described in the literature.

The proof of Theorem 1.4.2 is rather long. The main idea is to construct a quadratic differential ϖ on $\mathcal{R}$ (in a similar way as it is done in Theorem 1.3.2) and, for $t_1 = 0$, embed the support Σ_* of the mother body on its critical graph. We then apply the techniques developed in Chapter 3 to analyze the critical graph of ϖ when t_1 is deformed, keeping track of Σ_*. Projecting the critical graph of ϖ to the complex plane, we are thus able to determine Σ_* as stated in Theorem 1.4.2.

Asymptotics of multiple orthogonal polynomials

The algebraic equation (1.51) has three singular points $\hat{z}_0, \hat{z}_1$ and $\hat{z}_2$, that we label so that $\hat{z}_0 \in \mathbb{R}$, $\operatorname{Im}\hat{z}_1 < 0$ and $\overline{\hat{z}_2} = \hat{z}_1$.

Following Bleher and Kuijlaars [38] and Kuijlaars and López [90], we associate to the model a sequence of multiple orthogonal polynomials as in (1.48). In the present setting, the multiple orthogonality takes the explicit form

$$\begin{aligned}
&\sum_{l=0}^{2} \int_{\Sigma_l} P_{n,n}(z) z^k e^{\frac{n}{t_0}V(z)} y_l(c_n(z-t_1))dz = 0, \quad k = 0, \dots, \left\lceil \frac{n}{2} \right\rceil - 1, \\
&\sum_{l=0}^{2} \int_{\Sigma_l} P_{n,n}(z) z^k e^{\frac{n}{t_0}V(z)} y_l'(c_n(z-t_1))dz = 0, \quad k = 0, \dots, \left\lfloor \frac{n}{2} \right\rfloor - 1.
\end{aligned} \tag{1.53}$$

where each Σ_l is an oriented analytic arc starting at a common point z_* and ending at $\hat{z}_l$, and for $\omega = e^{2\pi i/3}$,

$$y_l(z) = \omega^l \operatorname{Ai}(\omega^l z),\ l = 0, 1, 2, \quad c_n = \left(\frac{n}{t_0}\right)^{2/3}.$$

The multipleorthogonal polynomial $P_{n,n}$ is characterized in terms of a 3×3 Riemann-Hilbert problem. In Chapter 4 we apply the Deift-Zhou nonlinear steepest descent method to this Riemann-Hilbert problem, which among other consequences yields

Theorem 1.4.3 (see Theorem 4.2.14)**.** *The sequence of zero counting measures* $(\mu(P_{n,n}))$ *converges weakly to the mother body* μ_* *of* Ω*.*

In virtue of the previous discussion, Theorem 1.4.3 thus indicates that the sequence $(P_{n,n})$ in (1.53) captures, at the level of the limiting zero distribution, the behavior expected to hold for the sequence $(q_{n,n})$ in (1.44).

1.5 Overview of the thesis

The rest of this thesis is organized as follows. Chapter 2, based on the joint work [94] with Arno Kuijlaars, is dedicated to the study of the max-min problem for non-hermitian orthogonal polynomials that was discussed in Section 1.2. Chapter 3 is based on the joint work with Andrei Martínez-Finkelshtein [107], and corresponds to the systematic study of the critical vector-valued measures that we briefly discussed in Section 1.3. Chapter 4 is based on the joint work with Pavel Bleher [42], and deals with the mother body problem in the normal matrix model with cubic plus linear potential, and the associated multiple orthogonal polynomials, as discussed in Section 1.4.

As it will become clear later, quadratic differentials play a fundamental role in this thesis. As such, in Appendix A we include a gentle introduction to quadratic differentials, in a form suitable to our needs.

Chapter 2

S-curves in polynomial external field

Curves in the complex plane that satisfy the S-property were first introduced by Stahl [130, 131] and they were further studied by Gonchar and Rakhmanov [71] in the 1980s. Rakhmanov [116] recently showed the existence of curves with the S-property in a harmonic external field by means of a max-min variational problem in logarithmic potential theory. This is done in a fairly general setting, which however does not include the important special case of an external field $\operatorname{Re} V$ where V is a polynomial of degree ≥ 2. In this chapter, based on the joint work [94] with A. Kuijlaars, we give a detailed proof of the existence of a curve with the S-property in the external field $\operatorname{Re} V$ within the collection of all curves that connect two or more pre-assigned directions at infinity in which $\operatorname{Re} V \to +\infty$. Our method of proof is very much based on the works of Rakhmanov on the max-min variational problem [116] and of Martínez-Finkelshtein and Rakhmanov [104] on critical measures.

2.1 Introduction

The concept of *S-property* for logarithmic potentials appeared for the first time in the works of H. Stahl [128, 129, 130, 131], in the study of the limiting distribution of poles of Padé approximants, see also [127] for a recent survey and extension of these results.

Inspired by Stahl's works, Gonchar and Rakhmanov extended the S-property

to situations with external field [71]. They then characterized the limiting distribution of zeros of certain *non-hermitian* orthogonal polynomials, subject to the existence of a certain curve with the S-property in an external field - the *S-curve*, see Section 2.2.2 below for a precise definition.

Very recently, Rakhmanov returned to the question of existence of S-curves from a general perspective [116]. He considered an associated *max-min equilibrium problem* in logarithmic potential theory, and in an "ideal" situation he proved that this max-min problem has a solution and the solution has the S-property. This general approach by Rakhmanov is very similar in spirit to his previous work with Kamvissis [87], where a max-min problem for Green energy in a particular external field was considered.

In [116], Rakhmanov also pointed out some examples where his proposed "ideal" situation does not apply, although similar considerations should also lead to the existence of a curve with the S-property. The present chapter is aimed at studying this problem in a very particular, but important, model, namely when the external field is given by the real part of a polynomial.

Following the approach of Rakhmanov, for a polynomial V we consider a max-min problem of the form

$$\max_{\Gamma} \min_{\substack{\operatorname{supp}\mu\subset\Gamma \\ \mu(\mathbb{C})=1}} \left[\iint \log \frac{1}{|x-y|} d\mu(x) d\mu(y) + \int \operatorname{Re} V(x)\, d\mu(x) \right],$$

where the maximum is taken over a suitable class of contours Γ (see Section 2.2.3 below for precise definitions), and the infimum is taken over the set of Borel probability measures μ on Γ. The aim of this chapter is to prove that the max-min problem has a solution, and this solution leads to an S-curve Γ.

The max-min approach is not the only possible approach to the existence of the S-curve. In some particular cases, it is possible to construct the S-curve explicitly from specific properties of the problem at hand, see e.g. [2, 7, 15, 28, 47, 49] for recent contributions. In general, the explicit determination of the S-curve - or more specifically the determination of the support of its equilibrium measure - is a hard problem, and some numerical studies have also been carried out, see [2, 28].

Motivated by questions in Random Matrix Theory, Bertola [24] also studied the existence of the S-curve for a polynomial external field in the same framework as the present chapter. By using deformation techniques, Bertola was able to show the existence of the S-curve. However, his approach only works when the underlying equilibrium measure vanishes as a square root at the endpoints of its support, although it is very likely that his approach could also be adapted to remove this restriction. It is worth emphasizing that in our setup there is no

restriction on the underlying equilibrium measure - so we get the same result as Bertola but valid in the general situation.

An extension of the concept of S-curves to vector equilibrium problems appears in the context of Hermite-Padé approximation, see e.g. [11, 112, 117]. Vector equilibrium problems also appear in certain problems in random matrix theory, for example for random matrix models with external source [9, 33] and coupled random matrices [63], see [89] for an overview. The asymptotic analysis has been mostly restricted to cases with enough symmetry so that the relevant contours are contained in the real or imaginary axis. A suitable existence theory for curves with S-property appropriate to vector equilibrium problems with external fields, and possibly also upper constraints, would be a major step towards the analysis of situations with less symmetry. See [13] for a first example in this direction.

2.2 Background and statement of the main result

To state our main result, we first need to introduce a few notations and notions.

Throughout this chapter, V always denotes a complex polynomial of degree $N \geq 2$ and

$$\varphi = \operatorname{Re} V.$$

Also, we denote

$$D_R(z_0) = \{z \in \mathbb{C} \mid |z - z_0| < R\}, \qquad D_R = D_R(0).$$

2.2.1 Notions from potential theory

Given a finite Borel measure μ on $\mathbb{C}$, its *logarithmic potential* at $x \in \mathbb{C}$ is defined by

$$U^\mu(x) = \int \log \frac{1}{|x-y|}\, d\mu(y),$$

and its *logarithmic energy* by

$$I(\mu) = \iint \log \frac{1}{|x-y|}\, d\mu(x) d\mu(y) = \int U^\mu(x)\, d\mu(x),$$

whenever these integrals make sense.

For a closed set $F \subset \mathbb{C}$ and φ the real part of a polynomial as before, we define $\mathcal{M}_1(F)$ as the set of Borel probability measures μ supported on F, satisfying

the growth condition

$$\int \log(1+|x|)d\mu(x) < +\infty, \tag{2.1}$$

and by $\mathcal{M}_1^{\varphi}(F)$ we denote the subset of $\mathcal{M}_1(F)$ consisting of all measures μ for which $I(\mu)$ is finite and $\varphi \in L^1(\mu)$. The condition (2.1) assures the quantities $U^{\mu}(z), I(\mu)$ are well defined elements of $(-\infty, +\infty]$ and $U^{\mu}(z)$ is finite for a.e. $z \in \mathbb{C}$ with respect to planar Lebesgue measure.

For $\mu \in \mathcal{M}_1^{\varphi}(F)$, the quantity

$$I^{\varphi}(\mu) = I(\mu) + \int \varphi(x)d\mu(x),$$

is called the *weighted logarithmic energy of μ in the external field φ*, or just weighted energy of μ.

The following minimization problem is classical [120]: find a measure $\mu^{\varphi} = \mu^{\varphi,F} \in \mathcal{M}_1^{\varphi}(F)$ for which the infimum

$$I^{\varphi}(F) = \inf_{\mu \in \mathcal{M}_1^{\varphi}(F)} I^{\varphi}(\mu) \tag{2.2}$$

is attained, i.e., for which $I^{\varphi}(\mu^{\varphi}) = I^{\varphi}(F)$. The measure μ^{φ} is called the *equilibrium measure* of the set F in the external field φ. For the case without external field, that is, when $\varphi \equiv 0$, the measure μ^0 is also called the *Robin measure* of F, the value $I(F)$ is the *Robin constant* of F, the constant $e^{-I(F)}$ is called *(logarithmic) capacity* of F and denoted by $\operatorname{cap} F$.

For φ the real part of a polynomial as before, if Γ is a contour in $\mathbb{C}$ satisfying the growth condition

$$\lim_{\substack{z\to\infty \\ z\in\Gamma}} \varphi(z) = +\infty, \tag{2.3}$$

the equilibrium measure $\mu^{\varphi,\Gamma}$ uniquely exists [120] and can be characterized through the *Euler - Lagrange variational conditions*. It is the only measure in $\mathcal{M}_1^{\varphi}(\Gamma)$ for which there exists a constant l satisfying

$$U^{\mu}(z) + \frac{1}{2}\varphi(z) = l, \quad z \in \operatorname{supp}\mu, \tag{2.4}$$

$$U^{\mu}(z) + \frac{1}{2}\varphi(z) \geq l, \quad z \in \Gamma. \tag{2.5}$$

2.2.2 S-property

Definition 2.2.1. A contour Γ satisfying the growth condition (2.3) is said to possess the *S-property in the external field φ* if its equilibrium measure $\mu = \mu^{\varphi,\Gamma}$

in the external field satisfies the following. There is a finite set E such that $\operatorname{supp}\mu \setminus E$ is locally an analytic arc at each of its points, and its potential $U^\mu = U^{\mu^{\varphi,\Gamma}}$ satisfies

$$\frac{\partial}{\partial n_+}\left(U^\mu + \frac{1}{2}\varphi\right)(z) = \frac{\partial}{\partial n_-}\left(U^\mu + \frac{1}{2}\varphi\right)(z), \quad z \in \operatorname{supp}\mu \setminus E, \tag{2.6}$$

where $n_\pm$ are the unit normal vectors to $\operatorname{supp}\mu$ at z.

If a contour has the S-property in the external field φ, we also call it an *S-curve* in the external field φ. If the external field φ is clear from the context (as it is in this chapter), we briefly call it an S-curve.

As it is clear already from the Definition 2.2.1, the S-property is intrinsic to the equilibrium measure in the external field of the contour. If we modify the contour away from the support, keeping the equilibrium measure in the external field the same for the modified contour, the S-property is preserved.

Although in the present thesis we are just interested in the S-property stated in terms of logarithmic potentials, its analogue for potentials coming from other kernels, such as the Green potential, have also their own interest [87, 105, 117].

2.2.3 The class of admissible contours

There exist N sectors $S_1, \dots, S_N$ in the complex plane along which $\varphi(z) = \operatorname{Re} V(z) \to +\infty$ as $z \to \infty$ in S_j. These sectors are determined by the leading coefficient of V. If $V(z) = a_0 z^N + \cdots$, $a_0 \neq 0$, then

$$S_j = \left\{ z \in \mathbb{C} \mid |\arg z - \theta_j| < \frac{\pi}{2N} \right\}, \qquad \theta_j = -\frac{\arg a_0}{N} + \frac{2\pi(j-1)}{N}, \tag{2.7}$$

for $j = 1, \dots, N$.

We say that a set $F \subset \mathbb{C}$ *stretches out to infinity* in the sector S_j if there exist $\epsilon > 0$ and $r_0 > 0$ such that for every $r > r_0$ there is $z \in F$ with

$$|z| = r, \qquad |\arg z - \theta_j| < \frac{\pi}{2N} - \epsilon.$$

Thus in particular we have $\varphi(z) \to +\infty$ if $z \to \infty$ within $S_j \cap F$.

A partition $\mathcal{P}$ of $\{1, \dots, N\}$ is called *noncrossing* if it satisfies the following property:

$$j \overset{\mathcal{P}}{\sim} j' \ \wedge \ k \overset{\mathcal{P}}{\sim} k' \ \wedge j < k < j' < k' \Longrightarrow j \overset{\mathcal{P}}{\sim} k.$$

Here $\overset{\mathcal{P}}{\sim}$ denotes the equivalence relation that is associated with the partition $\mathcal{P}$.

Figure 2.1: Graphical representation of the crossing partition $\mathcal{P} = \{\{1, 4, 5\}, \{2, 3, 6\}\}$ (on the left) and of the noncrossing partition $\mathcal{P} = \{\{1, 5, 6\}, \{2, 3\}, \{4\}\}$ (on the right).

The term *noncrossing* becomes more evident in a graphical representation of a partition, see Figure 2.1.

To any noncrossing partition we associate a collection $\mathcal{T}$ of admissible contours.

Definition 2.2.2. Let $\mathcal{P}$ be a noncrossing partition of $\{1, \dots, N\}$ and $\mathcal{P}_0$ the subset of $\mathcal{P}$ obtained by removing from $\mathcal{P}$ all singleton sets. We assume $\mathcal{P}_0 \neq \emptyset$. We associate with $\mathcal{P}$ the collection $\mathcal{T}(\mathcal{P})$ of admissible contours Γ defined as follows.

i) Each $\Gamma \in \mathcal{T}(\mathcal{P})$ is a finite union of C^1 Jordan arcs.

ii) Each $\Gamma \in \mathcal{T}(\mathcal{P})$ has at most $|\mathcal{P}_0|$ connected components, all of them unbounded and stretching out to infinity in at least two of the sectors $S_1, \dots, S_N$.

iii) For each $A \in \mathcal{P}_0$ there is a connected component Γ_A of Γ that stretches out to infinity in each sector S_j with $j \in A$.

iv) If $A \in \mathcal{P} \setminus \mathcal{P}_0$ then there exists $R > 0$ for which

$$\Gamma \cap (S_j \setminus D_R) = \emptyset, \quad j \in A.$$

For simplicity, we will mostly write $\mathcal{T}$ instead of $\mathcal{T}(\mathcal{P})$.

Figure 2.2 shows all noncrossing partitions (up to rotation) for a polynomial of degree $N = 5$ and representative contours Γ from each of the collections $\mathcal{T}(\mathcal{P})$.

The restriction to noncrossing partitions in Definition 2.2.2 is not essential. We could as well have defined the admissible contours for arbitrary partitions, but then the class of admissible contours obtained for a given crossing partition would coincide with the class of admissible contours for some noncrossing partition.

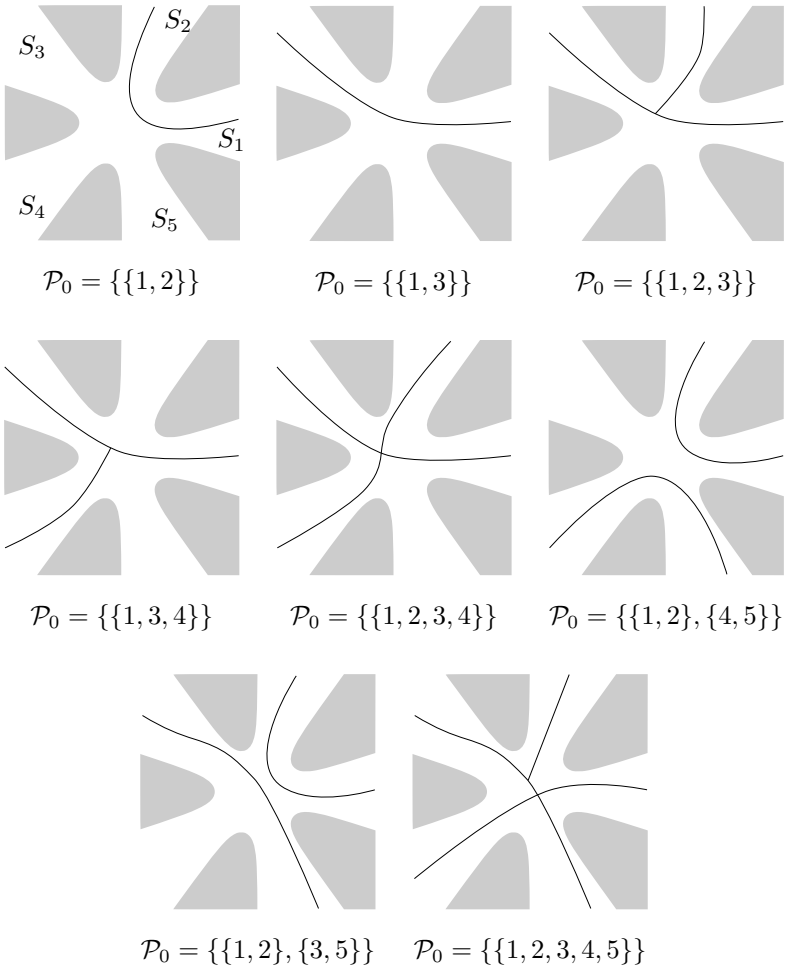

Figure 2.2: All possible choices of $\mathcal{P}$ and representative contours in $\mathcal{T}(\mathcal{P})$ for a polynomial V of degree 5 and positive leading coefficient. The sectors $S_1, \ldots, S_5$ are indicated on the top left figure. In gray is represented the region where φ is very negative.

2.2.4 The main theorem

For the polynomial V and a fixed noncrossing partition $\mathcal{P}$ as above, the *max-min energy problem* for the pair $(V, \mathcal{T}(\mathcal{P}))$ asks for finding a contour $\Gamma_0 \in \mathcal{T}$ for which $I^\varphi(\cdot)$, see (2.2), attains its maximum on $\mathcal{T}$. That is,

$$I^\varphi(\Gamma_0) = \max_{\Gamma \in \mathcal{T}} I^\varphi(\Gamma) = \max_{\Gamma \in \mathcal{T}} \min_{\mu \in \mathcal{M}_1^\varphi(\Gamma)} I^\varphi(\mu). \tag{2.8}$$

In what follows we use

$$C^\mu(z) = \int \frac{d\mu(x)}{x - z} \tag{2.9}$$

to denote the Cauchy transform of a measure μ. The main result of this chapter is the following.

Theorem 2.2.3. *Let V be a polynomial of degree $N \geq 2$ and let $\mathcal{P}$ be a noncrossing partition with class $\mathcal{T}(\mathcal{P})$ of admissible contours as in Definition 2.2.2. Then there exists a solution $\Gamma_0 \in \mathcal{T}(\mathcal{P})$ to the max-min energy problem (2.8) for $(V, \mathcal{T}(\mathcal{P}))$.*

The contour Γ_0 has the S-property in the external field $\varphi = \operatorname{Re} V$.

The equilibrium measure $\mu_0 := \mu^{\varphi, \Gamma_0}$ of Γ_0 in the external field φ is supported on a finite union of analytic arcs that are critical trajectories of the quadratic differential $-R(z)dz^2$, where

$$R(z) = \left(C^{\mu_0}(z) + \frac{V'(z)}{2} \right)^2, \quad z \in \mathbb{C} \setminus \operatorname{supp} \mu_0, \tag{2.10}$$

is a polynomial of degree $2N - 2$.

Furthermore μ_0 is absolutely continuous with respect to arclength and

$$d\mu_0(s) = \frac{1}{\pi i} R_+(s)^{1/2} ds. \tag{2.11}$$

See the Appendix A for a brief discussion on quadratic differentials and their critical trajectories.

In (2.11) we use a complex line element ds on Γ_0, which induces an orientation on Γ_0. Then $R_+(s)^{1/2}$ denotes the limiting value of

$$R(z)^{1/2} = \int \frac{d\mu_0(x)}{x - z} + \frac{V'(z)}{2}$$

as $z \to s \in \Gamma_0$ from the left-hand side.

The contour Γ_0 that is the maximizer for the max-min energy property in Theorem 2.2.3 is not unique. We can modify the contour Γ_0 outside the support of μ_0 slightly, preserving the equilibrium measure in the external field. In this way we obtain a new contour that also solves the max-min problem for $(V, \mathcal{T}(\mathcal{P}))$.

Although the contour is not unique, the equilibrium measure in the external field μ_0 and its support turn out to be uniquely determined by V and $\mathcal{P}$. We do not know of a direct way to prove this, but there is an indirect way using orthogonal polynomials. Assume for simplicity that $\mathcal{P}_0 = \{\{i, j\}\}$ for some $1 \leq i < j \leq N$. This means that any contour $\Gamma \in \mathcal{T}(\mathcal{P})$ connects two fixed distinguished sectors at infinity where $\operatorname{Re} V(z) \to +\infty$.

The (non hermitian) bilinear form defined on polynomials p and q,

$$\langle p, q \rangle = \langle p, q \rangle_{V,n} = \int_\Gamma p(z) q(z) e^{-nV(z)} dz$$

is then well defined and independent of the choice of contours $\Gamma \in \mathcal{T}(\mathcal{P})$. A polynomial p_n of degree at most n is *orthogonal* with respect to $\langle \cdot, \cdot \rangle$ if

$$\langle p_n, q \rangle = 0,$$

for any polynomial q of degree $\leq n - 1$. Associated to the polynomial p_n is its normalized zero counting measure χ_n

$$\chi_n = \frac{1}{\deg p_n} \sum_{p_n(z)=0} \delta_z.$$

In studying (χ_n), Gonchar and Rakhmanov proved

Theorem 2.2.4 ([71, Theorem 3]). *If there exists $\Gamma \in \mathcal{T}(\mathcal{P})$ with the S-property in the external field $\varphi = \operatorname{Re} V$ and $\mathbb{C} \setminus \operatorname{supp} \mu^{\varphi,\Gamma}$ is connected, then*

$$\chi_n \xrightarrow{*} \mu^{\varphi,\Gamma}.$$

In other words, if a contour $\Gamma \in \mathcal{T}(\mathcal{P})$ has the S-property, then its equilibrium measure in the external field is the weak limit of (χ_n).

By Theorem 2.2.3 any contour $\Gamma \in \mathcal{T}(\mathcal{P})$ with the max-min property has the S-property. Also $\mathbb{C} \setminus \operatorname{supp} \mu^{\varphi,\Gamma}$ is connected, since otherwise we could remove self-intersecting subarcs of Γ and increase its energy. Thus, if Γ_0, Γ_1 are two solutions to the max-min problem $(V, \mathcal{T}(\mathcal{P}))$, then by Theorem 2.2.4 both equilibrium measures μ^{φ,Γ_0} and μ^{φ,Γ_1} are the weak limit of the sequence (χ_n). By uniqueness of limits, it follows that $\mu^{\varphi,\Gamma_0} = \mu^{\varphi,\Gamma_1}$.

The above argument applies if $\mathcal{P}_0 = \{\{i, j\}\}$ for some $1 \leq i < j \leq N$. For other choices of $\mathcal{P}_0$, we need to modify the bilinear form $\langle \cdot, \cdot \rangle$ to get the appropriate family of orthogonal polynomials (p_n). For more details, we refer to [24, 27].

2.2.5 Rakhmanov's results and overview of the rest of the chapter

As mentioned in the Introduction, our contribution is very much influenced by the work of Rakhmanov [116], which we now explain.

The first result obtained by Rakhmanov in [116], which is relevant to us is the following.

Theorem 2.2.5 ([116, Theorem 9.2]). *Suppose F is closed in $\overline{\mathbb{C}}$. If*

$$-\infty < I^{\varphi}(F) < +\infty,$$

then the equilibrium measure $\mu^{\varphi,F}$ in external field φ exists and is unique.

In contrast with previous results, Theorem 2.2.5 does not contain any assumption on the growth of φ at ∞. Actually the theorem in [116] is more general as it also deals with situations where the external field is continuous except at a finite number of points, and no growth restriction near these singularities.

Rakhmanov considers the energy functional

$$F \mapsto I^{\varphi}(F)$$

defined on a metric space of compacts, which we explain next.

The Riemann sphere $\overline{\mathbb{C}}$ is mapped to the sphere $\mathcal{S} \subset \mathbb{R}^3$ centered at $(0, 0, 1/2)$ with radius $\frac{1}{2}$,

$$\mathcal{S} = \left\{ (x_1, x_2, x_3) \in \mathbb{R}^3 \mid x_1^2 + x_2^2 + (x_3 - \tfrac{1}{2})^2 = \tfrac{1}{4} \right\},$$

via the inverse stereographic map $L : \overline{\mathbb{C}} \to \mathcal{S}$ given by $L(\infty) = (0, 0, 1)$ and

$$L(z) = \left(\frac{\operatorname{Re} z}{1 + |z|^2}, \frac{\operatorname{Im} z}{1 + |z|^2}, \frac{|z|^2}{1 + |z|^2} \right), \qquad z \in \mathbb{C}.$$

The *hyperbolic metric* on $\overline{\mathbb{C}}$ is then given by

$$\mathrm{d}(z, w) = \|L(z) - L(w)\|,$$

where the norm $\|\cdot\|$ on the right-hand side above is the Euclidean norm in $\mathbb{R}^3$. The following relation holds

$$\mathrm{d}(z,w) = \frac{|z-w|}{\sqrt{1+|z|^2}\sqrt{1+|w|^2}}, \quad z,w \in \mathbb{C}.$$

This metric induces a metric on compact subsets of $\overline{\mathbb{C}}$. If $K_1, K_2 \subset \overline{\mathbb{C}}$ are compacts, the *Hausdorff metric* between them is given by the formula

$$\mathrm{d_H}(K_1,K_2) = \max\left\{\sup_{x\in K_1} \operatorname{dist}(x,K_2), \sup_{y\in K_2} \operatorname{dist}(y,K_1)\right\}, \tag{2.12}$$

where the distance between points and sets above is the usual one induced by d,

$$\operatorname{dist}(x,K) = \inf_{y\in K} \mathrm{d}(x,y).$$

Alternatively, denoting

$$(K)_\delta = \{x \in \overline{\mathbb{C}} \mid \ \operatorname{dist}(x,K) < \delta\},$$

it can be equivalently defined by

$$\mathrm{d_H}(K_1,K_2) = \inf\left\{\delta > 0 \mid K_1 \subset (K_2)_\delta,\ K_2 \subset (K_1)_\delta\right\}.$$

The Hausdorff metric is thus defined on closed sets of $\overline{\mathbb{C}}$. Naturally it induces a metric on closed sets of $\mathbb{C}$ by adding the point at infinity to unbounded closed sets. In what follows, when we talk about the Hausdorff metric on closed subsets of $\mathbb{C}$, we mean the metric obtained with this natural identification to closed subsets of $\overline{\mathbb{C}}$.

We equip $\mathcal{T}$ with the Hausdorff metric (2.12) induced by the hyperbolic distance. So when we refer to a topological notion on $\mathcal{T}$ such as convergence or continuity, we always mean with respect to the Hausdorff metric just introduced.

Suppose $\mathcal{F}$ is a class of closed subsets of $\mathbb{C}$ for which there exists an absolute constant c such that every compact set in $\mathcal{F}$ has at most c connected components. Equip $\mathcal{F}$ with the Hausdorff metric just introduced. For such classes $\mathcal{F}$, Rakhmanov proves the following.

Theorem 2.2.6 ([116, Theorem 3.2]). *The energy functional $I^\varphi : \mathcal{F} \to [-\infty, +\infty]$ is upper semicontinuous.*

If the class $\mathcal{F}$ is closed, then it follows from Theorem 2.2.6 that there exists a set $F_0 \in \mathcal{F}$ maximizing I^φ. However, it is easy to see that the class of

admissible contours $\mathcal{T} = \mathcal{T}(\mathcal{P})$ introduced in Definition 2.2.2 is not closed in the Hausdorff metric. An easy way to see this is through space-filling curves. One can approximate sets of large planar measure with smooth contours, and the limiting set is not a smooth contour anymore.

A natural idea would then be to work with the closure $\overline{\mathcal{T}}$ of the class $\mathcal{T}$ in the Hausdorff metric. There is however an issue with that, since sets in $\overline{\mathcal{T}}$ may stretch out to infinity in unlikely directions, and we might then recover the S-curve for the admissible class $\mathcal{T}(\mathcal{P}')$ corresponding to another choice of partition $\mathcal{P}'$.

Our technique to overcome this last issue is to introduce a suitable subclass $\mathcal{T}_M \subset \mathcal{T}$, see (2.63), consisting of contours that do not enter a "forbidden region" Δ_M. Then we take the closure $\mathcal{F}_M = \overline{\mathcal{T}}_M$, see also (2.64). For the closed class $\mathcal{F}_M$, Theorem 2.2.6 assures us that there exists a set F_0 maximizing the energy functional $I^\varphi(\cdot)$ on $\mathcal{F}_M$. Moreover, with M chosen large enough, we can guarantee that the set F_0 does not come to the boundary of the forbidden region Δ_M, which implies that small deformations of F_0 in any direction also belong to $\mathcal{F}_M$.

Any C^2_c function $h : \mathbb{C} \to \mathbb{C}$ generates a one-parameter deformation F_0^t of this maximizer set by

$$F_0^t = \{z + th(z) \mid z \in F\}, \qquad t \in \mathbb{R}. \tag{2.13}$$

Now, since F_0^t also belongs to $\mathcal{F}$ for t sufficiently close to 0, we have that (the limit actually exists)

$$\lim_{t\to 0} \frac{I^\varphi(F_0^t) - I^\varphi(F_0)}{t} = 0.$$

because F_0 is a maximizer set. Rakhmanov [116] then proves that this limit implies that the equilibrium measure μ^{φ,F_0} in the external field φ is critical, in the sense introduced by Martínez-Finkelshtein and Rakhmanov [104], see also Section 2.3 below.

As it was already observed by Martínez-Finkelshtein and Rakhmanov [104], the Cauchy transform of a critical measure is an algebraic function. In the present context, this means that the Cauchy transform C^{μ_0} of the equilibrium measure in external field satisfies an algebraic equation of the form

$$\left(C^{\mu_0}(z) + \frac{V'(z)}{2}\right)^2 = R(z), \qquad \text{for a.e. } z \in \mathbb{C},$$

where R is a polynomial of degree $2n-2$, see Proposition 2.3.7 below. The main technical difference between [104] and the present framework is that in [104] this is obtained under the assumption that the critical measure is compactly

supported, while here we obtain the algebraic equation first, and as one of its consequences we find that μ_0 must be compactly supported. As in [104], the algebraic equation also implies that the measure μ_0 is supported on a finite union of analytic arcs and its density can be recovered from the polynomial R, see Propositions 2.3.8, 2.3.9. Also, the S-property ultimately follows from the algebraic equation, see Corollary 2.3.11.

As a final step, once some properties of the equilibrium measure in external field μ_0 of the maximizer set F_0 are known, we drop the parts of F_0 that do not belong to $\operatorname{supp}\mu_0$, and we give in Section 2.5.3 a construction of a curve $\Gamma_0 \in \mathcal{T}(\mathcal{P})$ whose equilibrium measure in the external field φ is the desired measure μ_0.

The rest of the chapter is organized as follows. In Section 2.3 we discuss critical measures. The results therein presented are similar to the ones obtained for the first time by Martínez-Finkelshtein and Rakhmanov [104]. However, as mentioned before and further explained later, the setup in [104] is not the same as ours, so we preferred to present detailed proofs in Section 2.3. In Section 2.4 we explain the link between critical measures and critical sets, following the lines of [116]. Section 2.5 is devoted to the proof of Theorem 2.2.3.

2.3 Critical Measures

As before, V is a polynomial of degree $N \geq 2$ and the external field φ is given by

$$\varphi(z) = \operatorname{Re} V(z), \qquad z \in \mathbb{C}. \tag{2.14}$$

With proper modifications, all the results and proofs in this section are also valid for external fields given by the real part of an analytic function, possibly multivalued, with rational (and so single-valued) derivative, but for our purposes it is enough to consider the polynomial case.

The results we are going to show here were proven before by Martínez-Finkelshtein and Rakhmanov [104] under the assumption that the measures involved are a priori compactly supported and the external field has a rational derivative with simple poles. The techniques we are using are also similar, but sometimes simplified and adapted to our needs. The main difference here is that we do not impose a priori that a critical measure must have compact support. Ultimately, we do find that critical measures must be compactly supported (for external fields as in (2.14)), and then the results here are the same as the ones obtained in [104].

2.3.1 Derivative of the energy functional

Consider the set of test functions C_c^2, consisting of C^2 complex-valued functions in $\mathbb{C}$ with compact support. For a function $h \in C_c^2$ and $t \in \mathbb{R}$ denote

$$h_t(z) = z + th(z), \quad z \in \mathbb{C}. \tag{2.15}$$

Any function $h \in C_c^2$ generates local variations of sets $F \mapsto F^t = h_t(F)$ and also of measures $\mu \mapsto \mu^t$, where μ^t is the pushforward measure induced by h_t. If μ has finite weighted logarithmic energy then the same is true for μ^t.

For a measure $\mu \in M_1^\varphi(\mathbb{C})$ and $h \in C_c^2$, we define the *derivative* of the weighted energy functional at μ in the direction of h by

$$D_h I^\varphi(\mu) = \lim_{t \to 0} \frac{I^\varphi(\mu^t) - I^\varphi(\mu)}{t}, \tag{2.16}$$

whenever the limit exists. A first result is that $D_h I^\varphi(\mu)$ indeed always exists.

Proposition 2.3.1. *Given $\mu \in \mathcal{M}_1^\varphi(\mathbb{C})$ and $h \in C_c^2$, the derivative $D_h I^\varphi(\mu)$ exists and is given by*

$$D_h I^\varphi(\mu) = -\operatorname{Re}\left(\iint \frac{h(x) - h(y)}{x - y}\, d\mu(x) d\mu(y) - \int V'(x) h(x)\, d\mu(x) \right). \tag{2.17}$$

Proof. The proof here is the same as in [104, Proof of Lemma 3.7]. By the change of variables formula

$$I^\varphi(\mu^t) = \iint \log \frac{1}{|x - y + t(h(x) - h(y))|}\, d\mu(x) d\mu(y) + \int \varphi(x + th(x))\, d\mu(x),$$

which implies

$$I^\varphi(\mu^t) - I^\varphi(\mu) = -\iint \log \left| 1 + t \frac{h(x) - h(y)}{x - y} \right| d\mu(x) d\mu(y) + \int \left(\varphi(x + th(x)) - \varphi(x) \right) d\mu(x). \tag{2.18}$$

Since $h \in C_c^2$, we have for $t \to 0$,

$$\log\left|1 + t\frac{h(x)-h(y)}{x-y}\right| = \operatorname{Re}\left[\log\left(1 + t\frac{h(x)-h(y)}{x-y}\right)\right]$$
$$= t\operatorname{Re}\left(\frac{h(x)-h(y)}{x-y}\right) + \mathcal{O}(t^2), \tag{2.19}$$

with the implicit constant in $\mathcal{O}(t^2)$ uniform in $x, y \in \mathbb{C}$, and analogously

$$V(x + th(x)) - V(x) = tV'(x)h(x) + \mathcal{O}(t^2),$$

where again the $\mathcal{O}$ term is uniform in $x \in \mathbb{C}$. This implies

$$\varphi(x + th(x)) - \varphi(x) = t\operatorname{Re}(h(x)V'(x)) + \mathcal{O}(t^2) \quad \text{as } t \to 0,$$

and the result follows by plugging this last equation and (2.19) into (2.18). □

2.3.2 Critical measures

Definition 2.3.2. We say a measure $\mu \in \mathcal{M}_1^{\varphi}(\mathbb{C})$ is *φ-critical* if

$$D_h I^{\varphi}(\mu) = 0$$

for every $h \in C_c^2$.

The definition of φ-critical measures introduced in [104] allows the external field to have singularities. In that situation, the test functions h appearing in Definition 2.3.2 should also vanish on a set $\mathcal{A}$ of zero capacity containing the singular points of φ, leading to the notion of $(\varphi, \mathcal{A})$-critical measures. In [104] it is also imposed that critical measures must have compact support. In the case considered here the only singularity of the external field is at $z = \infty$, and for convenience we are initially considering functions that are not just vanishing at infinity but also in a neighborhood of it, that is, compactly supported functions.

Considering h and ih separately, we easily obtain the following from Proposition 2.3.1.

Corollary 2.3.3. *A measure $\mu \in \mathcal{M}_1^{\varphi}(\mathbb{C})$ is φ-critical if, and only if,*

$$\iint \frac{h(x)-h(y)}{x-y} d\mu(x) d\mu(y) = \int V'(x)h(x)d\mu(x) \tag{2.20}$$

for every $h \in C_c^2$.

Equation (2.20) appears frequently in the context of random matrices, although usually in different forms and names as for example *Loop equations*, *Schwinger-Dyson equations* or *Ward identities*, see [5, 59, 67].

We need to extend (2.20) to larger classes of test functions.

Lemma 2.3.4. *Let μ be a φ-critical measure. Then equation (2.20) remains valid for $h \in C^2$ satisfying*

$$h(z) = \mathcal{O}\left(\frac{1}{z^{N-1}}\right), \quad z \to \infty. \tag{2.21}$$

Proof. Introduce the function $\Theta_n : [0, +\infty) \to \mathbb{R}$ by

$$\Theta_n(t) = \begin{cases} 1, & t \le n, \\ \frac{1}{16n^5}(3n-t)^3(2n^2-3nt+3t^2) & n < t < 3n, \\ 0, & t \ge 3n. \end{cases}$$

Then $\Theta_n \in C_c^2$, $\Theta_n(t) \overset{n\to\infty}{\to} 1$ and

$$0 \le \Theta_n(t) \le 1, \qquad |\Theta_n'(t)| < \frac{1}{n}, \quad t \ge 0. \tag{2.22}$$

For $h \in C^2$ satisfying (2.21), define

$$h_n(x) = \Theta_n(|x|)h(x), \quad x \in \mathbb{C}.$$

Then h_n belongs to C_c^2, so that equation (2.20) is valid for it. From assumption (2.21) and the fact that $\deg V = N$, we see

$$V'(x)h(x) = \mathcal{O}(1), \quad x \to \infty,$$

and from the definition of h_n and the Dominated Convergence Theorem, it is easily seen

$$\int V'(x)h_n(x)d\mu(x) \overset{n\to\infty}{\to} \int V'(x)h(x)d\mu(x). \tag{2.23}$$

The measure μ has finite logarithmic energy, so it has no mass points. In particular, the diagonal $\{(x,x) \mid x \in \mathbb{C}\}$ has zero $\mu \times \mu$ measure, implying

$$\frac{h_n(x)-h_n(y)}{x-y} \overset{n\to\infty}{\to} \frac{h(x)-h(y)}{x-y}, \quad \mu\times\mu\text{-a.e.}$$

Using (2.22), we get

$$\left|\frac{h_n(x)-h_n(y)}{x-y}\right| = \left|\frac{h(x)-h(y)}{x-y}\Theta_n(|x|) + \frac{\Theta_n(|x|)-\Theta_n(|y|)}{x-y}h(y)\right|$$

$$\leq \left|\frac{h(x)-h(y)}{x-y}\right| + |h(y)|.$$

From (2.21) we find that both terms on the right-hand side are bounded, and therefore $\mu\times\mu$-integrable. The Dominated Convergence Theorem can be applied, yielding

$$\iint \frac{h_n(x)-h_n(y)}{x-y}d\mu(x)d\mu(y) \overset{n\to\infty}{\to} \iint \frac{h(x)-h(y)}{x-y}d\mu(x)d\mu(y),$$

and (2.20) for h follows from this last limit and (2.23), keeping in mind that (2.20) is valid for each h_n. □

Lemma 2.3.5. *Let μ be a φ-critical measure. If $z\in\mathbb{C}$ is such that*

$$\int \frac{d\mu(x)}{|x-z|} < +\infty, \tag{2.24}$$

then (2.20) is valid for every function of the form

$$h(x) = \frac{g(x)}{x-z}, \qquad g\in C_c^2.$$

Proof. The same idea used to prove Lemma 2.3.4 can also be used here, namely approximating h by a sequence of functions for which (2.20) is valid. But now the approximating sequence needs to be modified. By translating $x\mapsto x-z$ we can assume $z=0$, and then we rewrite

$$h(x) = \frac{g(x)\overline{x}}{|x|^2}.$$

Define

$$h_n(x) = \frac{g(x)\overline{x}}{|x|^2+\epsilon_n^2},$$

where (ϵ_n) is a sequence of positive numbers converging to zero. Clearly $h_n\in C_c^2$, and so equation (2.20) is valid for it.

Note that (2.24) assures us that h is μ-integrable. Proceeding then similarly as in the proof of Lemma 2.3.4,

$$\int V'(x)h_n(x)d\mu(x) \overset{n\to\infty}{\to} \int V'(x)h(x)d\mu(x), \tag{2.25}$$

and also

$$\frac{h_n(x)-h_n(y)}{x-y} \overset{n\to\infty}{\to} \frac{h(x)-h(y)}{x-y}, \quad \mu\times\mu\text{-a.e.} \tag{2.26}$$

Moreover,

$$\begin{aligned}
|h_n(x)-h_n(y)| &\le \left|\frac{|y|^2\overline{x}g(x)-|x|^2\overline{y}g(y)}{(|x|^2+\epsilon_n^2)(|y|^2+\epsilon_n^2)}\right| + \frac{\epsilon_n^2\,|\overline{x}g(x)-\overline{y}g(y)|}{(|x|^2+\epsilon_n^2)(|y|^2+\epsilon_n^2)} \\
&\le \left|\frac{|y|^2\overline{x}g(x)-|x|^2\overline{y}g(y)}{|x|^2|y|^2}\right| \\
&\quad + \frac{|\overline{x}g(x)-\overline{y}g(y)|}{|x||y|}\frac{1}{\left(\frac{|x|}{\epsilon_n}+\frac{\epsilon_n}{|x|}\right)\left(\frac{|y|}{\epsilon_n}+\frac{\epsilon_n}{|y|}\right)} \\
&\le \left|\frac{yg(x)-xg(y)}{xy}\right| + \left|\frac{\overline{x}g(x)-\overline{y}g(y)}{xy}\right|,
\end{aligned} \tag{2.27}$$

where in the last inequality we used $t+1/t>1$ for $t\ge 0$.

Now, using the trivial decompositions

$$\frac{yg(x)-xg(y)}{xy(x-y)} = \frac{1}{y}\frac{g(x)-g(y)}{x-y} - \frac{g(x)}{xy},$$

$$\frac{\overline{x}g(x)-\overline{y}g(y)}{\overline{x}\overline{y}(\overline{x}-\overline{y})} = \frac{1}{\overline{x}}\frac{g(x)-g(y)}{\overline{x}-\overline{y}} + \frac{g(x)}{\overline{x}\overline{y}}$$

in (2.27), we get

$$\left|\frac{h_n(x)-h_n(y)}{x-y}\right| \le \left(\frac{1}{|x|}+\frac{1}{|y|}\right)\left|\frac{g(x)-g(y)}{x-y}\right| + \frac{2}{|y|}\left|\frac{g(x)}{x}\right|$$

Since $g\in C_c^2$, the quotient

$$\frac{g(x)-g(y)}{x-y},$$

is bounded, as well as g, say both by M. This last inequality then implies

$$\left|\frac{h_n(x)-h_n(y)}{x-y}\right| \le \frac{M}{|x|}+\frac{M}{|y|}+\frac{2M}{|x||y|}.$$

From assumption (2.24) the right-hand side above is $\mu\times\mu$-integrable. From the Dominated Convergence Theorem and (2.26) we conclude

$$\iint \frac{h_n(x)-h_n(y)}{x-y}d\mu(x)d\mu(y) \overset{n\to\infty}{\to} \iint \frac{h(x)-h(y)}{x-y}d\mu(x)d\mu(y).$$

Since (2.20) is valid for the h_n's, this last limit together with (2.25) implies (2.20) for h. □

A combination of Lemmas 2.3.4 and 2.3.5 leads to the following.

Corollary 2.3.6. *Let μ be a φ-critical measure. Suppose $z_1, z_2, \dots, z_{N-1}$ are distinct points such that*

$$\int \frac{d\mu(x)}{|x - z_j|} < +\infty, \qquad j = 1, \dots, N-1. \tag{2.28}$$

Then equation (2.20) is valid for the function

$$h(x) = \prod_{j=1}^{N-1} \frac{1}{x - z_j}.$$

Proof. Let $\delta = \frac{1}{4} \min\{|z_j - z_k| \mid 1 \le j < k \le N-1\}$. For each $j = 1, \dots, N-1$, we can take a C^2_c function $\chi_j : \mathbb{C} \to [0,1]$ supported in $D(z_j, 2\delta)$ with $\chi_j \equiv 1$ in $D(z_j, \delta)$. Then $h_j = \chi_j h$ satisfies the condition of Lemma 2.3.5 and $h - \sum_{j=1}^{N-1} h_j$ satisfies the condition of Lemma 2.3.4. Thus the equality (2.20) holds for these functions, and then by linearity it also holds for h. □

Given a finite positive Borel measure μ, consider the function $\mathbb{C} \to [0, +\infty]$

$$z \mapsto \int \frac{d\mu(x)}{|x - z|}.$$

It is the convolution of a finite Borel measure with the function $x \mapsto \frac{1}{|x|}$, which is in $L^1_{loc}(\mathbb{C}, m_2)$, where m_2 is the planar Lebesgue measure. Thus Tonelli's Theorem tells us it also belongs to $L^1_{loc}(\mathbb{C}, m_2)$, being then finite m_2-a.e. This implies that the Cauchy transform C^μ of μ,

$$C^\mu(z) = \int \frac{d\mu(x)}{x - z}, \qquad z \in \mathbb{C},$$

is well-defined and finite m_2-a.e., and

$$C^\mu(z) = \mathcal{O}(z^{-1}), \quad z \to \infty. \tag{2.29}$$

As observed by Martínez-Finkelshtein and Rakhmanov [104, Lemma 5.1], an essential feature of critical measures is the fact that their Cauchy Transform satisfies an algebraic equation of degree 2.

Proposition 2.3.7. *Let μ be a φ-critical measure. Then there exists a polynomial R of degree $2N-2$ such that*

$$\left(C^{\mu}(z)+\frac{1}{2}V'(z)\right)^2 = R(z), \qquad m_2\text{-a.e.} \tag{2.30}$$

where m_2 is the Lebesgue measure on $\mathbb{C}$.

As we will see later, one of the consequences of Proposition 2.3.7 is that φ-critical measures are always compactly supported (see Proposition 2.3.9 below). However, since we cannot assume this *a priori*, our proof, at the technical level, is different from the one given in [104, Proof of Lemma 5.1], although the key ideas are similar.

Proof. Since $\int \frac{d\mu(x)}{|x-z|}$ is finite m_2-a.e., we can fix $N-2$ distinct points $z_1,\dots,z_{N-2}$ for which

$$\int \frac{d\mu(x)}{|x-z_j|} < \infty, \quad j=1,\dots,N-2. \tag{2.31}$$

Take $z \in \mathbb{C}\setminus\{z_1,\dots,z_{N-2}\}$. Since we want to have (2.30) m_2-a.e. and $\int \frac{d\mu(x)}{|x-z|}$ is finite m_2-a.e., it is enough to prove the identity (2.30) under the assumption

$$\int \frac{d\mu(x)}{|x-z|} < \infty. \tag{2.32}$$

Define

$$h(x)=\frac{A(x)}{x-z}, \qquad A(x)=\prod_{j=1}^{N-2}(x-z_j)^{-1}. \tag{2.33}$$

Then h satisfies the conditions of Corollary 2.3.6 (with $z=z_{N-1}$) and so (2.20) is valid for this h. We can write

$$\int V'(x)h(x)\,d\mu(x) = A(z)V'(z)C^{\mu}(z)+D_1(z), \tag{2.34}$$

where D_1 is the rational function

$$D_1(z)=\int \frac{A(x)V'(x)-A(z)V'(z)}{(x-z)}\,d\mu(x),$$

whose only possible poles are the points $z_1,\dots,z_{N-2}$, all of them simple, and

$$D_1(z)=\mathcal{O}(1), \qquad z\to\infty. \tag{2.35}$$

On the other hand, we can write

$$\frac{h(x)-h(y)}{x-y} = \frac{(x-y)A(z)+(z-x)A(y)+(y-z)A(x)}{(x-y)(x-z)(y-z)} - \frac{A(z)}{(x-z)(y-z)}.$$

The first term on the right-hand side is bounded away from $z_1, \dots, z_{N-2}$, and since we are assuming (2.31) this term is $d\mu(x) \times d\mu(y)$-integrable. The second term is also $d\mu(x) \times d\mu(y)$-integrable because of assumptions (2.31) and (2.32). From this we conclude

$$\iint \frac{h(x)-h(y)}{x-y}\, d\mu(x)d\mu(y) = -A(z)(C^\mu(z))^2 + D_2(z), \tag{2.36}$$

where

$$D_2(z) = \iint \frac{(x-y)A(z)+(z-x)A(y)+(y-z)A(x)}{(x-y)(x-z)(y-z)}\, d\mu(x)d\mu(y),$$

is also a rational function with simple poles at $z_1, \dots, z_{N-2}$ and no other poles. Moreover,

$$D_2(z) = \mathcal{O}(z^{-1}), \quad z \to \infty. \tag{2.37}$$

As (2.20) is valid for this h, equations (2.34) and (2.36) give us

$$-A(z)(C^\mu(z))^2 + D_2(z) = A(z)V'(z)C^\mu(z) + D_1(z),$$

which is equivalent to (2.30) if we set

$$R(z) = \frac{D_2(z)-D_1(z)}{A(z)} + \frac{1}{4}\left(V'(z)\right)^2. \tag{2.38}$$

Note that the poles of A cancel out the possible poles of $D_1 - D_2$, and due also to the behavior of D_1 and D_2 at infinity given in (2.35), (2.37) we see that R is indeed a polynomial of degree $2N-2$. □

From the polynomial R in (2.30), we can recover μ.

Proposition 2.3.8. *Suppose μ is a measure on $\mathbb{C}$ for which there exist polynomials Q and R such that*

$$\left(C^\mu(z) + Q(z)\right)^2 = R(z), \qquad m_2\text{-a.e.} \tag{2.39}$$

Then μ is supported on a union of analytic arcs, which are maximal trajectories of the quadratic differential $-R(z)\,dz^2$. Moreover, in the interior of any arc of $\operatorname{supp}\mu$*, the measure μ is absolutely continuous with respect to the arclength measure, with density given by*

$$d\mu(s) = \frac{1}{\pi i}\sqrt{R(s)}\, ds, \tag{2.40}$$

where ds is the complex line element, chosen according to a fixed orientation of the arcs of $\operatorname{supp}\mu$.

Observe that by Proposition 2.3.7, the condition (2.39) is valid for φ-critical measures with the choice $Q(z) = \frac{V'(z)}{2}$.

Since Proposition 2.3.8 is essentially about local properties of the measure μ, it is not important if the measure μ has unbounded support or not. So the proof presented here is essentially the same as the one given in [104, Lemma 5.2] for measures with bounded support, which in turn is modelled after a result in [23]. We decided to give a full detailed proof here for the benefit of the reader, and also to correct a sign misprint in [104]: in the first centered formula following formula (5.23) in [104] the right-hand side should have a $-$-sign.

Proof. Let G be a simply connected domain not containing zeros of R and intersecting $\operatorname{supp}\mu$. Fix a point $z_0 \in \operatorname{supp}\mu \cap G$ and select a branch of $\sqrt{R}$ in G, and define

$$\xi(z) = \int_{z_0}^{z} \sqrt{R(s)}\, ds, \quad z \in G.$$

Reducing G if necessary, we can assume ξ is a conformal mapping between G and $\xi(G) = I \times iJ = \widehat{G}$, $I, J \subset \mathbb{R}$ intervals both containing $z = 0$.

For this same branch of $\sqrt{R}$, define for m_2-a.e. $z \in G$ a function χ by the formula

$$\chi(z) = \frac{C^{\mu}(z) + Q(z)}{\sqrt{R(z)}}.$$

Due to (2.39) χ assumes values in $\{-1, 1\}$. A simple application of the Cauchy-Green Formula [72, pg. 491] gives us

$$\frac{\partial C^{\mu}}{\partial \overline{z}} = -\pi d\mu$$

in the sense of distributions, and we conclude (also in the sense of distributions)

$$\frac{\partial}{\partial \overline{z}} \left(\sqrt{R(z)}\chi(z) \right) = \sqrt{R(z)}\, \frac{\partial \chi}{\partial \overline{z}}(z) = -\pi d\mu(z). \tag{2.41}$$

Now, ξ is a conformal map from G onto $\widehat{G}$, with inverse denoted by $z = z(\xi)$, which induces a map between distributions in the z-variable and the ξ-variable, say $u \mapsto u_*$, where u_* is the distribution acting on test functions in $\widehat{G}$ via the formula

$$\langle u, \phi \rangle = \langle u_*, \psi \rangle,$$

where $\psi(\xi) = \phi(z)$.

Now we will calculate the (distributional) derivative of $\chi_*(\xi) = \chi(z(\xi))$. If μ_* is the pushforward measure of μ induced by ξ in $\widehat{G}$ then (2.41) and the chain rule applied to $\psi(\xi) = \phi(z)$ imply

$$\begin{aligned}
\langle \mu_*, \psi \rangle &= \langle \mu, \phi \rangle \\
&= -\frac{1}{\pi} \left\langle \frac{\partial}{\partial \overline{z}} \left(\sqrt{R}\, \chi \right), \phi \right\rangle \\
&= \frac{1}{\pi} \int \frac{\partial \phi}{\partial \overline{z}}(z) \sqrt{R(z)}\, \chi(z)\, dm_2(z) \\
&= \frac{1}{\pi} \int \frac{\partial}{\partial \overline{z}} \left(\psi(\xi(z)) \right) \sqrt{R(z)}\, \chi(z)\, dm_2(z) \\
&= \frac{1}{\pi} \int \left(\frac{\partial \psi}{\partial \xi}(\xi(z)) \frac{\partial \xi}{\partial \overline{z}}(z) + \frac{\partial \psi}{\partial \overline{\xi}}(\xi(z)) \overline{\frac{\partial \xi}{\partial z}(z)} \right) \sqrt{R(z)} \chi(z)\, dm_2(z) \\
&= \frac{1}{\pi} \int \frac{\partial \psi}{\partial \overline{\xi}}(\xi(z)) \left| \sqrt{R(z)} \right|^2 \chi(z)\, dm_2(z),
\end{aligned}$$

since $\frac{\partial \xi}{\partial \overline{z}} = 0$ and $\frac{\partial \xi}{\partial z} = \sqrt{R(z)}$. Thus by the change of variables formula for the Lebesgue measure

$$\begin{aligned}
\langle \mu_*, \psi \rangle &= \frac{1}{\pi} \int \frac{\partial \psi}{\partial \overline{\xi}}(\xi) \left| \sqrt{R(z(\xi))} \right|^2 \chi_*(\xi)\, \left| z'(\xi) \right|^2 dm_2(\xi) \\
&= \frac{1}{\pi} \int \frac{\partial \psi}{\partial \overline{\xi}}(\xi)\, \chi_*(\xi)\, dm_2(\xi),
\end{aligned}$$

where we used that $z'(\xi) = \frac{1}{\xi'(z)} = \frac{1}{\sqrt{R(z)}}$. The result is that $\langle \mu_*, \psi \rangle = -\frac{1}{\pi} \left\langle \frac{\partial \chi_*}{\partial \overline{\xi}}, \psi \right\rangle$ which can be rewritten as

$$\frac{\partial \chi_*}{\partial \overline{\xi}} = \frac{1}{2} \frac{\partial \chi_*}{\partial x} + \frac{i}{2} \frac{\partial \chi_*}{\partial y} = -\pi d\mu_*, \tag{2.42}$$

where $\xi = x + iy$ with $x, y \in \mathbb{R}$. As μ is a real measure, we conclude $\frac{\partial \chi_*}{\partial y} = 0$, which means $\chi_*(\xi) = g(\operatorname{Re} \xi)$, for a real function g defined on the interval I.

If λ is the pushforward measure of μ_* induced by $\xi \mapsto \operatorname{Re} \xi$, using (2.42) we can conclude in a similar fashion that

$$\frac{dg}{dx} = -\alpha d\lambda,$$

where α is a positive constant, and so

$$g(x) = \beta - \alpha \int_{-\infty}^{x} d\lambda,$$

for some real constant β. But g only assumes values in $\{1, -1\}$, and since $\int_{-\infty}^{x} d\lambda$ is non-decreasing, we conclude g is non-increasing and also that there exists x_0 in I for which $\lambda = c\delta_{x_0}$, where c is a positive constant, and then

$$g(x) = 1 - 2 \int_{-\infty}^{x} d\delta_{x_0}.$$

In terms of μ_* and χ_*, this means that there exists a vertical segment $L = \{x_0\} \times iJ$ in $\widehat{G}$ with χ_* equal to 1 at the left side of L and -1 at the right side of L, and $\operatorname{supp} \mu_*$ is contained in L. But for such χ_* a direct computation shows

$$\frac{\partial \chi_*}{\partial \bar{\xi}} = \frac{1}{2} \frac{\partial \chi_*}{\partial x} = -dy,$$

where dy is the Lebesgue measure on L, so by (2.42)

$$d\mu_* = \frac{1}{\pi} dy = \frac{1}{i\pi} dt.$$

where dt is the line element in L, oriented such that $\chi_* = 1$ on the positive side of L. Since ξ is a conformal map we can pullback the measures $d\mu_*$ and dt, obtaining

$$d\mu(s) = \frac{1}{\pi i} \sqrt{R(s)}\, ds,$$

where ds is the complex line element on the trajectory $\gamma = \xi^{-1}(L)$ chosen with orientation such that $\xi(z) = 1$ on the positive side (i.e., on the left-hand side) of γ.

Finally, the trajectory arcs of $\operatorname{supp} \mu$ must be maximal, because the arguments above show that $\operatorname{supp} \mu$ is an analytic arc in a neighborhood of any point of its support that is not a zero of R. □

For the next proposition, it is important that $\varphi = \operatorname{Re} V$ with V polynomial.

Proposition 2.3.9. *For any φ-critical measure μ, the support* $\operatorname{supp} \mu$ *is compact and can be written as*

$$\operatorname{supp} \mu = \bigcup_j \alpha_j, \tag{2.43}$$

where each α_j is an analytic arc and the union is taken over a finite set of indices. Each α_j is a critical trajectory of the quadratic differential $-R(z)dz^2$.

Proof. Propositions 2.3.7 and 2.3.8 tell us that the measure μ is supported on maximal trajectories of the quadratic differential

$$-R(z)dz^2 = -\left(C^\mu(z) + \frac{1}{2}V'(z)\right)^2 dz^2,$$

which has a pole of order $2N+2$ at $z=\infty$. The general theory of quadratic differentials assures us that there exists a neighborhood U of $z=\infty$ such that every trajectory intersecting U ends up at $z=\infty$ in at least one direction [133, Theorem 7.4]. In particular, if $\gamma \cap U \neq \emptyset$ for some maximal trajectory γ of $\operatorname{supp}\mu$, then γ would be unbounded, and due to (2.40) the measure μ would not be finite.

Since R is a polynomial, the only bounded trajectories are critical trajectories that connect two different zeros of R. Since there are only finitely many zeros of R, the union in (2.43) is certainly over a finite number of arcs. □

It is worth noting that the expression (2.38) for R in terms of the function A defined in (2.33), depends on the chosen points $z_1, \ldots, z_{N-2}$ at which the Cauchy transform of μ is convergent. Since we now know by Proposition 2.3.9 that $\operatorname{supp}\mu$ is compact, we can take the constant function $A(x)=1$ in (2.33), and the rest of the proof of (2.30) then works fine for this A. Repeating all the computations, we also end up with a nicer representation for R,

$$R(z) = \left(\frac{V'(z)}{2}\right)^2 - \int \frac{V'(x)-V'(z)}{x-z}\,d\mu(x), \tag{2.44}$$

which is well-known for equilibrium problems in polynomial external fields on the real line, see e.g. [55]. This representation also allows us to derive some extra properties for R. For example, from (2.44) one easily sees that $R(z) - \frac{(V'(z))^2}{4}$ is a polynomial of degree $n-2$, whose leading coefficient coincides with minus the leading coefficient of V'.

Also, if V is quadratic, say

$$V(z) = az^2 + bz + c, \qquad a \neq 0,$$

then (2.44) reduces to

$$R(z) = \left(\frac{2az+b}{2}\right)^2 - 2a,$$

since μ is a probability measure. Then the zeros of R are

$$z_\pm = \frac{-b \pm 2\sqrt{2a}}{2a},$$

for some choice of the branch of the square root, and the support of the φ-critical measure is the segment from z_- to z_+.

For V cubic, the polynomial $R(z) - \frac{(V'(z))^2}{4}$ is linear, so there is one free parameter to be determined by the requirement of extra conditions, see for instance [2, 49, 84]. See also [48] for a similar situation.

2.3.3 Critical measures and the S-property

By Proposition 2.3.8, the support of a φ-critical measure μ consists of analytic arcs and their endpoints. The analytic arcs are trajectories of the quadratic differential $-R(z)dz^2$. Each regular point $z \in \operatorname{supp}\mu$ has a neighborhood, say G, for which $G \cap \operatorname{supp}\mu$ is an analytic arc. The only non-regular points are the zeros of R.

The next result is taken from [104].

Proposition 2.3.10. *Let μ be a φ-critical measure, with $\operatorname{supp}\mu = \bigcup \alpha_j$ as in Proposition 2.3.9.*

i) Then there exist constants $\omega_j \in \mathbb{R}$ such that

$$U^\mu(z) + \frac{1}{2}\varphi(z) = \omega_j, \qquad z \in \alpha_j.$$

ii) If $z \in \operatorname{supp}\mu$ is regular, then

$$\frac{\partial}{\partial n_+}\left(U^\mu + \frac{1}{2}\varphi\right)(z) = \frac{\partial}{\partial n_-}\left(U^\mu + \frac{1}{2}\varphi\right)(z),$$

where $n_\pm$ are the normal vectors to $\operatorname{supp}\mu$ at z pointing in opposite directions.

Proof. See Lemma 5.4 of [104]. □

An immediate consequence of part ii) of Proposition 2.3.10 is the following.

Corollary 2.3.11. *If V is a polynomial, $\varphi = \operatorname{Re} V$ and $\Gamma \subset \mathbb{C}$ is a contour satisfying the growth condition (2.3) and whose equilibrium measure $\mu^{\varphi,\Gamma}$ is a φ-critical measure, then Γ has the S-property in the external field φ.*

As a final remark, we notice that the cornerstone of the present section is Proposition 2.3.7, which gives us that the Cauchy transform of a φ-critical

measure is an algebraic function. One could also analyze (2.30) from another perspective, namely given V', find a polynomial R and a probability measure μ such that the algebraic equation (2.30) is satisfied. This is the spirit of some works already present in the literature, e.g. [82, 104, 123, 124]. It is expected that the pairs (R, μ) satisfying (2.30) depend on continuous parameters, but as it follows from our analysis, only for a finite number of pairs (R, μ) the measure μ is an equilibrium measure (of some admissible contour) in the external field $\varphi = \operatorname{Re} V$. More precisely, just for a finite number of pairs (R, μ) obtained in this way, all the constants ω_j appearing in Proposition 2.3.10 i) coincide. In such a case there is a choice of partition $\mathcal{P}$ and a contour $\mathcal{T}(\mathcal{P})$ for which μ is the equilibrium measure of Γ in the external field φ.

2.4 Critical sets

We continue to use the notation introduced in the beginning of Section 2.3. So for $h \in C_c^2$ we have h_t as in (2.15), and we denote by μ^t the pushforward of a measure μ induced by h_t. For a subset $F \subset \mathbb{C}$, we denote $F^t = h_t(F)$.

In Section 2.3 we studied variations of the energy functional I^φ induced by h, viewed as acting on measures, see (2.16). But we might as well study variations of I^φ when viewed as acting on sets, that is, we might consider the limit

$$D_h I^\varphi(F) = \lim_{t \to 0} \frac{I^\varphi(F^t) - I^\varphi(F)}{t}. \tag{2.45}$$

Just as the vanishing of $D_h I^\varphi(\mu)$ defines critical measures, the vanishing of $D_h I^\varphi(F)$ defines critical sets.

Definition 2.4.1. We say that a closed set F is a φ-critical set (or simply a critical set) if the limit in (2.45) exists for every $h \in C_c^2$, and

$$D_h I^\varphi(F) = 0$$

for every $h \in C_c^2$.

The remarkable fact is that the limit (2.45) coincides with the derivative of I^φ at the equilibrium measure in external field of F.

Proposition 2.4.2. *Let $F \subset \mathbb{C}$ be a closed set with $-\infty < I^\varphi(F) < +\infty$. Then the limit in (2.45) exists and*

$$D_h I^\varphi(F) = D_h I^\varphi(\mu^{\varphi, F}). \tag{2.46}$$

The existence of the equilibrium measure in the external field $\mu^{\varphi,F}$ is guaranteed by Theorem 2.2.5. Proposition 2.4.2 is due to Rakhmanov, who gives a proof in [116, Section 9.10] and refers to an unpublished manuscript where the argument is first given. We found that one of the steps in the proof in [116], namely the equivalent of (2.55), requires some additional explanation, and therefore we decided to present here a detailed proof.

To prove Proposition 2.4.2, we will need an auxiliary lemma. We use $\mathcal{M}_0$ to denote the set of signed measures defined on $\mathbb{C}$, whose positive and negative parts belong to $\mathcal{M}_1(\mathbb{C})$ (see the beginning of Section 2.2.1 for the definition of $\mathcal{M}_1(\mathbb{C})$). Recall that a sequence of finite signed measures (σ_n) converges vaguely to a finite signed measure σ if

$$\int f d\sigma_n \overset{n\to\infty}{\to} \int f d\sigma,$$

for every continuous functions f with compact support.

Lemma 2.4.3. *The functional*

$$\mathcal{M}_0 \ni \sigma \mapsto I(\sigma) = \iint \log|x-y|^{-1} d\sigma(x) d\sigma(y)$$

is well-defined on $\mathcal{M}_0$ and strictly positive for $\sigma \neq 0$. If (σ_n) is a sequence of signed measures in $\mathcal{M}_0$ with

$$I(\sigma_n) \overset{n\to\infty}{\to} 0,$$

then the sequence (σ_n) converges vaguely to the null measure.

Proof. The lemma is well known if we consider signed measures supported in the unit disc, see for example [97, pg. 80, Theorem 1.16, pg. 88, Lemma 1.3]. The main issue here is that we are dealing with signed measures with possibly unbounded support. The proof we are going to give is actually obtained by collecting known results together and fitting them to our needs here.

Given two measures μ, ν with finite energies $I(\mu)$, $I(\nu)$, the integral

$$I(\mu,\nu) = \iint \log \frac{1}{|x-y|} d\mu(x) d\nu(y),$$

is well defined and finite [108, Theorem 2.2], that is, $|\log|x-y|^{-1}| \in L^1(\mu\times\nu)$. In particular, if $\sigma = \sigma_+ - \sigma_- \in \mathcal{M}_0$, then the value

$$I(\sigma) = I(\sigma_+) + I(\sigma_-) - 2I(\sigma_+,\sigma_-)$$

is also well defined and finite. Due to a result of Mattner [108, Theorem 2.2] it is positive, i.e., $I(\sigma) \geq 0$ and $I(\sigma) = 0$ if and only if σ is the zero measure.

For $\sigma \in \mathcal{M}_0$ compactly supported and absolutely continuous with respect to the Lebesgue measure m_2, say $d\sigma = f dm_2$, with $f \in C_c^\infty$ and real-valued satisfying $\int f dm_2 = 0$, Cegrell et al. [44, Lemma 2.4] obtained the representation

$$I(\sigma) = 2\pi \int \frac{|\hat{f}(x)|^2}{|x|^2}\, dm_2(x), \tag{2.47}$$

for $I(\sigma)$, where

$$\hat{f}(z) = \int f(x) e^{-2\pi i \operatorname{Re}(x\overline{z})}\, dm_2(x)$$

is the Fourier transform of f (induced by $\mathbb{R}^2$, so that $\operatorname{Re}(x\overline{z}) = \operatorname{Re} x \operatorname{Re} z + \operatorname{Im} x \operatorname{Im} z$ is just the inner product in $\mathbb{R}^2$). For $\sigma = \sigma_+ - \sigma_- \in \mathcal{M}_0$ and a given sequence of approximation to the identity (ψ_n) (ψ_n is smooth and independent of σ) satisfying

$$\int \psi_n\, dm_2 = 1, \quad \psi_n(z) \geq 0, \quad \text{for } z \in \mathbb{C}, \quad \text{and} \quad \psi_n(z) \equiv 0 \ \text{ for } |z| > \frac{1}{n},$$

Cegrell et al. constructed a sequence of absolutely continuous signed measures $\mu_n = \psi_n * \lambda_n \in \mathcal{M}_0$ with $\lim_{n\to\infty} I(\mu_n) = I(\sigma)$, where

$$\lambda_n = \sigma\big|_{\Sigma_n} - \sigma(\Sigma_n)\lambda, \tag{2.48}$$

and λ is the normalized Lebesgue measure on the unit disc and (Σ_n) a sequence of discs $\Sigma_n = D_{R_n}$ whose respective sequence of radii (R_n) converges to $+\infty$ when $n \to \infty$.

So now consider a sequence (σ_m) in $\mathcal{M}_0$ with $I(\sigma_m) \to 0$. For each m consider the measures $\lambda_{n,m}$ defined as in (2.48) for $\sigma = \sigma_m$. For each m, we can take $n = n(m)$ large enough, such that for $\mu_m := \lambda_{n,m} * \psi_n$,

$$|I(\mu_m) - I(\sigma_m)| < \frac{1}{m}, \tag{2.49}$$

and we can make sure that $n(m+1) > n(m)$, for all m. The explicit form of μ_m and this last condition on the indices imply in particular

$$\mu_m - \sigma_m \to 0 \text{ vaguely.} \tag{2.50}$$

The measures μ_m are absolutely continuous w.r.t. m_2 with a smooth and compactly supported density, say $d\mu_m = f_m dm_2$. Equations (2.47) and (2.49) and the convergence $I(\sigma_m) \to 0$ then imply

$$\frac{\hat{f}_m(x)}{x} \to 0 \ \text{ in } L^2(m_2) \qquad \text{as } m \to \infty.$$

If $h = h_1 + ih_2 \in C_c^\infty$, then $h_j, f_m \in L^1(m_2) \cap L^2(m_2)$ and also $x\hat{h}_j \in L^2(m_2)$, and the Plancherel Theorem and Cauchy-Schwarz inequality imply for $j = 1, 2$,

$$\begin{aligned}\left|\int h_j \, d\mu_m\right| &= \left|\int h_j(x) f_m(x) \, dm_2(x)\right| \\ &= \left|\int \hat{h}_j(z) \hat{f}_m(z) \, dm_2(z)\right| \\ &\leq \|x\hat{h}_j\|_2 \left\|\frac{\hat{f}_m}{x}\right\|_2 \to 0, \qquad \text{as } m \to \infty,\end{aligned}$$

so that

$$\lim_{m\to\infty} \int h \, d\mu_m = 0. \tag{2.51}$$

Finally, since C_c^∞ is dense in C_c w.r.t. the uniform norm and $|\int f_m \, dm_2|$ is uniformly bounded, the inequality

$$\left|\int h \, d\mu\right| \leq \|h - h_n\|_\infty \left|\int f_m \, dm_2\right| + \left|\int h_n \, d\mu_m\right|$$

for a sequence (h_n) of functions in C_c^∞ converging to $h \in C_c$ in the uniform norm shows the limit (2.51) is also true for $h \in C_c$, that is, $\mu_m \to 0$ vaguely. In virtue of (2.50) this is equivalent to the vague convergence $\sigma_m \to 0$. □

Proof of Proposition 2.4.2. For t small enough and h_t as in (2.15), the inverse map h_t^{-1} is a well defined C_c^2 function which satisfies

$$h_t^{-1}(x) = x - th(x) + o(t), \tag{2.52}$$

$$\frac{h_t^{-1}(x) - h_t^{-1}(y)}{x - y} = 1 - t\frac{h(x) - h(y)}{x - y} + o(t), \tag{2.53}$$

with the o terms uniform in $x, y \in \mathbb{C}$.

For simplicity, denote by μ_F and μ_{F^t} the equilibrium measures in the external field φ of F and F^t, respectively. By Rakhmanov's Theorem 2.2.5 and the assumption $h \in C_c^2$ these measures certainly exist.

Clearly, in view of the definitions (2.16) and (2.45) and Proposition 2.3.1, it is enough to prove that

$$I^\varphi(F^t) - I^\varphi(F) = I^\varphi(\mu_F^t) - I^\varphi(\mu_F) + o(t), \quad t \to 0,$$

which comes down to proving

$$I^{\varphi}(\mu_{F^t}) - I^{\varphi}(\mu_F^t) = o(t), \quad t \to 0.$$

For a given t, denote by $\mu_{F^t}^{-t}$ the pushforward measure of μ_{F^t} induced by the inverse mapping h_t^{-1}. Bearing in mind equations (2.52), (2.53) and mimicking the proof of Proposition 2.3.1 we obtain

$$I^{\varphi}(\mu_{F^t}^{-t}) - I^{\varphi}(\mu_{F^t}) = -tD_h I^{\varphi}(\mu_{F^t}) + o(t), \quad t \to 0,$$

and also from Proposition 2.3.1,

$$I^{\varphi}(\mu_F^t) - I^{\varphi}(\mu_F) = tD_h I^{\varphi}(\mu_F) + o(t), \quad t \to 0.$$

This in turn implies

$$\begin{aligned} 0 &\le I^{\varphi}(\mu_F^t) - I^{\varphi}(\mu_{F^t}) \\ &= I^{\varphi}(\mu_F) - I^{\varphi}(\mu_{F^t}^{-t}) + t(D_h I^{\varphi}(\mu_F) - D_h I^{\varphi}(\mu_{F^t})) + o(t) \\ &\le t(D_h I^{\varphi}(\mu_F) - D_h I^{\varphi}(\mu_{F^t})) + o(t), \quad t \to 0, \end{aligned} \tag{2.54}$$

so we are done if we can show

$$\lim_{t\to 0} D_h I^{\varphi}(\mu_{F^t}) = D_h I^{\varphi}(\mu_F). \tag{2.55}$$

To obtain (2.55), assume for a moment

$$\int f \, d\mu_{F^t} \overset{t\to 0}{\to} \int f \, d\mu_F, \quad f \in C_c, \tag{2.56}$$

that is, $\mu_{F^t} \to \mu_F$ vaguely, to be proved later. Since $h \in C_c^2$ the function

$$(x, y) \mapsto \frac{h(x) - h(y)}{x - y}$$

is continuous with compact support, so that by (2.56)

$$\iint \frac{h(x) - h(y)}{x - y} \, d\mu_{F^t}(x) d\mu_{F^t}(y) \overset{t\to 0}{\to} \iint \frac{h(x) - h(y)}{x - y} \, d\mu_F(x) d\mu_F(y). \tag{2.57}$$

The function hV' belongs also to C_c^2, so again by (2.56)

$$\int h(x)V'(x) \, d\mu_{F^t}(x) \overset{t\to 0}{\to} \int h(x)V'(x) \, d\mu_F(x). \tag{2.58}$$

Using Proposition 2.3.1 and (2.57), (2.58), the limit (2.55) follows and the proof is done, provided that we have (2.56).

The proof of (2.56) will be done in two steps, namely $\mu_F^t \to \mu_F$ and $\mu_{F^t} - \mu_F^t \to 0$ vaguely.

The first of these limits follows directly from the change of variables formula,

$$\int f \, d\mu_{F^t} = \int f \circ h_t \, d\mu \to \int f \, d\mu, \qquad t \to 0,$$

because f has compact support, and so it is bounded, and $h_t(z) \to z$ as $t \to 0$, and the dominated convergence theorem can be applied.

The difference $D_h I^\varphi(\mu_F) - D_h I^\varphi(\mu_{F^t})$ is bounded, thanks to Proposition 2.3.1, so (2.54) implies $I^\varphi(\mu_F^t) - I^\varphi(\mu_{F^t}) \to 0$. Now, following notations of the previous Lemma,

$$\begin{aligned} 0 \le I(\mu_F^t - \mu_{F^t}) &= 2I^\varphi(\mu_F^t) + 2I^\varphi(\mu_{F^t}) - 4I^\varphi\left(\frac{\mu_F^t + \mu_{F^t}}{2}\right) \\ &\le 2I^\varphi(\mu_F^t) + 2I^\varphi(\mu_{F^t}) - 4I^\varphi(\mu_{F^t}) \\ &= 2I^\varphi(\mu_F^t) - 2I^\varphi(\mu_{F^t}) \to 0 \end{aligned} \tag{2.59}$$

as $t \to 0$. The inequality in (2.59) is obtained by noting that $\frac{1}{2}(\mu_F^t + \mu_{F^t}) \in \mathcal{M}_1^\varphi(F^t)$, so its weighted energy is larger than $I^\varphi(\mu_{F^t})$. Lemma 2.4.3 then implies $\mu_F^t - \mu_{F^t} \to 0$ vaguely. □

An immediate consequence of Proposition 2.4.2 is the following.

Corollary 2.4.4. *The equilibrium measure $\mu^{\varphi,F}$ in the external field φ of a φ-critical set F is a φ-critical measure.*

2.5 Proof of Theorem 2.2.3

In this section we are going to prove Theorem 2.2.3. Recall we are assuming that V is a polynomial of degree N, $\varphi = \operatorname{Re} V$ and $\mathcal{T} = \mathcal{T}(\mathcal{P})$ is the class of admissible contours associated to a fixed noncrossing partition $\mathcal{P}$, as given in Definition 2.2.2. This setup defines the max-min problem $(V, \mathcal{T})$, see (2.8).

2.5.1 The collection $\mathcal{T}_M$

In the first step we are going to restrict the class of contours $\mathcal{T}$. The contours in $\mathcal{T}$ stretch out to infinity in certain directions in which $\varphi \to +\infty$, as specified by the partition $\mathcal{P}$. However, it is not forbidden that some parts of $\Gamma \in \mathcal{T}$ are in regions of the plane where φ is very negative. Then also $I^{\varphi}(\Gamma)$ will be very negative, and so such Γ will be far from optimal for the max-min problem (2.8).

Here we are going to make this precise, and we show that for M large enough we can restrict to a certain subclass $\mathcal{T}_M$ of $\mathcal{T}$ that we are going to define first.

For $M > 0$ large enough, the level set

$$\varphi^{-1}(-M) = \{z \in \mathbb{C} \mid \varphi(z) = -M\}. \tag{2.60}$$

consists of N disjoint analytic arcs, each of them stretching out to infinity in its both ends. This is so because φ is the real part of a polynomial of degree N. Then, if $M > 0$ is large enough,

$$\Delta_M = \varphi^{-1}(-\infty, -M) \cap \{z \in \mathbb{C} \mid \operatorname{dist}(z, \varphi^{-1}(-M)) > 8\} \tag{2.61}$$

is an open non-empty set and its boundary consists of a union of N pairwise disjoint analytic arcs. The distance in (2.61) is the usual Euclidean distance

$$\operatorname{dist}(z, X) = \inf_{x \in X} |z - x|.$$

The set Δ_M is indicated by the gray regions in Figures 2.2 and 2.3. We also assume M satisfies

$$-M < \sup_{\Gamma \in \mathcal{T}} I^{\varphi}(\Gamma). \tag{2.62}$$

Then for such M we consider the subclass

$$\mathcal{T}_M = \{\Gamma \in \mathcal{T} \mid \Gamma \cap \Delta_M = \emptyset\}, \tag{2.63}$$

and its closure

$$\mathcal{F}_M = \overline{\mathcal{T}_M} \tag{2.64}$$

with respect to Hausdorff metric on closed subsets of $\mathbb{C}$ with the hyperbolic distance. The sets in $\mathcal{F}_M$ are closed subsets of $\mathbb{C}$, but they are not necessarily finite unions of contours, since this property is not preserved under taking closure in the Hausdorff metric.

However, because of Definition 2.2.2 ii), each $F \in \mathcal{F}_M$ has at most $|\mathcal{P}_0|$ components that are all unbounded in $\mathbb{C}$, since this property is preserved by taking closure in the Hausdorff metric. Also

$$F \cap \Delta_M = \emptyset, \qquad \text{for all } F \in \mathcal{F}_M. \tag{2.65}$$

Proposition 2.5.1. *We have*

$$\sup_{\Gamma\in\mathcal{T}\setminus\mathcal{T}_M} I^\varphi(\Gamma) < \sup_{\Gamma\in\mathcal{T}_M} I^\varphi(\Gamma) \le \sup_{F\in\mathcal{F}_M} I^\varphi(F) < +\infty. \tag{2.66}$$

Proof. The inequality in (2.66) between the supremum over $\mathcal{T}_M$ and the supremum over $\mathcal{F}_M$ is trivial.

We start with the proof of the first inequality in (2.66). To prove this we take $\Gamma \in \mathcal{T} \setminus \mathcal{T}_M$. Since all connected components of Γ are unbounded, see item ii) of Definition 2.2.2, and Γ intersects the set Δ_M from (2.61), we have that Γ contains a connected subset Γ_0 satisfying

$$\Gamma_0 \subset \varphi^{-1}(-\infty, -M) \quad \text{and} \quad \operatorname{diam}\Gamma_0 \ge 8.$$

Then $\operatorname{cap}(\Gamma_0) \ge \frac{\operatorname{diam}\Gamma}{4} \ge 2$, which means that $I(\Gamma_0) \le \log\frac{1}{2}$, see for example [118, page 138]. Let ω be the equilibrium measure on Γ_0 (without external field). Then $I(\omega) = I(\Gamma_0) \le \log\frac{1}{2}$, and

$$I^\varphi(\Gamma_0) \le I^\varphi(\omega) = I(\omega) + \int \varphi\, d\omega \le \log\frac{1}{2} - M,$$

because Γ_0 is contained in the region where $\varphi < -M$. Then by (2.62)

$$I^\varphi(\Gamma) \le I^\varphi(\Gamma_0) \le \log\frac{1}{2} + \sup_{\Gamma'\in\mathcal{T}} I^\varphi(\Gamma').$$

Since $\Gamma \in \mathcal{T} \setminus \mathcal{T}_M$ is arbitrary, and $\log\frac{1}{2} < 0$, we find the first inequality in (2.66).

It remains to prove that $\sup_{F\in\mathcal{F}_M} I^\varphi(F)$ is finite. To this end, we construct a closed curve γ, contained in $\mathbb{C} \setminus \Delta_M$ and intersecting all the connected components of $\partial\Delta_M$, see Figure 2.3 for a pictorial configuration of γ.

Recall that by item ii) of Definition 2.2.2 the connected components of sets in $\mathcal{T}$ are unbounded and stretch out to infinity in at least two of the sectors $S_1, \dots, S_N$. Assuming in addition that $\Gamma \in \mathcal{T}_M$, that is, $\Gamma \cap \Delta_M = \emptyset$, it is easy to see that $\Gamma_A \cap \gamma \neq \emptyset$ for any connected component Γ_A of Γ. This property is preserved by taking closures with respect to Hausdorff metric, that is, it is also valid

$$F_A \cap \gamma \neq \emptyset \tag{2.67}$$

for any connected component F_A of a set F belonging to $\mathcal{F}_M$.

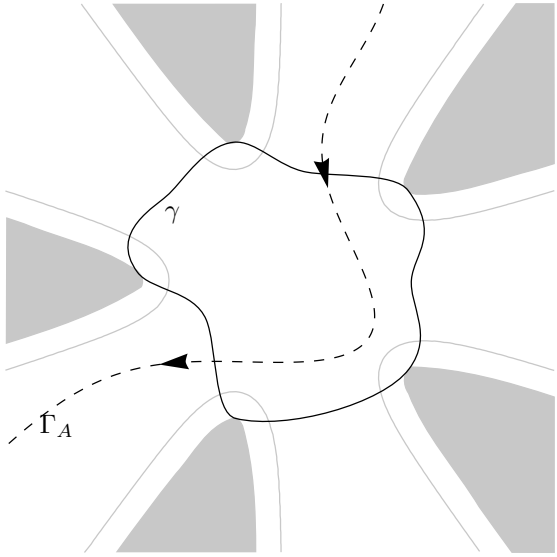

Figure 2.3: A possible choice for γ in the proof of Proposition 2.5.1 for the case $V(z) = z^5 + z$. The level curves $\varphi(z) = -M$ are shown in gray solid lines and the set Δ_M is the shaded region. Sets in $\mathcal{F}_M$ cannot intersect the shaded region. The contour Γ_A, shown in black dashed line, is part of an admissible curve Γ for $A = \{2, 4\}$.

Fix $R > 4$ for which $\gamma \subset D_{R-4}$. A similar reasoning as the one that led to (2.67) shows that

$$F_A \cap \partial D_R \neq \emptyset, \tag{2.68}$$

for any connected component F_A of $F \in \mathcal{F}_M$. From (2.67) and (2.68) we see that there exists a connected compact $F_0 \subset F$ with

$$F_0 \cap \gamma \neq \emptyset, \quad F_0 \cap \partial D_R \neq \emptyset, \quad F_0 \subset \overline{D}_R.$$

This means that $\operatorname{diam} F_0 \geq 4$, because $\gamma \subset D_{R-4}$. Then $\operatorname{cap} F_0 \geq 1$, which implies $I(F_0) \leq 0$, and then

$$I^\varphi(F) \leq I^\varphi(F_0) \leq I(F_0) + \sup_{z \in F_0} \varphi(z) \leq \sup_{z \in \overline{D}_R} \varphi(z) < +\infty.$$

Since R is independent of $F \in \mathcal{F}_M$, the inequality $\sup_{F \in \mathcal{F}_M} I^\varphi(F) < +\infty$ follows. □

2.5.2 A maximizer set F_0

The following is an immediate consequence of Proposition 2.5.1.

Corollary 2.5.2. *There exists $F_0 \in \mathcal{F}_M$ such that*

$$I^{\varphi}(F_0) = \sup_{F \in \mathcal{F}_M} I^{\varphi}(F). \tag{2.69}$$

Proof. The class $\mathcal{F}_M$ is closed in the Hausdorff metric. The upper semicontinuity of I^{φ} given by Theorem 2.2.6 and Proposition 2.5.1 gives the desired result. □

The next lemma assures that small variations of F_0 are still in $\mathcal{F}_M$.

Lemma 2.5.3. *Let $F_0 \in \mathcal{F}_M$ be a maximizer set given by Corollary 2.5.2. For every $h \in C_c^2$, there exists $t_0 > 0$ such that $F_0^t \in \mathcal{F}_M$, for every $t \in (-t_0, t_0)$.*

Proof. Since $F_0 \in \mathcal{F}_M$, we already observed that $F_0 \cap \Delta_M = \emptyset$, see (2.65). The same argument that was used to prove the first inequality in Proposition 2.5.1 shows that

$$F_0 \cap \overline{\Delta}_M = \emptyset.$$

Let $h \in C_c^2$ be a test function. Since h is compactly supported, it follows that there is a $t_0 > 0$ such that

$$F_0^t \cap \overline{\Delta}_M = \emptyset \qquad \text{for all } t \in (-t_0, t_0). \tag{2.70}$$

We also take t_0 small enough so that $x \mapsto h_t(x) = x + th(x)$ is a C^2-diffeomorphism on $\mathbb{C}$ for $t \in (-t_0, t_0)$.

Let $t \in (-t_0, t_0)$, and let (Γ_n) be a sequence in $\mathcal{T}_M$ that converges to F_0 in Hausdorff metric. It is then an easy fact that the convergence

$$\Gamma_n^t \to F_0^t \qquad \text{as } n \to \infty \tag{2.71}$$

in the Hausdorff metric also holds true.

Take $R > 0$ such that $\operatorname{supp} h \subset D_R$. Since h_t is a diffeomorphism that leaves $\mathbb{C} \setminus D_R$ invariant, we then have

$$\Gamma_n^t \cap (\mathbb{C} \setminus D_R) = \Gamma_n \cap (\mathbb{C} \setminus D_R), \tag{2.72}$$

for all n. Since $\Gamma_n \in \mathcal{T}_M$, it does not intersect Δ_M, and so by (2.72)

$$\Gamma_n^t \cap (\mathbb{C} \setminus D_R) \cap \Delta_M = \emptyset. \tag{2.73}$$

The convergence (2.71), together with the fact that F_0^t does not intersect the closed set $\overline{\Delta}_M$, see (2.70), implies that for large enough n,

$$\Gamma_n^t \cap D_R \cap \Delta_M = \emptyset. \tag{2.74}$$

Then by (2.73) and (2.74) we have

$$\Gamma_n^t \cap \Delta_M = \emptyset$$

for n large enough, and so $\Gamma_n^t \in \mathcal{T}_M$ by the definition (2.63) of the class $\mathcal{T}_M$. Because of (2.71), we then conclude that $F_0^t \in \overline{\mathcal{T}}_M = \mathcal{F}_M$. □

From Lemma 2.5.3 it follows that the maximizer F_0 is a φ-critical set. Thus by Corollary 2.4.4 its equilibrium measure in the external field φ is a φ-critical measure and the results of Section 2.3 apply to this measure. Thus we obtain the following proposition that summarizes the work we did so far.

Proposition 2.5.4. *The equilibrium measure $\mu_0 = \mu^{\varphi,F_0}$ of F_0 is φ-critical. There exists a polynomial R such that*

$$\left(C^{\mu_0}(z) + \frac{1}{2}V'(z)\right)^2 = R(z), \quad m_2\text{-a.e.} \tag{2.75}$$

Moreover, $\operatorname{supp}\mu_0$ *is compact and consists of a finite union of analytic arcs, which are maximal trajectories of the quadratic differential $-R(z)dz^2$, with each trajectory connecting two distinct zeros of R. The measure μ_0 is absolutely continuous with respect to the arclength measure on those arcs and*

$$d\mu_0(s) = \frac{1}{\pi i}\sqrt{R(s)}\,ds \tag{2.76}$$

where ds is the complex line element. At any point $z \in \operatorname{supp}\mu_0$ which is not a zero of R, its logarithmic potential satisfies

$$\frac{\partial}{\partial n_+}\left(U^{\mu_0} + \frac{1}{2}\varphi\right)(z) = \frac{\partial}{\partial n_-}\left(U^{\mu_0} + \frac{1}{2}\varphi\right)(z), \tag{2.77}$$

where $n_\pm$ are the unit normal vectors to $\operatorname{supp}\mu_0$ *at z pointing in opposite directions.*

Thus by (2.77) we have that the support of μ_0 satisfies the S-property in the external field φ.

2.5.3 Proof of Theorem 2.2.3

Having in hands the equilibrium measure in the external field $\mu_0 = \mu^{\varphi,F_0}$ of the maximizer set F_0 given by Corollary 2.5.2, our final task is to construct a contour $\Gamma_0 \in \mathcal{T}$ for which $\mu^{\varphi,\Gamma_0} = \mu_0$. Note that we know that the support of μ_0 consists of a finite union of analytic arcs, but we do not know that the full set F_0 is a contour. There is actually no reason why this should be the case, and so we will modify F_0 outside of the support of its equilibrium measure in the external field, while preserving the equilibrium measure in the external field. We also have to show that the contour Γ_0 that we obtain this way belongs to the class $\mathcal{T}$.

To this end, we consider the set

$$\Lambda = \left\{ z \in \mathbb{C} \mid U^{\mu_0}(z) + \frac{1}{2}\varphi(z) > l_0 \right\}, \tag{2.78}$$

for the variational constant l_0 of μ_0 appearing in the Euler-Lagrange variational conditions (2.4) and (2.5) for μ_0.

Lemma 2.5.5.

For any $\epsilon > 0$, there exists $R_\epsilon > 0$ such that for every $R \geq R_\epsilon$ the following holds. The set $\Lambda \setminus D_R$ has exactly N connected components, each of them contained in precisely one of the sectors

$$\left\{ z \in \mathbb{C} \mid |z| \geq R, |\arg z - \theta_j| \leq \frac{\pi}{2N} + \epsilon \right\}, \quad j = 1, \ldots, N, \tag{2.79}$$

and containing in its interior the half-rays

$$L_{j,R} = \{ z \in \mathbb{C} \mid |z| \geq R, \ \arg z = \theta_j \}, \quad j = 1, \ldots, N. \tag{2.80}$$

Recall that the angles θ_j are given in (2.7) and they are determined by the polynomial V.

Proof. The boundary of Λ consists of level curves of $U^{\mu_0} + \frac{1}{2}\varphi$, and these are exactly the trajectories of the quadratic differential $-R(z)dz^2$ given in (2.75). The quadratic differential has a pole of order $2N + 2$ at $z = \infty$. Lemma 2.5.5 then follows from the local behavior of trajectories of a quadratic differential near a pole of order ≥ 4, see [133, Theorem 7.4]. □

Fix a number

$$0 < \epsilon < \frac{\pi}{2N} \tag{2.81}$$

and also $R > R_\epsilon$ for which

$$\operatorname{supp} \mu_0 \subset D_R. \tag{2.82}$$

For $j = 1, \ldots, N$, let $\Lambda(j)$ be the connected component of $\overline{\Lambda} \cup \operatorname{supp} \mu_0$ for which

$$L_{j,R} \subset \Lambda(j). \tag{2.83}$$

Then $\Lambda(j)$ is pathwise connected, and we can connect any point in $\Lambda(j)$ to infinity through a curve entirely contained in $\Lambda(j)$ and stretching out to infinity in the sector S_j (see (2.7) for the definition of S_j).

The sets $\Lambda(j)$ for $j = 1, \ldots, N$, need not be disjoint. It can happen that $\Lambda(j) = \Lambda(k)$ for some pair of distinct numbers j, k. Of course, if their intersection is non-empty then $\Lambda(j) = \Lambda(k)$.

The next lemma is the key for completing the proof of Theorem 2.2.3.

Lemma 2.5.6. *If $A \in \mathcal{P}_0$ and $j, k \in A$, then $\Lambda(j) = \Lambda(k)$.*

The proof of Lemma 2.5.6 is postponed to Section 2.5.4. We first show how to complete the proof of Theorem 2.2.3, assuming the lemma.

Proof of Theorem 2.2.3. Let ϵ and $R > R_\epsilon$ be given as in (2.81) and (2.82). For the angles $\theta_1, \ldots, \theta_N$ in (2.7), denote

$$z_j = Re^{i\theta_j}, \quad j = 1, \ldots, N.$$

From (2.82) and Lemma 2.5.5 we see that $z_j \in \Lambda$. Given $A \in \mathcal{P}_0$, we have by Lemma 2.5.6 that the points z_j with $j \in A$, belong to the same connected component of $\overline{\Lambda} \cup \operatorname{supp} \mu_0$. Then there exists a connected set $\gamma_A \subset \overline{\Lambda} \cup \operatorname{supp} \mu_0$ which is a finite union of bounded C^1 Jordan arcs satisfying

$$z_j \in \gamma_A, \quad \text{for every } j \in A.$$

For $L_{j,R}$ given by (2.80), define

$$\Gamma_A = \gamma_A \cup \bigcup_{j \in A} L_{j,R}.$$

Each Γ_A is then a finite union of C^1 arcs. Γ_A is connected and Γ_A stretches out to infinity in each sector S_j with $j \in A$. The union

$$\Gamma_0 = \bigcup_{A \in \mathcal{P}_0} \Gamma_A$$

then satisfies all the requirements in Definition 2.2.2 and it follows that

$$\Gamma_0 \in \mathcal{T}(\mathcal{P}).$$

Hence

$$I^{\varphi}(\Gamma_0) \leq \sup_{\Gamma \in \mathcal{T}(\mathcal{P})} I^{\varphi}(\Gamma). \tag{2.84}$$

Since $\Gamma_0 \subset \Gamma_0 \cup \operatorname{supp} \mu_0$, we also have that

$$I^{\varphi}(\Gamma_0 \cup \operatorname{supp} \mu_0) \leq I^{\varphi}(\Gamma_0). \tag{2.85}$$

On the other hand, since $\Gamma_0 \subset \overline{\Lambda} \cup \operatorname{supp} \mu_0$, the variational conditions (2.4), (2.5) are valid for $\Gamma_0 \cup \operatorname{supp} \mu_0$, which means that μ_0 is the equilibrium measure of $\Gamma_0 \cup \operatorname{supp} \mu_0$ in the external field φ. Thus

$$I^{\varphi}(\Gamma_0 \cup \operatorname{supp} \mu_0) = I^{\varphi}(\mu_0) = I^{\varphi}(F_0), \tag{2.86}$$

since μ_0 is the equilibrium measure in the external field of F_0 as well. Then we recall that F_0 is the maximizer of I^{φ} over the class $\mathcal{F}_M$ which contains $\mathcal{T}_M$. Then by Proposition 2.5.1

$$I^{\varphi}(F_0) \geq \sup_{\Gamma \in \mathcal{T}_M} I^{\varphi}(\Gamma) = \sup_{\Gamma \in \mathcal{T}} I^{\varphi}(\Gamma) \tag{2.87}$$

Combining the inequalities in (2.84)–(2.87), we finally get

$$I^{\varphi}(\Gamma_0) \leq \sup_{\Gamma \in \mathcal{T}} I^{\varphi}(\Gamma) \leq I^{\varphi}(F_0) = I^{\varphi}(\Gamma_0 \cup \operatorname{supp} \mu_0) \leq I^{\varphi}(\Gamma_0) \tag{2.88}$$

and so equality holds throughout in (2.88).

Let $\mu_1 = \mu^{\varphi, \Gamma_0}$ be the equilibrium measure in the external field φ of Γ_0. Then because of the equalities in (2.88), we have

$$I^{\varphi}(\mu_1) = I^{\varphi}(\Gamma_0) = I^{\varphi}(\Gamma_0 \cup \operatorname{supp} \mu_0)$$

Thus μ_1 is a measure supported on $\Gamma_0 \subset \Gamma_0 \cup \operatorname{supp} \mu_0$ whose energy in external field φ is equal to the minimal energy for measures on $\Gamma_0 \cup \operatorname{supp} \mu_0$. By uniqueness of equilibrium measure it follows that $\operatorname{supp} \mu_0 \subset \Gamma_0$ and $\mu_0 = \mu_1$ is the equilibrium measure in external field φ of Γ_0.

Then $\Gamma_0 \in \mathcal{T}$ has the S-property in external field φ, see (2.77) in Proposition 2.5.4. Also the remaining statements of Theorem 2.2.3 follow from Proposition 2.5.4. This completes the proof of Theorem 2.2.3, assuming the validity of Lemma 2.5.6. □

2.5.4 Proof of Lemma 2.5.6

What remains is the proof of Lemma 2.5.6.

Proof of Lemma 2.5.6. We take $A \in \mathcal{P}_0$ and $j, k \in A$ with $j \neq k$ and our task is to prove that $\Lambda(j) = \Lambda(k)$.

In the proof we make use of the maximizer $F_0 \in \mathcal{F}_M$ and we know that μ_0 is the equilibrium measure of F_0 in the external field φ. Thus by the variational conditions (2.4), (2.5),

$$F_0 \subset \{z \in \mathbb{C} \mid U^{\mu_0}(z) + \frac{1}{2}\varphi(z) \geq l_0\}.$$

If $z \in F_0 \setminus \operatorname{supp} \mu_0$ then $U^{\mu_0} + \frac{1}{2}\varphi$ is harmonic near z, and so cannot have a local maximum at z. It follows that

$$F_0 \subset \overline{\Lambda} \cup \operatorname{supp} \mu_0. \tag{2.89}$$

where we recall that Λ is defined in (2.78).

Since $\mathcal{F}_M$ is the closure of $\mathcal{T}_M$, there exists a sequence $(\Gamma_n)_n$ in $\mathcal{T}_M$ such that

$$\Gamma_n \to F_0 \quad \text{in Hausdorff metric.} \tag{2.90}$$

Let $n \in \mathbb{N}$. From item iii) of Definition 2.2.2 it follows that Γ_n has a connected component that stretches out to infinity in the sectors S_j and S_k. Then by dropping parts of that component that go to infinity in other sectors, and parts that make loops, we can find a subset $\widetilde{\Gamma}_n \subset \Gamma_n$ that is a simple piecewise C^1 contour that goes from infinity in the sector S_j to infinity in the sector S_k. Here simple means that it has no points of self-intersection. We consider $\widetilde{\Gamma}_n$ as an oriented contour, and we talk about points on the contour that lie before or after other points. From the definition of $\mathcal{T}_M$, see (2.63), we know that

$$\widetilde{\Gamma}_n \cap \Delta_M = \emptyset. \tag{2.91}$$

The region Δ_M consists of N connected components, all of them stretching out to infinity, as shown with the gray shaded regions in Figure 2.3 for the case $N = 5$.

Let R be large enough such that the circle $|z| = R$ intersects each of the components of Δ_M along a circular arc. Then there are also N circular subarcs of $|z| = R$ outside of Δ_M, that we call $\alpha_1, \ldots, \alpha_N$ where α_i is in the direction

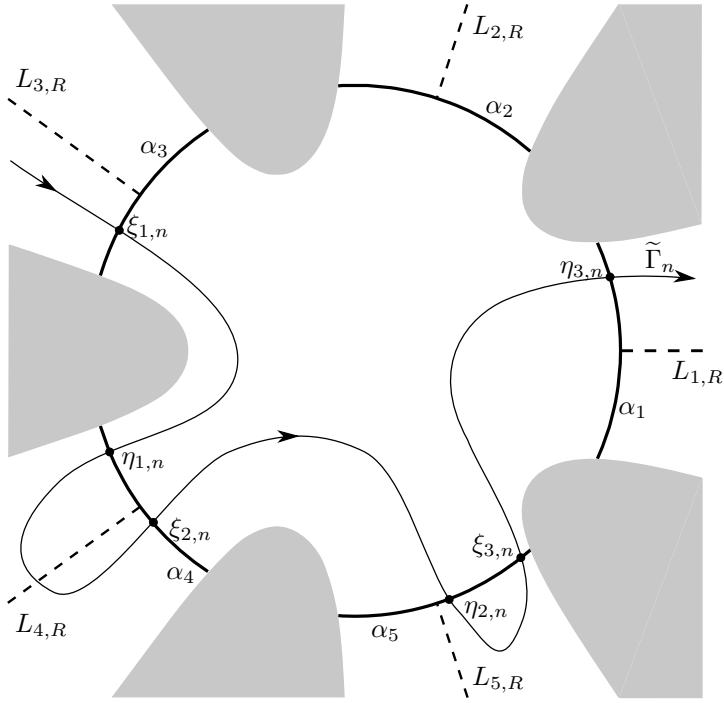

Figure 2.4: Pictorial example for the proof of Lemma 2.5.6, considering a polynomial V of degree 5. The shaded region is Δ_M. The black thick arcs belonging to a circle are the curves α_i. The oriented contour is an example of $\widetilde{\Gamma}_n$ for some Γ_n in (2.90). The points $\xi_{i,n}, \eta_{i,n}$, $j = 1, \dots, l$ are also represented in the figure, in this case with value $l = 3$.

of the sector S_i, for $i = 1, \dots, N$. By taking R large enough, we can also make sure that

$$\{z \in \alpha_i \mid U^{\mu_0}(z) + \frac{1}{2}\varphi(z) \geq l_0\} \subset \Lambda(i) \tag{2.92}$$

for each i, where $\Lambda(i)$ is as in (2.83).

We now follow the contour $\widetilde{\Gamma}_n$ starting at infinity in the sector S_j. It will meet the arc α_j. We let $\xi_{1,n}$ be the *last point* on $\widetilde{\Gamma}_n$ that is on α_j. Then $\widetilde{\Gamma}_n$ enters into $D_R \setminus \Delta_M$ and never returns to α_j. Since it ends up at infinity again, the contour has to leave $D_R \setminus \Delta_M$ again, and it will do so along one of the arcs α_i, with $i \neq j$. We let $\eta_{1,n}$ be the *first point* after $\xi_{1,n}$ which is on one of the α_i again, say $\eta_{1,n} \in \alpha_{j_1}$. If $j_1 = k$, then we stop. If $j_1 \neq k$, then we continue and we let $\xi_{2,n}$ be the *last point* on $\widetilde{\Gamma}_n$ that is on α_{j_1}. After $\xi_{2,n}$ the contour is

going into $D_R \setminus \Delta_M$ again, since the contour has to end in the sector S_k and $j_1 \neq k$. The contour will meet one of the α_i again, and we let $\eta_{2,n}$ be the *first point* after $\xi_{2,n}$ which is on one of the α_i, say $\eta_{2,n} \in \alpha_{j_2}$. Then $j_2 \neq j$ and $j_2 \neq j_1$, since $\xi_{1,n}$ is the last point on α_j and $\xi_{2,n}$ is the last point on α_{j_1}, and $\eta_{2,n}$ comes after these two points. If $j_2 = k$ then we stop, and otherwise we continue, see Figure 2.4 for an illustration.

Continuing this process, we find a sequence of distinct indices $j_0, j_1, \ldots, j_l$ for some $l \in \{1, \ldots, N-1\}$, where

$$j_0 = j, \qquad j_l = k,$$

and points $\xi_{1,n}, \eta_{1,n}, \ldots, \xi_{l,n}, \eta_{l,n}$ on the contour $\widetilde{\Gamma}_n$ with

$$\xi_{i,n} \in \alpha_{j_{i-1}}, \quad \text{and} \quad \eta_{i,n} \in \alpha_{j_i} \qquad \text{for } i = 1, \ldots, l. \tag{2.93}$$

Furthermore, if we use $\widetilde{\Gamma}_n(\xi, \eta)$ to denote the part of $\widetilde{\Gamma}_n$ lying strictly between two points ξ and η of the contour, then

$$\widetilde{\Gamma}_n(\xi_{i,n}, \eta_{i,n}) \subset D_R \setminus \Delta_M \qquad \text{for } i = 1, \ldots, l. \tag{2.94}$$

The numbers $l, j_1, \ldots, j_{l-1}$ depend on the contour $\widetilde{\Gamma}_n$ and so they depend on n. But these numbers are always positive integers less than or equal to N, so there are just finite possible choices for them. By passing to a subsequence of the sequence (Γ_n), we may assume they are independent of n.

The set

$$\widetilde{\Gamma}_n[\xi_{i,n}, \eta_{i,n}] = \widetilde{\Gamma}_n(\xi_{i,n}, \eta_{i,n}) \cup \{\xi_{i,n}, \eta_{i,n}\}$$

is a connected closed subset of $\widetilde{\Gamma}_n$ lying in the compact set $\overline{D_R} \setminus \Delta_M$. By completeness of the Hausdorff metric, there is a subsequence, say $N_1 \subset \mathbb{N}$, such that the limit

$$F_i = \lim_{n \to \infty, n \in N_1} \widetilde{\Gamma}_n[\xi_{i,n}, \eta_{i,n}]. \tag{2.95}$$

exists in the Hausdorff metric for every $i = 1, \ldots, l$.

The limit F_i is connected, because this property is preserved by taking limits in the Hausdorff metric if all the sets involved are contained in a large, but fixed, compact set of $\mathbb{C}$, in this case $\overline{D}_R$, see (2.94). Also

$$F_i \subset F_0 \qquad \text{for } i = 1, \ldots, l, \tag{2.96}$$

as follows from (2.90) and the fact $\widetilde{\Gamma}_n[\xi_{i,n}, \eta_{i,n}] \subset \Gamma_n$.

By compactness of α_i we may also assume (by taking a further subsequence, if necessary) that the sequences $(\xi_{i,n})_n$ and $(\eta_{i,n})_n$ for $i = 1, \dots, l$ converge along the same subsequence N_1, say

$$\xi_i = \lim_{n\to\infty, n\in N_1} \xi_{i,n}, \qquad \eta_i = \lim_{n\to\infty, n\in N_1} \eta_{i,n}, \qquad \text{for } i = 1, \dots, l.$$

Then by (2.93) and (2.95)

$$\xi_i \in F_i \cap \alpha_{j_{i-1}}, \quad \text{and} \quad \eta_i \in F_i \cap \alpha_{j_i}, \tag{2.97}$$

for every $i = 1, \dots, l$. From (2.97) and (2.92) it follows that

$$\xi_i \in \Lambda(j_{i-1}) \qquad \eta_i \in \Lambda(j_i).$$

Each F_i is a connected subset of F_0 and by (2.89) and (2.97) we see that ξ_i and η_i belong to the same connected component of $\overline{\Lambda} \cap \operatorname{supp} \mu_0$, which means that

$$\Lambda(j_{i-1}) = \Lambda(j_i) \quad \text{for } i = 1, \dots, l.$$

Thus $\Lambda(j_0) = \Lambda(j_l)$ which gives us $\Lambda(j) = \Lambda(k)$ as required. □

Chapter 3

Critical measures for vector energy: global structure of trajectories of quadratic differentials

Saddle points of a vector logarithmic energy with a vector polynomial external field on the plane are known as the *critical vector-valued measures*, a notion that finds a natural motivation in several branches of analysis. In this chapter, based on the joint project [107] with A. Martínez-Finkelshtein, we study in depth the case of measures $\vec{\mu} = (\mu_1, \mu_2, \mu_3)$ when the mutual interaction comprises both attracting and repelling forces.

For arbitrary vector polynomial external fields we establish general structural results about critical measures, such as their characterization in terms of an algebraic equation solved by an appropriate combination of their Cauchy transforms, and the symmetry properties (or the S-properties) exhibited by such measures. In consequence, we conclude that critical vector-valued measures are supported on a finite number of analytic arcs, that are trajectories of a quadratic differential globally defined on a three-sheeted Riemann surface. The complete description of the so-called critical graph for such a differential is the key to the construction of the critical measures.

We illustrate these connections studying in depth a one-parameter family of critical measures under the action of a cubic external field. This choice is

motivated by the asymptotic analysis of a family of (non-hermitian) multiple orthogonal polynomials, that will be the subject of a forthcoming study. Here we compute explicitly the Riemann surface and the corresponding quadratic differential, and analyze the dynamics of its critical graph as a function of the parameter, giving a detailed description of the occurring phase transitions. When projected back to the complex plane, this construction gives us the complete family of critical vector-valued measures, that in this context turn out to be vector-valued equilibrium measures.

3.1 Introduction

Statistical systems of many particles have been the object of intense analysis for a long time, both from the perspective of physics and mathematics. The study of a particular type of interacting particle systems, the so-called determinantal point processes, has been especially fruitful in the past thirty years. This success can be explained both by the ubiquitous character and flexibility of these models (describing the eigenvalues of several random matrix ensembles, non-intersecting diffusion paths, random growth models, random tilings, to mention a few) and the introduction of new tools, intrinsically related with the analytic theory of orthogonal polynomials and their generalizations.

A common feature of these models is that either the joint probability density, the correlation functions, the normalization constant or the generating function can be expressed as a determinant, and the right selection of the functions appearing in these determinants unveils the integrable structure of the underlying processes. Another unified property of these models is the possibility to put them in the framework of the so-called log gases, where the particles behave as charges on one or two dimensional sets, subject to the logarithmic interaction.

The best known case is the spectrum of unitary matrix models (1.1), described in terms of classical families of orthogonal polynomials on the real line, as it was briefly mentioned in the introduction. Their zeros, all real and simple, satisfy an electrostatic model that goes all the way back to Stieltjes [132], and in the large degree limit solve the minimization problem for the associated weighted logarithmic energy (1.6). In other words, the zeros provide an equilibrium configuration on the conducting real line. A similar situation occurs for some non-intersecting paths models or for the six-vertex model in statistical mechanics [40], to mention some more examples.

Further immediate generalizations of the problems above oblige us to leave the real line, extending the notion of orthogonality and the associated log gas models

to the complex plane, and the introduction of non-hermitian orthogonality becomes crucial.

Non-hermitian orthogonal polynomials appear naturally in approximation theory, as denominators of rational (e.g. Padé) approximants to analytic functions [71, 111], or equivalently, in the study of continued fractions. Electrostatic models on a conducting plane are also associated with the polynomial solutions of certain linear differential equations [103, 104]. Recently, non-hermitian orthogonality found its way to areas with a much more "modern" flavor as well, playing the crucial role in the description of the rational solutions to Painlevé equations [18,25], in theoretical physics [2,3,19,20,31,32], in numerical analysis [49] and in percolation theory [16].

The available log gas models on the conducting plane suggest to extend the analysis of the equilibrium distributions (local energy minima on the prescribed sets) to the study of saddle points of the logarithmic energy on the plane. This yields the notion of *critical measures*, studied systematically in [104], following the original ideas in the unpublished manuscript [113]. The advantage of dealing with saddle points of the energy is the possibility to avoid the complications of the free boundaries, as well as to use variational techniques that go back to the work of Löwner and Schiffer.

Returning to our motivation rooted in the interacting particle systems, recent works have showed that more general models, such as the hermitian matrix model with an external source [33,35,36], the two-matrix model [17,26,60,62,63], some classes of non-intersecting paths [89,91] or the normal matrix model [38,90] require considering log gases with more than one group of charges. In this case, standard orthogonal polynomials are not enough, and we must turn to the so-called *multiple orthogonal polynomials* and to the associated vector equilibrium problems [70]. The connection of these two notions was put forward first by Gonchar and Rakhmanov [69,70], motivated by the analytic theory of Hermite–Padé approximants. The reader interested in further details is advised to look into the monograph by Nikishin and Sorokin [111], which features a nice introduction to vector equilibrium problems from the approximation theory's perspective.

Although the analytic theory of multiple orthogonal polynomial is still in its infancy, two somewhat extreme cases are fairly well understood (see e.g. [10,134]). The first one, known as the Angelesco system, corresponds to orthogonality with respect to measures living on disjoint sets, whose asymptotics is described by a vector equilibrium for repelling systems of charges. The other one, called the Nikishin system, where on the contrary the orthogonality is defined on the same set for all measures, is governed by a system of mutually attracting charges. In both situations the size of the charged ensembles is fixed. From

the recent works of Aptekarev [6] and Rakhmanov [115] it became apparent that the "intermediate" cases require more complex log-gases models for their asymptotic descriptions, mixing both attracting and repelling charges, as well as allowing for charges "flowing" from one ensemble to another, see Sections 3.2.1 and 3.3 below.

In the context of the non-hermitian orthogonality, multiple orthogonal polynomials yield naturally the notion of the *critical vector-valued measures*, defined again as saddle points for the total logarithmic energy, and which are the central object in this chapter.

3.2 Main results

3.2.1 General polynomial external fields

Assume we are given a vector of three non-negative measures $\vec{\mu} = (\mu_1, \mu_2, \mu_3)$, compactly supported on the plane. For the interaction matrix A and vector of real-valued functions ("external fields") $\vec{\phi} = (\phi_1, \phi_2, \phi_3)$

$$A = (a_{j,k}) = \begin{pmatrix} 1 & \frac{1}{2} & \frac{1}{2} \\ \frac{1}{2} & 1 & -\frac{1}{2} \\ \frac{1}{2} & -\frac{1}{2} & 1 \end{pmatrix}, \quad \phi_j = \operatorname{Re} \Phi_j, \quad j = 1, 2, 3, \tag{3.1}$$

where Φ_1, Φ_2, Φ_3 are polynomials[1], and denoting by

$$I(\mu, \nu) := \iint \log \frac{1}{|x - y|} d\mu(x) d\nu(y)$$

the logarithmic energy of two compactly supported measures μ and ν, we consider the total energy functional of the form [70]

$$E(\vec{\mu}) = E(\vec{\mu}, \vec{\phi}) = \sum_{j,k=1}^{3} a_{j,k} I(\mu_j, \mu_k) + \sum_{j=1}^{3} \int \phi_j d\mu_j. \tag{3.2}$$

The matrix A is symmetric, singular and positive-semidefinite. Its only non-zero eigenvalue (of order 2) is $3/2$, and the corresponding eigenspace is given by

[1] Although our methodology is, generally speaking, valid also for general positive-semidefinite interaction matrices and when Φ_j' are rational, we restrict ourselves here to the given matrix A and the polynomial external fields; these choices avoid some technicalities related to cumbersome notation and the order or coincidence of the poles.

the vectors $(v_1, v_2, v_3)^T \in \mathbb{C}^3$ (in what follows, $(\cdot)^T$ stands for the transpose) satisfying

$$v_1 - v_2 - v_3 = 0.$$

As it will be seen below, the external fields in (3.1) must satisfy the compatibility condition of $\vec{\Phi}' = (\Phi_1', \Phi_2', \Phi_3')^T$ being an eigenvector for the eigenvalue $3/2$, that is,

$$\Phi_1'(z) - \Phi_2'(z) = \Phi_3'(z), \quad z \in \mathbb{C}. \tag{3.3}$$

We complete the description of the electrostatic model by introducing the constraints on vector-valued measures under consideration: given a parameter $\alpha \in [0, 1]$, we require that $\vec{\mu} = (\mu_1, \mu_2, \mu_3)$ satisfies

$$|\mu_1| + |\mu_2| = 1, \quad |\mu_1| + |\mu_3| = \alpha, \quad |\mu_2| - |\mu_3| = 1 - \alpha. \tag{3.4}$$

Here $|\mu|$ denotes the total mass (total variation) of the measure μ.

It should be pointed out that a particular case of this model (with all $\Phi_j \equiv 0$ and $\alpha = 1/2$) appears in the work of Aptekarev [6] and Rakhmanov [115] in their study of Hermite-Padé approximants [8, 11, 115]. Notice that A in (3.1) contains submatrices that are the interaction matrices both for the Angelesco and for the Nikishin cases.

Let us denote by m_2 the plane Lebesgue measure on $\mathbb{C}$. We are interested in the existence of critical vector-valued measures within a family $\mathcal{M}_\alpha$ of measures $\vec{\mu} = (\mu_1, \mu_2, \mu_3)$ satisfying (3.4) plus the following conditions:

- each μ_j, $j = 1, 2, 3$, is a non-negative Borel measure, supported on a compact set in $\mathbb{C}$ of zero plane Lebesgue measure,

  $$m_2(\operatorname{supp} \mu_j) = 0, \quad j = 1, 2, 3,$$

  and such that the energy $E(\vec{\mu})$, defined in (3.2), is finite.

- the set

  $$S_\alpha := \bigcup_{1 \le j < k \le 3} (\operatorname{supp} \mu_j \cap \operatorname{supp} \mu_k) \tag{3.5}$$

  is finite,

  $$\operatorname{card} S_\alpha < \infty. \tag{3.6}$$

The *vector equilibrium problems* deal with the minimizers of the energy functional (3.2) over a family of measures $\vec{\mu}$ living on prescribed (and fixed) subsets of $\mathbb{C}$, see e.g. [22, 70, 79] and the references therein. As it follows from [22], the equilibrium measure (global minimizer of $E(\vec{\mu})$), if it exists in the class $\mathcal{M}_\alpha$, is unique.

Here we consider a natural extension of the notion of vector equilibrium for the conducting plane: the *critical vector-valued measures*, defined as follows. For $t \in \mathbb{C}$ and $h \in C^2(\mathbb{C})$, denote by μ^t the pushforward measure of μ induced by the variation of the plane $z \mapsto h_t(z) = z + th(z)$, $z \in \mathbb{C}$.

Definition 3.2.1. We say that for $\alpha \in [0,1]$, $\vec{\mu} = (\mu_1, \mu_2, \mu_3)$ is an *α-critical measure* (or a saddle point of the energy $E(\cdot)$) if $\vec{\mu} \in \mathcal{M}_\alpha$, and

$$\lim_{t \to 0} \frac{E(\vec{\mu}^t) - E(\vec{\mu})}{t} = 0, \tag{3.7}$$

for every function $h \in C^2(\mathbb{C})$.

Sometimes, when the value of α is irrelevant or is clear from the context, we will simplify the terminology speaking simply about *critical measures*.

In order to formulate our first results we introduce some notation. Given a (scalar) non-negative Borel measure λ, compactly supported on the plane, we denote by

$$U^\lambda(z) := \int \log \frac{1}{|x - z|} d\lambda(x)$$

its logarithmic potential, which is harmonic in $\mathbb{C} \setminus \operatorname{supp} \lambda$ and superharmonic in $\mathbb{C}$. Additionally, the principal value of the Cauchy transform

$$C^\lambda(z) := \lim_{\epsilon \to 0+} \int_{|z-x|>\epsilon} \frac{1}{x - z}\, d\lambda(x) \tag{3.8}$$

is analytic in $\mathbb{C} \setminus \operatorname{supp} \lambda$, and

$$2\, \frac{\partial U^\lambda}{\partial z}(z) = C^\lambda(z), \quad z \in \mathbb{C} \setminus \operatorname{supp} \lambda, \tag{3.9}$$

with

$$\frac{\partial}{\partial z} = \frac{1}{2} \left(\frac{\partial}{\partial x} - i \frac{\partial}{\partial y} \right).$$

The interaction matrix A in (3.1) satisfies the following identities:

$$2A = B^T B = 3I_3 - bb^T, \quad B = \begin{pmatrix} 1 & 1 & 0 \\ -1 & 0 & -1 \\ 0 & -1 & 1 \end{pmatrix}, \quad b = \begin{pmatrix} 1 \\ -1 \\ -1 \end{pmatrix}, \tag{3.10}$$

where I_3 is the 3×3 identity matrix. For a vector of measures $\vec{\mu} = (\mu_1, \mu_2, \mu_3) \in \mathcal{M}_\alpha$, define the vector of functions $\vec{\xi} = (\xi_1, \xi_2, \xi_3)^T$ through the equality

$$\vec{\xi} = B \left(\frac{1}{3} \vec{\Phi}' + \vec{C} \right), \tag{3.11}$$

where $\vec{C} = (C^{\mu_1}, C^{\mu_2}, C^{\mu_3})^T$. Alternatively, the functions ξ_1, ξ_2, ξ_3 are given explicitly as

$$\begin{aligned}
\xi_1(z) &= \frac{\Phi_1'(z)}{3} + \frac{\Phi_2'(z)}{3} + C^{\mu_1}(z) + C^{\mu_2}(z), \\
\xi_2(z) &= -\frac{\Phi_1'(z)}{3} - \frac{\Phi_3'(z)}{3} - C^{\mu_1}(z) - C^{\mu_3}(z), \\
\xi_3(z) &= -\frac{\Phi_2'(z)}{3} + \frac{\Phi_3'(z)}{3} - C^{\mu_2}(z) + C^{\mu_3}(z).
\end{aligned} \tag{3.12}$$

It was proved in [104, Section 5] (see also [94]) that the Cauchy transform of a scalar critical measure is a solution of a quadratic equation m_2-a.e. on $\mathbb{C}$, which is a characterizing property of such measures. Our first result is a natural generalization of this property to the critical vector-valued measures:

Theorem 3.2.2. *Suppose that for $\alpha \in [0,1]$, $\vec{\mu} = (\mu_1, \mu_2, \mu_3) \in \mathcal{M}_\alpha$ is an α-critical measure in the sense of Definition 3.2.1. Then there exist a polynomial R and a rational function D with poles of order at most 2 such that the functions ξ_1, ξ_2, ξ_3 in (3.11) satisfy m_2-a.e. on $\mathbb{C}$ the algebraic equation*

$$\xi^3 - R(z)\xi + D(z) = 0. \tag{3.13}$$

The polynomial R is given by

$$R(z) = \frac{1}{9}\sum_{j,k=1}^{3} a_{j,k}\Phi_j'(z)\Phi_k'(z) - \sum_{j=1}^{3}\int \frac{\Phi_j'(x) - \Phi_j'(z)}{x - z}\, d\mu_j(x), \quad z \in \mathbb{C}. \tag{3.14}$$

Moreover, each of the measures μ_1, μ_2, μ_3 is supported on a finite union of analytic arcs, and they are absolutely continuous with respect to the arclength measure of their supports.

Each pole p of D, if exists, belongs to the support of at least two of the measures μ_1, μ_2, μ_3, and for each such a measure μ_k its density satisfies

$$\frac{d\mu_k}{|dz|}(z) = |z - p|^{-\nu}(c + o(1)), \qquad \text{as } z \to p \text{ along } \operatorname{supp}\mu_k, \tag{3.15}$$

for some nonzero constant c (which may depend on p and k), where 3ν is the order of p as a pole of D.

We also prove a converse to Theorem 3.2.2.

Theorem 3.2.3. *Suppose that for $\alpha \in [0,1]$, $\vec{\mu} = (\mu_1, \mu_2, \mu_3) \in \mathcal{M}_\alpha$ is such that the measures μ_1, μ_2, μ_3 are supported on a finite union of analytic arcs, and are absolutely continuous with respect to the arclength.*

If for some polynomials V_1, V_2, V_3 with

$$V_1'(z) + V_2'(z) + V_3'(z) = 0, \quad z \in \mathbb{C}, \tag{3.16}$$

the functions

$$\begin{aligned} \xi_1(z) &= V_1'(z) + C^{\mu_1}(z) + C^{\mu_2}(z), \quad z \in \mathbb{C} \setminus (\operatorname{supp}\mu_1 \cup \operatorname{supp}\mu_2), \\ \xi_2(z) &= V_2'(z) - C^{\mu_1}(z) - C^{\mu_3}(z), \quad z \in \mathbb{C} \setminus (\operatorname{supp}\mu_1 \cup \operatorname{supp}\mu_3), \\ \xi_3(z) &= V_3'(z) - C^{\mu_2}(z) + C^{\mu_3}(z), \quad z \in \mathbb{C} \setminus (\operatorname{supp}\mu_2 \cup \operatorname{supp}\mu_3). \end{aligned} \tag{3.17}$$

satisfy an algebraic equation of the form (3.13) for a polynomial R and a rational function D, then $\vec{\mu}$ is a critical measure for the energy functional (3.1)–(3.2) and the external fields defined by

$$\Phi_1(z) := V_1(z) - V_2(z), \quad \Phi_2(z) := V_1(z) - V_3(z), \quad \Phi_3(z) := V_3(z) - V_2(z). \tag{3.18}$$

Notice that with the definition (3.18) and the compatibility condition (3.16) the equalities (3.17) take the form (3.12).

A few remarks are in order.

Theorems 3.2.2 and 3.2.3 show that there is a clear connection between critical measures and cubic equations of a specific form. The fact that the equation is cubic has to do with the rank of the interaction matrix A in (3.1), which is 2: from the proofs it is natural to expect that critical measures (with ≥ 3 components) for an energy functional with an interaction matrix of rank r should be related to algebraic equations of degree $r+1$.

Furthermore, the compatibility condition (3.16) has to do with the structure of the interaction matrix (3.1), and finds its expression also in the absence of the ξ^2 term in the algebraic equation (3.13). Equation (3.16) and the structure of (3.17) should be seen as normalization conditions, ensuring that the underlying energy functional is of the precise form (3.2). Different choices for these identities would lead to a different interaction matrix in (3.2).

The notion of critical vector-valued measures can be extended to accommodate also log-rational external fields and domains with non-trivial boundaries ("hard edges", in the terminology of random matrix theory). The variations of the energy in these situations must allow for fixed points, see [104] for the scalar

case. Fixed points and singularities of the external fields will appear among possible points of blow-up of the density of the critical measures, and also as possible poles of the coefficients R and D in (3.13).

Finally, a reader familiar with the notion of the scalar equilibrium and scalar critical measures might be puzzled by the fact that we allow for a blow-up of the densities of such measures in the case of polynomial external fields. Indeed, in the scalar case all critical measures in such circumstances have uniformly bounded densities on the whole complex plane [94]. This is no longer the case in the vector case, as the following two examples illustrate: they show that the components of the critical vector-valued measures can create "artificial hard edges", obstructing each other and presenting unbounded densities when it was not expected, i.e. not created by the external field or by the boundaries of the conducting domain.

Example 3.2.4 (Repulsive or Angelesco interaction)**.** Consider the algebraic equation

$$\xi^3 - \xi - \frac{1}{z} = 0.$$

It has simple branch points at $\pm 3\sqrt{3}/2$, and a double branch point at $z = 0$, and three solutions ξ_j specified by their behavior as $z \to \infty$:

$$\xi_1(z) = -\frac{1}{z} + \mathcal{O}\left(\frac{1}{z^2}\right),$$

$$\xi_2(z) = 1 + \frac{1}{2z} + \mathcal{O}\left(\frac{1}{z^2}\right),$$

$$\xi_3(z) = -1 + \frac{1}{2z} + \mathcal{O}\left(\frac{1}{z^2}\right),$$

with $\xi_1(z) + \xi_2(z) + \xi_3(z) = 0$. A direct calculation shows that there are two measures, μ_1, living on $[-3\sqrt{3}/2, 0]$, and $\mu_2(x) = \mu_1(-x)$, such that $|\mu_1| = |\mu_2| = 1/2$, and

$$C^{\mu_1}(z) = 1 - \xi_2(z), \quad z \in \mathbb{C} \setminus [-3\sqrt{3}/2, 0],$$

$$C^{\mu_2}(z) = -1 - \xi_3(z), \quad z \in \mathbb{C} \setminus [0, 3\sqrt{3}/2].$$

Hence Theorem 3.2.3 shows that $\vec{\mu} = (\mu_1, \mu_2, 0) \in \mathcal{M}_{1/2}$ is a $1/2$-critical vector-valued measure, according to Definition 3.2.1, corresponding to the interaction matrix (3.1) and the polynomial external fields given by

$$\Phi_1(z) = -z = -\Phi_2(z), \quad \Phi_3(z) = -2z.$$

Notice however that the densities of both measures μ_j, $j = 1, 2$, blow up at $z = 0$ as $|z|^{-1/3}$.

It is worth mentioning that the same pair of measures (μ_1, μ_2) solves the Angelesco-type vector *equilibrium* problem of minimizing (3.2) under the assumptions

$$\operatorname{supp}\mu_1 \subset (-\infty, 0], \quad \operatorname{supp}\mu_2 \subset [0, +\infty), \quad |\mu_1| = |\mu_2| = \frac{1}{2}, \quad \mu_3 = 0.$$

This equilibrium problem does exhibit a hard edge at the origin, and the proof is based on the same type of energy variation, but leaving $z = 0$ as a fixed point. It should be pointed out that a similar problem (but on finite intervals) was analyzed first by Kalyagin in [86].

Example 3.2.5 (Attractive or Nikishin interaction)**.** Let us consider now the following cubic equation, which (up to a certain rescaling) has appeared already in [17]:

$$\xi^3 - \frac{1}{3}\xi - \frac{1}{z^2} + \frac{2}{27} = 0. \tag{3.19}$$

As in the Example 3.2.4, it has simple branch points at $\pm 3\sqrt{3}/2$, and a double branch point at $z = 0$.

Let $(81 - 12z^2)^{1/2}$ denote the branch of the square root in $\mathbb{C} \setminus [-3\sqrt{3}/2, 3\sqrt{3}/2]$ with positive boundary values on $(-3\sqrt{3}/2, 3\sqrt{3}/2)$ from the upper half plane, and let

$$\Upsilon(z) := \left(-1 + \frac{3(81 - 12z^2)^{1/2}}{2z^2}\right)^{1/3}$$

also have positive boundary values on the same interval from the upper half plane. Then Υ is holomorphic in $\mathbb{C} \setminus [-3\sqrt{3}/2, 3\sqrt{3}/2]$, and

$$\xi_1(z) = \frac{1}{3}\left(e^{\pi i/3}\Upsilon(z) + \frac{1}{e^{\pi i/3}\Upsilon(z)}\right) = \frac{1}{3} - \frac{1}{z} + \mathcal{O}\left(\frac{1}{z^2}\right) \text{ as } z \to \infty$$

is holomorphic in $\mathbb{C} \setminus [0, 3\sqrt{3}/2]$. Moreover, Cardano's formula shows that ξ_1 is a solution of (3.19); the other two solutions are given by

$$\xi_2(z) = \xi_1(-z) \quad \text{and} \quad \xi_3(z) = -\xi_1(z) - \xi_2(z).$$

For the selected branch of Υ, the $\xi_{1,\pm}$ boundary values of ξ_1 on $(0, 3\sqrt{3}/2)$ from the upper and lower half plane, respectively, satisfy

$$w(x) := \frac{1}{2\pi i}\left(\xi_{1,+} - \xi_{1,-}\right)(x) > 0, \quad x \in (0, 3\sqrt{3}/2).$$

Thus, $d\mu_2(x) := w(x)dx$ is a positive unit Borel measure on $[0, 3\sqrt{3}/2]$, and its Cauchy transform is

$$C^{\mu_2}(z) = \xi_1(z) - \frac{1}{3}, \quad z \in \mathbb{C} \setminus [0, 3\sqrt{3}/2)].$$

Analogously, $\mu_3(z) := \mu_2(-z)$ is a positive unit Borel measure on $[-3\sqrt{3}/2, 0]$, and

$$C^{\mu_3}(z) = -\xi_2(z) + \frac{1}{3}, \quad z \in \mathbb{C} \setminus [-3\sqrt{3}/2), 0].$$

Theorem 3.2.3 shows that $\vec{\mu} = (0, \mu_2/2, \mu_3/2) \in \mathcal{M}_{1/2}$ is a 1/2-critical vector-valued measure, according to Definition 3.2.1, corresponding to the interaction matrix (3.1) and the polynomial external fields given by

$$\Phi_1(z) = 0, \quad \Phi_2(z) = z = -\Phi_3(z).$$

Notice that now the densities of both measures μ_j, $j = 2, 3$, blow up at $z = 0$ as $|z|^{-2/3}$.

The next example illustrates that in Theorem 3.2.3 we cannot discard the degenerate cases when the coefficient D in (3.13) is identically zero, or other situations when (3.13) becomes reducible over the field of rational functions:

Example 3.2.6. If μ is a scalar critical measure for the external field $\operatorname{Re} V$, where V is a polynomial, then there exists a polynomial Q for which [94, 104]

$$\left(C^{\mu}(z) + \frac{1}{2}V'(z)\right)^2 = Q(z), \quad m_2\text{– a.e. } z \in \mathbb{C}. \tag{3.20}$$

If we set

$$\mu_1 = \mu_3 = 0, \quad \mu_2 = \mu, \quad \Phi_2 = V, \quad \Phi_1 = -\Phi_3 = \frac{V}{2},$$

then

$$E(\vec{\mu}^t) = I(\mu^t, \mu^t) + \int \operatorname{Re} V \, d\mu^t, \tag{3.21}$$

which shows that the vector-valued measure $\vec{\mu} = (\mu_1, \mu_2, \mu_3)$ is α-critical for $\alpha = 0$. The function ξ_2 in (3.12) becomes zero, whereas ξ_1, ξ_3 are analytic continuations of each other across $\operatorname{supp} \mu$. From the proof of Theorem 3.2.2 in Section 3.3 we conclude that the corresponding algebraic equation (3.74) is then reducible and has the form

$$\xi(\xi^2 - Q(z)) = 0, \tag{3.22}$$

where Q is the polynomial in (3.20).

Conversely, if the Cauchy transform of a probability measure μ satisfies an algebraic equation of the form (3.20) for some polynomials V and Q, then the construction just carried out combined with Theorem 3.2.3 gives us that μ is a scalar critical measure for the external field $\operatorname{Re} V$.

In very much the same spirit, if we now set

$$\mu_2 = \mu_3 = \mu, \quad \mu_1 = 0, \quad \Phi_1 = 2\Phi_2 = 2\Phi_3 = V, \tag{3.23}$$

then the energy of $\vec{\mu}^t$ is also given by (3.21), showing again that $\vec{\mu}^t$ is α-critical, now for $\alpha = 1$. The respective functions ξ_1, ξ_2 are analytic continuation of each other across $\operatorname{supp}\mu$, whereas $\xi_3 \equiv 0$ on $\mathbb{C}$, and the corresponding algebraic equation is reducible to the form (3.22).

The critical measure in (3.23) violates the assumption (3.6), but the conclusions of Theorem 3.2.2 still hold. However, condition (3.6) cannot be simply dropped, as the following example shows:

Example 3.2.7. Let Φ_1, Φ_2 be two arbitrary polynomials. For $\alpha = 1/2$ and the polynomial vector external field $\vec{\phi} = (\phi_1, \phi_2, \phi_1 - \phi_2)^T$, $\phi_j = \operatorname{Re}\Phi_j$, satisfying (3.3), consider the vector-valued measure $\vec{\mu} = (\mu_1, \mu_2, \mu_3)$, with

$$\mu_1 = \mu_2 = \frac{1}{2}\mu, \quad \mu_3 = 0.$$

The total energy of $\vec{\mu}$ is

$$E(\vec{\mu}) = \frac{3}{4}\left(I(\mu,\mu) + \frac{2}{3}\int(\phi_1 + \phi_2)d\mu\right).$$

Thus, if μ is a *scalar* probability critical measure in the external field

$$\phi = \frac{2}{3}(\phi_1 + \phi_2).$$

then (3.7) for $\vec{\mu}$ takes place. In other words, $\vec{\mu}$ is 1/2-critical in the external field $\vec{\phi}$. However, the statement of Theorem 3.2.2 does not hold: each of the corresponding functions ξ_1, ξ_2, ξ_3 in (3.12) satisfies an algebraic equation of degree 2, but if $\phi_1 \neq \phi_2$, these equations cannot be combined into a single algebraic equation of degree 3. To be more precise, calculations in the spirit of the proof of Theorem 3.2.2 in Section 3.3 below show that if Q is the polynomial in the right hand side of the equation (3.20) for μ (with $V' = (\Phi_1' + \Phi_2')/3$), then

$$\xi_1^2 = Q, \quad \xi_2 = -\frac{1}{2}(\xi_1 + \Phi_1' - \Phi_2'), \quad \xi_3 = -\frac{1}{2}(\xi_1 - \Phi_1' + \Phi_2').$$

Clearly, the only assumption not satisfied by the measure $\vec{\mu}$ in this example is (3.6).

A consequence of Theorem 3.2.2 is that the set

$$\Xi_\alpha = (\operatorname{supp}\mu_1 \cup \operatorname{supp}\mu_2 \cup \operatorname{supp}\mu_3) \setminus S_\alpha \tag{3.24}$$

is a finite union of disjoint analytic arcs, each of them contained in exactly one of the supports $\operatorname{supp}\mu_1, \operatorname{supp}\mu_2, \operatorname{supp}\mu_3$.

Any orientation of an arc $\Sigma \in \Xi_\alpha$ defines its left and right sides, as well as the left (or $+$) and right (or $-$) continuous boundary values of each ξ_j on Σ, that we denote by $\xi_{j\pm}$. In what follows, we use extensively (and without further warning) the notation mod 3, so that $\xi_0 = \xi_3$, $\xi_4 = \xi_1$ and so forth.

Since ξ_j's are the three branches of the cubic equation (3.13), assumption (3.6) implies that for any curve $\Sigma \subset \Xi_\alpha$ there exists an index $j \in \{1,2,3\}$ such that

$$\xi_{j+}(z) = \xi_{j-}(z), \quad \xi_{(j+1)\pm}(z) = \xi_{(j-1)\mp}(z), \quad z \in \Sigma. \tag{3.25}$$

Critical measures are intimately connected with vector equilibrium problems and the vector symmetry (S-property), as it is evidenced by the next theorem.

Theorem 3.2.8. *Given $j \in \{1,2,3\}$, let Σ be an open analytic arc in $\operatorname{supp}\mu_j \setminus S_\alpha$, not containing any branch point of (3.13). There exists a constant $l = l(\Sigma) \in \mathbb{R}$ for which both the Euler-Lagrange variational equation (*equilibrium condition*)*

$$\sum_{k=1}^{3} a_{j,k} U^{\mu_k}(z) + \frac{\phi_j(z)}{2} = l, \tag{3.26}$$

and the S-property

$$\frac{\partial}{\partial n_+}\left(\sum_{k=1}^{3} a_{jk} U^{\mu_k}(z) + \frac{\phi_j(z)}{2}\right) = \frac{\partial}{\partial n_-}\left(\sum_{k=1}^{3} a_{jk} U^{\mu_k}(z) + \frac{\phi_j(z)}{2}\right)$$

hold true for $z \in \Sigma$, where $n_\pm$ are the unit normal vectors to Σ, pointing in opposite directions.

If the constants $l(\Sigma)$ above are independent of the connected component Σ of $\operatorname{supp}\mu_j$, and this property holds for $j = 1,2,3$, then the critical vector-valued measure is the equilibrium measure for the vector of contours $(\operatorname{supp}\mu_1, \operatorname{supp}\mu_2, \operatorname{supp}\mu_3)$, see [22, Theorem 1.8].

The S-property is the natural generalization of the scalar S-property, taking into account that in those arcs the potentials of the measures μ_{j-1} and μ_{j+1} are harmonic.

Critical vector-valued measures $\vec{\mu}$ are also closely connected with trajectories of a quadratic differential on the Riemann surface $\mathcal{R} = \mathcal{R}_1 \cup \mathcal{R}_2 \cup \mathcal{R}_3$ of the algebraic equation (3.13), with

$$\begin{aligned} \mathcal{R}_1 &= \overline{\mathbb{C}} \setminus (\operatorname{supp}\mu_1 \cup \operatorname{supp}\mu_2), \\ \mathcal{R}_2 &= \overline{\mathbb{C}} \setminus (\operatorname{supp}\mu_1 \cup \operatorname{supp}\mu_3), \\ \mathcal{R}_3 &= \overline{\mathbb{C}} \setminus (\operatorname{supp}\mu_2 \cup \operatorname{supp}\mu_3). \end{aligned} \tag{3.27}$$

The sheets are connected across arcs in Ξ_α according to the following rule: if for $\Sigma \subset \Xi_\alpha$ the condition (3.25) holds, then we connect the sheets $\mathcal{R}_{j+1}$ and $\mathcal{R}_{j-1}$ through Σ crosswise, identifying the $\pm$-side of Σ on $\mathcal{R}_{j+1}$ with its $\mp$-side on $\mathcal{R}_{j-1}$.

As usual, we regard the solutions ξ_1, ξ_2, ξ_3 in (3.12) as branches of the same meromorphic function $\xi : \mathcal{R} \to \overline{\mathbb{C}}$, defined by (3.13), so that function ξ_j is the restriction of ξ to the sheet $\mathcal{R}_j$ of the Riemann surface $\mathcal{R}$.

Theorem 3.2.9. *Let*

$$Q(z) = \begin{cases} \xi_2(z) - \xi_3(z), & \text{on } \mathcal{R}_1, \\ \xi_1(z) - \xi_3(z), & \text{on } \mathcal{R}_2, \\ \xi_1(z) - \xi_2(z), & \text{on } \mathcal{R}_3. \end{cases}$$

Then Q^2 extends to a meromorphic function on $\mathcal{R}$. Moreover,

$$\varpi = -Q^2(z)dz^2 \tag{3.28}$$

is a meromorphic quadratic differential on $\mathcal{R}$ with possible poles only at the points at ∞. Finally, for $j = 1, 2, 3$, each arc of $\operatorname{supp}\mu_j$ is an arc of trajectory of ϖ.

As it was mentioned in Section 3.1, the connection between quadratic differentials and critical (or equilibrium) measures is not new. For scalar critical measures, the quadratic differential can be globally projected on the complex plane, so it is not necessary to consider it on a non-trivial Riemann surface. Even for vector-valued measures, this connection has been exploited before, see for instance [95,96], but only locally on the plane. To our knowledge, Theorem 3.2.9 is the first time this connection is stated on the whole surface $\mathcal{R}$, which provides a powerful tool for the construction of critical measures.

Remark 3.2.10. Assume that at $z = p$ we have (3.15) with $\nu \in \{1/3, 2/3\}$ (see Theorem 3.2.2). Then p is a triple branch point of $\mathcal{R}$, so that the local

coordinate for $\mathcal{R}$ at $z = p$ is $z = p + w^3$. Theorem 3.2.9 asserts that $\operatorname{supp}\mu_j$ lives on trajectories of the quadratic differential ϖ defined in (3.28), which in this local coordinate takes the form $\varpi = w^{4-6\nu}(\text{const} + o(1))dw^2$, const $\neq 0$.

If $\nu = 1/3$ (or equivalently if the polynomial D in (3.13) has a simple pole at p), then by the local structure of the trajectories, their canonical projection from $\mathcal{R}$ onto $\mathbb{C}$ consists of two analytic arcs intersecting at p perpendicularly (a "cross"). As Example 3.2.4 shows, this configuration can correspond to the interaction of two repulsive measures, and p can potentially belong to the intersection of the three components μ_j.

However, for $\nu = 2/3$ (which means that D has a double pole at p) the canonical projection of the trajectories from $\mathcal{R}$ onto $\mathbb{C}$ at p consists of a single analytic arc through this point. It implies, due to (3.6), that in this case p belongs to the intersection of at most two (and then, exactly two) components of $\vec{\mu}$; moreover, it will be the endpoint of an arc in each of the supports. A quick analysis of the cubic branching shows that these two positive measures cannot interact repulsively ("Angelesco" interaction), and hence, must attract each other ("Nikishin" interaction). Thus, Example 3.2.5 represents (at least, locally) the most generic case of the 2/3-blowup of the density of a critical vector-valued measure.

Remark 3.2.11. We should point out that (3.6) plays a substantial role for Theorem 3.2.2, but the conclusion of Theorem 3.2.3 still holds true even if we drop (3.6) completely. In this situation, if Σ is an analytic arc contained in the support of at least two of the measures μ_1, μ_2, μ_3, and $\mu_2 \neq \mu_3$ on Σ, then we can choose an orientation on Σ for which

$$\xi_{1+}(z) = \xi_{3-}(z), \quad \xi_{2+}(z) = \xi_{1-}(z), \quad \xi_{3+}(z) = \xi_{2-}(z), \quad z \in \Sigma. \tag{3.29}$$

The Euler-Lagrange equation (3.26) holds true for the three measures μ_1, μ_2, μ_3 (and possibly different constants l), and with respect to the orientation (3.29) the S-property now becomes

$$\frac{\partial}{\partial n_+}\left(\sum_{k=1}^{3} a_{jk}U^{\mu_k}(z) + \frac{\phi_j(z)}{2}\right) = (-1)^{j+1}\frac{\partial}{\partial n_-}\left(\sum_{k=1}^{3} a_{j+1,k}U^{\mu_k}(z) + \frac{\phi_{j+1}(z)}{2}\right).$$

The conclusion of Theorem 3.2.9 is also valid in this situation (with appropriate gluing of the sheets of $\mathcal{R}$ across the overlaps of the supports). However, we

do not know whether there are positive measures with non-trivial overlapping supports for which the functions (3.12) are the three solutions to the same cubic equation as in Theorem 3.2.3.

3.2.2 The cubic case

In order to illustrate the results stated above we analyze in depth the interesting and highly non-trivial cubic case, corresponding to the energy functional (3.1)–(3.2), with

$$\Phi_1(z) = \Phi_2(z) = z^3, \quad \Phi_3(z) = 0, \quad z \in \mathbb{C}, \tag{3.30}$$

so that the external fields are

$$\phi(z) = \phi_1(z) = \phi_2(z) = \operatorname{Re} z^3, \quad \phi_3(z) = 0, \quad z \in \mathbb{C}; \tag{3.31}$$

in what follows, we consider only the values of the parameter $\alpha \in [0, 1/2)$; see the discussion in the Remark 3.2.15 and also in the introduction to Section 3.4.

We build a continuous one-parameter family of critical vector-valued measures $\vec{\mu}$ by choosing in (3.13) the coefficients

$$R(z) = 3z^4 - 3z - c, \quad D(z) = -2z^6 + 3z^3 + cz^2 - 3\alpha(1-\alpha), \tag{3.32}$$

where $c = c(\alpha)$ is the real parameter given by

$$c = -\left(\frac{243}{64}(1 - 4\alpha(1-\alpha))^2\right)^{\frac{1}{3}}. \tag{3.33}$$

Theorem 3.2.12. *For $\alpha \in [0, 1/2)$, there exists a one-parameter family $\vec{\mu} = \vec{\mu}_\alpha \in \mathcal{M}_\alpha$ of critical measures for the potentials (3.31) for which the corresponding algebraic equation (3.13) has coefficients (3.32).*

Moreover, for any such a critical measure, if the associated algebraic equation (3.13) defines a Riemann surface of genus 0, then its coefficients are given by (3.32) for some choice of the cubic root in (3.33).

Remark 3.2.13. As it follows from the proof of this theorem in Section 3.4.1 (see also Remark 3.4.2), there are other choices for the coefficient c that yield critical vector-valued measures, but for which the associated Riemann surface is of genus 1. We do not consider this case here.

For the critical measure $\vec{\mu}_\alpha$ given by Theorem 3.2.12, the algebraic function ξ defined by (3.13) has two real branch points $a_1 < b_1$ and two nonreal branch points b_2, $a_2 = \overline{b_2}$ ($\operatorname{Im} b_2 > 0$). The support of the components μ_j of the critical measure $\vec{\mu}_\alpha = (\mu_1, \mu_2, \mu_3)$ can be easily described; we show that it exhibits a phase transition for a certain value of α:

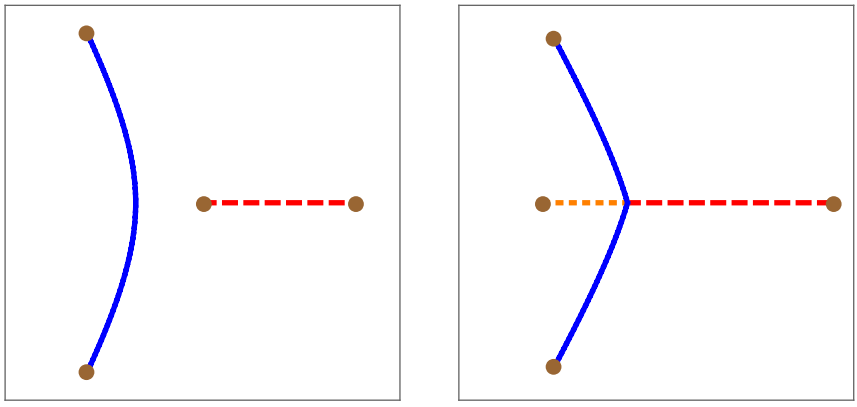

Figure 3.1: For $\tau \approx 0.126 < \tau_c$ (left panel) and for $\tau \approx 0.227 > \tau_c$ (right panel), numerical evaluation of the supports of the measures μ_1 (long dashed line), μ_2 (continuous line) and μ_3 (short dashed line - only on the right panel).

Theorem 3.2.14. *There exists a critical value $\alpha_c \in (0, 1/2)$, determined by*

$$\mathrm{Im} \int_{b_2}^{a_1} (\xi_1(s) - \xi_3(s)) ds = 0, \tag{3.34}$$

where ξ_1, ξ_3 are the functions in (3.12), such that

- *If $\alpha < \alpha_c$ then $\mu_3 = 0$, $\mathrm{supp}\, \mu_1 = [a_1, b_1]$, and $\mathrm{supp}\, \mu_2$ is an analytic arc, disjoint from $\mathrm{supp}\, \mu_1$ and connecting the branch points a_2, b_2.*
- *If $\alpha_c < \alpha < 1/2$ then none of the measures is zero, and there exists a value $a_* \in (a_1, b_1)$, determined by the condition*

$$\mathrm{Im} \int_{b_2}^{a_*} (\xi_1(s) - \xi_3(s)) ds = 0, \tag{3.35}$$

for which $\mathrm{supp}\, \mu_1 = [a_*, b_1]$, $\mathrm{supp}\, \mu_3 = [a_1, a_*]$ and $\mathrm{supp}\, \mu_* = \gamma_1 \cup \gamma_2$, where γ_1 is an analytic arc on the upper half plane connecting b_2 to a_*, and γ_2 is its complex conjugate arc.

We refer to Figure 3.1 for an actual numerical evaluation of the supports of the measures μ_1, μ_2, μ_3 in Theorem 3.2.14.

Remark 3.2.15. The restriction $\alpha < 1/2$ arises somewhat naturally in our analysis. For $\alpha = 1/2$, the algebraic equation (3.13) with coefficients (3.32)–(3.33) still defines a vector-valued measure $\vec{\mu}_{1/2}$ in the sense of Theorem 3.2.3, but the support of its third component is unbounded; hence, strictly speaking the measure $\vec{\mu}_{1/2}$ does not belong to $\mathcal{M}_{1/2}$.

In rough terms, Theorems 3.2.2 and 3.2.3 induce a map

$$\{\text{critical vector-valued measures}\} \mapsto \{\text{algebraic equations}\}$$

and Theorems 3.2.12 and 3.2.14 characterize this map completely for a subclass of algebraic equations and the cubic potential (3.30).

The existence of the critical measure $\vec{\mu}$ assured by Theorem 3.2.12 and the topological description of its support given by Theorem 3.2.14 follow after a careful analysis of the associated quadratic differential ϖ in (3.28). We describe the critical graph of ϖ for $\alpha = 0$ and indicate its subsets corresponding to the supports $\operatorname{supp}\mu_1, \operatorname{supp}\mu_2, \operatorname{supp}\mu_3$. In other words, we lift the supports to the associated Riemann surface, embedding them into the critical graph of ϖ. We then deform the parameter α in the interval $(0, 1/2)$, observing the dynamics of the critical graph and keeping track of the supports of the measures.

During this deformation procedure, the critical graph of ϖ displays several transitions, described in Sections 3.5.5.2–3.5.5.7, but only one of such transitions, governed by equation (3.34), has direct impact on the topology of $\operatorname{supp}\mu_1, \operatorname{supp}\mu_2, \operatorname{supp}\mu_3$.

It should be stressed that there are not many tools for such an analysis (we have summarized the basic facts about quadratic differentials in the Appendix A), and that it can be extremely complicated, even on the Riemann sphere. The situation becomes even more involved when we consider trajectories on a more general compact Riemann surface. We believe that the methodology we have developed is of independent interest, and can be applied in other situations as well.

3.2.3 Critical measures and max-min problems

The critical measure given by Theorem 3.2.12 is crucial in the study of multiple orthogonal polynomial $P_{n,m}(z) = z^N + \dots$ defined through

$$\begin{aligned} \int_{\Sigma_1} z^j P_{n,m}(z) e^{-Nz^3} dz = 0, \quad j = 0, \dots, n-1, \\ \int_{\Sigma_2} z^j P_{n,m}(z) e^{-Nz^3} dz = 0, \quad j = 0, \dots, m-1, \end{aligned} \tag{3.36}$$

where $N = n + m$ and Σ_1, Σ_2 are contours extending to ∞ with angles $-\frac{2\pi}{3}$, 0 and $-\frac{2\pi}{3}$, $\frac{2\pi}{3}$, respectively. It turns out that the asymptotic behavior of $P_{n,m}$ as $m, n \to \infty$ in such a way that $n/N \to \alpha \in (0, 1/2)$, is governed by this critical vector-valued measures $\vec{\mu} \in \mathcal{M}_\alpha$: under this regime, the sequence of

zero counting measures associated with $(P_{n,m})$ converges to the sum of the first two components of $\vec{\mu}$. The two extremal cases, $\alpha = 0$ and $\alpha = 1/2$, have been proved in [49] and [68], respectively, and the general case $\alpha \in (0, 1/2)$ will be addressed in a follow-up publication [106].

As we already mentioned, zeros of orthogonal polynomials on the real line are characterized as solutions to logarithmic equilibrium problems. The measure $\vec{\mu}$ given by Theorem 3.2.12, and hence the zeros of the multiple orthogonal polynomials (3.36), also admits a vector equilibrium problem characterization, as explained next.

Let $\mathcal{T}$ be the class of contours Σ extending to ∞ with angles $-\frac{2\pi}{3}, \frac{2\pi}{3}$ and intersecting the real axis exactly once, say at $a_* = a_*(\Sigma)$. Denote by $\mathcal{M}_\alpha(\Sigma)$ the subset of measures $\vec{\nu} = (\nu_1, \nu_2, \nu_3) \in \mathcal{M}_\alpha$ that further satisfy

$$\operatorname{supp} \nu_1 \subset [a_*, +\infty), \quad \operatorname{supp} \nu_2 \subset \Sigma, \quad \operatorname{supp} \nu_3 \subset (-\infty, a_*].$$

The *α-equilibrium measure* $\vec{\nu}_\alpha = \vec{\nu}_{\alpha,\Sigma}$ of $\Sigma \in \mathcal{T}$ (for the energy functional $E(\cdot)$ given in (3.2) with (3.30)–(3.31)) is the unique measure $\vec{\nu}_\alpha \in \mathcal{M}_\alpha(\Sigma)$ for which

$$E(\vec{\nu}_\alpha) = \inf_{\vec{\nu} \in \mathcal{M}_\alpha(\Sigma)} E(\nu) =: E_\alpha(\Sigma).$$

Theorem 3.2.16. *For $\alpha \in (0, 1/2)$, there exists a contour $\Gamma \in \mathcal{T}$ for which its α-equilibrium measure is the α-critical measure $\vec{\mu}$ given by Theorem 3.2.12.*

We conjecture that the contour Γ is characterized by the max-min property

$$E_\alpha(\Gamma) = \sup_{\Sigma \in \mathcal{T}} E_\alpha(\Sigma).$$

This characterization would be analogous to the max-min property for non-hermitian orthogonal polynomials [94,116,130,131]. Furthermore, an adaptation of the methods in [94,104] shows that the α-equilibrium measure of any contour solving this max-min problem is in fact an α-critical measure.

3.2.4 Structure of the rest of the chapter

Theorems 3.2.2, 3.2.8, 3.2.9, and a simplified version of Theorem 3.2.3 are proven in Section 3.3 (the complete proof of Theorem 3.2.3 is rather technical and thus deferred to Section 3.6). In Section 3.4.1 we derive the coefficients (3.32)–(3.33) and prove the second part of Theorem 3.2.12. Assuming the existence of certain short trajectories (fact proved later, in Section 3.5), we derive the first part of

Theorem 3.2.12 and Theorem 3.4.7 in Section 3.4.2, which yields Theorem 3.2.16. Section 3.5 is devoted to the analysis of the global structure of the quadratic differential (3.28) for the cubic potentials (3.30), which also provides a proof of Theorem 3.2.14 (or equivalently, of Theorem 3.5.4, where the structure of the support of the critical vector-valued measure is rephrased in the terminology of quadratic differentials). Finally, the final Section 3.7 contains the description of the numerical experiments and procedures used in this chapter.

3.3 Critical vector-valued measures

Critical measures were defined in the previous section in terms of the vanishing of the total energy (3.7). Here we use an alternative characterization, more convenient for calculations. When $\vec{\mu} = \mu$ is a scalar measure, the following Proposition 3.3.1 coincides with [104, Lemma 3.1]. The proof extends trivially to vectors of measures $\vec{\mu}$ and polynomial external fields as considered here. We skip the details.

Proposition 3.3.1. *For any vector of measures $\vec{\mu} \in \mathcal{M}_\alpha$, it is valid*

$$E(\vec{\mu}^t) = E(\vec{\mu}) + t \operatorname{Re} \mathcal{D}_h(\vec{\mu}) + \mathcal{O}(t^2), \quad t \to 0,$$

where

$$\mathcal{D}_h(\vec{\mu}) = -\sum_{j,k=1}^{3} a_{j,k} \iint \frac{h(x)-h(y)}{x-y} d\mu_j(x) d\mu_k(y) + \sum_{j=1}^{3} \int \Phi_j'(x) h(x) d\mu_j(x). \quad (3.37)$$

Although the definition of critical measures only requires to evaluate $\mathcal{D}_h(\vec{\mu})$ for test functions $h \in C^2(\mathbb{C})$, the quantity $\mathcal{D}_h(\vec{\mu})$ as defined above will be used for any function defined on $\operatorname{supp}\mu_1 \cup \operatorname{supp}\mu_2 \cup \operatorname{supp}\mu_3$, as long as the integrals on the right-hand side of (3.37) exist.

In particular, considering h and $-ih$, we get from Proposition 3.3.1

Corollary 3.3.2. *A measure $\vec{\mu} \in \mathcal{M}_\alpha$ is critical if, and only if,*

$$\mathcal{D}_h(\vec{\mu}) = 0,$$

for every function $h \in C^2(\mathbb{C})$.

The following lemma is inspired by [104], where a similar situation (but involving only one measure) was analyzed, and borrowed in the following form from [94, Lemma 3.5], where a simplified proof is given. The proof from [94] is easily extended to our situation by simply choosing $g \equiv 1$ therein and mimicking the arguments.

Lemma 3.3.3. *Suppose $\vec{\mu}$ is a critical vector-valued measure. If $z \in \mathbb{C}$ satisfies*

$$\int \frac{d\mu_j(x)}{|x-z|} < \infty, \quad j = 1, 2, 3, \tag{3.38}$$

then $\mathcal{D}_{h_z}(\vec{\mu}) = 0$ for the meromorphic function

$$h_z(x) = \frac{1}{x-z}, \quad x \in \mathbb{C}. \tag{3.39}$$

The next result is straightforward, and we skip its proof:

Lemma 3.3.4. *Let f be holomorphic in a punctured neighborhood of $p \in \mathbb{C}$. If $|f(z)|^r$ is m_2-locally integrable at p for some $r > 0$, then p is either a removable singularity or a pole of f of order $< 2/r$.*

For any finite Borel measure μ, it follows from Tonelli's theorem that the function

$$z \mapsto \int \frac{d\mu(x)}{|x-z|}$$

is locally m_2-integrable and in particular finite m_2-a.e.; that is, (3.38) is satisfied for m_2-a.e. $z \in \mathbb{C}$. Hence the Cauchy transform C^μ of the measure μ is finite m_2-a.e. In particular, the functions ξ_1, ξ_2, ξ_3 in (3.12) are finite m_2-a.e. and locally integrable with respect to m_2, so that

$$\sum_{j=1}^{3} \xi_j^2(z) \tag{3.40}$$

is well-defined m_2-a.e. and is analytic on open subsets of $\mathbb{C} \setminus (\operatorname{supp}\mu_1 \cup \operatorname{supp}\mu_2 \cup \operatorname{supp}\mu_3)$.

Recall the quantities R, $\mathcal{D}_h(\vec{\mu})$ and h_z defined in (3.14), (3.37) and (3.39), respectively. The next lemma is crucial for what comes later:

Lemma 3.3.5. *If $\vec{\mu} \in \mathcal{M}_\alpha$, then the functions ξ_j defined in (3.12) satisfy the identity*

$$\frac{1}{2}\left(\xi_1^2 + \xi_2^2 + \xi_3^2\right)(z) = R(z) + \mathcal{D}_{h_z}(\vec{\mu}) \quad m_2\text{-a.e.} \tag{3.41}$$

Moreover, the statements

(i) $\sum_{j=1}^{3} \xi_j^2(z)$ *is a polynomial,*

(ii) $\sum_{j=1}^{3} \xi_j^2(z) = 2R(z)$ m_2*-a.e.*

(iii) $\mathcal{D}_{h_z}(\vec{\mu}) = 0$ *for every* z *satisfying* (3.38)*,*

are equivalent.

Proof. For $h = h_z$,

$$\begin{aligned} \iint \frac{h_z(x) - h_z(y)}{x - y} d\mu_j(x) d\mu_k(y) &= -\iint \frac{1}{(x - z)(y - z)} d\mu_j(x) d\mu_k(y) \\ &= -C^{\mu_j}(z) C^{\mu_k}(z), \end{aligned} \tag{3.42}$$

and

$$\int h_z(x) \Phi_j'(x) d\mu_j(x) = \Phi_j'(z) C^{\mu_j}(z) - Q_j(z), \tag{3.43}$$

where

$$Q_j(z) = -\int \frac{\Phi_j'(x) - \Phi_j'(z)}{x - z} d\mu_j(x). \tag{3.44}$$

Notice that the integrand in the right-hand side of (3.44) is a polynomial both in x and in z, and thus (since μ_j is finite and compactly supported) it is also $d\mu_j(x)$-integrable for all z. Hence, Q_j is a bona fide polynomial. Additionally, (3.42) and (3.43) also show that $D_{h_z}(\vec{\mu})$ is finite whenever (3.38) holds true.

Using (3.42) and (3.43) in (3.37), we get that

$$\mathcal{D}_{h_z}(\vec{\mu}) = \sum_{j,k=1}^{3} a_{j,k} C^{\mu_j}(z) C^{\mu_k}(z) + \sum_{j=1}^{3} \Phi_j'(z) C^{\mu_j}(z) - \sum_{j=1}^{3} Q_j(z),$$

or equivalently,

$$\mathcal{D}_{h_z}(\vec{\mu}) = \vec{C}(z)^T A \vec{C}(z) + (\vec{\Phi}'(z))^T \vec{C}(z) - \sum_{j=1}^{3} Q_j(z), \tag{3.45}$$

with the previously used notation $\vec{C} = (C^{\mu_1}, C^{\mu_2}, C^{\mu_3})^T$ and $\vec{\Phi}' = (\Phi_1', \Phi_2', \Phi_3')^T$.

On the other hand, by (3.11) (and taking also into account both identities from (3.10)) we get

$$\frac{1}{2}\left(\xi_1^2 + \xi_2^2 + \xi_3^2\right) = \frac{1}{2}\vec{\xi}^T \vec{\xi} = \left(\frac{1}{3}\vec{\Phi}' + \vec{C}\right)^T A \left(\frac{1}{3}\vec{\Phi}' + \vec{C}\right)$$

$$= \frac{1}{9}(\vec{\Phi}')^T A\vec{\Phi}' + \vec{C}^T A\vec{C} + \frac{2}{3}\left(\vec{\Phi}'\right)^T A\vec{C}$$

$$= \frac{1}{9}(\vec{\Phi}')^T A\vec{\Phi}' + \vec{C}^T A\vec{C} + \frac{1}{3}\left(\vec{\Phi}'\right)^T \left(3I_3 - bb^T\right)\vec{C}$$

$$= \left\{\vec{C}^T A\vec{C} + \left(\vec{\Phi}'\right)^T \vec{C}\right\} + \frac{1}{9}(\vec{\Phi}')^T A\vec{\Phi}' - \frac{1}{3}\left(b^T\vec{\Phi}'\right)^T \left(b^T\vec{C}\right).$$

Notice that the compatibility condition (3.3) means precisely that $b^T\vec{\Phi}' = \vec{0}$, so that

$$\frac{1}{2}\left(\xi_1^2 + \xi_2^2 + \xi_3^2\right) = \frac{1}{9}(\vec{\Phi}')^T A\vec{\Phi}' + \left\{\vec{C}^T A\vec{C} + \left(\vec{\Phi}'\right)^T \vec{C}\right\},$$

and using (3.45) we can simplify the expression between brackets above to conclude that

$$\frac{1}{2}\left(\xi_1^2 + \xi_2^2 + \xi_3^2\right) = \mathcal{D}_{h_z}(\vec{\mu}) + \frac{1}{9}(\vec{\Phi}')^T A\vec{\Phi}' + \sum_{j=1}^{3} Q_j = \mathcal{D}_{h_z}(\vec{\mu}) + R,$$

where R was defined in (3.14). This identity is valid for values of z satisfying (3.38), which proves (3.41), as well as the equivalence of *(ii)* and *(iii)*.

Clearly, *(ii)* implies *(i)*. On the other hand, by (3.42),

$$\lim_{z\to\infty} \iint \frac{h_z(x) - h_z(y)}{x - y} d\mu_j(x) d\mu_k(y) = 0,$$

and since function $h_z(\cdot)$ converges uniformly to 0 as $z \to \infty$, by the Dominated Convergence Theorem we conclude that

$$\lim_{z\to\infty} \int h_z(x)\Phi_j'(x) d\mu_j(x) = 0.$$

Thus,

$$\lim_{z\to\infty} \mathcal{D}_{h_z}(\vec{\mu}) = 0. \tag{3.46}$$

Measures μ_1, μ_2 and μ_3 are compactly supported, so that (3.41) holds for all z sufficiently large, and with (3.46),

$$\lim_{z\to\infty} \left(\xi_1^2 + \xi_2^2 + \xi_3^2 - 2R\right)(z) = 0.$$

This establishes that *(i)* implies *(ii)*. □

Proof of Theorem 3.2.2. A combination of Corollary 3.3.2 and Lemma 3.3.5 shows that if $\vec{\mu}$ is critical, then the polynomial R in (3.14) is alternatively expressed as

$$R(z) = \frac{1}{2}(\xi_1(z)^2 + \xi_2(z)^2 + \xi_3(z)^2).$$

From the expressions (3.12) it follows that

$$\xi_1 + \xi_2 + \xi_3 = 0, \tag{3.47}$$

and as a consequence

$$R = \frac{1}{2}\left(\xi_1^2 + \xi_2^2 + \xi_3^2\right) = \xi_1^2 + \xi_1\xi_2 + \xi_2^2 = \xi_2^2 + \xi_2\xi_3 + \xi_3^2 = \xi_3^2 + \xi_3\xi_1 + \xi_1^2. \tag{3.48}$$

Multiplying the identities in (3.48) by appropriate factors $(\xi_j - \xi_k)$, it follows that

$$\xi_1(z)^3 - \xi_1(z)R(z) = \xi_2(z)^3 - \xi_2(z)R(z) = \xi_3(z)^3 - \xi_3(z)R(z). \tag{3.49}$$

Define

$$D(z) = -\xi_j(z)^3 + \xi_j(z)R(z). \tag{3.50}$$

Due to (3.49), D does not depend on the choice of $j \in \{1, 2, 3\}$. When we choose $j = 1$, we see that D is analytic on $\mathbb{C} \setminus (\operatorname{supp}\mu_1 \cup \operatorname{supp}\mu_2)$. Similarly, when we choose $j = 2, 3$, we see that D should be analytic on $\mathbb{C} \setminus (\operatorname{supp}\mu_1 \cup \operatorname{supp}\mu_3)$ and $\mathbb{C} \setminus (\operatorname{supp}\mu_2 \cup \operatorname{supp}\mu_3)$, respectively. Consequently, D can only have singularities at S_α, defined in (3.5), so from (3.6) these singularities are all isolated and in a finite number.

Moreover,

$$\begin{aligned} |D(z)|^{1/3} &\leq \left(|\xi_j(z)|^3 + |\xi_j(z)||R(z)|\right)^{1/3} \\ &\leq |\xi_j(z)| + |\xi_j(z)|^{1/3}|R(z)|^{1/3}, \end{aligned}$$

where for the last inequality we used $(x+y)^{1/3} \leq x^{1/3} + y^{1/3}$, which is valid for any non negative numbers x, y.

The function ξ_j is locally m_2-integrable (see the comments after Lemma 3.3.4). Hence the function D satisfies the conditions of Lemma 3.3.4 for $r = 1/3$ and any choice of $p \in S_\alpha$, so the points in S_α are not essential singularities of D. Moreover, from the behavior of the ξ_j's and R when $z \to \infty$, it follows that D has polynomial growth at ∞. We conclude that D is rational (although it could be identically zero).

In summary, we have shown that under the assumptions of Theorem 3.2.2, there exist a polynomial R, defined in (3.14), and a rational function D with possible poles in S_α, such that the functions ξ_1, ξ_2, ξ_3 satisfy

$$\xi_j(z)^3 - R(z)\xi_j(z) + D(z) = 0, \quad m_2 - \text{a.e.}$$

The fact that all the components μ_j are supported on a finite union of analytic arcs, and that they are absolutely continuous with respect to the arclength measure of their supports is then a direct consequence of [30, Theorem 2].

Let p be a pole of D. The functions ξ_1, ξ_2, ξ_3 satisfy the cubic equation (3.13), so their local behavior near p is of the form

$$\xi_j(z) = (z-p)^{-\nu_j}(\kappa_j + o(1)), \qquad \text{as } z \to p, \quad j = 1, 2, 3, \tag{3.51}$$

where $\nu_1, \nu_2, \nu_3 \in \mathbb{Q}$ and $\kappa_1, \kappa_2, \kappa_3$ are nonzero constants. Since p is a pole of D and R is a polynomial, from (3.50) we learn the ν_j's are all equal, say to ν, and 3ν should be equal to the order of p as a pole of D. Moreover, we further get that none of the functions ξ_1, ξ_2 and ξ_3 is analytic near p, so p has to belong to the support of at least two of the measures μ_1, μ_2 and μ_3. On the other hand, since ξ_j is a linear combination of polynomials and Cauchy transforms of finite measures, we must also have $\nu < 1$, so we conclude

$$\nu \in \left\{ \frac{1}{3}, \frac{2}{3} \right\}.$$

The behavior (3.15) then follows from Plemelj's formula and (3.51), concluding the proof. □

Remark 3.3.6. The fact that (scalar) finite measures, whose Cauchy transform satisfies a quadratic equation m_2-q.e., live on a finite set of analytic curves was established in [104] without any additional constraint on the measure (the proof was inspired by [23]). This was extended to an arbitrary algebraic equation in [30], but with a crucial assumption on the measure that its support has a zero plane Lebesgue measure (this assumption is embedded in the definition of the class $\mathcal{M}_\alpha$ in Section 3.2.1). Nevertheless, we believe that the assertion about the support is still true even if we drop this a priori restriction on $\vec{\mu}$.

Our next goal is to prove Theorem 3.2.3. In other words, for a vector of measures $\vec{\mu} \in \mathcal{M}_\alpha$ we assume that the components of $\vec{\mu}$ are supported on a finite union of analytic arcs, and the associated functions ξ_j in (3.17) satisfy an algebraic equation of the form (3.13) for some polynomial R and some rational function D. As we already pointed out after the statement of Theorem 3.2.3, these assumptions allow us to write $\vec{\xi}$ as in (3.12) for the vector of external fields $\vec{\Phi} = (\Phi_1, \Phi_2, \Phi_3)$ given by (3.18). In particular, it follows that ξ_j's satisfy (3.47) and consequently

$$R = \xi_1\xi_2 + \xi_1\xi_3 + \xi_2\xi_3 = \frac{1}{2}(\xi_1^2 + \xi_2^2 + \xi_3^2).$$

From Lemma 3.3.5 we get immediately the following result:

Corollary 3.3.7. *Under the assumptions of Theorem 3.2.3, the vector of measures $\vec{\mu}$ satisfies*

$$\mathcal{D}_{h_z}(\vec{\mu}) = 0$$

for $z \in \mathbb{C} \setminus (\operatorname{supp}\mu_1 \cup \operatorname{supp}\mu_2 \cup \operatorname{supp}\mu_3)$, where h_z is as in (3.39).

Hence, the proof of Theorem 3.2.3 is reduced basically to extending the conclusion of Corollary 3.3.7 to the whole class of functions $h \in C^2(\mathbb{C})$. Although this is relatively straightforward for h analytic in a neighborhood of the union of $\operatorname{supp}\mu_j$, it takes more effort beyond the analyticity due to the integrand $(h(x) - h(y))/(x - y)$ in (3.37). In this case we need to appeal to a "refined" version of the celebrated Mergelyan theorem that would allow for an approximation of a given sufficiently smooth function by a sequence of analytic ones, and in such a way that the sequence of derivatives is uniformly bounded. The complete proof we were able to find is rather technical, so for the sake of readability we postpone it to Section 3.6, and present here the arguments valid for the case when h vanishes in a neighborhood of the set of double poles of D (or when this set is empty). We formulate it as an independent proposition:

Proposition 3.3.8. *Let $\vec{\mu} \in \mathcal{M}_\alpha$ be a vector of measures satisfying the conditions of Theorem 3.2.3. Suppose that $h \in C^2(\mathbb{C})$ satisfies*

$$\operatorname{supp} h \cap \widehat{S}_\alpha = \emptyset,$$

where $\widehat{S}_\alpha$ is the set of double poles of D. Then $\mathcal{D}_h(\vec{\mu}) = 0$.

Proof. Recall that the union of the support of the components of $\vec{\mu}$ is a finite union of analytic arcs, whose points of intersection are denoted by S_α (see (3.5)), and the poles of the coefficient D in (3.13) belong to S_α, as it follows from the arguments in (3.51) *et seq.* Furthermore, if $p \in S_\alpha \setminus \widehat{S}_\alpha$, then

$$\frac{d\mu_j}{ds}(z) = \mathcal{O}\left(|z - p|^{-\nu}\right), \quad \text{as } z \to p, \quad j = 1, 2, 3, \tag{3.52}$$

for some $\nu \leq 1/3$ (possibly $\nu < 0$).

Given h as above, let us define

$$\vec{g}(z) = (g_1(z), g_2(z), g_3(z))^T \quad \text{and} \quad \vec{H}(z) = (H_1(z), H_2(z), H_3(z))^T,$$

with

$$g_j(z) = \int \frac{h(x)}{x - z} d\mu_j(x), \quad H_j(z) = \int \frac{h(x) - h(z)}{x - z} d\mu_j(x), \quad j = 1, 2, 3,$$

where as usual we understand $g_j(z)$ in terms of its principal value (as in (3.8)), for $z \in \operatorname{supp}\mu_j$. With this convention and recalling (3.24), on any open analytic

arc Σ from Ξ_α, not containing any branch point of (3.13), by the Sokhotsky–Plemelj's formula we have

$$g_{j\pm}(z) = \pm\pi i h(z)\mu_j'(z) + g_j(z), \quad z \in \Sigma, \tag{3.53}$$

where $\mu_j' = d\mu_j/ds$ is the Radon-Nikodym derivative of μ_j with respect to the line element on Σ, so that if $\Sigma \cap \operatorname{supp}\mu_j = \emptyset$, we have $\mu_j' = 0$.

Let Σ be an open analytic arc from $\operatorname{supp}\mu_1 \cup \operatorname{supp}\mu_2 \cup \operatorname{supp}\mu_3$, not containing any branch point of (3.13). Observe that the matrix B in (3.10) satisfies the identity $B^T = M_1 - M_2$, where

$$M_1 = \begin{pmatrix} 1 & 0 & 0 \\ 0 & 0 & -1 \\ 0 & -1 & 0 \end{pmatrix}, \quad M_2 = \begin{pmatrix} 0 & 1 & 0 \\ -1 & 0 & 0 \\ 0 & 0 & -1 \end{pmatrix}.$$

Since $\vec{H}$ is continuous across Σ, by (3.10),

$$2A\vec{H}(z) = (M_1 - M_2)\, B\vec{H}(z) = M_1 B\vec{H}_-(z) - M_2 B\vec{H}_+(z), \quad z \in \Sigma. \tag{3.54}$$

Furthermore, the identity

$$\vec{H}(z) = \vec{g}(z) - h(z)\vec{C}(z)$$

holds for all $z \in \mathbb{C} \setminus (\operatorname{supp}\mu_1 \cup \operatorname{supp}\mu_2 \cup \operatorname{supp}\mu_3)$, and we obtain that

$$2A\vec{H}(z) = (M_1 B\vec{g}_- - M_2 B\vec{g}_+)(z) - h(z)\left(M_1 B\vec{C}_- - M_2 B\vec{C}_+\right)(z). \tag{3.55}$$

Recall that Equation (3.16) allows us to rewrite (3.17) as (3.12) with the external fields given in (3.18). From (3.11),

$$B\vec{C} = \vec{\xi} - \frac{1}{3}B\vec{\Phi}',$$

so that

$$\begin{aligned} M_1 B\vec{C}_-(z) - M_2 B\vec{C}_+(z) &= \left(M_1(\vec{\xi}_- - \frac{1}{3}B\vec{\Phi}') - M_2(\vec{\xi}_+ - \frac{1}{3}B\vec{\Phi}')\right)(z) \\ &= M_1\vec{\xi}_-(z) - M_2\vec{\xi}_+(z) - \frac{2}{3}A\vec{\Phi}'(z). \end{aligned} \tag{3.56}$$

Because the functions ξ_j's satisfy a cubic equation, the boundary conditions (3.25) are valid and imply the equality

$$XM_1\vec{\xi}_-(z) = XM_2\vec{\xi}_+(z), \quad z \in \Sigma, \tag{3.57}$$

where

$$X = X(z) = \begin{pmatrix} \chi_1(z) & 0 & 0 \\ 0 & \chi_2(z) & 0 \\ 0 & 0 & \chi_3(z) \end{pmatrix},$$

and χ_j is the characteristic function of $\operatorname{supp}\mu_j$, $j = 1, 2, 3$. The matrix X is piecewise constant; for ease of notation we suppress its z-dependence in the following computations.

Since $\vec{\Phi}'$ is an eigenvector of A corresponding to the eigenvalue $3/2$ (see Section 3.2.1), we learn from (3.56) and (3.57)

$$XM_1B\vec{C}_-(z) - XM_2B\vec{C}_+(z) = -X\vec{\Phi}'(z), \quad z \in \Sigma. \tag{3.58}$$

An immediate consequence of this identity, combined with Sokhotsky–Plemelj's formula $\vec{C}_+ = 2\pi i\vec{\mu}' + \vec{C}_-$, is

$$\begin{aligned} &XM_1B\vec{C}_+(z) - XM_2B\vec{C}_-(z) \\ &\qquad = -X\vec{\Phi}'(z) + 2\pi iX(M_1 + M_2)B\vec{\mu}'(z), \quad z \in \Sigma, \end{aligned} \tag{3.59}$$

where, as usual, $\vec{\mu} = (\mu_1, \mu_2, \mu_3)^T$.

Multiplying (3.55) by X and using (3.58), we conclude that

$$2XA\vec{H}(z) = X\left(M_1B\vec{g}_- - M_2B\vec{g}_+\right)(z) + h(z)X\vec{\Phi}'(z), \quad z \in \Sigma.$$

Since

$$(M_1B)^T = -M_2B, \quad X^T = X,$$

we can write it equivalently as

$$2\left(\left(A\vec{H}\right)^T X\right)(z) = \left(\vec{g}_+^T M_1BX - \vec{g}_-^T M_2BX\right)(z) + h(z)\left(\vec{\Phi}'(z)\right)^T X, \quad z \in \Sigma. \tag{3.60}$$

Recall that $\Sigma \subset \Xi_\alpha$ was arbitrary, so we can integrate this formula along $\operatorname{supp}\mu_1 \cup \operatorname{supp}\mu_2 \cup \operatorname{supp}\mu_3$.

By (3.53), for $j \in \{1, 2, 3\}$ we get

$$\int g_{j\pm}(y)d\mu_k(y) = \pm\pi i \int h(y)\mu_j'(y)d\mu_k(y) + \int g_j(y)d\mu_k(y), \tag{3.61}$$

where we recall that if g_j is discontinuous across $\operatorname{supp}\mu_k$, we understand the second integral in the right hand side above in terms of its principal value. By

assumption, $\operatorname{supp} h$ does not contain double poles of the coefficient D, and we use the condition (3.52) to get the behavior

$$h(y)\mu_j'(y) = \mathcal{O}(|y-p|^{-\nu}), \qquad \text{as } y \to p \tag{3.62}$$

for some $\nu = \nu(p) \leq 1/3$ and any endpoint p of the support of μ_k. In particular, this implies that $h\mu_j'$ and g_j are μ_k-integrable, so the integrals in the right-hand side of (3.61) are convergent. Moreover, the behavior (3.62) allows us to interchange the order of integration for the second integral in the right-hand side of (3.61) (see [110, Equation (20), page 25]) in order to get

$$\int g_j(y)d\mu_k(y) = -\int h(y)C^{\mu_k}(y)d\mu_j(y).$$

Again by Sokhotsky–Plemelj's formula,

$$\int h(y)C^{\mu_k}(y)d\mu_j(y) = \mp\pi i \int h(y)\mu_k'(y)d\mu_j(x) + \int h(y)C_{\pm}^{\mu_k}(y)d\mu_j(y),$$

and using it in (3.61), we finally conclude that

$$\int g_{j\pm}(y)d\mu_k(y) = \pm 2\pi i \int \mu_j'(y)\mu_k'(y)h(y)dy - \int h(y)\mu_j'(y)C_{\pm}^{\mu_k}(y)dy.$$

A direct consequence of this formula is that for any 3×3 constant matrix $\mathcal{M}$,

$$\int \vec{g}_{\pm}^{T}\mathcal{M}d\vec{\mu} = \pm 2\pi i \int h(y)(\vec{\mu}'(y))^T\mathcal{M}\vec{\mu}'(y)dy - \int h(y)(\vec{\mu}'(y))^T\mathcal{M}\vec{C}_{\pm}(y)dy.$$

In particular, we have

$$\begin{aligned}
\int \left(\vec{g}_{+}^{T}M_1B - \vec{g}_{-}^{T}M_2B\right)d\vec{\mu} &= 2\pi i \int h(y)(\vec{\mu}'(y))^T\left(M_1+M_2\right)B\vec{\mu}'(y)dy \\
&\quad - \int h(y)(\vec{\mu}'(y))^T\left(M_1B\vec{C}_{+}(y) - M_2B\vec{C}_{-}(y)\right)dy \\
&= 2\pi i \int h(y)(\vec{\mu}'(y))^T X(y)\left(M_1+M_2\right)B\vec{\mu}'(y)dy \\
&\quad - \int h(y)(\vec{\mu}'(y))^T X(y)\left(M_1B\vec{C}_{+}(y) - M_2B\vec{C}_{-}(y)\right)dy \\
&= \int h(y)(\vec{\mu}'(y))^T\vec{\Phi}'(y)dy,
\end{aligned}$$

where we have used the trivial identity $\vec{\mu}'^T X = \vec{\mu}'^T$ for the last two equalities, and also (3.59) for the last equality. Thus, integrating (3.60) with respect to $d\vec{\mu}$, observing that $X d\vec{\mu} = d\vec{\mu}$ and applying this last identity, we arrive at

$$\int \left(A\vec{H}\right)^T (z) d\vec{\mu}(z) = \int h(z) \left(\vec{\Phi}'(z)\right)^T d\vec{\mu}(z),$$

which is a compact form of writing the condition $\mathcal{D}_h(\vec{\mu}) = 0$. □

Proof of Theorem 3.2.8. For a vector-valued function $\vec{f}$ we understand by

$$\int \vec{f}(z) dz$$

the term by term integration, and we denote by $\vec{\mu}' = (\mu_1', \mu_2', \mu_3')$ the vector whose components are the densities of μ_1, μ_2, μ_3 (with respect to the complex line element) along the arcs of Ξ_α. Because the supports of the components of $\vec{\mu}$ are made of analytic arcs, and $\vec{\mu}'$ has analytic components, we conclude that $\vec{U} = (U^{\mu_1}, U^{\mu_2}, U^{\mu_3})^T$ is continuous across the arcs of Ξ_α.

Integrating (3.11) and using (3.9) we get

$$\operatorname{Re} \int^z \vec{\xi}(y) dy = \operatorname{Re} \left(\frac{1}{3} B\vec{\Phi}(z)\right) + B\vec{U}(z) - \vec{d},$$

where $\vec{d}$ is a real constant vector which only depends on the connected component of $\mathbb{C} \setminus \operatorname{supp} \mu_1 \cup \operatorname{supp} \mu_2 \cup \operatorname{supp} \mu_3$.

Let Σ be an open analytic arc from Ξ_α, not containing any branch point of (3.13). Reasoning as for (3.54), we have

$$2A\vec{U}(z) = (M_1 - M_2)\, B\vec{U}(z) = M_1 B\vec{U}_-(z) - M_2 B\vec{U}_+(z), \quad z \in \Sigma.$$

Thus, for $z \in \Sigma$ and $\vec{d}_\pm$ the vector of constants for the component on the $\pm$-side of Σ,

$$\begin{aligned} 2A\vec{U}(z) &= M_1 \left(\operatorname{Re} \int^z \vec{\xi}_-(y) dy - \operatorname{Re} \left(\frac{1}{3} B\vec{\Phi}(z)\right) + \vec{d}_-\right) \\ &\quad - M_2 \left(\operatorname{Re} \int^z \vec{\xi}_+(y) dy - \operatorname{Re} \left(\frac{1}{3} B\vec{\Phi}(z)\right) + \vec{d}_+\right) \\ &= \operatorname{Re} \int^z \left(M_1 \vec{\xi}_-(y) - M_2 \vec{\xi}_+(y)\right) dy - \frac{2}{3} \operatorname{Re} A\vec{\Phi}(z) + M_1 \vec{d}_- - M_2 \vec{d}_+. \end{aligned}$$

Recalling that $A\vec{\Phi}' = (3/2)\vec{\Phi}'$ this last equation implies

$$2A\vec{U}(z) = \operatorname{Re}\int^z \Big(M_1\vec{\xi}_-(y) - M_2\vec{\xi}_+(y)\Big)\,dy - \operatorname{Re}\vec{\Phi}(z) + M_1\vec{d}_- - M_2\vec{d}_+, \quad z \in \Sigma.$$

If $\Sigma \subset \operatorname{supp}\mu_{4-j}$, then ξ_j continuous across Σ, and (3.25) tells us that the $(4-j)$-th entry of $M_1\xi_- - M_2\xi_+$ vanishes, which in turn yields (3.26) (with j replaced by $4-j$).

Note that due to (3.26) the S-property on $\operatorname{supp}\mu_{4-j}$ is equivalent to

$$\left[\frac{\partial}{\partial z}\left(\sum_{k=1}^{3} a_{4-j,k}U^{\mu_k} + \frac{\phi_{4-j}}{2}\right)\right]_+ = -\left[\frac{\partial}{\partial z}\left(\sum_{k=1}^{3} a_{4-j,k}U^{\mu_k} + \frac{\phi_{4-j}}{2}\right)\right]_-, \tag{3.63}$$

Equation (3.11) means that for $z \notin \Xi_\alpha$,

$$2\frac{\partial}{\partial z}\left(A\vec{U}(z) + \frac{1}{2}\vec{\phi}(z)\right) = A\vec{C}(z) + \frac{1}{2}\vec{\Phi}'(z) = \frac{1}{2}B^T\vec{\xi}(z),$$

where we also used the identity involving A and B in (3.10) and $A\vec{\Phi}' = (3/2)\vec{\Phi}'$. As before, the boundary conditions (3.25) imply that the entry $(4-j)$ of $B^T(\vec{\xi}_- + \vec{\xi}_+)$ vanishes, and the equation above then implies (3.63). □

Proof of Theorem 3.2.9. We denote the restriction of Q to the sheet $\mathcal{R}_j$ by Q_j. In cyclic notation mod 3, Q_j^2 can be expressed as

$$Q_j^2(z) = (\xi_{j-1}(z) - \xi_{j+1}(z))^2, \quad z \in \mathcal{R}_j, \quad j = 1, 2, 3.$$

Clearly Q_j^2 is meromorphic in $\overline{\mathbb{C}} \setminus (\operatorname{supp}\mu_1 \cup \operatorname{supp}\mu_2 \cup \operatorname{supp}\mu_3)$. We first prove that each Q_j^2 is meromorphic on the sheet $\mathcal{R}_j$. If $\Gamma \subset \operatorname{supp}\mu_3$, then due to (3.6) the function ξ_1 is analytic across Γ, hence

$$\xi_{2\pm}(s) = \xi_{3\mp}(s), \quad s \in \Gamma,$$

implying that

$$Q_{1+}^2(s) = (\xi_{2+}(s) - \xi_{3+}(s))^2 = (\xi_{3-}(s) - \xi_{2-}(s))^2 = Q_{1-}^2(s), \quad s \in \Gamma,$$

so Q_1^2 is analytic across Γ and, as a consequence, it follows that Q_1^2 is meromorphic on the whole sheet $\mathcal{R}_1$. Similarly we prove Q_j^2 is meromorphic on $\mathcal{R}_j$, $j = 2, 3$.

We now show that Q^2 is globally defined, that is, the function Q^2_{j+1} is the analytic continuation of Q^2_j from $\mathcal{R}_j$ to $\mathcal{R}_{j+1}$, $j = 1, 2, 3$.

Consider an arc $\Gamma \subset \Xi_\alpha$. For the construction of $\mathcal{R}$ we know that Γ connects exactly two sheets, which we assume to be $\mathcal{R}_1$ and $\mathcal{R}_2$, the remaining cases are analogous. Then $\Gamma \subset \operatorname{supp}\mu_1 \setminus (\operatorname{supp}\mu_2 \cup \operatorname{supp}\mu_3)$, so the function ξ_3 is analytic across Γ, hence $\xi_{1\pm} = \xi_{2\mp}$ on Γ and

$$Q^2_{1\pm}(s) = (\xi_{2\pm}(s) - \xi_3(s))^2 = (\xi_{1\mp}(s) - \xi_3(s))^2 = Q^2_{2\mp}(s),$$

so Q^2_2 is the analytic continuation of Q^2_1 to $\mathcal{R}_2$ across Γ.

Thus, Q^2 is meromorphic along any arc connecting the sheets. It is clear that the functions ξ_1, ξ_2, ξ_3, and hence Q^2, can only be unbounded at the points at ∞ and also at the poles of the coefficient D in (3.13). If p is such a pole, then the three functions ξ_1, ξ_2, ξ_3 are branched at p, and the local coordinate of $\mathcal{R}$ at $z = p$ is of the form $z = p + u^3$, $u \in \mathbb{C}$, and hence

$$dz^2 = 9u^4 du^2. \tag{3.64}$$

Since p is at most a double pole of D, it follows from the identities

$$D(z) = -\xi_j(z)^3 + R(z)\xi_j(z), \quad j = 1, 2, 3,$$

that the functions ξ_1, ξ_2, ξ_3 all blow up with the same order $\nu/3$, $\nu \in \{1, 2\}$, that is

$$\xi_j(z) = \frac{\kappa_j}{z^{\nu/3}}(1 + o(1)), \qquad \text{as } z \to p, \quad j = 1, 2, 3,$$

for some nonzero constants $\kappa_1, \kappa_2, \kappa_3$, so

$$Q^2(z) = \frac{c}{z^{2\nu/3}}(1 + o(1)) = \frac{c}{u^{2\nu}}(1 + o(1)), \qquad \text{as } z \to p,$$

for some constant c. Combining with (3.64), we get

$$-Q(z)^2 dz^2 = \tilde{c} u^{4-2\nu}(1 + o(1)) du^2,$$

for some constant $\tilde{c}$. Since $\nu \leq 2$, we get that ϖ has to remain bounded near p, and hence ϖ can only have poles at the points at ∞.

Let $\Sigma \subset \Xi_\alpha \cap \operatorname{supp}\mu_1$ be an open arc. Due to assumption (3.6), function ξ_3 is analytic across Σ. Now the definition of function ξ_1 in (3.12), the Sokhotsky-Plemelj's formula and (3.25) yield that for $s \in \Sigma$,

$$\begin{aligned} d\mu_1(s) = d\mu_1(s) + d\mu_2(s) &= \frac{1}{2\pi i}\left(\xi_{1+}(s) - \xi_{1-}(s)\right) ds \\ &= \frac{1}{2\pi i}\left(\xi_{1+}(s) - \xi_{2+}(s)\right) ds. \end{aligned}$$

Analogously, if $\Sigma \subset \Xi_\alpha \cap \operatorname{supp} \mu_2$, then ξ_2 is analytic across Σ, and for $s \in \Sigma$,

$$d\mu_2(s) = d\mu_1(s) + d\mu_2(s) = \frac{1}{2\pi i} \left(\xi_{1+}(s) - \xi_{1-}(s)\right) ds$$
$$= \frac{1}{2\pi i} \left(\xi_{1+}(s) - \xi_{3+}(s)\right) ds.$$

Finally, if $\Sigma \subset \Xi_\alpha \cap \operatorname{supp} \mu_3$, then ξ_1 is analytic across Σ, and using again the definition of ξ_3 in (3.12) and the Sokhotsky-Plemelj's formula, we get that for $s \in \Sigma$,

$$d\mu_3(s) = d\mu_3(s) - d\mu_1(s) = \frac{1}{2\pi i} \left(\xi_{3+}(s) - \xi_{3-}(s)\right) ds$$
$$= \frac{1}{2\pi i} \left(\xi_{3+}(s) - \xi_{2+}(s)\right) ds.$$

This shows that the measures μ_j must be supported on arcs of trajectories of ϖ. □

3.4 The cubic case

In the following two sections we deal with the cubic case, and describe a one-parameter family of critical vector-valued measures for the energy functional (3.1)–(3.2) and for the choice (3.30), so that the external fields are given by (3.31). Although the α-critical measures were defined for $\alpha \in [0, 1]$, here we restrict our attention to $\alpha \in [0, 1/2]$. As it will follow from our analysis below, as $\alpha \nearrow 1/2$, the support of the component μ_3 of the α-critical measure becomes unbounded. Furthermore, our original motivation was the asymptotic analysis of the multiple orthogonal polynomials (3.36), for which the case of $\alpha \in [1/2, 1]$ can be easily reduced to $\alpha \in [0, 1/2]$ by an appropriate rotation of the plane. Thus, the selection of this interval for α is natural in the present situation, although our method carries over without any special difficulty to the whole range of α.

3.4.1 The spectral curve

Recall that by Theorem 3.2.2 the shifted resolvents, defined in (3.12), of any critical vector-valued measure $\vec{\mu} = (\mu_1, \mu_2, \mu_3)$ satisfy the algebraic equation ("spectral curve") (3.13). As a first step, we deduce the expressions (3.32)–(3.33) for its coefficients.

For the potentials as in (3.31), the coefficient R in (3.14) reduces to

$$R(z) = 3z^4 - 3z - c, \tag{3.65}$$

where at this moment the constant c is given in the form

$$c = \int x(d\mu_1(x) + d\mu_2(x)).$$

Since $D(z) = -\xi_1^3 + R(z)\xi_1 = \xi_1\xi_2(\xi_1 + \xi_2)$, comparing the expansions of both expressions at ∞ and using (3.4), we further get that

$$C^{\mu_1}(z) + C^{\mu_2}(z) = -\frac{1}{z} - \frac{c}{3z^2} + \frac{1-\alpha(1-\alpha)}{3z^4} + \mathcal{O}\left(\frac{1}{z^5}\right), \quad z \to \infty,$$

and

$$D(z) = -2z^6 + 3z^3 + cz^2 - 3\tau, \quad \tau := \alpha(1-\alpha). \tag{3.66}$$

Observe that $\tau = \alpha(1-\alpha)$ is an equivalent parametrization that gives a bijection between the interval $\alpha \in [0, \frac{1}{2}]$ and $\tau \in [0, \frac{1}{4}]$. As it was mentioned in Section 3.2.3, the extremal cases, $\tau = 0$ and $\tau = \frac{1}{4}$, were studied in [49] and [68], respectively, in their connection to the multiple orthogonal polynomials (3.36), for the choices $n = 0$ and $n = m$, respectively, and the family of critical measures depending on $\alpha \in (0, 1/2)$ are also relevant to the asymptotic analysis of these polynomials for general n, m. From a different perspective, we are studying a continuous deformation of the critical measures, interpolating the extremal cases of $\tau = 0$ and $\tau = \frac{1}{4}$.

The discriminant of (3.13) with respect to the variable ξ is

$$\begin{aligned}\operatorname{Discr}(z) &= 4R^3(z) - 27D^2(z)\\ &= (81 - 324\tau)z^6 + 54cz^5 + 9c^2z^4 + 54(9\tau - 2)z^3\\ &\quad + 54c(3\tau - 2)z^2 - 36c^2z - 4c^3 - 243\tau^2.\end{aligned}$$

Since $\operatorname{Discr}(z)$ is a polynomial in z of degree 6, if the Riemann surface of (3.13) has genus 0 then, by the Riemann-Hurwitz theorem, $\operatorname{Discr}(z)$ must have a multiple root. In particular, the discriminant Discr_1 of $\operatorname{Discr}(z)$ must vanish. A cumbersome but straightforward calculation (that can be carried out with the aid of a symbolic algebra software such as Mathematica) shows that

$$\operatorname{Discr}_1 = a\tau p_1(c)p_2(c)^3$$

for a nonzero real constant a and

$$\begin{aligned} p_1(c) &= 64c^3 + 243(1-4\tau)^2, \\ p_2(c) &= c^6 - 486c^3\tau(1+\tau) + 2187\tau(3\tau-1)^3, \end{aligned} \tag{3.67}$$

so we expect c to be a root of either p_1 or p_2. For the case $\tau = \frac{1}{4}$ studied in [68], the algebraic equation (3.13) reduces to

$$\xi^3 - (3z^4 - 3z)\xi - 2z^6 + 3z^3 - \frac{3}{4} = 0,$$

showing that $c = 0$, which is a root of p_1. By continuity, we expect c to be a root of p_1 for every choice of $\tau \in (0, \frac{1}{4})$, concluding that

$$c^3 = -\frac{243}{64}(1-4\tau)^2,$$

or

$$c = -\left(\frac{243}{64}(1-4\tau)^2\right)^{\frac{1}{3}}. \tag{3.68}$$

which is the same as (3.33).

Obviously, c defined by (3.68) can take three possible values; for the rest of the chapter we choose c to be real (and thus, negative), so that the algebraic equation (3.13) is also real. It should be pointed out that a different choice of c would lead to an algebraic equation corresponding to another triplet of critical measures $\vec{\mu}$, that can be obtained from the original one by rotation by $\pm 2\pi/3$.

For the choice of c in (3.68), we can rewrite $\mathrm{Discr}(z)$ as

$$\mathrm{Discr}(z) = \frac{243}{256} q_1(z) q_2(z)^2, \tag{3.69}$$

where q_1, q_2 are given by

$$\begin{aligned} q_1(z) =& \frac{256}{3^{5/3}}(1-4\tau)^{1/3}z^4 + \frac{128}{9}z^3 + \frac{16}{3^{1/3}}(1-4\tau)^{2/3}z^2 \\ & - 3^{1/3}32(1-4\tau)^{1/3}z + 16(1-8\tau), \end{aligned} \tag{3.70}$$

$$q_2(z) = 3^{1/3}(1-4\tau)^{1/3}z - 1. \tag{3.71}$$

For $\tau < \frac{1}{4}$ the discriminant of q_1 is

$$\text{const} \times \tau(1-\tau)^2(27-100\tau)^3,$$

which never vanishes, and we conclude that q_1 has always four distinct roots. For the choice $\tau = \frac{1}{8}$, q_1 has two complex conjugate roots and two real roots, so this also holds for any τ.

The resultant of q_1 and q_2 is

$$\text{const} \times (1 - 12\tau)^4 (1 - 4\tau)^{2/3},$$

so that in the interval $0 < \tau < 1/4$, the polynomials q_1, q_2 share a root only when $\tau = 1/12$. It then follows that for $\tau \neq 1/12$ the roots of q_1 are branch points of multiplicity 2 of (3.13).

If the double zero b_* of Discr (that is, the zero of q_2) is a branch point of (3.13), then its multiplicity (as a branch point) has to be three. This means that the three solutions to (3.13) should coincide for $z = b_*$, so (3.13) has to share a root with its second ξ-derivative, and hence $\xi_j(b_*) = 0$, $j =, 1, 2, 3$. Plugging this back into (3.13) we see that $D(b_*) = 0$. But

$$D(b_*) = -\frac{(12\tau - 1)^3}{36(1 - 4\tau)^2},$$

so $D(b_*) = 0$ only for $\tau = 1/12$. Hence for $\tau \neq 1/12$ the point b_* is a regular point of (3.74), that is, the algebraic equation (3.13) is not branched at $z = b_*$. We already observed that the simple zeros of Discr are always branch points of multiplicity 2, so the Riemann-Hurwitz formula says that for $\tau \neq 1/12$ the associated algebraic equation has genus 0. Continuity with respect to τ assures that the genus cannot increase for $\tau = 1/12$, and hence the genus is also zero for this value.

The discussion above can be summarized in the following proposition:

Proposition 3.4.1. *The algebraic equation* (3.13) *with coefficients given by* (3.65), (3.66) *and* (3.68), *has four branch points (the zeros of the polynomial* q_1 *in* (3.70)*) and a double point (the zero of* q_2 *in* (3.71)*). Two of the branch points are real and the other two form a complex conjugate pair. For* $\tau \neq 1/12$ *all these points are distinct, while when* $\tau = 1/12$, *the double point and one of the real branch points of* (3.13) *coalesce. The associated Riemann surface has always genus* 0.

Although the choice of c in (3.68), as a root of p_1 instead of p_2, was mostly motivated by the construction of a continuous one-parameter family of critical measures $\vec{\mu}$ interpolating the extremal cases $\alpha = 0$ and $\alpha = 1/2$ studied in [49,68], formulas (3.65), (3.66) and (3.68) can also be explained in terms of the genus 0 ansatz stated in Theorem 3.2.12 that we prove next.

Proof of the second part of Theorem 3.2.12. We already noted that if the Riemann surface has genus 0, then c must be a root of at least one of the polynomials p_1 and p_2 in (3.67), and Proposition 3.4.1 assures that the roots of p_1 give rise to Riemann surfaces of genus 0. It thus suffices to show that zeros of p_2 give rise to a surface of genus 1.

Consider c to be a root of the polynomial p_2. As before, c can be assumed to be real, the remaining nonreal choices of c as a root of p_2 can be reduced to the real ones with suitable change of variables. Hence,

$$c = 3(9\tau + 9\tau^2 + \sqrt{3}(1 + 9\tau)\tau^{1/2})^{1/3} \tag{3.72}$$

or

$$c = 3(9\tau + 9\tau^2 - \sqrt{3}(1 + 9\tau)\tau^{1/2})^{1/3}. \tag{3.73}$$

Making the change of variables $\tau = u^6/3$, this can be written as

$$c = c(u) = 3u(u + 1)(u^2 - u + 1), \quad 0 < |u| \leq \left(\frac{3}{4}\right)^{1/6},$$

where $u > 0$ corresponds to the value of c in (3.72) and $u < 0$ corresponds to the choice of c in (3.73).

With this identification, the discriminant $\mathrm{Discr}(z)$ simplifies to

$$\mathrm{Discr}(z) = -27(u + z)^2 q(z),$$

where

$$q(z) = z^4(4u^6 - 3) - z^3(8u^7 + 6u^4) + z^2(9u^8 + 6u^5) \\ - z(10u^9 + 12u^6 - 4) + 5u^{10} + 12u^7 + 12u^4 + 4u.$$

The discriminant of q is given by

$$-6912(u^3 + 1)^6 \left(10u^3 + 9\right) \left(3u^6 + 1\right)^3 \neq 0 \quad \text{for } |u| \in (0, (3/4)^{1/6}).$$

Moreover,

$$q(-u) = 9u^4 \left(2u^3 + 1\right)^2,$$

hence $q(-u) \neq 0$, unless $u = -1/2^{1/3}$, which corresponds to $\tau = 1/12$. But for this latter choice, the corresponding value of c in (3.73) coincides with the value of c in (3.68), hence the coefficients R and D are given by (3.32).

Thus, let $u \neq -1/2^{1/3}$. Then $\mathrm{Discr}(z)$ has four simple roots, which have to be branch points of the equation, and one double root $z = -u$. At this double root, the algebraic equation (3.13) simply reduces to $\xi^3 = 0$, so its three solutions coincide. This is only compatible with the fact that $\mathrm{Discr}(z)$ has a double root at $z = -u$ if the three solutions are branched at this point. Hence we have four branch points of multiplicity 2 and one branch point of multiplicity 3, and the Riemann-Hurwitz formula gives us that the Riemann surface has genus 1. □

The first part of Theorem 3.2.12, claiming existence of α-critical measures, will be given by Corollary 3.4.6.

Remark 3.4.2. Obviously the quadratic differential (3.28) still makes sense if c is a root of p_2 as in the proof above. Numerical experiments performed to compute its critical graph indicate that the corresponding algebraic equation should also give rise to α-critical measures as in Theorem 3.2.3.

3.4.2 Equilibrium problem from the spectral curve

In this section, starting from the algebraic equation

$$\xi^3 - R(z)\xi + D(z) = 0, \tag{3.74}$$

where it is assumed that the coefficients R and D are given by (3.65)–(3.68), we find a vector of measures $\vec{\mu} = (\mu_1, \mu_2, \mu_3) \in \mathcal{M}_\alpha$ for which the respective ξ-functions in (3.12) satisfy (3.74), and consequently we prove Theorems 3.2.14 and 3.2.16. A central object for this analysis is the associated quadratic differential (3.28) (see also (3.76) *et seq.* below) and its critical graph, whose description is postponed to Section 3.5.

According to Proposition 3.4.1, the spectral curve (3.74) has two real branch points $a_1 < b_1$, two non real branch points $b_2 = \overline{a}_2$, with $\mathrm{Re}\, b_2 > 0$, and a double point

$$b_* = \frac{1}{(3(1-4\tau))^{1/3}} > 0 \quad \text{for } \tau \in (0, 1/4).$$

Since

$$q_1(b_*) = \frac{32(1-12\tau)^2}{9(1-4\tau)} \geq 0 \quad \text{for } \tau \in (0, 1/4),$$

we easily conclude that $b_* \geq b_1$ for $\tau \in (0, 1/4)$, with $b_* = b_1$ if and only if $\tau = 1/12$.

Moreover, equation (3.74) defines a three-sheeted Riemann surface $\mathcal{R}$ of genus 0 for every value of the parameter $\tau \in (0, 1/4)$. In contrast to (3.27), where the cuts for the Riemann surface are defined in terms of the supports of the critical

measures, here the cuts that split $\mathcal{R}$ into the sheets $\mathcal{R}_1, \mathcal{R}_2, \mathcal{R}_3$ can be chosen in a somewhat arbitrary way, as long as they connect the branch points. In our case, the sheet structure will be given by two cuts: the interval of the real line connecting the real branch points a_1, b_1 of $\mathcal{R}$ and a Jordan arc (to be defined precisely below) that joins the complex-conjugate branch points a_2, b_2. This arc intersects $\mathbb{R}$ in a unique point a_*, whose location depends on the value of the parameter τ. Namely, there is a certain critical value $\tau_c \approx 0.19$, defined later, such that $a_* \in (a_1, b_1)$ if and only if $\tau_c < \tau < 1/4$ (what we call the *supercritical regime*), see Figure 3.2. It is important to stress here that $\tau_c > 1/12$.

Obviously, it ultimately follows from our arguments that this cut structure coincides with (3.27) for the critical measure given by Theorem 3.2.14.

Using these cuts we define three oriented sets, Δ_1, Δ_2 and Δ_3 on $\mathbb{C}$. Namely, Δ_2 is always the projection onto $\mathbb{C}$ of the cut joining the complex-conjugate branch points a_2, b_2 and oriented from a_2 to b_2. In the subcritical regime ($0 < \tau < \tau_c$) we denote by $\Delta_1 = [a_1, b_1] \subset \mathbb{R}$ oriented from a_1 to b_1, and set $\Delta_3 = \emptyset$. In the supercritical regime ($\tau_c < \tau < 1/4$), $\Delta_1 = [a_*, b_1] \subset \mathbb{R}$ and $\Delta_3 = [a_1, a_*] \subset \mathbb{R}$, both with the natural orientation. The orientation induces the left (denoted by the subscript "+") and right (with the subscript "−") boundary values of functions defined on $\mathbb{C}$ or $\mathcal{R}$.

We define

$$\mathcal{R}_1 = \overline{\mathbb{C}} \setminus (\Delta_1 \cup \Delta_2), \quad \mathcal{R}_2 = \overline{\mathbb{C}} \setminus (\Delta_1 \cup \Delta_3), \quad \mathcal{R}_3 = \overline{\mathbb{C}} \setminus (\Delta_2 \cup \Delta_3),$$

and build the Riemann surface $\mathcal{R} = \mathcal{R}_1 \cup \mathcal{R}_2 \cup \mathcal{R}_3$, associated to the algebraic equation (3.74), connecting each pair of sheets $\mathcal{R}_j$ crosswise across the cuts as follows: Δ_1 connects $\mathcal{R}_1$ with $\mathcal{R}_2$, Δ_2 connects $\mathcal{R}_1$ with $\mathcal{R}_3$, and Δ_3 connects $\mathcal{R}_2$ with $\mathcal{R}_3$ (this last condition is clearly non-trivial only in the supercritical regime, when $\tau_c < \tau < 1/4$), see again Figure 3.2.

As we will see soon, the cuts $\Delta_1, \Delta_2, \Delta_3$ can be specified in such a way that we will be able to define positive measures living on Δ_j's, and the construction of the sheet structure will coincide with (3.27).

The three solutions ξ_1, ξ_2, ξ_3 of (3.74) are enumerated according to their asymptotic expansion at infinity:

$$\begin{aligned} \xi_1(z) &= 2z^2 - \frac{1}{z} + \mathcal{O}(z^{-2}), \\ \xi_2(z) &= -z^2 + \frac{\alpha}{z} + \mathcal{O}(z^{-2}), \\ \xi_3(z) &= -z^2 + \frac{1-\alpha}{z} + \mathcal{O}(z^{-2}). \end{aligned} \tag{3.75}$$

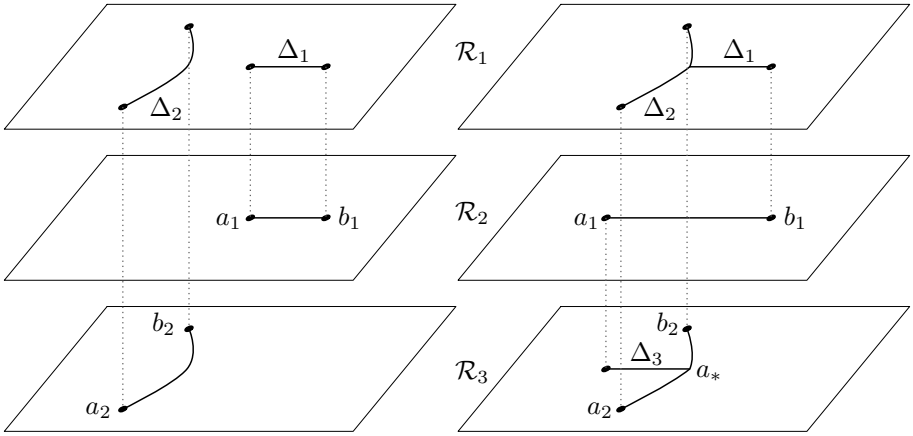

Figure 3.2: Sheet structure in the *precritical* $0 < \tau < \tau_c$ (left) and *supercritical* $\tau_c < \tau < 1/4$ (right) regimes.

As before, the functions ξ_1, ξ_2, ξ_3 are regarded as branches of the same meromorphic function $\xi : \mathcal{R} \to \overline{\mathbb{C}}$, defined by (3.74). As it is rigorously given by Proposition 3.5.3 below, the function ξ_j is the restriction of ξ to the sheet $\mathcal{R}_j$ of the Riemann surface $\mathcal{R}$.

Due to the explicit geometric description of the sets Δ_j's and sheets $\mathcal{R}_j$'s, it is straightforward to check that with

$$Q(z) = \begin{cases} \xi_2(z) - \xi_3(z), & \text{on } \mathcal{R}_1, \\ \xi_1(z) - \xi_3(z), & \text{on } \mathcal{R}_2, \\ \xi_1(z) - \xi_2(z), & \text{on } \mathcal{R}_3, \end{cases} \tag{3.76}$$

Q^2 extends as a single-valued meromorphic function on $\mathcal{R}$, and

$$\varpi = -Q^2(z)\, dz^2 \tag{3.77}$$

is the corresponding rational quadratic differential on $\mathcal{R}$. The details are also carried out in the general setting of Theorem 3.2.9 in its proof.

One of the main outcomes of the discussion in Section 3.5 (see Theorem 3.5.4 and Remark 3.5.11) is that we can choose the cut Δ_2 connecting a_2, b_2 to coincide with the trajectory along which

$$\operatorname{Re} \int^z (\xi_{1+}(s) - \xi_{3+}(s)) ds = \text{const}, \quad z \in \Delta_2. \tag{3.78}$$

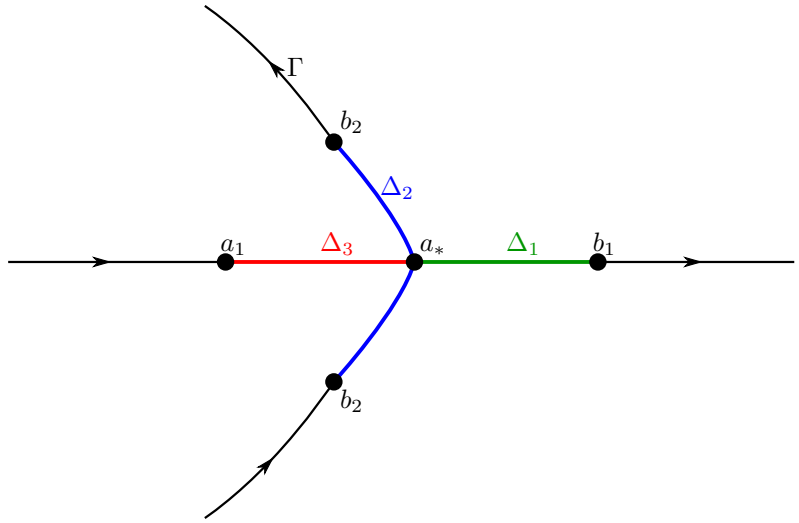

Figure 3.3: Pictorial representation of the sets Δ_1, Δ_2, Δ_3 and Γ in the supercritical regime.

Furthermore, Δ_2 can be extended to an analytic arc Γ from $e^{-\frac{2\pi i}{3}}\infty$ to $e^{\frac{2\pi i}{3}}\infty$ in such a way that

$$\operatorname{Im} \int^z (\xi_{1+}(s) - \xi_{3+}(s))ds = \text{const}, \quad z \in \Gamma \setminus \Delta_2, \tag{3.79}$$

and

$$\xi_1(z) - \xi_3(z) \neq 0, \quad z \in \Gamma \setminus \{a_2, b_2\}, \tag{3.80}$$

see Figure 3.3.

Further,

$$\operatorname{Re} \int^z (\xi_{1+}(s) - \xi_{2+}(s))ds = \text{const}, \quad z \in \Delta_1, \tag{3.81}$$

and

$$\xi_{1+}(z) - \xi_{2+}(z) \neq 0, \quad z \in \Delta_1 \setminus \{a_1, b_1\}, \tag{3.82}$$

and in the supercritical regime $\tau_c < \tau < 1/4$, also

$$\operatorname{Re} \int^z (\xi_{2+}(s) - \xi_{3+}(s))ds = \text{const}, \quad z \in \Delta_3, \tag{3.83}$$

and

$$\xi_{2+}(s) - \xi_{3+}(s) \neq 0, \quad z \in \Delta_3 \setminus \{a_1, a_*\},$$

for which we refer to Proposition 3.5.3.

Finally, it also holds

$$\begin{aligned} &\xi_1(z) - \xi_2(z) > 0, \quad z > b_1, \\ &\xi_2(z) - \xi_3(z) > 0, \quad z < \min\{a_1, a_*\}, \end{aligned} \tag{3.84}$$

and in the precritical regime $\tau < \tau_c$,

$$\xi_1(z) - \xi_2(z) < 0, \quad z \in (a_*, a_1), \tag{3.85}$$

for which again we refer to Proposition 3.5.3.

We define measures μ_1, μ_2, μ_3 on Δ_1, Δ_2, Δ_3, respectively, through the formulas

$$\begin{aligned} d\mu_1(s) &= \frac{1}{2\pi i}(\xi_{1+}(s) - \xi_{2+}(s))ds, \quad s \in \Delta_1, \\ d\mu_2(s) &= \frac{1}{2\pi i}(\xi_{1+}(s) - \xi_{3+}(s))ds, \quad s \in \Delta_2, \end{aligned} \tag{3.86}$$

and

$$d\mu_3(s) = \begin{cases} 0, & \text{if } 0 < \tau < \tau_c, \\ \dfrac{1}{2\pi i}(\xi_{3+}(s) - \xi_{2+}(s))ds, \quad s \in \Delta_3, & \text{if } \tau_c < \tau < 1/4, \end{cases}$$

where ds denotes the complex line element on the respective arc. Due to their construction, the supports of the measures μ_1, μ_2, μ_3 satisfy the claims of Theorem 3.2.14 (see also Theorem 3.5.4).

Remark 3.4.3. Using the definition in (3.76) we can describe formulas (3.86) saying that we build μ_j from the values of Q on the sheet $\mathcal{R}_{4-j}$, $j = 1, 2, 3$.

Proposition 3.4.4. *Expressions* (3.86) *define positive measures* μ_1, μ_2, μ_3.

Proof. We prove the statement for the supercritical regime $\tau_c < \tau < 1/4$; the precritical regime, somewhat simpler, can be analyzed similarly.

From (3.78) and (3.81) it follows that the measures μ_1, μ_2, μ_3 are real. Moreover, the densities of μ_1, μ_3 with respect to the complex line element ds are continuous and non vanishing in the interior of Δ_1, Δ_3, so the respective measures do not change sign. As for μ_2, its density with respect to ds is continuous when restricted to either the upper or the lower half plane, but not across $\mathbb{R}$.

We start now with μ_1. For $x \in \Delta_1$, we can write

$$\mu_1([x, b_1]) = -\frac{1}{2\pi i}\psi_{1+}(x), \tag{3.87}$$

where

$$\psi_1(z) = \int_{b_1}^{z} (\xi_1(s) - \xi_2(s))ds, \quad z \in \mathbb{C} \setminus ((-\infty, b_1] \cup \Delta_2)\,.$$

By the asymptotic expansion (3.75), we have that

$$\psi_1(z) = z^3 + \mathcal{O}(z), \quad z \to \infty,$$

and since $\xi_1 - \xi_2$ does not change sign on $[b_1, +\infty)$, see (3.82), we conclude that

$$\psi_1(x) > 0, \quad x > b_1.$$

The function ψ_1 vanishes at the point $z = b_1$ with order $3/2$. Since we already know that ψ_1 should map Δ_1 to $i\mathbb{R}$, from its order of vanishing we further get that the imaginary part of $\psi_{1+}(x)$ is negative when $x \in \Delta_1$ is sufficiently close to the endpoint b_1. From (3.82), we conclude

$$\psi_{1+}(x) \in i\mathbb{R}_-, \quad x \in \Delta_1.$$

By (3.87), this establishes the positivity of μ_1.

Furthermore, the density $d\mu_3/ds$ is the analytic continuation of $d\mu_1/ds$ across Δ_2, hence $d\mu_3$ is also positive.

Finally, in order to establish the sign of μ_2, consider first $x \in \Delta_2 \cap \mathbb{C}_-$, $\mathbb{C}_- = \{z \in \mathbb{C} : \operatorname{Im}(z) < 0\}$. Denote by $\Delta_2[a_2, x]$ the subarc of Δ_2 from a_2 to x. Then

$$\mu_2(\Delta_2[a_2, x]) = \frac{1}{2\pi i}\psi_{2+}(x), \tag{3.88}$$

where

$$\psi_2(z) = \int_{a_2}^{z} (\xi_{1+}(s) - \xi_{3+}(s))ds, \quad z \in \mathbb{C} \setminus ((-\infty, b_1] \cup \Delta_2).$$

From (3.79) and (3.80) we learn that $\operatorname{Re}(\psi_2)$ is monotone on $\Gamma(e^{-\frac{3\pi i}{2}}\infty, a_2)$. The asymptotics

$$\psi_2(z) = z^3 + \mathcal{O}(z), \quad z \to \infty,$$

shows that

$$\operatorname{Re}\psi_2(z) \to +\infty, \quad z \to \infty \text{ along } \Gamma,$$

hence $\operatorname{Re}(\psi_2)$ is strictly decreasing on $\Gamma(^{-\frac{3\pi i}{2}}\infty, a_2)$, $\psi_2(a_2) = 0$. Since ψ_2 vanishes with order $3/2$ on a_2, we conclude that

$$\psi_{2+}(x) \in i\mathbb{R}_+, \quad x \in \Delta_2 \cap \mathbb{C}_-.$$

Thus, by (3.88) measure μ_2 is positive on $\Delta_2 \cap \mathbb{C}_-$.

The positivity of μ_2 on $\Delta_2 \cap \mathbb{C}_+$ can be obtained by similar arguments or using the real symmetry of the density of μ_2; we leave the details to the interested reader.

The proposition is proved. □

Our next goal is an expression for the Cauchy transforms of combinations of measures μ_1, μ_2, μ_3:

Proposition 3.4.5. *The Cauchy transform of the measures μ_1, μ_2, μ_3 defined in (3.86) are related to the ξ-functions in (3.75) through*

$$C^{\mu_1}(z) + C^{\mu_2}(z) + 2z^2 = \xi_1(z), \quad z \in \mathbb{C} \setminus (\Delta_1 \cup \Delta_2), \tag{3.89}$$

$$C^{\mu_1}(z) + C^{\mu_3}(z) + z^2 = -\xi_2(z), \quad z \in \mathbb{C} \setminus (\Delta_1 \cup \Delta_3), \tag{3.90}$$

$$C^{\mu_2}(z) - C^{\mu_3}(z) + z^2 = -\xi_3(z), \quad z \in \mathbb{C} \setminus (\Delta_2 \cup \Delta_3). \tag{3.91}$$

In particular, the total masses of the measures μ_1, μ_2, μ_3 satisfy (3.4), namely

$$|\mu_1| + |\mu_2| = 1, \quad |\mu_1| + |\mu_3| = \alpha, \quad |\mu_2| - |\mu_3| = 1 - \alpha.$$

Proof. This is a straightforward consequence of residues calculations. For instance,

$$\begin{aligned} C^{\mu_1}(z) + C^{\mu_2}(z) &= \frac{1}{2\pi i} \int_{\Delta_1} \frac{\xi_{1+}(s) - \xi_{1-}(s)}{s - z} ds + \frac{1}{2\pi i} \int_{\Delta_2} \frac{\xi_{1+}(s) - \xi_{1-}(s)}{s - z} ds \\ &= -\frac{1}{2\pi i} \int_C \frac{\xi_1(s)}{s - z} ds \\ &= \operatorname{Res}\left(\frac{\xi_1(s)}{s - z}, s = z\right) + \operatorname{Res}\left(\frac{\xi_1(s)}{s - z}, s = \infty\right), \end{aligned}$$

where C is a positively oriented closed contour which encircles $\Delta_1 \cup \Delta_2$ and does not encircle z. Using the expansion (3.75), we compute the residue at infinity and thus conclude

$$C^{\mu_1}(z) + C^{\mu_2}(z) = -2z^2 + \xi_1(z).$$

Analogously,

$$\begin{aligned} C^{\mu_1}(z) + C^{\mu_3}(z) &= -\operatorname{Res}\left(\frac{\xi_2(s)}{s - z}, s = z\right) - \operatorname{Res}\left(\frac{\xi_2(s)}{s - z}, s = \infty\right) \\ &= -z^2 - \xi_2(z), \end{aligned}$$

and taking the difference of these last two equations,

$$C^{\mu_2}(z) - C^{\mu_3}(z) = -z^2 + \xi_1(z) + \xi_2(z) = -z^2 - \xi_3(z).$$

Finally, (3.4) is a direct consequence of the asymptotic expansion (3.75). □

A combination of Proposition 3.4.5 with Theorem 3.2.3 yields the first part of Theorem 3.2.12, namely

Corollary 3.4.6. *The vector of measures* $\vec{\mu} = (\mu_1, \mu_2, \mu_3) \in \mathcal{M}_\alpha$ *defined through* (3.86) *is* α*-critical for the potentials* (3.31).

Recalling (3.9), the potential U^μ of a compactly supported signed measure μ for which $\mathbb{C} \setminus \operatorname{supp} \mu$ is connected is the real part of a primitive of C^μ, that is

$$U^\mu(z) = \operatorname{Re} \int^z C^\mu(s)ds + c, \quad z \in \mathbb{C} \setminus \operatorname{supp} \mu, \tag{3.92}$$

where the constant is chosen so as to have

$$\lim_{z\to\infty} \left(\operatorname{Re} \int^z C^\mu(s)ds + c \right) = 0.$$

Let us apply this to the measures μ_1, μ_2, μ_3 given in (3.86). From (3.89),

$$\int_{b_1}^z (C^{\mu_1}(s) + C^{\mu_2}(s))ds + \frac{2}{3}z^3 - \frac{2}{3}b_1^3 = \int_{b_1}^z \xi_1(s)ds, \quad z \in \mathbb{C} \setminus (\Delta_1 \cup \Delta_2),$$

and from (3.90),

$$\int_{b_1}^z (C^{\mu_1}(s) + C^{\mu_3}(s))ds + \frac{1}{3}z^3 - \frac{1}{3}b_1^3 = -\int_{b_1}^z \xi_2(s)ds, \quad z \in \mathbb{C} \setminus (\Delta_1 \cup \Delta_3).$$

Summarizing,

$$\int_{b_1}^z (2C^{\mu_1}(s) + C^{\mu_2}(s) + C^{\mu_3}(s))ds + z^3 - b_1^3$$
$$= \int_{b_1}^z (\xi_1(s) - \xi_2(s))ds, \quad z \in \mathbb{C} \setminus (\Delta_1 \cup \Delta_2 \cup \Delta_3),$$

where we must use the same paths of integration in the left and in the right hand sides. By (3.92) we then conclude

$$2U^{\mu_1}(z)+U^{\mu_2}(z)+U^{\mu_3}(z)+\phi(z)-l_1 \\ = \operatorname{Re}\int_{b_1}^{z}(\xi_1(s)-\xi_2(s))ds, \quad z\in\mathbb{C}\setminus\Delta, \tag{3.93}$$

for some constant l_1, the external field ϕ given in (3.31) and $\Delta=\Delta_1\cup\Delta_2\cup\Delta_3$. Since the ξ_j's have purely imaginary periods, the right hand side above is well defined regardless the path chosen.

In a completely analogous way, for $z\in\mathbb{C}\setminus\Delta$ we get

$$\begin{aligned} 2U^{\mu_2}(z)+U^{\mu_1}(z)-U^{\mu_3}(z)+\phi(z)-l_2 &= \operatorname{Re}\int_{a_2}^{z}(\xi_1(s)-\xi_3(s))ds,\\ 2U^{\mu_3}(z)+U^{\mu_1}(z)-U^{\mu_2}(z)-l_3 &= \operatorname{Re}\int_{\min\{a_1,a_*\}}^{z}(\xi_3(s)-\xi_2(s))ds. \end{aligned} \tag{3.94}$$

Combining (3.93) with (3.81), we conclude that

$$2U^{\mu_1}(z)+U^{\mu_2}(z)+U^{\mu_3}(z)+\phi(z)-l_1=0, \quad z\in\Delta_1. \tag{3.95}$$

Moreover, from the first equation in (3.84) we also get

$$2U^{\mu_1}(z)+U^{\mu_2}(z)+U^{\mu_3}(z)+\phi(z)-l_1>0, \quad z\in(b_1,+\infty). \tag{3.96}$$

Furthermore, in the precritical case $\tau<\tau_c$ and $z\in[a_*,a_1)$,

$$\begin{aligned} 2U^{\mu_1}(z)+U^{\mu_2}(z)+U^{\mu_3}(z)+\phi(z)-l_1 &= \operatorname{Re}\int_{b_1}^{a_1}(\xi_{1+}(s)-\xi_{2+}(s))ds\\ &\quad+\operatorname{Re}\int_{a_1}^{z}(\xi_1(s)-\xi_2(s))ds\\ &= -\int_{z}^{a_1}(\xi_1(s)-\xi_2(s))ds>0, \end{aligned} \tag{3.97}$$

where for the second equality we used (3.81) and for the final inequality we used (3.85).

Analogously,

$$2U^{\mu_2}(z) + U^{\mu_1}(z) - U^{\mu_3}(z) + \phi(z) - l_2 = 0, \quad z \in \Delta_2, \tag{3.98}$$

$$2U^{\mu_3}(z) + U^{\mu_1}(z) - U^{\mu_2}(z) - \tilde{l}_3 = 0, \quad z \in \Delta_3, \tag{3.99}$$

$$2U^{\mu_3}(z) + U^{\mu_1}(z) - U^{\mu_2}(z) - \tilde{l}_3 > 0, \quad z < \min\{a_*, a_1\}, \tag{3.100}$$

$$2U^{\mu_3}(a_*) + U^{\mu_1}(a_*) - U^{\mu_2}(a_*) = \tilde{l}_3. \tag{3.101}$$

If $\tau \geq \tau_c$, we evaluate (3.95),(3.98), (3.99) at the common point $a_* \in \Delta_1 \cap \Delta_2 \cap \Delta_3$ and take differences in order to get

$$l_1 - l_2 - \tilde{l}_3 = 0.$$

On the other hand, if $\tau < \tau_c$, we use (3.97) to get

$$2U^{\mu_1}(a_*) + U^{\mu_2}(a_*) + U^{\mu_3}(a_*) + \phi(a_*) > l_1.$$

We now combine this inequality with (3.98) evaluated at $z = a_* \in \Delta_2$ and (3.101), and conclude

$$\tilde{l}_3 > l_1 - l_2.$$

Hence, for both the precritical and supercritical cases we can define

$$l_3 := l_1 - l_2,$$

and with this definition, it follows that

$$2U^{\mu_3}(z) + U^{\mu_1}(z) - U^{\mu_2}(z) - l_3 > 0, \quad z < \min\{a_*, a_1\},$$

$$2U^{\mu_3}(z) + U^{\mu_1}(z) - U^{\mu_2}(z) - l_3 = 0, \quad z \in \Delta_3.$$

One more variational inequality is based on the fact that we deal with a critical trajectory of our quadratic differential. Recall that by (3.94),

$$2U^{\mu_2}(z) + U^{\mu_1}(z) - U^{\mu_3}(z) + \phi(z) - l_2 = \operatorname{Re}\psi_2(z), \quad z \in \mathbb{C} \setminus \Delta,$$

where

$$\psi_2(z) = \int_{a_2}^{z} (\xi_1(s) - \xi_3(s))ds.$$

From (3.79), we know that ψ_2 is real-valued on $\Gamma \setminus \Delta_2$. Hence,

$$2U^{\mu_2}(z) + U^{\mu_1}(z) - U^{\mu_3}(z) + \phi(z) - l_2 = \psi_2(z), \quad z \in \Gamma \setminus \Delta_2.$$

Moreover, by (3.80), the real-valued function ψ_2 is monotone on each connected component of $\Gamma \setminus \Delta_2$. Analyzing at ∞, we see that

$$\psi_2(z) = z^3 + \mathcal{O}(z),$$

hence ψ_2 tends to $+\infty$ along Γ. Since it is zero at the endpoints a_2, b_2 of the connected components of $\Gamma \setminus \Delta_2$, we conclude that Ψ_2 is always positive on $\Gamma \setminus \Delta_2$, and hence

$$2U^{\mu_2}(z) + U^{\mu_1}(z) - U^{\mu_3}(z) + \phi(z) - l_2 > 0, \quad z \in \Gamma \setminus \Delta_2.$$

We summarize our findings in the following theorem:

Theorem 3.4.7. *Let measures μ_1, μ_2, μ_3 be defined in (3.86). Then there exist real constants l_1, l_2 and*

$$l_3 := l_1 - l_2,$$

such that the following variational conditions are satisfied:

$$\begin{aligned}
&2U^{\mu_1}(z) + U^{\mu_2}(z) + U^{\mu_3}(z) + \phi(z) - l_1 = 0, \quad z \in \Delta_1,\\
&2U^{\mu_1}(z) + U^{\mu_2}(z) + U^{\mu_3}(z) + \phi(z) - l_1 > 0, \quad z \in \Gamma_1 \setminus \Delta_1,\\
&2U^{\mu_2}(z) + U^{\mu_1}(z) - U^{\mu_3}(z) + \phi(z) - l_2 = 0, \quad z \in \Delta_2,\\
&2U^{\mu_2}(z) + U^{\mu_1}(z) - U^{\mu_3}(z) + \phi(z) - l_2 > 0, \quad z \in \Gamma_2 \setminus \Delta_2\\
&2U^{\mu_3}(z) + U^{\mu_1}(z) - U^{\mu_2}(z) - l_3 = 0, \quad z \in \Delta_3,\\
&2U^{\mu_3}(z) + U^{\mu_1}(z) - U^{\mu_2}(z) - l_3 > 0, \quad z \in \Gamma_3 \setminus \Delta_3.
\end{aligned} \tag{3.102}$$

where $\Gamma_1 = [a_*, +\infty)$, $\Gamma_2 = \Gamma$, $\Gamma_3 = (-\infty, a_*]$.

Remark 3.4.8. In the pre-critical case ($\tau < \tau_c$), $\Delta_3 = \emptyset$, thus the equality on Δ_3 in (3.102) is void.

The equalities in (3.102) are the same as those in (3.26). The extra information in Theorem 3.4.7 is coming from the remaining equations, which assure that the triplet (μ_1, μ_2, μ_3) is the (unique) minimizer of the energy functional (3.2) over measures (ν_1, ν_2, ν_3) satisfying (3.4) (with μ_j replaced by ν_j) and $\operatorname{supp} \mu_j \subset \Gamma_j$, $j = 1, 2, 3$, see [22, Theorem 1.8]. This is equivalent to Theorem 3.2.16 with $\Gamma = \Gamma_2$.

3.5 Global structure of the trajectories in the cubic case

3.5.1 Dynamics of the singularities

A natural first step in the study of the structure of the trajectories of a quadratic differential is to clarify the position and the character of its singular points. In the case of the quadratic differential (3.77) we have to analyze the location and the dynamics of the branch points and the double point of the Riemann surface $\mathcal{R}$ (corresponding to the spectral curve (3.74)) as functions of the parameter τ.

Recall that in Section 3.4.2 we have denoted the branch points of (3.74) by a_1, a_2, b_1, b_2, with the conventions

$$a_1, b_1 \in \mathbb{R}, \quad a_1 < b_1, \quad a_2 = \bar{b}_2, \quad \operatorname{Im} a_2 < 0,$$

and the double point of (3.74) by b_*.

Proposition 3.5.1. *The main parameters of the Riemann surface $\mathcal{R}$ associated to the algebraic equation (3.74) exhibit the following behavior: as τ grows from 0 to $1/4$,*

(i) the coefficient c in (3.68) increases monotonically from $-3^{5/3}/4$ to 0;

(ii)
- *the branch point a_1 decreases monotonically from $3^{2/3}/4$ to $-\infty$;*
- *the branch point b_1 increases monotonically from $3^{2/3}/4$ to $3^{2/3}/2$;*
- *the double point b_* increases monotonically from $3^{-1/3}$ to $+\infty$.*

(iii) Always

$$b_1 \le b_*,$$

and the equality is attained only for $\tau = 1/12$.

Proof. Recall that we chose c in (3.68) to be real, thus (i) follows directly from the definition of c.

Any branch point $z = \zeta$ of $\mathcal{R}$ is a zero of the polynomial q_1 of degree 4 and real coefficients, defined in (3.70), so that

$$\partial_\tau \zeta = -\frac{\partial_\tau q_1(\zeta)}{\partial_z q_1(\zeta)}. \tag{3.103}$$

It is easy to check that the resultant of q_1 and $\partial_\tau q_1$ (with respect to the variable z) is

$$\text{const} \times (1-4\tau)^{-\frac{5}{3}} (27 - 100\tau)^3 \neq 0 \quad \text{for } \tau \in (0, 1/4),$$

which implies that for any root ζ of q_1, $\partial_\tau q_1(\zeta) \neq 0$, and thus preserves its sign in the whole range of values of $\tau \in (0, 1/4)$.

On the other hand, since a_1 (resp., b_1) is the smallest (resp., largest) real root of q_1, and the leading coefficient of q_1 is positive, we know that

$$\partial_z q_1(a_1) < 0, \quad \partial_z q_1(b_1) > 0.$$

Straightforward calculations show that for $\tau = 1/8$, $a_1 = 0 < b_1$ and

$$\partial_\tau q_1(z) = -256\, u^4 - 64\left((u-1)^2 + 1\right), \quad u = \left(\frac{2}{3}\right)^{2/3} z.$$

In particular, $\partial_\tau q_1(z) \leq -64$, and we conclude that in this case,

$$\partial_\tau q_1(a_1) = -128, \quad \partial_\tau q_1(b_1) < 0.$$

Hence, $\partial_\tau q_1(a_1), \partial_\tau q_1(b_1) < 0$ for all $\tau \in (0, 1/4)$, and by (3.103), a_1 is a decreasing and b_1 is an increasing function of τ.

From the expression (3.71) it follows that

$$b_* = \frac{1}{3^{1/3}(1-4\tau)^{1/3}}.$$

Replacing it in (3.70) we get

$$q_1(b_*) = \frac{32(1-12t)^2}{9(1-4t)} > 0 \text{ for } \tau \in (0, 1/4), \quad \tau \neq 1/12.$$

Since for $\tau = 0$,

$$a_1 = b_1 = \frac{3^{2/3}}{4} < b_* = 3^{-1/3}, \tag{3.104}$$

this concludes the proof of (iii). Finally, it remains to observe that for $\tau = 1/4$,

$$q_1(z) = \frac{128}{9}\left(z^3 - \frac{9}{8}\right),$$

which has one real positive root $(3^{2/3}/2)$ and two complex conjugate ones. This shows that

$$\lim_{\tau \to 1/4-} a_1 = -\infty, \quad \lim_{\tau \to 1/4-} b_1 = \frac{3^{2/3}}{2}.$$

□

We finish this section with a technical lemma that will be used later.

Proposition 3.5.2. *For $0 < \tau < 1/12$, the polynomial D in (3.66) does not have zeros on (a_1, b_1), whereas for $1/12 < \tau < 1/4$, D has exactly one zero on (a_1, b_1). Moreover, for $0 < \tau < 1/12$, $D(b_1) = 0$ only for $\tau = 1/12$, and $D(a_1)$ is never zero.*

Proof. On one hand, the discriminant of the polynomial D with respect to z is

$$f(\tau) = \text{const}\, \tau(1 - 12\tau)^2 \left(128\tau^2 - 32\tau - 1\right)$$

which shows that for $\tau \in (0, 1/4)$, polynomial D has no multiple roots as long as $\tau \neq 1/12$.

On the other hand, we have seen in Section 3.4.1 that the branch points of $\mathcal{R}$ are the zeros of the polynomial q_1 defined in (3.70). The resultant (also w.r.t. z) of D and q_1 is

$$g(\tau) = \text{const}(1 - 12\tau)^3(27 - 100\tau)^3,$$

so again, for $\tau \in (0, 1/4)$, polynomials D and q_1 have no common roots as long as $\tau \neq 1/12$, in particular implying that D does not vanish at a_1, b_1 for $\tau \neq 1/12$. For $\tau = 1/12$, we compute $b_1 = b_* = 2^{-1/3}$ and factor

$$D(z) = -(z - b_*)^2(2z^4 + 2^{5/3}z^3 + 3\ 2^{1/3}z^2 + z + 2^{-4/3}),$$

so for $\tau = 1/12$ we have $D(b_1) = 0$ and $D(a_1) < 0$.

It is worth pointing out that both f and g can be easily found by means of any computer algebra software.

Having in mind that D and q_1 do not share roots for $\tau \neq 1/12$, it is sufficient to establish the assertion concerning the zeros of D for a single value of τ in $(0, 1/12)$, and for a single value of τ in $(1/12, 1/4)$.

For $\tau = 1/4$, D is a quadratic polynomial in z^3 so its roots can be explicitly computed; we get that its only real roots are

$$z_1 = \left(\frac{3 - \sqrt{3}}{4}\right)^{1/3}, \quad z_2 = \left(\frac{3 + \sqrt{3}}{4}\right)^{1/3}.$$

Since

$$\left(\frac{3 - \sqrt{3}}{4}\right)^{1/3} < \frac{3^{2/3}}{2} < \left(\frac{3 + \sqrt{3}}{4}\right)^{1/3},$$

from Proposition 3.5.1 (ii) we see that for $\tau = 1/4 - \epsilon$, for a certain small value of $\epsilon > 0$,

$$a_1 < z_1 < b_1 < z_2.$$

On the other hand, it is easy to check that for $\tau = 0$,

$$D(a_1) = D(b_1) = D(3^{2/3}/4) < 0,$$

so that for $\tau = \epsilon$, for a certain small value of $\epsilon > 0$, D does not vanish on (a_1, b_1). □

3.5.2 The Riemann surface associated to the algebraic equation

In Section 3.4.2 we described the construction of the three-sheeted Riemann surface $\mathcal{R} = \mathcal{R}_1 \cup \mathcal{R}_2 \cup \mathcal{R}_3$ and of the branch cuts in such a way that the three solutions ξ_j of (3.74), specified by the asymptotic conditions (3.75), become meromorphic on the respective sheet $\mathcal{R}_j$, with poles only at $z = \infty$. They are also pairwise distinct as long as $\mathrm{Discr}(z)$, defined in (3.69), does not vanish, i.e. for $z \notin \{a_1, b_1, a_2, b_2, b_*\}$.

The arc Δ_2 intersects $\mathbb{R}$ in a unique point a_*; there is a critical value $\tau_c \in (1/12, 1/4)$, to be specified later, such that $a_* < a_1$ for $0 < \tau < \tau_c$ (what we called the precritical regime), and $a_* \in (a_1, b_1)$ for $\tau_c < \tau < 1/4$ (the supercritical regime).

As a first result we establish some relations between the solutions $\xi_j(z)$.

Proposition 3.5.3. *Let $\tau \in (0, 1/4)$, $\tau \neq \tau_c$. Then*

(i) for $x \in \mathbb{R} \setminus (\Delta_1 \cup \Delta_2 \cup \Delta_3)$,

$$\xi_3(x) < \xi_2(x) < \xi_1(x), \quad x < \min(a_*, a_1), \tag{3.105}$$

$$\xi_2(x) < \xi_3(x) < \xi_1(x), \quad x > b_*, \tag{3.106}$$

$$\xi_1(x) < \xi_2(x) < \xi_3(x), \quad a_* < x < a_1, \quad \text{if } \tau < \tau_c, \tag{3.107}$$

$$\xi_2(x) < \xi_1(x) < \xi_3(x), \quad b_1 < x < b_*, \quad \text{if} \quad 0 < \tau < 1/12, \tag{3.108}$$

$$\xi_3(x) < \xi_2(x) < \xi_1(x), \quad b_1 < x < b_*, \quad \text{if} \quad 1/12 < \tau < 1/4. \tag{3.109}$$

Additionally,

$$\begin{aligned} &\xi_2(b_*) < \xi_3(b_*) = \xi_1(b_*), \quad \text{for} \quad 0 < \tau < 1/12, \\ &\xi_2(b_*) = \xi_3(b_*) < \xi_1(b_*), \quad \text{for} \quad 1/12 < \tau < 1/4. \end{aligned} \tag{3.110}$$

(ii) on $\Delta_1 \cup \Delta_2 \cup \Delta_3$,

- *for* $x \in \overset{\circ}{\Delta}_1 := \Delta_1 \setminus \{\max(a_1, a_*), b_1\}$,

$$\xi_2(x) = \overline{\xi_1(x)} \in \mathbb{C} \setminus \mathbb{R}, \quad \xi_3(x) \in \mathbb{R}, \tag{3.111}$$

and

$$\xi_{1\pm}(x) = \xi_{2\mp}(x), \quad \xi_{3+}(x) = \xi_{3-}(x). \tag{3.112}$$

- *for* $z \in \overset{\circ}{\Delta}_2 := \Delta_2 \setminus \{a_2, b_2, \max(a_1, a_*)\}$,

$$\xi_{1\pm}(z) = \xi_{3\mp}(z), \quad \xi_{2+}(z) = \xi_{2-}(z). \tag{3.113}$$

- *for* $x \in \overset{\circ}{\Delta}_3 := \Delta_3 \setminus \{a_1, a_*\}$ *(when* $\tau > \tau_c$*)*,

$$\xi_2(x) = \overline{\xi_3(x)} \in \mathbb{C} \setminus \mathbb{R}, \quad \xi_1(x) \in \mathbb{R}, \tag{3.114}$$

and

$$\xi_{2\pm}(z) = \xi_{3\mp}(z), \quad \xi_{1+}(z) = \xi_{1-}(z). \tag{3.115}$$

Moreover,

$$\xi_1(a_1) = \xi_2(a_1), \quad \textit{if } \tau < \tau_c, \tag{3.116}$$

$$\xi_3(a_1) = \xi_2(a_1), \quad \textit{if } \tau > \tau_c, \tag{3.117}$$

$$\xi_1(b_1) = \xi_2(b_1), \tag{3.118}$$

$$\xi_1(a_2) = \xi_3(a_2) \quad \textit{and} \quad \xi_1(b_2) = \xi_3(b_2). \tag{3.119}$$

Proof. Recall that we deal with the case $\alpha \in (0, 1/2)$, so that $0 < \alpha < 1-\alpha < 1$. The behavior at infinity in (3.75) gives (3.105) and also (3.106). Furthermore, we have established in Proposition 3.5.1 that if $\tau \neq 1/12$ then $b_* \notin \{a_1, b_1, a_2, b_2\}$, and in this case b_* is a double zero of $\mathrm{Discr}(z)$. This means that when $\tau \neq 1/12$, only two of the three values $\xi_1(b_*)$, $\xi_2(b_*)$, $\xi_3(b_*)$ coincide, and since

$$\xi_1(b_*) + \xi_2(b_*) + \xi_3(b_*) = 0,$$

the coincident two differ in sign from the third one. Furthermore, since also

$$(\xi_1\xi_2\xi_3)(b_*) = -D(b_*),$$

we see that the sign of this third one is opposite to the sign of $D(b_*)$. But direct calculations show that

$$D(b_*) = -\frac{(12\tau - 1)^3}{36(1 - 4\tau)^2} \begin{cases} > 0, & \text{for } 0 < \tau < 1/12, \\ < 0, & \text{for } 1/12 < \tau < 1/4, \end{cases}$$

which means that for $0 < \tau < 1/12$ the two coincident values of $\xi_j(b_*)$ are the largest two, and the other way around if $1/12 < \tau < 1/4$. It remains to use (3.106) in order to establish (3.110).

Inequalities (3.108)–(3.109) follow by noticing that b_* is a double zero of $\mathrm{Discr}(z)$, so it is a simple zero of $\xi_1 - \xi_3$ (for $0 < \tau < 1/12$) and of $\xi_2 - \xi_3$ (for $1/12 < \tau < 1/4$).

From Proposition 3.5.2 we know that $D(a_1) \neq 0$, $D(b_1) \neq 0$ for $\tau \neq 1/12$. In particular, since for $\tau = 0$ (see (3.104)), $a_1 = b_1 = 3^{2/3}/4$ and $D(a_1) = D(b_1) = -81/2048 < 0$, we conclude that $D(a_1) < 0$ and $D(b_1) < 0$ for $0 \leq \tau < 1/12$. In other words, the smallest two of the three solutions ξ_j come together at a_1 and at b_1. Now (3.108) implies (3.118) for $0 \leq \tau < 1/12$.

On the other hand, recall that by Proposition 3.5.1, $D(a_1) \to -\infty$ as $\tau \to 1/4$, and that for $\tau = 1/4$,

$$D(z) = -2z^6 + 3z^3 - \frac{3}{4}, \quad b_1 = 3^{2/3}/2,$$

so that $D(b_1) = 3/32 > 0$. Using the same arguments we conclude that for $1/12 < \tau < 1/4$, the largest two of the three solutions ξ_j come together at b_1 (and (3.109) yields (3.118)), and the smallest two become confluent at a_1 (and (3.117) follows from (3.105)).

The discriminant $\mathrm{Discr}(x)$ is negative for $a_1 < x < b_1$, so just one of the solutions ξ_j is real on $a_1 < x < b_1$, and the other two are complex-conjugates of each other. Since we have ruled out the coincidence of the three branches, equality (3.118) implies that ξ_1, ξ_2 are non-real on $\overset{\circ}{\Delta}_1$, which yields (3.111)–(3.112). By the same argument we also have (3.116), as well as (now using (3.105)) the identities (3.114)–(3.115).

Recall that we already established that the smallest two of the three solutions ξ_j come together at a_1, and (3.116) shows that for $\tau < \tau_c$,

$$\xi_1(x) < \xi_3(x), \quad \xi_2(x) < \xi_3(x), \quad \text{for } a_* < x < a_1. \tag{3.120}$$

For $\tau < \tau_c$, when crossing Δ_2 two of the three solutions ξ_j are swapped, and the third one remains invariant. But the only option compatible both with (3.105) and (3.120) is (3.107).

Finally, for $\tau < \tau_c$, the inequalities (3.105) and (3.107) show that ξ_2 is continuous across Δ_2, and as a consequence (3.113) has to hold, obviously for the full range of $\tau \in (0, 1/4)$. This, in turn, implies the last identity (3.119). □

Proposition 3.5.1 gives the formal proof of the fact that the Riemann surface $\mathcal{R}$, described in Section 3.4.2, is actually the Riemann surface of the cubic equation

(3.74), and with this construction the function ξ_j is meromorphic on $\mathcal{R}_j$ and satisfies the asymptotic expansion (3.75). Moreover, $\xi : \mathcal{R} \to \mathbb{C}$, given by $\xi \equiv \xi_j$ on $\mathcal{R}_j$, is meromorphic on $\mathcal{R}$, giving the global solution to the algebraic equation (3.74). From Theorem 3.2.12, or alternatively Proposition 3.4.1, the Riemann surface $\mathcal{R}$ has genus 0.

Let $\pi : \mathcal{R} \to \overline{\mathbb{C}}$ be the canonical projection on the Riemann surface $\mathcal{R}$. For a point $p \in \overline{\mathbb{C}} \setminus (\Delta_1 \cup \Delta_2 \cup \Delta_3)$, we denote by $p^{(j)}$, $j = 1, 2, 3$, its preimage by π on $\mathcal{R}_j$, that is,

$$\{p^{(j)}\} = \pi^{-1}(\{p\}) \cap \mathcal{R}_j, \quad j = 1, 2, 3.$$

This notation is trivially extended to $p \in \Delta_1 \cup \Delta_2 \cup \Delta_3$ by taking boundary values.

Notice that for the branch points it is valid

$$b_1^{(1)} = b_1^{(2)}, \quad a_2^{(2)} = a_2^{(3)}, \quad b_2^{(2)} = b_2^{(3)},$$

and

$$a_1^{(1)} = a_1^{(2)} \ (\tau \le \tau_c), \quad a_1^{(2)} = a_1^{(3)} \ (\tau > \tau_c),$$

whereas if p belongs to a cut connecting exactly two sheets, say $\mathcal{R}_j$ and $\mathcal{R}_k$, then

$$p_{\pm}^{(j)} = p_{\mp}^{(k)}.$$

We insist that the construction of $\mathcal{R}$ is independent of the concrete choice of the cut Δ_2; this freedom will be used latter to specify an appropriate Δ_2. Namely, in the next section we will show that Δ_2 can be made coincident with a critical trajectory of the quadratic differential ϖ, defined in (3.77),which connects a_2 and b_2, see Definition 3.5.5 below.

3.5.3 Computation of width parameters

Certain integrals of the function Q defined in (3.76) will play a crucial role in the upcoming analysis of the dynamics of the trajectories of the quadratic differential $\varpi = -Q^2(z)\,dz^2$ on $\mathcal{R}$. They can be also formulated in terms of certain Abelian integrals on $\mathcal{R}$.

Namely, we are interested in

$$\begin{aligned} \omega_1 = \omega_1(\tau) &= \operatorname{Re} \int_{b_2^{(1)}}^{a_1^{(1)}} Q(s)ds = \operatorname{Re} \int_{b_2}^{a_1} (\xi_2(s) - \xi_3(s))ds, \\ \omega_2 = \omega_2(\tau) &= \operatorname{Re} \int_{b_2^{(2)}}^{a_1^{(2)}} Q(s)ds = \operatorname{Re} \int_{b_2}^{a_1} (\xi_1(s) - \xi_3(s))ds, \end{aligned} \tag{3.121}$$

and

$$\begin{aligned}\omega_3 = \omega_3(\tau) &= \operatorname{Re}\int_{b_2^{(3)}}^{a_1^{(3)}} Q(s)ds = \operatorname{Re}\int_{b_2}^{a_1} (\xi_1(s) - \xi_2(s))ds,\\ \omega_4 = \omega_4(\tau) &= \operatorname{Re}\int_{b_2^{(1)}}^{b_*^{(1)}} Q(s)ds = \operatorname{Re}\int_{b_2}^{b_*} (\xi_2(s) - \xi_3(s))ds,\end{aligned} \tag{3.122}$$

with $\omega_4(\tau)$ defined for $\tau \geq 1/12$. In this definition we understand that we integrate between two points on a sheet $\mathcal{R}_j$ along a path that stays entirely in $\mathcal{R}_j$.

The values ω_j are correctly defined regardless of the precise choice of the integration paths. Indeed, the residues of the functions ξ_1, ξ_2, ξ_3 at ∞ are real (and independent of the value of τ), see (3.75), so the integral of Q along a big loop on either $\mathcal{R}_j$ encircling $\infty^{(j)}$ is purely imaginary. It remains to notice that the genus of $\mathcal{R}$ is zero, so that any closed contour around either branch cut Δ_j can be deformed to such a big loop.

Analytic computation of ω_j's is a formidable task. Instead, we have computed them numerically, see Figure 3.4 for the result. Since the integrands in (3.121)–(3.122) are multivalued functions, the numerical integration requires to implement an analytic continuation of each branch of ξ. We give further details in Section 3.7.

The functions ω_1, ω_2, have two and one zeros on $(0, 1/4)$, respectively, whereas ω_3 and ω_4 do not vanish on the intervals $(0, 1/4)$ and $(1/12, 1/4)$, respectively.

We denote the zeros of ω_1 by τ_1, τ_2 and of ω_2 by τ_c. We have

$$\tau_1 \approx 0.12487351, \quad \tau_c \approx 0.1913565, \quad \tau_2 \approx 0.2289555,$$

so that they satisfy

$$0 < \frac{1}{12} < \tau_1 < \tau_c < \tau_2 < 1/4. \tag{3.123}$$

We point out that the value τ_c is the one used in Section 3.4.2 in the construction of the Riemann surface $\mathcal{R}$, and it is equivalently determined by (3.34).

It is also clear from Figure 3.4 that $\omega_1 \neq \omega_4$ for $\tau > 1/12$.

3.5.4 Critical points of the quadratic differential

We follow the construction (3.28), (3.77) and define the meromorphic quadratic differential $\varpi = -Q^2(z)\,dz^2$ on the Riemann surface $\mathcal{R}$.

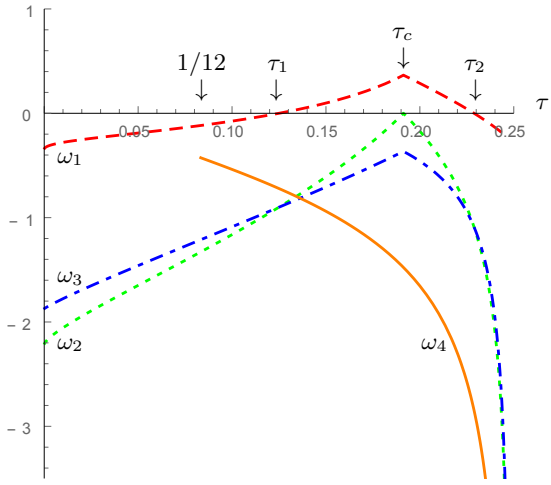

Figure 3.4: The graphics of the functions ω_1 (upper dashed line), ω_2 (short dashed line), ω_3 (dashed line with dots) and ω_4 (continuous line).

We start by analyzing the character of the critical points of ϖ. For instance, the local parameter at $z = a_1^{(1)}$ is

$$z = a_1^{(1)} + u^2,$$

so that $dz^2 = 4u^2 du^2$. In consequence, $(\xi_j - \xi_k)^2(z)dz^2$ has a double zero at $z = a_1^{(1)}$ if and only if $\xi_j(a_1^{(1)}) \neq \xi_k(a_1^{(1)})$. A similar analysis at the rest of the points of $\mathcal{R}$ yields the following classification of the critical points of ϖ on the Riemann surface (see Figure 3.5):

(a) For $0 < \tau < \tau_c$:

  (i) Simple zeros at $a_1^{(3)}$, $b_1^{(3)}$, $a_2^{(2)}$, $b_2^{(2)}$;
  (ii) Double zeros at $a_1^{(1)}$, $b_1^{(1)}$ (only for $\tau \neq 1/12$), $a_2^{(1)}$, $b_2^{(1)}$;
  (iii) Double zero at $b_*^{(2)}$ if $\tau < 1/12$ and a double zero at $b_*^{(1)}$ if $\tau > 1/12$;
  (iv) Zero of order 4 at $b_1^{(1)} = b_*^{(1)}$ if $\tau = 1/12$;
  (v) Double pole at $\infty^{(1)}$ with a real residue;
  (vi) Poles of order 8 at $\infty^{(2)}$, $\infty^{(3)}$.

(b) For $\tau_c \leq \tau < 1/4$:

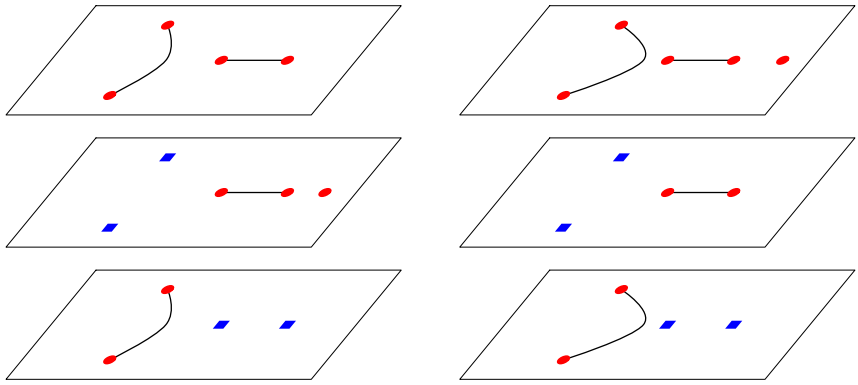

$0 < \tau < 1/12$ $\qquad$ $1/12 < \tau < \tau_c$

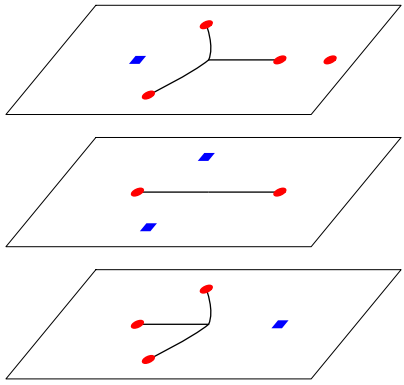

$\tau_c < \tau < 1/4$

Figure 3.5: The finite critical points of ϖ in each case. Simple and double zeros are represented, respectively, with squares and dots.

(i) Simple zeros at $a_1^{(1)}$, $b_1^{(3)}$, $a_2^{(2)}$, $b_2^{(2)}$;

(ii) Double zeros at $a_1^{(2)}$, $b_1^{(1)}$, $a_2^{(1)}$, $b_2^{(1)}$;

(iii) Double zero at $b_*^{(1)}$;

(iv) Double pole at $\infty^{(1)}$ with a real residue;

(v) Poles of order 8 at $\infty^{(2)}$, $\infty^{(3)}$.

It is instructive to think of the critical points as evolving dynamically with τ. Under this perspective, Propositions 3.5.1 and 3.5.3 show that for τ small the

double point (node) b_* corresponds to the double zero $b_*^{(2)}$ on the second sheet. When $\tau = 1/12$, the points b_*, b_1 coalesce, giving rise to a higher order zero at the branch point $b_1^{(1)} = b_1^{(2)}$. For larger values of τ, the double point emerges on the first sheet: now $b_*^{(2)}$ is a regular point whereas $b_*^{(1)}$ is a double zero.

In the same spirit, the simple zero a_1 of the discriminant of (3.74) carries two critical points of ϖ. For $\tau < \tau_c$ these are the simple zero $a_1^{(3)}$ and the double zero $a_1^{(1)} = a_1^{(2)}$. For values of τ larger than τ_c, these points interchange their roles: $a_1^{(1)}$ is a simple zero and $a_1^{(3)} = a_1^{(2)}$ is a double zero.

3.5.5 Analyzing the global structure of trajectories

3.5.5.1 General principles

The rest of this section is devoted to the description of the critical graph of the quadratic differential (3.77) for the whole range $0 \le \tau < 1/4$. One of the outcomes of our analysis is the following theorem:

Theorem 3.5.4. *For the quadratic differential $\varpi = -Q^2(z)\,dz^2$ and for all values of the parameter $0 \le \tau \le \tau_c$ there exists a critical trajectory of ϖ joining $a_2^{(2)}$ and $b_2^{(2)}$ on $\mathcal{R}_2$, whose projection by π on $\mathbb{C}$ is a real-symmetric analytic arc Δ_2 joining a_2 and b_2.*

For $\tau_c \le \tau \le 1/4$, there is an arc of critical trajectory of ϖ joining $a_2^{(2)}$ with a point $a_*^{(2)}$ on the interval $[a_1^{(2)}, b_1^{(2)}]$ which is determined by (3.35), and the conjugate symmetric arc of trajectory joining $b_2^{(2)}$ with the same point. The projection by π on $\mathbb{C}$ of the union of these two arcs of trajectories is also denoted by Δ_2.

Recall that τ_c was formally introduced in Section 3.5.3. In virtue of the results in Section 3.4.2, in particular Corollary 3.4.6, Theorem 3.5.4 implies Theorem 3.2.14.

We remind the reader that up to now the branch cut, separating the sheets $\mathcal{R}_1$ and $\mathcal{R}_3$, was free (see Figure 3.2). In what follows we agree in the following:

Definition 3.5.5. The curve, connecting a_2 and b_2 as part of the branch cut separating the sheets $\mathcal{R}_1$ and $\mathcal{R}_3$, is always given by the lift of Δ_2 (from Theorem 3.5.4) to the sheets $\mathcal{R}_1$ and $\mathcal{R}_3$.

In the next sections we will show that this definition is consistent with our construction of the Riemann surface $\mathcal{R}$.

One important fact is that the residues of ϖ at the poles at infinity (and the local behavior of the trajectories there) are independent of τ: at $\infty^{(1)}$ they are closed analytic curves (so that $\infty^{(1)}$ is the center of a circle domain, see Appendix A), while $\infty^{(2)}, \infty^{(3)}$ attract trajectories in 6 asymptotic directions, given by the angles

$$\theta_j^{(\infty)} = \frac{2j-1}{6}\,\pi, \quad j = 1, \dots, 6. \tag{3.124}$$

Critical values (3.123) split the interval $(0, 1/4)$ into subintervals $(0, 1/12)$, $(1/12, \tau_1)$, (τ_1, τ_c), (τ_c, τ_2) and $(\tau_2, 1/4)$. We will show that the topology of the critical graph remains invariant in each of these intervals.

The methodology we use can be summarized as follows:

(i) Compute the critical graph for τ equal to one of the critical values (3.123).

(ii) Analyze the possible deformation of the trajectories for the values $\tau + \varepsilon$, with $\varepsilon > 0$ small, identifying the trajectories that display a phase transition.

(iii) Prove that the topology of the critical graph is invariant inside the subinterval of interest, by analyzing the behavior of the widths ω_j's and showing that the corresponding strip and ring domains can not disappear.

Along the way, will use some general *principles* that we enumerate here:

P.1 Quadratic differential ϖ has no recurrent trajectory for any value of τ, see Jenkin's Three Poles Theorem in Section A.3.

P.2 If γ is an arc of trajectory of ϖ, then $\overline{\gamma}$, corresponding to the lift of the complex conjugate of $\pi(\gamma)$ to the same sheet, is also an arc of trajectory.

P.3 The complement of the critical graph of ϖ on $\mathcal{R}$ cannot have a simply connected component without poles on its boundary: that would contradict Corollary A.3.3 or the maximum principle for harmonic functions on a compact Riemann surface.

P.4 The meromorphic function Q^2 depends analytically on the parameter τ. Hence the critical graph of ϖ, and in particular all its critical trajectories, depend continuously (in any reasonable topology, for instance, in the Hausdorff distance) from τ.

P.5 If for a certain value $\tau = A$, the point p belongs to the half plane domain for $\infty^{(k)}$ determined by the angles $\theta_j^{(\infty)}, \theta_{j+1}^{(\infty)}$, then the same holds true

for a small neighborhood of values $\tau \in (A-\varepsilon, A+\varepsilon)$, $\varepsilon > 0$. The point p is also allowed to depend continuously on τ.

P.6 If for a certain value $\tau = A$, an arc of trajectory emanating from a given point p intersects the real line at a *regular* point, then the same holds true for $\tau \in (A-\varepsilon, A+\varepsilon)$, $\varepsilon > 0$. As before, the point p is allowed to depend continuously on τ.

There will be one more useful tool that we will employ several times in our analysis, formulated as Proposition 3.5.7 below.

When describing the structure and the evolution of the trajectories of the quadratic differential ϖ we face the dilemma of either a formalization of each statement, with a precise formulation of the behavior of every trajectory in every situation, or a much more visual description, with rigorous proofs but illustrated by a number of figures. We opted for the second choice[2].

Next, we agree on some convention about trajectories. Let $p^{(j)} \in \mathcal{R}_j$ be a zero of ϖ. We denote by $\gamma_1(p^{(j)})$, $\gamma_2(p^{(j)})$, ..., the trajectories of ϖ *emanating* from p *on* $\mathcal{R}_j$, in such a way that their canonical projections $\pi(\gamma_n(p^{(j)}))$, see Section 3.5.2, are enumerated in an anti-clockwise direction starting from the positive OX semiaxis[3]. Notice that when $p^{(j)}$ is a branch point of $\mathcal{R}$, so that $p^{(j)} = p^{(k)}$ for some $j \neq k$, trajectories $\gamma_n(p^{(j)})$ and $\gamma_n(p^{(k)})$ are different because they emerge from $p^{(j)} = p^{(k)}$ on different sheets of $\mathcal{R}$. Otherwise, when $p^{(j)}$ belongs to a single sheet $\mathcal{R}_j$, we occasionally drop the superindex (j) when it cannot lead us into confusion.

Given two points $p, q \in \mathbb{R}$, the integral

$$\int_p^q \sqrt{-\varpi}$$

along a contour γ connecting p and q is understood to be the integral of any analytic continuation of the meromorphic differential $\sqrt{-\varpi}$ along γ. This is well defined up to the branch of the square root, which will be clear in each context.

[2]We confess we might have been influenced by the famous quote of Vladimir Arnold [136]:

> It is almost impossible for me to read contemporary mathematicians who, instead of saying "Petya washed his hands," write simply: "There is a $t_1 < 0$ such that the image of t_1 under the natural mapping $t_1 \mapsto \mathrm{Petya}(t_1)$ belongs to the set of dirty hands, and a t_2, $t_1 < t_2 \leq 0$, such that the image of t_2 under the above-mentioned mapping belongs to the complement of the set defined in the preceding sentence."

[3]This notation is not correctly defined only if the direction of a trajectory coincides with a branch cut, situation that will be explicitly avoided in what follows.

3.5.5.2 Degenerate case $\tau = 0$

For $\tau = 0$, the algebraic equation (3.74) reduces to

$$\left(\xi + z^2\right)\left(4\xi^2 - 8z^4 - 4\xi z^2 + 12z - 3 \times 3^{2/3}\right) = 0,$$

whose solutions, denoted in accordance with (3.75), are

$$\xi_1(z) = \frac{z^2 + \sqrt{3}\sqrt{h(z)}}{2}, \quad \xi_2(z) = -z^2, \quad \xi_3(z) = \frac{z^2 - \sqrt{3}\sqrt{h(z)}}{2},$$

where the branch of the square root is chosen to be positive for large real values,

$$h(z) = 3z^4 - 4z + 3^{2/3} = 3\left(z - a_2\right)\left(z - b_2\right)\left(z - b_*\right)^2,$$

and the points a_1, b_1, a_2, b_2, b_* are given explicitly by

$$a_1 = b_1 = \frac{3^{2/3}}{4}, \quad b_2 = \overline{a_2} = \frac{1}{3^{1/3}}(-1 + i\sqrt{2}), \quad b_* = \frac{1}{3^{1/3}}.$$

The cut Δ_1 is reduced to a single point a_1, and the sheet $\mathcal{R}_2$ is detached from the others. Since (3.74) is reducible, its Riemann surface is in fact the union of two Riemann surfaces,

$$\mathcal{R}_2 = \overline{\mathbb{C}} \quad \text{and} \quad \widetilde{\mathcal{R}} = \mathcal{R}_1 \cup \mathcal{R}_3.$$

Here $\mathcal{R}_1 = \mathcal{R}_3 = \overline{\mathbb{C}} \setminus \Delta_2$, and Δ_2 is a simple curve connecting the points a_2, b_2, to be precisely specified later. The quadratic differential (3.76) degenerates into two quadratic differentials ϖ_1 on $\overline{\mathbb{C}}$ and ϖ_2 on $\widetilde{\mathcal{R}}$, namely

$$\begin{aligned} \varpi_1 &= -3h(z)dz^2 \quad \text{on } \overline{\mathbb{C}}, \\ \varpi_2 &= \begin{cases} -\frac{1}{4}(3z^2 - \sqrt{3}\sqrt{h(z)})^2 dz^2 & \text{on } \mathcal{R}_1, \\ -\frac{1}{4}(3z^2 + \sqrt{3}\sqrt{h(z)})^2 dz^2 & \text{on } \mathcal{R}_3. \end{cases} \end{aligned} \tag{3.125}$$

We analyze the structure of their critical graphs next.

Trajectories of ϖ_1, whose only critical points are as follows:

- Simple zeros at $z = a_2, b_2$;
- Double zero at $z = b_*$;
- Pole of order 8 at $z = \infty$.

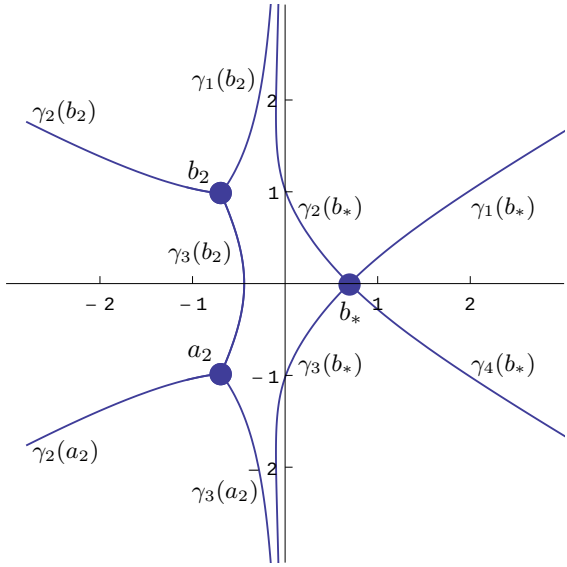

Figure 3.6: $\tau = 0$: the critical graph of ϖ_1.

Under the change of variables $z \mapsto \frac{i}{\sqrt[3]{3}} z$, the quadratic differential ϖ_1 becomes $-q(z)dz^2$, where

$$q(z) = -(z^2 - 2iz - 3)(z + i)^2$$

is, up to a multiplicative factor $\frac{1}{4}$, the same polynomial obtained in [49, eq. (2.1)]. Having in mind this identification, it was proven in [49, Theorem 2.1] that the trajectory $\gamma_3(b_2)$ of ϖ_1 connects b_2 and a_2: in the notation introduced above, $\gamma_3(b_2) = \gamma_1(a_2)$, see Figure 3.6.

From [49] we also know that $\gamma_3(b_2)$ intersects the real axis at a point $a_* < b_*$, which can be calculated numerically: by

$$a_* \approx -0.441782. \tag{3.126}$$

The rest of the critical graph of ϖ_1 is as follows. Notice that due to the symmetry, we only need to describe the trajectories in the upper half plane.

The trajectories $\gamma_j(b_*)$, $\gamma_j(b_2)$, $j = 1, 2$, cannot be finite, see Principle **P.3** above. Hence, they all diverge to ∞ along the asymptotic directions (3.124), and according Theorem A.3.1, all directions are represented. There are 3 asymptotic directions for 4 trajectories in the upper half plane, so necessarily the divergence angle for $\gamma_1(b_*)$ is $\theta_1^{(\infty)}$, while the divergence angle for $\gamma_2(b_2)$ is

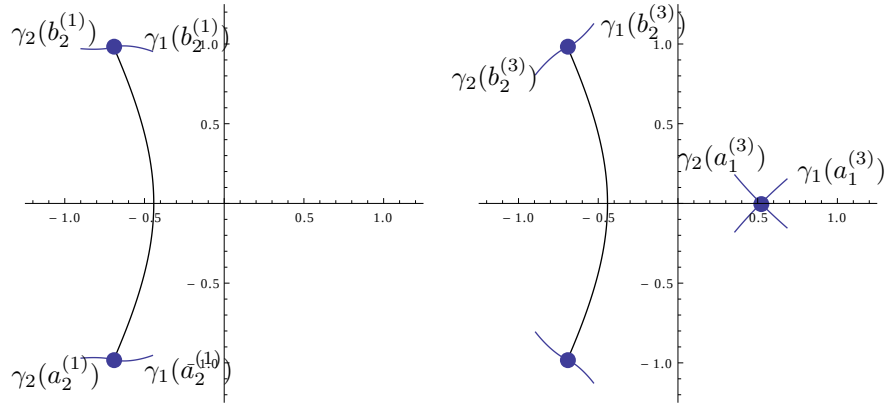

Figure 3.7: On the left it is represented the critical trajectories of ϖ_2 on $\mathcal{R}_1$ and on the right its critical trajectories on $\mathcal{R}_3$, all of them in blue and just locally at the critical points. The black curve is the cut Δ_2 connecting $\mathcal{R}_1$ and $\mathcal{R}_3$.

$\theta_3^{(\infty)}$. Since two consecutive trajectories emanating from a zero cannot diverge to ∞ in the same direction (this would contradict Theorem A.3.2), we conclude that both $\gamma_2(b_*)$ and $\gamma_1(b_2)$ must diverge in the direction $\theta_2^{(\infty)}$, see Figure 3.6.

Trajectories of ϖ_2, whose only critical points are as follows:

- Double zeros at $z = a_1^{(3)}$, $z = b_2^{(1)}$ and $z = a_2^{(1)}$;
- Double pole at $z = \infty^{(1)}$ with real residue;
- Pole of order 8 at $\infty^{(3)}$.

The double zeros $b_2^{(1)} = b_2^{(3)}$ $a_2^{(1)} = a_2^{(3)}$ are also branch points of $\widetilde{\mathcal{R}}$, and the critical graph of ϖ_2 is made of trajectories $\gamma_j(a_2^{(1)})$, $\gamma_j(b_2^{(1)})$, $j = 1, 2$, emanating on $\mathcal{R}_1$, and of trajectories $\gamma_j(a_2^{(3)})$, $\gamma_j(b_2^{(3)})$, $j = 1, 2$, along with $\gamma_j(a_1^{(3)})$, $j = 1, \dots, 4$, emanating on $\mathcal{R}_3$, see Figure 3.7.

The branch cut Δ_2 connecting the sheets $\mathcal{R}_1$ and $\mathcal{R}_3$, so far arbitrary, is chosen as $\Delta_2 = \gamma_3(b_2)$, where $\gamma_3(b_2)$ is the critical trajectory of ϖ_1 connecting b_2 to a_2, as described above.

Lemma 3.5.6. *With the branch cut Δ_2 specified above, the critical trajectories $\gamma_j(b_2^{(1)})$ and $\gamma_j(a_2^{(1)})$ of ϖ_2 belong entirely to the sheet $\mathcal{R}_1$.*

Proof. Suppose that one of the trajectories $\gamma_j(b_2^{(1)})$ emanating from b_2 intersects the cut Δ_2 for the fist time at a point x. Clearly, this point (actually, its canonical projection) must lie in the upper half plane: otherwise we readily get that $\gamma_j(b_2^{(1)}) = \gamma_j(a_2^{(1)})$ and no intersection with Δ_2 occur.

Integrating from b_2 to x along $\gamma_j(b_2^{(1)})$ and using the definition of a trajectory we get

$$0 = \operatorname{Re} \int_{b_2^{(1)}}^{x^{(1)}} \sqrt{-\varpi} = \frac{3}{4} \operatorname{Re} \int_{b_2}^{x} s^2 ds - \frac{\sqrt{3}}{4} \operatorname{Re} \int_{b_2}^{x} \sqrt{h(s)}_{\pm} ds \tag{3.127}$$

where the $\pm$ sign in the last integrand depends on the side of the cut Δ_2 to which x belongs. However, Δ_2 projects onto the trajectory $\gamma_3(b_2)$ of ϖ_1, so the second integral in the right-hand side of (3.127) is purely imaginary. Hence, this equation reduces to

$$\operatorname{Re} x^3 = \operatorname{Re} b_2^3 = \frac{5}{3}. \tag{3.128}$$

It was proved in [49] that the trajectory Δ_2 is contained in the domain bounded by the triangle with vertices b_2, $3^{-1/3}(\sqrt{2}-1)$ and a_2. In particular, the part of Δ_2 on the upper half plane, and hence x, is contained in the domain bounded by the triangle T determined by the vertices b_2, $\operatorname{Re} b_2$ and $3^{-1/3}(\sqrt{2}-1)$. The function $z \mapsto \operatorname{Re} z^3$ has a unique maximum on T at the point $z = b_2$. Since $\operatorname{Re} z^3$ is harmonic, it cannot attain a maximum on the domain bounded by T, hence (3.128) can only occur if $x = b_2$, showing that $\gamma_j(b_2^{(1)}) \setminus \{b_2^{(1)}\}$ does not intersect the cut Δ_2. □

Recall that $\infty^{(1)}$ is the center of a circle domain, which means that all trajectories of ϖ_2 passing through sufficiently distant points on $\mathcal{R}_1$ are closed Jordan curves. In particular, no trajectory diverges to $\infty^{(1)}$, and every trajectory entirely contained in $\mathcal{R}_1$ has to be closed. Consequently, both trajectories $\gamma_j(b_2^{(1)})$ are closed as well, $\gamma_j(b_2^{(1)}) = \gamma_j(a_2^{(1)})$, and $\gamma_1(b_2^{(1)})$ (respectively $\gamma_2(b_2^{(1)})$) intersects the real line, say at the point c_* (respectively d_*). We claim that

$$d_* < a_* < c_* < a_1, \tag{3.129}$$

with a_* defined in (3.126).

Indeed, both c_* and d_* cannot lie on the same side of the cut Δ_2 without running into contradiction with the general principle **P.3** above. Hence, either $d_* < a_* < c_*$ or $c_* < a_* < d_*$. The latter is impossible without $\gamma_1(b_2^{(1)})$ and $\gamma_2(b_2^{(1)})$ intersecting somewhere in the upper half plane, which again contradicts **P.3**. We conclude that $d_* < a_* < c_*$.

Let us prove the inequality $c_* < a_1$. Using the definition of trajectory and (3.122) we get

$$0 = \operatorname{Re} \int_{b_2^{(1)}}^{c_*^{(1)}} Q(s)ds = \operatorname{Re} \int_{b_2}^{c_*} (\xi_2(s) - \xi_3(s))ds = \omega_3 + \int_{a_1}^{c_*} (\xi_2(s) - \xi_3(s))ds.$$

But $\omega_3 = \omega_3(0) < 0$, see Figure 3.4, so that

$$\int_{a_1}^{c_*} (\xi_2(s) - \xi_3(s))ds > 0.$$

Function $\xi_2 - \xi_3$ is continuous and non-vanishing on $(a_*, +\infty)$, and by (3.75) it is negative for large real parameters, so it is negative on the whole interval $(a_*, +\infty)$. Since $c_* \in (a_*, +\infty)$, the equality above is only possible if $c_* < a_1$. This proves (3.129).

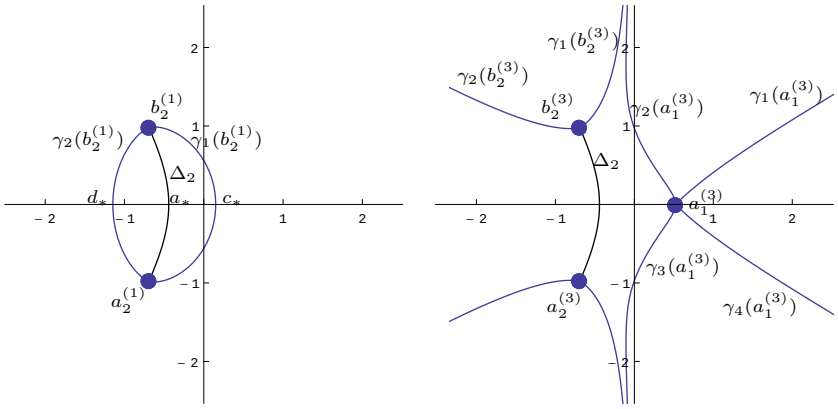

Figure 3.8: $\tau = 0$: blue lines represent the critical graph of ϖ_2 on $\mathcal{R}_1$ (left) and $\mathcal{R}_3$. The black curve is the branch cut Δ_2 connecting $\mathcal{R}_1$ and $\mathcal{R}_3$.

The discussion of the structure of the trajectories $\gamma_1(a_1^{(3)})$, $\gamma_2(a_1^{(3)})$, $\gamma_1(b_2^{(3)})$, $\gamma_2(b_2^{(3)})$ is identical to the analysis of the trajectories $\gamma_j(b_*)$, $\gamma_j(b_2)$, $j = 1, 2$, on $\mathcal{R}_2$ for ϖ_1 above, so we omit the details.

The global structure of the critical graph on ϖ_2 on both sheets is presented in Figure 3.8. The basic conclusion is that with the branch cut Δ_2 specified above, the critical graph splits into two sets: a closed Jordan curve on $\mathcal{R}_1$, containing $a_2^{(1)}$ and $b_2^{(1)}$, and 4 analytic arcs on $\mathcal{R}_3$, starting and ending at $\infty^{(3)}$, each passing through one of the branch points $a_2^{(3)}$, $b_2^{(3)}$ and $a_1^{(3)}$.

3.5.5.3 Trajectories for $0 < \tau < \frac{1}{12}$

A combination of the general principles **P.2** and **P.6** assures us that the finite critical trajectories for $\tau = 0$ remain finite for small perturbations of τ, and that the behavior of the trajectories described for $\tau = 0$ is preserved for τ small.

Let $\varepsilon > 0$ be sufficiently small. The general principle **P.4** above tells us that if we consider the domains $\Omega_\varepsilon^{(1)}$, (respectively $\Omega_\varepsilon^{(2)}$ and $\Omega_\varepsilon^{(3)}$), swept by trajectories of (3.125) passing through points in the ε-neighborhood of $a_1^{(1)}$ (respectively $a_1^{(2)}$ and $a_1^{(3)}$), then there exists a $\delta > 0$ such that the critical trajectories for ϖ and $0 < \tau < \delta$, passing through $a_1^{(j)}$, $j = 1, 2, 3$, belong to $\Omega_\varepsilon = \Omega_\varepsilon^{(1)} \cup \Omega_\varepsilon^{(2)} \cup \Omega_\varepsilon^{(3)}$. These domains are depicted schematically on Figure 3.9.

We should keep in mind that the branch cut Δ_2 now is completely specified by Definition 3.5.5, which is consistent as long as the critical trajectory $\gamma_3(b_2^{(2)})$ joining $a_2^{(2)}$ and $b_2^{(2)}$, *exists* and *remains on* $\mathcal{R}_2$ for the full range of the parameter τ under consideration. The forthcoming analysis shows that this is the case for $\tau \leq \tau_c$.

According to the general principle **P.4**, there exists a $\delta > 0$ small enough such that for $0 < \tau < \delta$, both $a_1^{(j)}, b_1^{(j)} \in \Omega_\varepsilon^{(j)}$, $j = 1, 2, 3$, and the critical trajectories emerging from $a_1^{(j)}, b_1^{(j)}$ stay in $\Omega_\varepsilon^{(j)}$.

For instance, since for $\tau = 0$ the critical trajectories $\gamma_j(a_1^{(3)})$, $j = 1, \ldots, 4$, define three half-plane domains (bounded by $\gamma_1(a_1^{(3)}) \cup \gamma_2(a_1^{(3)})$, $\gamma_3(a_1^{(3)}) \cup \gamma_4(a_1^{(3)})$ and $\gamma_1(a_1^{(3)}) \cup \gamma_4(a_1^{(3)})$, see Figure 3.8, right), they must be persistent under small perturbation of τ, and either $a_1^{(3)}$ or $b_1^{(3)}$, or both, must belong to their boundaries. Taking into account the structure of $\Omega_\varepsilon^{(3)}$ it is straightforward to conclude that for $0 < \tau < \delta$, the trajectories of ϖ through $a_1^{(3)}$ and $b_1^{(3)}$ are as shown in Figure 3.10.

We now examine the trajectories from $a_1^{(1)}$ and $b_1^{(1)}$. The following result comes in very handy:

Proposition 3.5.7. *Defne*

$$\begin{aligned} h(x, y) &= \int_x^y \operatorname{Re}(\xi_{1+}(s) - \xi_3(s))\, ds \\ &= \int_x^y \operatorname{Re}(\xi_{2+}(s) - \xi_3(s))\, ds, \quad \textit{if } x, y \in \Delta_1, \end{aligned} \tag{3.130}$$

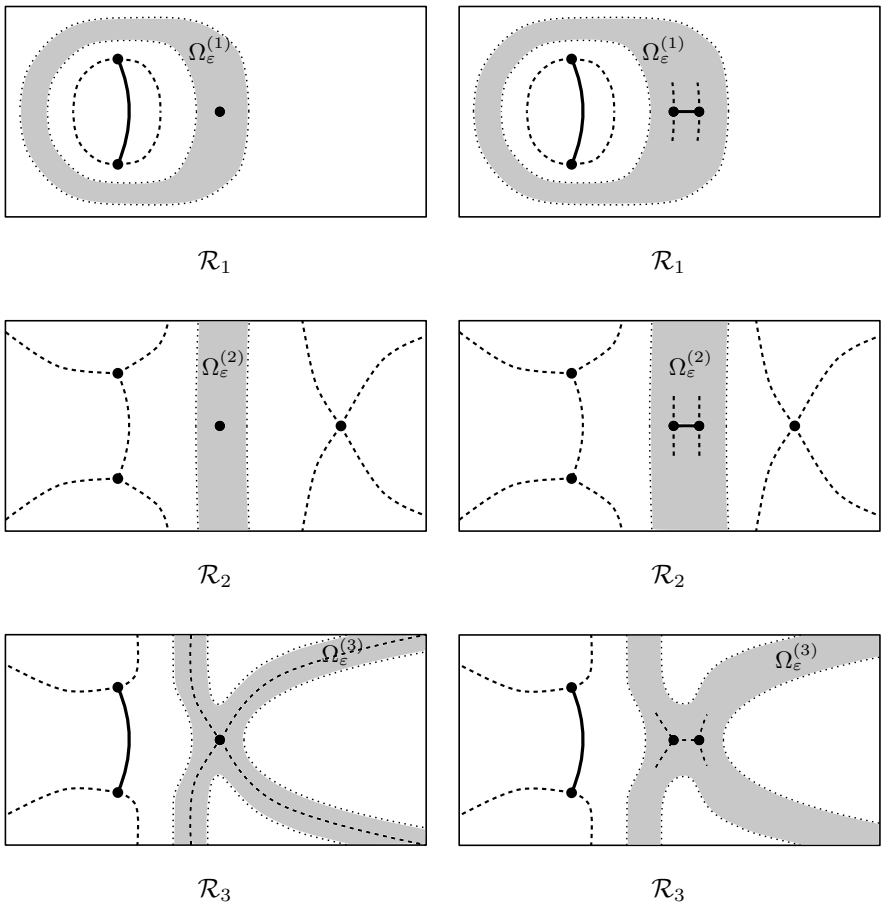

Figure 3.9: Left: critical graph of ϖ for $\tau = 0$, with the domains $\Omega_\varepsilon^{(j)}$, $j = 1, 2, 3$, in gray. Right: local behavior or the critical trajectories for ϖ and $\tau = \delta > 0$, passing through $a_1^{(j)}$, $j = 1, 2, 3$, with the same domains superimposed.

and

$$\begin{aligned} h(x,y) &= \int_x^y \operatorname{Re}(\xi_1(s) - \xi_{2+}(s))\, ds \\ &= \int_x^y \operatorname{Re}(\xi_1(s) - \xi_{3+}(s))\, ds, \quad \textit{if } x, y \in \Delta_3, \end{aligned} \tag{3.131}$$

where we integrate along each interval.

If $0 < \tau < 1/12$, then there exists no pair of values $x \neq y$, $x, y \in \Delta_1$, such that $h(x, y) = 0$.

If $1/12 < \tau < 1/4$, and there exists a pair of values $x \neq y$, $x, y \in \Delta_1$ (resp., $x, y \in \Delta_3$) such that $h(x, y) = 0$, then there exists no such pair of values on Δ_3 (resp., on Δ_1).

Furthermore, if $x_1 < y_1$, $x_2 < y_2$ are two such pairs, $(x_1, y_1) \cap (x_2, y_2) \neq \emptyset$.

Notice that h is well defined on Δ_1 and Δ_3 due to the symmetry relations (3.111) and (3.114), and that $\Delta_3 = \emptyset$ for $1/12 < \tau < \tau_c$.

Proof. Assume that there does exist a pair of values $x < y$, $x, y \in \Delta_1$, such that $h(x, y) = 0$ (same analysis is valid for $x, y \in \Delta_3$). By the mean value theorem, there exists a $u \in (x, y)$ such that

$$\operatorname{Re} \xi_{1+}(u) = \operatorname{Re} \xi_{2+}(u) = \xi_3(u),$$

hence,

$$0 = \operatorname{Re} \xi_{1+}(u) + \operatorname{Re} \xi_{2+}(u) + \xi_3(u) = 3\xi_3(u).$$

But

$$D(u) = -\xi_{1+}(u)\xi_{2+}(u)\xi_3(u) = 0,$$

and the assertion follows from Proposition 3.5.2, keeping in mind that D has exactly one zero on $\Delta_1 \cup \Delta_3$ for $1/12 < \tau < 1/4$. □

One of the consequences of Proposition 3.5.7 is that for $0 < \tau < \delta$, the trajectories emanating from $a_1^{(1)}$ and $b_1^{(1)}$ cannot cut Δ_1 and must stay on the sheet $\mathcal{R}_1$. Thus, using again the general principle **P.4** we conclude that the trajectories $\gamma_k(a_1^{(1)})$, $\gamma_k(b_1^{(1)})$, $k = 1, 2$, are closed and encircle the cut Δ_2, see Figure 3.10.

Similar considerations can be applied to get the behavior for the trajectories emanating from $a_1^{(2)}$, $b_1^{(2)}$, and the final result for τ small is seen in Figure 3.10. We skip the details.

The outcome of our analysis is that the critical graph of ϖ has the structure showed in Figure 3.10, at least for $0 < \tau < \delta$. Our next goal is to prove that this is actually valid for $\tau \in (0, 1/12)$. The continuity principle **P.4** yields that this is the case as long as

(i) No collision of the critical points occur: this is true indeed for $\tau \in (0, 1/12)$, see Section 3.5.4.

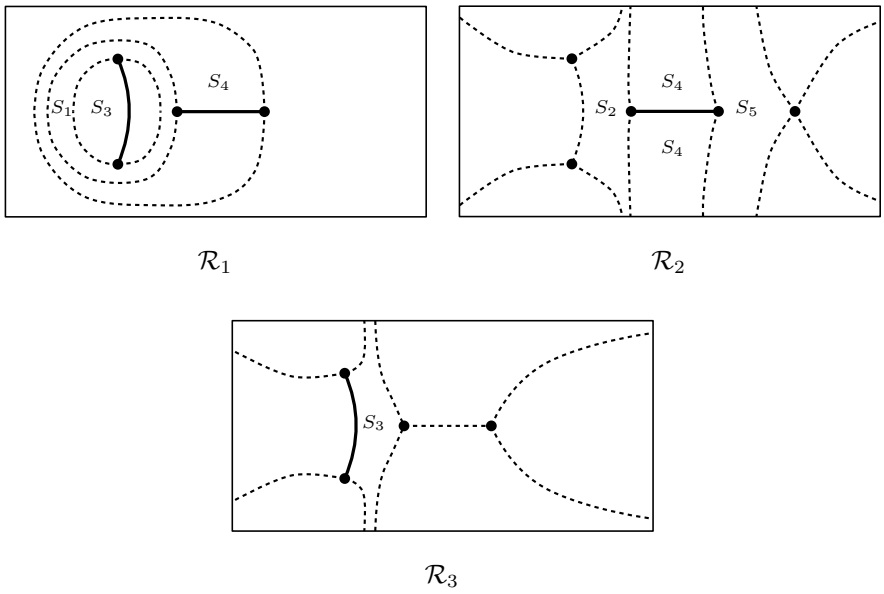

Figure 3.10: Critical graph of ϖ for $0 < \tau < 1/12$, with the strip and ring domains labeled by S_j's. Notice that some of these domains intersect more than one sheet.

(ii) No new domains emerge, which amounts to say that the finite trajectories for $0 < \tau < \delta$ remain critical for $0 < \tau < 1/12$: this is assured by a combination of **P.2** and **P.6**.

(iii) No connected components of the complement of the critical graph "disappear". More precisely, it means that no width of any strip or ring domain becomes zero. These domains for $0 < \tau < \delta$ are identified on Figure 3.10: there is one ring domain S_1 and 4 strip domains, $S_2, \dots, S_5$. There widths $\sigma(S_j)$ (see the definition (A.6) in Section A.3) are given by:

- $\sigma(S_j) = |\omega_j|$, $j = 1, 2, 3$, with ω_j defined in (3.121)–(3.122). They do not vanish for $\tau \in (0, 1/12)$, see Figure 3.4.
- $\sigma(S_4) = |h(a_1, b_1)|$, with h defined in (3.130)–(3.131), which does not vanish for $\tau \in (0, 1/12)$, see Proposition 3.5.7.
- $\sigma(S_5) = \left|\int_{b_1}^{b_*} (\xi_1(s) - \xi_3(s))ds\right|$, which does not vanish for $\tau \in (0, 1/12)$, see (3.108).

We conclude that the critical graph of ϖ, depicted in Figure 3.10, is valid for the whole range $0 < \tau < 1/12$. In particular, the critical trajectory $\gamma_1(a_2^{(2)})$ connects the points $a_2^{(2)}$ and $b_2^{(2)}$, which proves Theorem 3.5.4 for $0 < \tau < 1/12$.

3.5.5.4 Trajectories for $\frac{1}{12} < \tau < \tau_1$

When $\tau = 1/12$, the double point b_* coincides with b_1, and the strip domain S_5 disappears ($\sigma(S_5) \searrow 0$ as $\tau \nearrow 1/12$), see Figure 3.11, left. Clearly, this transition has no impact on the structure of trajectories on the third sheet. Moreover, again a combination of **P.2** and **P.6** assures the finite trajectories for $\tau = 1/12$ remain finite for $1/12 < \tau < 1/12 + \delta$.

Let $\varepsilon > 0$ be sufficiently small. Similarly to what has been done in the previous interval, the general principle **P.4** tells us that if we consider the domains $\Omega_\varepsilon^{(1)}$ and $\Omega_\varepsilon^{(2)}$, swept by trajectories of ϖ passing through points in the ε-neighborhood of $b_1^{(1)}$ and $b_1^{(2)} = b_*^{(2)}$, then there exists a $\delta > 0$ such that the critical trajectories for $1/12 < \tau < 1/12 + \delta$, passing through $b_1^{(j)}$, $j = 1, 2$, and $b_*^{(1)}$, belong to $\Omega_\varepsilon = \Omega_\varepsilon^{(1)} \cup \Omega_\varepsilon^{(2)}$. These domains are also depicted schematically on Figure 3.11, left.

For $1/12 < \tau < 1/12 + \delta$ we consider the first sheet and the trajectories emanating from $b_1^{(1)}$ and $b_*^{(1)}$; thanks to principle **P.2**, we concentrate on the upper half plane $\mathbb{C}_+$ (or to be precise, on its pre-image by π on $\mathcal{R}_1$), namely $\gamma_1(b_*^{(1)})$, $\gamma_2(b_*^{(1)})$, $\gamma_1(b_1^{(1)})$, see Figure 3.11, right. These trajectories must stay in Ω_ε, so they have to intersect $\pi^{-1}(\mathbb{R})$ on $\mathcal{R}_1$. Let us denote the points of intersection of $\gamma_1(b_*^{(1)})$, $\gamma_2(b_*^{(1)})$, $\gamma_1(b_1^{(1)})$ by $x_1^{(1)}$, $x_2^{(1)}$, $x_3^{(1)}$, respectively. Using the general principles **P.2** and **P.3** we must immediately discard the following possibilities: (i) $x_j \geq b_1$ for some j, (ii) $x_1 \leq a_*^{(1)}$ and $x_2 \leq a_*^{(1)}$ (recall that $a_* = \Delta_2 \cap \mathbb{R}$). Since trajectories cannot intersect, it holds $x_1 < x_2 < x_3$ and we conclude that necessarily $x_2 \in (a_1, b_1)$, and consequently, $x_3 \in (a_1, b_1)$ as well. In particular, $h(x_3, b_1) = 0$, in the notation (3.130)–(3.131).

Since x_1 and x_2 belong to trajectories with a common point $b_*^{(1)}$, the assumption $x_1 \in (a_1, b_1)$ yields that $h(x_1, x_2) = 0$, and since $(x_1, x_2) \cap (x_3, b_1) = \emptyset$, this contradicts Proposition 3.5.7.

From the considerations above, it follows that $\gamma_1(b_*^{(1)})$ is closed, stays on $\mathcal{R}_1$, and intersects $\pi^{-1}(\mathbb{R})$ to the left of Δ_2, and the trajectories $\gamma_2(b_*^{(1)})$, $\gamma_1(b_1^{(1)})$ intersect the cut Δ_1 and move to the second sheet $\mathcal{R}_2$. We keep denoting these points of intersection by x_2, x_3 as before. Clearly, $x_3 > x_2$, and Proposition 3.5.7

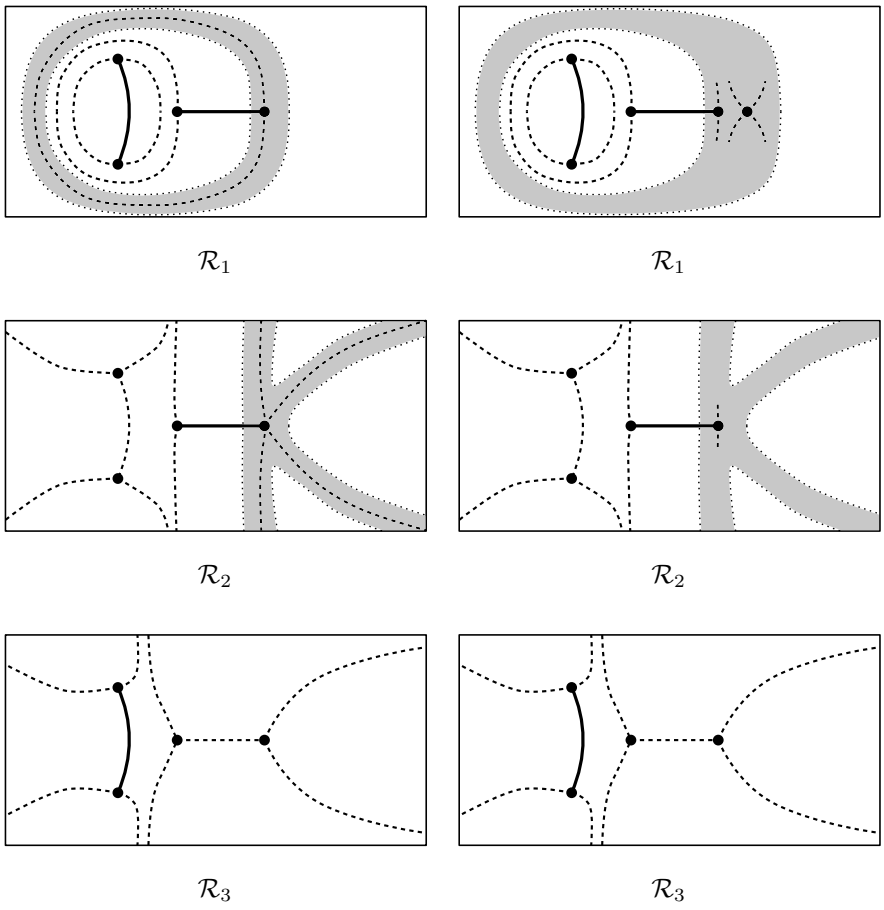

Figure 3.11: Left: critical graph of ϖ for $\tau = 1/12$, with the domains $\Omega_\varepsilon^{(j)}$, $j = 1, 2$, in gray. Right: local behavior or the critical trajectories for ϖ and $\tau = 1/12 + \delta > 0$, passing through $b_1^{(j)}$, $j = 1, 2$, and $b_*^{(1)}$, with the same domains superimposed.

implies that these are the only points of intersection of these trajectories with the interval (a_1, b_1).

Let us turn to the second sheet, $\mathcal{R}_2$ and consider $\gamma_1(b_1^{(2)})$: from the structure of $\Omega_\varepsilon^{(2)}$ it is clear that it either diverges to $\infty^{(2)}$, or intersects the branch cut between a_1 and b_1 and moves to $\mathcal{R}_1$. If we assume the latter, $\Omega_\varepsilon^{(1)}$ shows that

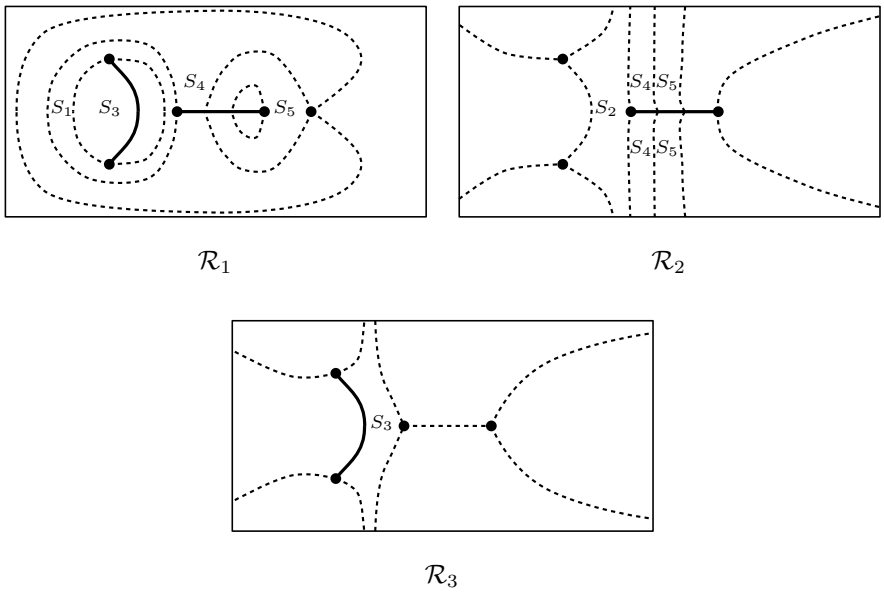

Figure 3.12: Critical graph of ϖ for $1/12 < \tau < \tau_1$, with the strip and ring domains labeled by S_j's. Notice that some of these domains intersect more than one sheet.

either it will return to $\mathcal{R}_2$ at a different point in (a_1, b_1) (in contradiction with Proposition 3.5.7), or it bounds a simply connected domain, which contradicts **P.3**. Hence, $\gamma_1(b_1^{(2)})$ must diverge to $\infty^{(2)}$, and thus $b_1^{(2)}$ lies on the boundary of the half plane domain bounded for $\tau = 1/12$ by $\gamma_1(b_1^{(2)})$ and $\gamma_4(b_1^{(2)})$. In particular, by **P.5**, for $1/12 < \tau < 1/12 + \delta$, $\gamma_1(b_1^{(2)})$ diverges to $\infty^{(2)}$ in the same asymptotic direction given by the angle $\theta_1^{(\infty)}$ from (3.124).

Recall that we concluded that the trajectory $\gamma_1(b_1^{(1)})$ enters $\mathcal{R}_2$ through the cut (a_1, b_1) at a point x_3. The only possibility left for it is to go to $\infty^{(2)}$. Applying Theorem A.3.2 to the ϖ-polygon bounded by the trajectories $\gamma_1(b_1^{(1)})$ and $\gamma_2(b_1^{(2)})$, we get that $\gamma_1(b_1^{(1)})$ goes to $\infty^{(2)}$ in the asymptotic direction given by the angle $\theta_5^{(\infty)}$, and consequently $\gamma_1(b_*^{(1)})$ extends to $\infty^{(2)}$ with angle θ_5 as well.

The outcome of our analysis is that for $1/12 < \tau < 1/12 + \delta$ the critical graph of ϖ has the structure showed in Figure 3.12. We prove that this is actually valid for $\tau \in (1/12, \tau_1)$. Again, the continuity principle **P.4** yields that this

is the case as long as (i) no collision of the critical points occur (this is true indeed for $\tau \in (1/12, 1/4)$, see Section 3.5.4), (ii) finite critical trajectories for $1/12 < \tau < 1/12 + \delta$ remain finite for $1/12 < \tau < \tau_1$ (assured by a combination of **P.2** and **P.6**); and (iii) no width of any strip and ring domains become zero. These domains for $1/12 < \tau < 1/12 + \delta$ are identified on Figure 3.12: there is one ring domain S_1 and 4 strip domains, $S_2, \ldots, S_5$. There widths $\sigma(S_j)$ are given by:

- $\sigma(S_j) = |\omega_j|$, $j = 1, 2, 3$, with ω_j defined in (3.121)–(3.122). They do not vanish for $1/12 < \tau < \tau_1$, see Figure 3.4, although $\sigma(S_1)$ does vanish for $\tau = \tau_1$.
- $\sigma(S_4)$ is given by the absolute value of

$$\operatorname{Re} \int_{a_1}^{b_*} (\xi_2(s) - \xi_3(s)) = \operatorname{Re} \int_{a_1}^{b_2} (\xi_2(s) - \xi_3(s)) ds \tag{3.132}$$

$$+ \operatorname{Re} \int_{b_2}^{b_*} (\xi_2(s) - \xi_3(s)) ds$$

$$= -\omega_1 + \omega_4, \tag{3.133}$$

  and $\omega_1 \neq \omega_4$ for $\tau > 1/12$, see Figure 3.4 in Section 3.5.3.
- $\sigma(S_5) = \left| \int_{b_1}^{b_*} (\xi_2(s) - \xi_3(s)) ds \right|$, which does not vanish for $\tau > 1/12$, see (3.109).

We conclude that the critical graph of ϖ, depicted in Figure 3.12, is valid for the whole range $1/12 < \tau < \tau_1$. In particular this yields Theorem 3.5.4 in the mentioned range of τ.

3.5.5.5 Trajectories for $\tau_1 < \tau < \tau_c$

At the value $\tau = \tau_1$ the critical trajectory $\gamma_1(b_2^{(1)})$ on the first sheet hits the branch point $a_1^{(1)}$, so that the ring domain S_1 disappears ($\sigma(S_1) \searrow 0$ as $\tau \nearrow \tau_1$), see Figure 3.12. From the analysis of the behavior of the rest of the widths $\sigma(S_j)$ and the other finite critical trajectories, it follows that this fact does not affect the rest of the strip domains - note that there are no other ring domains. In particular, the trajectories emerging from a_1, a_2, and b_2 on the sheets $\mathcal{R}_2$, $\mathcal{R}_3$ do not display any phase transition.

The critical graph for $\tau = \tau_1$ is depicted in Figure 3.13. In accordance with the methodology we have followed so far, we fix an $\varepsilon > 0$

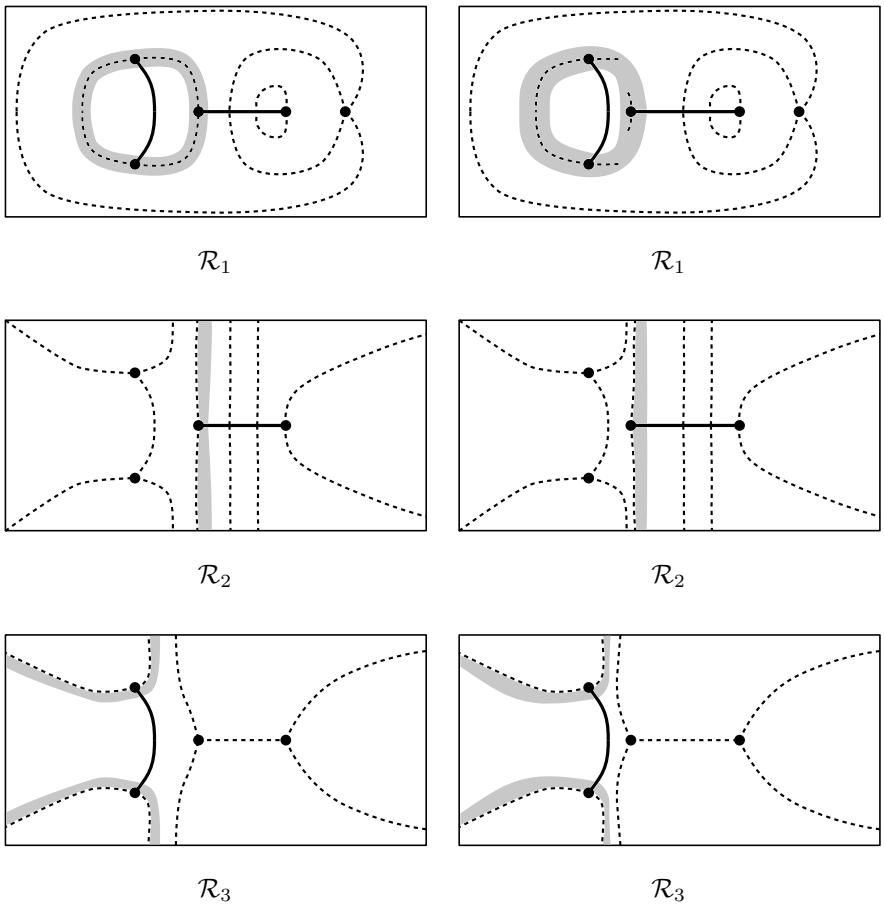

Figure 3.13: Left: critical graph of ϖ for $\tau = \tau_1$, with the domain Ω_ε in gray. Right: local behavior or the critical trajectories for ϖ and $\tau = \tau_1 + \delta > 0$, passing through $b_2^{(1)}$ and $a_1^{(1)}$, with the same domain superimposed.

sufficiently small and consider the domain Ω_ε swept by trajectories of ϖ passing through points in the ε-neighborhood of $b_2^{(1)}$ and $a_1^{(1)} = a_*^{(1)}$. Notice that Ω_ε no longer lives on the single sheet, and its boundary now also contains critical trajectories, namely $\gamma_j(a_1^{(2)})$, $\gamma_j(a_2^{(3)})$, $\gamma_j(b_2^{(3)})$, $j = 1, 2$. This is so because, as already mentioned, there is no transition for these trajectories. Observe also that when $\tau \nearrow \tau_1$ the trajectory $\gamma_2(b_2^{(1)}) = \gamma_2(a_2^{(1)})$ does not collide with any

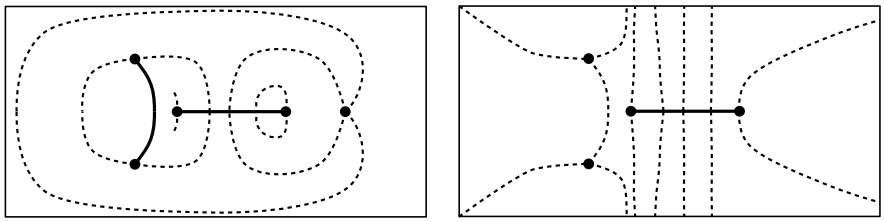

Figure 3.14: Some trajectories of ϖ on the first two sheets, for $\tau_1 < \tau < \tau_c$.

critical point other than its endpoints, hence its topology is unchanged under small perturbations of τ around τ_1. In fact, there exists a $\delta > 0$ such that the critical trajectories for $\tau_1 < \tau < \tau_1 + \delta$, passing through $b_1^{(1)}$, belong to Ω_ε. This domain is also depicted schematically on Figure 3.13, left.

We now consider the possible behavior of $\gamma_1(b_2^{(1)})$ for $\tau_1 < \tau < \tau_1 + \delta$, having in mind that it cannot leave the shaded region Ω_ε, which shows that either $\gamma_1(b_2^{(1)})$ moves immediately to $\mathcal{R}_3$ through Δ_2, or it intersects the (preimage of) the real line near a_1.

In the first case, $\gamma_1(b_2^{(1)})$ extends to $\infty^{(3)}$ with angle $\theta_3^{(\infty)}$. Thus $\gamma_1(b_2^{(1)}) \cup \gamma_2(b_2^{(3)})$ is the boundary of a ϖ-polygon for which $\kappa = 1$ and $\lambda = 0$, contradicting (A.7).

Assume otherwise, so that $\gamma_1(b_2^{(1)})$ intersects the (preimage of the) real line at a point $x^{(1)}$, x close to a_1. If $x \le a_1$, we integrate from b_2 to x over $\gamma_1(b_2^{(1)})$ and then from x to a_1 over the real line to get

$$\begin{aligned} \omega_1 &= \operatorname{Re} \int_{b_2}^{x} (\xi_2(s) - \xi_3(s))ds + \int_{x}^{a_1} (\xi_2(s) - \xi_3(s))ds \\ &= \int_{x}^{a_1} (\xi_2(s) - \xi_3(s))ds. \end{aligned} \tag{3.134}$$

In the range of τ considered, $\omega_1 > 0$, while the last integral is ≤ 0, see (3.107), which leads us into a contradiction. Hence, $x \in (a_1, b_1)$, so that $\gamma_1(b_2^{(1)})$ moves to the second sheet. Recall that if $x_3^{(1)}$ is the point of intersection of $\gamma_2(b_1^{(1)})$ with Δ_1, we already have $h(x_3, b_1) = 0$, so by Proposition 3.5.7, $\gamma_1(b_2^{(1)})$ cannot return to $\mathcal{R}_1$; in consequence, it stays on the second sheet and diverges to $\infty^{(2)}$ in the asymptotic direction corresponding to the angle $\theta_5^{(\infty)}$, see Figure 3.14.

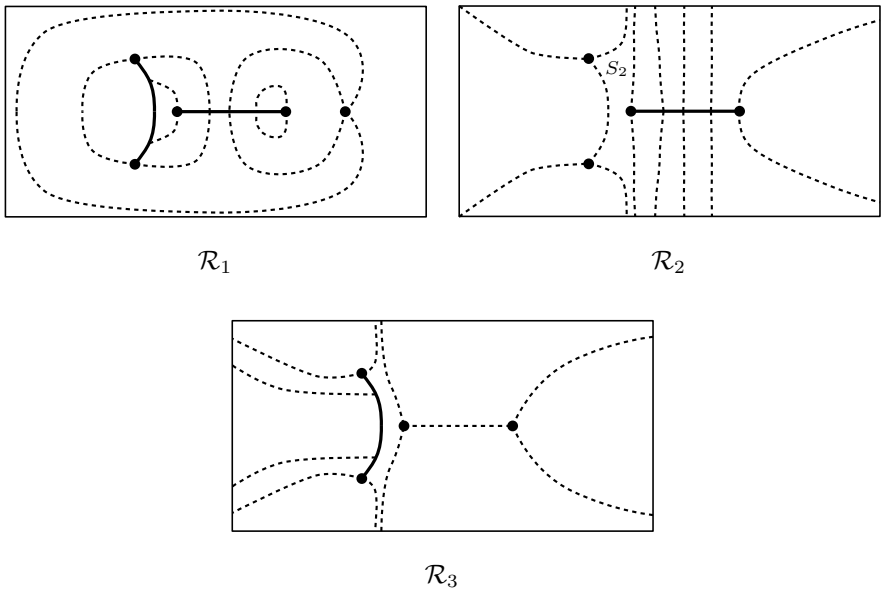

Figure 3.15: Global structure of trajectories for $\tau_1 < \tau < \tau_c$.

On the other hand, trajectories $\gamma_j(a_1^{(1)})$, $j = 1, 2$, are "trapped" between $\gamma_1(b_2^{(1)})$ and the branch cut $\Delta_2^{(2)}$, see Figure 3.14, left. Thus, they cannot stay on $\mathcal{R}_1$ without violating the general principle **P.3**, so they move to the third sheet and diverge to $\infty^{(3)}$ in the asymptotic directions corresponding to the angles $\theta_3^{(\infty)}$ and $\theta_4^{(\infty)}$, respectively.

The outcome of our analysis is that for $\tau_1 < \tau < \tau_1 + \delta$ the critical graph of ϖ has the structure showed in Figure 3.15. Same analysis as in the previous section shows that this is actually valid for the whole range $\tau_1 < \tau < \tau_c$, in particular implying Theorem 3.5.4 for this range of τ.

3.5.5.6 Trajectories for $\tau_c < \tau < \tau_2$

We come to the topologically most important phase transition. According to Definition 3.5.5, we use the lift of the trajectory joining $a_2^{(2)}$ and $b_2^{(2)}$ on $\mathcal{R}_2$ as the branch cut connecting the sheets $\mathcal{R}_1$ and $\mathcal{R}_3$. When $\tau = \tau_c$, the strip domain S_2 disappears ($\sigma(S_2) \searrow 0$ as $\tau \nearrow \tau_c$), and this trajectory finally reaches the branch point $a_1^{(2)}$, see Figure 3.15. Note that this transition corresponds to

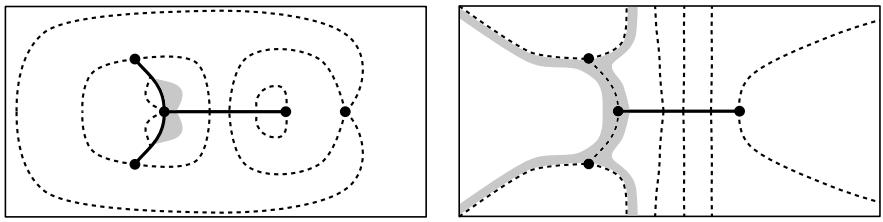

$\mathcal{R}_1$ $\mathcal{R}_2$

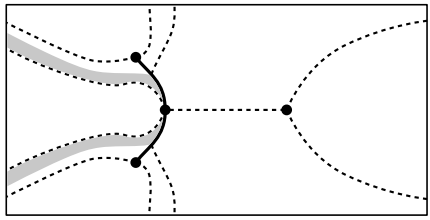

$\mathcal{R}_3$

Figure 3.16: Critical graph of ϖ for $\tau = \tau_c$, with the domain Ω_ε in gray, consisting of the trajectories for ϖ passing through the ε-neighborhood of $a_1^{(2)}$, $a_2^{(2)}$, and $b_2^{(2)}$.

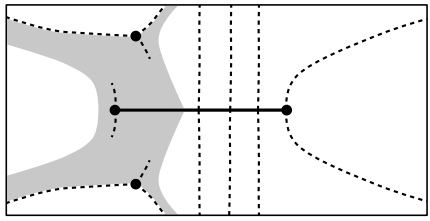

Figure 3.17: The domain Ω_ε on $\mathcal{R}_2$ for $\tau_c < \tau < \tau_c + \delta$.

(3.34). We fix an $\varepsilon > 0$ sufficiently small and consider the domain Ω_ε swept by trajectories of ϖ passing through points in the ε-neighborhood of $a_1^{(2)}$, $a_2^{(2)}$, and $b_2^{(2)}$. The critical graph for $\tau = \tau_c$ along with Ω_ε is displayed in Figure 3.16.

For $\tau_c < \tau < \tau_c + \delta$ we examine first the second sheet and the trajectories emanating from $a_1^{(2)}$, $a_2^{(2)}$, and $b_2^{(2)}$. For a sufficiently small $\delta > 0$, these trajectories must stay in Ω_ε, see Figure 3.17.

Analyzing $\gamma_1(a_1^{(2)})$ we have to discard the following possibilities:

- $\gamma_1(a_1^{(2)})$ cannot intersect (the preimage by π of) the real line to the left of a_1 without violating the general principle **P.3**.
- it cannot intersect (the preimage by π of) the real line to on the cut (a_1, b_1) either: otherwise the equation $h(x, a_1) = 0$ has a solution in $x \in (a_1, b_1)$, along with the identity $h(x_3, b_1) = 0$, where $x_3^{(1)}$ is the point of intersection of $\gamma_2(b_1^{(1)})$ with Δ_1, and since $(a_1, x) \cap (x_3, b_1) = \emptyset$, this would contradict Proposition 3.5.7.
- $\gamma_1(a_1^{(2)}) \neq \gamma_3(b_2^{(2)})$, because $\omega_2 \neq 0$ for $\tau > \tau_c$, see Figure 3.4.
- $\gamma_1(a_1^{(2)})$ cannot diverge to $\infty^{(2)}$ in the asymptotic direction $\theta_2^{(\infty)}$. Indeed, otherwise either $\gamma_3(b_2^{(2)})$ also diverges to $\infty^{(2)}$ in the same direction, or it intersects the real axis to the left of $a_1^{(2)}$. In the former case, we get a ϖ-polygon for which $\kappa = 1$ and $\lambda = 0$, contradicting (A.7), and in the latter one we proceed as in (3.134) (with ω_1 replaced by ω_2) to get a contradiction.

The only possibility left for $\gamma_1(a_1^{(2)})$ is to diverge to $\infty^{(2)}$ in the asymptotic direction $\theta_3^{(\infty)}$. Since it was already observed that $\gamma_3(b_1^{(2)})$ cannot diverge to $\infty^{(2)}$, it must intersect $\pi^{(-1)}(\mathbb{R})$ to the right of a_1.

The outcome of our analysis on the second sheet, as well as the region Ω_ε on the remaining sheets, is displayed in Figure 3.18. The cut Δ_2 is chosen in such a way that its projection on $\mathcal{R}_2$ coincides with $\left(\gamma_3(b_2^{(2)}) \cup \gamma_1(a_2^{(2)})\right) \cap \mathcal{R}_2$.

What is left is to describe the behavior of $\gamma_3(b_2^{(2)})$ on the rest of the sheets. We already saw that this trajectory has to move to $\mathcal{R}_1$ through the cut Δ_1. It cannot intersect Δ_1 again (see Proposition 3.5.7), and it must stay in the region Ω_ε displayed in Figure 3.18. Hence, the only possibility is that $\gamma_3(b_2^{(2)})$ intersects the cut Δ_2, moves to the sheet $\mathcal{R}_3$ and diverges to $\infty^{(3)}$ in the asymptotic direction $\theta_4^{(\infty)}$.

The critical graph of ϖ for $\tau_c < \tau < \tau_c + \delta$ has the structure showed in Figure 3.19, and we now prove that this is actually valid for $\tau \in (\tau_c, \tau_2)$. Again, the continuity principle **P.4** yields that this is the case as long as (i) no collision of the critical points occur (this is true indeed for $\tau \in (\tau_c, \tau_2)$, see Section 3.5.4); (ii) finite trajectories for $\tau_c < \tau < \tau_c + \delta$ remain finite for $\tau \in (\tau_c, \tau_2)$ (assured by a combination of **P.2** and **P.6**) and (iii) no width of any strip domains become zero. These domains for $\tau_c < \tau < \tau_c + \delta$ are identified on Figure 3.19; observe that there are now 7 strip domains S_j, and no ring domains. Let us compute their widths $\sigma(S_j)$.

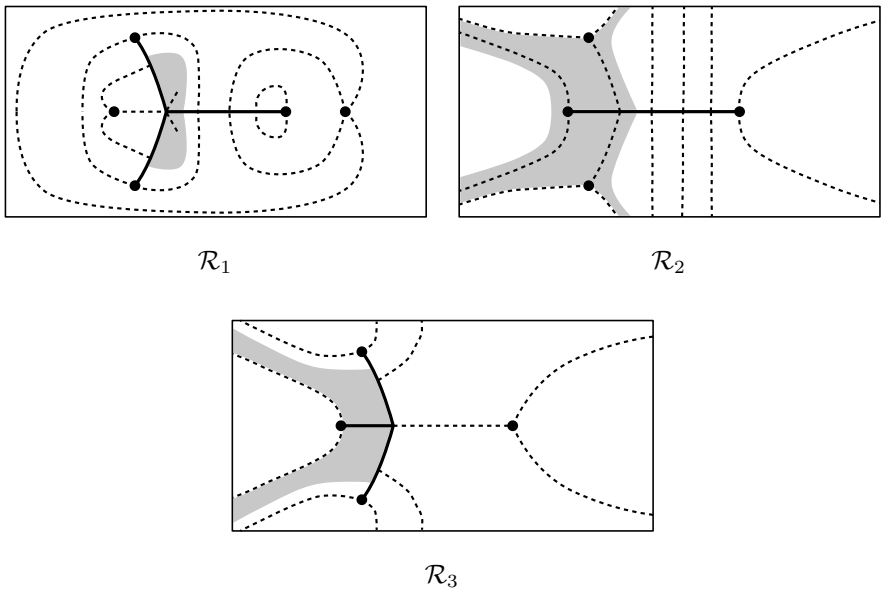

Figure 3.18: Part of the critical graph of ϖ for $\tau_c < \tau < \tau_c + \delta$, with the domain Ω_ε in gray, consisting of the trajectories for ϖ passing through the ε-neighborhood of $a_1^{(2)}$, $a_2^{(2)}$ and $b_2^{(2)}$.

Lemma 3.5.8. *For $\tau_c < \tau < \tau_2$,*

$$\sigma(S_1) = \sigma(S_2) = \sigma(S_3) = |\omega_1(\tau)|,$$

with $\omega_1(\tau)$ defined in (3.121).

Proof. The fact that $\sigma(S_1) = |\omega_1|$ is the straightforward consequence of the definition of ω_1. Also $\sigma(S_2) = \sigma(S_3)$ by the symmetry under conjugation. So, it remains to compute the width $\sigma(S_2)$, given by the absolute value of the real part of the integral

$$\begin{aligned}\int_{b_2^{(2)}}^{a_2^{(1)}=a_2^{(3)}} \sqrt{-\varpi} &= \int_{b_2^{(2)}}^{a_1^{(2)}=a_1^{(3)}} Q(s)ds + \int_{a_1^{(3)}}^{a_2^{(3)}} Q(s)ds \\ &= \int_{b_2}^{a_1} (\xi_1(s) - \xi_3(s))ds + \int_{a_1}^{a_2} (\xi_1(s) - \xi_2(s))ds.\end{aligned}$$

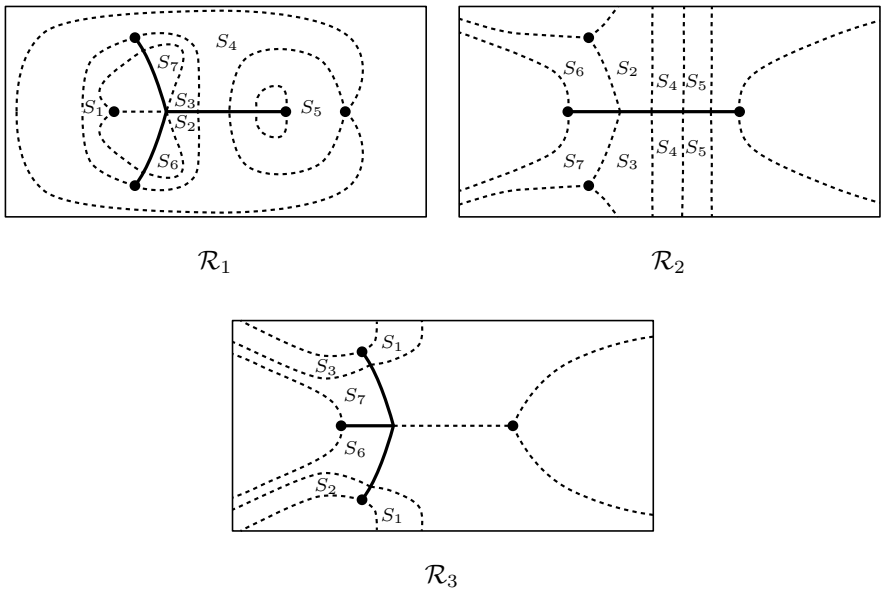

Figure 3.19: Critical graph of ϖ for $\tau_c < \tau < \tau_2$, with the strip domains labeled by S_j's.

Symmetry under conjugation tells us

$$\operatorname{Re}\int_{a_1}^{a_2}(\xi_1(s)-\xi_2(s))ds = \operatorname{Re}\int_{a_1}^{b_2}(\xi_1(s)-\xi_2(s))ds,$$

and using it in the previous identity, we get

$$\begin{aligned}\sigma(S_2) &= \left|\operatorname{Re}\int_{b_2}^{a_1}(\xi_1(s)-\xi_3(s))ds - \operatorname{Re}\int_{b_2}^{a_1}(\xi_1(s)-\xi_2(s))ds\right| \\ &= \left|\operatorname{Re}\int_{b_2}^{a_1}(\xi_3(s)-\xi_2(s))ds\right| = |\omega_1|.\end{aligned}$$

□

Lemma 3.5.8 implies that $\sigma(S_j) \neq 0$, $j = 1, 2, 3$, for $\tau_c \leq \tau < \tau_2$, although $\sigma(S_j) \searrow 0$ as $\tau \nearrow \tau_2$, $j = 1, 2, 3$, see Figure 3.4.

Regarding the rest of the strip domains,

- $\sigma(S_4) = |\omega_4| \neq 0$ for $\tau_c \leq \tau \leq \tau_2$, see again Figure 3.4.

- $\sigma(S_5) = \left|\int_{b_1}^{b_*}(\xi_2(s) - \xi_3(s))ds\right|$, which does not vanish for $\tau > 1/12$, see (3.109).
- From the symmetry by complex conjugation, $\sigma(S_6) = \sigma(S_7)$, and the structure of S_6 on $\mathcal{R}_2$ shows that $\sigma(S_6) = |\omega_2|$, so that $\sigma(S_6) = \sigma(S_7) \neq 0$ for $\tau_c < \tau \leq \tau_2$.

Consequently, the critical graph displayed in Figure 3.19 is valid for $\tau_c < \tau < \tau_2$. In particular it implies Theorem 3.5.4 for $\tau_c \in (\tau_c, \tau_2)$.

3.5.5.7 Trajectories for $\tau_2 < \tau < 1/4$

Lemma 3.5.8 shows that at $\tau = \tau_2$, the strip domains S_1, S_2 and S_3 displayed in Figure 3.19 disappear *simultaneously*, which happens because at that moment the branch point $a_1^{(1)}$ hits the critical trajectory $\gamma_1(a_2^{(1)}) = \gamma_2(b_2^{(1)})$ and the point a_* of intersection of Δ_2 with the real line collides with the critical trajectories $\gamma_2(a_2^{(1)})$ and $\gamma_1(b_2^{(1)})$. The resulting critical graph is shown in Figure 3.20.

As before, we fix an $\varepsilon > 0$ sufficiently small and consider the domain Ω_ε swept by trajectories of ϖ passing through points in the ε-neighborhood of $a_1^{(1)}$, $a_2^{(1)}$, $b_2^{(1)}$ and $a_*^{(j)}$. Observe that for a small perturbation of $\tau = \tau_2$, $\gamma_3(b_2^{(2)}) \cap \mathcal{R}_2$ does not coalesce with critical points other than the starting point $b_2^{(2)}$, hence this arc of critical trajectory displays the same structure as for $\tau = \tau_2$. In particular, the cut Δ_2 is well defined as the projection of $(\gamma_3(b_2^{(2)}) \cup \gamma_1(a_2^{(2)})) \cap \mathcal{R}_2$ on the other sheets. Thus, there exists a $\delta > 0$ such that the critical trajectories for $\tau_2 < \tau < \tau_2 + \delta$, passing through the above mentioned critical points, belong to Ω_ε. This domain is also depicted schematically on Figure 3.20, left.

Lemma 3.5.9. *Let t be a point on the part of the curve $\Delta_2^{(1)}$ joining $b_2^{(1)}$ with $a_*^{(1)}$, and γ a Jordan curve on $\mathcal{R}_1$ connecting the boundary values $t_\pm$ on $\Delta_2^{(1)}$ and containing the only branch point $b_2^{(1)}$ inside. Then*

$$\operatorname{Re}\int_\gamma Q(s)ds = \operatorname{Re}\int_\gamma (\xi_{2+}(s) - \xi_{3+}(s))ds = 0.$$

Proof. We can deform γ to the cut Δ_2. If we denote by $\Delta_2(t)$ the arc of Δ_2 from b_2 to t, we get

$$\operatorname{Re}\int_\gamma Q(s)ds = \operatorname{Re}\int_{\Delta_2(t)} (\xi_{2+}(s) - \xi_{3+}(s))ds - \operatorname{Re}\int_{\Delta_2(t)} (\xi_{2-}(s) - \xi_{3-}(s))ds.$$

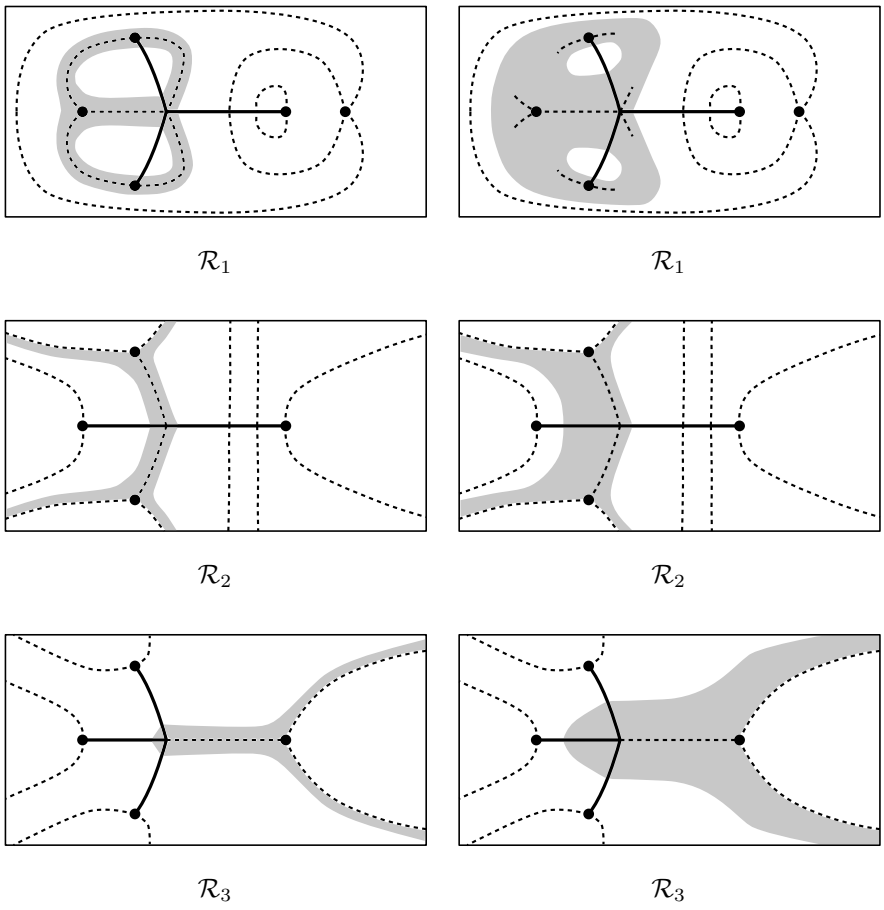

Figure 3.20: Left: critical graph of ϖ for $\tau = \tau_2$, with the domain Ω_ε in gray. Right: local behavior or the critical trajectories for ϖ and $\tau = \tau_2 + \delta > 0$, passing through $a_1^{(1)}$, $a_2^{(1)}$, $b_2^{(1)}$ and a_*, with the same domain superimposed.

Using the jump condition (3.113) and the fact that $\Delta_2^{(2)}$ is an arc of trajectory of ϖ, we thus conclude

$$\begin{aligned}\operatorname{Re}\int_\gamma Q(s)ds &= \operatorname{Re}\int_{\Delta_2(t)} (\xi_{3-}(s) - \xi_{3+}(s))ds \\ &= \operatorname{Re}\int_{\Delta_2(t)} (\xi_{1+}(s) - \xi_{3+}(s))ds \\ &= \operatorname{Re}\int_{\Delta_2^{(2)}(t)} Q_+(s)ds = 0,\end{aligned}$$

and the proof is complete. □

Now we describe the critical trajectories for $\tau_2 < \tau < \tau_2 + \delta$, starting with $\gamma_2(a_1^{(1)})$. Notice first that in this case $\omega_1 \neq 0$, so that $\gamma_2(a_1^{(1)})$ cannot contain $b_2^{(1)}$. Furthermore, if $\gamma_2(a_1^{(1)})$ intersects the cut Δ_2 (and thus diverges to $\infty^{(2)}$ in the asymptotic direction $\theta_1^{(\infty)}$), then $\gamma_1(a_1^{(1)}) \cup \gamma_2(a_1^{(1)}) \cup \gamma_1(b_1^{(3)})$ determines a ϖ-polygon for which $\kappa = 1$ and $\lambda = 0$, in a contradiction with (A.7).

Keeping in mind that $\gamma_2(a_1^{(1)})$ must belong to Ω_ε we conclude that it has to intersect the real axis in one of the sheets. Let us denote by x the point of the first intersection of this trajectory with $\pi^{-1}(\mathbb{R})$. Again, we discard some cases:

- x cannot be on $\mathcal{R}_1$ to the left of a_1: this yields (by the general principle **P.2**) that $\gamma_2(a_1^{(1)}) = \gamma_3(a_1^{(1)})$, violating **P.3**.
- x cannot be on $\mathcal{R}_1$ to the right of a_*.

  Indeed, if $x > a_*$, we form a curve γ given by the union of three pieces: γ_1 is the arc of $\gamma_1(a_1^{(1)})$ from $a_*^{(1)}$ to $a_1^{(1)}$, γ_2 is the arc of $\gamma_2(a_1^{(1)})$ from $a_1^{(1)}$ to x, and γ_3 is the interval from x to $a_*^{(1)}$. This curve satisfies the assumptions of Lemma 3.5.9, so that

$$\operatorname{Re} \int_\gamma (\xi_{2+}(s) - \xi_{3+}(s))ds = 0.$$

  Since

$$\operatorname{Re} \int_{\gamma_1 \cup \gamma_2} (\xi_{2+}(s) - \xi_{3+}(s))ds = 0$$

  by the definition of trajectories, we conclude that

$$\operatorname{Re} \int_{a_*}^{x} (\xi_{2+}(s) - \xi_{3+}(s))ds = 0,$$

  that is, $h(a_*, x) = 0$, in the notation (3.130)–(3.131). But if $x_3^{(1)}$ is the point of intersection of $\gamma_2(b_1^{(1)})$ with Δ_1, we also have $h(x_3, b_1) = 0$, and since $(a_*, x) \cap (x_3, b_1) = \emptyset$, this would contradict Proposition 3.5.7.
- x cannot be on $\mathcal{R}_2$ to the left of a_* (in other words, x cannot belong to Δ_3, which could occur if the trajectory $\gamma_2(a_1^{(1)})$ had slipped to the second sheet through the cut Δ_2 before hitting the real line): this yields

$$\operatorname{Re} \int_{x}^{a_*} (\xi_{1+}(s) - \xi_{3+}(s))ds = 0,$$

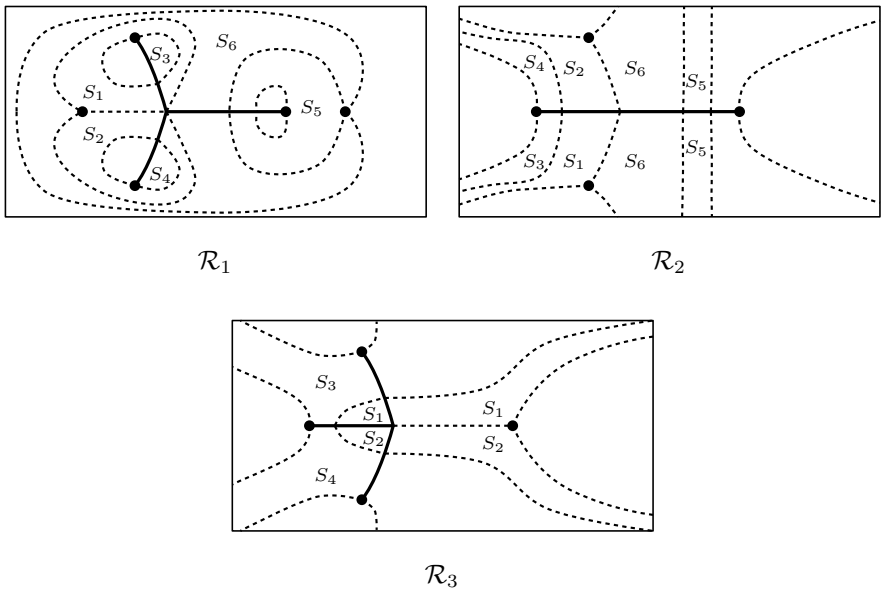

Figure 3.21: Critical graph of ϖ for $\tau_2 < \tau < 1/4$, with the strip domains labeled by S_j's.

that is, $h(x, a_*) = 0$, in the notation (3.130)–(3.131), with $x, a_* \in \Delta_3$. But if $x_3^{(1)}$ is the point of intersection of $\gamma_2(b_1^{(1)})$ with Δ_1, we also have $h(x_3, b_1) = 0$, in contradiction with Proposition 3.5.7.

The only possibility left is that $\gamma_2(a_1^{(1)})$ hits the real line *precisely* at the point a_*. This means also that $\gamma_2(a_1^{(1)}) = \gamma_1(a_2^{(2)})$, as shown in Figure 3.21.

Regarding trajectories $\gamma_1(b_2^{(1)})$ and $\gamma_2(b_2^{(1)})$, they cannot satisfy $\gamma_1(b_2^{(1)}) = \gamma_2(b_2^{(1)})$, and due to principle **P.3** they must belong to Ω_ε. Hence, they have to behave as shown in Figure 3.21. We skip the details.

The critical graph of ϖ for $\tau_2 < \tau < \tau_2 + \delta$ has the structure showed in Figure 3.21, and we prove that this is actually valid for $\tau \in (\tau_2, 1/4)$. The continuity principle **P.4** yields that this is the case as long as (i) no collision of the critical points occur (this is true indeed for $\tau \in (\tau_2, 1/4)$, see Section 3.5.4), (ii) the finite critical trajectories for $\tau_2 < \tau < \tau_2 + \delta$ remain finite in the range $\tau \in (\tau_2, 1/4)$ (certainly true by a combination of **P.2** and **P.6**) and (iii) no width of any strip domains become zero. These domains for $\tau_2 < \tau < \tau_2 + \delta$ are identified on Figure 3.21; observe that there are now 6 strip domains S_j,

and no ring domains. Their widths $\sigma(S_j)$ are:

- $\sigma(S_1) = \sigma(S_2) = |\omega_1| \neq 0$ for $\tau \in (\tau_2, 1/4)$.
- $\sigma(S_3) = \sigma(S_4) = |\omega_3| \neq 0$ for $\tau \in (\tau_2, 1/4)$.
- $\sigma(S_5) = \left|\int_{b_1}^{b_*} (\xi_2(s) - \xi_3(s))ds\right|$, which does not vanish for $\tau > 1/12$, see (3.109).
- As in (3.133), we get that $\sigma(S_6) = |\omega_4 - \omega_1|$, and $\omega_1 \neq \omega_4$ for $\tau > 1/12$, see Figure 3.4 in Section 3.5.3.

We conclude that the structure of the critical graph of ϖ, depicted in Figure 3.21, is actually valid for the whole range $\tau \in (\tau_2, 1/4)$. This finishes the proof of Theorem 3.5.4.

Remark 3.5.10. The attentive reader might notice that in Figure 3.19, for instance, the critical trajectories $\gamma_1(a_2^{(2)})$ and $\gamma_2(a_1^{(1)})$ intersect the cut Δ_2 in $\mathcal{R}_1$ on pairs of opposite points $t_\pm$. This phenomenon, which also occurs in Figure 3.21, is easily explained by Lemma 3.5.9.

Remark 3.5.11. It follows from the results of Sections 3.5.5.3–3.5.5.7 that the trajectories $\gamma_1(b_2^{(2)})$ and $\gamma_2(b_2^{(2)})$ determine a half plane domain H. In particular, this implies that there is an orthogonal critical trajectory γ_1 emerging from $b_2^{(2)}$ which is entirely contained in H and extends to $\infty^{(2)}$ along the angle $2\pi/3$. Similarly, there is an orthogonal critical trajectory γ_2 (which is the complex conjugate of γ_1) emerging from $a_2^{(2)}$ and extending to $\infty^{(2)}$ along the angle $-2\pi/3$. Then the projected contour

$$\Gamma = \pi(\gamma_1 \cup \gamma_2) \cup \Delta_2$$

satisfies the conditions stated in (3.78)–(3.80).

3.6 Proof of Theorem 3.2.3 in the general case

The proof of Theorem 3.2.3 presented in Section 3.3 is valid when the set $\widehat{S}_\alpha \subset S_\alpha$ of double poles of the coefficient D in (3.13) is empty (see Proposition 3.3.8). Our goal now is to show that for a vector of measures $\vec{\mu} \in \mathcal{M}_\alpha$ whose components are supported on a finite union of analytic arcs, and such that the associated functions ξ_j in (3.17) satisfy (3.13) for a polynomial R and a rational function D, the equality

$$\mathcal{D}_h(\vec{\mu}) = 0 \tag{3.135}$$

is valid for every function $h \in C^2(\mathbb{C})$, without any further restriction on the poles of D. Recall that this fact was established so far for the Cauchy kernels h_z defined in (3.39), and when $\operatorname{supp} h \cap \widehat{S}_\alpha = \emptyset$, see Proposition 3.3.8.

As a first step, we extend (3.135) to polynomials:

Lemma 3.6.1. *Under the assumptions of Theorem 3.2.3, $\mathcal{D}_q(\vec{\mu}) = 0$ for every algebraic polynomial q.*

Proof. Fix $\rho > 0$ for which

$$\operatorname{supp}\mu_1 \cup \operatorname{supp}\mu_2 \cup \operatorname{supp}\mu_3 \subset V_\rho := \{x \in \mathbb{C} \mid |x| < \rho\}.$$

For $x \in V_\rho$ and z sufficiently large, we can expand

$$h_z(x) = -\sum_{j=0}^{\infty} \frac{x^j}{z^{j+1}},$$

which implies the identity

$$p_{n-1}(x,z) - z^{n+1}h_z(x) = x^n + w_z(x), \tag{3.136}$$

where the function

$$w_z(x) = \sum_{j=n+1}^{\infty} \frac{x^j}{z^{j-n}}$$

converges to 0 as $z \to \infty$ uniformly for $x \in V_\rho$, and $p_{n-1}(x,z)$ is a polynomial of degree $n-1$ in x, given explicitly by

$$p_{n-1}(x,z) = -\sum_{j=0}^{n-1} x^j z^{n-j}.$$

Set $p_{-1} \equiv 0$. If

$$q(x) = \sum_{n=0}^{N} a_n x^n$$

is a polynomial of degree N, then (3.136) shows that

$$q(x) = -zq(z)h_z(x) + Q_z(x) + W_z(x), \tag{3.137}$$

where

$$Q_z(x) = \sum_{n=0}^{N} a_n p_{n-1}(x,z), \quad W_z(x) = -\sum_{n=0}^{N} a_n w_z(x).$$

Note that Q is a polynomial of degree $N-1$ in x.

Moreover, W_z and W_z' both converge to 0 as $z \to \infty$ uniformly for $x \in V_\rho$. Hence, the convergences

$$\frac{W_z(x) - W_z(y)}{x - y} \to 0, \quad \Phi'(x) W_z(x) \to 0 \quad \text{as } z \to \infty$$

hold uniformly for $x, y \in V_\rho$, and from the definition of $\mathcal{D}_h$ in (3.37) we get

$$\mathcal{D}_{W_z}(\vec{\mu}) \to 0 \quad \text{as } z \to \infty.$$

The quantity $\mathcal{D}_h(\vec{\mu})$ is linear in h, so (3.136) implies

$$\mathcal{D}_q(\vec{\mu}) = -zq(z)\mathcal{D}_{h_z}(\vec{\mu}) + \mathcal{D}_{Q_z}(\vec{\mu}) + \mathcal{D}_{W_z}(\vec{\mu}) = \mathcal{D}_{Q_z}(\vec{\mu}) + \mathcal{D}_{W_z}(\vec{\mu}),$$

where for the last equality we used Corollary 3.3.7, and hence from the previous limit we get

$$\mathcal{D}_q(\vec{\mu}) = \lim_{z \to \infty} \mathcal{D}_{Q_z}(\vec{\mu}).$$

The result now follows easily by induction on the degree N of q. If $N = 0$, then Q_z is identically zero, and the equality above implies that $\mathcal{D}_q(\vec{\mu}) = 0$. Assuming now that $\mathcal{D}_h(\vec{\mu}) = 0$ for every polynomial h of degree at most $N-1$, we get that $\mathcal{D}_{Q_z}(\vec{\mu}) = 0$ because $Q_z(x)$ is a polynomial of degree at most $N-1$ in x, and the equality above implies $\mathcal{D}_q(\vec{\mu}) = 0$, concluding the proof. □

If $p \in \widehat{S}_\alpha$, then as it is discussed in Remark 3.2.10, the point p belongs to exactly two of the supports of μ_1, μ_2 and μ_3, and locally the union of these sets is an analytic arc. That is, there exists an open disk U_p centered at p such that

$$\gamma_p = U_p \cap (\operatorname{supp}\mu_1 \cup \operatorname{supp}\mu_2 \cup \operatorname{supp}\mu_3) \tag{3.138}$$

is an analytic arc passing through p.

Additionally, given any point $z \in (\operatorname{supp}\mu_1 \cup \operatorname{supp}\mu_2 \cup \operatorname{supp}\mu_3) \setminus \widehat{S}_\alpha$, there exists a small disk B_z centered z, disjoint from $\widehat{S}_\alpha$ and such that the set

$$B_z \cap (\operatorname{supp}\mu_1 \cup \operatorname{supp}\mu_2 \cup \operatorname{supp}\mu_3)$$

is a finite union of analytic arcs, which can only intersect at the common point z. In case $z \notin S_\alpha$, this intersection reduces to a single analytic arc. The collection

$$\{B_z\} \cup \{U_p\}$$

constructed above is an open cover of the compact set $\operatorname{supp}\mu_1 \cup \operatorname{supp}\mu_2 \cup \operatorname{supp}\mu_3$, from which we extract a finite subcover

$$\{B_j\}_{j=1}^{m} \cup \{U_p\}_{p\in\widehat{S}_p},$$

where for $j = 1, \dots, m$ we have $B_j = B_z$ for some $z = z_j \in (\operatorname{supp}\mu_1 \cup \operatorname{supp}\mu_2 \cup \operatorname{supp}\mu_3) \setminus \widehat{S}_\alpha$. Set

$$B = \bigcup_{j=1}^{m} B_j, \quad U = \bigcup_{p\in\widehat{S}_\alpha} U_p.$$

It follows from their construction that these sets satisfy

$$B \cap \widehat{S}_\alpha = \emptyset, \quad \operatorname{supp}\mu_1 \cup \operatorname{supp}\mu_2 \cup \operatorname{supp}\mu_3 \subset B \cup U. \tag{3.139}$$

Consider a smooth partition of unity $\{\psi_k\}$ of $\operatorname{supp}\mu_1 \cup \operatorname{supp}\mu_2 \cup \operatorname{supp}\mu_3$ subordinated to the open cover $B \cup U$. That is, each function ψ_k is real, belongs to $C_\infty(\mathbb{C})$ and additionally satisfies the following properties.

- $0 \le \psi_k(z) \le 1$, for every $z \in \mathbb{C}$.
- For every k, either $\operatorname{supp}\psi_k \subset U$ or $\operatorname{supp}\psi_k \subset B$.
- Every $z \in \operatorname{supp}\mu_1 \cup \operatorname{supp}\mu_2 \cup \operatorname{supp}\mu_3$ belongs to the support of a finite number of functions in the collection $\{\psi_k\}$.
- $\sum_k \psi_k(z) = 1$, for every $z \in \operatorname{supp}\mu_1 \cup \operatorname{supp}\mu_2 \cup \operatorname{supp}\mu_3$.

Since $\operatorname{supp}\mu_1 \cup \operatorname{supp}\mu_2 \cup \operatorname{supp}\mu_3$ is compact, the collection $\{\psi_k\}$ can be assumed to be finite. Moreover, we can refine $\{\psi_k\}$ and assume that $\operatorname{supp}\psi_k \subset U$ whenever $\operatorname{supp}\psi_k \cap \widehat{S}_\alpha \neq \emptyset$. Set

$$\widehat{\psi}(z) = \sum_{\operatorname{supp}\psi_k \cap \widehat{S}_\alpha \neq \emptyset} \psi_k(z), \quad \psi(z) = \sum_k \psi_k(z) - \widehat{\psi}(z).$$

The functions ψ and $\widehat{\psi}$ belong to $C_\infty(\mathbb{C})$, satisfy

$$\operatorname{supp}\psi \cap \widehat{S}_\alpha = \emptyset, \quad \operatorname{supp}\widehat{\psi} \subset U \tag{3.140}$$

and

$$\psi(z) + \widehat{\psi}(z) = 1, \quad z \in \operatorname{supp}\mu_1 \cup \operatorname{supp}\mu_2 \cup \operatorname{supp}\mu_3. \tag{3.141}$$

Lemma 3.6.2. *Under the conditions of Theorem 3.2.3, if q is a polynomial, then $\mathcal{D}_{\widehat{\psi}q}(\vec{\mu}) = 0$, where $\widehat{\psi}$ is the function constructed above.*

Proof. From (3.141), it follows that $q \equiv \psi q + \widehat{\psi} q$ on $\operatorname{supp}\mu_1 \cup \operatorname{supp}\mu_2 \cup \operatorname{supp}\mu_3$. From the definition of $\mathcal{D}_h$ in (3.37) we then get

$$\mathcal{D}_{\widehat{\psi q}}(\vec{\mu}) = \mathcal{D}_q(\vec{\mu}) - \mathcal{D}_{\psi q}(\vec{\mu}).$$

Using the first condition in (3.140), we get $\operatorname{supp}(\psi q) \cap \widehat{S}_\alpha = \emptyset$, so Lemma 3.3.8 gives us $\mathcal{D}_{\psi q}(\vec{\mu}) = 0$. Since q is a polynomial, we learn from Lemma 3.6.1 that $\mathcal{D}_q(\vec{\mu}) = 0$, concluding the proof. □

We are finally able to prove Theorem 3.2.3 in its full generality.

Proof of Theorem 3.2.3. Recall the definition of the arcs $\{\gamma_p\}$, $p \in \widehat{S}_\alpha$, given in (3.138). Each of these arcs is a simple contour on the complex plane, and we can find a smooth arc $\gamma \subset \mathbb{C}$ for which $\cup\gamma_p \subset \gamma$ and $\mathbb{C} \setminus \gamma$ is connected. In particular, the second condition in (3.140) implies

$$\operatorname{supp}(\widehat{\psi}) \cap (\operatorname{supp}\mu_1 \cup \operatorname{supp}\mu_2 \cup \operatorname{supp}\mu_3) \subset \bigcup_{p \in \widehat{S}_\alpha} \gamma_p \subset \gamma. \tag{3.142}$$

Consider a parametrization $\gamma : [0,1] \to \mathbb{C}$ of γ by arc length, set $a = \gamma(0)$ and define a continuous function $g : \gamma \to \mathbb{C}$ by $g(z) = \gamma'(\gamma^{-1}(z))$. That is, $g(z)$ is a unit vector tangent to γ at the point z, varying continuously with z. Given $h \in C^2(\mathbb{C})$, define

$$G : \gamma \to \mathbb{C}, \quad G(z) = \frac{1}{g(z)} \left(\frac{\partial h}{\partial x}(z) \operatorname{Re} g(z) + \frac{\partial h}{\partial y}(z) \operatorname{Im} g(z) \right)$$

γ is a simple smooth arc, so it has empty interior. Since $\mathbb{C} \setminus \gamma$ is connected and G is continuous, Mergelyan's Theorem tells us that there exists a sequence of polynomials (p_n) converging to G uniformly on γ. In particular, for $\gamma(t) = z$ this implies that the convergence

$$\begin{aligned} p_n(\gamma(t))\gamma'(t) &= p_n(z)g(z) \\ &\to \frac{\partial h}{\partial x}(z) \operatorname{Re} g(z) + \frac{\partial h}{\partial y}(z) \operatorname{Im} g(z) = \frac{d}{dt}(h(\gamma(t)))\Big|_{t=\gamma^{-1}(z)} \end{aligned}$$

holds uniformly on γ, and as a consequence the sequence of polynomials

$$q_n(z) = \int_a^z p_n(s)ds + h(a)$$

converges to

$$\int_0^t \frac{d}{du}(h(\gamma(u)))du + h(a) = h(z)$$

uniformly for $z \in \gamma$.

In summary, we constructed a sequence of polynomials (q_n) converging uniformly to h on γ, and for which the sequence of derivatives $(q_n') = (p_n)$ converges to G uniformly on γ; in particular there exists $M > 0$, independent of n, such that

$$|q_n'(x)| \leq M, \quad x \in \gamma, \quad n \geq 1. \tag{3.143}$$

Hence, the convergence

$$\widehat{\psi}(x)q_n(x) \to \widehat{\psi}(x)h(x) \tag{3.144}$$

holds true uniformly along γ. Due to (3.142), this is enough to conclude that the convergence above holds uniformly on $\operatorname{supp}\mu_1 \cup \operatorname{supp}\mu_2 \cup \operatorname{supp}\mu_3$, so that

$$\int \Phi_j'\widehat{\psi}q_n \, d\mu_j \to \int \Phi_j'\widehat{\psi}h \, d\mu_j, \quad j = 1, 2, 3. \tag{3.145}$$

The measures μ_1, μ_2 and μ_3 do not have point masses, so the diagonal $\{x = y\}$ has zero $\mu_j \times \mu_k$ measure. Thus the limit (3.144) also implies that the convergence

$$\frac{\widehat{\psi}(x)q_n(x) - \widehat{\psi}(y)q_n(y)}{x - y} \to \frac{\widehat{\psi}(x)h(x) - \widehat{\psi}(x)h(y)}{x - y} \tag{3.146}$$

holds true pointwise $(\mu_j \times \mu_k)$-a.e.

Since the arc γ is connected, we also know that

$$\left|\frac{\widehat{\psi}(x)q_n(x) - \widehat{\psi}(y)q_n(y)}{x - y}\right| \leq \sup_{s\in[0,1]} \left|\frac{d}{dt}\left(\left((\widehat{\psi}q_n) \circ \gamma\right)(t)\right)\right|_{t=s}$$

whenever $x, y \in \gamma$. In virtue of (3.143) and (3.144), the right-hand side in the inequality above is uniformly bounded in n. Hence the left-hand side of (3.146) is uniformly bounded along γ, and using (3.142) and once again (3.144), we can extend this conclusion to $\operatorname{supp}\mu_1 \cup \operatorname{supp}\mu_2 \cup \operatorname{supp}\mu_3$. Using the Dominated Convergence Theorem and (3.146) we conclude

$$\iint \frac{\widehat{\psi}(x)q_n(x) - \widehat{\psi}(y)q_n(y)}{x - y} d\mu_j(x)d\mu_k(y)$$

$$\longrightarrow \iint \frac{\widehat{\psi}(x)h(x) - \widehat{\psi}(y)h(y)}{x - y} d\mu_j(x)d\mu_k(y),$$

for $j,k=1,2,3$. Combined with (3.145), we finally get

$$\mathcal{D}_{\widehat{\psi q_n}}(\vec{\mu}) \to \mathcal{D}_{\widehat{\psi h}}(\vec{\mu}).$$

From Lemma 3.6.2, we know that $\mathcal{D}_{\widehat{\psi q_n}}(\vec{\mu})=0$ for every n, hence $\mathcal{D}_{\widehat{\psi h}}(\vec{\mu})=0$. On the other hand, due to the first condition in (3.140), we have $\operatorname{supp}(\psi h)\cap\widehat{S}_\alpha=\emptyset$, so from Lemma 3.3.8 we get $\mathcal{D}_{\psi h}(\vec{\mu})=0$. Thus,

$$\mathcal{D}_h(\vec{\mu}) = \mathcal{D}_{\widehat{\psi h}}(\vec{\mu}) + \mathcal{D}_{\psi h}(\vec{\mu}) = 0,$$

where for the first equality we used (3.141). Since $h\in C^2(\mathbb{C})$ is arbitrary, Corollary 3.3.2 gives us that the measure $\vec{\mu}$ is critical, concluding the proof. □

3.7 Numerical experiments

In this Section we look under the hood of the calculation of the functions ω_j in (3.121), as well as of the numerical procedures used to find and plot the trajectories of the quadratic differential ϖ from Section 3.5.

As it was mentioned, Figure 3.4 was obtained by means of a numerical evaluation of the integrals defining the functions ω_j in (3.121)–(3.122). For that, we compute the integrals of the form

$$\int_{z_1}^{z_2} \xi_j(s)ds$$

along the line segment joining chosen roots z_1, z_2 of the discriminant in (3.69) by means of the composite trapezoidal rule.

For τ fixed, we compute the points $z_k=z_k(\tau)$, choose a value $m\in\mathbb{N}$, and consider a grid of $m+1$ equally spaced nodes $\{p_j\}_{j=1}^{m+1}$,

$$p_j = z_1 + \frac{j-1}{m}(z_2-z_1), \quad j=1,\cdots,m+1,$$

that will be used as the quadrature nodes for the composite trapezoidal rule. At each $z=p_j$ we solve (3.74) numerically, obtaining an (unordered) set of three solutions $\xi_k(p_j)$. Comparing their values at consecutive quadrature points, we collect them into a sequence of (ordered) vectors $\vec{v}_j=(\xi_{\sigma(1)},\xi_{\sigma(2)},\xi_{\sigma(3)})^T(p_j)$, $j=1,\dots,m+1$, where σ is a permutation of $\{1,2,3\}$ that does not depend on j. We can then determine the permutation σ using equations (3.110) and (3.116)–(3.119) as boundary conditions.

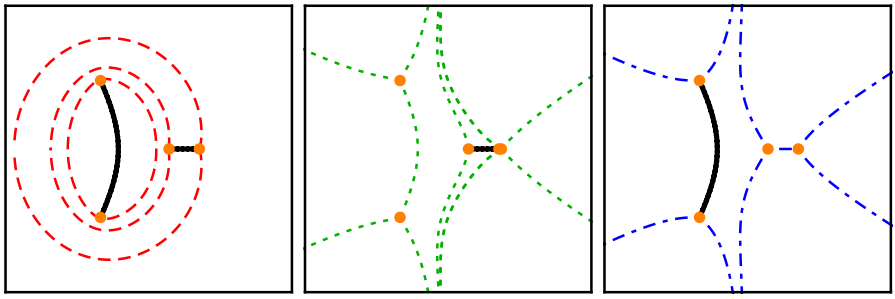

Figure 3.22: Numerical evaluation of the critical graph for $\tau = 1/25$.

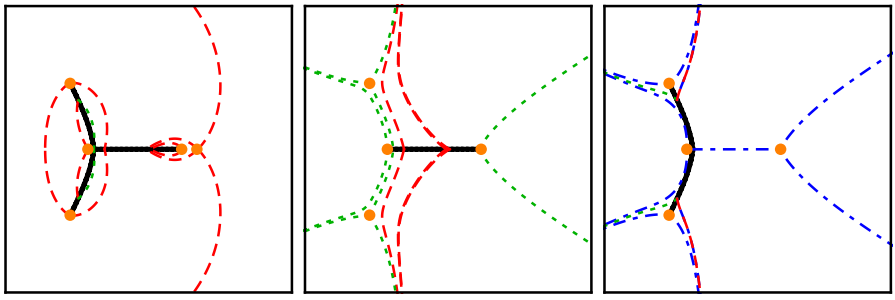

Figure 3.23: Numerical evaluation of the critical graph for $\tau = 1/5$.

This procedure is repeated for n equally spaced values of τ,

$$\tau = \tau_k = \frac{k}{4(n+1)}, \quad k = 1, \dots, n,$$

(notice that $\tau_k \in [0, 1/4)$; we stop at $k = n$ in order to avoid the degenerate situation at $\tau = 1/4$ for which some of the endpoints of integration diverge to ∞).

The result of these calculations with $n = 1000$ and $m = 10000$ is plotted in Figure 3.4.

On the other hand, we also performed numerical experiments that helped us to build the intuition to predict (and confirm) the structure of the critical graphs in Section 3.5. A sample of such graphs is presented in Figures 3.22–3.24.

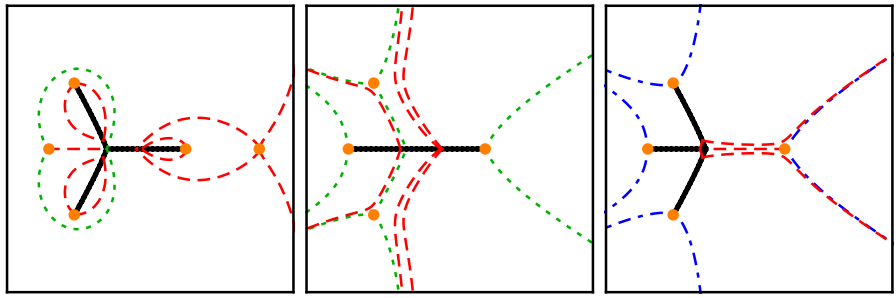

Figure 3.24: Numerical evaluation of the critical graph for $\tau = 1/5$.

The numerical procedure used for these pictures is as follows. If $\gamma(t), t \in J \subset \mathbb{R}$, is a parameterization of a trajectory of $\varpi = Q^2(z)dz^2$, then

$$Q^2(\gamma(t))\gamma'(t) = if(t), \quad t \in J,$$

where f is some real valued function. A different choice of f correspond just to a reparameterization of γ. In a natural (arc-length) parametrization of γ the equation above takes the form

$$\gamma'(t) = i\frac{\overline{Q^2(\gamma(t))}}{|Q^2(\gamma(t))|}, \quad t \in J. \tag{3.147}$$

This is an ordinary differential equation for γ that can be solved by standard methods (e.g. the family of Runge-Kutta algorithms).

We should bewared of two aspects when implementing this method. The first one concerns the initial values, that usually are at branch points of (3.74), and thus, at zeros of Q, from where more than one trajectory emanates. This can be resolved by perturbing the initial point along the prescribed direction, which can be obtained from a local analysis of Q at the singular point.

The second aspect concerns the choice of branches of Q^2 in (3.147), where we take advantage of the fact that all the branch points of (3.74) are quadratic. The value of Q^2 is found numerically by solving (3.74), which gives us the three possible values ξ_k. Near a branch point two of these values are close (corresponding to the two solutions coinciding at this branch point), allowing us to distinguish the third solution. This, in turn, allows to recognize on the the possible branches of Q^2, but not the other two.

For instance, at $z = b_2$ we will have $\xi_1 \approx \xi_3$ (see (3.119)), which singles out the branch ξ_2 and makes the branch $Q^2 = (\xi_1 - \xi_3)^2$ easily distinguishable. In

order to identify the remaining two branches (i.e., $(\xi_2 - \xi_1)^2$ and $(\xi_2 - \xi_3)^2$) we must use further results about the local and global structure of the critical graph of ϖ, established in Section 3.5.

Chapter 4

The mother body phase transition in the normal matrix model

The normal matrix model with algebraic potential has gained a lot of attention recently, partially in virtue of its connection to several other topics as quadrature domains, inverse potential problems and the Laplacian growth.

In the present chapter, based on the joint work [42] with Pavel Bleher, we consider the normal matrix model with cubic plus linear potential. In order to regularize the model, we follow Elbau & Felder and introduce a cut-off. In the large size limit, the eigenvalues of the model accumulate uniformly within a certain domain Ω that we determine explicitly by finding the rational parametrization of its boundary.

We also study in detail the mother body problem associated to Ω. It turns out that the mother body measure μ_* displays a novel phase transition that we call the *mother body phase transition*: although $\partial\Omega$ evolves analytically, the mother body measure undergoes a "one-cut to three-cut" phase transition.

To construct the mother body measure, we define a quadratic differential ϖ on the associated spectral curve, and embed μ_* into its critical graph. Using deformation techniques for quadratic differentials, we are able to get precise information on μ_*. In particular, this allows us to determine the phase diagram for the mother body phase transition explicitly.

Following previous works of Bleher & Kuijlaars and Kuijlaars & López, we consider multiple orthogonal polynomials associated with the normal matrix model. Applying the Deift-Zhou nonlinear steepest descent method to the associated Riemann-Hilbert problem, we obtain strong asymptotic formulas for these polynomials. Due to the presence of the linear term in the potential, there are no rotational symmetries in the model. This makes the construction of the associated g-functions significantly more involved, and the critical graph of ϖ becomes the key technical tool in this analysis as well.

4.1 Introduction

We are interested in the eigenvalues of the normal matrix model given by the probability distribution

$$d\pi_n(M) = \frac{1}{\widetilde{Z}_n} e^{-n \operatorname{Tr} \mathcal{V}(M)} dM, \tag{4.1}$$

where M is an $n \times n$ normal matrix and $\mathcal{V}$ is a given function of M. Its induced joint probability distribution on the eigenvalues $\lambda = (\lambda_1, \ldots, \lambda_n) \in \mathbb{C}^n$ is given explicitly by

$$d\pi_n(\lambda) = \frac{1}{Z_n} \prod_{j<k} |\lambda_j - \lambda_k|^2 e^{-n \sum_{j=1}^n \mathcal{V}(\lambda_j)} d\lambda, \tag{4.2}$$

where $d\lambda$ is the Lebesgue measure on $\mathbb{C}^n$ and Z_n is the corresponding partition function [45, 65].

This model has been studied in the literature for different choices of the potential $\mathcal{V}$ and under various perspectives [4, 5, 45, 81, 99, 100, 101, 119]. Of particular interest is the choice

$$\mathcal{V}(z) = \frac{1}{t_0}(|z|^2 - V(z) - \overline{V(z)}), \quad z \in \mathbb{C}, \quad V(z) = \sum_{k=1}^{d+1} \frac{t_k}{k} z^k, \quad t_{d+1} \neq 0. \tag{4.3}$$

As formally observed by Kostov, Krichever, Mineev-Weinstein, Wiegmann and Zabrodin [88], in this situation the eigenvalues should accumulate on a domain $\Omega = \Omega(t_0, t_1, \ldots, t_d)$, whose boundary $\partial\Omega$ evolves in time $t_0 > 0$ according to the Laplacian growth model with given harmonic moments

$$\operatorname{Area}(\Omega) = \pi t_0, \qquad -\frac{1}{\pi} \int_{\mathbb{C}\setminus\Omega} \frac{dA(z)}{z^k} = t_k, \quad k = 1, 2, 3, \ldots, \tag{4.4}$$

where we set $t_j = 0$, for $j \geq d+2$, and dA is the Lebesgue measure on $\mathbb{C}$.

However, the model (4.1) for $\mathcal{V}$ given by (4.3) is in general purely formal. If $d \geq 2$, the density in (4.1) is not integrable, hence the normal matrix model is ill-defined. To overcome this essential issue, Elbau and Felder [65] proposed to consider a *cut off* model. Instead of integrating (4.1) over the whole set of normal matrices, they consider (4.1) as a distribution over normal matrices whose eigenvalues are constrained to lie within a fixed bounded domain $D \subset \mathbb{C}$. In this setup, the model becomes well-defined and the eigenvalue density (4.2) can be rewritten as

$$d\pi_n(\lambda) = \frac{1}{Z_n} \prod_{j<k} |\lambda_j - \lambda_k|^2 \prod_{j=1}^{n} \chi_D(\lambda_j) e^{-n\mathcal{V}(\lambda_j)} d\lambda, \tag{4.5}$$

where χ_D is the characteristic function of D. Let

$$\mu_\lambda = \frac{1}{n} \sum_{j=1}^{n} \delta_{\lambda_j}$$

be a probability atomic measure on D with atoms at the points λ_j of an eigenvalue configuration λ and

$$H(\mu) = \iint_{x \neq z} \log \frac{1}{|z-x|} d\mu(x) d\mu(z) + \int \mathcal{V}(z) d\mu(z) \tag{4.6}$$

the Coulomb gas Hamiltonian, where μ is an arbitrary probability measure on D, giving a distribution of the Coulomb gas particles. Then formula (4.5) can be written as

$$d\pi_n(\lambda) = \frac{1}{Z_n} e^{-n^2 H(\mu_\lambda)} d\lambda,$$

The factor n^2 in the exponent suggests that, as $n \to \infty$, the measure $d\pi_n(\lambda)$ concentrates in a shrinking neighborhood of the equilibrium measure μ_0, which is the probability measure minimizing

$$\iint \log \frac{1}{|z-x|} d\mu(x) d\mu(z) + \int \mathcal{V}(z) d\mu(z) \tag{4.7}$$

over all probability measures supported on D. This concentration phenomenon has been proved rigorously for instance in [65, 81] under different assumptions.

Under the additional requirements that

1. the boundary ∂D of the cut off is sufficiently smooth,
2. the potential $\mathcal{V}$ has exactly one minimum in the cut off D, and
3. the time parameter t_0 is *sufficiently small*,

Elbau and Felder proved that the (unique) probability measure on D minimizing (4.7) has the form

$$d\mu_0(z) = \frac{1}{\pi t_0}\chi_\Omega(z)dA(z), \tag{4.8}$$

where χ_Ω is the characteristic function of a simply connected domain $\Omega = \Omega(t_0, V)$ contained in D, whose boundary $\partial\Omega$ is a *polynomial curve* of degree d: there exists a rational function of the form

$$h(w) = rw + a_0 + \frac{a_1}{w} + \cdots + \frac{a_d}{w^d}, \quad w \in \mathbb{C}, \quad r > 0,\ a_d \neq 0, \tag{4.9}$$

which is injective on the boundary of the unit disc $\mathbb{D}$ and such that $\partial\Omega = h(\partial\mathbb{D})$. Moreover, h gives a conformal map of $\mathbb{C} \setminus \mathbb{D}$ onto $\mathbb{C} \setminus \Omega$. Furthermore, still for sufficiently small time t_0, Elbau and Felder proved rigorously the connection of Ω with the Laplacian growth as in (4.4).

Concerning local statistics, Elbau [64] pointed out that the eigenvalue distribution (4.5) is a bona fide determinantal point process with kernel

$$K_n(z, w) = e^{-\frac{n}{2}(\mathcal{V}(z)+\mathcal{V}(w))} \sum_{j=0}^{n} \frac{q_{j,n}(z)\overline{q_{j,n}(w)}}{h_{n,j}},$$

where $q_{j,n}(z) = z^j + \ldots$ are *planar orthogonal polynomials in the external field* $\mathcal{V}$ (or simply POP's)

$$\int_D q_{j,n}(z)\overline{q_{k,n}(z)}e^{-n\mathcal{V}(z)}dA(z) = h_{n,j}\delta_{j,k}, \quad j, k \in \mathbb{N}. \tag{4.10}$$

A natural question is to understand the behavior of the polynomials $(q_{n,n})$, and in particular of their zeros, as $n \to \infty$. Elbau showed that any weak limit μ_* of the zero counting measures

$$\mu_n = \frac{1}{n} \sum_{q_{n,n}(w)=0} \delta_w$$

should be supported in D and satisfy the mother body property for μ_0, namely

$$\int \log|s - z|d\mu_0(s) = \int \log|s - z|d\mu_*(s), \quad z \in \mathbb{C} \setminus D. \tag{4.11}$$

The goal of the present chapter is to study in detail the cubic plus linear model

$$\mathcal{V}(z) = \frac{1}{t_0}(|z|^2 - 2\,\mathrm{Re}\,V(z)), \qquad V(z) = \frac{z^3}{3} + t_1 z, \quad -\frac{3}{4} < t_1 < \frac{1}{4}\ , \tag{4.12}$$

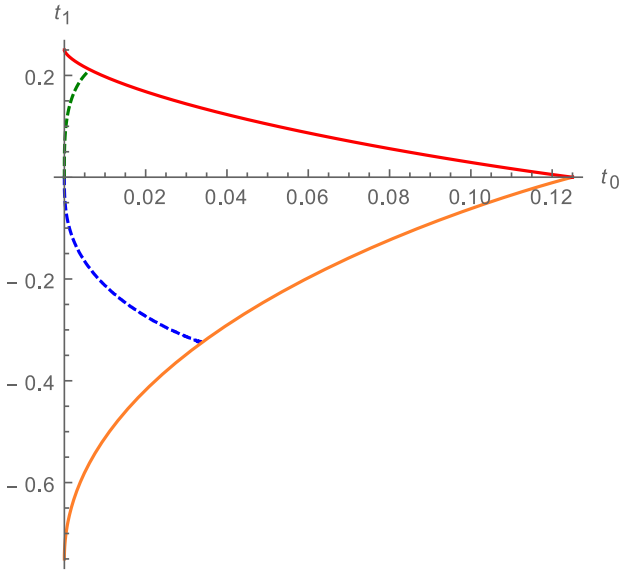

Figure 4.1: Phase diagram on the (t_0, t_1)-plane: the solid curves are the pairs $(t_{0,crit}, t_1)$, which correspond to the cusp phase transition. The dashed curves are the points of the form $(\tilde{t}_{0,crit}, t_1)$ and they correspond to the mother body phase transition. We should remark that the dashed curves on the upper and lower half planes are *not analytic continuation of each other*: the curve on the upper half plane is algebraic, whereas the one on the lower half plane is transcendental.

for values of t_0 up to a critical time $t_{0,crit} = t_{0,crit}(t_1)$. The restriction on t_1 above comes from the corresponding potential $\mathcal{V}$: as a simple analysis shows, if either $t_1 \leq -3/4$ or $t_1 \geq 1/4$, then the potential $\mathcal{V}$ has no local minimum. Consequently, for any choice of cut off D, the corresponding eigenvalues should accumulate on the boundary of D as $n \to \infty$, so that the limiting shape of eigenvalues Ω intersects ∂D and is very sensitive to the precise choice of D.

For t_1 as in (4.12), we are able to determine precisely the underlying phase diagram in the (t_0, t_1)-plane, as is shown in Figure 4.1. Given t_1 as above and for all positive values of t_0 up to the critical time $t_{0,crit} = t_{0,crit}(t_1)$, we find the parametrization h in (4.9) of the corresponding polynomial curve $\partial\Omega$, and consequently we obtain the associated limiting eigenvalue distribution (4.8) explicitly. When $t_0 \to t_{0,crit}$, the boundary of $\partial\Omega$ creates either one (if $t_1 > 0$) or two (if $t_1 < 0$) cusps: we call this phenomenon the *cusp phase transition*. We are able to compute the critical curve $(t_{0,crit}, t_1)$ explicitly.

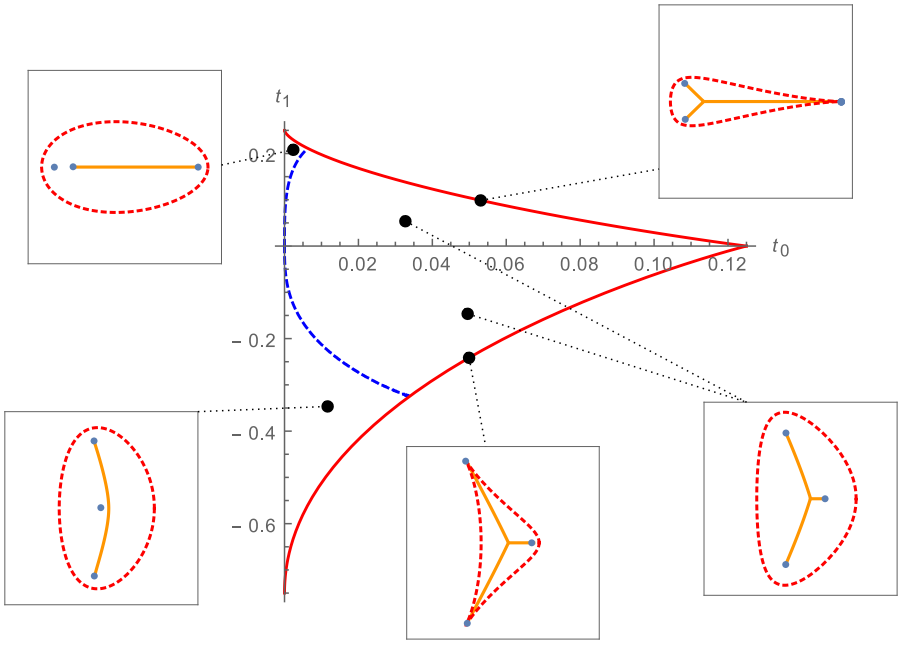

Figure 4.2: The phase diagram and the various topological configurations of $\partial\Omega$ (dashed lines in each frame) and $\operatorname{supp}\mu_*$ (solid lines in each frame). The dots inside each frame are the branch points of the associated spectral curve.

For all values of (t_0, t_1) in our phase diagram, we also study the mother body equation (4.11) in detail. We construct a measure μ_* satisfying (4.11) and whose support consists of a finite union of analytic arcs. Furthermore, we find another critical time $\tilde{t}_{0,crit} = \tilde{t}_{0,crit}(t_1) < t_{0,crit}$ such that if $t_0 < \tilde{t}_{0,crit}$, then $\operatorname{supp}\mu_*$ consists of one analytic arc, whereas for $t_0 > \tilde{t}_{0,crit}$ the set $\operatorname{supp}\mu_*$ consists of three analytic arcs meeting at a common point. We call this transition the *mother body phase transition*.

The critical value $\tilde{t}_{0,crit}$ is depicted in Figure 4.1. We emphasize that the boundary of $\partial\Omega$ depends analytically on the parameters (t_0, t_1) in the phase diagram. So what our results show is that the measure μ_* solving the mother body problem (4.11) displays a phase transition that is not felt by $\partial\Omega$. We refer to Figure 4.2 for a visualization of this transition. To our knowledge, this is the first time such a phenomenon is described.

The construction of the measure μ_* is, in our opinion, our main technical contribution. We construct a quadratic differential on the three-sheeted Riemann surface (a.k.a. spectral curve) associated with the model, and lift the problem

(4.11) to the trajectories of this quadratic differential. Following the techniques already employed in Chapter 3, we use deformation techniques to describe the critical graph of this quadratic differential. When we project some of these trajectories back to the complex plane, we recover the measure μ_*. This critical graph displays some phase transitions; these transitions are determined by the critical value $\tilde{t}_{0,crit}$ and correspond to the phase transitions of $\operatorname{supp}\mu_*$.

We follow previous works of Bleher and Kuijlaars [38] and Kujlaars and López [90] and introduce a new sequence of polynomials $(P_{n,n})$ which has, at the heuristic level, the same asymptotic behavior as the sequence $(q_{n,n})$ in (4.10). We characterize this sequence $(P_{n,n})$ in terms of multiple orthogonality of non-hermitian type, and using the Deift-Zhou steepest descent method we obtain strong asymptotic formulas for these polynomials. As one of the consequences, we prove that the sequence of zero counting measures for $(P_{n,n})$ converges weakly to the measure μ_*.

The case $t_1 = 0$ was studied before by Bleher and Kuijlaars [38], and it plays a substantial role here as well. Many auxiliary results require separate proofs depending whether $t_1 < 0$ or $t_1 > 0$, and a complete analysis would make the already lengthy chapter much longer. So our main focus is on the case $t_1 > 0$, whose main results are stated in Section 4.2. The corresponding main results for $t_1 < 0$ are stated and discussed in Section 4.2.10, but their proofs are analogous and not provided.

4.2 Statement of main results

4.2.1 Phase diagram of the cubic model

For the choice of potential (4.3) with V as in (4.12), the rational function h in (4.9) assumes the form

$$h(w) = rw + a_0 + \frac{a_1}{w} + \frac{a_2}{w^2}.$$

According to Elbau and Felder [65, page 442], the coefficients of h should be related to the normal matrix model (4.1) with cubic potential (4.12) through the system of equations

$$\begin{cases} \dfrac{a_2}{r^2} = 1, & \dfrac{a_1}{r} - \dfrac{2a_0a_2}{r^2} = 0, \\[2ex] a_0 - \dfrac{a_0a_1}{r} - \dfrac{a_2(2a_1r - a_0^2)}{r^2} = t_1, & r^2 - a_1^2 - 2a_2^2 = t_0. \end{cases} \tag{4.13}$$

This system of equations is obtained by computing the (expected) exterior harmonic moments of $\partial\Omega$ in terms of the rational function h. Solving in terms of r, it gives us

$$a_1 = 2ra_0, \quad a_2 = r^2, \quad a_0 = \frac{1 - 4r^2 + \delta\sqrt{(1-4r^2)^2 - t_1}}{2}. \tag{4.14}$$

where $\delta = \pm 1$. When $t_1 \to 0$, we expect $a_0 = 0$ [38]; thus $\delta = -1$, and h reduces to

$$h(w) = rw + a_0 + \frac{2a_0 r}{w} + \frac{r^2}{w^2}, \tag{4.15}$$

where

$$a_0 = a_0(t_0, t_1) = \frac{1 - 4r^2 - \sqrt{(1-4r^2)^2 - 4t_1}}{2}, \tag{4.16}$$

and $r = r(t_0, t_1)$ is to be determined. Using the values (4.14) in the last equation in (4.13), after a lengthy calculation we conclude that r should be a root of the polynomial

$$p(x) = 128x^{10} - 124x^8 + (64t_0 - 16t_1 + 36)x^6 + \left(16t_1^2 + 8t_1 - 28t_0 - 3\right)x^4 + t_0(2 - 8t_1)x^2 + t_0^2 \tag{4.17}$$

When $t_1 \to 0$, we compare again with the results by Bleher and Kuijlaars [38] to get that r should be the smallest positive root of p. An analysis of the discriminant of p then leads us to consider the domain $\mathcal{F}$ on the (t_0, t_1)-plane, bounded by the segments

$$(t_0, 0), \quad 0 \le t_0 \le 1/8,$$

$$(0, t_1), \quad 0 \le t_1 \le 1/4,$$

and the critical curve Γ_c, parametrized by

$$\Gamma_c : \quad t_0 = -6s^4 + 4s^3, \quad t_1 = 4s^3 - 3s^2 + 1/4, \quad 0 \le s \le 1/2. \tag{4.18}$$

Proposition 4.2.1. *For $(t_0, t_1) \in \mathcal{F}$, the polynomial p in (4.17) has a smallest positive root $r = r(t_0, t_1)$, which is simple.*

Proposition 4.2.1 is part of Theorem 4.3.6, which is proved in Section 4.3.1.

The curve Γ_c corresponds to the cusp phase transition for $t_1 > 0$. A plot of the region $\mathcal{F}$ and the critical curve Γ_c are displayed in Figure 4.3.

Since the function $r = r(t_0, t_1)$ is a simple root of the polynomial p, it is analytic with respect to both variables t_0, t_1, as long as $(t_0, t_1) \in \mathcal{F}$, and it is continuous up to the boundary of $\mathcal{F}$. The function r plays a fundamental role in the rest of the chapter.

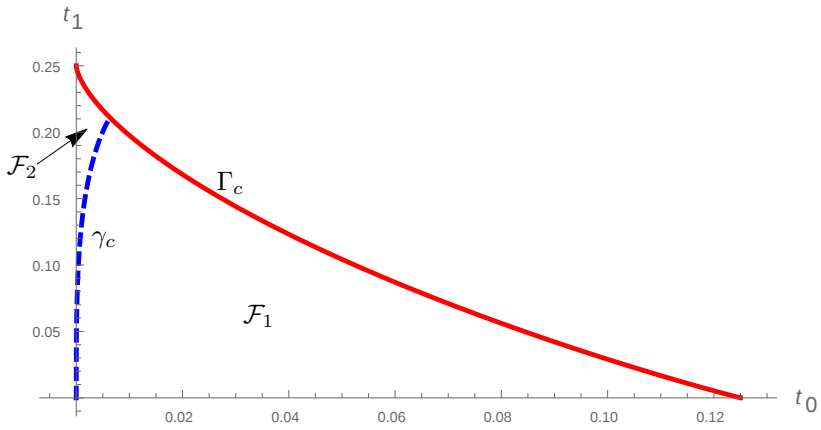

Figure 4.3: Phase diagram on the (t_0, t_1)-plane: The solid curve is Γ_c given in (4.18) and the dashed curve is γ_c given in (4.30). The region determined by Γ_c, γ_c and the t_0-axis is the three-cut region $\mathcal{F}_1$, whereas the region between Γ_c, γ_c and the t_1-axis is the one-cut region $\mathcal{F}_2$. Axes are scaled differently.

4.2.2 The limiting boundary of eigenvalues as a polynomial curve

As it was heuristically explained in Section 4.2.1, the rational function h in (4.15), with coefficients a_0 and r as in (4.16) and Proposition 4.2.1, should give the parametrization of the polynomial curve $\partial\Omega$ for the potential (4.12). This is rigorously established by our next result.

Theorem 4.2.2. *For $(t_0, t_1) \in \mathcal{F}$ and r, a_0 given respectively by Proposition 4.2.1 and equation (4.16), the rational function h is injective on $\overline{\mathbb{C}} \setminus \mathbb{D}$. The image $h(\partial\mathbb{D})$ is an analytic curve whose interior is a simply connected domain Ω with area given by*

$$\operatorname{Area}(\Omega) = \pi t_0.$$

Moreover, the exterior harmonic moments of Ω with respect to any point $\zeta \in \Omega$ are given by

$$\frac{1}{2\pi i}\int_{\partial\Omega} \frac{\overline{z}}{(z-\zeta)^k} dz = \begin{cases} t_1 + \zeta^2, & k = 1, \\ 2\zeta, & k = 2, \\ 1, & k = 3, \\ 0, & k \geq 4. \end{cases} \tag{4.19}$$

Theorem 4.2.2 is proved in Section 4.3.2.

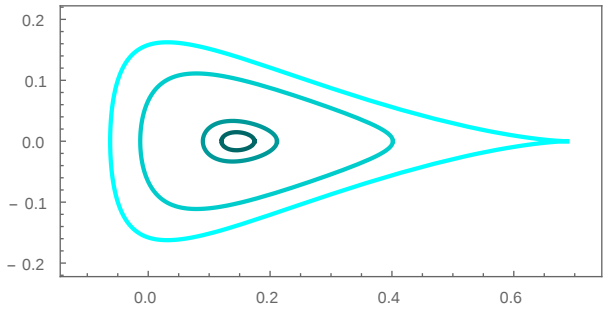

Figure 4.4: The boundary $\partial\Omega$ corresponding to $t_1 = \frac{1}{8}$ and $t_0 = \frac{1}{2500}, \frac{1}{500}, \frac{1}{50}, \frac{5}{128}$ (from dark to bright color, respectively). For the pair $(t_0, t_1) = (\frac{5}{128}, \frac{1}{8})$, which belongs to the critical curve Γ_c, a cusp is created at the boundary. Numerical output.

The equality $\partial\Omega = h(\partial\mathbb{D})$ with h rational and injective on $\partial\mathbb{D}$ says that $\partial\Omega$ is a *polynomial curve*, in the sense of Elbau and Felder [65]. We refer to Figure 4.4 for examples.

If $0 \in \Omega$ and $k \geq 3$, then the integrals in (4.4) are convergent for $\zeta = 0$ and Green's Theorem applied to $\mathbb{C} \setminus \Omega$ gives us the formula

$$-\frac{1}{\pi}\int_{\mathbb{C}\setminus\Omega} \frac{dA(z)}{z^k} = \frac{1}{2\pi i}\int_{\partial\Omega} \frac{\overline{z}}{z^k}\, dz,$$

leading to the connection previously mentioned in (4.4).

For a measure ν on the complex plane, we denote by

$$U^{\nu}(z) = \int \log\frac{1}{|s-z|} d\nu(s), \quad z \in \mathbb{C}, \tag{4.20}$$

its logarithmic potential, which is harmonic in $\mathbb{C} \setminus \operatorname{supp}\nu$ and superharmonic in $\mathbb{C}$ [120].

Define the measure μ_0 by the formula

$$d\mu_0(z) = \frac{1}{\pi t_0}\chi_{\Omega}(z) dA(z). \tag{4.21}$$

Theorem 4.2.3. *Suppose $(t_0, t_1) \in \mathcal{F}$. Consider the potential $\mathcal{V}$ in (4.3) for the cubic polynomial V in (4.12). There exist an open neighborhood D of $\overline{\Omega}$ and a constant l such that*

$$2U^{\mu_0}(z) + \mathcal{V}(z) = l, \quad z \in \overline{\Omega}, \tag{4.22}$$

$$2U^{\mu_0}(z) + \mathcal{V}(z) > l, \quad z \in D \setminus \overline{\Omega}. \tag{4.23}$$

As an immediate consequence, we recover the connection with the normal matrix model.

Theorem 4.2.4. *Suppose $(t_0, t_1) \in \mathcal{F}$, and $\mathcal{V}$ and V are as in Theorem 4.2.3. Suppose in addition that a given domain D contains $\overline{\Omega}$ and satisfies the conclusions of Theorem 4.2.3. Then the measure μ_0 in (4.21) is the limiting eigenvalue distribution of the normal matrix model with cubic potential (4.12) and cut off D.*

Theorems 4.2.3 and 4.2.4 are proved in Section 4.6. The evolution of the domain Ω in time $t_0 > 0$ is displayed in Figure 4.4.

4.2.3 Spectral curve

The pairs of points

$$(\xi, z) = (h(w^{-1}), h(w)), \quad w \in \overline{\mathbb{C}}$$

are expected to be solutions of an algebraic equation of the form

$$F(\xi, z) = 0,$$

where F is a symmetric polynomial in ξ and z, with $\deg_z F = \deg_\xi F = 3$. This equation is known in random matrix terminology as the *spectral curve* or *master loop equation*. Using equations (4.13)–(4.16), after a lengthy calculation we arrive at

$$F(\xi, z) := \xi^3 + z^3 - z^2\xi^2 - t_1(\xi^2 + z^2) - (1+t_0)z\xi + (B+t_1)(\xi+z) + A = 0, \quad (4.24)$$

where

$$B = 4a_0^3 r^2 + 4a_0^2 r^4 + 4a_0 r^4 - a_0 r^2 \quad (4.25)$$

and

$$A = -\Big(a_0^4\left(1-4r^2\right) - 2a_0^3\left(1-2r^2\right)^2 + a_0^2\left(-4r^6+6r^4-3r^2+1\right) + r^2\left(r^2-1\right)^3\Big), \quad (4.26)$$

$r = r(t_0, t_1)$ is as in Proposition 4.2.1 and a_0 is given in (4.16).

For each z, there are three solutions ξ_1, ξ_2, ξ_3 to (4.24), labeled according to the expansions

$$\begin{aligned}
\xi_1(z) &= z^2 + t_1 + \frac{t_0}{z} + \mathcal{O}(z^{-2}), \\
\xi_2(z) &= -z^{1/2} + \frac{t_1}{2z^{1/2}} - \frac{t_0}{2z} + \mathcal{O}(z^{-3/2}), \qquad \text{as } z \to \infty, \\
\xi_3(z) &= z^{1/2} - \frac{t_1}{2z^{1/2}} - \frac{t_0}{2z} + \mathcal{O}(z^{-3/2}),
\end{aligned} \tag{4.27}$$

where the square root is considered with a branch cut along the negative axis, and the branch is chosen such that $z^{1/2} > 0$ along the positive axis. In particular, the solution ξ_1 is meromorphic at $z = \infty$, whereas ξ_2, ξ_3 are branched at $z = \infty$.

A map $w \mapsto (\psi(w), \phi(w))$, ψ, ϕ rational, is a *rational parametrization* of (4.24) if

$$F(\psi(w), \phi(w)) = 0, \quad w \in \overline{\mathbb{C}}.$$

A rational parametrization as above is called *proper* if every but a finite number of pairs (ξ, z) satisfying (4.24) is generated by $(\xi, z) = (\psi(w), \phi(w))$ for exactly one choice $w \in \overline{\mathbb{C}}$.

Theorem 4.2.5. *Suppose that $(t_0, t_1) \in \mathcal{F}$. The map*

$$w \mapsto (\xi, z) = (h(w^{-1}), h(w)), \quad w \in \overline{\mathbb{C}}, \tag{4.28}$$

where h is given in (4.15), is a proper rational parametrization of the algebraic equation (4.24).

Moreover, the function ξ_1 is the Schwarz function of $\partial\Omega$. That is, there exists a simply connected domain $E \subset \overline{\mathbb{C}}$, containing $\partial\Omega$ and the point ∞, and such that ξ_1 admits a meromorphic continuation to E, with pole only at ∞, and satisfies

$$\xi_1(z) = \overline{z}, \quad z \in \partial\Omega. \tag{4.29}$$

Theorem 4.2.5 is proved in Section 4.3.2.

When $(t_0, t_1) \in \Gamma_c$, the function ξ_1 becomes branched in $\partial\Omega$ (see Section 4.2.8 below).

In particular, the existence of the Schwarz function implies that $\overline{\mathbb{C}} \setminus \overline{\Omega}$ is a quadrature domain, we refer the reader to [1, 98] for more details.

4.2.4 Phase transition of the spectral curve

The curve

$$\gamma_c: \quad t_0 = -2s^{12} + s^6 - 9s^{10}, \quad t_1 = \frac{3}{2}s^2 - \frac{9}{4}s^4 - 6s^8, \quad 0 \le s \le \frac{1}{2} \tag{4.30}$$

splits the parameter region $\mathcal{F}$ into two parts $\mathcal{F}_1$, $\mathcal{F}_2$. The first part, $\mathcal{F}_1$, consists of points (t_0, t_1) that lie to the right of γ_c, whereas the second part, $\mathcal{F}_2$, consists of points that lie to the left of γ_c, see Figure 4.3. For reasons that will become apparent later, we call $\mathcal{F}_1$ the *three-cut* region and $\mathcal{F}_2$ the *one-cut* region.

Theorem 4.2.6. *For $(t_0, t_1) \in \mathcal{F} \setminus \gamma_c$, the spectral curve (4.24) has three branch points z_0, z_1, z_2 of order two, and no other branch points. These points are located as follows.*

(i) For $(t_0, t_1) \in \mathcal{F}_1$,

$$\operatorname{Im} z_1 < 0, \quad \overline{z}_2 = z_1, \quad z_0 > 0, \quad z_0, z_1, z_2 \in \Omega.$$

(ii) For $(t_0, t_1) \in \mathcal{F}_2$,

$$z_2 < z_1 < z_0, \quad z_0 > 0, \quad z_0, z_1 \in \Omega.$$

(iii) For $(t_0, t_1) \in \gamma_c$, (4.24) has a branch point $z_0 > 0$ of order two and a branch point $z_1 = z_2 \in \mathbb{R}$ of order three, with $z_1 < z_0$. Furthermore, $z_0, z_1 \in \Omega$.

Moreover, ∞ is always a branch point of order two of (4.24).

Finally, for $(t_0, t_1) \in \mathcal{F}$, (4.24) has three critical points $\hat{z}_0, \hat{z}_1, \hat{z}_2 \in \mathbb{C} \setminus \overline{\Omega}$, satisfying

$$\hat{z}_0 > z_0, \quad \hat{z}_1, \hat{z}_2 \in \mathbb{C} \setminus \mathbb{R}, \quad \operatorname{Im} \hat{z}_1 < 0, \quad \overline{\hat{z}}_2 = z_1.$$

The proof of Theorem 4.2.6 is provided in Section 4.4. In Theorem 4.2.6, by a critical point $\hat{z}_j$ we mean that it satisfies

$$\frac{\partial F}{\partial \xi}(\xi_k, \hat{z}_j) = \frac{\partial F}{\partial z}(\xi_k, \hat{z}_j) = 0,$$

for some choice of $\xi_k = \xi_k(\hat{z}_j)$ for which the pair $(\xi_k, \hat{z}_j)$ satisfies (4.24).

Theorem 4.2.6 can be summarized in the following manner. The critical curve γ_c determines two different regimes for the spectral curve: for pairs (t_0, t_1) to the left of γ_c the spectral curve has three real branch points, whereas for (t_0, t_1) to the right of γ_c the spectral curve has one real and two non real branch points. At γ_c, these non real branch points coalesce. We refer the reader to Figure 4.5 for a depiction of the branch points and critical points.

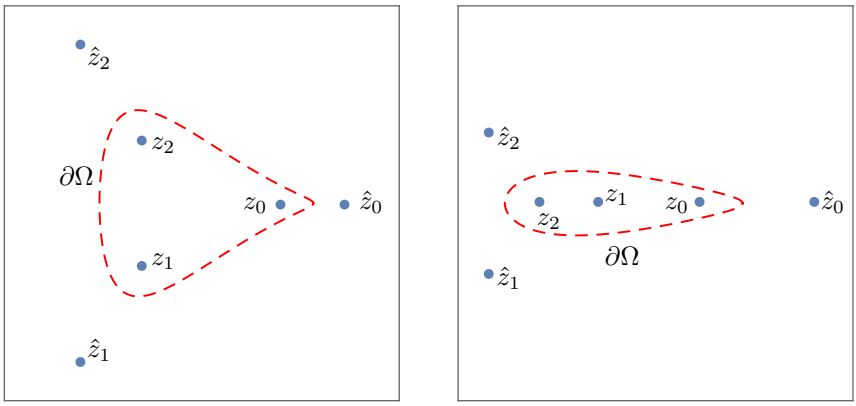

Figure 4.5: The boundary of Ω and the branch points and critical points in the three-cut (left-hand panel) and one-cut (right-hand panel) cases.

4.2.5 The parameters (r, a_0) as a change of variables

The functions $r = r(t_0, t_1)$ and $a_0 = a_0(t_0, t_1)$, given by Proposition 4.2.1 and equation (4.16), respectively, can be seen as a change of variables. It turns out that we can express the inverse change of coordinates $(r, a_0) \mapsto (t_0, t_1)$ explicitly.

Proposition 4.2.7. *Suppose $(t_0, t_1) \in \overline{\mathcal{F}}$. The functions r and a_0 satisfy the nonlinear system*

$$2r^4 - r^2(1 - 4a_0^2) = -t_0 \tag{4.31}$$

$$a_0^2 - (1 - 4r^2)a_0 = -t_1 \tag{4.32}$$

The equations (4.31)–(4.32) are nothing but the last two equations in (4.13), taking into account the values of a_1 and a_2 in (4.14).

As a consequence of Proposition 4.2.7, we can compute our phase diagram in the (r, a_0)-plane, as it is established by the next Theorem and it is shown in Figure 4.6.

Theorem 4.2.8. *On the (r, a_0)-plane, the curve Γ_c assumes the form*

$$r = s, \quad a_0 = \frac{1 - 2s}{2}, \qquad 0 < s < \frac{1}{2}, \tag{4.33}$$

and the curve γ_c assumes the form

$$r = s^3, \quad a_0 = \frac{3}{2}s^2, \qquad 0 < s < \frac{1}{2}. \tag{4.34}$$

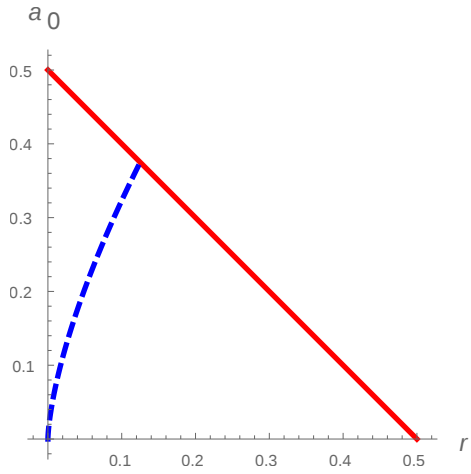

Figure 4.6: Image of the phase diagram in Figure 4.3 through the change of variables $(t_0, t_1) \mapsto (r, a_0)$. The solid curve is the image of Γ_c and the dashed curve is the image of γ_c. The region determined by the solid and dashed curves and the r-axis corresponds to $\mathcal{F}_1$, whereas the region between the solid and dashed curves and the a_0-axis corresponds to $\mathcal{F}_2$.

The proofs of Proposition 4.2.7 and Theorem 4.2.8 are given in Section 4.3.2.

4.2.6 The mother body problem

We now focus our attention on the mother body problem (4.11). In what follows, given a set $E \subset \mathbb{C}$ we denote

$$E^* = \{z \in \mathbb{C} \mid \overline{z} \in E\} \quad \text{and} \quad \mathbb{C}_\pm = \{z \in \mathbb{C} \mid \pm \operatorname{Im} z > 0\}. \tag{4.35}$$

Recall also that, according to Theorem 4.2.6, z_0, z_1 and z_2 are the branch points of the spectral curve (4.24).

Theorem 4.2.9. *There exists a contour Σ_* with*

$$\Sigma_* \subset \Omega, \tag{4.36}$$

and for which the solution ξ_1 in (4.27) admits an analytic continuation to $\mathbb{C} \setminus \Sigma_*$ that satisfies

$$(\xi_{1+}(s) - \xi_{1-}(s))ds \in i\mathbb{R}, \quad s \in \Sigma_*, \tag{4.37}$$

where ds is a tangent vector to Σ_* at the point s. The contour Σ_* is symmetric with respect to the real axis

$$(\Sigma_*)^* = \Sigma_*$$

and has the following geometric properties.

(i) (Three-cut case) For $(t_0, t_1) \in \mathcal{F}_1$, the contour Σ_* can be decomposed into

$$\Sigma_* = \Sigma_{*,0} \cup \Sigma_{*,1} \cup \Sigma_{*,2},$$

where each $\Sigma_{*,j}$ is a smooth oriented contour from a common point $z_* \in (-\infty, z_0)$ to the branch point z_j and

$$\Sigma_{*,0} = [z_*, z_0], \quad (\Sigma_{*,2})^* = \Sigma_{*,1} \subset \overline{\mathbb{C}}_-.$$

(ii) (One-cut case) For $(t_0, t_1) \in \mathcal{F}_2$, the contour Σ_* is given by

$$\Sigma_* = [z_1, z_0].$$

Moreover, the measure

$$d\mu_*(z) = \frac{1}{2\pi i t_0}(\xi_{1-}(z) - \xi_{1+}(z))dz, \quad z \in \Sigma_* \tag{4.38}$$

is a probability measure on Σ_*.

The phase diagram displayed in Figure 4.2 shows several configurations of $\operatorname{supp}\mu_*$, and we refer to Figure 4.7 for more detailed numerical evaluations of $\operatorname{supp}\mu_*$, displaying the evolution of $\operatorname{supp}\mu_*$ in time t_0 while t_1 is kept fixed.

As we mentioned in the introduction, the construction of the measure μ_* in Theorem 4.2.9 is our main technical contribution, and it is quite involved. The first step, carried out in Section 4.4, is to construct the Riemann surface $\mathcal{R}$ for (4.24); along the way we also collect several results that are used later on. The sheet structure of $\mathcal{R}$ depends, in the terminology of Theorem 4.2.9, on whether we are in the three-cut or one-cut cases, and are explicitly given in Sections 4.4.3.1 and 4.4.3.2, respectively. In Section 4.5, we introduce a certain quadratic differential ϖ that encodes μ_* on some of its trajectories. The main goal of Section 4.5 is to describe the critical graph $\mathcal{G}$ of ϖ. This is done by first computing $\mathcal{G}$ for $t_1 = 0$ by "brute force", and then deforming the parameter $t_1 > 0$, keeping track of all fundamental domains of $\mathcal{G}$. It turns out that the three-cut–to–one-cut phase transition for μ_* can be interpreted in terms of a phase transition for $\mathcal{G}$, and furthermore $\mathcal{G}$ also plays a fundamental role in the asymptotic analysis of the multiple orthogonal polynomials that will be

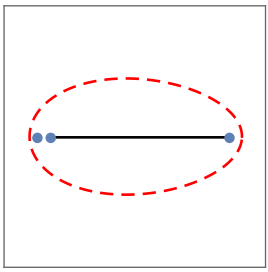

$(t_0, t_1) = (\frac{1}{2500}, \frac{1}{8}) \in \mathcal{F}_2$

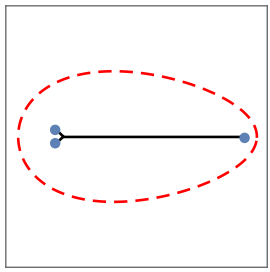

$(t_0, t_1) = (\frac{1}{500}, \frac{1}{8}) \in \mathcal{F}_1$

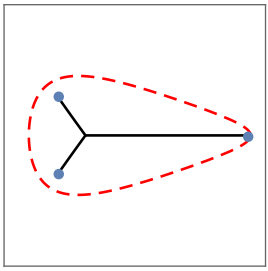

$(t_0, t_1) = (\frac{1}{50}, \frac{1}{8}) \in \mathcal{F}_1$

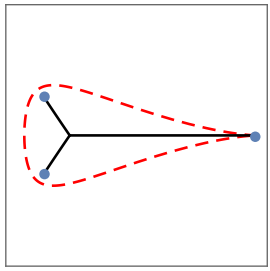

$(t_0, t_1) = (\frac{5}{128}, \frac{1}{8}) \in \Gamma_c$

Figure 4.7: For the given values of (t_0, t_1), the boundary $\partial\Omega$ (dashed contour), the support of the measure μ_* (solid lines) and the branch points z_0, z_1, z_2 (dots) are shown (the panels here are scaled differently - compare with Figure 4.4). Note the transition when we move from $\mathcal{F}_2$ to $\mathcal{F}_1$. We stress that the contours of $\operatorname{supp}\mu_*$ outside the real line are not straight line segments. Numerical outputs.

introduced in a moment. In Section 4.6 we use this critical graph $\mathcal{G}$ to recover the measure μ_*.

It is a consequence of this analysis that the support Σ_* of μ_*, and in particular the point z_*, is determined as the projection of certain trajectories of ϖ. Roughly speaking, there are a number of points $y \in (-\infty, z_0)$ which are solutions to

$$\operatorname{Re} \int_{z_2}^{y} (\xi_1(s) - \xi_2(s)) ds = 0,$$

where ξ_1, ξ_2 are (appropriate analytic continuations of) the functions in (4.27); the value $y = z_*$ is the largest of those solutions. We refer the reader to Sections 4.5 and 4.6 for details.

The measure μ_* is connected to the normal matrix model by the following theorem.

Theorem 4.2.10. *The measure μ_* in (4.38) relates to the limiting measure of eigenvalues μ_0 (4.8) through the conditions*

$$U^{\mu_0}(z) = U^{\mu_*}(z), \quad z \in \mathbb{C} \setminus \Omega, \tag{4.39}$$

$$U^{\mu_0}(z) < U^{\mu_*}(z), \quad z \in \Omega. \tag{4.40}$$

The proof of Theorem 4.2.10 is given in Section 4.6.

Given a domain $G \subset \mathbb{C}$, a measure ν is called a *mother body* (or also *potential-theoretic skeleton*) of G if [75]

(M1) $\operatorname{supp} \nu$ has null area measure;

(M2) $\mathbb{C} \setminus \operatorname{supp} \nu$ is connected;

(M3) $\operatorname{supp} \nu \subset G$;

(M4) for μ_G the normalized area measure of G, one has

$$U^{\mu_G}(z) \leq U^{\nu}(z), \quad z \in \mathbb{C},$$

$$U^{\mu_G}(z) = U^{\nu}(z), \quad z \in \mathbb{C} \setminus G.$$

Conditions (M1)–(M4) are, generally speaking, quite demanding, and consequently domains with mother bodies are somewhat rare. Cases where the existence of the mother body is known include discs, convex polyhedra [74] and ellipses [125], and mother bodies have also been obtained numerically for certain oval shapes [121]. Mother body measures appear in the context of quadrature domains [73], inverse problems in geophysics [137], zero distribution of orthogonal polynomials [77, 109], among others. We refer the reader to the lecture notes [75] by Gustafsson for more details.

Conditions (M1), (M2) and (M3) are satisfied for $\nu = \mu_*$ and $G = \Omega$. Equation (4.39) is the same as (4.11), and together with (4.40) they give (M4) and thus express that μ_* is a mother body for the domain Ω. For this reason, we call the "one-cut–to–three-cuts" phase transition for $\operatorname{supp} \mu_*$ the *mother body phase transition.*

When the (boundary of the) domain G displays some topological transition, it is natural to expect that its mother body measure displays some phase transition as well. In fact, this has already been described in several previous works in

the context of random normal matrices [19, 20, 38, 95], although in some cases without explicit mention. However, in our situation it is very interesting that the transition for μ_* occurs before any transition for Ω. In other words, the limiting domain for the eigenvalues of the normal matrix model (4.1) does not feel the mother body phase transition: as it is assured by Theorem 4.2.2, the boundary Ω depends analytically on the parameters (t_0, t_1) even across the critical curve γ_c.

To our knowledge, this is the first time a phase transition for the mother body, without any phase transition on the boundary of the underlying domain, is described in the literature. A somewhat related situation has already appeared in the work of Gustafsson and Lin [76, Example 5.2], where the authors identified, indirectly and without any detailed analysis, a phase transition for the branch points of the Schwarz function for a curve moving analytically in time: the branch points of the Schwarz function thus play the role of the end points of the mother body. Another similar phenomenon has been described in a previous work of Bleher and Liechty [41, Section X], where they identified a phase transition for the zero distribution of the underlying orthogonal polynomials that is not reflected in the asymptotics of the partition function studied therein. In virtue of this latter work, it is also natural to expect that the partition function of (4.1) for the cubic potential (4.12) should not "feel" the mother body phase transition.

4.2.7 Associated multiple orthogonality

We follow [19, 38] and replace the planar orthogonality to an orthogonality over contours.

Construct a piecewise smooth curve

$$\Sigma = \Sigma_0 \cup \Sigma_1 \cup \Sigma_2, \tag{4.41}$$

where each set Σ_j is a smooth oriented arc, starting at a common point $a_* \in \mathbb{R}$ and ending at the critical point $\hat{z}_j$ given by Theorem 4.2.6, $j = 0, 1, 2$. Recalling the notations introduced in (4.35), we assume

$$a_* < \hat{z}_0, \quad \Sigma_0 = [a_*, \hat{z}_0], \quad \Sigma_1 \subset \mathbb{C}_- \cup \{a_*\}, \quad \Sigma_2 \subset \mathbb{C}_+ \cup \{a_*\}. \tag{4.42}$$

we refer for instance to Figure 4.8 for a possible configuration of Σ. At this moment the contour Σ is rather arbitrary; in fact the conditions in (4.42) are made for simplicity and could even be loosen. But later the contour Σ will be chosen in an optimal way.

As a general notational convention, for the rest of the chapter we use cyclic notation mod 3 without further mention when clear from the context. So for

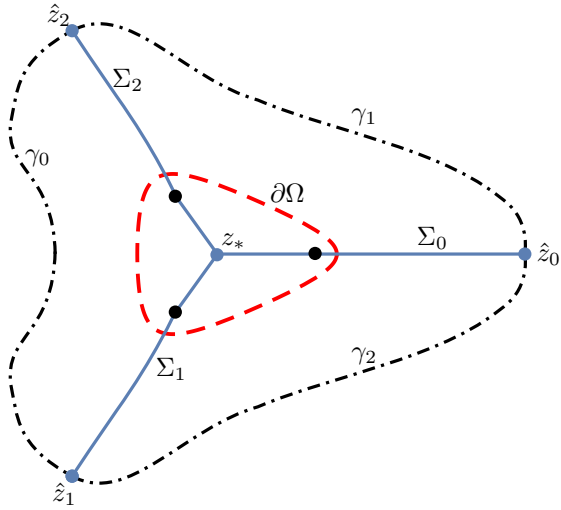

Figure 4.8: The dashed curve is $\partial\Omega$ and the dots inside it are the branch points z_0, z_1 and z_2 and the point z_*. The dot-dashed line is a possible configuration for $\partial D = \gamma_0 \cup \gamma_1 \cup \gamma_2$, and the points on ∂D are the critical points $\hat{z}_0$, $\hat{z}_1$ and $\hat{z}_2$. The solid contour is a possible extension $\Sigma = \Sigma_0 \cup \Sigma_1 \cup \Sigma_2$ of the support Σ_* of the mother body measure Σ_*.

instance

$$\hat{z}_3 = \hat{z}_0, \quad \hat{z}_4 = \hat{z}_1, \quad \hat{z}_5 = \hat{z}_2,$$

and similarly for other quantities appearing later on.

Consider a compact, connected set $D \subset \mathbb{C}$, assuming in addition

$$\Sigma, \Omega \subset D, \quad \hat{z}_l \in \partial D, \ l = 0, 1, 2,$$

where Σ is a curve as just explained above and Ω is the domain given by Theorem 4.2.2. The domain D should be interpreted as the cut off region in (4.10).

The points $\hat{z}_0, \hat{z}_1, \hat{z}_2$ split the boundary ∂D into three curves $\gamma_0, \gamma_1, \gamma_2$. For $l = 0, 1, 2$ (and again with cyclic notation mod 3), the curve γ_l is the oriented sub arc of ∂D going from $\hat{z}_{l+2}$ to $\hat{z}_{l+1}$ that does not contain $\hat{z}_l$, see Figure 4.8 for an example of a configuration of D, Σ and Ω.

For the third root of unity ω and the directions at infinity ∞_l given by

$$\omega = e^{\frac{2\pi i}{3}}, \quad \infty_l = -\omega^{-l}\infty, \quad l = 0, 1, 2, \tag{4.43}$$

let Γ_l be any unbounded oriented contour from ∞_{l+1} to ∞_{l+2}, $l = 0, 1, 2$. Also for $l = 0, 1, 2$ and any non negative integer k, define

$$w_{l,k,n}(z) = \int_{\Gamma_l} s^k e^{-\frac{n}{t_0}(sz - V(s) - V(z))} ds, \quad z \in \mathbb{C}, \tag{4.44}$$

$$\widetilde{w}_{l,k,n}(z) = \int_{\infty_l}^{\overline{z}} s^k e^{-\frac{n}{t_0}(sz - V(s) - V(z))} ds, \quad z \in \mathbb{C}.$$

where we recall that V is given in (4.12).

For $l = 0, 1, 2$, the union of contours $\gamma_l \cup \Sigma_{l+1} \cup \Sigma_{l+2}$ is the boundary of a domain $D_l \subset D$. An application of Green's Theorem to each of the pieces D_0, D_1, D_2 yields

Proposition 4.2.11. *For any polynomial Q and any integer $k \geq 0$, it is valid*

$$2i \int_D Q(z) \overline{z}^k e^{-\frac{n}{t_0}\left(|z|^2 - 2 \operatorname{Re} V(z)\right)} dA(z)$$

$$= \sum_{l=0}^{2} \int_{\Sigma_l} Q(z) w_{l,k,n}(z) dz + \sum_{l=0}^{2} \int_{\gamma_l} Q(z) \widetilde{w}_{l,k,n}(z) dz. \tag{4.45}$$

The analogue to Proposition 4.2.11 for the monomial case $V(z) = \frac{z^d}{d}$, $d \geq 3$, is treated in [90, Proposition 1.1]. For the benefit of the reader we include the proof for V as in (4.12), which follows the same arguments presented in [90].

Proof. Let us apply the complex Green's theorem

$$2i \int_S \frac{\partial f}{\partial \overline{z}} \, dA = \int_{\partial S} f \, dz$$

with $S = D_l$ and $f = Q(z)\widetilde{w}_{l,k,n}(z)$. Then we obtain that

$$2i \int_{D_l} Q(z) \overline{z}^k e^{-\frac{n}{t_0}\left(|z|^2 - V(\overline{z}) - V(z)\right)} \, dA(z) = \int_{\partial D_l} Q(z) \widetilde{w}_{l,k,n}(z) \, dz.$$

Summing over $l = 0, 1, 2$, we get that

$$2i \int_D Q(z) \overline{z}^k e^{-\frac{n}{t_0}\left(|z|^2 - V(\overline{z}) - V(z)\right)} \, dA(z) = \sum_{l=0}^{2} \int_{\partial D_l} Q(z) \widetilde{w}_{l,k,n}(z) \, dz. \tag{4.46}$$

The sum on the right can be partitioned as

$$\sum_{l=0}^{2}\int_{\partial D_l} Q(z)\widetilde{w}_{l,k,n}(z)\,dz = \sum_{l=0}^{2}\left[\int_{\gamma_l} Q(z)\widetilde{w}_{l,k,n}(z)\,dz + \int_{\Sigma_{l+2}} Q(z)\widetilde{w}_{l,k,n}(z)\,dz - \int_{\Sigma_{l+1}} Q(z)\widetilde{w}_{l,k,n}(z)\,dz\right].$$

Combining integrals over Σ_l, we obtain that

$$\sum_{l=0}^{2}\int_{\partial D_l} Q(z)\widetilde{w}_{l,k,n}(z)\,dz = \sum_{l=0}^{2}\int_{\gamma_l} Q(z)\widetilde{w}_{l,k,n}(z)\,dz + \sum_{l=0}^{2}\int_{\Sigma_l} Q(z)\left[\widetilde{w}_{l+1,k,n}(z) - \widetilde{w}_{l+2,k,n}(z)\right]\,dz.$$

We now observe that

$$\begin{aligned}\widetilde{w}_{l+1,k,n}(z) - \widetilde{w}_{l+2,k,n}(z) &= \int_{\infty_{l+1}}^{\overline{z}} s^k e^{-\frac{n}{t_0}(sz-V(s)-V(z))}ds \\ &\quad - \int_{\infty_{l+2}}^{\overline{z}} s^k e^{-\frac{n}{t_0}(sz-V(s)-V(z))}ds \\ &= \int_{\Gamma_l} s^k e^{-\frac{n}{t_0}(sz-V(s)-V(z))}ds \\ &= w_{l,k,n}(z),\end{aligned}$$

hence

$$\sum_{l=0}^{2}\int_{\partial D_l} Q(z)\widetilde{w}_{l,k,n}(z)\,dz = \sum_{l=0}^{2}\int_{\gamma_l} Q(z)\widetilde{w}_{l,k,n}(z)\,dz + \sum_{l=0}^{2}\int_{\Sigma_l} Q(z)w_{l,k,n}(z)\,dz. \quad (4.47)$$

Equation (4.45) then follows from (4.46) and (4.47). □

In particular, if $Q = q_{j,n}$ is the planar orthogonal polynomial (4.10), we conclude

$$\sum_{l=0}^{2} \int_{\Sigma_l} q_{j,n}(z) w_{l,k,n}(z) dz \; + \; \sum_{l=0}^{2} \int_{\gamma_l} q_{j,n}(z) \widetilde{w}_{l,k,n}(z) dz = 0, \quad k = 0, \dots, j-1. \tag{4.48}$$

Led by the fact that the integrals coming from $\partial D = \cup \gamma_l$ should be negligible compared to the integrals over Σ when $n \to \infty$, we follow [38, 90] and neglect the integrals over ∂D in (4.48). This motivates the introduction of the following family of polynomials.

Definition 4.2.12. We define $P_{j,n}$ to be the monic polynomial of degree j, if it exists, that satisfies

$$\sum_{l=0}^{2} \int_{\Sigma_l} P_{j,n}(z) w_{l,k,n}(z) dz = 0, \quad k = 0, \dots, j-1, \tag{4.49}$$

where the weights $w_{l,k,n}$, $k, n \in \mathbb{N}$, $l = 0, 1, 2$, are given in (4.44).

Proposition 4.2.13. *The polynomial $P_{j,n}$, if it exists, fulfills the non-hermitian multiple orthogonality conditions*

$$\begin{aligned} \sum_{l=0}^{2} \int_{\Sigma_l} P_{j,n}(z) z^k w_{l,0,n}(z) dz = 0, \quad k = 0, \dots, \left\lceil \frac{j}{2} \right\rceil - 1, \\ \sum_{l=0}^{2} \int_{\Sigma_l} P_{j,n}(z) z^k w_{l,1,n}(z) dz = 0, \quad k = 0, \dots, \left\lfloor \frac{j}{2} \right\rfloor - 1. \end{aligned} \tag{4.50}$$

For a proof when $t_1 = 0$, we refer to [38, Lemma 5.1]. The case $t_1 \neq 0$ is treated similarly. For the sake of completeness we give the proof.

Proof. Equation (4.49) reads

$$\sum_{l=0}^{2} \int_{\Sigma_l} P_{j,n}(z) \int_{\Gamma_l} s^k e^{-\frac{n}{t_0}(sz - V(s) - V(z))} ds dz = 0, \quad k = 0, \dots, j-1. \tag{4.51}$$

Let $Q(s)$ be any polynomial. Integration by parts gives the identity

$$\begin{aligned} &\int_{\Gamma_l} Q'(s) e^{-\frac{n}{t_0}(sz - V(s) - V(z))} ds \\ &\qquad = \frac{n}{t_0} \int_{\Gamma_l} Q(s) \left(z - V'(s)\right) e^{-\frac{n}{t_0}(sz - V(s) - V(z))} ds, \end{aligned}$$

hence

$$z\int_{\Gamma_l} Q(s)e^{-\frac{n}{t_0}(sz-V(s)-V(z))}ds$$
$$= \int_{\Gamma_l}\left(V'(s)Q(s)+\frac{t_0}{n}Q'(s)\right)e^{-\frac{n}{t_0}(sz-V(s)-V(z))}ds. \quad (4.52)$$

Introduce the linear differential operator

$$\mathcal{A}: Q(s)\mapsto V'(s)Q(s)+\frac{t_0}{n}Q'(s). \quad (4.53)$$

Then the identity (4.52) can be written as

$$z\int_{\Gamma_l} Q(s)e^{-\frac{n}{t_0}(sz-V(s)-V(z))}ds = \int_{\Gamma_l}\mathcal{A}(Q)(s)e^{-\frac{n}{t_0}(sz-V(s)-V(z))}ds.$$

Applying it k times, we obtain that

$$z^k\int_{\Gamma_l} Q(s)e^{-\frac{n}{t_0}(sz-V(s)-V(z))}ds = \int_{\Gamma_l}\mathcal{A}^k(Q)(s)e^{-\frac{n}{t_0}(sz-V(s)-V(z))}ds,$$

thus

$$\sum_{l=0}^{2}\int_{\Sigma_l} P_{j,n}(z)z^k\int_{\Gamma_l} Q(s)e^{-\frac{n}{t_0}(sz-V(s)-V(z))}dsdz$$
$$= \sum_{l=0}^{2}\int_{\Sigma_l} P_{j,n}(z)\int_{\Gamma_l}\mathcal{A}^k(Q)(s)e^{-\frac{n}{t_0}(sz-V(s)-V(z))}dsdz.$$

Observe that if $Q(s)$ is a polynomial, then $\mathcal{A}^k(Q)(s)$ is a polynomial as well, and since $\deg V'=2$, we obtain from (4.53) that

$$\deg\mathcal{A}^k(Q)=\deg Q+2k,$$

hence if $Q(s)\equiv 1$ and $2k<j$, then orthogonality condition (4.51) implies that

$$\sum_{l=0}^{2}\int_{\Sigma_l} P_{j,n}(z)z^k\int_{\Gamma_l} e^{-\frac{n}{t_0}(sz-V(s)-V(z))}dsdz$$
$$= \sum_{l=0}^{2}\int_{\Sigma_l} P_{j,n}(z)\int_{\Gamma_l}\mathcal{A}^k(1)(s)e^{-\frac{n}{t_0}(sz-V(s)-V(z))}dsdz=0.$$

This proves the first identity in (4.50). To prove the second one, we take $Q(s) \equiv s$ and any k such that $2k+1 < j$. Then the orthogonality condition (4.51) implies that

$$\sum_{l=0}^{2} \int_{\Sigma_l} P_{j,n}(z) z^k \int_{\Gamma_l} s e^{-\frac{n}{t_0}(sz - V(s) - V(z))} ds dz$$

$$= \sum_{l=0}^{2} \int_{\Sigma_l} P_{j,n}(z) \int_{\Gamma_l} \mathcal{A}^k(z)(s) e^{-\frac{n}{t_0}(sz - V(s) - V(z))} ds dz = 0.$$

This proves (4.50). □

We are mostly interested in the *diagonal* polynomials $P_{n,n}$. From Proposition 4.2.13 we obtain that the polynomial $P_{n,n}$ fulfills the non-hermitian multiple orthogonality conditions

$$\begin{aligned} \sum_{l=0}^{2} \int_{\Sigma_l} P_{n,n}(z) z^k w_{l,0,n}(z) dz = 0, \quad k = 0, \dots, \left\lceil \frac{n}{2} \right\rceil - 1, \\ \sum_{l=0}^{2} \int_{\Sigma_l} P_{n,n}(z) z^k w_{l,1,n}(z) dz = 0, \quad k = 0, \dots, \left\lfloor \frac{n}{2} \right\rfloor - 1. \end{aligned} \tag{4.54}$$

We remark that there is no complex conjugation on the integrands in (4.54). Consequently, it follows from the construction of the functions $w_{l,k,n}$ that the orthogonality conditions (4.54) do not depend on the precise choice of the contour Σ as in (4.41), but only on its endpoints $\hat{z}_0, \hat{z}_1$ and $\hat{z}_2$.

As a consequence of Proposition 4.2.13, $P_{n,n}$ is additionally characterized through a Riemann-Hilbert problem (shortly RHP). We apply the nonlinear Deift/Zhou steepest descent analysis [50,53] to this RHP and obtain the existence and asymptotic information for the polynomial $P_{n,n}$ for n sufficiently large. This analysis is carried out in Sections 4.7 and 4.8 for the three-cut and one-cut cases, respectively, and we refer the reader to these sections for more details. We also stress that several trajectories of the quadratic differential ϖ constructed in Section 4.5 play a fundamental role in this asymptotic analysis. One of the outcomes of it is regarding the zero counting measure

$$\mu_n = \frac{1}{n} \sum_{P_{n,n}(w)=0} \delta_w. \tag{4.55}$$

Theorem 4.2.14. *Suppose $(t_0, t_1) \in \mathcal{F} \setminus \gamma_c$. The sequence of zero counting measures (μ_n) converges weakly to the measure μ_* given by (4.38).*

By Theorem 4.2.2, we know that the restriction of h to $\overline{\mathbb{C}} \setminus \mathbb{D}$ admits an inverse $\psi_1 : \overline{\mathbb{C}} \setminus \Omega \to \overline{\mathbb{C}} \setminus \mathbb{D}$. The function ψ_1 is alternatively characterized as the conformal map from $\mathbb{C} \setminus \overline{\Omega}$ to $\mathbb{C} \setminus \overline{\mathbb{D}}$ that is uniquely determined by the conditions

$$\lim_{z\to\infty} \psi_1(\infty) = \infty, \quad \lim_{z\to\infty} \psi_1'(z) = \frac{1}{r},$$

where r is as in Proposition 4.2.1.

In addition, define the multivalued analytic function

$$G(z) = \int_{z_0}^{z} \xi_1(s)ds, \quad z \in \mathbb{C} \setminus \Sigma_*, \tag{4.56}$$

where z_0 is as in Theorem 4.2.6, ξ_1 is as in (4.27) and the path of integration is taken in $\mathbb{C} \setminus \Sigma_*$. As can be seen from the expansion (4.27), the residue of the function ξ_1 at ∞ is $-t_0$. In particular, this implies that G is well defined modulo $2\pi i t_0$.

As for the uniform asymptotics for $P_{n,n}$, one of the consequences of our asymptotic analysis is given by the following result.

Theorem 4.2.15. *Suppose $(t_0, t_1) \in \mathcal{F} \setminus \gamma_0$. The map ψ_1 admits an analytic continuation to $\mathbb{C} \setminus \Sigma_*$, and for a certain constant c, the asymptotic formula*

$$P_{n,n}(z) = \sqrt{r\psi_1'(z)}e^{\frac{n}{t_0}(G(z)-V(z)+c)}(1 + \mathcal{O}(n^{-1})), \tag{4.57}$$

holds uniformly on compacts of $\mathbb{C} \setminus \Sigma_*$, where the branch of the square root is chosen with branch cut on Σ_* and so that $\sqrt{r\psi_1'(z)} \to 1$ as $z \to \infty$.

Theorems 4.2.14 and 4.2.15 are proven in Section 4.10, after the conclusion of the steepest descent analysis.

Relation (4.39) is comparable with results by Elbau [64, Lemma 5.1 and Theorem 5.3]. As mentioned in the introduction, Elbau shows that any weak limit ν of the sequence of zero counting measures for the polynomials $(q_{n,n})$ in (4.10) should also satisfy (4.39) (with μ_* replaced by ν). Hence, what Theorem 4.2.14 says is that, at the level of weak asymptotics, our multiple orthogonal polynomials $(P_{n,n})$ have the same behavior as expected for the planar orthogonal polynomials $(q_{n,n})$. We also expect the formula (4.57) to hold true if we replace $P_{n,n}$ by the polynomial $q_{n,n}$.

The restriction $(t_0, t_1) \in \mathcal{F} \setminus \gamma_c$ in Theorems 4.2.14 and 4.2.15 is of technical nature. For these values of (t_0, t_1), the density of μ_* vanishes as square root at

the endpoints of its support, and as a consequence the required local parametrices in the steepest descent analysis are constructed out of solutions to the Airy differential equation. However, in the critical case $(t_0, t_1) \in \gamma_c$ the density of μ_* vanishes with order $1/3$ at the endpoint $z_1 = z_2$, and a different parametrix is required to complete the steepest descent analysis. This order of vanishing indicates that the local parametrix near $z_1 = z_2$ should be constructed in terms of solutions to the Pearcey differential equation (see for instance [37] and the references therein), but the rest of the analysis carried out here should work, after cosmetic changes, in this critical case as well. In particular, the conclusions of Theorems 4.2.14 and 4.2.15 should also hold true for $(t_0, t_1) \in \gamma_c$.

4.2.8 Behavior at the boundary of the phase diagram

When $(t_0, t_1) \in \Gamma_c$, the branch point z_0 and the double point $\hat{z}_0$ described in Theorem 4.2.6 come together at the boundary $\partial\Omega$. This corresponds to a branching of the Schwarz function ξ_1 on $\partial\Omega$, and explains the emerging of the cusp in $\partial\Omega$, as can be seen, for instance, in Figures 4.2, 4.4 and 4.7.

Consequently, when $(t_0, t_1) \in \Gamma_c$ the support of $\operatorname{supp}\mu_*$ comes to the boundary of Ω as well, and the density of the measure μ_* vanishes with order $3/2$ at the endpoint $z_0 = \hat{z}_0$. This coalescence (for $t_1 = 0$) is already described in the literature (see for instance [38, 95, 99]), and the local behavior of the polynomial $P_{n,n}$ (after suitable regularization in terms of bilinear forms instead of a cut-off) near this point is expected to be given in terms of solutions to the Painlevé I equation, see for instance [32, 61] for related works. When $t_1 > 0$, nothing special happens near the other endpoints z_1, z_2 of $\operatorname{supp}\mu_*$.

4.2.9 The S-property

Thanks to the precise manner we constructed the weights for the integrals in each contour Σ_l, the sum of integrals in (4.54) neither depends on the precise choice of contours Σ_1, Σ_2 and Σ_3 nor on their common point a_*. This freedom is reflected in Theorem 4.2.14, which says that the zeros of $P_{n,n}$ accumulate on $\operatorname{supp}\mu_*$ regardless of the precise choice of the contour Σ. Furthermore, although the orthogonality conditions (4.54) do depend on the choice of endpoints $\hat{z}_0, \hat{z}_1$ and $\hat{z}_2$ for Σ, it becomes clear from our RH analysis that there is some flexibility in the choice of these points: in the large n limit the behavior of $P_{n,n}$ does not depend on these endpoints, as long as they are selected within some regions determined by certain critical trajectories of the underlying quadratic differential.

This freedom in the choice of the contour Σ is characteristic for non-hermitian orthogonality, and it is reflected in the behavior of the zeros of the respective orthogonal polynomials. Among all possible choices of contours, the zeros, in the large n limit, accumulate on a very particular one, determined by the so called *S-property*, as we discuss next.

Given a contour Σ for the orthogonality (4.54), construct three other oriented contours L_j, $j = 0, 1, 2$, starting at the point a_* in the inner sector between Σ_{j-1} and Σ_{j+1}, and extending to ∞ along the directions ∞_j, $j = 0, 1, 2$, as defined in (4.43). Assume in addition $L_j \cap L_k = L_j \cap \Sigma = \{a_*\}$ for $j \neq k$ and set $L = L_0 \cup L_1 \cup L_2$. We refer to Figure 4.29 in Section 4.7.3 for an example of the configuration of L and Σ.

To any pair of contours (Σ, L) as above, we associate a class of pairs of measures $\mathcal{M}(\Sigma, L) = \{(\nu_1, \nu_2)\}$, where each pair (ν_1, ν_2) satisfies the constraints

$$|\nu_1| = 2|\nu_2| = 1, \quad \operatorname{supp} \nu_1 \subset \Sigma, \quad \operatorname{supp} \nu_2 \subset L.$$

For a pair $(\nu_1, \nu_2) \in \mathcal{M}(\Sigma, L)$, we denote by

$$I(\nu_1, \nu_2) = \iint \log \frac{1}{|s - z|} d\nu_1(s) d\nu_2(s)$$

their mutual logarithmic energy and define the *vector energy*

$$E(\nu_1, \nu_2) = I(\nu_1, \nu_1) + I(\nu_2, \nu_2) - I(\nu_1, \nu_2) - \frac{1}{t_0} \int \operatorname{Re}(V(x) - \Psi(x)) d\nu_1(x),$$

where $\Psi(z)$ is an appropriate branch of $\frac{2}{3}(z - t_1)^{3/2}$.

The *vector equilibrium problem* for the pair (Σ, L) and the energy $E(\cdot)$ asks for minimizing this vector energy on $\mathcal{M}(\Sigma, \Gamma)$. That is, asks for finding a pair $(\lambda_1, \lambda_2) \in \mathcal{M}(\Sigma, L)$, the so-called *vector equilibrium measure*, satisfying

$$E(\lambda_1, \lambda_2) = \inf_{(\mu_1, \mu_2) \in \mathcal{M}(\Sigma, L)} E(\mu_1, \mu_2).$$

We stress that the vector equilibrium measure (λ_1, λ_2) depends on the pair of contours (Σ, L). Finally, the *S-property problem* asks for finding a pair of contours (Σ, L) for which the respective vector equilibrium measure (λ_1, λ_2) satisfies the *S-properties*

$$\frac{\partial}{\partial n_+} \left(2U^{\lambda_1}(z) - U^{\lambda_2}(z) - \frac{1}{t_0} \operatorname{Re}(V(z) - \Psi(z)) \right) =$$

$$\frac{\partial}{\partial n_-} \left(2U^{\lambda_1}(z) - U^{\lambda_2}(z) - \frac{1}{t_0} \operatorname{Re}(V(z) - \Psi(z)) \right), \quad z \in \operatorname{supp} \lambda_1$$

and

$$\frac{\partial}{\partial n_+}\left(2U^{\lambda_2}(z)-U^{\lambda_1}(z)\right)=\frac{\partial}{\partial n_-}\left(2U^{\lambda_2}(z)-U^{\lambda_1}(z)\right),\quad z\in\operatorname{supp}\lambda_2,$$

where $n_\pm$ are the normal vectors to $\Sigma\cup L$ and U^{λ_j} is defined in (4.20). If the pair (Σ,L) has the S-property as above, we call it a pair of *S-contours*

The S-property has been originally introduced in the context of Padé approximants by H. Stahl [128,129,130] and further extended by A. Gonchar and E. Rakhmanov [71] to non-hermitian orthogonality with varying weights, see also [21,24,84,94,104,116] for a more recent account of results when dealing with non-hermitian orthogonality.

However, the S-property for multiple orthogonality is much less clear. To our knowledge, the cases which have been studied so far are either restricted to multiple orthogonality with fixed (non varying) weights [11] or make strong symmetry assumptions for the weights [9, 33, 35, 38]. For all of those, the S-property followed directly from the symmetry at hand.

In the present setting, given a pair of contours (Σ,L) as above, the vector equilibrium energy exists, is unique and can be further characterized in terms of certain (Euler-Lagrange) variational conditions [22,79]. However, finding the pair of S-contours is a much more delicate matter. To recover the S-property in our setting, we recall the condition (4.37), which allows us to define the *positive* measure μ_* as in (4.38). From our analysis of the underlying quadratic differential in Section 4.5, it is possible to construct two contours (Σ,L) such that the respective vector equilibrium measure is of the form (μ_*,λ_*), where the measure μ_* is the one given by Theorem 4.2.9. The contour L satisfies the auxiliary condition

$$(\xi_{2+}(z)-\xi_{3+}(z))dz\in i\mathbb{R},\quad z\in L,\tag{4.58}$$

and the measure λ_* can be constructed from this condition. It then follows that the S-property for this pair of contours (Σ,L) is actually equivalent to the conditions (4.37) and (4.58). Consequently, the measure μ_* can also be interpreted in terms of the S-property above, and conditions (4.37) and (4.58) can be regarded as *algebraic* S-properties. As we will see later, (4.37) and (4.58) also play a fundamental role in the construction of the g-functions used in the forthcoming RH analysis.

4.2.10 Statement of Results - $t_1<0$

As we mentioned in the introduction, after appropriate modifications the results of Sections 4.2.1–4.2.9 are also valid for $t_1\in(-3/4,0)$, as we discuss next.

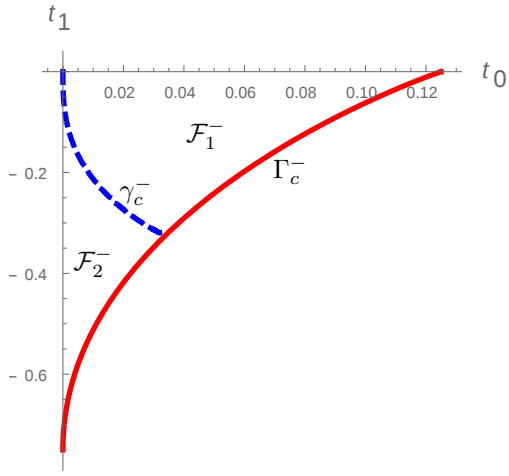

Figure 4.9: Phase diagram for t_1 negative. The dashed curve is γ_c^-, whereas the solid curve is Γ_c^-. The region to the right of γ_c^- is $\mathcal{F}_1^-$, whereas the region to the left of γ_c^- is $\mathcal{F}_2^-$.

The curve

$$\Gamma_c^- : \quad t_0 = -16s^6 + 6s^4, \quad t_1 = -12s^4 + 6s^2 - \frac{3}{4}, \quad 0 \le s \le \frac{1}{2},$$

together with the horizontal and vertical axes determine a bounded domain $\mathcal{F}^-$ on the (t_0, t_1)-plane, see Figure 4.9. Note in particular that $t_1 < 0$, whenever $(t_0, t_1) \in \mathcal{F}^-$.

When $(t_0, t_1) \in \mathcal{F}^-$, Proposition 4.2.1 still holds true. That is, the polynomial p still has a smallest positive root, always simple, that we keep denoting by $r = r(t_0, t_1)$. The coefficient a_0 in (4.16) is well-defined, but now it becomes negative. Nevertheless, the rational function h in (4.15) is also well-defined, and Theorems 4.2.2, 4.2.3 and 4.2.4 hold true without any modification in their statements. However, we emphasize that the behavior of the roots of p and of the coefficients r and a_0, as functions of (t_0, t_1), change when compared to $t_1 > 0$, so all the auxiliary results needed in their proofs have to be modified. We refer the reader to Figure 4.10 where, for a certain choice of $t_1 < 0$, the evolution in time $t_0 > 0$ of the boundary $\partial\Omega$ is displayed.

The quantities $B = B(t_0, t_1)$, $A = A(t_0, t_1)$, given respectively in equations (4.25) and (4.26), are still meaningful, and so is the spectral curve in (4.24), and Theorem 4.2.5 also holds true for $(t_0, t_1) \in \mathcal{F}^-$. As for the branch points and critical points of the spectral curve, we have the following result.

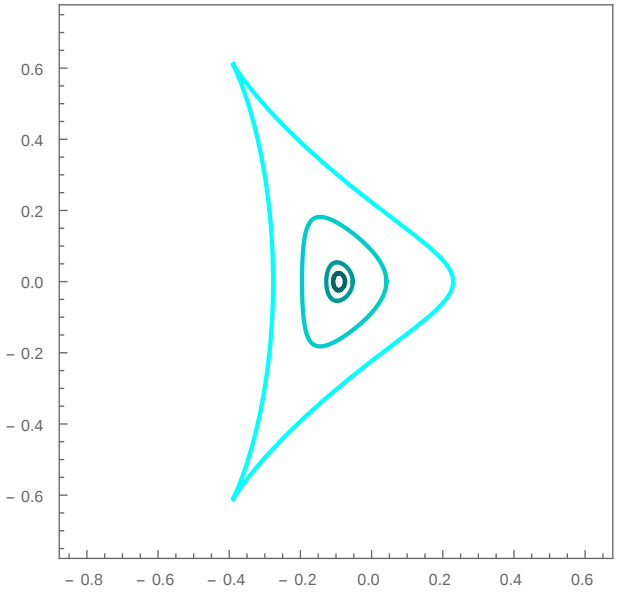

Figure 4.10: The boundary $\partial\Omega$ corresponding to $t_1 = -\frac{1}{10}$ and $t_0 = \frac{1}{2500}, \frac{1}{500}, \frac{1}{50}$ and $\frac{35+4\sqrt{30}}{1800}$. (respectively from dark to bright color). For the pair given by $(t_0, t_1) = (\frac{35+4\sqrt{30}}{1800}, -\frac{1}{10})$, which belongs to the critical curve Γ_c^-, cusps are created at the boundary. Numerical output.

Theorem 4.2.16. *For $(t_0, t_1) \in \mathcal{F}^-$, the spectral curve (4.24) has three simple branch points $z_0, z_1, z_2 \in \mathbb{C}$ with*

$$z_0 \in \mathbb{R}, \quad z_1 \in \mathbb{C}_-, \quad z_2 = \overline{z}_1, \quad z_1, z_2 \in \Omega,$$

and three singular points $\hat{z}_0, \hat{z}_1, \hat{z}_2 \in \mathbb{C} \setminus \overline{\Omega}$ which satisfy

$$\hat{z}_0 \in \mathbb{R}, \quad \hat{z}_1 \in \mathbb{C}_-, \quad z_2 = \overline{z}_1.$$

Comparing Theorem 4.2.16 with the three-cut case $(t_0, t_1) \in \mathcal{F}_1$ in Theorem 4.2.6, the essential difference here is that the point z_0 is not always in the domain Ω. For t_1 negative and small, the three points z_0, z_1 and z_2 are branch points of the Schwarz function ξ_1 of $\partial\Omega$. However, when t_1 decreases (while $t_0 > 0$ is kept fixed), this point z_0 becomes a branch point of the other two solutions ξ_2, ξ_3 of the spectral curve (4.24), but it is not anymore a branch point of ξ_1. If we keep decreasing t_1 the branch point z_0 might leave the domain Ω, even before t_1 reaches the critical value $-3/4$. This phenomenon is reflected in the mother body measure μ_*, as will be explained in a moment.

Theorem 4.2.17. *Suppose $(t_0, t_1) \in \mathcal{F}^-$ and z_0 and z_2 are the branch points given by Theorem 4.2.16. The implicit equation*

$$\operatorname{Re} \int_{z_0}^{z_2} (\xi_1(s) - \xi_2(s)) ds = 0 \tag{4.59}$$

defines an analytic curve γ_c^- on the (t_0, t_1)-plane, which connects the boundary Γ_c^- to the origin.

A plot of the curve γ_c^- can be seen in Figure 4.9. This curve determines two regions $\mathcal{F}_1^-, \mathcal{F}_2^- \subset \mathcal{F}^-$, labeled such that $\mathcal{F}_1^-$ ($\mathcal{F}_2^-$) consists of the points in $\mathcal{F}^-$ that are above (below) γ_c^-.

Proposition 4.2.7 holds true for $(t_0, t_1) \in \mathcal{F}_-$ without any modification, and Theorem 4.2.8 assumes the following form.

Theorem 4.2.18. *On the (r, a_0)-plane, the critical curve Γ_c^- is expressed as*

$$r = s, \quad a_0 = -\frac{1 - 4s^2}{2}, \qquad 0 < s < \frac{1}{2},$$

and the curve γ_c^- is implicitly given by

$$\begin{aligned} &(r + w_0^3) \left[(30 a_0^2 r^2 + 4 a_0^3) w_0^3 + r a_0 (r^2 (12 - 8 a_0) + 10 a_0) w_0^2 \right. \\ &\left. + 6 a_0 r^2 (5 - r^2) w_0 + 12 r^3 + 3 r^5 \right] + 3 w_0^6 r^2 (1 - 4 a_0^2 - 2 r^2) \log \frac{w_0^3}{r} = 0, \end{aligned} \tag{4.60}$$

where $w_0 = w_0(r, a_0)$ is the unique real solution to $h'(w) = 0$.

The critical curves Γ_c^- and γ_c^- on the (r, a_0)-plane are displayed in Figure 4.11.

The function w_0 is algebraic in r and a_0, and the presence of the log term in (4.60) indicates that the curve γ_c^- is transcendental. In particular, γ_c^- is not the analytic continuation of γ_c (see also Section 4.2.11 below). For an indication on how to get (4.59)–(4.60), we refer to Remark 4.11.6.

We are ready to state the result equivalent to Theorem 4.2.9.

Theorem 4.2.19. *For $(t_0, t_1) \in \mathcal{F}^-$, there exists a contour $\Sigma_* \subset \Omega$ for which the function ξ_1 in (4.27) admits an analytic continuation to $\mathbb{C} \setminus \Sigma_*$ that satisfies the property*

$$(\xi_{1+}(s) - \xi_{1-}(s)) ds \in i\mathbb{R}, \quad z \in \Sigma_*.$$

The contour Σ_* is symmetric with respect to the real axis, and

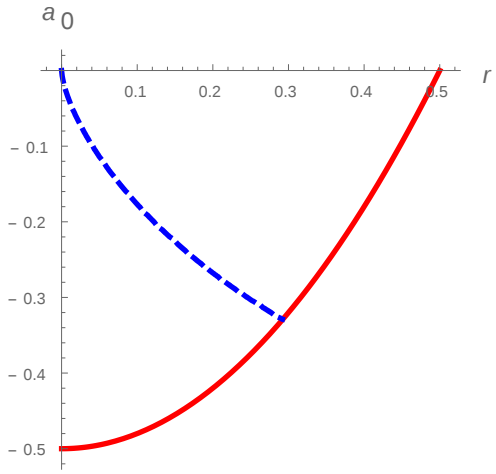

Figure 4.11: Image of the phase diagram in Figure 4.3 through the change of variables $(t_0, t_1) \mapsto (r, a_0)$. The solid curve is the image of Γ_c^- and the dashed curve is the image of γ_c^-. The region determined by the solid and dashed curves and the r-axis corresponds to $\mathcal{F}_1^-$, whereas the region between the solid and dashed curves and the a_0-axis corresponds to $\mathcal{F}_2^-$.

(i) (Three-cut case) For $(t_0, t_1) \in \mathcal{F}_1^-$, the contour Σ_* decomposes as

$$\Sigma_* = \Sigma_{*,0} \cup \Sigma_{*,1} \cup \Sigma_{*,2},$$

where $\Sigma_{*,l}$ is a smooth oriented contour from a common point $z_* \in (-\infty, z_0)$ to the branch point z_l and

$$\Sigma_{*,0} = [z_*, z_0], \quad (\Sigma_{*,2})^* = \Sigma_{*,1} \subset \overline{\mathbb{C}}_-.$$

(ii) (One-cut case) For $(t_0, t_1) \in \mathcal{F}_1^-$, the contour Σ_* is a single analytic arc which connects the branch points z_1 and z_2 and intersects the real axis at a point $z_* > z_0$.

Furthermore, the measure

$$d\mu_*(z) = \frac{1}{2\pi i t_0}(\xi_{1-}(z) - \xi_{1+}(z))dz, \quad z \in \Sigma_*$$

is a probability measure on Σ_*.

The arc Σ_* for various choices of the parameter (t_0, t_1) is displayed in Figure 4.12.

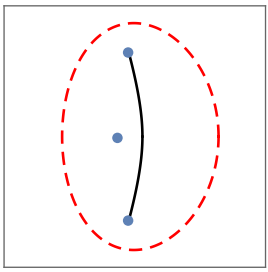

$(t_0, t_1) = (\frac{1}{2500}, -\frac{1}{10}) \in \mathcal{F}_2^-$

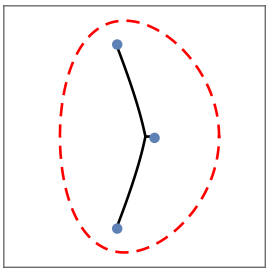

$(t_0, t_1) = (\frac{1}{500}, -\frac{1}{10}) \in \mathcal{F}_1^-$

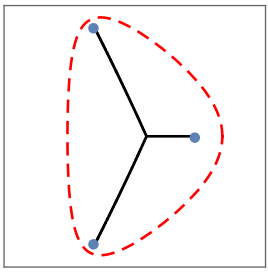

$(t_0, t_1) = (\frac{1}{50}, -\frac{1}{10}) \in \mathcal{F}_1^-$

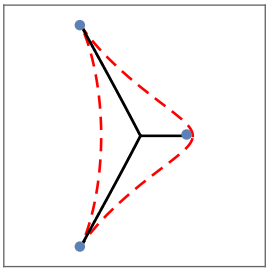

$(t_0, t_1) = (\frac{135+4\sqrt{30}}{1800}, -\frac{1}{10}) \in \Gamma_c^-$

Figure 4.12: For the given values of (t_0, t_1), the boundary $\partial\Omega$ (dashed contour), the support of the mother body measure μ_* (solid lines) and the branch points z_0, z_1, z_2 (dots) are shown (the panels here are scaled differently - compare with Figure 4.4). Note the transition when we move from $\mathcal{F}_2^-$ to $\mathcal{F}_1^-$. We stress that the contours of $\operatorname{supp}\mu_*$ outside the real line are not straight line segments. Numerical outputs.

In the three-cut cases for $(t_0, t_1) \in \mathcal{F}_1$ and $(t_0, t_1) \in \mathcal{F}_1^-$ the geometry of the support Σ_* of μ_* is essentially the same. However, when (t_0, t_1) crosses γ_c^- and we move to the one-cut case for $t_1 < 0$, the part of Σ_* on the real line disappears, and we are only left with a single analytic arc, which is symmetric with respect to the real line. This is in contrast with the one-cut case for $t_1 > 0$, which corresponds to the shrinking of the arc outside the real line and reduction of Σ_* to a real interval.

The point z_* in Theorem 4.2.19 moves continuously with (t_0, t_1) and it is determined as one of the finitely many real solutions $y = z_*$ to the implicit equation

$$\int_{z_1}^{y} (\xi_1(s) - \xi_2(s))ds = 0. \tag{4.61}$$

The critical curve γ_c^- is then determined by the condition $z_* = z_0$ (compare (4.61) with (4.59)).

To conclude this section, we remark that Theorem 4.2.10 also extends to $(t_0, t_1) \in \mathcal{F}^-$ for the respective measure μ_0 and the measure μ_* given by Theorem 4.2.19.

4.2.11 Phase transition along the mother body critical curve

As we mentioned above, the critical curves γ_c and γ_c^- are not analytical continuation of each other. More precisely, if we consider them as functions $t_0(t_1)$, then they are both analytic at $t_1 = 0$ and their values and their first two derivatives are equal to 0 at $t_1 = 0$, but their third derivatives at $t_1 = 0$ are different. This can be characterized as a phase transition of the third order. To see this phase transition, let us evaluate the asymptotic behavior of the function $t_0(t_1)$ as $t_1 \to +0$ and $t_1 \to -0$.

We start with γ_c. When we approach the origin, we take into account the leading terms in (4.30) in order to get

$$t_0 = s^6(1 + \mathcal{O}(s^4)), \quad t_1 = \frac{3}{8}s^2(1 + \mathcal{O}(s^2)), \qquad \text{as } s \to 0.$$

Hence we have the approximation

$$t_0 = \frac{8}{27}t_1^3(1 + \mathcal{O}(t_1)), \tag{4.62}$$

as we approach the origin along γ_c, where the implicit term is analytic in t_1.

The similar analysis for γ_c^- is more involved. The relation $h'(w_0) = 0$ gives us that

$$a_0 = \frac{w_0^3 - 2r}{w_0}. \tag{4.63}$$

Replacing this expression into (4.60) we arrive at

$$\begin{aligned}\left(r + w_0^3\right)\left(-24r^3 + 2r^5 + 36r^4 w_0 + \left(10r^4 + 22r^2\right) w_0^3\right.\\ \left. -48r^3 w_0^4 - \left(4r^3 + r\right) w_0^6 + 15r^2 w_0^7 + w_0^9\right)\\ - 6r^2 w_0^4 \left(4r^2 + \left(2r^2 - 1\right) w_0^2 - 4r w_0^3 + w_0^6\right) \log \frac{w_0^3}{r} = 0.\end{aligned} \tag{4.64}$$

We now make the Ansatz, to be verified in a moment, that w_0 can be expressed as

$$w_0 = (Cr)^{1/3} \tag{4.65}$$

along γ_c^-, where $C = C(r)$ is a positive function, to be determined later, which remains bounded away from 0 and ∞ when $r \to 0$. Using the change of variables (4.65) in (4.64), we get

$$r^4(1+C)\left(-24+22C-C^2+C^3+\left(2+10C-4C^2\right)r^2\right.$$
$$\left.+C^{1/3}\left(36-48C+15C^2\right)r^{4/3}\right)$$
$$+r^4\left(6C^2-C^{1/3}\left(24C-24C^2+6C^3\right)r^{4/3}-12C^2r^2\right)\log C=0,$$

that is, $C = C(r)$ should satisfy

$$(1+C)(-24+22C-C^2+C^3)+6C^2\log C=-Q(r,C(r)) \tag{4.66}$$

where

$$Q(r,c):=\left(2+10c-4c^2\right)r^2+c^{1/3}\left(36-48c+15c^2\right)r^{4/3}$$
$$-\left(c^{1/3}\left(24c-24c^2+6c^3\right)r^{4/3}+12c^2r^2\right)\log C$$

A simple application of the implicit function theorem tells us that there exists a function $C = C(r)$ satisfying (4.66). Consequently, we get that along γ_c^-, we can express w_0 as a function of r as in (4.65). Furthermore, when $r \to 0$ it is easily seen that $Q(r, c) \to 0$, thus the constant $C_0 = C(0)$ solves

$$(1+C_0)(-24+22C_0-C_0^2+C_0^3)+6C_0^2\log C_0=0.$$

Numerically, we see that

$$C_0 = 1.075\ldots. \tag{4.67}$$

Hence, in virtue of (4.65) and (4.63) we get the first order approximation

$$w_0=C_0^{1/3}r^{1/3}(1+\mathcal{O}(r)),\quad a_0=\frac{(C_0-2)}{2C_0^{1/3}}r^{2/3}(1+\mathcal{O}(r)), \tag{4.68}$$

valid as $r \to 0$ along γ_c^-, where the implicit terms are analytic in r. By (4.31)–(4.32), we know that

$$t_0=-2r^4+r^2-\frac{(C_0-2)^2}{C_0^{2/3}}r^{10/3}(1+\mathcal{O}(r))=r^2(1+\mathcal{O}(r)),$$

$$t_1=a_0(1-a_0-4r^2)=\frac{(C_0-2)}{2C_0^{1/3}}r^{2/3}(1+\mathcal{O}(r)),$$

so by the second equation in (4.68) we get the first order approximation

$$t_0 = \frac{8C_0}{(C_0-2)^3} t_1^3 (1 + \mathcal{O}(t_1)), \tag{4.69}$$

as $(t_0, t_1) \to (0,0)$ along γ_c^-, and the implicit term is analytic in t_1. Using (4.67) we also get

$$\frac{8}{27} < \left| \frac{8C_0}{(C_0-2)^3} \right|.$$

Thus, comparing (4.62) with (4.69), we see that the tangent vector and the curvature of γ_c and γ_c^- coincide at the origin, but the derivative of their curvatures do not coincide. In the terminology of statistical mechanics, the origin $(t_0, t_1) = (0,0)$ determines a third order phase transition along the critical curve $\gamma_c \cup \gamma_c^-$.

4.2.12 Setup for the remainder of the chapter

The rest of the chapter is organized as follows.

In Section 4.3 we derive several technical results on the functions r and a_0, which are extensively used in the rest of the chapter. Propositions 4.2.1 and 4.2.7 and Theorems 4.2.2, 4.2.5 and 4.2.8 are proved in Section 4.3.

In Section 4.4 we study the spectral curve (4.24) and construct its associated Riemann surface $\mathcal{R}$ as a three-sheeted cover of the complex plane. This sheet structure depends on whether we are in the three-cut (Section 4.4.3.1) or one-cut (Section 4.4.3.2) cases. Along the way, we also prove Theorem 4.2.6 in Section 4.4.

In Section 4.5 we introduce the quadratic differential ϖ on the Riemann surface $\mathcal{R}$ (which was already mentioned after Theorem 4.2.9), and describe its critical graph. Using its critical graph, in Section 4.6 we prove Theorems 4.2.3, 4.2.4, 4.2.9 and 4.2.10.

In Sections 4.7 and 4.8 we carry out the asymptotic analysis of the Riemann-Hilbert problem characterizing the multiple orthogonal polynomial $P_{n,n}$ in Proposition 4.2.13, in the three-cut and one-cut cases, respectively. This analysis also heavily relies on the critical graph of the quadratic differential ϖ. The final ingredient in the analysis of this Riemann-Hilbert problem is the so-called global parametrix, whose construction is provided in Section 4.7.6.

In Section 4.10 we use the outcome of the asymptotic analysis in order to prove Theorems 4.2.14 and 4.2.15.

Finally, in Section 4.11 we study the width parameters used in Section 4.5 to perform the deformation of the critical graph of ϖ.

4.3 Limiting boundary of eigenvalues. Proofs of Propositions 4.2.1 and 4.2.7 and Theorems 4.2.2, 4.2.5 and 4.2.8

In this section we prove Proposition 4.2.1 and Theorem 4.2.2. To do so, we need some technical lemmas, which are also used in the next sections.

4.3.1 Analysis of the algebraic function r. Proof of Proposition 4.2.1

It is convenient to change variables for the polynomial p in (4.17) and instead consider

$$\widetilde{p}(x) = p(\sqrt{x}) = 128x^5 - 124x^4 + (-16t_1 + 64t_0 + 36)x^3 + \left(16t_1^2 + 8t_1 - 28t_0 - 3\right)x^2 + t_0(2 - 8t_1)x + t_0^2. \quad (4.70)$$

With the help of Mathematica, the discriminant of $\widetilde{p}$ with respect to x is computed

$$\operatorname{Discr}(\widetilde{p}; x) = 16384\, t_0^2\, p_1(t_0)p_2(t_0)p_3(t_0), \quad (4.71)$$

where

$$\begin{aligned} p_1(s) &= 8192s^3 + 192(64t_1 - 7)s^2 - 48(1 - 4t_1)^2 s + (108t_1 - 11)(4t_1 - 1)^3 \\ p_2(s) &= 1728s^2 - 432(1 + 4t_1)s + (3 + 4t_1)^2(3 + 16t_1), \\ p_3(s) &= (8s - 8t_1 - 1)^2. \end{aligned} \quad (4.72)$$

Lemma 4.3.1. *For $t_1 > 0$, the polynomials p_2, p_3 in (4.72) do not have zeros on $(0, 1/8)$.*

Proof. The discriminant of p_2 in s is

$$-1769472\, t_1^3,$$

which is clearly negative for $t_1 > 0$, and hence p_2 does not have real zeros. The Lemma for p_3 follows trivially from the inequality

$$8s - 8t_1 - 1 < -8t_1 < 0,$$

which is valid if $0 < s < 1/8$. □

Lemma 4.3.2. *The three roots $s_1, s_2, t_{0,crit}$ of the polynomial p_1 in (4.72) satisfy*

$$s_1 < 0 < s_2 < t_{0,crit}, \quad 0 < t_1 < \frac{11}{108}; \tag{4.73}$$

$$s_1 < s_2 = 0 < t_{0,crit}, \quad t_1 = \frac{11}{108}; \tag{4.74}$$

$$s_1 \le s_2 < 0 < t_{0,crit}, \quad \frac{11}{108} < t_1 < \frac{1}{4}; \quad \text{and } s_1 = s_2 \text{ only for } t_1 = \frac{1}{8}. \tag{4.75}$$

Moreover, the function

$$t_1 \mapsto t_{0,crit} = t_{0,crit}(t_1), \quad 0 < t_1 < 1/4,$$

is decreasing and

$$t_{0,crit}(0) = 1/8, \quad t_{0,crit}(1/4) = 0. \tag{4.76}$$

Finally, the curve Γ_c in (4.18) is parameterized by $(t_{0,crit}, t_1)$, that is,

$$\Gamma_c : \ (t_0, t_1) = (t_{0,crit}(t_1), t_1), \quad 0 < t_1 < \frac{1}{4}. \tag{4.77}$$

Proof. For a positive constant c, the discriminant of p_1 (with respect to s) is given by

$$\mathrm{Discr}(p_1; s) = c\, t_1^3 (1 - 8t_1)^2 (1 - 4t_1)^3.$$

In particular, $\mathrm{Discr}(p_1; s) \ge 0$ for $0 < t_1 < 1/4$, so p_1 has always three real roots for $0 < t_1 < 1/4$, and these are all distinct if $t_1 \ne 1/8$. For $t_1 = 1/8$, p_1 simply factors as

$$p_1(s) = \frac{1}{12}(1 + 32s)^2 (128s - 5), \tag{4.78}$$

so the largest positive root $t_{0,crit}$ of p_1 is always simple if $0 < t_1 < 1/4$, and also $s_1 = s_2 = -\frac{1}{32} < 0$ for $t_1 = 1/8$. Evaluating explicitly,

$$p_1(0) = (1 - 4t_1)^3 (11 - 108t_1),$$

which means that $p_1(0) < 0$ for $t_1 < \frac{11}{108}$, and $p_1(0) \geq 0$ otherwise. Therefore, combining continuity and what we already have, we get the inequalities claimed in (4.73)–(4.75).

We now verify that $t_{0,crit} < 1/8$. For $t_1 \in (11/108, 1/4)$, the value $t_{0,crit}$ is the unique positive root of p_1. Since also

$$p_1(1/8) = 64t_1^2(108t_1^2 - 92t_1 + 27) > 0, \quad 0 < t_1 < \frac{1}{4},$$

and the leading coefficient of p_1 is positive, we use continuity to conclude that the inequality $t_{0,crit} < 1/8$ always holds true.

The derivative of $t_{0,crit}$ is computed via the chain rule,

$$\frac{\partial}{\partial t_1} t_{0,crit} = -\frac{\frac{\partial p_1}{\partial t_1}}{\frac{\partial p_1}{\partial s}}. \tag{4.79}$$

Since $t_{0,crit}$ is the largest root of p_1,

$$\frac{\partial p_1}{\partial s}(t_{0,crit}) > 0, \quad 0 < t_1 < \frac{1}{4}. \tag{4.80}$$

The derivative of p_1 with respect to t_1 is explicitly computed to be

$$\frac{\partial p_1}{\partial t_1}(s) = 48(256s^2 + s(8 - 32t_1) - (1 - 4t_1)^2(5 - 36t_1)).$$

For $t_1 = 1/8$, (4.78) gives

$$t_{0,crit} = \frac{5}{128}, \quad \frac{\partial p_1}{\partial t_1}(t_{0,crit})\Big|_{t_1=1/8} = \frac{81}{24}. \tag{4.81}$$

We claim that $\frac{\partial p_1}{\partial t_1}(t_{0,crit})$ is never zero. To the contrary, the discriminant $\mathrm{Discr}(p_1; t_1)$ with respect to t_1 would be zero, and it is thus enough to show that $\mathrm{Discr}(p_1; t_1)$ is different from zero. For a positive constant c,

$$\mathrm{Discr}(p_1; t_1) = c\, s^2(8s - 1)^3(1 + 32s)^2;$$

and since $t_{0,crit} < 1/8$ we conclude

$$\mathrm{Discr}(p_1; t_1)\Big|_{s=t_{0,crit}} \neq 0,$$

so $\frac{\partial p_1}{\partial t_1}(t_{0,crit})$ is never zero for $0 < t_1 < 1/4$. From (4.81) and continuity,

$$\frac{\partial p_1}{\partial t_1}(t_{0,crit}) > 0, \quad 0 < t_1 < \frac{1}{4}.$$

Combining this last equation with (4.79) and (4.80), we finally get that $t_{0,crit}$ is a decreasing function of t_1.

The limits (4.76) now follow directly from a combination of (4.73)–(4.75) and the explicitly expressions

$$p_1(s)\Big|_{t_1=0} = (1-8s)^2(11+128s), \quad p_1(s)\Big|_{t_1=1/4} = 64s^2(27+128s).$$

To conclude, we prove (4.77). Plugging the parametrization (4.18) into the definition of p_1, one can easily verify

$$p_1(t_0) = 0, \quad (t_0, t_1) \in \Gamma_c,$$

so t_0 is always a root of p_1 if $(t_0, t_1) \in \Gamma_c$. For $s = 1/4$ in (4.18), we compute explicitly $(t_0, t_1) = (5/128, 1/8) = (t_{0,crit}, t_1)$, hence Γ_c intersects $(t_0, t_{0,crit})$ at $(5/128, 1/8)$. Since $t_{0,crit}$ is always a simple root and the pair $(t_0, t_1) \in \Gamma_c$ must always give rise to a root of p_1, by continuity we conclude (4.77). □

As as consequence of Lemma 4.3.2, the parameter region $\mathcal{F}$ is alternatively described as

$$\mathcal{F} = \{(t_0, t_1) \mid 0 < t_1 < 1/4, \quad 0 < t_0 < t_{0,crit}(t_1)\}.$$

Lemma 4.3.3. *For $(t_0, t_1) \in \mathcal{F} \cup \Gamma_c$, $t_1 \neq 0, 1/4$, the polynomial $\widetilde{p}$ in (4.71) never has a triple root.*

Proof. If $\widetilde{p}$ has a triple root, then $\widetilde{p}, \widetilde{p}', \widetilde{p}''$ share a common root, say x_0. This means that $t_0 \mapsto \widetilde{p}(x_0), \widetilde{p}'(x_0), \widetilde{p}''(x_0)$ all share a common root. We compute two of their resultants with the help of Mathematica. Their full expressions are rather long, but we exhibit their first coefficients,

$$\text{Resultant}(p(x), p''(x); t_0) = -44040192\, x^7 + 56033280\, x^6 + \dots,$$

$$\text{Resultant}(p'(x), p''(x); t_0) = 245760\, x^5 - 202752\, x^4 + \dots,$$

and since $t_0 \mapsto \widetilde{p}(x_0), \widetilde{p}'(x_0), \widetilde{p}''(x_0)$ all share a common root,

$$\text{Resultant}(p'(x_0), p''(x_0); t_0) = 0 = \text{Resultant}(p(x_0), p''(x_0); t_0).$$

We now see $\text{Resultant}(p(x), p''(x); t_0), \text{Resultant}(p'(x), p''(x); t_0)$ as functions of x. The equation above says that these polynomials share a common root x_0, so their resultant with respect to x must be zero. Again with the help of Mathematica, we compute their resultant with respect to x to get

$$-c\, t_1^6(1+t_1)^3(1-4t_1)^4(3+4t_1)^3(27+4t_1)^2(775+864t_1+13824t_1^2)^2$$

for some large positive constant c. It is then not hard to see that this last expression is never zero for $0 < t_1 < 1/4$, and the Lemma follows. □

Lemma 4.3.4. *For $(t_0, t_1) \in \mathcal{F}$, the polynomial $\widetilde{p}$ defined in (4.71) has a smallest positive root $\widetilde{r}$, which is simple. When $(t_0, t_1) \to \Gamma_c$, $\widetilde{r}$ becomes a root of higher multiplicity, given explicitly as $\widetilde{r} = s^2$, where s is the parameter on (4.18).*

Proof. When $t_0 \to 0$, the polynomial $\widetilde{p}$ factors into

$$\widetilde{p}(x) = x^2 q(x), \quad q(x) := 128x^3 - 124x^2 + (36 - 16t_1)x + 16t_1^2 + 8t_1 - 3. \tag{4.82}$$

The discriminant and value at $x = 0$ of q are respectively given by

$$\mathrm{Discr}(q; x) = -1024(1 + 8t_1)^2(3 + 16t_1)(108t_1 - 11), \tag{4.83}$$

$$q(0)\big|_{t_0=0} = 16t_1^2 + 8t_1 - 3 < 0, \quad 0 < t_1 < \frac{1}{4}. \tag{4.84}$$

For the sake of clarity, we split the rest of the proof into three parts, the last of those being a limiting case of the others.

1st Case: $0 < t_1 < \frac{11}{108}$.

In this case, the discriminant (4.83) is positive, so q has three real roots. For $t_1 = 1/16$, these are given by

$$\left\{ \frac{3}{8}, \frac{1}{64}(19 - 3\sqrt{17}), \frac{1}{64}(19 + 3\sqrt{17}) \right\},$$

so in particular they are all positive. Since $q(0)$ is never zero, see (4.84), we conclude that these three roots are all positive for any choice $t_1 \in (0, 11/108)$. This is the same as saying that in the present situation and $t_0 = 0$, the polynomial $\widetilde{p}$ has a double root $x_1 = \widetilde{r} = 0$ and three simple positive roots $x_2 < x_3 < x_4$.

Recall that s_2 is a root of p_1 as in Lemma (4.3.2). For $0 < t_0 < s_2$, a combination of Equation (4.71), Lemma 4.3.1 and Equation (4.73) assures $\widetilde{p}$ has only simple roots. By continuity from t_0 and the further observations $\widetilde{p}(0) = t_0^2 > 0$ and $\widetilde{p}(x) < 0$ when $x \to -\infty$, we learn that for $0 < t_0 < s_2$, the double root of $\widetilde{p}$ at $x = 0$ splits into two simple roots $x_1 < 0 < \widetilde{r}$ and the remaining roots still satisfy $\widetilde{r} < x_2 < x_3 < x_4$.

We now approach $t_0 \nearrow s_2$. In this situation, two roots of $\widetilde{p}$ collide, because p_1 - hence $\mathrm{Discr}(\widetilde{p}; x)$, see (4.71) - is zero for $t_0 = s_2$. For $t_1 = 1/16$, $t_0 = s_2$, the

roots of $\widetilde{p}$ are computed numerically

$$s_2 = 0.0512061,\ \{x_1, \widetilde{r}, x_2, x_3, x_4\} \approx \{-0.0169, 0.0607, 0.1235, 0.4007, 0.4007\},$$

so in this case $x_3 = x_4$ and $\widetilde{r}$ is a simple root. By continuity and Lemma 4.3.3, we conclude $x_3 = x_4$ whenever $t_0 = s_2$, and hence $\widetilde{r}$ is always a simple root for $t_0 \leq s_2$. Again by Equation (4.71), Lemma 4.3.1 and Equation (4.73), we know that $\widetilde{p}$ does not have multiple roots for $s_2 < t_0 < t_{0,crit}$, and we finally conclude that $\widetilde{r}$ is always a simple root in the present case.

2nd Case: $\frac{11}{108} < t_1 < \frac{1}{4}$.

This case is somewhat simpler than the previous one. In the present case, the discriminant (4.83) is negative, so q has one real root and two non real roots. From (4.84) we see that this real root is positive. Similarly as before, it means $\widetilde{p}$ has a double root $\widetilde{r} = x_1 = 0$, and simple roots $x_2 > 0$, $x_3, x_4 \in \mathbb{C} \setminus \mathbb{R}$.

As before, we compute $p(0) = t_0^2$, $\widetilde{p}(x) < 0$ for $x \to -\infty$ and conclude that for $t_0 > 0$ and small, the double root splits into two simple roots $x_1 < 0 < \widetilde{r}$ and the remaining roots still satisfy $x_2 > 0$, $x_3, x_4 \in \mathbb{C} \setminus \mathbb{R}$.

From Equation (4.71), Lemma 4.3.1 and Equation (4.73) we know $\widetilde{p}$ has no multiple roots for $0 < t_0 < t_{0,crit}$, so we conclude the smallest positive root $\widetilde{r}$ is always simple.

3rd Case: $t_1 = \frac{11}{108}$.

In this case the polynomial q simply factors as

$$q(x) = \frac{4}{729}(9x - 4)^2(288x - 23),$$

and it clearly has three positive roots. The rest follows the same lines as 2nd Case.

In either of the cases above, we consider the limit $(t_0, t_1) \to (t_{0,crit}, t_1) \in \Gamma_c$ and plug the parametrization (4.18) into the expression for $\tilde{p}$ in (4.70), arriving at

$$\widetilde{p}(x) = 4(s^2 - x)^2 \left[32x^3 + (64s^2 - 31)x^2 + (48s^3 - 50s^2 + 8) + 9s^4 - 12s^3 + 4s^2\right],$$

so s^2 is a root of $\tilde{p}$ for $(t_0, t_1) \in \Gamma_c$. The discriminant (in x) of the polynomial inside brackets above is

$$144(1 - 2s)^3(2 - 3s)^2(8s^2 - 4s - 1)(64s^2 + 35s + 7) < 0, \quad 0 < s < 1/4,$$

so that polynomial has only one real root. Its value at $x = 0$ is $9s^4 - 12s^3 + 4s^2$, which is positive for $0 < s < 1/4$, hence this root is negative.

Comparing to what we proved before, it means that for $(t_0, t_1) \in \Gamma_c$, the root $\widetilde{r}$ collides with the root x_2, becoming the double root $\widetilde{r} = s^2$, as we want. □

Lemma 4.3.5. *The function*

$$t_1 \mapsto \widetilde{r} = \widetilde{r}(t_0, t_1), \quad (t_0, t_1) \in \mathcal{F},$$

is increasing and satisfies the inequalities

$$\widetilde{r} < \frac{1}{4}, \tag{4.85}$$

$$4t_1 < (1 - 4\widetilde{r})^2. \tag{4.86}$$

Proof. The chain rule tells us

$$\frac{\partial}{\partial t_1}\widetilde{r} = -\frac{\frac{\partial \widetilde{p}}{\partial t_1}}{\frac{\partial \widetilde{p}}{\partial x}}. \tag{4.87}$$

As it followed from the calculations in the proof of Lemma 4.3.4, $\widetilde{r}$ is the second smallest real root of $\widetilde{p}$, hence

$$\frac{\partial \widetilde{p}}{\partial x}(\widetilde{r}) < 0. \tag{4.88}$$

Moreover,

$$\frac{\partial \widetilde{p}}{\partial t_1} = -8x(2x^2 - (4t_1 + 1)x + t_0).$$

For $t_1 = 1/8$, $t_0 = 1/32 < t_{0,crit} = 5/128$, we compute

$$\widetilde{r} \approx 0.040736, \quad \frac{\partial \widetilde{p}}{\partial t_1}(\widetilde{r}) \approx 0.00864782 > 0,$$

thus the monotonicity follows from (4.87), (4.88) and the previous inequality once we prove that $\frac{\partial \widetilde{p}}{\partial t_1}(\widetilde{r})$ is never zero.

If $\frac{\partial \widetilde{p}}{\partial t_1}(\widetilde{r})$ were zero, then the polynomials $\widetilde{p}$, $\frac{\partial \widetilde{p}}{\partial t_1}$ would share a zero, hence their resultant with respect to x would be zero. But

$$\text{Resultant}\left(\widetilde{p}, \frac{\partial \widetilde{p}}{\partial t_1}(\widetilde{r}); x\right) = c\, t_1^2 t_0^4 (1 + 8t_1 - 8t_0)^2,$$

and this last expression is never zero for $0 < t_1 < 1/4$, $0 < t_0 < t_{0,crit} < 1/8$.

We now prove (4.85). In the proof of Lemma 4.3.4, we already observed that $\widetilde{r} \to 0$ when $t_0 \to 0$, see (4.82). In particular (4.85) is valid for t_0 very small. In addition

$$\widetilde{p}(1/4) = \frac{1}{64}(1 + 8t_1 - 8t_0)^2 \neq 0,$$

because $0 < t_1 < 1/4$, $0 < t_0 < t_{0,crit} < 1/8$, implying that $\widetilde{r} \neq 1/4$. By continuity from the case $t_0 = 0$, we get (4.85).

For (4.86), define

$$f(x) := (1 - 4x)^2 - 4t_1, \quad x \in \mathbb{C}.$$

We want to prove that $f(\widetilde{r}) > 0$. Using (4.85) and the monotonicity of $\widetilde{r}$

$$\frac{\partial}{\partial t_1}(f(\tilde{r})) = -8(1 - 4\widetilde{r})\frac{\partial \widetilde{r}}{\partial t_1} - 4 < 0,$$

hence $t_1 \mapsto f(\tilde{r})$ is decreasing, so it is enough to prove $f(\widetilde{r}) \geq 0$ for $(t_0, t_1) \in \Gamma_c$. But for this choice, we know that $\widetilde{r} = s^2$, where s is the parameter in (4.18), and in this case

$$f(\widetilde{r}) = 4s^2(1 - 2s^2)^2 > 0, \quad (t_0, t_1) \in \Gamma_c, \quad t_1 \neq 0, 1/4,$$

as desired. □

As a consequence of Lemmas 4.3.4 and 4.3.5, we get the following refinement of Proposition 4.2.1.

Theorem 4.3.6. *For $(t_0, t_1) \in \mathcal{F}$, the polynomial p in (4.17) has a smallest positive root r. The function $t_1 \mapsto r$ is increasing and satisfies*

$$0 < r < \frac{1}{2}, \quad 4t_1 < (1 - 4r^2)^2, \quad (t_0, t_1) \in \mathcal{F}. \tag{4.89}$$

In the limit $(t_0, t_1) \to (t_{0,crit}, t_1) \in \Gamma_c$, r becomes a root of higher multiplicity of p, explicitly given as $r = s$, where s is the parameter in (4.18).

Proof. The Theorem follows directly as a consequence of Lemmas 4.3.4 and 4.3.5, having in mind the identification (4.70). □

Proposition 4.3.7. *For $(t_0, t_1) \in \mathcal{F}$, the quantity $a_0 = a_0(t_0, t_1)$ in (4.16) is well defined and positive. Moreover, the function $t_1 \mapsto a_0$ is increasing.*

Proof. The positivity of a_0 follows directly from (4.16) and (4.89).

Simple computations show that a_0 is the smallest root of

$$q(x) := x^2 + x(4r^2 - 1) + t_1.$$

This implies

$$\frac{\partial a_0}{\partial t_1} = -\frac{\frac{\partial q}{\partial t_1}}{\frac{\partial q}{\partial x}} = -\frac{8a_0 r \frac{\partial r}{\partial t_1} + 1}{\frac{\partial q}{\partial x}(a_0)}.$$

Note that the discriminant of q is given by $(1 - 4r^2)^2 - 4t_1$, which is strictly positive due to (4.89). So a_0 is always a simple root, and since it is the smallest one,

$$\frac{\partial q}{\partial x}(a_0) < 0.$$

Moreover, since $t_1 \mapsto r$ is increasing by Theorem 4.3.6, we also know that $\frac{\partial r}{\partial t_1} > 0$. Recalling that we already proved $a_0 > 0$, we conclude from the last two equations

$$\frac{\partial a_0}{\partial t_1} > 0.$$

□

Lemma 4.3.8. *For $(t_0, t_1) \in \mathcal{F}$, it is valid*

$$0 < 2a_0 + 2r < 1.$$

In addition, the equality

$$2a_0 + 2r = 1$$

is attained when $(t_0, t_1) \in \Gamma_c$.

Proof. The positivity of $2a_0 + 2r$ is trivial since both a_0, r are positive for $(t_0, t_1) \in \mathcal{F}$. From the monotonicity given by Theorem 4.3.6 and Proposition 4.3.7, it is enough to prove that the equality is attained for $(t_0, t_1) \in \Gamma_c$. The later then follows from the definition of a_0 in (4.16), Equation (4.18) and the value $r = s$ given by Theorem 4.3.6. □

4.3.2 Analysis of the rational parametrization h. Proofs of Theorems 4.2.2, 4.2.5 and 4.2.8 and Proposition 4.2.7

We proceed to the analysis of the rational function h given in (4.15).

Denote by

$$R_0 = R_0(h) = \sup\{|w| \mid h'(w) = 0\},$$

the *critical radius* of h. The relevance of R_0 comes from the fact that the rational function h is injective on $\overline{\mathbb{C}} \setminus \overline{D}_{R_0}$, where D_R denotes the open disc centered at 0 and radius R.

Lemma 4.3.9. *For the rational function h in (4.15) and $(t_0, t_1) \in \mathcal{F}$, the inequality $R_0 < 1$ holds true.*

Proof. Note that

$$h'(w) = r - \frac{2a_0 r}{w^2} - \frac{2r^2}{w^3},$$

so the zeros of h' are solutions to the equation

$$w^3 - 2a_0 w - 2r = 0.$$

Using Lemma 4.3.8, we get

$$|(w^3 - 2a_0 w - 2r) - w^3| \leq 2a_0 + 2r < 1 = |w^3|, \quad w \in \partial\mathbb{D}.$$

By Rouché's Theorem we conclude that all the roots of h' are on $\mathbb{D}$. □

Corollary 4.3.10. *For $(t_0, t_1) \in \mathcal{F}$, h is a biholomorphism from $\overline{\mathbb{C}} \setminus \overline{\mathbb{D}}$ to $h(\overline{\mathbb{C}} \setminus \overline{\mathbb{D}})$.*

Proof. From Lemma 4.3.9, we know that $R_0 < 1$. In particular $\overline{\mathbb{C}} \setminus \overline{\mathbb{D}} \subset \overline{\mathbb{C}} \setminus \overline{D}_{R_0}$, and the result follows. □

As a consequence of Corollary 4.3.10, the set $h(\partial\mathbb{D})$ is an analytic closed curve that splits $\overline{\mathbb{C}}$ into two simply connected domains; only one of which is bounded and henceforth denoted by Ω.

Proof of Theorem 4.2.5. A straightforward computation shows that

$$F(h(w^{-1}), h(w)) = 0, \quad w \in \mathbb{C},$$

where F is as in (4.24). For a rational function $\chi = \frac{\chi_1}{\chi_2}$, its *degree* is defined as

$$\deg \chi = \max\{\deg \chi_1, \deg \chi_2\}.$$

Since

$$\max\{\deg_\xi F, \deg_z F\} = 3 = \max\{\deg h(w), \deg h(w^{-1})\},$$

it follows from [122, Theorem 4.21] that $(h(w^{-1}), h(w))$ is a proper parametrization.

From Corollary 4.3.10 we know that h maps $V := \overline{\mathbb{C}} \setminus \overline{D}_{R_0}$ biholomorphically to an open simply connected set $G \subset \overline{\mathbb{C}}$ with $(\overline{\mathbb{C}} \setminus \Omega) \subset G$. This means that h admits a meromorphic inverse $g : G \to V$, so that

$$h(g(z)) = z, \quad z \in G. \tag{4.90}$$

From its definition, it follows that g maps $\partial\Omega$ to $\partial\mathbb{D}$, and we conclude

$$\overline{g(z)} = \frac{1}{g(z)}, \quad z \in \partial\Omega. \tag{4.91}$$

Furthermore,

$$F\big(h(1/g(z)), h(g(z))\big) = 0,$$

so that the meromorphic function

$$S(z) = h\left(\frac{1}{g(z)}\right), \quad z \in G, \tag{4.92}$$

is a solution to the algebraic equation (4.24). Since ξ_1 is the only solution in (4.27) that is not branched at ∞, we conclude that S has to be a meromorphic continuation of ξ_1 to the neighborhood G of $\overline{\mathbb{C}} \setminus \Omega$. Thus using the fact that h has real coefficients and (4.90)–(4.91)

$$\overline{z} = \overline{h(g(z))} = h(\overline{g(z)}) = h\left(\frac{1}{g(z)}\right) = S(z), \quad z \in \partial\Omega,$$

which shows that the meromorphic continuation S of ξ_1 is the Schwarz function of $\partial\Omega$. □

Corollary 4.3.11. *The Riemann surface $\mathcal{R}$ defined by (4.24) has genus 0.*

Proof. From Theorem 4.2.5, we learn the rational parametrization h defines a biholomorphism between $\mathcal{R}$ and $\overline{\mathbb{C}}$. Since the genus of $\overline{\mathbb{C}}$ is 0, the same holds true for $\mathcal{R}$ [122, pg. 90, Remark (2)]. □

Proof of Theorem 4.2.2. After Corollary 4.3.10, it only remains to compute the area and harmonic moments (4.19). The computations are very much the same as in [38, pg. 1290]. We include them here for completeness.

Using Green's formula on Ω,

$$2i\,\mathrm{Area}(\Omega) = 2i\int_\Omega dA(z) = \int_{\partial\Omega} \overline{z}\, dz. \tag{4.93}$$

By (4.29),

$$2i\,\mathrm{Area}(\Omega) = \int_{\partial\Omega} \xi_1(z)\,dz.$$

We now deform the above integral to $z = \infty$ and use the expansion (4.27) and the residue theorem to get that this last integral is equal to $2\pi i t_0$.

Having in mind the identity

$$\frac{1}{2\pi i}\int_{\partial\Omega} \frac{\overline{z}}{(z-z_0)^k}\,dz = \frac{1}{2\pi i}\int_{\partial\Omega} \frac{\xi_1(z)}{(z-z_0)^k}\,dz,$$

the equalities in (4.19) follow in a similar fashion. □

Proof of Proposition 4.2.7. Equation (4.32) follows directly from identity (4.16). In fact, it was already used in the proof of Proposition 4.3.7.

Recall Equation (4.93),

$$2\pi i t_0 = 2i\,\mathrm{Area}(\Omega) = \int_{\partial\Omega} \overline{z} dz.$$

We now change coordinates $z = h(w)$ in the integral above, and the formula becomes

$$\begin{aligned} 2\pi i t_0 &= \int_{\partial\mathbb{D}} \overline{h(w)} h'(w) dw \\ &= \int_{\partial\mathbb{D}} h(\overline{w}) h'(w) dw \\ &= \int_{\partial\mathbb{D}} h(w^{-1}) h'(w) dw \end{aligned}$$

Expanding the integrand $h(w^{-1})h'(w)$ and using the residue theorem, we get

$$2\pi i t_0 = 2\pi i\,\mathrm{Res}(h(w^{-1})h'(w), w = 0) = 2\pi i(-4a_0^2 r^2 - 2r^4 + r^2),$$

which is equivalent to (4.31) □

Recall the curve γ_c splitting our phase diagram $\mathcal{F}$ into two parts $\mathcal{F}_1$, $\mathcal{F}_2$, see (4.30). Lemma 4.3.9 assures us the critical points of h are on the unit disc, but it is important for later to have a better control on the position of these points, as it is stated in the next two lemmas.

Lemma 4.3.12. *The zeros w_0, w_1, w_2 of the function h' satisfy*

- *For $(t_0, t_1) \in \mathcal{F}_1$,*

$$w_0 \in (0,1), \quad \overline{w}_2 = w_1, \quad w_1 \in \mathbb{D} \setminus \mathbb{R}.$$

- *For $(t_0, t_1) \in \mathcal{F}_2$,*

$$w_0 \in (0,1), \quad -1 < w_1 < w_2 < 0.$$

- *For $(t_0, t_1) \in \gamma_c$, h' has a simple root $w_0 \in (0,1)$ and a double root $w_1 = w_2 \in (-1,0)$.*

Furthermore,

$$h\left(\frac{1}{w_j}\right) \neq 0, \quad j = 0, 1, 2. \tag{4.94}$$

Proof. The zeros of h' are the same as the zeros of the polynomial $\tilde{h}$ given by

$$\tilde{h}(w) = \frac{w^3}{r} h'(w) = w^3 - 2a_0 w - 2r. \tag{4.95}$$

For $t_1 = 0$, $\tilde{h}$ reduces to $w^3 - 2r$, which has three simple zeros, only one of them real. The discriminant of $\tilde{h}$ is given by

$$\operatorname{Discr}(\tilde{h}; w) = 4(8a_0^3 - 27r^2) \tag{4.96}$$

so h' has a zero with multiplicity iff $a_0 = \frac{3}{2} r^{2/3}$. Plugging this into (4.31)–(4.32), we get that t_0, t_1 are given by (4.30) for $s = r^{1/3}$. In particular, this is only possible for $0 < r < 1/8$.

Furthermore, $\operatorname{Discr}(\tilde{h}; w)$ does not change sign in each of the sets $\mathcal{F}_1, \mathcal{F}_2$. When we keep t_0 fixed and send $t_1 \to 0$, we know from (4.16) that $a_0 \to 0$, whereas r remains positive, so $\operatorname{Discr}(\tilde{h}; w) < 0$ on $\mathcal{F}_1$. On the other hand, if we keep t_1 fixed and send $t_0 \to 0$, it follows from (4.31)–(4.32) that a_0 remains positive, whereas $r \to 0$, and hence $\operatorname{Discr}(\tilde{h}; w) > 0$ on $\mathcal{F}_2$.

In virtue of (4.96), the discussion above means that $\tilde{h}$ - and thus h' - has exactly one real zero for $(t_0, t_1) \in \mathcal{F}_1$, and three real zeros for $(t_0, t_1) \in \mathcal{F}_2$.

From Lemma 4.3.9, we already know that all the zeros of h' belong to $\mathbb{D}$. Since $a_0 \geq 0, r > 0$, see Theorem 4.3.6 and Proposition 4.3.7, from Descartes rule of signs we learn that h' has exactly one positive real zero for $(t_0, t_1) \in \mathcal{F}$.

It only remains to prove (4.94). Suppose to the contrary that $h(w_j^{-1}) = 0$ for some j. This means that the polynomial

$$\hat{h}(w) = w^2 h(w^{-1}) = r^2 w^3 + 2a_0 r w^2 + a_0 w + r$$

has the common root w_j with the polynomial $\tilde{h}$ in (4.95). But,

$$\begin{aligned}&\text{Resultant}(\tilde{h}, \hat{h})\\ &\quad = -r^3[1 - 4a_0^2 + r^2(6 - 16a_0^2) + r^4(12 - 16a_0^2) + 8r^6 + 32a_0^3 r^2],\end{aligned}$$

and because $0 < r < 1/2$ and $0 \le a_0 < 1/2$ (see Lemma 4.3.8), it is not hard to see that the term between brackets above is always positive, thus the resultant above is nonzero and consequently $\tilde{h}$ and $\hat{h}$ do not have common roots. The proof is complete. □

Proof of Theorem 4.2.8. Equation (4.33) follows directly from the equality given by Lemma 4.3.8 for $(t_0, t_1) \in \Gamma_c$.

Equation (4.96) and the arguments thereafter immediately show that in the coordinate system (r, a_0), the critical curve γ_c is described as in (4.34). □

4.4 Geometry of the spectral curve. Proof of Theorem 4.2.6

An important role for the analysis of the spectral curve (4.24) is played by the discriminant

$$\mathcal{D}(z) = \text{Discr}(F(\xi, z); \xi), \tag{4.97}$$

$\mathcal{D}$ is a polynomial of degree 9 in z. It can be computed with the help of Mathematica, but its explicit expression is rather complicated to be dealt with directly. Its first coefficients are

$$\mathcal{D}(z) = 4z^9 - 4t_1 z^8 + (4B + 16t_1)\, z^7 + \cdots, \quad z \in \mathbb{C},$$

where B is as in (4.25).

Theorem 4.2.6 can be restated in terms of the discriminant $\mathcal{D}$.

Theorem 4.4.1. *For $(t_0, t_1) \in \mathcal{F}$ the discriminant $\mathcal{D}$ in (4.97) has three double zeros $\hat{z}_0$, $\hat{z}_1$, $\hat{z}_2 \in \mathbb{C} \setminus \overline{\Omega}$ satisfying*

$$\hat{z}_0 > 0, \quad \operatorname{Im} \hat{z}_1 < 0, \quad \overline{\hat{z}}_2 = \hat{z}_1. \tag{4.98}$$

In addition, $\mathcal{D}$ always has a real simple zero $z_0 > 0$, $z_0 \in \Omega$. Its remaining zeros z_1, z_2 also belong to Ω and are located as follows.

(i) For $(t_0, t_1) \in \mathcal{F}_1$,

$$\operatorname{Im} z_1 < 0, \quad \overline{z}_2 = z_1.$$

(ii) For $(t_0, t_1) \in \mathcal{F}_2$,

$$z_2 < z_1 < z_0.$$

(iii) For $(t_0, t_1) \in \gamma_c$,

$$z_1 = z_2 < z_0$$

that is, $\mathcal{D}$ has a double zero at $z_1 = z_2$.

Assuming Theorem 4.4.1, we now prove Theorem 4.2.6. The proof of Theorem 4.4.1 is given in Section 4.4.2

Proof of Theorem 4.2.6. The zeros z_0, z_1, z_2 of $\mathcal{D}$ given by Theorem 4.4.1 correspond to the branch points given by Theorem 4.2.6. The branch point at ∞ follows from the asymptotics (4.27) for the solutions ξ_1, ξ_2, ξ_3. In virtue of Lemma 4.4.2 below, the double zeros $\hat{z}_0, \hat{z}_1, \hat{z}_2$ of $\mathcal{D}$ are singular points of (4.24). □

The spectral curve (4.24) can be seen as a (branched) three-sheeted cover $\mathcal{R}$ of the Riemann sphere $\overline{\mathbb{C}}$. The main goal of the rest of the present section is to describe the three sheets $\mathcal{R}_1$, $\mathcal{R}_2$, $\mathcal{R}_3$ of $\mathcal{R}$. As an analytic counterpart, we ultimately prove Theorem 4.4.1. During this Section, t_0 is always considered to be a fixed parameter, and every deformation is taken with respect to the parameter t_1.

4.4.1 The spectral curve for $t_1 = 0$

We briefly discuss the case $t_1 = 0$ studied by Bleher and Kuijlaars [38], describing their results in a suitable form for our needs. Besides being instructive, both to fix notation and keep in mind the main lines of the rest of the section, this particular case is also used later.

For $t_1 = 0$ the quantities r, a_0, A, B appearing in Proposition 4.2.1, (4.16), (4.25) and (4.26), respectively, are explicitly given by

$$r = \frac{\sqrt{1-\sqrt{1-8t_0}}}{2}, \tag{4.99}$$

$$a_0 = 0,$$

$$A = \frac{1+20t_0-8t_0^2-(1-8t_0)^{3/2}}{32}, \tag{4.100}$$

$$B = 0.$$

The spectral curve (4.24) is invariant under rotation $(\xi, z) \mapsto (\omega^2\xi, \omega z)$, $\omega = e^{2\pi i/3}$, and this symmetry is carried over to all related quantities. For instance, in this situation it is easy to see that $h(\omega w) = \omega h(w)$.

The discriminant $\mathcal{D}$ in (4.97) is a cubic polynomial in z^3, thus reflecting the aforementioned three-fold rotational symmetry. It has a simple real zero z_0 and a double real zero $\hat{z}_0 > z_0$ given by

$$z_0 = \frac{3}{4}\left(1-\sqrt{1-8t_0}\right)^{2/3}, \quad \hat{z}_0 = \frac{3+\sqrt{1-8t_0}}{4}, \tag{4.101}$$

and the remaining zeros are

$$z_j = \omega^{-j} z_0, \quad \hat{z}_j = \omega^{-j}\hat{z}_0, \quad j = 1, 2. \tag{4.102}$$

In terms of the rational parametrization h, the branch points z_0, z_1, z_2 are obtained as

$$z_j = h(w_j), \quad j = 0, 1, 2, \tag{4.103}$$

where $w_0 \in (0,1), w_j = \omega^{2j} w_0$, $j = 1, 2$, are the zeros of h' as in Lemma 4.3.12.

Regarding Theorem 4.2.9, we are always in the three-cut situation and

$$\Sigma_* = \Sigma_{*,0} \cup \Sigma_{*,1} \cup \Sigma_{*,2}, \quad \Sigma_{*,j} = [0, z_j], \quad j = 0, 1, 2. \tag{4.104}$$

For

$$\mathcal{R}_1 = \overline{\mathbb{C}} \setminus \Sigma_*, \quad \mathcal{R}_2 = \overline{\mathbb{C}} \setminus ([-\infty, 0] \cup \Sigma_{*,1} \cup \Sigma_{*,2}), \quad \mathcal{R}_3 = \overline{\mathbb{C}} \setminus [-\infty, z_0], \tag{4.105}$$

the Riemann Surface $\mathcal{R}$ is the resulting surface after gluing $\mathcal{R}_1$ to $\mathcal{R}_2$ along $\Sigma_{*,1} \cup \Sigma_{*,2}$, $\mathcal{R}_1$ to $\mathcal{R}_3$ along $\Sigma_{*,0}$ and $\mathcal{R}_2$ to $\mathcal{R}_3$ along $[-\infty, 0]$, always in the usual crosswise manner.

Each function ξ_j in (4.27) has an analytic continuation to the whole sheet $\mathcal{R}_j$, and for the values of z_0, z_1, z_2 as above, they satisfy

$$\xi_1(z_0) = \frac{r^{2/3}\left(2r^2+1\right)}{2^{1/3}} = \xi_3(z_0), \qquad \xi_1(z_j) = \omega^{-j}\xi_1(z_0) = \xi_2(z_j), \quad j = 1, 2, \tag{4.106}$$

$$\xi_1(\hat{z}_0) = \hat{z}_0 = \xi_3(\hat{z}_0), \qquad \xi_1(\hat{z}_j) = \omega^{-j}\hat{z}_j = \xi_2(\hat{z}_j), \quad j = 1, 2. \tag{4.107}$$

Careful readers may notice this sheet structure differs from the one given in [38], where the authors construct the sheets respecting the underlying three-fold symmetry. But for us it is more convenient to do it this way, because for $t_1 \neq 0$ the symmetry is unavoidably broken.

The preimage of a point $z \in \overline{\mathbb{C}}$ through the canonical projection $\pi : \mathcal{R} \to \overline{\mathbb{C}}$ on the sheet $\mathcal{R}_j$ is denoted by $z^{(j)}$, $j = 1, 2, 3$. Equivalently, a point $z^{(j)} \in \mathcal{R}_j$ can be seen as the pair $(\xi_j(z), z)$ - we use both representations without further explanation.

At the branch points of $\mathcal{R}$, two of the preimages coincide. More precisely, $\mathcal{R}$ is branched at the points

$$z_0^{(1)} = z_0^{(3)}, \quad z_1^{(1)} = z_1^{(2)}, \quad z_2^{(1)} = z_2^{(2)}, \quad \infty^{(2)} = \infty^{(3)},$$

and for $z \in \mathbb{C} \setminus \{z_0, z_1, z_2\}$ the points $z^{(1)}, z^{(2)}, z^{(3)}$ are all distinct.

4.4.2 The spectral curve for $t_1 > 0$. Proof of Theorem 4.4.1

We now focus on the case when t_1 is positive.

Consider the system of equations

$$F(\xi, z) = 0, \tag{4.108}$$

$$\frac{\partial F}{\partial \xi}(\xi, z) = 3\xi^2 - 2z^2\xi - 2t_1\xi - (1+t_0)z + B + t_1 = 0, \tag{4.109}$$

$$\frac{\partial F}{\partial z}(\xi, z) = 3z^2 - 2z\xi^2 - 2t_1 z - (1+t_0)\xi + B + t_1 = 0. \tag{4.110}$$

Lemma 4.4.2. *If $z \in \mathbb{C}$ is a zero of $\mathcal{D}$ but the point $z^{(j)} \in \mathcal{R}$ is not a branch point of $\mathcal{R}$, then $(\xi_j(z), z)$ satisfies the system (4.108)–(4.110).*

Proof. For a generic point $(\xi, z) = (h(w^{-1}), h(w))$ satisfying (4.108) it is true

$$-\frac{h'(w^{-1})}{w^2}\frac{\partial F}{\partial \xi}(h(w^{-1}), h(w)) + h'(w)\frac{\partial F}{\partial z}(h(w^{-1}), h(w)) = 0.$$

If $z^{(j)}$ is a zero of the discriminant $\mathcal{D}$, then $(\xi_j(z), z)$ satisfies (4.109), hence from the previous equation

$$h'(w)\frac{\partial F}{\partial z}(h(w^{-1}), h(w)) = 0.$$

Since $z^{(j)}$ is not a branch point, $h'(w) \neq 0$, and the Lemma follows. □

Subtracting Equation (4.110) from Equation (4.109), we get

$$(\xi - z)(3\xi + 3z + 2z\xi + 1 + t_0 - 2t_1) = 0,$$

and as a corollary of Lemma 4.4.2

Corollary 4.4.3. *If $z \in \mathbb{C}$ is a zero of $\mathcal{D}$ but the point $z^{(j)} \in \mathcal{R}$ is not a branch point of $\mathcal{R}$, then the pair $(\xi_j(z), z)$ satisfies at least one of the equations below,*

$$\xi - z = 0, \tag{4.111}$$

$$3\xi + 3z + 2z\xi + 1 + t_0 - 2t_1 = 0. \tag{4.112}$$

Corollary 4.4.2 gives us an analytic tool for studying the dynamics of the singular points $\hat{z}_0, \hat{z}_1, \hat{z}_2$ when deforming t_1, namely through the system (4.111)–(4.112). When $t_1 = 0$, $(\xi_1(\hat{z}_0), \hat{z}_0), (\xi_2(\hat{z}_0), \hat{z}_0)$ satisfy (4.111), whereas $(\xi_1(\hat{z}_j), \hat{z}_j), (\xi_3(\hat{z}_j), \hat{z}_j)$, $j = 1, 2$, satisfy (4.112), as can be verified by simply plugging the values (4.101),(4.102),(4.107) into (4.111)–(4.112).

Writing $(\xi, z) = (h(w^{-1}), h(w))$, equations (4.111)–(4.112) respectively become

$$\left(w - \frac{1}{w}\right) g(w) = 0, \tag{4.113}$$

$$f(w) = 0, \tag{4.114}$$

where

$$g(w) = 1 - 2a_0 - r\left(w + \frac{1}{w}\right), \tag{4.115}$$

$$f(w) = \widetilde{f}\left(w + \frac{1}{w}\right), \tag{4.116}$$

with

$$\widetilde{f}(w) = 2r^3w^3 + 3r^2(1+2a_0)w^2 + r(3+8a_0+4a_0^2+4a_0r^2-6r^2)w \\ + 6a_0 + 2a_0^2 - 4r^2 - 12a_0r^2 + 8a_0^2r^2 + 2r^4 + 1 + t_0 - 2t_1. \quad (4.117)$$

Lemma 4.4.4. *For $(t_0,t_1) \in \mathcal{F}$, the function g in (4.115) has exactly one zero $\hat{w}_0$ on $(1,+\infty)$ and exactly one zero $\hat{w}_0^{-1}$ on $(0,1)$.*

Proof. We notice that $w \mapsto w + 1/w$ is a bijection from $(1,+\infty)$ to $(2,+\infty)$. Since $(1-2a_0)/r > 2$, see Lemma 4.3.8, the equation

$$w + \frac{1}{w} = \frac{1-2a_0}{r}$$

has precisely one solution $\hat{w}_0$ on $(1,+\infty)$. □

For $t_1 = 0$, g simplifies to

$$g(w) = 1 - r\left(w + \frac{1}{w}\right),$$

so the point $\hat{w}_0$ and its images $h(\hat{w}_0), h(\hat{w}_0^{-1})$ in this case are given by

$$\hat{w}_0 = \frac{\sqrt{1-4r^2}+1}{2r}, \quad h(\hat{w}_0^{-1}) = h(\hat{w}_0) = 1 - r^2 = \hat{z}_0, \quad (4.118)$$

where $\hat{z}_0$ is given in (4.101) and we used the explicit expression for r in (4.99).

Lemma 4.4.5. *For $(t_0,t_1) \in \mathcal{F}$, the polynomial $\widetilde{f}$ in (4.117) has exactly one root on $(-\infty,0)$ and no other real roots.*

Proof. The function $(\widetilde{f})'$ is a polynomial of degree 2, whose discriminant is given by

$$\mathrm{Discr}((\widetilde{f})') = 12r^2\left(12r^2 - 3 - 4a_0\left(1 + 2r^2 - a_0\right)\right).$$

Using the upper bound $r < 1/2$ given by Theorem 4.3.6 and the inequality given in Lemma 4.3.8, we get

$$12r^2 - 3 < 0, \quad 1 + 2r^2 - a_0 > 1 - a_0 \geq 2r + a_0 > 0,$$

so $\mathrm{Discr}((\widetilde{f})') < 0$ and hence $(\widetilde{f})'$ has no real zeros. This implies that $\widetilde{f}$ has exactly one real root.

Moreover,

$$\begin{aligned}\widetilde{f}(0) &= a_0^2\left(8r^2+2\right)+a_0\left(6-12r^2\right)+1+2r^4-4r^2+t_0-2t_1\\ &\geq 1+2r^4-4r^2+t_0-2t_1,\end{aligned}\tag{4.119}$$

where we used $a_0 \geq 0$ and $0 < r < 1/2$, see Proposition 4.3.7 and Theorem 4.3.6. The derivative of the right-hand side is given by

$$\frac{\partial}{\partial t_1}(1+2r^4-4r^2+t_0-2t_1) = -8r(1-r^2)\frac{\partial r}{\partial t_1}-2<0,$$

where again we used Theorem 4.3.6. This implies the minimum of the right-hand side in (4.119) is attained when $(t_0,t_1)\in\Gamma_c$, hence using (4.18) with parameter $s=r$ given by Theorem 4.3.6,

$$1+2r^4-4r^2+t_0-2t_1 > -4r^4-4r^3+2r^2+\frac{1}{2}>0, \quad 0<r<\frac{1}{2}.$$

Returning this conclusion back to (4.119), we get $\widetilde{f}(0)>0$, so the only real root of $\widetilde{f}$ needs to be negative. □

As a consequence,

Corollary 4.4.6. *For $(t_0,t_1)\in\mathcal{F}$, the function f in (4.116) has two simple zeros $\hat{w}_1$, $\hat{w}_2=\overline{\hat{w}_1}$, $\operatorname{Im}\hat{w}_1<0$, on $\mathbb{D}\backslash\mathbb{R}$, two simple zeros $\hat{w}_1^{-1},\hat{w}_2^{-1}$ on $\mathbb{C}\backslash(\mathbb{D}\cup\mathbb{R})$ and two zeros on $(-\infty,0)\cup\partial\mathbb{D}$, the latter not necessarily distinct.*

Proof. The Corollary is a direct consequence of Lemma 4.4.5 and the 2-to-1 correspondence between the zeros of f and the zeros of $\tilde{f}$ induced by the map $w\mapsto w+w^{-1}$. □

Corollary 4.4.7. *The functions f, g given by (4.115)–(4.117) do not have a common root.*

Proof. This result follows directly from Lemma 4.4.4 and Corollary 4.4.6. □

For $t_0=0$, f reduces to

$$\begin{aligned}f(w) = 2r^4+2r^3w^3+\frac{2r^3}{w^3}+3r^2w^2+\frac{3r^2}{w^2}+2r^2\\ +\left(6r^3+\left(3-6r^2\right)r\right)w+\frac{6r^3+\left(3-6r^2\right)r}{w}+t_0+1\end{aligned}$$

and the root $\hat{w}_1$ and the values $h(\hat{w}_1), h(\hat{w}_1^{-1})$ are given by

$$\begin{aligned} \hat{w}_1 &= \omega^2 \hat{w}_0, \\ h(\hat{w}_1) &= \omega^2 h(\hat{w}_0) = \omega^2 \hat{z}_0 = \hat{z}_1, \\ h(\hat{w}_1^{-1}) &= \omega h(\hat{w}_0^{-1}) = \omega \hat{z}_0 = \omega^2 \hat{z}_1 \end{aligned} \tag{4.120}$$

where we recall that $\omega = e^{\frac{2\pi i}{3}}$ and $\hat{z}_0, \hat{z}_1$ and $\hat{w}_0$ are given in (4.101), (4.102) and (4.118).

To get started to the deformation argument used for the proof of Theorem 4.4.1, we state the following weak form of Theorem 4.4.1 as a Lemma.

Lemma 4.4.8. *For $t_1 > 0$ small, the discriminant $\mathcal{D}$ has three simple zeros, which are branch points of $\mathcal{R}$, and three double zeros, which are not branch points of $\mathcal{R}$.*

Proof. As explained in Section 4.4.1, the result is true for $t_1 = 0$. As a general fact that follows by continuity arguments, for small perturbations of t_1, the multiplicity of a zero of $\mathcal{D}$ cannot increase. That is, simple zeros of $\mathcal{D}$ for $t_1 = 0$ stay simple for small t_1, and double zeros of $\mathcal{D}$ for $t_1 = 0$ either keep being double zeros or else split into two distinct simple zeros.

In particular, we get that for small perturbation of t_1, $\mathcal{D}$ still has *at least* three simple zeros.

By Riemann-Hurwitz formula and the genus 0 condition given by Corollary 4.3.11, we know that $\mathcal{R}$ has four branch points. One of those is the point $z = \infty$, see (4.27), and each simple zero of $\mathcal{D}$ is also a branch point. Hence, $\mathcal{D}$ must have *at most* three simple zeros, and by the remarks above it follows that $\mathcal{D}$ has exactly three simple zeros and exactly three double zeros for small perturbations of t_1. □

Remark 4.4.9. The discriminant $\mathcal{D}$ can be expressed as

$$\mathcal{D}(z) = (\xi_1 - \xi_2)^2 (\xi_1 - \xi_3)^2 (\xi_2 - \xi_3)^2,$$

where ξ_j's are the solutions to (4.24). In particular, at least two of the ξ_j's coincide at each zero of $\mathcal{D}$. By continuity from the case $t_1 = 0$, it follows that for t_1 small, the solution ξ_1 coincides with one of the other two solutions at each zero of $\mathcal{D}$.

After this preparation, we can proceed to

Proof of Theorem 4.4.1. For $w_j, \hat{w}_j$, $j = 0, 1, 2$, the points given by Lemmas 4.3.12, 4.4.4 and Corollary 4.4.6, define

$$z_j = h(w_j), \quad \hat{z}_j = h(\hat{w}_j), \quad j = 0, 1, 2. \tag{4.121}$$

Our goal is to prove that these points satisfy the conclusions of Theorem 4.4.1. As a first step we prove their geometric properties *(i)–(iii)*, and afterwards we prove that these points are zeros of $\mathcal{D}$ with the claimed multiplicities. At the end, we prove that $z_0, z_1, z_2 \in \Omega$ in the three-cut case and $z_0, z_1 \in \Omega$ in the one-cut case.

First note that $\hat{z}_0, \hat{z}_1, \hat{z}_2 \in \mathbb{C} \setminus \overline{\Omega}$, because $|\hat{w}_j| > 1$ and h maps $\mathbb{C} \setminus \mathbb{D}$ to $\mathbb{C} \setminus \Omega$, see Corollary 4.3.10 and also Lemma 4.4.4 and Corollary 4.4.6.

We verify (4.98). For $t_1 = 0$, (4.98) follows from (4.118) and (4.120). Since $\hat{w}_0 \in (1, +\infty)$ (Lemma 4.4.4) and h maps $(1, +\infty)$ to $(0, +\infty) \setminus \Omega$ (Corollary 4.3.10), it follows that $\hat{z}_0 \in (0, +\infty) \setminus \Omega$, and in particular $z_0 > 0$. Because $\hat{w}_1$ is never real and $|\hat{w}_1| > 1$, see Corollary 4.4.6, the point $\hat{z}_1$ cannot be real neither, again due to Corollary 4.3.10. Thus by continuity with respect to t_1 we get $\operatorname{Im} \hat{z}_1 < 0$. The equality $\hat{z}_2 = \overline{\hat{z}_1}$ is trivial from (4.121) and the definition of $\hat{w}_1, \hat{w}_2$ given by Corollary 4.4.6.

We now prove that *(i)-(iii)* are satisfied by the points z_0, z_1, z_2.

For $t_1 = 0$, *(i)* follows from (4.103). When we tune up t_1, the point z_1 cannot become real for $(t_0, t_1) \in \mathcal{F}_1$. Indeed, the value w_j is a double zero of

$$z_j = h(w).$$

If z_1 becomes real for $(t_0, t_1) \in \mathcal{F}_1$ - hence also $z_2 = \overline{z_1}$ - then the equation $z_1 = h(w)$ has two distinct solutions w_1, w_2 with multiplicity two, see Lemma 4.3.12, which cannot occur because of the explicit form of h. By continuity, we get *(i)*.

When $(t_0, t_1) \in \gamma_c$, we know that $w_1 = w_2 \in (-1, 0)$, see Lemma 4.3.12. This automatically implies $z_1 = z_2$. Choosing $s = 1/4$ in (4.34), we compute explicitly

$$w_0 = 1/2, \quad w_1 = w_2 = \frac{1}{4}, \quad z_0 = \frac{111}{1024} > \frac{21}{256} = z_1 = z_2,$$

so for the respective choice of parameters $(t_0, t_1) \in \gamma_c$ *(iii)* holds true. Since h' never has triple roots, see Lemma 4.3.12, by continuity we conclude *(iii)* holds true for every choice of parameters $(t_0, t_1) \in \gamma_c$.

When (t_0, t_1) enters $\mathcal{F}_2$, we learn from *(iii)* and continuity that $z_1, z_2 < z_0$, so to get *(ii)* it only remains to prove that in this situation $z_2 < z_1$, or equivalently $h(w_2) < h(w_1)$.

The function $w \mapsto h(w)$ goes to $-\infty$ when $w \to -\infty$. On the negative axis its derivative has two simple zeros $w_1 < w_2$ and no others. This implies h is increasing in $(-\infty, w_1)$ and decreasing in (w_1, w_2), and hence $h(w_1) > h(w_2)$, so finally *(ii)* is proven.

For $(t_0, t_1) \in \mathcal{F} \setminus \gamma_c$, we now prove z_0, z_1, z_2 are simple zeros of $\mathcal{D}$ and $\hat{z}_0$, $\hat{z}_1$, $\hat{z}_2$ are double zeros of $\mathcal{D}$.

The points z_0, z_1, z_2 are the only branch points of $\mathcal{R}$, so surely they are zeros of $\mathcal{D}$. The remaining zeros of $\mathcal{D}$ must be of multiplicity at least two, because they are not branch points. Since we already know the points $\hat{z}_1, \hat{z}_2, \hat{z}_3$ are pairwise distinct, a total counting of zeros (according to multiplicity) shows it is enough to prove $\hat{z}_1, \hat{z}_2, \hat{z}_3$ are always zeros of $\mathcal{D}$, and their multiplicity properties will follow.

For $t_1 = 0$, $\mathcal{D}$ is given by

$$\mathcal{D}(z) = 4z^9 + (t_0^2 + 4A + 12t_0 - 8)z^6 + (4t_0^3 + 18At_0 + 12t_0^2 - 36A + 12t_0 + 4)z^3 - 27A^2,$$

where A is given in (4.100). Using (4.118), (4.120), after a lengthy calculation it follows that $\hat{z}_j$ is a double zero of $\mathcal{D}$, $j = 0, 1, 2$.

From Lemma 4.4.8, we know $\mathcal{D}$ has three double zeros for t_1 small, and these are not branch points. Let $h(\tilde{w}) = \tilde{z}$ be one of these zeros. We can assume $h(\tilde{w}^{-1}) = \xi_1(\tilde{z})$, see Remark 4.4.9, so in particular

$$|\tilde{w}| > 1. \tag{4.122}$$

From Corollary 4.4.3 we know the pair $(\xi, \tilde{z}) = h((\tilde{w}^{-1}), h(\tilde{w}))$ satisfies one of Equations (4.111)–(4.112), and hence $\tilde{w}$ must satisfy at least one of equations (4.113)–(4.114). Combining Equation (4.122) with Lemma 4.4.4 and Corollary 4.4.6, we thus get that $\tilde{w}_j$ must be one of the points $\hat{w}_0, \hat{w}_1, \hat{w}_2$, so $\tilde{z}$ must be one of the points $\hat{z}_1, \hat{z}_2, \hat{z}_3$.

Although carried out for t_1 small, the argument above works as long as none of the points $z_j, \hat{z}_j$ pairwise coincide. But we already proved (4.98), *(i)-(iii)* are valid, so the only coalescence that can happen is $z_1 = z_2$, and only for $(t_0, t_1) \in \gamma_c$. By continuity it means that in this case $\mathcal{D}$ has a unique simple zero z_0 and the other points $\hat{z}_0, \hat{z}_1, \hat{z}_2$, $z_1 = z_2$ are double zeros of $\mathcal{D}$ - the double zero $z_1 = z_2$ is still a branch point of $\mathcal{R}$. When we move beyond γ_c, the double zero $z_1 = z_2$ splits into the two simple zeros z_1, z_2 and the point z_1 is still a simple zero. The genus 0 constraint then guarantees that the remaining zeros

should still be of multiplicity at least two, and by analytic continuation these must be given by $\hat{z}_0, \hat{z}_1, \hat{z}_2$.

We now verify that $z_0, z_1, z_2 \in \Omega$ for $(t_0, t_1) \in \mathcal{F}_1$. For $t_1 = 0$ we know from (4.106) that

$$\xi_1(z_0) = \xi_3(z_0), \qquad \xi_1(z_j) = \xi_2(z_j), \quad j = 1, 2,$$

where ξ_1, ξ_2, ξ_3 are (analytic continuations of) the solutions to (4.24) as in (4.27). Since we already proved that the points z_0, z_1 and z_2 do not pairwise coincide for $(t_0, t_1) \in \mathcal{F}_1$, we conclude that these equalities are valid for every choice $(t_0, t_1) \in \mathcal{F}_1$. Hence ξ_1 is branched at each of the points z_0, z_1 and z_2. But from Theorem 4.2.5 we know that ξ_1 is the Schwarz function of $\partial\Omega$, hence ξ_1 is meromorphic on $\overline{\mathbb{C}} \setminus \Omega$ and consequently its branch points z_0, z_1 and z_2 have to belong to Ω.

It only remains to prove that $z_0, z_1 \in \Omega$ in the one-cut case $(t_0, t_1) \in \mathcal{F}_2$. When we cross γ_c, the branch point z_0 does not coalesce with any other zero of $\mathcal{D}$; thus by continuity we get that $\xi_1(z_0) = \xi_3(z_0)$ for every $(t_0, t_1) \in \mathcal{F}_2$. The discriminant $\mathcal{D}$ is a polynomial of degree 9 with positive leading coefficient, and for $(t_0, t_1) \in \mathcal{F}_2$ we already know that its only real zeros are z_2, z_1, z_0 and $\hat{z}_0$, the first three of multiplicity one, and the last one of multiplicity two. Hence

$$\begin{aligned} &\mathcal{D}(z) < 0, \quad z \in (-\infty, z_2), \\ &\mathcal{D}(z) > 0, \quad z \in (z_2, z_1), \\ &\mathcal{D}(z) < 0, \quad z \in (z_1, z_0), \\ &\mathcal{D}(z) > 0, \quad z \in (z_0, \hat{z}_0) \cup (\hat{z}_0, +\infty). \end{aligned} \tag{4.123}$$

We already know that $\xi_1(z_2) = \xi_3(z_2)$. The third inequality in (4.123) then implies that the boundary values of the analytic continuations of ξ_1 and ξ_2 are complex conjugate of each other in the interval (z_1, z_0). Combining with the second inequality in (4.123) we get that $\xi_1(z_1) = \xi_3(z_1)$, that is, the function ξ_1 is branched at z_1 as well. Since we already know from Theorem 4.2.5 that ξ_1 is the Schwarz function of $\partial\Omega$, the branch points of ξ_1 have to be in Ω, that is, $z_0, z_1 \in \Omega$, concluding the proof. □

Remark 4.4.10. We stress that the proof of Theorem 4.4.1 also shows that the points z_j and $\hat{z}_j$, $j = 0, 1, 2$, given by Theorem 4.2.6 can be obtained through the equalities

$$h(w_j) = z_j, \quad h(\hat{w}_j) = \hat{z}_j, \qquad j = 0, 1, 2,$$

where w_0, w_1 and w_2 are the zeros of h' as in Lemma 4.3.12, and $\hat{w}_0$, $\hat{w}_1$ and $\hat{w}_2$ are given by Lemma 4.4.4 and Corollary 4.4.6. We will use this fact extensively in the next sections.

4.4.3 Sheet structure for $\mathcal{R}$

To construct the sheet structure of $\mathcal{R}$, we make use of the following proposition.

Proposition 4.4.11. *For $(t_0, t_1) \in \mathcal{F}$, the (meromorphic continuation of) the functions ξ_1, ξ_2 and ξ_3 in (4.27) satisfy*

$$\xi_1(\hat{z}_0) = \xi_3(\hat{z}_0), \qquad \xi_1(\hat{z}_j) = \xi_2(\hat{z}_j), \quad j = 1, 2.$$

Furthermore,

(i) for $(t_0, t_1) \in \mathcal{F}_1$,

$$\xi_1(z_0) = \xi_3(z_0), \qquad \xi_1(z_j) = \xi_2(z_j), \quad j = 1, 2;$$

(ii) for $(t_0, t_1) \in \mathcal{F}_2$,

$$\xi_1(z_j) = \xi_3(z_j), \quad j = 0, 1, \qquad \xi_2(z_2) = \xi_3(z_3);$$

(iii) for $(t_0, t_1) \in \gamma_c$,

$$\xi_1(z_0) = \xi_3(z_0), \qquad \xi_1(z_1) = \xi_2(z_1) = \xi_3(z_1).$$

Proof. The first equality in (ii) was explicitly verified in the final part of the proof of Theorem 4.4.1. The other properties claimed by the proposition follow from similar continuity arguments. We skip the details. □

Using Proposition 4.4.11 we are ready to construct the sheet structure of the Riemann surface $\mathcal{R}$ associated with the algebraic equation (4.24). We see $\mathcal{R}$ as a branched three-sheeted cover of $\mathbb{C}$ and denote its sheets by $\mathcal{R}_1$, $\mathcal{R}_2$ and $\mathcal{R}_3$, so that

$$\mathcal{R} = \mathcal{R}_1 \cup \mathcal{R}_2 \cup \mathcal{R}_3.$$

The explicit construction of $\mathcal{R}_1, \mathcal{R}_2, \mathcal{R}_3$ is carried out below and depends on whether we are in the three-cut or one-cut case. In both situations, for $j = 1, 2, 3$, the function ξ_j in (4.27) admits a meromorphic continuation to the whole sheet $\mathcal{R}_j$. As usual, these functions ξ_1, ξ_2, ξ_3 are regarded as branches of the same meromorphic function

$$\xi : \mathcal{R} \to \overline{\mathbb{C}}, \quad \xi \equiv \xi_j \text{ on } \mathcal{R}_j,$$

which is the global solution to (4.24).

Moreover, given the sheet structure $\mathcal{R} = \mathcal{R}_1 \cup \mathcal{R}_2 \cup \mathcal{R}_3$, we denote the restriction of the canonical projection $\pi : \mathcal{R} \to \overline{\mathbb{C}}$ to $\mathcal{R}_j$ by π_j, $j = 1, 2, 3$. With this notation, the function π_j is invertible outside the branch cuts connecting the sheets, and its inverse π_j^{-1} extends continuously to the branch cuts if one considers appropriate limiting boundary values. As at the end of Section 4.4.1, we denote by $p^{(j)}$ the inverse image of a point $p \in \overline{\mathbb{C}}$ through π_j. That is, $p^{(j)}$ denotes the point in $\mathcal{R}_j$ which is uniquely defined through the relation

$$\{p^{(j)}\} = \pi_j^{-1}(\{p\}), \quad j = 1, 2, 3.$$

The point $p^{(j)}$ is also well defined at branch points. However, if p belongs to the projection of the open arcs constituting the branch cuts of $\mathcal{R}_j$, then the set $\pi_j^{-1}(\{p\})$ contains two points on $\mathcal{R}_j$, one on each side of the branch cut. We denote these two points by $p_+^{(j)}, p_-^{(j)} \in \mathcal{R}_j$, labeled according to

$$\{p_+^{(j)}\} = \pi_{j+}^{-1}(\{p\}), \quad \{p_-^{(j)}\} = \pi_{j-}^{-1}(\{p\}).$$

In particular, if p belongs to the branch cut connecting two sheets $\mathcal{R}_j$ and $\mathcal{R}_k$, then $p_\pm^{(j)} = p_\mp^{(k)}$.

4.4.3.1 Sheet structure in the three-cut case

Consider a Jordan arc γ_0 connecting z_1 to z_2 and intersecting $\mathbb{R}$ exactly once, say at the point z_*. Assume in addition $\gamma_0^* = \gamma_0$ and $z_* < z_0$. Set

$$\Sigma_* = \gamma_0 \cup [z_*, z_0]$$

and define

$$\mathcal{R}_1 = \overline{\mathbb{C}} \setminus \Sigma_*, \quad \mathcal{R}_2 = \overline{\mathbb{C}} \setminus (\gamma_0 \cup [-\infty, z_0]), \quad \mathcal{R}_3 = \overline{\mathbb{C}} \setminus [-\infty, z_0].$$

We construct the three-sheeted Riemann surface

$$\mathcal{R} = \mathcal{R}_1 \cup \mathcal{R}_2 \cup \mathcal{R}_3$$

connecting $\mathcal{R}_1$ to $\mathcal{R}_2$ along γ_0, $\mathcal{R}_1$ to $\mathcal{R}_3$ along $[z_*, z_0]$ and $\mathcal{R}_2$ to $\mathcal{R}_3$ along $[-\infty, z_*]$, always in the usual crosswise manner. For $t_1 = 0$ and the choice $\gamma_0 = [0, z_1] \cup [0, z_2]$, this is in agreement with the sheet structure for $t_1 = 0$ carried over in Section 4.4.1. This sheet structure is illustrated in Figure 4.13.

The Riemann surface $\mathcal{R}$ is branched at the points

$$z_0^{(1)} = z_0^{(3)}, \quad z_1^{(1)} = z_1^{(2)}, \quad z_2^{(1)} = z_2^{(2)}, \quad \infty^{(2)} = \infty^{(3)}.$$

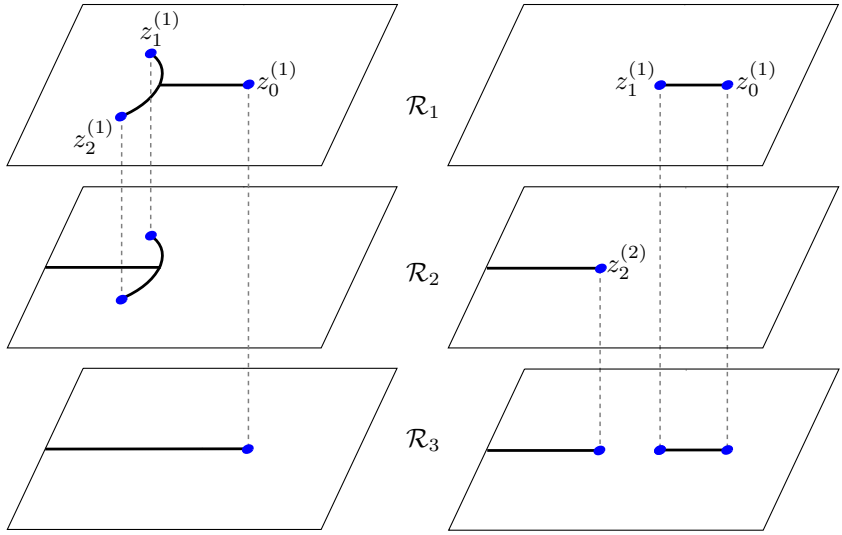

Figure 4.13: Sheet structure of $\mathcal{R}$ for $(t_0, t_1) \in \mathcal{F}_1$ (left) and $(t_0, t_1) \in \mathcal{F}_2$ (right).

We emphasize here the freedom in the choice of γ_0. This freedom is exploited later. We also remark that this sheet structure preserves the equalities

$$\begin{aligned} &\xi_1(\hat{z}_0) = \xi_3(\hat{z}_0), \quad \xi_1(\hat{z}_j) = \xi_2(\hat{z}_j), \ j = 1, 2, \\ &\xi_1(z_0) = \xi_3(z_0), \quad \xi_1(z_j) = \xi_2(z_j), \ j = 1, 2, \end{aligned} \tag{4.124}$$

claimed by Proposition 4.4.11. In addition, the following properties hold true

$$\xi_2(x) < \xi_3(x) < \xi_1(x), \qquad x > \hat{z}_0, \tag{4.125}$$

$$\xi_2(x) < \xi_1(x) < \xi_3(x), \qquad z_0 < x < \hat{z}_0, \tag{4.126}$$

$$\xi_{1\pm}(x) = \overline{\xi_{3\pm}(x)} = \xi_{3\mp}(x), \quad \operatorname{Im} \xi_2(x) = 0, \qquad z_* < x < z_0, \tag{4.127}$$

$$\xi_{2\pm}(x) = \overline{\xi_{3\pm}(x)} = \xi_{3\mp}(x), \quad \operatorname{Im} \xi_1(x) = 0, \qquad x < z_*, \tag{4.128}$$

as it follows from the asymptotic behavior (4.27) and an analysis of the sign of the discriminant $\mathcal{D}$ as in (4.123). We skip the details.

Furthermore, from the construction of the Riemann surface, it also holds true

$$\begin{aligned} &\xi_{1\pm}(z) = \xi_{3\mp}(z), \quad z \in [z_*, z_0], \\ &\xi_{1\pm}(z) = \xi_{2\mp}(z), \quad z \in \gamma_0. \end{aligned}$$

4.4.3.2 Sheet structure in the one-cut case

For $(t_0, t_1) \in \mathcal{F}_2$, we define

$$\mathcal{R}_1 = \overline{\mathbb{C}} \setminus [z_1, z_0], \quad \mathcal{R}_2 = \overline{\mathbb{C}} \setminus [-\infty, z_2], \quad \mathcal{R}_3 = \overline{\mathbb{C}} \setminus ([-\infty, z_2] \cup [z_1, z_0]).$$

In the present case, $\mathcal{R}_1$ is connected to $\mathcal{R}_3$ along $[z_1, z_0]$ and $\mathcal{R}_2$ is connected to $\mathcal{R}_3$ along $[-\infty, z_2]$, in the usual crosswise way. This sheet structure is shown in Figure 4.13.

The branch points of $\mathcal{R}$ are given by

$$z_0^{(1)} = z_0^{(3)}, \quad z_1^{(1)} = z_1^{(3)}, \quad z_2^{(2)} = z_2^{(3)}, \quad \infty^{(2)} = \infty^{(3)},$$

see Figure 4.13. In the same spirit as in (4.124)–(4.128), we also have the following equalities,

$$\begin{aligned} &\xi_1(\hat{z}_0) = \xi_3(\hat{z}_0), \quad \xi_1(\hat{z}_j) = \xi_2(\hat{z}_j), \ j = 1, 2, \\ &\xi_2(z_2) = \xi_3(z_2), \quad \xi_1(z_j) = \xi_3(z_j), \ j = 0, 1, \end{aligned} \tag{4.129}$$

and the relations

$$\begin{aligned} &\xi_2(x) < \xi_3(x) < \xi_1(x), && && x > \hat{z}_0, \\ &\xi_2(x) < \xi_1(x) < \xi_3(x), && && z_0 < x < \hat{z}_0, \\ &\xi_{1\pm}(x) = \overline{\xi_{3\pm}(x)} = \xi_{3\mp}(x), && \operatorname{Im} \xi_2(x) = 0, && z_1 < x < z_0, \\ &\xi_{2\pm}(x) = \overline{\xi_{3\pm}(x)} = \xi_{3\mp}(x), && \operatorname{Im} \xi_1(x) = 0, && x < z_2. \end{aligned} \tag{4.130}$$

4.5 Meromorphic quadratic differential on $\mathcal{R}$

Given any point $p \in \mathcal{R}$ which is not a branch point, we define the following function element in a neighborhood of p

$$Q(z) = \begin{cases} \xi_2(z) - \xi_3(z), & \text{if } p \in \mathcal{R}_1, \\ \xi_1(z) - \xi_3(z), & \text{if } p \in \mathcal{R}_2, \\ \xi_1(z) - \xi_2(z), & \text{if } p \in \mathcal{R}_3. \end{cases} \tag{4.131}$$

The function element Q cannot be extend to a (single-valued) meromorphic function on the whole Riemann surface $\mathcal{R}$, but it admits an analytic extension

along any path on $\mathcal{R}$. Hence given any path γ on $\mathcal{R}$, it is meaningful to talk about contour integrals of Q along γ. More importantly, the square Q^2 extends to a (single-valued!) meromorphic function on the whole Riemann surface $\mathcal{R}$, as it is shown in a general framework in [107, Theorem 1.8]. Due to our explicit sheet structure, this can also be verified directly, but we skip the details.

We are interested in the associated quadratic differential

$$\varpi = -(Q(z))^2 dz^2. \tag{4.132}$$

Zeros and poles of ϖ are the zeros and poles of Q^2, along with their multiplicities, and also the branch points of $\mathcal{R}$. Simple poles and zeros are called finite critical points, whereas poles of order at least 2 are called infinite critical points. An arc $\gamma \subset \mathcal{R}$ is said to be an *arc of trajectory* of ϖ if

$$\operatorname{Re} \int^z \sqrt{-\varpi} = \operatorname{Re} \int^z Q(s)ds = \text{const}, \quad z \in \gamma. \tag{4.133}$$

A trajectory is a maximal arc of trajectory, and it is called critical if it extends to a finite critical point of ϖ on at least one of its ends. Two trajectories can only intersect at the critical points. The union of all critical trajectories of ϖ is denoted by $\mathcal{G} = \mathcal{G}(\varpi)$ and is called the *critical graph* of ϖ.

The main goal of this Section is to describe the critical graph $\mathcal{G}$. As we will see later on, the critical graph plays a substantial role in the Riemann-Hilbert/Steepest Descent analysis carried over in Sections 4.7 and 4.8. Some of its trajectories also encode Equation (4.37): Theorem 4.2.9 will follow almost immediately once we describe the critical graph $\mathcal{G}$.

To describe the trajectories of ϖ, we follow the methodology used in Chapter 3. The main conclusion of this analysis is that the topology of the critical graph of ϖ only depends on whether (t_0, t_1) belongs to $\mathcal{F}_1$ or $\mathcal{F}_2$.

In our setting, the analysis works as follows. We first describe the trajectories for $t_1 = 0$, for which the underlying rotational symmetry plays a fundamental role. It turns out that in this case $\mathcal{R} \setminus \mathcal{G}$ consists only of strip and half plane domains, and no short trajectories. When we increase t_1, the critical graph is deformed, and we control its dynamics by means of analyzing the widths of the strip domains, showing that they do not vanish on $\mathcal{F}_1$, and thus the critical graph is preserved for values of (t_0, t_1) in this domain. When we cross γ_c, moving from $\mathcal{F}_1$ to $\mathcal{F}_2$, we are able to identify the phase transitions for the trajectories, and describe the critical graph for values of $(t_0, t_1) \in \mathcal{F}_2$ that are sufficiently close to γ_c. Once again the critical graph consists only of strip and half plane domains, but now there are also short trajectories. We again analyze

the widths of the strip domains, and also the short trajectories, and prove that the critical graph remains unchanged on $\mathcal{F}_2$.

The standard references on quadratic differentials are the books by Strebel [133] and by Jenkins [85]. We follow closely the notions described Appendix A, where the reader can find a discussion on the general theory of quadratic differentials in a form suitable for our needs.

The present Section is organized in the following manner. In Sections 4.5.1 and 4.5.2 we derive some technical lemmas that are needed for the computation of the critical graph, first for the three-cut case $(t_0, t_1) \in \mathcal{F}_1$ and then for the one-cut case $(t_0, t_1) \in \mathcal{F}_2$. In Section 4.5.3 we compute the zeros and poles of ϖ, and discuss some general principles that are used for the computation of the critical graph. Finally, in Sections 4.5.4 and 4.5.5 we derive the critical graph in the three-cut and one-cut cases, respectively.

When describing the trajectories and dynamics of the critical graph of ϖ, instead of a precise formulation of the behavior of each trajectory we opt for a more "reader friendly" approach, with visual description and illustration of the results by a number of pictures. And of course, we always provide rigorous proofs of the results.

4.5.1 Technical computations for the three-cut case

When $t_1 = 0$, the sheet structure constructed in Section 4.4.3.1 is consistent with the sheet structure in Section 4.4.1. However, for the analysis of the trajectories of ϖ when $t_1 = 0$, it is more convenient (although, strictly speaking, not necessary) to construct the sheets in a different way that better reflects the underlying discrete rotational symmetry.

According to Theorem 4.2.6, $z_j, \hat{z}_j$, $j = 1, 2, 3$, denote the branch points and the singular points of (4.24), respectively. In the case $t_1 = 0$, these points are explicitly given in (4.101)–(4.102).

We set

$$L_j = [0, \infty e^{\frac{(2j+3)\pi i}{3}}], \quad j = 0, 1, 2, \qquad L = \bigcup_{j=0}^{2} L_j, \tag{4.134}$$

and recalling the set Σ_* given explicitly for $t_1 = 0$ in (4.104), we define

$$\widetilde{\mathcal{R}}_1 = \overline{\mathbb{C}} \setminus \Sigma_*, \quad \widetilde{\mathcal{R}}_2 = \overline{\mathbb{C}} \setminus (\Sigma_* \cup L), \quad \widetilde{\mathcal{R}}_3 = \overline{\mathbb{C}} \setminus L. \tag{4.135}$$

We then connect the sheets $\widetilde{\mathcal{R}}_1$ and $\widetilde{\mathcal{R}}_2$ along Σ_* and the sheets $\widetilde{\mathcal{R}}_2$ and $\widetilde{\mathcal{R}}_3$ along L, always in the crosswise manner, and denote by $\widetilde{\mathcal{R}}$ the resulting three-sheeted

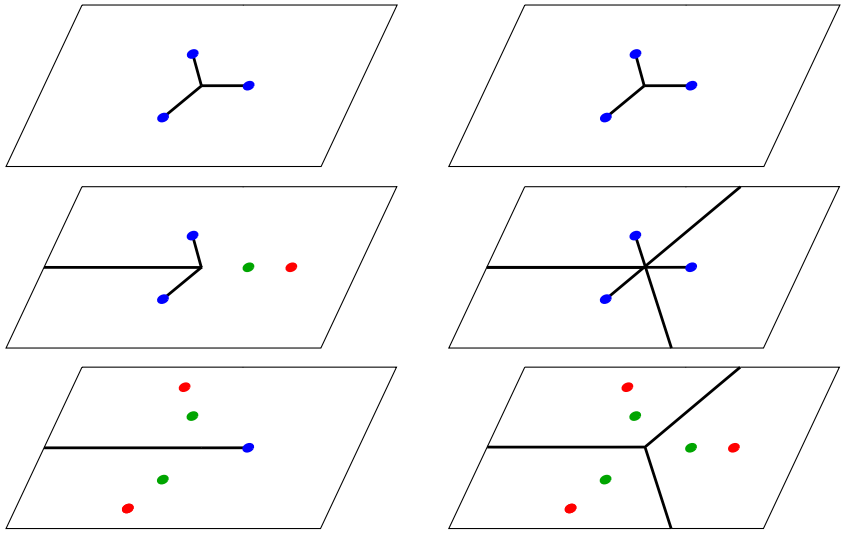

Figure 4.14: For $t_1 = 0$, the cut structure and the zeros of ϖ before (left) and after (right) the regluing $\mathcal{R}_j \mapsto \widetilde{\mathcal{R}}_j$.

Riemann surface,

$$\widetilde{\mathcal{R}} = \widetilde{\mathcal{R}}_1 \cup \widetilde{\mathcal{R}}_2 \cup \widetilde{\mathcal{R}}_3.$$

This construction can be compared to (4.105) through the identities

$$\begin{aligned}
\widetilde{\mathcal{R}}_1 &= \mathcal{R}_1, \\
\widetilde{\mathcal{R}}_2 &= \begin{cases} \mathcal{R}_3, & -\frac{\pi}{3} < \arg z < \frac{\pi}{3}, \\ \mathcal{R}_2, & \text{otherwise}, \end{cases} \\
\widetilde{\mathcal{R}}_3 &= \begin{cases} \mathcal{R}_2, & -\frac{\pi}{3} < \arg z < \frac{\pi}{3}, \\ \mathcal{R}_3, & \text{otherwise}. \end{cases}
\end{aligned} \tag{4.136}$$

That is, we interchange the sectors $-\pi/3 < \arg z < \pi/3$ between the sheets $\mathcal{R}_2$ and $\mathcal{R}_3$. We refer the reader to Figure 4.14 for a comparison of these sheets structures.

Clearly this new sheet structure also affects the analytic continuation of the function germs in (4.27). Each function germ in (4.27) admits an analytic continuation to the whole sheet $\widetilde{\mathcal{R}}_j$, and these analytic continuations satisfy the equalities

$$\xi_1(z_j) = \xi_2(z_j), \quad \xi_1(\hat{z}_j) = \xi_2(\hat{z}_j), \quad j = 0, 1, 2,$$

and the identities

$$\xi_3(x) < \xi_2(x) < \xi_1(x), \qquad x > \hat{z}_0, \tag{4.137}$$

$$\xi_3(x) < \xi_1(x) < \xi_2(x), \qquad z_0 < x < \hat{z}_0, \tag{4.138}$$

$$\xi_{1\pm}(x) = \overline{\xi_{2\pm}(x)} = \xi_{2\mp}(x), \quad \operatorname{Im}\xi_3(x) = 0, \qquad 0 < x < z_0, \tag{4.139}$$

$$\xi_{2\pm}(x) = \overline{\xi_{3\pm}(x)} = \xi_{3\mp}(x), \quad \operatorname{Im}\xi_1(x) = 0, \qquad x < 0, \tag{4.140}$$

which are compatible with (4.124)–(4.128), keeping in mind (4.136). During Section 4.5, for $t_1 = 0$ we always use the analytic continuations of the functions ξ_1, ξ_2, ξ_3 in accordance to the sheet structure for $\widetilde{\mathcal{R}}$, unless otherwise stated. For $t_1 > 0$ we keep using the sheet structure constructed in Sections 4.4.3.1 and 4.4.3.2.

For $t_1 = 0$, define

$$h_j(x, y) = \int_x^y (\operatorname{Re}\xi_{j+}(s) - \operatorname{Re}\xi_{3+}(s))ds, \quad x, y \in \mathbb{R}, \quad j = 1, 2, \tag{4.141}$$

where the integrals above are computed along the real axis. We emphasize that the functions ξ_1, ξ_2, ξ_3 in the expression above correspond to the sheet structure $\widetilde{R}_1, \widetilde{R}_2, \widetilde{R}_3$.

Lemma 4.5.1. *Suppose that $t_1 = 0$. For $j = 1, 2$, the following properties hold true for h_j.*

(i) If $x, y \in [0, z_0]$, $x \neq y$, then $h_j(x, y) \neq 0$.

(ii) If $h(x_j, y_j) = 0$, for $x_j < y_j \leq 0$, $j = 1, 2$, then $(x_1, y_1) \cap (x_2, y_2) \neq \emptyset$.

Proof. We first prove (i). If $h_j(x, y) = 0$ for $x, y \in [0, z_0]$, then we conclude that there exists u_0 between x and y for which

$$\operatorname{Re}\xi_{j+}(u_0) = \operatorname{Re}\xi_{3+}(u_0).$$

It follows from the first equation in (4.101) that $z_0 < 1$. In particular, this implies

$$0 < u_0 < z_0 < 1. \tag{4.142}$$

From (4.139) we know that $\overline{\xi_{1+}(u_0)} = \xi_{2+}(u_0)$, so

$$\operatorname{Re}\xi_{2+}(u_0) = \operatorname{Re}\xi_{1+}(u_0) = \xi_3(u_0).$$

For $t_1 = 0$, the coefficient of ξ^2 in (4.24) is $-z^2$. Using Vieta's relations we hence conclude

$$u_0^2 = \xi_{1+}(u_0) + \xi_{2+}(u_0) + \xi_3(u_0) = 3\xi_3(u_0).$$

Plugging in the pair $(\xi_3(u_0), u_0) = (u_0^2/3, u_0)$ back to (4.24), we see that u_0 must be a root of

$$\phi(u) = \frac{2}{27}u^6 - \left(\frac{2}{3} - t_0\right)u^3 - A = 0,$$

where the coefficient A, given explicitly in (4.100), is positive because $t_0 \in (0, 1/8)$. Due to the rotational symmetry $\phi(\omega u) = \phi(u)$, the polynomial ϕ has at most two real roots. Straightforward computations show

$$\phi(0) = -A < 0, \qquad \phi(1) = t_0 - A - \frac{16}{27} < 0.$$

Since the degree of ϕ is even and its leading coefficient is positive, the inequalities above imply that ϕ does not have roots on the interval $[0, 1]$, thus $u_0 \in \mathbb{R} \setminus [0, 1]$. But this is in contradiction with (4.142).

To get (ii), we first note that arguments similar as the analysis above show that ϕ has a zero in each of the intervals (x_1, y_1) and (x_2, y_2). On the other hand, the inequality and comments above also show that ϕ has exactly one zero on $(-\infty, 0)$, so this zero must belong to both intervals (x_1, y_1) and (x_2, y_2). □

For $(t_0, t_1) \in \mathcal{F}_1$ and recalling the definition of the function germ Q in (4.131) and the sheet structure described in Section 4.4.3.2, the quantities

$$\tau_1 = \operatorname{Re} \int_{z_2^{(3)}}^{z_0^{(3)}} Q(s)ds = \operatorname{Re} \int_{z_2}^{z_0} (\xi_1(s) - \xi_2(s))ds, \tag{4.143}$$

$$\tau_2 = \operatorname{Re} \int_{z_0^{(2)}}^{z_2^{(2)}} Q(s)ds = \operatorname{Re} \int_{z_0}^{z_2} (\xi_1(s) - \xi_3(s))ds, \tag{4.144}$$

$$\tau_3 = \operatorname{Re} \int_{z_2^{(3)}}^{\hat{z}_2^{(3)}} Q(s)ds = \operatorname{Re} \int_{z_2}^{\hat{z}_2} (\xi_1(s) - \xi_2(s))ds, \tag{4.145}$$

$$\tau_4 = \operatorname{Re} \int_{z_2^{(3)}}^{z_1^{(2)}} Q(s)ds = \operatorname{Re} \int_{z_2}^{x_*} (\xi_1(s) - \xi_2(s))ds + \operatorname{Re} \int_{x_*}^{z_1} (\xi_1(s) - \xi_3(s))ds \tag{4.146}$$

and

$$\tau_5 = \int_{z_0^{(2)}}^{\hat{z}_0^{(2)}} Q(s)ds = \int_{z_0}^{\hat{z}_0} (\xi_1(s) - \xi_3(s))ds \tag{4.147}$$

are of interest for what comes later. In the formulas above, the paths of integration are taken in $\mathbb{C} \setminus (-\infty, z_*] \cup \Sigma_*$ and x_* is any point in the interval $(-\infty, z_*)$: the value τ_4 does not depend on the precise choice of x_*, as it is indicated by the first integral defining it.

What is important here is that τ_j, $j = 1, \dots, 5$, do not vanish for $(t_0, t_1) \in \mathcal{F}_1$. The analysis of these quantities is carried out in the Section 4.11.1.

4.5.2 Technical computations for the one-cut case

It is a simple observation that if you fix $(\tilde{t}_0, \tilde{t}_1) \in \gamma_c$, then any pair of the form $(\tilde{t}_0, t_1) \in \mathcal{F}$, with t_1 larger than $\tilde{t}_1$, actually belongs to $\mathcal{F}_2$, as can be seen in Figure 4.3. In other words, $\mathcal{F}_2$ consists of points in $\mathcal{F}$ of the form $(\tilde{t}_0, t_1)$, where $(\tilde{t}_0, \tilde{t}_1) \in \gamma_c$ for some $\tilde{t}_1$ and $t_1 > \tilde{t}_1$. We use this fact without further mention.

Recall that w_0, w_1, w_2 denote the zeros of h' (see Lemma 4.3.12) and, moreover, $w_1 = w_2$ for $(t_0, t_1) \in \gamma_c$. For $(t_0, t_1) \in \mathcal{F}_2$, denote additionally by $\tilde{w}_j$ the simple root of $h(w) - z_j = h(w) - h(w_j)$, $j = 0, 1, 2$, and extend $\tilde{w}_j$ for values $(t_0, t_1) \in \gamma_c$ by continuity.

When $(t_0, t_1) \in \gamma_c$, we recall that r, a_0 are given in terms of $s \in (0, 1/2)$ by (4.34), so that

$$h'(w) = r - \frac{2a_0 r}{w^2} - \frac{2r^2}{w^3} = -\frac{s^3(2s - w)(s + w)^2}{w^3}.$$

In particular $w_0 = 2s$, so

$$h(w) - h(w_0) = \frac{s^3(2s - w)^2(s + 4w)}{4w^2}.$$

Summarizing, the last two equations tell us that when $(t_0, t_1) \in \gamma_c$, the quantities w_0, w_1, w_2 and $\tilde{w}_0$ mentioned above are given in terms of the parameter $s \in (0, 1/2)$ by

$$w_1 = -s = w_2, \quad \tilde{w}_0 = -\frac{s}{4}, \quad w_0 = 2s. \tag{4.148}$$

For the choice $a_0 = \frac{1}{4}$, $r = \frac{1}{32}$, corresponding to the pair $(t_0, t_1) = (\frac{639}{524288}, \frac{191}{1024}) \in \mathcal{F}_2$, we compute numerically

$$\begin{array}{lll} z_2 \approx 0.18352, & w_2 \approx -0.12932, & \tilde{w}_2 \approx -1.86844, \\ z_1 \approx 0.20797, & w_1 \approx -0.63351, & \tilde{w}_1 \approx -0.07786, \\ z_0 \approx 0.29599, & w_0 \approx 0.76284, & \tilde{w}_0 \approx -0.05370. \end{array}$$

so for this choice

$$\tilde{w}_2 < w_1 < w_2 < \tilde{w}_1 < \tilde{w}_0 < w_0. \tag{4.149}$$

If $(t_0, t_1) \in \mathcal{F}_2$, then none of the points $w_j, \tilde{w}_j$'s can pairwise coincide. Indeed, we already know from Lemma 4.3.12 that the points w_0, w_1 and w_2 do not pairwise coincide. If $\tilde{w}_j = \tilde{w}_k$ (or also $\tilde{w}_j = w_k$) for some pair j, k, then consequently

$$z_j = h(w_j) = h(\tilde{w}_j) = h(\tilde{w}_k) = h(w_k) = z_k,$$

which cannot occur on $\mathcal{F}_2$ (see Theorem 4.4.1). Hence by continuity we conclude that (4.149) holds for every pair $(t_0, t_1) \in \mathcal{F}_2$.

Lemma 4.5.2. *Fix $(\tilde{t}_0, \tilde{t}_1) \in \gamma_c$. Then*

$$\lim_{t_1 \to \tilde{t}_1 +} \frac{\partial w_1}{\partial t_1} = -\infty, \qquad \lim_{t_1 \to \tilde{t}_1 +} \frac{\partial w_2}{\partial t_1} = +\infty$$

Proof. We deal with the equality for w_1. The case w_2 is analogous. Let $(\tilde{t}_0, t_1) \in \mathcal{F}_2$, so $t_1 > \tilde{t}_1$. In this situation, w_1 is a simple zero of h', so

$$\frac{\partial w_1}{\partial t_1} = -\frac{\frac{\partial h'}{\partial t_1}(w_1)}{h''(w_1)}. \tag{4.150}$$

We see $(t_0, t_1) \mapsto (r, a_0)$ as a change of coordinates, so that from the chain rule

$$\left(\frac{\partial h'}{\partial t_0}, \frac{\partial h'}{\partial t_1} \right) = \left(\frac{\partial h'}{\partial r}, \frac{\partial h'}{\partial a_0} \right) \frac{D(r, a_0)}{D(t_0, t_1)}, \tag{4.151}$$

where $D(r, a_0)/D(t_0, t_1)$ is the Jacobian of the change of coordinates. From the Inverse Function Theorem,

$$\begin{aligned} \frac{D(r, a_0)}{D(t_0, t_1)} &= \left(\frac{D(t_0, t_1)}{D(r, a_0)} \right)^{-1} \\ &= \det \left(\frac{D(t_0, t_1)}{D(r, a_0)} \right)^{-1} \begin{pmatrix} \partial t_1/\partial a_0 & -\partial t_0/\partial a_0 \\ -\partial t_1/\partial r & \partial t_0/\partial r \end{pmatrix}. \end{aligned}$$

We use this expression to compute the second component in (4.151), arriving at

$$\frac{\partial h'}{\partial t_1} = \det\left(\frac{D(t_0,t_1)}{D(r,a_0)}\right)^{-1}\left(\frac{\partial t_0}{\partial r}\frac{\partial h'}{\partial a_0} - \frac{\partial t_0}{\partial a_0}\frac{\partial h'}{\partial r}\right). \tag{4.152}$$

Using (4.31)–(4.32), we compute explicitly

$$\frac{\partial t_0}{\partial r} = 2\left(1-4a_0^2\right)r - 8r^3, \qquad \frac{\partial t_0}{\partial a_0} = -8a_0r^2,$$

$$\frac{\partial t_1}{\partial r} = -8a_0r, \qquad \frac{\partial t_1}{\partial a_0} = 1-2a_0-4r^2,$$

and after a lengthy calculation

$$\det\left(\frac{D(t_0,t_1)}{D(r,a_0)}\right) = 2r\left(8a_0^3 - 4a_0^2\left(4r^2+1\right) + a_0\left(8r^2-2\right) + \left(1-4r^2\right)^2\right).$$

Similarly,

$$\frac{\partial t_0}{\partial r}\frac{\partial h'}{\partial a_0} - \frac{\partial t_0}{\partial a_0}\frac{\partial h'}{\partial r} = -\frac{4r^2\left(8ar - 2aw^3 - 4r^2w + w\right)}{w^3}$$

We are interested in the values of $\partial h'/\partial t_1$ for parameters on γ_c, so using (4.34) and (4.148) in the last two equations, we get

$$\frac{D(t_0,t_1)}{D(r,a_0)} = 2s^3\left(1-s^2\right)^3\left(2s^2+1\right)^2\left(1-4s^2\right) > 0, \quad s\in(0,1/2)$$

and

$$\frac{\partial t_0}{\partial r}\frac{\partial h'}{\partial a_0} - \frac{\partial t_0}{\partial a_0}\frac{\partial h'}{\partial r} = -4s^4(1-15s^4-4s^6) < 0, \quad s\in(0,1/2).$$

In virtue of (4.152), we conclude

$$\frac{\partial h'}{\partial t_1}(w_1) < 0, \quad (\tilde{t}_0,\tilde{t}_1)\in\gamma_c.$$

Additionally, since w_1 is the smallest root of the continuous function h' on $(-\infty,0)$ and $h'(w)\to r>0$ when $w\to-\infty$, we conclude

$$h''(w_1) < 0, \quad (t_0,t_1)\in\mathcal{F}_2.$$

When t_1 approaches $\tilde{t}_1$, w_1 becomes a double root of h', and hence $h''(w_1)$ approaches zero. The result then follows by combining the last two inequalities with (4.150). □

Having in mind (4.32), set

$$\begin{aligned} G(w) &= h\left(\frac{1}{w}\right) - \frac{t_1 + h(w)^2}{3} \\ &= \frac{2r^2w^2}{3} + \frac{4a_0rw}{3} + \frac{2a_0}{3} + \frac{r(3-4a_0^2-2r^2)}{3w} \\ &\quad - \frac{2a_0r^2(1+2a_0)}{3w^2} - \frac{4a_0r^3}{3w^3} - \frac{r^4}{3w^4}, \quad w \in \mathbb{C}. \end{aligned}$$

When $(t_0, t_1) \in \gamma_c$ we use (4.34) and (4.148) to compute

$$G(w_1) = 0 = G(w_2), \quad G(\tilde{w}_0) = -\frac{3}{8}s^2\left(7s^6 + 12s^4 + 8\right) < 0. \tag{4.153}$$

Lemma 4.5.3. *If $(\tilde{t}_0, \tilde{t}_1) \in \gamma_c$, then $G'(w) < 0$ on $(-\infty, 0)$.*

Proof. On γ_c, the quantities a_0 and r are explicitly given in terms of $s \in (0, 1/2)$ by (4.34). Substituting these values in the definition of G, we can rewrite

$$\begin{aligned} G'(w) &= \frac{s^3}{3w^5}p(w), \\ p(w) &= 4s^3w^6 + 6s^2w^5 + (2s^6 + 9s^4 - 3)w^3 \\ &\quad + 6s^5(1+3s^2)w^2 + 18s^8w + 4s^9. \end{aligned}$$

The discriminant of p can be decomposed as

$$\mathrm{Discr}(p; w) = c\,(s^2-1)^3 s^{24}(s^{30} + \ldots),$$

where the polynomial between parentheses has rational coefficients and is symbolically computed with Mathematica. Its zeros are computed numerically and verified to not belong to $(0, 1/2)$.

As a consequence, we conclude that p - and hence G' - does not have zeros with multiplicity on $(-\infty, 0)$. For $s = 1/2$,

$$p(w) = \frac{(w-1)\left(64w^5 + 256w^4 + 256w^3 - 52w^2 - 10w - 1\right)}{1024}$$

and the set of zeros (with nonnegative imaginary part) of the polynomial between parentheses above is numerically computed to be

$$\{-4.14697 + 1.16757i, -0.144709 + 0.158865i, 0.58336\}.$$

so in particular $p(w)$ has no negative zeros for $s = 1/2$, and the same holds true for G'. Since G' is never zero at $w = 0$ and, as we just observed, G' does not have zeros with multiplicity, by continuity of the zeros of G' with respect of s we get that G' is never zero on $(-\infty, 0)$. The result then follows from the extra observation that $G'(w) \to -\infty$ when $w \to -\infty$. □

Lemma 4.5.4. *Fix $(\tilde{t}_0, \tilde{t}_1) \in \gamma_c$. There exists $\varepsilon > 0$ such that for any pair $(\tilde{t}_0, t_1) \in \mathcal{F}_2$ with $0 < t_1 - \tilde{t}_1 < \varepsilon$, the following inequalities hold true*

$$G(w_2) < 0 < G(w_1).$$

Proof. We will prove

$$\lim_{t_1 \to \tilde{t}_1 +} \frac{\partial}{\partial t_1}(G(w_1)) = +\infty, \qquad \lim_{t_1 \to \tilde{t}_1 +} \frac{\partial}{\partial t_1}(G(w_2)) = -\infty. \tag{4.154}$$

By continuity, it then follows that $t_1 \mapsto G(w_1)$ ($t_1 \mapsto G(w_2)$) is increasing (decreasing) for t_1 sufficiently close to $\tilde{t}_1$. Since $G(w_1) = 0 = G(w_2)$ for $t_1 = \tilde{t}_1$ (see (4.153)), the result will follow.

From the definition of G and $j = 1, 2$,

$$\frac{\partial}{\partial t_1}(G(w_j)) = -\frac{1}{w_j^2} h'\left(\frac{1}{w_j}\right) \frac{\partial w_j}{\partial t_1} + \frac{\partial h}{\partial t_1}\left(\frac{1}{w_j}\right) - \frac{2}{3} h(w_j) \frac{\partial h}{\partial t_1}(w_j) - \frac{1}{3}, \tag{4.155}$$

where we also used $h'(w_j) = 0$. Additionally, we use (4.148) to get

$$h'\left(\frac{1}{w_j}\right) \to h'\left(-\frac{1}{s}\right) = 2s^9 - 3s^7 + s^3 > 0, \qquad \text{as } t_1 \to \tilde{t}_1.$$

From Lemma 4.5.2 and the inequality above, we know that the first term on the right hand side of (4.155) goes to $(-1)^{j+1}\infty$ when $t_1 \searrow \tilde{t}_1$. Since $w_j \to -s \neq 0$ in the limit $t_1 \searrow \tilde{t}_1$, the remaining terms remain bounded, concluding the proof of (4.154). □

Proposition 4.5.5. *Suppose $(\tilde{t}_0, \tilde{t}_1) \in \gamma_c$. There exists $\varepsilon > 0$ such that for every choice $(\tilde{t}_0, t_1) \in \mathcal{F}_2$ with $0 < t_1 - \tilde{t}_1 < \varepsilon$, the function G has no zeros on the intervals $(-\infty, w_1]$ and $[w_2, \tilde{w}_0]$.*

Proof. Since $\tilde{w}_0 < 0$, it follows from continuity and Lemma 4.5.3 that

$$G'(w) < 0, \quad w \in (-\infty, \tilde{w}_0], \quad 0 < t_1 - \tilde{t}_1 < \varepsilon,$$

so if $0 < t_1 - \tilde{t}_1 < \varepsilon$, then G is strictly decreasing on the interval $(-\infty, \tilde{w}_0]$, and as a consequence G has at most one zero in this interval. From Lemma 4.5.4, this zero has to be on the subinterval (w_1, w_2), thus G is never zero on $(-\infty, w_1] \cup [w_2, \tilde{w}_0]$. □

Corollary 4.5.6. *Suppose $(\tilde{t}_0, \tilde{t}_1) \in \gamma_c$. There exists $\varepsilon > 0$ such that for every choice $(\tilde{t}_0, t_1) \in \mathcal{F}_2$ with $0 < t_1 - \tilde{t}_1 < \varepsilon$, the functions*

$$z \mapsto \xi_1(z) - \frac{t_1 + z^2}{3}, \quad z \mapsto \xi_2(z) - \frac{t_1 + z^2}{3},$$

do not vanish, respectively, on the intervals $(-\infty, z_2], [z_1, z_0]$.

Proof. Under the mapping $z = h(w)$, the functions

$$z \mapsto \xi_1(z) - \frac{t_1 + z^2}{3}, \quad z \in (-\infty, z_2], \qquad z \mapsto \xi_2(z) - \frac{t_1 + z^2}{3}, \quad z \in [z_1, z_0]$$

transform to

$$w \mapsto G(w), \quad w \in (-\infty, \tilde{w}_2], \qquad w \mapsto G(w), \quad w \in [\tilde{w}_1, \tilde{w}_0]$$

respectively, where we recall that $\tilde{w}_j$, $j = 1, 2$, is the simple root of $h(w) = z_j$. From (4.149) we know $(-\infty, \tilde{w}_2] \subset (-\infty, w_1], [\tilde{w}_1, \tilde{w}_0] \subset [w_2, \tilde{w}_0]$, and the result follows from Proposition 4.5.5. □

Similarly as it is done in (4.141) for $t_1 = 0$, we now define

$$h_j(x, y) = \int_x^y (\operatorname{Re} \xi_{j+}(s) - \operatorname{Re} \xi_{3+}(s)) ds, \quad x, y \in \mathbb{R}, \quad j = 1, 2, \quad (t_0, t_1) \in \mathcal{F}_2.$$

The next result is the analogous of Lemma 4.5.1 for the one-cut case, and its proof is also similar.

Lemma 4.5.7. *Suppose $(\tilde{t}_0, \tilde{t}_1) \in \gamma_c$. There exists $\varepsilon > 0$ such that for any pair $(\tilde{t}_0, t_1) \in \mathcal{F}$ with $0 < t_1 - \tilde{t}_1 < \varepsilon$, the following properties hold true.*

(i) If $x, y \in (-\infty, z_2]$, $x \neq y$, then $h_1(x, y) \neq 0$.

(ii) If $x, y \in [z_1, z_0]$, $x \neq y$, then $h_2(x, y) \neq 0$.

Proof. For simplicity, denote $J_1 = (-\infty, z_2]$, $J_2 = [z_1, z_0]$. If $h_j(x, y) = 0$ for some points $x, y \in J_j$, $x \neq y$, then there exists a point $u_0 \in J_j$ for which

$$\operatorname{Re} \xi_{j+}(u_0) = \operatorname{Re} \xi_{3+}(u_0).$$

Using the equalities in (4.130) we conclude

$$\operatorname{Re} \xi_{1+}(u_0) = \operatorname{Re} \xi_{2+}(u_0) = \operatorname{Re} \xi_{3+}(u_0).$$

According to the sheet structure constructed in Section 4.4.3.2, the function ξ_j is real on J_j and continuous across J_j, so the equality above implies

$$\operatorname{Re}\xi_{1+}(u_0) + \operatorname{Re}\xi_{2+}(u_0) + \operatorname{Re}\xi_{3+}(u_0) = 3\xi_j(u_0).$$

On the other hand, the sum $\xi_1 + \xi_2 + \xi_3$ is equal to minus the coefficient of ξ^2 in (4.24), that is,

$$\xi_j(u_0) = \frac{1}{3}(\operatorname{Re}\xi_{1+}(u_0) + \operatorname{Re}\xi_{2+}(u_0) + \operatorname{Re}\xi_{3+}(u_0)) = \frac{t_1 + u_0^2}{3}.$$

This last equality implies that the function

$$z \mapsto \xi_j(z) - \frac{t_1 + z^2}{3}$$

is zero at the point $u_0 \in J_j$, contradicting Corollary 4.5.6. □

In the same spirit as at the end of Section 4.5.2, for $(t_0, t_1) \in \mathcal{F}_2$ we introduce the quantities

$$\tau_1 = \operatorname{Re}\int_{z_2^{(3)}}^{z_1^{(3)}} Q(s)ds = \operatorname{Re}\int_{z_2}^{z_1} (\xi_1(s) - \xi_2(s))ds, \tag{4.156}$$

$$\tau_2 = \operatorname{Re}\int_{z_2^{(2)}}^{z_1^{(2)}} Q(s)ds = \operatorname{Re}\int_{z_2}^{z_1} (\xi_1(s) - \xi_3(s))ds, \tag{4.157}$$

$$\tau_3 = \operatorname{Re}\int_{z_2^{(3)}}^{\hat{z}_2^{(3)}} Q(s)ds = \operatorname{Re}\int_{z_2}^{\hat{z}_2} (\xi_1(s) - \xi_2(s))ds, \tag{4.158}$$

$$\tau_4 = \operatorname{Re}\int_{z_2^{(1)}}^{z_1^{(1)}} Q(s)ds = \operatorname{Re}\int_{z_2}^{z_1} (\xi_2(s) - \xi_3(s))ds, \tag{4.159}$$

$$\tau_5 = \operatorname{Re}\int_{z_0^{(2)}}^{\hat{z}_0^{(2)}} Q(s)ds = \operatorname{Re}\int_{z_0}^{\hat{z}_0} (\xi_1(s) - \xi_3(s))ds \tag{4.160}$$

and

$$\tau_6 = -\operatorname{Re}\int_{z_1^{(1)}}^{z_0^{(1)}} Q(s)ds = \operatorname{Re}\int_{z_1}^{z_0} (\xi_3(s) - \xi_2(s))ds. \tag{4.161}$$

The analysis of these quantities is carried over in the Section 4.11.2. The important fact for what comes later is that these quantities never vanish for $(t_0, t_1) \in \mathcal{F}_2$.

4.5.3 Quadratic differential on the spectral curve: general principles

For a point $p \in \overline{\mathbb{C}}$, recall that $p^{(j)}$ denotes its preimage under the canonical projection $\pi : \mathcal{R} \mapsto \overline{\mathbb{C}}$ that lies on the sheet $\mathcal{R}_j$. Additionally, the points $z_j, \hat{z}_j$, $j = 0, 1, 2$, are given by Theorem 4.4.1.

We use Theorem 4.4.1, equations (4.124), (4.129) and the asymptotics (4.27) to find all critical points of ϖ. For $(t_0, t_1) \in \mathcal{F}_1$ they are as follows

- Double zeros at the branch points $z_0^{(1)} = z_0^{(3)}$, $z_1^{(1)} = z_1^{(2)}$, $z_2^{(1)} = z_2^{(2)}$;
- Double zeros at $\hat{z}_0^{(2)}$, $\hat{z}_1^{(3)}$, $\hat{z}_2^{(3)}$;
- Simple zeros at $z_0^{(2)}$, $z_1^{(3)}$, $z_2^{(3)}$;
- A pole of order 5 at $\infty^{(1)}$ and a pole of order 14 at $\infty^{(2)} = \infty^{(3)}$,

whereas for $(t_0, t_1) \in \mathcal{F}_2$ the critical points are given by

- Double zeros at the branch points $z_0^{(1)} = z_0^{(3)}$, $z_1^{(1)} = z_1^{(3)}$, $z_2^{(2)} = z_2^{(3)}$;
- Double zeros at $\hat{z}_0^{(2)}$, $\hat{z}_1^{(3)}$, $\hat{z}_2^{(3)}$;
- Simple zeros at $z_0^{(2)}$, $z_1^{(2)}$, $z_2^{(1)}$;
- A pole of order 5 at $\infty^{(1)}$ and a pole of order 14 at $\infty^{(2)} = \infty^{(3)}$.

These critical points are shown in Figure 4.15. From the general theory, it is known that there are $n + 2$ trajectories emanating from a given zero of order n, and any two consecutive trajectories form an angle $2\pi/(n + 2)$ at the zero.

It is time to recall some notation that was already used in Chapter 3. From a given zero $p^{(j)} \in \mathcal{R}_j$ emanate a number of critical trajectories on $\mathcal{R}_j$, which we denote by $\gamma_0(p^{(j)}), \gamma_1(p^{(j)}), \ldots$; we make the convention that these trajectories are labeled in such a way that their canonical projections $\pi(\gamma_0(p^{(j)})), \pi(\gamma_1(p^{(j)})), \ldots$, are enumerated in the anti-clockwise direction, starting on the positive horizontal direction. This is well defined as long as there are no trajectories emanating along branch cuts, situation that will not occur. We also note that if $p^{(k)} = p^{(j)}$ is a branch point joining two sheets $\mathcal{R}_j$ and $\mathcal{R}_k$, the trajectories $\gamma_l(p^{(j)}), \gamma_l(p^{(k)})$ are different, because they emanate from different sheets. We refer the reader to Figure 4.16 for an example.

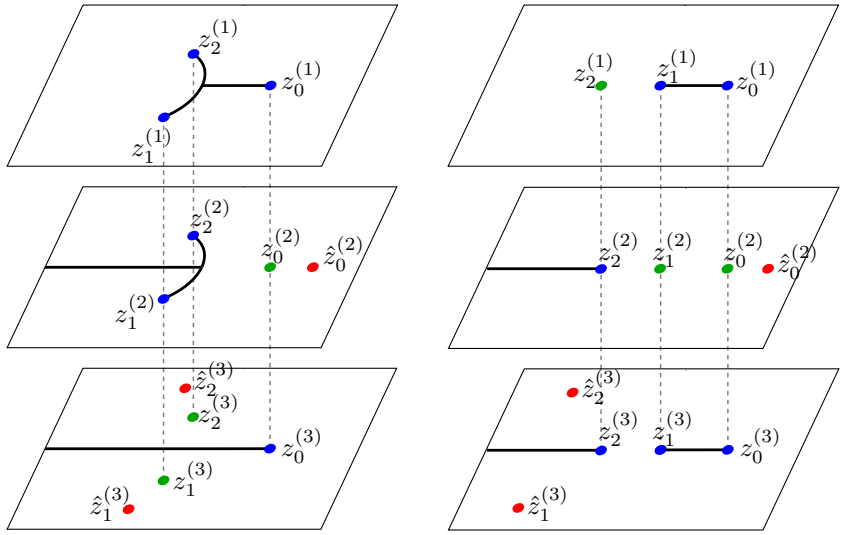

Figure 4.15: The critical points of ϖ: on the left for $(t_0, t_1) \in \mathcal{F}_1$ and on the right for $(t_0, t_1) \in \mathcal{F}_2$. Blue dots represent the zeros that are also branch points, red dots represent the remaining double zeros, and green dots represent simple zeros. In addition, there are also poles at the points at infinity.

Similar notation is adopted at the poles $\infty^{(1)}$, $\infty^{(2)} = \infty^{(3)}$. In this case, there are certain directions, henceforth called *critical directions* and denoted $\theta_0^{(k)}$, $\theta_1^{(k)}, \ldots$, along which any trajectory extending to $\infty^{(k)}$ has to do so along one of the critical directions $\theta_0^{(k)}, \theta_1^{(k)}, \ldots$. These directions are easily computed to be given by the angles

$$\theta_j^{(1)} = \frac{\pi}{3} + \frac{2\pi}{3} j, \quad j = 0, 1, 2, \qquad \theta_j^{(2)} = \theta_j^{(3)} = \frac{\pi}{6} + \frac{\pi}{3} j, \quad j = 0, \ldots, 5.$$

Note that $\mathcal{R}$ is branched at $\infty^{(2)} = \infty^{(3)}$, so in the same spirit as for finite branch points, although the numerical values for $\theta_j^{(2)}$ and $\theta_j^{(3)}$ are the same, we refer to $\theta_j^{(2)}$ as the critical direction on the sheet $\mathcal{R}_2$, whereas $\theta_j^{(3)}$ as the critical direction on the sheet $\mathcal{R}_3$.

Recall that $\pi_j : \mathcal{R}_j \to \overline{\mathbb{C}}$ denotes the restriction of the canonical projection $\pi : \mathcal{R} \to \overline{\mathbb{C}}$ to the sheet $\mathcal{R}_j$. We follow Chapter 3 and list some general principles regarding trajectories of quadratic differentials. These principles will be extensively used later on.

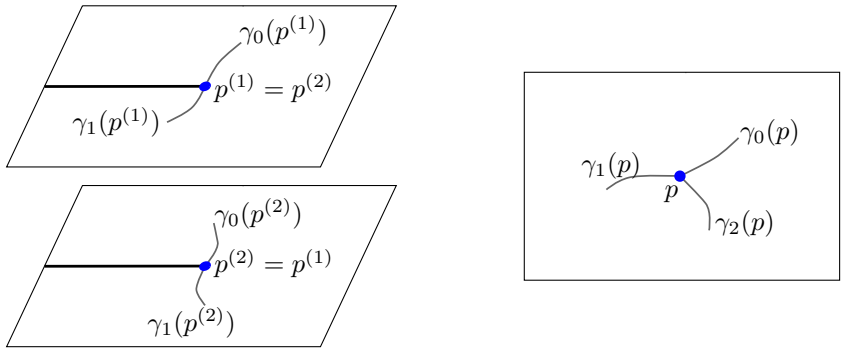

Figure 4.16: Example of critical trajectories' labeling around critical points. On the left-hand side, around the double zero $p^{(1)} = p^{(2)}$ connecting two sheets of the Riemann surface. On the right, around the simple zero p which is not a branch point.

P.1 The quadratic differential ϖ does not have recurrent trajectories, as it follows from Jenkins' Three Poles Theorem [114, Thm. 8.5, page 226]. Consequently, any trajectory γ of ϖ has a well defined limiting point along its two directions (possibly the same, in case γ is closed).

P.2 If $\gamma \subset \mathcal{R}_j$ is an arc of trajectory of ϖ, then the arc $\gamma^* = \pi_j^{-1}(\pi(\gamma)^*)$, obtained as the lift of the complex conjugate of $\pi(\gamma)$ to $\mathcal{R}_j$, is also an arc of trajectory.

P.3 If a ϖ-polygon does not have poles on its interior, then it has to have poles on its boundary. This is a consequence of (A.7).

P.4 The function Q^2 in (4.132) is analytic on the parameters (t_0, t_1). Consequently the trajectories of ϖ change continuously (in any reasonable topology) with the parameters (t_0, t_1). In our setting, it is enough to have the following observation. Choose a critical point p of ϖ, varying continuously with the parameter (t_0, t_1). Fix $(\tilde{t}_0, \tilde{t}_1)$ and assume that for small perturbations of $(\tilde{t}_0, \tilde{t}_1)$ the order of the critical point p is preserved and that a given open set $U \subset \mathcal{R}$ does not contain critical points of ϖ. If for $(\tilde{t}_0, \tilde{t}_1)$ the critical trajectory emanating from p along a given direction intersects the open set U, then the same holds true for small perturbations of $(\tilde{t}_0, \tilde{t}_1)$.

P.5 If for a given value $(\tilde{t}_0, \tilde{t}_1)$, a point p belongs to the half plane domain for the pole $\infty^{(k)}$ determined by the critical angles $\theta_j^{(k)}, \theta_{j+1}^{(k)}$, then the same holds true for parameters on a small neighborhood of $(\tilde{t}_0, \tilde{t}_1)$. The point p can depend continuously on (t_0, t_1).

P.6 If for a given value $(\tilde{t}_0, \tilde{t}_1)$, an arc of trajectory emerging from a certain point p intersects the real line at a *regular* point, then the same holds true for small perturbations of $(\tilde{t}_0, \tilde{t}_1)$. As before, the point p can depend continuously on the parameters.

When $t_1 = 0$ we will make use of one more principle, which will be enunciated in Section 4.5.4.

4.5.4 Critical graph in the three-cut case

This section is devoted to the description of the critical graph in the three-cut case $(t_0, t_1) \in \mathcal{F}_1$. We will use extensively the principle **P.1** without further mention. More precisely, in our situation this principle assures us that every trajectory has a limiting endpoint in its both directions, and our goal will be to, starting at a given critical trajectory emanating from a critical point, find its other endpoint.

4.5.4.1 Critical graph for $t_1 = 0$

We first describe the critical graph for $t_1 = 0$. To this end, we use the sheet structure in (4.135).

For $t_1 = 0$, the algebraic equation (4.24) is invariant under the action

$$(\xi, z) \mapsto (\omega^2 \xi, \omega z),$$

where we recall that $\omega = e^{2\pi i/3}$. With regard to the sheet structure (4.135), this discrete rotational symmetry is reflected on the trajectories of ϖ, and it leads to the following principle.

P.7 Suppose $t_1 = 0$. If $\gamma \subset \widetilde{\mathcal{R}}_j$ is an arc of trajectory, then the arc $\tilde{\gamma} = \pi_j^{-1}(\omega\pi(\gamma))$, obtained as the lift of $\omega\pi(\gamma)$ to $\widetilde{\mathcal{R}}_j$, is also an arc of trajectory.

Some of the trajectories of ϖ are straightforward to describe. On the interval $(-\infty, 0)$, the solutions ξ_2 and ξ_3 are complex conjugate of each other (see (4.140)), and the same is true for ξ_1 and ξ_2 on $(0, z_0)$ (see (4.139)). It thus follows from the definition of a trajectory in (4.133) that

$$\gamma_1(z_0^{(3)}) = \pi_1^{-1}((-\infty, 0]) \cup \pi_3^{-1}([0, z_0]), \tag{4.162}$$

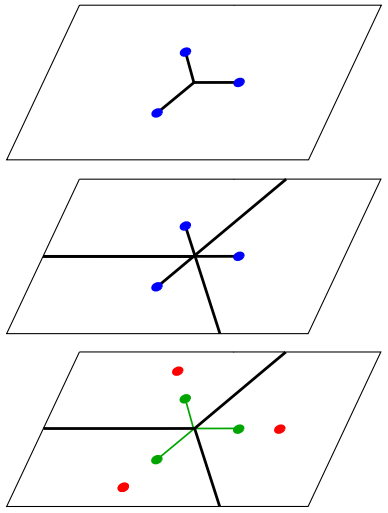

Figure 4.17: In thin lines the trivial trajectories of ϖ in the large are depicted; these are the trajectories described by equations (4.162)–(4.162). In thick lines the branch cuts for the Riemann surface.

that is, the trajectory $\gamma_1(z_0^{(3)})$ starts to the left of $z_0^{(3)}$, moves to the sheet $\widetilde{\mathcal{R}}_1$ and goes to $\infty^{(1)}$ along the negative axis. Using the principle **P.7**, we also get the trajectories $\gamma_0(z_1^{(3)})$ and $\gamma_2(z_2^{(3)})$. These are depicted in Figure 4.17.

We now focus on the trajectory $\gamma_0(z_0^{(1)})$.

Lemma 4.5.8. *The trajectory $\gamma_0(z_0^{(1)})$ goes to $\infty^{(1)}$ with angle $\theta_0^{(1)}$ and it is entirely contained in $\widetilde{\mathcal{R}}_1$*

Proof. We first claim that the trajectory $\gamma_0(z_0^{(1)})$ cannot intersect the interval $\pi_1^{-1}((z_0, +\infty))$. Indeed, to the contrary we use the principle **P.2** to get the equality $\gamma_0(z_0^{(1)}) = \gamma_1(z_0^{(1)})$. In particular, this implies that $\gamma_0(z_0^{(1)})$ is the boundary of a ϖ-polygon without poles on its closure, contradicting **P.3**.

The trajectory $\gamma_0(z_0^{(1)})$ cannot intersect the interval $\pi_{1+}^{-1}([0, z_0])$ neither. To see this, suppose it does, say at a point which projects to $x_0 \in [0, z_0]$. It then follows from (4.133) and the definition of ϖ (4.132) that

$$\operatorname{Re}\int_{x_0}^{z_0}(\xi_2(z)-\xi_3(z))dz = \int_{x_0}^{z_0}(\operatorname{Re}\xi_{2+}(x)-\operatorname{Re}\xi_{3+}(x))dx = 0, \qquad (4.163)$$

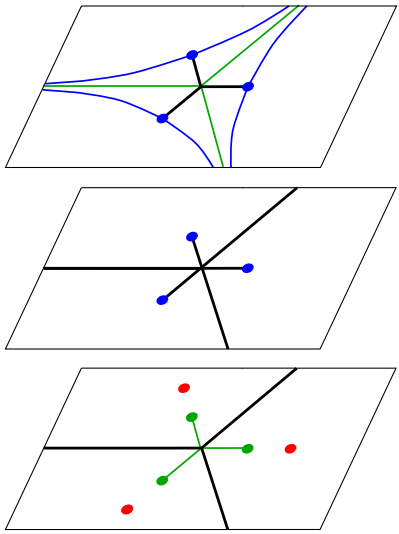

Figure 4.18: Trajectories of ϖ in the large after equations (4.162)–(4.162) and Lemma 4.5.8.

where the first integral is computed along $\pi(\gamma_0(z_0^{(1)}))$, and the second integral, obtained after deformation of the contour for the first one, is performed on $\mathbb{R}$. This is the same as saying that $h_2(x_0, z_0) = 0$, contradicting Lemma 4.5.1 (i).

In summary, we proved that the trajectory $\gamma_0(z_0^{(1)})$ does not intersect the arc $\pi_1^{-1}([0, +\infty))$. Since it cannot intersect the segment $\pi_1^{-1}([0, \infty e^{\pi i/3})$, because this is an arc of the trajectory $\gamma_0(z_1^{(3)}))$, the only possibility left is that it goes to $\infty^{(1)}$ with angle $\theta_0^{(1)}$, as we want. □

Using the principles **P.2** and **P.7**, we also get the behavior of the trajectories $\gamma_1(z_0^{(1)})$, $\gamma_j(z_k^{(1)})$, $k = 1, 2$, $j = 0, 1$. The outcome we have so far is displayed in Figure 4.18.

Recall that L_0, L_1 and L_2 denote the segments connecting the sheets $\widetilde{\mathcal{R}}_2$ and $\widetilde{\mathcal{R}}_3$ (see (4.134)).

Lemma 4.5.9. *The trajectory $\gamma_0(z_0^{(3)})$, intersects the cut L_2 exactly once, moves to the sheet $\widetilde{\mathcal{R}}_2$ and then extends to $\infty^{(2)}$ along the critical angle $\theta_1^{(2)}$.*

Proof. We first prove that $\gamma_0(z_0^{(3)})$ moves to $\widetilde{\mathcal{R}}_2$.

The trajectory $\gamma_0(z_0^{(3)})$ cannot intersect $\pi_3^{-1}([z_0,+\infty))$, otherwise the principle **P.2** tells us that $\gamma_0(z_0^{(3)}) = \gamma_2(z_0^{(3)})$, and this trajectory then determines a ϖ-polygon without poles on its closure, contradicting the principle **P.3**. So if we assume it does not move to $\widetilde{\mathcal{R}}_2$, it has to extend to $\infty^{(3)}$ with angle $\theta_0^{(3)}$, and as a consequence of the principle **P.2** we further get that $\gamma_2(z_0^{(3)})$ ends up at $\infty^{(3)}$ with angle $\theta_3^{(5)}$. We then apply Teichmüller's formula (A.7) to the ϖ-polygon determined by these two trajectories that contains $\hat{z}_0^{(3)}$. On the boundary there are two critical points, namely $z_0^{(3)}$ and $\infty^{(3)}$, and the sum on the left hand side of (A.7) is equal to 2. On the interior, there is only the double zero $\hat{z}_0^{(3)}$, so the sum on the right hand side of (A.7) is 4, a contradiction.

It is a conclusion of the last paragraph that the trajectory $\gamma_0(z_0^{(3)})$ goes to $\widetilde{\mathcal{R}}_2$. Combining **P.2** and **P.7**, we further get that the trajectories $\gamma_2(z_0^{(3)}), \gamma_j(z_1^{(3)})$ and $\gamma_{j-1}(z_2^{(3)})$ also move to $\widetilde{\mathcal{R}}_2$, $j = 1, 2$.

We now prove that $\gamma_0(z_0^{(3)})$ intersects L_2 exactly once. Again in virtue of the principles **P.2** and **P.7**, it is enough to verify that $\gamma_1(z_2^{(3)})$ intersects L_0 exactly once.

We already showed that $\gamma_1(z_2^{(3)})$ intersects L_0 at least once, say at a point projecting to $x \in (-\infty, 0)$. Suppose now that $\gamma_1(z_2^{(3)})$ intersects L_0 at another point, say projecting to $y \in (-\infty, 0)$. For simplicity, assume $x < y$, the case $x > y$ is analogous. Proceeding as in (4.163), we conclude that

$$h(x, y) = h(y, 0) = 0.$$

From Lemma 4.5.1 (ii), we learn that $(x, y) \cap (y, 0) \neq \emptyset$, which is certainly not true. We also remark that a combination of the principles **P.2** and **P.7** yield that $\gamma_0(z_2^{(3)})$ intersects the cut L_2 exactly once.

As a final step, we prove that $\gamma_0(z_0^{(3)})$ extends to $\infty^{(2)}$ with critical angle $\theta_1^{(2)}$. Again due to **P.2** and **P.7**, it is enough to prove that $\gamma_0(z_2^{(3)})$ extends to $\infty^{(2)}$ with angle $\theta_1^{(2)}$. The latter fact follows if we prove that $\gamma_0(z_2^{(3)})$ stays in the sector of $\widetilde{\mathcal{R}}_2$ determined by the positive real axis and L_2. Since we already noticed that $\gamma_0(z_2^{(3)})$ intersects L_0 exactly once and then enters this sector, it is enough to verify that $\gamma_0(z_2^{(3)})$ does not intersect the positive real axis on $\widetilde{\mathcal{R}}_2$.

Suppose the latter happens, say at a certain point projecting to $x \in [0, \infty)$. There are two possibilities, namely either $0 \leq x \leq z_0$ or $x > z_0$.

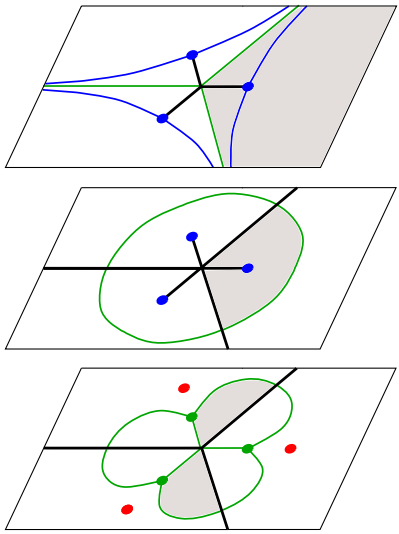

Figure 4.19: Figure for the hypothetical situation considered in the proof of Lemma 4.5.9. The shaded region is the ϖ-polygon contradicting Teichmüller's formula (A.7).

For the first situation, we note that in this case the integral

$$\int_{0^{(3)}}^{x^{(2)}} Q(s)ds,$$

computed along the contour $\gamma_2(z_2^{(3)}) \cup \gamma_0(z_2^{(3)})$, is purely imaginary. Deforming this integral to the interval $\pi_{2+}^{-1}([0,x])$ we conclude

$$\int_0^x (\operatorname{Re}\xi_{1+}(s) - \operatorname{Re}\xi_{3+}(s))ds = 0,$$

and the equation above contradicts Lemma 4.5.1 (i).

Now let us assume that $x > z_0$. Using **P.2**, this assumption implies that $\gamma_0(z_2^{(3)}) = \gamma_2(z_1^{(3)})$. The trajectories $\gamma_2(z_2^{(3)})$, $\gamma_0(z_2^{(3)})$, $\gamma_2(z_1^{(3)})$ then determine a ϖ-polygon whose only critical point in its interior is the double zero $z_0^{(1)} = z_0^{(2)}$ (this is the shaded domain in Figure 4.19). The right hand side of (A.7) is then 4, whereas the left hand side is 2, which is a contradiction. □

Again after an application of the principles **P.2** and **P.7**, we get the partial configuration in Figure 4.20.

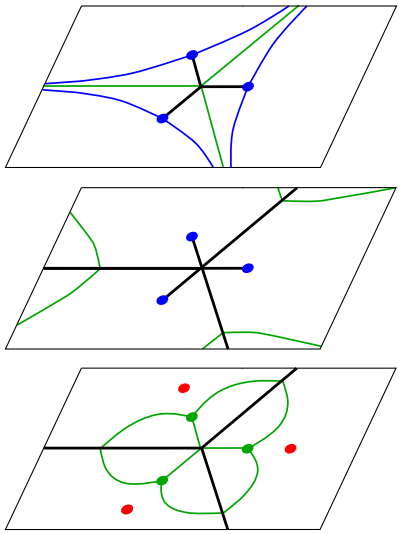

Figure 4.20: Trajectories of ϖ in the large after Lemma 4.5.9. Compare with the previous stage in Figure 4.18

Lemma 4.5.10. *The trajectories $\gamma_0(z_0^{(2)})$ and $\gamma_1(z_0^{(2)})$ extend to $\infty^{(2)}$ along critical angles $\theta_0^{(2)}$ and $\theta_5^{(2)}$, respectively.*

Proof. The trajectory $\gamma_0(z_0^{(2)})$ cannot intersect $\pi_{2+}^{-1}([0,z_0])$ neither. Otherwise, if it does so at a point $x_+^{(2)}$, then

$$0=\int_0^{x_+^{(2)}} Q(s)ds=\int_0^{x}(\operatorname{Re}\xi_{2+}(s)-\operatorname{Re}\xi_{3+}(s))ds,$$

where for the first integral we integrate over $\gamma_0(z_0^{(2)})$, and then we deform this contour of integration to the real line to get the second equality. Since $x\in(0,z_0]$, this is in contradiction with Lemma 4.5.1 (i).

Having in mind **P.2**, a consequence of the discussion above is that the trajectories $\gamma_0(z_0^{(2)})$ and $\gamma_1(z_0^{(2)})$ have to stay in the region on $\widetilde{\mathcal{R}}_2\cup\widetilde{\mathcal{R}}_3$ determined by the contour $\gamma_0(z_2^{(3)})\cup\gamma_2(z_2^{(3)})\cup\gamma_0(z_1^{(3)})\cup\gamma_2(z_1^{(3)})$. Additionally, the trajectory $\gamma_0(z_0^{(2)})$ cannot intersect $\pi_2^{-1}([z_0,\infty))$, otherwise using **P.2** we conclude that $\gamma_0(z_0^{(2)})=\gamma_1(z_0^{(2)})$, and this trajectory then determines a ϖ-polygon without poles on its closure, contradicting **P.3**. The only possibility left is the description claimed by the Lemma. □

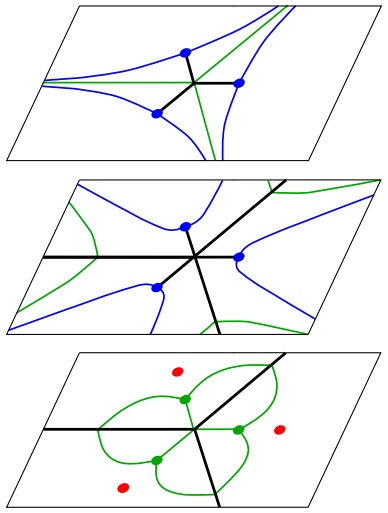

Figure 4.21: Trajectories of ϖ in the large after Lemma 4.5.10. Compare with the previous stage in Figure 4.20.

Again using **P.2** and **P.7**, we translate the previous Lemma to the trajectories emanating from $z_1^{(2)}$, $z_2^{(2)}$. The outcome is displayed in Figure 4.21.

Lemma 4.5.11. *The trajectory $\gamma_0(\hat{z}_0^{(3)})$ never leaves $\widetilde{\mathcal{R}}_3$ and extends to $\infty^{(3)}$ with critical angle $\theta_0^{(3)}$. The trajectory $\gamma_1(\hat{z}_0^{(3)})$ intersects the cut L_0 on $\widetilde{\mathcal{R}}_3$ exactly once, moves to the sheet $\widetilde{\mathcal{R}}_2$ and extends to $\infty^{(2)}$ along the critical direction $\theta_1^{(2)}$.*

Proof. An integral deformation argument similar to the one presented in the proof of Lemma 4.5.9 shows that any contour of the form $\gamma_k(\hat{z}_0^{(3)}) \cup \gamma_j(\hat{z}_0^{(3)})$, $j, k \in \{1, 2, 3, 4\}$, $j \neq k$, intersects each of the cuts L_0 and L_2 at most once. Moreover, these contours cannot be bounded closed loops in $\widetilde{\mathcal{R}}_3$, otherwise we would get a contradiction to **P.3**.

There are two critical directions in the sector $-\frac{\pi}{3} < \arg z < \frac{\pi}{3}$ in $\widetilde{\mathcal{R}}_3$, namely $\theta_0^{(3)}$ and $\theta_5^{(3)}$, so from the local behavior of trajectories near the pole $\infty^{(3)}$ we know that at most two trajectories from $\hat{z}_0^{(3)}$ can extend to $\infty^{(3)}$.

Combining the last two paragraphs, the only possibility left is that $\gamma_0(\hat{z}_0^{(3)})$ and $\gamma_3(\hat{z}_0^{(3)})$ stay in $\widetilde{\mathcal{R}}_3$ and go to $\infty^{(3)}$ along the critical directions $\theta_0^{(3)}$ and $\theta_5^{(3)}$,

respectively, and the trajectories $\gamma_1(\hat{z}_2^{(3)})$ and $\gamma_2(\hat{z}_2^{(3)})$ intersect the cuts L_0 and L_2, respectively, and move to $\widetilde{\mathcal{R}}_2$.

Consequently, we use **P.2** and **P.7** to get that $\gamma_1(\hat{z}_1^{(3)})$ has to intersect the branch cut L_0 on $\widetilde{\mathcal{R}}_3$ and move to the sheet $\widetilde{\mathcal{R}}_3$. Similarly as before, we also get that $\gamma_1(\hat{z}_1^{(3)})$ intersects L_0 at exactly one point. Indeed, due to the constrained geometry we have, this trajectory has to end up at a critical point on $\widetilde{\mathcal{R}}_1 \cup \widetilde{\mathcal{R}}_2$. Hence it has to cross L_0 an odd number of times. If $x_1 < y_1$ are any two points of intersection of $\gamma_1(\hat{z}_1^{(3)})$, we get $h(x_1, y_1) = 0$, as it follows from deformation of integrals as we did above. From Lemma 4.5.1 *(ii)* we then conclude that there can be at most two of such points x_1, y_1. Since the number of intersections is odd, we conclude that actually there is exactly one intersection point.

Using again **P.2** and **P.7**, we translate the outcome of the previous paragraph to the trajectory $\gamma_0(\hat{z}_0^{(3)})$, concluding that it intersects L_2 exactly once, and thus it has to stay in $\widetilde{\mathcal{R}}_2$. Consequently, the only possibility left for its behavior in the large is that it has to extend to $\infty^{(2)}$ along the critical direction $\theta_1^{(2)}$, concluding the proof. □

Using the principles **P.2** and **P.7**, it is straightforward to get from Lemma 4.5.11 the behavior of the trajectories emanating from the double zeros $\hat{z}_j^{(3)}$, $j = 0, 1, 2$, hence concluding the description of the critical graph of ϖ for $t_1 = 0$, as can be seen in Figure 4.22. For later convenience, we also reverse the regluing $\widetilde{\mathcal{R}}_j \mapsto \mathcal{R}_j$, and the result is also displayed in Figure 4.22.

4.5.4.2 Planar realization of the critical graph for $t_1 = 0$

A planar realization of $\mathcal{G}$ for $t_1 = 0$ can be seen in Figure 4.23. It consists of a rectangle whose top and bottom are identified, and whose left and right rims correspond, respectively, to the poles $\infty^{(2)} = \infty^{(3)}$ and $\infty^{(1)}$. On each of these rims, there are a number of marked points, corresponding to the critical directions at the respective poles.

From its planar realization, it is easy to identify the strip and end domains of $\mathcal{G}$. We denote the strip domains by $\mathcal{S}_j$, $j = 1, \cdots, 9$, labeling them according to Figure 4.23.

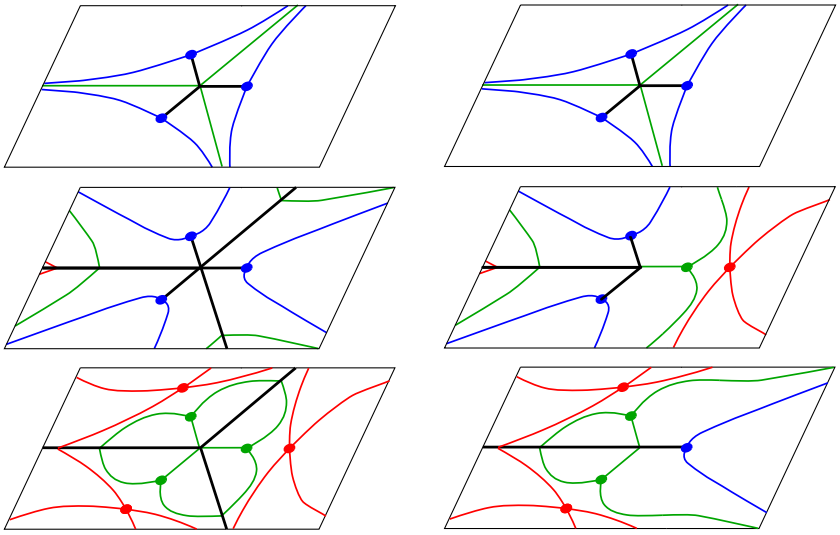

Figure 4.22: Critical graph of ϖ for $t_1 = 0$ before (left) and after (right) the regluing $\widetilde{\mathcal{R}} \mapsto \mathcal{R}$.

4.5.4.3 Deformation of the critical graph in the three-cut case

We now prove that the critical graph depicted in Figure 4.23 is always valid in the three-cut case, that is, for $(t_0, t_1) \in \mathcal{F}_1$. According to the principle **P.4**, this is the case as long as

(i) Existing zeros of ϖ do not coalesce and there are no new zeros appearing. This is the case as the discussion at the beginning of Section 4.5.3 assures us.

(ii) No new domains appear. Taking into account (i) above, this can only happen if a short trajectory changes its behavior. Since we do not have short trajectories for $t_1 = 0$, we are safe.

(iii) The existing strip domains do not shrink. This amounts to showing that their widths do not vanish. For $j = 1, \ldots, 5$, the identity $\sigma(\mathcal{S}_j) = |\tau_j|$ follows directly from (A.6) and the definition of τ_j given in (4.143)–(4.147). Consequently, $\sigma(\mathcal{S}_j) \neq 0$ for $j = 1, \cdots, 5$ and $(t_0, t_1) \in \mathcal{F}_1$. Moreover, the symmetry under conjugation shows that $\sigma(\mathcal{S}_j) = \sigma(\mathcal{S}_{j-5})$ for $j = 6, \ldots, 9$, thus $\sigma(\mathcal{S}_j) \neq 0$ for $j = 6, \ldots, 9$ as well.

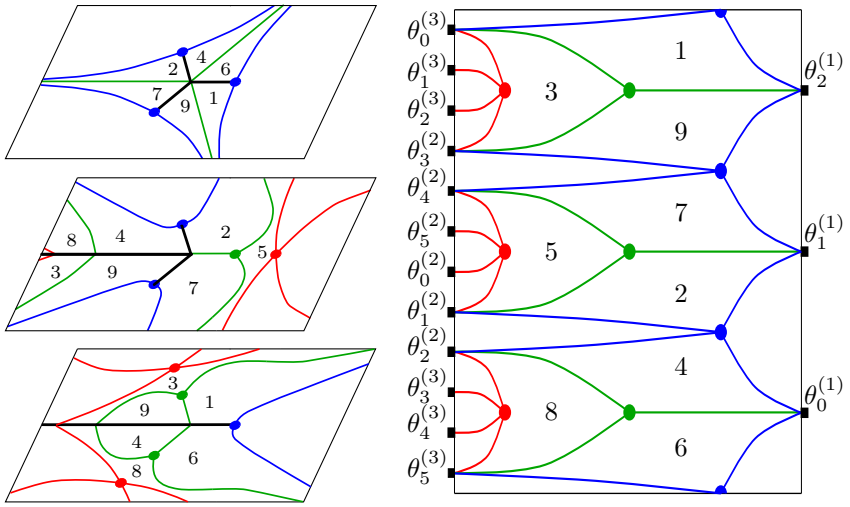

Figure 4.23: On the left panel the critical graph of ϖ in the three-cut case is displayed, and on the right panel its planar realization. The marked black dots on the rims of the rectangle correspond to the critical directions at the poles $\infty^{(1)}$ (right rim) and $\infty^{(2)} = \infty^{(3)}$ (left rim). In both pictures, the number j indicates the strip domain $\mathcal{S}_j$.

The considerations (i)–(iii) above hence show that the critical graph displayed in Figure 4.23 is valid for every choice $(t_0, t_1) \in \mathcal{F}_1$.

4.5.5 Critical graph in the one-cut case

We now describe the critical graph in the one-cut case $(t_0, t_1) \in \mathcal{F}_2$. We first describe the critical graph of ϖ for values of the parameter $(t_0, t_1) \in \mathcal{F}_2$ that are close to the critical curve γ_c and then prove that the topology of the critical graph remains unchanged when we deform the parameters (t_0, t_1) within $\mathcal{F}_2$.

4.5.5.1 Critical graph in the one-cut case - short range

When (t_0, t_1) approaches the critical curve $\in \gamma_c$ from $\mathcal{F}_1$, the critical points $z_1^{(j)}$ and $z_2^{(j)}$, $j = 1, 2$, of ϖ coalesce, thus the behavior of the critical trajectories emanating from these points can possibly (in fact, will) change. Choosing (t_0, t_1) sufficiently close to γ_c, the remaining trajectories emanating from the critical points $z_0^{(1)}$, $z_0^{(2)}$, $\hat{z}_0^{(2)}$, $\hat{z}_1^{(3)}$, $\hat{z}_2^{(3)}$ inherit their behavior already described

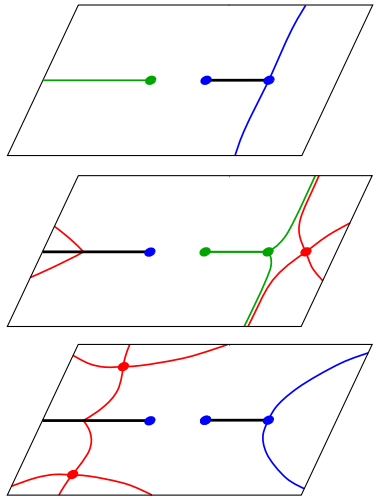

Figure 4.24: Trajectories that are preserved in the one-cut case when (t_0, t_1) is close to γ_c.

for parameters on $\mathcal{F}_1$. This is true because when we approach γ_c from $\mathcal{F}_1$, each of such trajectories do not coalesce with other zeros of ϖ, and from principle **P.4** they have to preserve their behavior.

Taking into account the relations in the last two equations in (4.130), we get

$$\gamma_1(z_2^{(1)}) = \pi_1^{-1}((-\infty, z_2]), \quad \gamma_1(z_0^{(2)}) = \pi_2^{-1}([z_1, z_0]) = \gamma_0(z_1^{(2)}),$$

so the starting configuration is the one displayed on Figure 4.24, which at this moment we know it is valid whenever $(t_0, t_1) \in \mathcal{F}_2$ is chosen sufficiently close to γ_c.

Lemma 4.5.12. *The trajectories $\gamma_0(z_1^{(1)}), \gamma_1(z_1^{(1)}), \gamma_0(z_1^{(3)})$ and $\gamma_1(z_1^{(3)})$ do not cross the branch cut $[z_1, z_0]$ connecting $\mathcal{R}_1$ and $\mathcal{R}_3$.*

The trajectories $\gamma_0(z_2^{(2)}), \gamma_1(z_2^{(2)}), \gamma_0(z_2^{(3)})$ and $\gamma_1(z_2^{(3)})$ do not cross the branch cut $(-\infty, z_2]$ connecting $\mathcal{R}_2$ and $\mathcal{R}_3$.

Proof. We deal with $\gamma_0(z_1^{(1)})$. The result for the remaining trajectories follow analogously.

Suppose $\gamma_0(z_1^{(1)})$ crosses the branch cut $[z_1, z_0]$ at a point projecting to x_0. Deforming the integral over $\gamma_0(z_1^{(1)})$ to the real line, we conclude

$$h_2(z_1, x_0) = \int_{z_1}^{x_0} \mathrm{Re}(\xi_2(x) - \xi_{3+}(x))dx = 0,$$

but this cannot occur, as it follows from Lemma 4.5.7 (ii) and our assumption that (t_0, t_1) is sufficiently close to γ_c. □

Lemma 4.5.13. *The trajectories $\gamma_0(z_1^{(1)})$ and $\gamma_0(z_2^{(1)})$ extend to $\infty^{(1)}$ along the critical angle $\theta_0^{(1)}$.*

The trajectories $\gamma_1(z_1^{(1)})$ and $\gamma_2(z_2^{(1)})$ extend to $\infty^{(1)}$ along the critical angle $\theta_2^{(1)}$.

Proof. From Lemma 4.5.12, we know that $\gamma_0(z_1^{(1)})$ must stay on the sheet $\mathcal{R}_1$, so either $\gamma_0(z_1^{(1)})$ intersects $\pi_1^{-1}([z_2, z_1])$ or it goes to $\infty^{(1)}$. If the former occurs, then we use **P.2** to get that $\gamma_0(z_1^{(1)}) = \gamma_3(z_1^{(1)})$, and consequently it determines a bounded ϖ polygon without poles on its closure, contradicting **P.3**. Hence we conclude that $\gamma_0(z_1^{(1)})$ extends to $\infty^{(1)}$, either along $\theta_0^{(1)}$ or $\theta_1^{(1)}$.

Consequently, the conclusion above forces $\gamma_0(z_2^{(1)})$ to stay in $\mathcal{R}_1$, so it also has to go to $\infty^{(1)}$ either along $\theta_0^{(1)}$ or $\theta_1^{(1)}$. We then apply (A.7) to the ϖ-polygon $D \subset \mathcal{R}_1$ determined by the trajectories $\gamma_0(z_2^{(1)})$ and $\gamma_1(z_2^{(1)})$. There are no critical points on D, so the right-hand side of (A.7) is equal to 2. Moreover, a simple computation shows that $\beta(z_2^{(1)}) = 0$, so

$$\beta(\infty^{(1)}) = 2 - \beta(z_2^{(1)}) = 2,$$

and then $\theta(\infty^{(1)}, D) = \frac{\pi}{3}$. Consequently, $\gamma_0(z_2^{(1)})$ extends to $\infty^{(1)}$ along $\theta^{(1)}$, and the same has to hold for $\gamma_0(z_1^{(1)})$.

Finally, we get the behavior of the trajectories $\gamma_1(z_1^{(1)})$ and $\gamma_2(z_2^{(1)})$ by simply applying the principle **P.2**. □

Very similar arguments as for the previous proof also work to describe the behavior of the trajectories emanating from $z_1^{(j)}$, $z_2^{(j)}$, $j = 2, 3$. We skip the details.

The final outcome is the critical graph displayed in Figure 4.25, where we remind the reader that we are assuming $(t_0, t_1) \in \mathcal{F}_2$ is sufficiently close to the critical curve γ_c. In this figure, the planar version of the critical graph (as

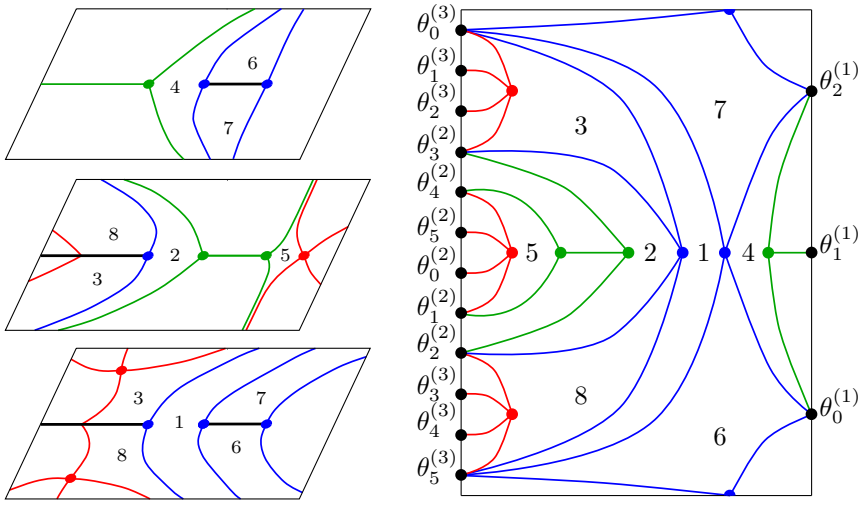

Figure 4.25: On the left the critical graph of ϖ for $(t_0, t_1) \in \mathcal{F}_2$, and on the right its planar realization. The marked black dots on the rims of the rectangle correspond to the critical directions at the poles $\infty^{(1)}$ (right rim) and $\infty^{(2)} = \infty^{(3)}$ (left rim). In both pictures, the number j indicates the strip domain $\mathcal{S}_j$.

explained in Section 4.5.4.2) is also displayed. We denote the strip domains by $\mathcal{S}_j$, $j = 1, \dots, 8$, labeled as displayed in Figure 4.25.

4.5.5.2 Deformation of the critical graph in the one-cut case

We now prove that the critical displayed in Figure 4.25 is always valid in the one-cut case, that is, for the whole range $(t_0, t_1) \in \mathcal{R}_2$. Similarly as in Section 4.5.4.3, we use the principle **P.4** to conclude that this is the case as long as

(i) The order of every critical point of ϖ is preserved and no new critical points appear. This is indeed the case, as discussed at the beginning of Section 4.5.3.

(ii) No new domains appear. Taking into account (i) above, this can only occur if a short trajectory changes its behavior. In the present situation, the only critical trajectory is $\gamma_0(z_1^{(2)}) = \gamma_2(z_0^{(2)})$, which lives on the real line, so from principle **P.2** it is clear that this trajectory does not change its behavior.

(iii) The strip domains do not shrink. As before, it is enough to verify that the widths $\sigma(\mathcal{S}_j)$, $j = 1, \dots, 8$, do not vanish for $(t_0, t_1) \in \mathcal{F}_2$. For $j = 1, \dots, 6$, these are given by $\sigma(\mathcal{S}_j) = |\tau_j|$, where τ_j is as in (4.156)–(4.161), so they do not vanish. Due to the symmetry under conjugation, the remaining widths satisfy $\sigma(\mathcal{S}_j) = \sigma(\mathcal{S}_{j-6})$, $j = 7, 8$, so these do not vanish as well.

From (i)–(iii) above, we finally conclude that the critical graph depicted in Figure 4.25 is valid for $(t_0, t_1) \in \mathcal{R}_2$.

4.6 The mother body measure. Proofs of Theorems 4.2.3, 4.2.4, 4.2.9 and 4.2.10

In Section 4.4.3 the Riemann surface $\mathcal{R}$ was constructed as a three-sheeted cover of $\overline{\mathbb{C}}$ with sheets $\mathcal{R}_1$, $\mathcal{R}_2$, $\mathcal{R}_3$. Up to this moment, the cut γ_0 used in the construction of $\mathcal{R}_1$ and $\mathcal{R}_2$ in the three-cut case (carried out in Section 4.4.3.1) was quite arbitrary, but in what follows it is important to choose it in an optimal way.

From the analysis of the quadratic differential carried over in Section 4.5.4 (see in particular Figure 4.23), we know that the arc of trajectory $\gamma_0(z_1^{(3)}) \cap \mathcal{R}_3$ connects $z_1^{(3)}$ to a point $z_*^{(3)}$, where $z_* \in (-\infty, z_0)$. We then define $\Sigma_{*,1}$ to be the contour on the complex plane obtained by the projection of this arc of trajectory, that is,

$$\Sigma_{*,1} = \pi\left(\gamma_0(z_1^{(3)}) \cap \mathcal{R}_3\right). \tag{4.164}$$

In this way $\Sigma_{*,1}$ is an arc with endpoints z_1 and z_*, and it is contained on the lower half plane. We additionally set

$$\Sigma_{*,2} = (\Sigma_{*,1})^* = \pi\left(\gamma_2(z_2^{(3)}) \cap \mathcal{R}_3\right), \tag{4.165}$$

so that $\Sigma_{*,2}$ is an arc with endpoints z_2 and z_* that is contained on the upper half plane. Furthermore, denote

$$\Sigma_{*,0} = [z_*, z_0], \tag{4.166}$$

where z_* is the point of intersection of $\Sigma_{*,1}$ with the real axis as above.

Following the construction carried out in Section 4.4.3.1, we then set

$$\gamma_0 = \Sigma_{*,1} \cup \Sigma_{*,2}$$

and

$$\Sigma_* = \Sigma_{*,0} \cup \Sigma_{*,1} \cup \Sigma_{*,2} \tag{4.167}$$

so that the cut for the sheet $\mathcal{R}_1$ is simply given by

$$\gamma_0 \cup [z_*, z_0] = \Sigma_*.$$

Note also that with this sheet structure, we can further characterize the interval $\Sigma_{*,0}$ by

$$\Sigma_{*,0} = \pi\left(\gamma_1(z_0^{(2)}) \cap \mathcal{R}_2\right).$$

For the rest of this chapter, whenever we refer to the sheet structure $\mathcal{R}_1 \cup \mathcal{R}_2 \cup \mathcal{R}_3$ for $\mathcal{R}$ in the three-cut case, we always assume the cut used in the sheet $\mathcal{R}_1$ to be given by Σ_* as in (4.167). Furthermore, we orient the arcs of Σ_* outwards, that is, $\Sigma_{*,j}$ is oriented from z_* to z_j, $j = 0, 1, 2$.

In the one-cut case, we keep denoting

$$\Sigma_* = [z_1, z_0].$$

In this case it follows from the analysis in Section 4.5.5 that Σ_* can be alternatively expressed through the identity

$$\Sigma_* = \pi\left(\gamma_0(z_1^{(2)})\right) = \pi\left(\gamma_1(z_0^{(2)})\right), \tag{4.168}$$

see in particular Figure 4.25.

Theorem 4.2.5 assures us that the function $w \mapsto h(w)$ is a conformal map from $\overline{\mathbb{C}}$ to $\mathcal{R}$. Standard arguments on conformal mappings allow us to recover the inverse image of each of the sheets $\mathcal{R}_1$, $\mathcal{R}_2$ and $\mathcal{R}_3$ under h. The outcome can be seen in Figure 4.26.

With these definitions, the set Σ_* satisfies all the geometric properties claimed by Theorem 4.2.9, except that we still have to prove the inclusion (4.36). Furthermore, the function ξ_1 in (4.27) admits a meromorphic continuation (that we keep denoting by ξ_1) to the whole sheet $\mathcal{R}_1 = \overline{\mathbb{C}} \setminus \Sigma_*$.

Recalling (4.92) *et seq.*, we also know that the function germ ξ_1 in (4.27) admits another meromorphic continuation S to a neighborhood G of $\overline{\mathbb{C}} \setminus \Omega$, which is also the Schwarz function of Ω. However, we emphasize that we do not know yet whether (4.36) is valid, and consequently we cannot be sure if $\xi_1 \equiv S$ in a full neighborhood of $\overline{\mathbb{C}} \setminus \Omega$.

Hence, for a moment we reserve the notation S for the meromorphic continuation of ξ_1 as the Schwarz function as above, and we use ξ_1 to denote the solution to (4.24) that is meromorphic in $\overline{\mathbb{C}} \setminus \Sigma_*$. Once we obtain (4.36), we can then conclude that these two meromorphic continuations coincide in a full neighborhood of $\overline{\mathbb{C}} \setminus \Omega$.

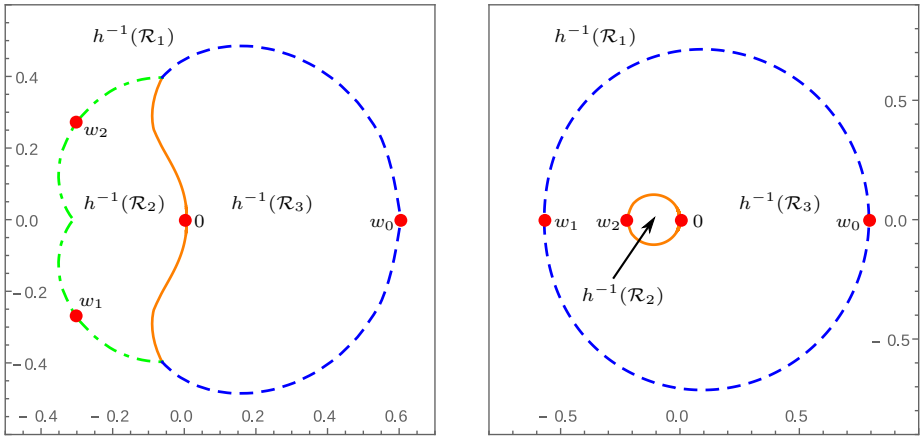

Figure 4.26: The partition of the w-plane into the inverse images of the sheets $\mathcal{R}_1$, $\mathcal{R}_2$ and $\mathcal{R}_3$ under the conformal map h. The dots are the points w_0, w_1, w_2 and 0, which are the inverse images of the branch points z_0, z_1, z_2 and $\infty^{(2)}$, respectively. In the left panel the three-cut case $\mathcal{F}_1$ is considered: the dashed line is the inverse image of the cut $\Sigma_{*,0}$ connecting $\mathcal{R}_1$ and $\mathcal{R}_3$, the dot-dashed line is the inverse image of the cut $\Sigma_{*,1} \cup \Sigma_{*,2}$ connecting $\mathcal{R}_1$ and $\mathcal{R}_2$ and the solid line is the inverse image of the cut $(-\infty, z_*)$ connecting $\mathcal{R}_2$ and $\mathcal{R}_3$. In the right panel the one-cut case $\mathcal{F}_2$ is considered: the dashed line is the inverse image of the cut (z_1, z_0) connecting $\mathcal{R}_1$ and $\mathcal{R}_3$ and the solid line is the inverse image of the cut $(-\infty, z_2)$ connecting $\mathcal{R}_2$ and $\mathcal{R}_3$. Numerical output for the choices $r = 1/20$ and $a_0 = 1/10$ (three-cut) and $a_0 = 1/4$ (one-cut).

Proof of Theorem 4.2.9. We now prove all the conclusions of Theorem 4.2.9, except for the inclusion (4.36).

From the construction of the set Σ_* as above, it follows that ξ_1 is meromorphic on $\overline{\mathbb{C}} \setminus \Sigma_*$, with pole only at ∞. Hence ξ_1 is analytic in $\mathbb{C} \setminus \Sigma_*$.

Suppose first that $(t_0, t_1) \in \mathcal{F}$. From the sheet structure constructed in Section 4.4.3.1 (and the cut Σ_* as in (4.167)), it holds true

$$\xi_{1-}(s) = \xi_{3+}(s), \quad s \in \Sigma_{*,0},$$

$$\xi_{1-}(s) = \xi_{2+}(s), \quad s \in \Sigma_{*,1} \cup \Sigma_{*,2}.$$

Since $\Sigma_{*,0}$, $\Sigma_{*,1}$ and $\Sigma_{*,2}$ are obtained as projections of arcs of the trajectories $\gamma_1(z_0^{(2)})$, $\gamma_0(z_1^{(3)})$ and $\gamma_2(z_2^{(3)})$, respectively (see (4.164)–(4.166)), we get

$$(\xi_{1+}(s) - \xi_{1-}(s))ds = (\xi_{1+}(s) - \xi_{3+}(s))ds \in i\mathbb{R}, \quad s \in \Sigma_{0,*}$$

and

$$(\xi_{1+}(s) - \xi_{1-}(s))ds = (\xi_{1+}(s) - \xi_{2+}(s))ds \in i\mathbb{R}, \quad s \in \Sigma_{1,*} \cup \Sigma_{2,*}.$$

This proves (4.37) in the three-cut case. Similarly, we use (4.168) to conclude that (4.37) is satisfied in the one-cut case as well. Furthermore, from its construction it immediately follows that Σ_* satisfies the properties claimed in (i) (in the three-cut case) and (ii) (in the one-cut case).

To prove that μ_* defined in (4.38) is a probability measure, first note that (4.37) automatically implies that it is a real measure. In the three-cut case, its density does not vanish on the arcs $\Sigma_{*,0}$, $\Sigma_{*,1}$ and $\Sigma_{*,2}$ of its support, so this measure has constant sign on each of these arcs. For $t_1 = 0$, we know that this density is positive in each of these arcs [38], so by continuity we conclude that this measure is positive for any pair $(t_0, t_1) \in \mathcal{F}_1$ as well. The total mass of μ_* is given by

$$\frac{1}{2\pi i t_0} \int_{\Sigma_*} (\xi_{1-}(z) - \xi_{1+}(z))dz = \frac{1}{2\pi i t_0} \oint_{\gamma} \xi_1(s)ds,$$

where γ is a contour positively oriented and encircling Σ_*. We deform γ to infinity and use the expansion (4.27) to get

$$\frac{1}{2\pi i t_0} \int_{\Sigma_*} (\xi_{1-}(z) - \xi_{1+}(z))dz = -\frac{1}{t_0} \operatorname{Res}(\xi_1, \infty) = 1,$$

so we conclude that in the three-cut case μ_* is indeed a probability measure.

To conclude that μ_* is positive in the one-cut case as well, note that the density of μ_* is continuous and does not vanish in the interval Σ_*, hence μ_* has constant sign along this interval. Calculations very similar as above show that the total mass of μ_* is 1, in particular μ_* has to be positive, and we then conclude that μ_* is a probability measure, as we want. □

We remind that to conclude the proof of Theorem 4.2.9 we still have to verify the inclusion (4.36). To do so, we first have to prove some auxiliary results, which are inspired from a similar analysis carried out by Balogh, Bertola, Lee and McLaughlin [19].

Recall that the principal value of the Cauchy transform C^λ of a finite and compactly supported measure λ is defined by

$$C^\lambda(z) = \lim_{\varepsilon \to 0} \int_{|s-z| \geq \varepsilon} \frac{d\lambda(s)}{s - z}, \quad z \in \mathbb{C}.$$

C^λ is analytic on the open sets of $\mathbb{C} \setminus \operatorname{supp} \lambda$ and satisfies the identity

$$2\frac{\partial U^\lambda}{\partial z}(z) = C^\lambda(z), \quad z \in \mathbb{C} \setminus \operatorname{supp} \lambda, \tag{4.169}$$

where U^λ is the potential of λ as in (4.20).

Lemma 4.6.1. *For $(t_0, t_1) \in \mathcal{F}$ and V the cubic polynomial (4.12), the Cauchy transform of the measure μ_0 in (4.21) satisfies*

$$C^{\mu_0}(z) = \begin{cases} -\frac{1}{t_0}(\overline{z} - V'(z)), & z \in \overline{\Omega}, \\ -\frac{1}{t_0}(S(z) - V'(z)), & z \in \mathbb{C} \setminus \Omega. \end{cases} \tag{4.170}$$

whereas the Cauchy transform of μ_* in (4.38) satisfies

$$C^{\mu_*}(z) = -\frac{1}{t_0}(\xi_1(z) - V'(z)), \quad z \in \mathbb{C} \setminus \Sigma_*. \tag{4.171}$$

Proof. Suppose $z \in \mathbb{C} \setminus \overline{\Omega}$. Using Green's Theorem and the definition of the Schwarz function S, we can write

$$\begin{aligned} C^{\mu_0}(z) &= \frac{1}{\pi t_0} \int_\Omega \frac{dA(s)}{s - z} \\ &= \frac{1}{2\pi i t_0} \int_{\partial\Omega} \frac{S(s)}{s - z} ds, \end{aligned}$$

where $\partial\Omega$ is oriented counterclockwise. The Schwarz function S is analytic on $\mathbb{C} \setminus \Omega$, so we can deform $\partial\Omega$ to ∞ in order to conclude

$$\begin{aligned} C^{\mu_0}(z) &= -\frac{1}{t_0} \operatorname{Res}\left(\frac{S(s)}{s - z}, s = z\right) - \frac{1}{t_0} \operatorname{Res}\left(\frac{S(s)}{s - z}, s = \infty\right) \\ &= -\frac{1}{t_0} \left(S(z) - V'(z)\right), \end{aligned}$$

where we computed the residue at ∞ using the fact that S is an analytic continuation of the function germ ξ_1 in (4.27). This is enough to prove the second equality in (4.170) for $z \in \mathbb{C} \setminus \overline{\Omega}$. Using continuity, this extends to $\partial\Omega$ as well.

Suppose now that $z \in \Omega$. Using the Cauchy-Green formula,

$$\begin{aligned} \overline{z} &= \frac{1}{2\pi i} \int_{\partial\Omega} \frac{\overline{s}}{s - z} ds - \frac{1}{\pi} \int_\Omega \frac{dA(s)}{s - z} \\ &= \frac{1}{2\pi i} \int_{\partial\Omega} \frac{S(s)}{s - z} ds - t_0 C^{\mu_0}(z). \end{aligned}$$

Proceeding as before, we can compute the contour integral on the right-hand side above, concluding that

$$\overline{z} = V'(z) - t_0 C^{\mu_0}(z),$$

which is equivalent to the first equation in (4.170).

Finally, (4.171) follows again by a residue calculation, having in mind the identity

$$C^{\mu_*}(z) = \frac{1}{2\pi i t_0} \int_{\Sigma_*} \frac{\xi_{1-}(s) - \xi_{1+}(s)}{s - z} ds = \frac{1}{2\pi i t_0} \int_{\gamma} \frac{\xi_1(s)}{s - z} ds,$$

where we recall that Σ_* is oriented outwards, and γ is any positively oriented contour encircling Σ_* and for which z is on the exterior region of γ. □

Recalling (4.12), denote by

$$\mathcal{U}_0(z) = 2U^{\mu_0}(z) + \mathcal{V}(z), \quad z \in \mathbb{C},$$

the total potential of μ_0, and by

$$\mathcal{U}_*(z) = 2U^{\mu_*}(z) + \mathcal{V}(z), \quad z \in \mathbb{C}, \tag{4.172}$$

the total potential of μ_*.

Proof of Theorem 4.2.3. Since the partial derivatives of U^{μ_0} are continuous and C^{μ_0} is absolutely convergent in $\mathbb{C}$, the identity (4.169) for μ_0 is actually valid on Ω as well, and the first equation in (4.170) then says

$$\frac{\partial \mathcal{U}_0}{\partial z}(z) = 0, \quad z \in \Omega.$$

This identity suffices to conclude that $\mathcal{U}_0$ is constant, say l, on $\overline{\Omega}$, which is the same as (4.22).

The second equality in (4.170) provides an harmonic extension $\widetilde{\mathcal{U}_0}$ of $\mathcal{U}_0$ to a neighborhood of $\partial\Omega$. More concretely, there is a neighborhood G of $\mathbb{C} \setminus \Omega$ and a constant c such that the harmonic function

$$\widetilde{\mathcal{U}_0}(z) = -\frac{1}{t_0} \operatorname{Re} \int^z S(s) ds + \frac{|z|^2}{t_0} + c, \quad z \in G,$$

coincides with $\mathcal{U}_0$ in $\mathbb{C} \setminus \Omega$. Note also that the primitive above does not depend on the path of integration chosen within G, because the residue of S at ∞ is real.

We will prove that

$$\widetilde{\mathcal{U}}_0(z_0+\varepsilon\eta) = l + \frac{2\varepsilon^2}{t_0^2} + \mathcal{O}(\varepsilon^3), \qquad \text{as } \varepsilon \to 0, \tag{4.173}$$

which is enough to conclude (4.23).

On $\partial\Omega$, we know that

$$\frac{\partial \widetilde{\mathcal{U}}_0}{\partial z}(z) = -\frac{1}{t_0}(S(z)-\overline{z}) = 0,$$

so the (real) gradient of $\widetilde{\mathcal{U}}_0$ vanishes on $\partial\Omega$. Furthermore, the Laplacian of $\widetilde{\mathcal{U}}_0$ is

$$\Delta\widetilde{\mathcal{U}}_0(z) = 4\frac{\partial^2 \widetilde{\mathcal{U}}_0}{\partial z \partial \overline{z}}(z) = \frac{4}{t_0}, \quad z \in \partial\Omega,$$

and the determinant of the Hessian $H(\widetilde{\mathcal{U}}_0)$ of $\widetilde{\mathcal{U}}_0$ is

$$\det H(\widetilde{\mathcal{U}}_0) = 4\left(\left(\frac{\partial^2 \widetilde{\mathcal{U}}_0}{\partial z \partial \overline{z}}\right)^2 - \frac{\partial^2 \widetilde{\mathcal{U}}_0}{\partial z^2}\frac{\partial^2 \widetilde{\mathcal{U}}_0}{\partial \overline{z}^2}\right) = \frac{4}{t_0}(1-|S'(z)|^2),$$

and the latter vanishes on $\partial\Omega$ because $|S'(z)| = 1$ there.

Hence we conclude that the eigenvalues of $H(\widetilde{\mathcal{U}}_0)$ are $4/t_0$ and 0. Taking into account that $\widetilde{\mathcal{U}}_0$ is constant along $\partial\Omega$, we see that the tangent vector to $\partial\Omega$ is an eigenvector for the eigenvalue 0, and consequently η is an eigenvector associated to $4/t_0$. This is enough to get (4.173). □

Proof of Theorem 4.2.4. The conditions (4.22)–(4.23) are enough to conclude that μ_0 is the equilibrium measure of D in the external field $\mathcal{V}$ [120, Theorem I.3.3]. The result is then an immediate consequence of [65, Theorem 4.1]. □

To prove the inclusion (4.36), we need two more lemmas.

Lemma 4.6.2. *Suppose $(t_0, t_1) \in \mathcal{F}$. The total potential $\mathcal{U}_*$ does not have a local minimum on Σ_*.*

Proof. Suppose first $z \notin \{z_*, z_0, z_1, z_2\}$. With respect to the outward orientation of Σ_*, denote by n_+ and n_- the normal vectors of Σ_* at z pointing to the

positive and negative sides of Σ_*, respectively. Combining (4.169) and (4.171), it follows that

$$\begin{aligned}\frac{\partial \mathcal{U}_*}{\partial n_\pm}(z) &= 2\,\mathrm{Re}\left(n_\pm \frac{\partial \mathcal{U}_{*\pm}}{\partial z}(z)\right)\\ &= \pm 2\,\mathrm{Re}\left(n_+\left(C_\pm^{\mu_*}(z)+\frac{1}{t_0}(\overline{z}-V'(z))\right)\right)\\ &= \pm\frac{2}{t_0}\,\mathrm{Re}\left(n_+\left(\overline{z}-\xi_{1\pm}(z)\right)\right).\end{aligned}$$

The vector tangent to Σ_* along its positive direction is $\tau_+ = -in_+$, and the equalities above then imply

$$\begin{aligned}\frac{\partial \mathcal{U}_*}{\partial n_+}(z)+\frac{\partial \mathcal{U}_*}{\partial n_-}(z) &= \frac{2}{t_0}\,\mathrm{Re}\left(n_+\big(\xi_{1-}(z)-\xi_{1+}(z)\big)\right)\\ &= -\frac{2}{t_0}\,\mathrm{Im}\left(\tau_+\big(\xi_{1-}(z)-\xi_{1+}(z)\big)\right). \qquad (4.174)\end{aligned}$$

Since the measure μ_* is positive, we learn from (4.38) and the last equality that

$$\frac{\partial \mathcal{U}_*}{\partial n_+}(z)+\frac{\partial \mathcal{U}_*}{\partial n_-}(z) < 0,$$

so at least one of these directional derivatives is negative, thus z cannot be a local minimum.

Suppose now $z \in \{z_0, z_1, z_2\}$, say $z = z_j$. Using (4.171) and the relation (4.169),

$$U^{\mu_*}(u) = -\frac{1}{t_0}\,\mathrm{Re}\int_{z_j}^{u}\xi_1(s)ds + \frac{1}{t_0}\,\mathrm{Re}(V(u)-V(z_j)), \quad u \in G\setminus\Sigma_*, \quad (4.175)$$

where G is a sufficiently small neighborhood of z and the path of integration lies in $G\setminus\Sigma_*$. On G the function ξ_1 admits an expansion of the form

$$\xi_1(u) = \xi_1(z_j) + \mathcal{O}((u-z_j)^{1/2}), \quad u \in G\setminus\Sigma_*.$$

Using this expansion in (4.175), we then get

$$\begin{aligned}\mathcal{U}_*(u) &= -\frac{2}{t_0}\,\mathrm{Re}\left(\xi_1(z_j)u\right)+\frac{|u|^2}{t_0}+c+\mathcal{O}((u-z_j)^{3/2}),\\ &= -\frac{2}{t_0}\,\mathrm{Re}\,u\,\mathrm{Re}\,\xi_1(z_j)+\frac{2}{t_0}\,\mathrm{Im}\,u\,\mathrm{Im}\,\xi_1(z_j)\\ &\quad+\frac{(\mathrm{Re}\,u)^2+(\mathrm{Im}\,u)^2}{t_0}+c+\mathcal{O}((u-z_j)^{3/2}), \quad u\in G\setminus\Sigma_*\end{aligned}$$

for some constant c. From (4.94) we know that $\xi_1(z_j) = h(w_j^{-1}) \neq 0$, so the leading contribution in the formula above is linear in $\operatorname{Re} u$ and $\operatorname{Im} u$, and consequently $\mathcal{U}_*$ cannot have a local minimum at z_j.

It remains to verify that $z = z_*$ cannot be a local minimum in the three-cut case $(t_0, t_1) \in \mathcal{F}_1$. Consider the angle θ between $\Sigma_{*,2}$ and $\Sigma_{*,0}$ on the upper half plane, so that $\theta \leq \pi$. Assume for the moment that $\theta > \pi/2$. In this case, for $\epsilon > 0$ sufficiently small, the point $z_* + \varepsilon i$ is in between $\Sigma_{*,0}$ and $\Sigma_{*,2}$, and using continuity we can conclude

$$\begin{aligned}\mathcal{U}_*(z_* + \varepsilon i) &= \lim_{\delta \to 0^+} \mathcal{U}_*(z_* + \varepsilon i + \delta) \\ &= U_*(z_*) + \varepsilon \lim_{\delta \to 0^+} \frac{\partial \mathcal{U}_*}{\partial n_+}(z_* + \delta) + \mathcal{O}(\varepsilon^2), \end{aligned} \tag{4.176}$$

where $n_+ = i$ is the normal to $\Sigma_{*,0}$, and the error term is uniform in δ. Similarly,

$$\begin{aligned}\mathcal{U}_*(z_* - \varepsilon i) &= \lim_{\delta \to 0^+} \mathcal{U}_*(z_* - \varepsilon i + \delta) \\ &= U_*(z_*) + \varepsilon \lim_{\delta \to 0^+} \frac{\partial \mathcal{U}_*}{\partial n_-}(z_* + \delta) + \mathcal{O}(\varepsilon^2). \end{aligned} \tag{4.177}$$

Proceeding as in (4.174) (and having in mind that in the present case $\tau_+ = 1$),

$$\begin{aligned}&\lim_{\delta \to 0^+} \left(\frac{\partial \mathcal{U}_*}{\partial n_+}(z_* + \delta) + \frac{\partial \mathcal{U}_*}{\partial n_-}(z_* + \delta) \right) \\ &\qquad = -\frac{2}{t_0} \lim_{\delta \to 0^+} \operatorname{Im} \big(\xi_{1-}(z_* + \delta) - \xi_{1+}(z_* + \delta) \big). \end{aligned}$$

As before, we use that the density of μ_* is positive on $\Sigma_{*,0}$ and does not vanish on z_* to conclude that the limit above is strictly negative. Taking into account (4.176)–(4.177), this is enough to conclude that z_* is not a point of minimum.

It only remains to prove the inequality $\theta > \pi/2$. When $t_1 = 0$, then $\theta = 3\pi/2$ and we are done. Since θ varies continuously with t_1, it is enough to prove that $\theta \neq \pi/2$.

To the contrary, suppose $\theta = \pi/2$. In this case, the vector tangent to $\Sigma_{*,2}$ converges to i as $z \to z_*$ along $\Sigma_{*,2}$, so that from (4.37) we learn

$$(\xi_{1+}(z_*) - \xi_{1-}(z_*)) \in \mathbb{R},$$

where the $\pm$ boundary values are with respect to $\Sigma_{*,2}$. But in this case $\xi_{1+}(z_*) \in \mathbb{R}$ as well, so we conclude that $\xi_{1-}(z_*) \in \mathbb{R}$, and consequently all the

solutions to (4.24) are real for $z = z_*$. But this cannot occur, because $z_* < z_0$ and we know from Theorem 4.4.1 that the discriminant of (4.24) is negative on the interval $(-\infty, z_0)$. □

Lemma 4.6.3. *The total potential $\mathcal{U}_*$ does not have a local minimum on Ω.*

Proof. From Lemma 4.6.2, we know that $\mathcal{U}_*$ does not attain a minimum on Σ_*, so if $p \in \Omega$ is a point of minimum of $\mathcal{U}_*$, then the gradient of $\mathcal{U}_*$ should vanish at p. This means that

$$0 = \frac{\partial \mathcal{U}_*}{\partial z}(p) = C^{\mu_*}(p) + \frac{1}{t_0}(\overline{p} - V'(p)) = \frac{1}{t_0}(\overline{p} - \xi_1(p)), \tag{4.178}$$

where for the first equality we used the definition of $\mathcal{U}_*$ given in (4.172) together with the identity (4.169), and for the last equality we used (4.171). That is, we conclude that the point p where $\mathcal{U}_*$ attains its minimum should satisfy $\xi_1(p) = \overline{p}$. Let w be such that

$$h(w) = p, \qquad h\left(\frac{1}{w}\right) = \xi_1(p) = \overline{p}. \tag{4.179}$$

We know from Theorem 4.2.2 that h maps $\partial\mathbb{D}$ to $\partial\Omega$. Since $p \in \Omega$, we learn from this that $|w| \neq 1$, so the point $\tilde{w} := 1/\overline{w}$ is different from w. Furthermore, because the rational function h has real coefficients,

$$h(\tilde{w}) = \overline{h(w^{-1})} = \overline{\xi_1(p)} = p = h(w), \tag{4.180}$$

and also

$$h\left(\frac{1}{\tilde{w}}\right) = \overline{h(w)} = \overline{p} = \xi_1(p) = h\left(\frac{1}{w}\right). \tag{4.181}$$

Since $\tilde{w} \neq w$, the pairs $(h(w^{-1}), h(w))$ and $(h(\tilde{w}^{-1}), h(\tilde{w}))$ represent distinct points on $\mathcal{R}$. In virtue of the equalities (4.179)–(4.181), we conclude that p is a zero of the discriminant of (4.24). But $p \notin \Sigma_*$, so in particular it cannot be a branch point. Thus $p = \hat{z}_j$ for some j, and from Theorem 4.2.6 we learn that p cannot be on Ω. Hence (4.178) cannot hold on $\Omega \setminus \Sigma_*$, and the proof is complete. □

Proof of (4.36). Fix t_0. When $t_1 = 0$, the set Σ_* is explicitly given by (4.104), and (4.36) is valid in this case. Suppose now that (4.36) is not valid for some value of t_1. Continuity arguments show that for the smallest of such value, say $\tilde{t}_1$, it holds true

$$\Sigma_* \subset \overline{\Omega} \qquad \text{and} \qquad \partial\Omega \cap \Sigma_* \neq \emptyset. \tag{4.182}$$

Recalling that ξ_1 and S coincide in a neighborhood of ∞, the inclusion in (4.182) implies $\xi_1 \equiv S$ on the whole set $\mathbb{C} \setminus \Omega$. Thus, still for the given pair $(t_0, \tilde{t}_1)$, the second identity in (4.170) combined with (4.171) then says that

$$C^{\mu_0}(z) = C^{\mu_*}(z), \quad z \in \mathbb{C} \setminus \Omega. \tag{4.183}$$

Taking into account (4.169), we further get

$$\mathcal{U}_*(z) - \mathcal{U}_0(z) = c, \quad z \in \mathbb{C} \setminus \Omega,$$

for some constant c. This constant is equal to

$$\begin{aligned} c &= \lim_{z\to\infty} \left(U^{\mu_*}(z) - U^{\mu_0}(z)\right) \\ &= \lim_{z\to\infty} \left(\int \log\left|1 - \frac{s}{z}\right| d\mu_0(s) - \int \log\left|1 - \frac{s}{z}\right| d\mu_*(s) \right) = 0. \end{aligned}$$

In particular, it follows from Theorem 4.2.3 that

$$\mathcal{U}_*(z) > l, \quad \text{for } z \in \mathbb{C} \setminus \overline{\Omega} \text{ sufficiently close to } \partial\Omega, \tag{4.184}$$

and

$$\mathcal{U}_*(z) = l, \quad z \in \partial\Omega. \tag{4.185}$$

The function $\mathcal{U}_*$ is continuous on $\overline{\Omega}$, so it has a minimum in this set. Using Lemma 4.6.3 and (4.185), we thus conclude

$$\mathcal{U}_*(z) > l, \quad z \in \Omega. \tag{4.186}$$

From (4.182), we know that there exists $p \in \partial\Omega \cap \Sigma_*$. From (4.184)–(4.186) we learn that p is a local minimum of $\mathcal{U}_*$, but this is in contradiction with Lemma 4.6.2.

Hence (4.36) always holds true, and the proof of Theorem 4.2.9 is complete. □

Proof of Theorem 4.2.10. Having in mind (4.36), we now know that $\xi_1 \equiv S$ on $\mathbb{C} \setminus \Omega$. Proceeding as in (4.183)–(4.186), we conclude

$$\mathcal{U}_*(z) = \mathcal{U}_0(z), \quad z \in \mathbb{C} \setminus \Omega, \tag{4.187}$$

$$\mathcal{U}_*(z) > l, \qquad z \in \Omega, \tag{4.188}$$

where l is the constant from Theorem 4.2.3. From the definition of $\mathcal{U}_0$ and $\mathcal{U}_*$ it follows that (4.187) is equivalent to (4.39). Furthermore, by Theorem 4.2.3 we know that $\mathcal{U}_0 \equiv l$ on Ω, and (4.188) then becomes (4.40). □

4.7 Riemann-Hilbert analysis in the three-cut case

In this section we perform the Riemann-Hilbert/Steepest Descent analysis for the multiple orthogonal polynomial $P_{n,n}$ (given in Definition 4.2.12) in the three-cut case $(t_0, t_1) \in \mathcal{F}_1$.

The analysis is similar to the one presented by Bleher and Kuijlaars in [38] for $t_1 = 0$. The main difference here is that we construct the g-functions only with the help of the ξ-functions, without relying on any vector equilibrium problem. Although our g-functions could also be given in terms of the solution to a vector equilibrium problem, we do not elaborate in this direction.

For $j = 0, 1, 2$, we extend $\Sigma_{*,j}$ given in Section 4.6 to a contour Σ_j in the following way. For $j = 0$, simply set $\Sigma_j = [z_*, \hat{z}_0]$. For $j = 2$, we take $\Sigma_2 \setminus \Sigma_{*,2}$ to be an arc from z_2 to $\hat{z}_2$ contained in the projection of the strip domain $\mathcal{S}_3$ of the quadratic differential ϖ, that is,

$$\Sigma_2 \setminus (\Sigma_{*,2} \cup \{\hat{z}_2\}) \subset \pi(\mathcal{S}_3), \tag{4.189}$$

where we recall that the strip domain $\mathcal{S}_3$ is labeled as in Figure 4.23. Lastly we extend $\Sigma_{*,1}$ imposing the conjugation property

$$\Sigma_1 \setminus \Sigma_{*,1} = (\Sigma_2 \setminus \Sigma_{*,2})^*. \tag{4.190}$$

In this way,

$$\Sigma_1 \setminus (\Sigma_{*,1} \cup \{\hat{z}_1\}) \subset \pi(\mathcal{S}_8), \tag{4.191}$$

where the strip domain $\mathcal{S}_8$ is given as in Figure 4.23. We refer the reader to Figure 4.27.

The arc Σ_j is oriented from z_* to $\hat{z}$. We then set

$$\Sigma = \Sigma_0 \cup \Sigma_1 \cup \Sigma_2,$$

and consider the multiple orthogonal polynomial $P_{n,n}$ in Definition 4.2.12 with this choice of Σ.

4.7.1 Multiple orthogonality in terms of Airy functions

The multiple orthogonality conditions (4.54) can be stated in terms of solutions to the Airy equation $y'' = zy$. The Airy function Ai is the special solution to the Airy equation determined by the asymptotic behavior

$$\operatorname{Ai}(z) = \frac{z^{-1/4}}{2\sqrt{\pi}} e^{-\frac{2}{3}z^{3/2}} (1 + \mathcal{O}(z^{-3/2}))$$

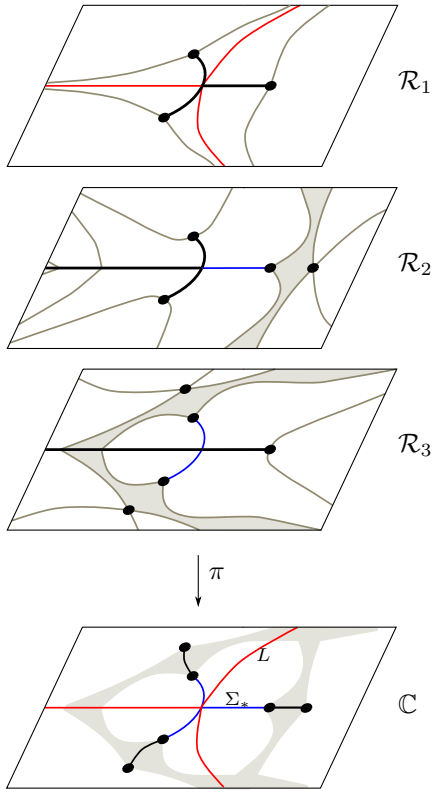

Figure 4.27: Illustration of properties (4.189) and (4.198). The trajectories highlighted on $\mathcal{R}$ in blue and red are projected onto $\mathbb{C}$ to the contours Σ_*, L, also respectively represented in blue and red. Σ_* consists of the union of the three trajectories projected from $\mathcal{R}_2$, $\mathcal{R}_3$, whereas L consists of the pieces projected from $\mathcal{R}_1$. In addition, we extend Σ_* to Σ by constraining $\Sigma \setminus \Sigma_*$ to lie within the shaded region on $\mathbb{C}$, which consists of the projections of the gray strip domains on $\mathcal{R}$. The arcs of $\Sigma \setminus \Sigma_*$ are depicted in black.

and

$$\mathrm{Ai}'(z) = -\frac{z^{1/4}}{2\sqrt{\pi}} e^{-\frac{2}{3}z^{3/2}} (1 + \mathcal{O}(z^{-3/2})), \tag{4.192}$$

which are valid when $z \to \infty, -\pi < \arg z < \pi$. It admits the integral representation

$$\mathrm{Ai}(z) = \frac{1}{2\pi i} \int_{\Gamma_0} e^{\frac{1}{3}s^3 - zs} ds, \quad z \in \mathbb{C},$$

where Γ_0 is a contour as in Section 4.2.7, see (4.43) *et seq.* For Γ_1, Γ_2, ω also given as in Section 4.2.7, set

$$y_j(z) = \omega^j \operatorname{Ai}(\omega^j z) = \frac{1}{2\pi i} \int_{\Gamma_j} e^{\frac{1}{3}s^3 - zs}, \quad z \in \mathbb{C}, \quad j = 0, 1, 2, \tag{4.193}$$

where we recall that $\omega = e^{2\pi i/3}$. Note that the integral representations above, in combination with contour deformation, immediately imply that

$$y_0(z) + y_1(z) + y_2(z) = \operatorname{Ai}(z) + \omega \operatorname{Ai}(\omega z) + \omega^2 \operatorname{Ai}(\omega^2 z) = 0. \tag{4.194}$$

Using the functions y_0, y_1 and y_2 in (4.193) and setting $c_n = (n/t_0)^{2/3}$, the conditions (4.54) can be rewritten as

$$\begin{aligned} &\sum_{l=0}^{2} \int_{\Sigma_l} P_{n,n}(z) z^k e^{\frac{n}{t_0} V(z)} y_l(c_n(z - t_1)) dz = 0, \quad k = 0, \dots, \left\lceil \frac{n}{2} \right\rceil - 1, \\ &\sum_{l=0}^{2} \int_{\Sigma_l} P_{n,n}(z) z^k e^{\frac{n}{t_0} V(z)} y_l'(c_n(z - t_1)) dz = 0, \quad k = 0, \dots, \left\lfloor \frac{n}{2} \right\rfloor - 1. \end{aligned} \tag{4.195}$$

4.7.2 The Riemann-Hilbert problem Y

For simplicity of presentation, we assume for now on n even. The case n odd can be treated similarly, after appropriate (and non essential) modifications.

Consider the following Riemann-Hilbert problem for Y.

- $Y : \mathbb{C} \setminus \Sigma \to \mathbb{C}^{3\times 3}$ is analytic;
- $Y_+(z) = Y_-(z) J_Y(z)$, $z \in \Sigma$, where

$$J_Y(z) = \begin{pmatrix} 1 & e^{\frac{n}{t_0} V(z)} y_j(c_n(z - t_1)) & e^{\frac{n}{t_1} V(z)} y_j'(c_n(z - t_1)) \\ 0 & 1 & 0 \\ 0 & 0 & 1 \end{pmatrix}, \quad z \in \Sigma_j;$$

- $Y(z) = (I + \mathcal{O}(z^{-1})) \begin{pmatrix} z^n & 0 & 0 \\ 0 & z^{-\frac{n}{2}} & 0 \\ 0 & 0 & z^{-\frac{n}{2}} \end{pmatrix}, \quad z \to \infty;$
- $Y(z) = \begin{pmatrix} \mathcal{O}(1) & \mathcal{O}(\log(z - \hat{z}_j)) & \mathcal{O}(\log(z - \hat{z}_j)) \\ \mathcal{O}(1) & \mathcal{O}(\log(z - \hat{z}_j)) & \mathcal{O}(\log(z - \hat{z}_j)) \\ \mathcal{O}(1) & \mathcal{O}(\log(z - \hat{z}_j)) & \mathcal{O}(\log(z - \hat{z}_j)) \end{pmatrix}, \ z \to \hat{z}_j, \ j = 0, 1, 2.$

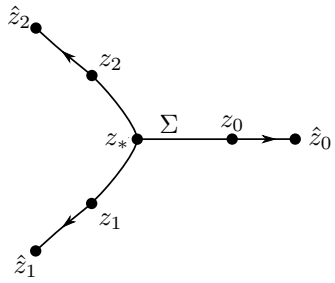

Figure 4.28: Contour Σ for the RHP for Y.

- $Y(z)$ is remains bounded when $z \to z_*$.

Here and in what follows, Σ is oriented outwards, that is, towards ∞, see Figure 4.28.

It turns out that the polynomial $P_{n,n}$ uniquely exists if, and only if, the Riemann Hilbert problem above has a solution. In such a case, the polynomial $P_{n,n}$ is recovered through

$$P_{n,n} = Y_{1,1}. \tag{4.196}$$

As one of the consequences of our analysis, we get that for sufficiently large n, the Riemann-Hilbert problem above has a solution, and thus the polynomial $P_{n,n}$ exists for n sufficiently large.

4.7.3 First transformation: $Y \mapsto X$

The first transformation, essentially the same as in [38], has the goal of reducing the jump matrix of Y to nontrivial 2×2 blocks. Define

$$y_3(z) = 2\pi i(\omega^2 \operatorname{Ai}(\omega z) - \omega \operatorname{Ai}(\omega^2 z)),$$

$$y_4(z) = \omega y_3(\omega z),$$

$$y_5(z) = \omega^2 y_3(\omega^2 z).$$

Using the identities $1-\omega = i\sqrt{3}\omega^2$ and $1-\omega^2 = -i\sqrt{3}\omega$, in combination with (4.194), we also get

$$\begin{aligned} y_3(z) &= \frac{2\pi}{\sqrt{3}}((1-\omega)\operatorname{Ai}(\omega z) + (1-w^2)\omega^2 \operatorname{Ai}(\omega^2 z)) \\ &= \frac{2\pi}{\sqrt{3}}(-\omega \operatorname{Ai}(\omega z) - \omega^2 \operatorname{Ai}(\omega^2 z) + \operatorname{Ai}(\omega z) + \operatorname{Ai}(\omega^2 z)) \\ &= \frac{2\pi}{\sqrt{3}}(\operatorname{Ai}(z) + \operatorname{Ai}(\omega z) + \operatorname{Ai}(\omega^2 z)) \end{aligned}$$

This last identity immediately implies that $y_3(\omega z) = y_3(z)$, and consequently $y_4(z) = \omega y_3(z)$ and $y_5(z) = \omega^2 y_3(z)$.

Additionally, set

$$L_0 = (-\infty, z_*] = \pi(\mathcal{R}_1 \cap \gamma_1(z_0^{(2)})) \tag{4.197}$$

and

$$L_2 = \pi(\mathcal{R}_1 \cap \gamma_0(z_1^{(3)})), \quad L_1 = L_2^* = \pi(\mathcal{R}_1 \cap \gamma_2(z_2^{(3)})), \tag{4.198}$$

where $\pi : \mathcal{R} \to \overline{\mathbb{C}}$ is the canonical projection as before, see Figure 4.27. L_1 and L_2 are unbounded analytic arcs with a common finite endpoint $z_* \in \mathbb{R}$, and they extend to ∞ along the angles $\frac{\pi}{3}$ and $-\frac{\pi}{3}$, respectively. We set the orientation on L_j to be outwards, that is, from z_* to ∞.

Remark 4.7.1. For ease of presentation, in what follows we assume that $L_j \cap \Sigma_* = \{z_*\}$. If L_j intersects Σ_* in more points, it is still possible to carry out the Riemann-Hilbert analysis along the same lines as we present here, with appropriate and non essential modifications. Numerical experiments indicate that the condition $L_j \cap \Sigma_* = \{z_*\}$ always holds true anyway.

The union $L = L_0 \cup L_1 \cup L_2$ divides the plane into three domains, henceforth denoted G_0, G_1, G_2, where G_j is uniquely defined through the condition that $\hat{z}_j$ is contained in G_j, see Figure 4.29.

We make the transformation

$$\begin{aligned} X(z) = \begin{pmatrix} 1 & 0 & 0 \\ 0 & \frac{c_n^{-1/4}}{\sqrt{2\pi}} & 0 \\ 0 & 0 & i\frac{c_n^{1/4}}{\sqrt{2\pi}} \end{pmatrix} Y(z) \begin{pmatrix} 1 & 0 & 0 \\ 0 & y'_{j+3}(c_n(z-t_1)) & -y'_j(c_n(z-t_1)) \\ 0 & -y_{j+3}(c_n(z-t_1)) & y_j(c_n(z-t_1)) \end{pmatrix} \\ \times \begin{pmatrix} 1 & 0 & 0 \\ 0 & 1 & 0 \\ 0 & 0 & -2\pi i \end{pmatrix}, \quad z \in G_j, \quad j = 0, 1, 2. \end{aligned} \tag{4.199}$$

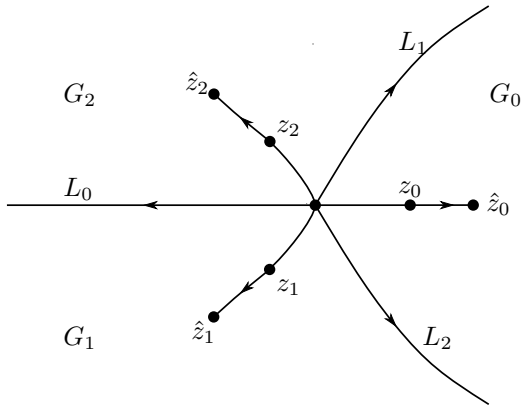

Figure 4.29: Contour $\Sigma \cup L$, $L = L_0 \cup L_1 \cup L_2$, for the RHP's for X and T, and the sectors G_0, G_1, G_2.

It follows as in [38, pp. 1297–1301] that X satisfies the following RHP

- $X : \mathbb{C} \setminus (\Sigma \cup L) \to \mathbb{C}^{3\times 3}$ is analytic;
- $X_+(z) = X_-(z)J_X(z)$, $z \in \Sigma \cup L$, where J_X is given by

$$J_X(z) = \begin{pmatrix} 1 & 0 & 0 \\ 0 & \omega^2 & 1 \\ 0 & 0 & \omega \end{pmatrix}, \ z \in L, \quad J_X(z) = \begin{pmatrix} 1 & e^{\frac{n}{t_0}V(z)} & 0 \\ 0 & 1 & 0 \\ 0 & 0 & 1 \end{pmatrix}, \ z \in \Sigma;$$

- X has the same endpoint conditions as Y at $z_*, \hat{z}_j$, $j = 0, 1, 2$;
- $X(z) = (I + \mathcal{O}(z^{-1}))A(z)Q(z), \quad z \to \infty,$
  where

$$A(z) = \begin{pmatrix} 1 & 0 & 0 \\ 0 & z^{1/4} & 0 \\ 0 & 0 & z^{-1/4} \end{pmatrix} \times \begin{cases} \begin{pmatrix} 1 & 0 & 0 \\ 0 & \frac{1}{\sqrt{2}} & -\frac{i}{\sqrt{2}} \\ 0 & -\frac{i}{\sqrt{2}} & \frac{1}{\sqrt{2}} \end{pmatrix}, & z \in G_0, \\ \begin{pmatrix} 1 & 0 & 0 \\ 0 & -\frac{i}{\sqrt{2}} & -\frac{1}{\sqrt{2}} \\ 0 & \frac{1}{\sqrt{2}} & \frac{i}{\sqrt{2}} \end{pmatrix}, & z \in G_1, \\ \begin{pmatrix} 1 & 0 & 0 \\ 0 & \frac{i}{\sqrt{2}} & \frac{1}{\sqrt{2}} \\ 0 & -\frac{1}{\sqrt{2}} & -\frac{i}{\sqrt{2}} \end{pmatrix}, & z \in G_2 \end{cases} \tag{4.200}$$

and

$$Q(z) = \begin{cases} \begin{pmatrix} z^n & 0 & 0 \\ 0 & z^{-\frac{n}{2}} e^{\frac{2n}{3t_0}(z-t_1)^{3/2}} & 0 \\ 0 & 0 & z^{-\frac{n}{2}} e^{-\frac{2n}{3t_0}(z-t_1)^{3/2}} \end{pmatrix} & z \in G_0, \\ \begin{pmatrix} z^n & 0 & 0 \\ 0 & z^{-\frac{n}{2}} e^{-\frac{2n}{3t_0}(z-t_1)^{3/2}} & 0 \\ 0 & 0 & z^{-\frac{n}{2}} e^{\frac{2n}{3t_0}(z-t_1)^{3/2}} \end{pmatrix} & z \in G_1 \cup G_2. \end{cases}$$

4.7.4 Second transformation: $X \mapsto T$

The second transformation has the goal of removing the n-dependence from the asymptotics of X.

Introduce the g-functions

$$\begin{aligned} g_1(z) &= \int_{z_0}^{z} \xi_1(s)ds + c_1, && z \in \mathbb{C} \setminus (\Sigma_* \cup L_0), \\ g_2(z) &= \int_{z_*}^{z} \xi_2(s)ds + c_2, && z \in \mathbb{C} \setminus (\Sigma_{*,1} \cup \Sigma_{*,2} \cup L_0), \\ g_3(z) &= \int_{z_0}^{z} \xi_3(s)ds + c_3, && z \in \mathbb{C} \setminus (\Sigma_{*,0} \cup L_0), \end{aligned} \tag{4.201}$$

where for g_2 the path of integration starts along $(z_*, +\infty)$ and

$$c_2 = -\pi i t_0 - \int_{\Sigma_{*,2}} (\xi_{1+}(s) - \xi_{2+}(s))ds, \quad c_1 = c_3 = \int_{z_*}^{z_0} \xi_{3-}(s)ds. \tag{4.202}$$

The constant c_2 can be alternatively expressed as

$$c_2 = -\pi i t_0 + 2\pi i t_0 \mu_*(\Sigma_{*,2}) = -\pi i t_0 + 2\pi i t_0 \mu_*(\Sigma_{*,1}) = -\pi i t_0 \mu_*(\Sigma_{*,0}), \tag{4.203}$$

where μ_* is given by Theorem 4.2.9. In particular, c_2 is purely imaginary.

We could as well express one of the g-functions in terms of the other two through $\sum \xi_j = V'$, but we found more convenient to work with three g-functions instead.

The asymptotics (4.27) can be rewritten as

$$\begin{aligned}
\xi_1(z) &= V'(z) + \frac{t_0}{z} + \mathcal{O}(z^{-2}),\\
\xi_2(z) &= -(z-t_1)^{1/2} - \frac{t_0}{2z} + \mathcal{O}(z^{-3/2}), \qquad z\to\infty,\\
\xi_3(z) &= (z-t_1)^{1/2} - \frac{t_0}{2z} + \mathcal{O}(z^{-3/2}),
\end{aligned}$$

which in turn give

$$\begin{aligned}
g_1(z) &= V(z) + l_1 + t_0\log z + \mathcal{O}(z^{-1}),\\
g_2(z) &= -\frac{2}{3}(z-t_1)^{3/2} + l_2 - \frac{t_0}{2}\log z + \mathcal{O}(z^{-1/2}), \qquad z\to\infty,\\
g_3(z) &= \frac{2}{3}(z-t_1)^{3/2} + l_3 - \frac{t_0}{2}\log z + \mathcal{O}(z^{-1/2}),
\end{aligned} \tag{4.204}$$

for some constants l_1, l_2, l_3.

Lemma 4.7.2. *For the constants l_2, l_3, c_2 and c_3 as in (4.201)–(4.204), it is valid*

$$l_3 = l_2, \qquad c_2 = i\,\mathrm{Im}\,c_3. \tag{4.205}$$

Proof. From the asymptotics (4.204),

$$\begin{aligned}
g_{3+}(z) - g_{2-}(z) &= \frac{2}{3}((z-t_1)_+^{3/2} + (z-t_1)_-^{3/2}) + l_3 - l_2\\
&\quad - \frac{t_0}{2}(\log z)_+ + \frac{t_0}{2}(\log z)_- + \mathcal{O}(z^{-1/2})\\
&= l_3 - l_2 + \pi i t_0 + \mathcal{O}(z^{-1/2}), \quad z\in L_0
\end{aligned}$$

On another hand, from the definition of g_2 and g_3,

$$\begin{aligned}
g_{3+}(z) - g_{2-}(z) &= c_3 - c_2 + \int_{z_0}^{z_*} \xi_{3-}(s)ds - \int_{z_*}^{z_2} (\xi_{1+}(s) - \xi_{2+}(s))ds\\
&= -c_2 + \int_{z_*}^{z_2} (\xi_{1-}(s) - \xi_{1+}(s))ds = \pi i t_0, \quad z\in L_0,
\end{aligned}$$

where for the second equality we used the jump condition $\xi_{1\pm} = \xi_{2\mp}$ in $\Sigma_{*,2}$, which follows from the sheet structure constructed in Section 4.4.3.1.

To get the second equality in (4.205), just note that

$$\begin{aligned} 2i\,\mathrm{Im}\, c_3 = c_3 + \overline{c_3} &= \int_{z_*}^{z_0} (\xi_{3-}(s) - \overline{\xi_{3-}(s)})ds \\ &= \int_{z_*}^{z_0} (\xi_{1+}(s) - \xi_{1-}(s))ds \\ &= -2\pi i t_0 \mu_*(\Sigma_{*,0}) = 2c_2, \end{aligned}$$

where for the second equality we used the jump equalities in (4.127) and for the last equality we used (4.203). □

The second transformation is given by

$$\begin{aligned} T(z) = &\begin{pmatrix} e^{\frac{n}{t_0}l_1} & 0 & 0 \\ 0 & e^{\frac{n}{t_0}l_2} & 0 \\ 0 & 0 & e^{\frac{n}{t_0}l_2} \end{pmatrix} X(z) \\ &\times \begin{cases} \begin{pmatrix} e^{\frac{n}{t_0}(V(z)-g_1(z))} & 0 & 0 \\ 0 & e^{-\frac{n}{t_0}g_3(z)} & 0 \\ 0 & 0 & e^{-\frac{n}{t_0}g_2(z)} \end{pmatrix}, & z \in G_0, \\ \begin{pmatrix} e^{\frac{n}{t_0}(V(z)-g_1(z))} & 0 & 0 \\ 0 & e^{-\frac{n}{t_0}g_2(z)} & 0 \\ 0 & 0 & e^{-\frac{n}{t_0}g_3(z)} \end{pmatrix}, & z \in G_1 \cup G_2. \end{cases} \end{aligned} \tag{4.206}$$

It follows that T is the solution to the following RHP,

- $T : \mathbb{C} \setminus (\Sigma \cup L) \to \mathbb{C}^{3\times 3}$ is analytic;
- $T_+(z) = T_-(z)J_T(z)$, $z \in \Sigma \cup L$, where J_T is given by

$$J_T = \begin{cases} \begin{pmatrix} e^{\frac{n}{t_0}(g_{1-}-g_{1+})} & e^{\frac{n}{t_0}(g_{1-}-g_{3+})} & 0 \\ 0 & e^{\frac{n}{t_0}(g_{3-}-g_{3+})} & 0 \\ 0 & 0 & e^{\frac{n}{t_0}(g_{2-}-g_{2+})} \end{pmatrix}, & \text{on } \Sigma_0, \\ \begin{pmatrix} e^{\frac{n}{t_0}(g_{1-}-g_{1+})} & e^{\frac{n}{t_0}(g_{1-}-g_{2+})} & 0 \\ 0 & e^{\frac{n}{t_0}(g_{2-}-g_{2+})} & 0 \\ 0 & 0 & e^{\frac{n}{t_0}(g_{3-}-g_{3+})} \end{pmatrix}, & \text{on } \Sigma_1 \cup \Sigma_2, \end{cases}$$

and

$$J_T = \begin{cases} \begin{pmatrix} e^{\frac{n}{t_0}(g_{1-}-g_{1+})} & 0 & 0 \\ 0 & \omega^2 e^{\frac{n}{t_0}(g_{2-}-g_{2+})} & e^{\frac{n}{t_0}(g_{2-}-g_{3+})} \\ 0 & 0 & \omega e^{\frac{n}{t_0}(g_{3-}-g_{3+})} \end{pmatrix}, & \text{on } L_0, \\ \begin{pmatrix} 1 & 0 & 0 \\ 0 & \omega^2 e^{-\frac{n}{t_0}(g_2-g_3)} & 1 \\ 0 & 0 & \omega e^{-\frac{n}{t_0}(g_3-g_2)} \end{pmatrix}, & \text{on } L_1, \\ \begin{pmatrix} 1 & 0 & 0 \\ 0 & \omega^2 e^{-\frac{n}{t_0}(g_3-g_2)} & 1 \\ 0 & 0 & \omega e^{-\frac{n}{t_0}(g_2-g_3)} \end{pmatrix}, & \text{on } L_2; \end{cases}$$

- T satisfies the same endpoint conditions as X when $z \to z_*, \hat{z}_j$, $j = 0, 1, 2$;
- $T(z) = (I + \mathcal{O}(z^{-1}))A(z)$, as $z \to \infty$.

Our next goal is to simplify the jump matrix J_T further. For this purpose it is convenient to introduce the functions

$$\begin{aligned} \Phi_0(z) &= \frac{1}{t_0}\int_{z_0}^{z} (\xi_1(s) - \xi_3(s))ds, \\ \Phi_1(z) &= \frac{1}{t_0}\int_{z_1}^{z} (\xi_1(s) - \xi_2(s))ds, \qquad z \in \mathbb{C} \setminus (\Sigma_* \cup L_0), \\ \Phi_2(z) &= \frac{1}{t_0}\int_{z_2}^{z} (\xi_1(s) - \xi_2(s))ds. \end{aligned} \tag{4.207}$$

and also

$$\begin{aligned} \Psi_j(z) &= \frac{1}{t_0}\int_{z_*}^{z} (\xi_2(s) - \xi_3(s))ds, \quad z \in \mathbb{C} \setminus (\Sigma_* \cup L_0), \quad j = 0, 1, \\ \Psi_2(z) &= \frac{1}{t_0}\int_{z_*}^{z} (\xi_3(s) - \xi_2(s))ds, \quad z \in \mathbb{C} \setminus (\Sigma_* \cup L_0). \end{aligned} \tag{4.208}$$

where the paths of integration for Ψ_0, Ψ_1 and Ψ_2 are as follows.

- If $\operatorname{Im} z \geq 0$, then the path of integration for Φ_0 emanates from z_* in the sector between L_0 and Σ_2 on the upper half plane. If $\operatorname{Im} z < 0$, then the path of integration for Φ_0 emanates from z_* in the sector between L_0 and Σ_1 on the lower half plane.

- For $j = 1, 2$, the path of integration for Ψ_j emanates from z_* in the sector between L_j and Σ_{j+1} on G_{j+1}.

The main properties of the functions Φ_j and Ψ_j are collected in the next proposition.

Proposition 4.7.3. *The functions g_j, Φ_j, Ψ_j, $j = 0, 1, 2$, satisfy*

(A) For $z \in \Sigma_{*,0}$,

$$\begin{aligned}
&\textit{(i)} && g_{1+}(z) - g_{1-}(z) = t_0\Phi_{0+}(z),\\
&\textit{(ii)} && g_{2+}(z) - g_{2-}(z) = 0,\\
&\textit{(iii)} && g_{3+}(z) - g_{3-}(z) = t_0\Phi_{0-}(z),\\
&\textit{(iv)} && g_{3+}(z) - g_{1-}(z) = 0,\\
&\textit{(v)} && \operatorname{Re}\Phi_{0\pm}(z) = 0,\\
&\textit{(vi)} && \Phi_{0+}(z) + \Phi_{0-}(z) = 0,\\
&\textit{(vii)} && \Psi_{1+}(z) + \Psi_{2-}(z) = \Phi_{0+}(z) + \frac{2c_2}{t_0}.
\end{aligned}$$

(B) For $j = 1, 2$ and $z \in \Sigma_{*,j}$,

$$\begin{aligned}
&\textit{(i)} && g_{1+}(z) - g_{1-}(z) = t_0\Phi_{j+}(z),\\
&\textit{(ii)} && g_{2+}(z) - g_{2-}(z) = t_0\Phi_{j-}(z),\\
&\textit{(iii)} && g_{3+}(z) - g_{3-}(z) = 0,\\
&\textit{(iv)} && g_{2+}(z) - g_{1-}(z) = (-1)^{j+1}\pi i t_0,\\
&\textit{(v)} && \operatorname{Re}\Phi_{j\pm} = 0,\\
&\textit{(vi)} && \Phi_{j+}(z) + \Phi_{j-}(z) = 0,\\
&\textit{(vii)} && \Phi_{j-1,-}(z) + (-1)^{j+1}\Psi_{j+1,+}(z) = \Phi_{j+}(z) - \frac{c_2}{t_0} - \pi i.
\end{aligned}$$

(C) For $z \in \Sigma_0 \setminus \Sigma_{j,0}$,

$$g_3(z) - g_1(z) = -t_0\Phi_0(z).$$

(D) For $j = 1, 2$, and $z \in \Sigma_j \setminus \Sigma_{*,j}$,

$$g_2(z) - g_1(z) = -t_0\Phi_j(z) + (-1)^{j+1}\pi i t_0.$$

(E) $\operatorname{Re}\Phi_j$ is negative on $\Sigma_j \setminus \Sigma_{*,j}$, $j = 0, 1, 2$.

(F) For $j = 0, 1, 2$, the functions $\operatorname{Im}\Phi_{j+}$ and $\operatorname{Im}\Phi_{j-}$ are decreasing and increasing, respectively, along the orientation of $\Sigma_{*.j}$.

(G) For $z \in L_0$,

(i) $\Psi_{0+}(z) + \Psi_{0-}(z) = 0$,
(ii) $\operatorname{Re} \Psi_{0\pm}(z) = 0$,
(iii) $g_{1+}(z) - g_{1-}(z) = -2\pi i t_0$,
(iv) $g_{2+}(z) - g_{2-}(z) = t_0 \Psi_{0+}(z) + 2c_2 + 2\pi i t_0$,
(v) $g_{3+}(z) - g_{3-}(z) = t_0 \Psi_{0-}(z) - 2c_2$,
(vi) $g_{3+}(z) - g_{2-}(z) = \pi i t_0$.
(vii) $\Phi_{2-}(z) - \Phi_{1+}(z) = \Psi_{0+}(z) + \dfrac{2c_2}{t_0} + 2\pi i$.

(H) For $j = 1, 2$, and $z \in L_j$,

(i) $\Psi_{j+}(z) = \Psi_{j-}(z)$,
(ii) $\operatorname{Re} \Psi_j(z) = 0$,
(iii) $g_3(z) - g_2(z) = (-1)^j t_0 \Psi_j(z) + (-1)^{j+1} c_2$
(iv) $\Phi_{j-1}(z) - \Phi_{j+1}(z) = \Psi_j(z) - \dfrac{c_2}{t_0} + \pi i$.

(I) For $j = 0, 1, 2$, the function $\operatorname{Im} \Psi_{j+}$ is decreasing along the orientation of L_j.

Proof. To see that the conditions (A)–(v) and (B)–(v) are true, note that from the sheet structure constructed in Section 4.4.3.1, it follows that

$$\Phi_{j\pm}(z) = \int_{z_j}^{z} (\xi_{1\pm}(s) - \xi_{1\mp}(s)) ds, \quad z \in \Sigma_*.$$

Since Σ_* satisfies (4.37), the right-hand side above has to be purely imaginary, leading to (A)–(v) and (B)–(v).

Similarly, to get (G)–(ii) and (H)–(ii) we note that (4.197)–(4.198) say that L_j coincides with the projection of a trajectory on the first sheet of the quadratic differential (4.132). From the definition of ϖ in (4.131)–(4.132) and of its trajectories (4.133), and taking also into account that $z_* \in L$, we thus get

$$\operatorname{Re} \int_{z_*}^{z} (\xi_{2+}(s) - \xi_{3+}(s)) ds = 0, \quad z \in L,$$

which is enough to conclude (G)–(ii) and (H)–(ii).

The remaining conditions claimed in (A)–(D) and (G)–(H) follow in a straightforward manner, once one has in mind the sheet structure for the spectral curve $\mathcal{R}$ (see Sections 4.4.3.1 and the beginning of Section 4.6), and also equations (4.202)–(4.203) and (4.205). We skip the details for these computations.

Recalling that $\xi_1 < \xi_3$ on $(z_0, \hat{z}_0)$, see (4.126), we get (E) for $j = 0$.

Note that the analytic continuation of the function Φ_2 (that we keep denoting by Φ_2) coincides (up to a multiplicative real factor) with the primitive Υ in (A.1) on the strip domain $\mathcal{U} = \mathcal{S}_3$. In particular, Φ_2 maps $\mathcal{S}_3$ to a vertical strip on $\mathbb{C}$ whose one of the boundary components is the imaginary axis, and consequently the sign of $\operatorname{Re}\Phi_2$ is constant on $\mathcal{S}_3$. The trajectory $\gamma_0(z_2^{(3)})$ is contained in one of the components of $\partial\mathcal{S}_3$, is mapped by Φ_2 to the imaginary axis and extends to ∞ along the angle $\theta_0^{(3)} = \pi/6$. Using the expansion (4.27) it follows that

$$\Phi_2(z) = \frac{z^3}{3t_0} + \mathcal{O}(z) = i\frac{|z|^3}{3t_0} + \mathcal{O}(z), \qquad \text{as } z \to \infty \text{ along } \gamma_0(z_2^{(3)}),$$

thus $\gamma_0(z_2^{(3)})$ is mapped by Φ_2 to $i\mathbb{R}_+$. Hence, because Φ_2 is conformal, we conclude that the left-hand side of $\gamma_0(z_2^{(3)})$ in the orientation from $z_2^{(3)}$ to ∞ (that is, $\mathcal{S}_3$) is mapped by Φ_2 to the left-hand side of $i\mathbb{R}_+$ in the natural orientation. Since the sign of $\operatorname{Re}\Phi_2$ is constant on $\mathcal{S}_3$, this is enough to conclude that $\operatorname{Re}\Phi_2(z) < 0$ on $\mathcal{S}_3$. In virtue of (4.191), we conclude (E) for $j = 2$. Finally, (E) for $j = 1$ follows in a similar fashion, or also noticing the symmetry relations $\overline{\Phi_2(z)} = \Phi_1(\bar{z})$ and (4.190).

For (F), denote by γ_z the sub arc of $\Sigma_{*,j}$ from z to z_j. It follows from (4.207) that we can write

$$\Phi_{j\pm}(z) = \frac{1}{t_0}\int_{z_j}^{z} (\xi_{1\pm}(s) - \xi_{1\mp}(s))ds = \pm 2\pi i \mu_*(\gamma_z).$$

The measure μ_* is positive, so $\mu_*(\gamma_z)$ is decreasing along $\Sigma_{*,j}$, and (F) follows from the equation above.

We now proceed to prove (I). We already know that

$$\operatorname{Im}\Psi_{j+}(z) = \Psi_{j+}(z), \quad z \in L_j, \tag{4.209}$$

as it follows from (G)–(ii) and (H)–(ii). The derivative of Ψ_{j+} is, up to a sign, equal to $\xi_{2+} - \xi_{3+}$, which does not vanish along L_j. Combining with (4.209) we learn that $\operatorname{Im}\Psi_{j+}$ is monotone along L_j. Taking into account that L_j extends

to ∞ with angle $\pi - 2j\pi/3$ and using the asymptotics (4.27), we learn

$$\begin{aligned}\Psi_{j+}(z) &= \epsilon\frac{4}{3}z^{3/2} + \mathcal{O}(z^{1/2}) \\ &= -\frac{4i}{3}|z|^{3/2} + \mathcal{O}(z^{1/2}), \qquad \text{as } z \to \infty \text{ along } L_j,\end{aligned}$$

where $\epsilon = -1$ for $j = 0, 1$ and $\epsilon = 1$ for $j = 2$. In virtue of the previous comments, this is enough to conclude (G)–(ii) and (H)–(ii). □

The jump matrix J_T can then be rewritten as

$$J_T(z) = \begin{cases} \begin{pmatrix} e^{-n\Phi_{j+}(z)} & 1 & 0 \\ 0 & e^{-n\Phi_{j-}(z)} & 0 \\ 0 & 0 & 1 \end{pmatrix}, & z \in \Sigma_{*,j},\ j = 0, 1, 2, \\ \begin{pmatrix} 1 & e^{n\Phi_j(z)} & 0 \\ 0 & 1 & 0 \\ 0 & 0 & 1 \end{pmatrix}, & z \in \Sigma_j \setminus \Sigma_{*,j},\ j = 0, 1, 2, \\ \begin{pmatrix} 1 & 0 & 0 \\ 0 & \omega^2 e^{-n(\Psi_{0+}(z)+\alpha_0)} & 1 \\ 0 & 0 & \omega e^{-n(\Psi_{0-}(z)-\alpha_0)} \end{pmatrix}, & z \in L_0, \\ \begin{pmatrix} 1 & 0 & 0 \\ 0 & \omega^2 e^{-n(\Psi_j(z)-\alpha_j)} & 1 \\ 0 & 0 & \omega e^{n(\Psi_j(z)-\alpha_j)} \end{pmatrix}, & z \in L_j, \quad j = 1, 2, \end{cases}$$

where we set

$$\alpha_0 = \frac{2c_2}{t_0}, \quad \alpha_1 = \alpha_2 = \frac{c_2}{t_0}.$$

Remark 4.7.4. Our second transformation $X \mapsto T$ should be compared with the sequence of transformations $X \mapsto V \mapsto U \mapsto T$ in [38].

4.7.5 Opening of lenses: $T \mapsto S$

Based on the properties of the functions Φ_j, Ψ_j, we now open lenses around the contours Σ_*, L. We denote by

$$\mathscr{S} = \mathscr{S}^+ \cup \mathscr{S}^-$$

the (open) lens around the contour Σ_*, with the convention that $\mathscr{S}^+$ and $\mathscr{S}^-$ are the parts of $\mathscr{S}$ lying on the upper and lower sides of Σ_*, respectively. Furthermore, $\partial\mathscr{S}^+$ and $\partial\mathscr{S}^-$ denote the parts of the boundary of $\mathscr{S}$ lying on the upper and lower sides of Σ_*, respectively. In addition, we assume that $\partial\mathscr{S}$ intersects $\Sigma_{*,j}$ only at the endpoint z_j and, moreover, $\partial\mathscr{S}^\pm$ is chosen so that it intersects the contour L_j, $j = 0, 1, 2$, at a point other than z_*. We also set $\mathscr{S}_j^\pm$ and $\partial\mathscr{S}_j^\pm$ to be the parts of $\mathscr{S}^\pm$ and $\partial\mathscr{S}^\pm$ on the $\pm$-sides of $\Sigma_{*,j}$, $j = 0, 1, 2$, respectively. We refer the reader to Figure 4.30 for a depiction of this lens.

We claim that the lens $\mathscr{S}$ can be chosen so that

$$\operatorname{Re}\Phi_j(z) > 0, \quad z \in \partial\mathscr{S}_j^\pm \setminus \{z_j\}, \quad j = 0, 1, 2. \tag{4.210}$$

To see this, we use Proposition 4.7.3 (F) and the Cauchy-Riemann equations to get that $\operatorname{Re}\Phi_j$ is increasing in both normal directions to $\Sigma_{*,j}$. Taking into account that $\operatorname{Re}\Phi_{j\pm} = 0$ along $\Sigma_{*,j}$ (see Proposition 4.7.3 (A)–(v) and (B)–(v)) and reducing $\mathscr{S}$ if necessary, (4.210) follows.

In the very same spirit, we construct the lens

$$\mathscr{L} = \mathscr{L}^+ \cup \mathscr{L}^-$$

around L, where $\mathscr{L}^\pm$ denotes the part of $\mathscr{L}$ on the $\pm$-side of L, and as before we use $\partial\mathscr{L}^\pm$ to denote the part of the boundary of $\mathscr{L}$ that is on the $\pm$-side of L, and $\mathscr{L}_j^\pm$, $\partial\mathscr{L}_j^\pm$ to denote the respective parts of $\mathscr{L}^\pm$, $\partial\mathscr{L}^\pm$ on the $\pm$-sides of L_j, $j = 0, 1, 2$. We additionally assume that $\partial\mathscr{L}_j^\pm$ does not intersect L_j and for some $\varepsilon > 0$ small,

$$\arg z \to \pi - \frac{2\pi i}{3} j \pm \varepsilon, \qquad \text{as } z \to \infty \text{ along } \partial\mathscr{L}_j^\pm.$$

In an analogous manner as in (4.210), we claim that $\mathscr{L}$ can be chosen so that

$$\begin{aligned} \operatorname{Re}\Psi_0(z) > 0, &\quad z \in \partial\mathscr{L}_0^\pm, \\ \pm\operatorname{Re}\Psi_j(z) > 0, &\quad z \in \partial\mathscr{L}_j^\pm, \ j = 1, 2. \end{aligned} \tag{4.211}$$

Indeed, similarly as before we combine Cauchy-Riemann equations and Proposition 4.7.3 (I) to conclude that $\operatorname{Re}\Psi_j$ is increasing in the direction normal to L_j (pointing towards the positive side of L_j). Taking into account that $\operatorname{Re}\Psi_{j+} = 0$ along L_j (see (G)–(ii) and (H)–(ii)), Ψ_j is continuous along L_j for $j = 1, 2$ (see (H)–(i)) and reducing $\mathscr{L}$ if necessary, this leads to the inequalities in (4.211) on $\partial\mathscr{L}_j^\pm$, $j = 1, 2$, and also on $\partial\mathscr{L}_0^+$. Finally, the inequality for $\partial\mathscr{L}_0^-$ then follows from the inequality on $\partial\mathscr{L}_0^+$ and the jump condition (G)–(i).

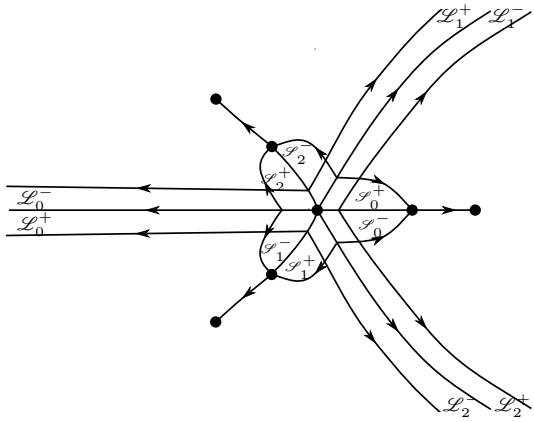

Figure 4.30: Lenses $\mathscr{S}$, $\mathscr{L}$ determining the contour Σ_S.

The lips $\partial\mathscr{S}_j^\pm$, $\partial\mathscr{L}_j^\pm$ of the lenses are oriented outwards, that is, towards ∞, see Figure 4.30.

We are finally ready to open lenses. Set

$$S = T\times$$

$$\begin{cases} I, & \text{on } \mathbb{C}\setminus(\mathscr{S}\cup\mathscr{L}),\\ \begin{pmatrix} 1 & 0 & 0\\ \mp e^{-n\Phi_j} & 1 & 0\\ 0 & 0 & 1\end{pmatrix}, & \text{on } \mathscr{S}_j^\pm\setminus\mathscr{L},\\ \begin{pmatrix} 1 & 0 & 0\\ 0 & 1 & 0\\ 0 & \mp\omega^\mp e^{-n(\Psi_0\pm\alpha_0)} & 1\end{pmatrix}, & \text{on } \mathscr{L}_0^\pm\setminus\mathscr{S},\\ \begin{pmatrix} 1 & 0 & 0\\ 0 & 1 & 0\\ 0 & \mp\omega^\mp e^{\mp n(\Psi_j-\alpha_j)} & 1\end{pmatrix}, & \text{on } \mathscr{L}_j^\pm\setminus\mathscr{S},\ j\neq 0.\\ \begin{pmatrix} 1 & 0 & 0\\ \pm e^{-n\Phi_{\pm1}} & 1 & 0\\ \omega^\pm e^{-n(\Psi_0+\Phi_{\pm1}\pm\alpha_0)} & \mp\omega^\mp e^{-n(\Psi_0\pm\alpha_0)} & 1\end{pmatrix}, & \text{on } \mathscr{L}_0^\pm\cap\mathscr{S}_{\pm1}^\mp \end{cases} \tag{4.212}$$

and

$$S = T\times \begin{pmatrix} 1 & 0 & 0 \\ \pm e^{-n\Phi_{j\pm1}} & 1 & 0 \\ \omega^{\pm} e^{\mp n(\Psi_j \pm \Phi_{j\pm1} - \alpha_j)} & \mp\omega^{\mp} e^{\mp n(\Psi_j - \alpha_j)} & 1 \end{pmatrix}, \quad \text{on } \mathscr{L}_j^{\pm} \cap \mathscr{S}_{j\pm1}^{\mp},\ j \neq 0, \tag{4.213}$$

where $\omega^+ = \omega$, $\omega^- = \omega^{-1} = \omega^2$ and all indices are understood modulo 3.

Denote

$$\Gamma_S = \Sigma \cup L \cup \partial\mathscr{S} \cup \partial\mathscr{L}.$$

The matrix S satisfies the following RHP.

- $S : \mathbb{C} \setminus \Gamma_S \to \mathbb{C}^{3\times3}$ is analytic;
- $S_+(z) = S_-(z)J_S(z)$, $z \in \Gamma_S$, where the jump matrix J_S is given by

$$J_S = \begin{cases} \begin{pmatrix} 0 & 1 & 0 \\ -1 & 0 & 0 \\ 0 & 0 & 1 \end{pmatrix}, & \text{on } \Sigma_* \\ \begin{pmatrix} 1 & 0 & 0 \\ 0 & 0 & 1 \\ 0 & -1 & 0 \end{pmatrix}, & \text{on } L \\ \begin{pmatrix} 1 & e^{n\Phi_j} & 0 \\ 0 & 1 & 0 \\ 0 & 0 & 1 \end{pmatrix}, & \text{on } \Sigma_j \setminus \Sigma_{*,j}, \\ \begin{pmatrix} 1 & 0 & 0 \\ e^{-n\Phi_j} & 1 & 0 \\ 0 & 0 & 1 \end{pmatrix}, & \text{on } \partial\mathscr{S}_j \setminus \mathscr{L}, \\ \begin{pmatrix} 1 & 0 & 0 \\ 0 & 1 & 0 \\ 0 & \omega^{\mp} e^{-n(\Psi_0 \pm \alpha_0)} & 1 \end{pmatrix}, & \text{on } \partial\mathscr{L}_0^{\pm} \setminus \mathscr{S}, \\ \begin{pmatrix} 1 & 0 & 0 \\ 0 & 1 & 0 \\ 0 & \omega^{\mp} e^{\mp n(\Psi_j + \alpha_j)} & 1 \end{pmatrix}, & \text{on } \partial\mathscr{L}_j^{\pm} \setminus \mathscr{S}, j \neq 0, \end{cases}$$

and

$$J_S = \begin{cases} \begin{pmatrix} 1 & 0 & 0 \\ e^{-n\Phi_{\pm 1}} & 1 & 0 \\ \mp e^{-n(\Psi_0+\Phi_{\pm 1}\pm\alpha_0)} & 0 & 1 \end{pmatrix}, & \text{on } \partial\mathscr{S}_{\pm 1}^{\mp} \cap \mathscr{L}, \\ \begin{pmatrix} 1 & 0 & 0 \\ e^{-n\Phi_{j\pm 1}} & 1 & 0 \\ \mp e^{\mp n(\Psi_j\pm\Phi_{j\pm 1}-\alpha_j)} & 0 & 1 \end{pmatrix}, & \text{on } \partial\mathscr{S}_{j\pm 1}^{\mp} \cap \mathscr{L}, \ j \neq 0, \\ \begin{pmatrix} 1 & 0 & 0 \\ 0 & 1 & 0 \\ \mp\omega^{\pm} e^{-n(\Psi_0+\Phi_{\pm 1}\pm\alpha_j)} & \omega^{\mp} e^{-n(\Psi_0\pm\alpha_0)} & 1 \end{pmatrix}, & \text{on } \partial\mathscr{L}_0^{\pm} \cap \mathscr{S}, \\ \begin{pmatrix} 1 & 0 & 0 \\ 0 & 1 & 0 \\ \mp\omega^{\pm} e^{\mp n(\Psi_j\pm\Phi_{j\pm 1}-\alpha_j)} & \omega^{\mp} e^{\mp n(\Psi_j-\alpha_j)} & 1 \end{pmatrix}, & \text{on } \partial\mathscr{L}_j^{\pm} \cap \mathscr{S}, \ j \neq 0; \end{cases}$$

- S has the same endpoint behavior as X when $z \to z_*, \hat{z}_j$, $j = 0, 1, 2$,
- $S(z) = (I + \mathcal{O}(z^{-1}))A(z)$, as $z \to \infty$.

The jump conditions above can be verified directly from the definition of S, once one has in hands Lemma 4.7.2 and Proposition 4.7.3. The remaining conditions on the RHP above follow directly from the RHP for T. We skip the details.

4.7.6 The global parametrix

As we will see in a moment, the jump matrix J_S converges to the identity matrix on $\Gamma_S \setminus (\Sigma_* \cup L)$. Hence, neglecting the jumps on $\Gamma_S \setminus (\Sigma_* \cup L)$, we are led to the Riemann-Hilbert problem for M, commonly called the *global parametrix*.

- $M : \mathbb{C} \setminus (\Sigma_* \cup L) \to \mathbb{C}^{3\times 3}$ is analytic;
- $M_+(z) = M_-(z)J_M(z)$, $z \in \Sigma_* \cup L$, where

$$J_M(z) = \begin{pmatrix} 0 & 1 & 0 \\ -1 & 0 & 0 \\ 0 & 0 & 1 \end{pmatrix}, \ z \in \Sigma_*, \quad J_M(z) = \begin{pmatrix} 1 & 0 & 0 \\ 0 & 0 & 1 \\ 0 & -1 & 0 \end{pmatrix}, \ z \in L; \tag{4.214}$$

- $M(z) = \mathcal{O}((z - z_j)^{-1/4})$ as $z \to z_j$, $j = 0, 1, 2$;
- M remains bounded as $z \to z_*$;
- $M(z) = (I + \mathcal{O}(z^{-1}))A(z)$ as $z \to \infty$;

We postpone the construction of the parametrix to Section 4.9.

4.7.7 The local parametrices

Denote by

$$D_\delta(z_j) = \{z \in \mathbb{C} \mid |z - z_j| < \delta\}, \quad j = 0, 1, 2,$$

the disk of radius $\delta > 0$ around z_j and set

$$D_\delta = \bigcup_{j=0}^{2} D_\delta(z_j). \tag{4.215}$$

For $\delta > 0$ sufficiently small, we search for a matrix P, called the *local parametrix*, solution to the following RHP.

- $P : D_\delta \setminus \Gamma_S \to \mathbb{C}^{3\times 3}$ is analytic;
- $P_+(z) = P_-(z)J_S(z)$, $z \in \Gamma_S \cap D_\delta$;
- $P(z) = (I + \mathcal{O}(n^{-1}))M(z)$, as $n \to \infty$ uniformly for $z \in \partial D_\delta$, where M is the global parametrix constructed in Section 4.7.6;

Note that the non trivial jumps for P only come on the upper left 2×2 corner of J_S, so this is essentially a 2×2 RHP.

As we are in the three-cut case $(t_0, t_1) \in \mathcal{F}_1$, the function Φ_j has order of vanishing $3/2$ at z_j, that is,

$$\Phi_j(z) = \text{const} \times (z - z_j)^{\frac{3}{2}}(1 + \mathcal{O}(z - z_j)^{1/2}), \quad \text{as } z \to z_j, \quad j = 0, 1, 2,$$

and the local parametrix can be constructed out of Airy functions, see for instance [50]. We skip this construction here.

4.7.8 Final transformation: $S \mapsto R$

We arrived at the final step of our analysis. For D_δ as in (4.215) and M and P the global and local parametrices considered in Sections 4.7.6 and 4.7.7, respectively, we make the final transformation

$$R(z) = \begin{cases} S(z)M(z)^{-1}, & z \in \mathbb{C} \setminus (\Gamma_S \cup D_\delta), \\ S(z)P(z)^{-1}, & z \in D_\delta \setminus \Gamma_S. \end{cases} \tag{4.216}$$

Since the jumps of M and P coincide with the jumps of S on $\Sigma_* \cup L$ and $\Gamma_S \cap D_\delta$, respectively, it follows that R satisfies a RHP on the contour

$$\Gamma_R = \partial D_\delta \cup (\Gamma_S \setminus (D_\delta \cup L \cup \Sigma_*)),$$

where each piece of ∂D_δ is oriented in the clockwise direction, see Figure 4.31. More precisely,

- $R : \mathbb{C} \setminus \Gamma_R \to \mathbb{C}^{3\times 3}$ is analytic;
- $R_+(z) = R_-(z)J_R(z)$, $z \in \Gamma_R$, where

$$J_R(z) = \begin{cases} M(z)J_S(z)M(z)^{-1}, & z \in \Gamma_R \setminus \partial D_\delta, \\ P(z)M(z)^{-1}, & z \in \partial D_\delta. \end{cases}$$

- $R(z) = I + \mathcal{O}(z^{-1}), \quad z \to \infty.$

It follows from (4.210), (4.211) and the definition of the jump J_S that for some positive constant c,

$$J_R(z) = I + \mathcal{O}(e^{-nc}), \quad z \in \Gamma_R \setminus \partial D_\delta,$$

whereas from the RHP for P it follows that

$$J_R(z) = I + \mathcal{O}(n^{-1}), \quad z \in \partial D_\delta,$$

where the implicit terms in the last two formulas above are uniform in z. As a consequence [50], we conclude that for n large enough the RHP for R is uniquely solvable and

$$R(z) = I + \mathcal{O}\left(\frac{1}{n(1+|z|)}\right), \quad n \to \infty, \tag{4.217}$$

uniformly on $\mathbb{C} \setminus \Gamma_R$.

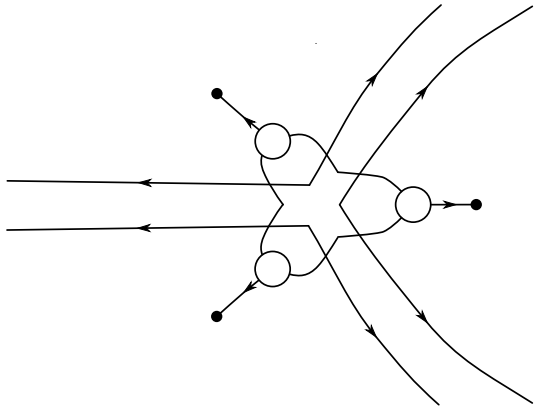

Figure 4.31: Contour Σ_R for the jump of the RHP for R.

Thus we can invert the series of transformations performed

$$Y \mapsto X \mapsto T \mapsto S \mapsto R$$

to conclude that the RHP for Y is uniquely solvable and, moreover, translate (4.217) into asymptotic information about Y (see Section 4.10 below for an example) concluding the steepest descent analysis.

4.8 Riemann-Hilbert analysis in the one-cut case

We proceed to the Riemann-Hilbert/Steepest Descent analysis in the one-cut case $(t_0, t_1) \in \mathcal{F}_2$. We do not give much details, and mostly highlight the main differences comparing to the three-cut case carried out in Section 4.7. The focus is on the jumps and parametrices, the remaining aspects of the steepest descent analysis are the same as in the three-cut case.

Following Theorem 4.2.9, for $(t_0, t_1) \in \mathcal{F}_2$ we denote $\Sigma_* = [z_1, z_0]$. The first step is to define the contours Σ and L in the same spirit as (4.189) and (4.198). As before, these are defined taking into account the critical graph of the quadratic differential ϖ. The parts of Σ and L lying on the real line are defined by

$$\Sigma_0 = [z_2, \hat{z}_0], \quad L_0 = (-\infty, z_2] = \pi\left(\gamma_1(z_2^{(1)})\right).$$

To construct Σ_1, Σ_2, L_1 and L_2, we rely on the critical graph of ϖ. For $\pi : \mathcal{R} \to \overline{\mathbb{C}}$ the canonical projection and $\mathcal{S}_3$ the strip domain determined by the condition that $\hat{z}_2^{(3)}$ and $z_2^{(3)}$ are the critical points on its boundary (see

Figure 4.25), we consider an oriented contour Σ_2 from z_2 to $\hat{z}_2$, contained in the upper half plane, and satisfying

$$\Sigma_2 \setminus \{z_2, \hat{z}_2\} \subset \pi\left(\mathcal{S}_3 \cap \mathcal{R}_3\right), \tag{4.218}$$

and set $\Sigma_1 = (\Sigma_2)^*$, $\Sigma = \Sigma_0 \cup \Sigma_1 \cup \Sigma_2$. Furthermore, define

$$L_1 = \pi\left(\gamma_0(z_2^{(1)})\right), \quad L_2 = (L_1)^* = \pi\left(\gamma_2(z_2^{(1)})\right), \tag{4.219}$$

and then set $L = L_0 \cup L_1 \cup L_2$, see Figure 4.32. Choosing Σ_1 and Σ_2 appropriately, we can also be sure that $L \cap \Sigma = \{z_2\}$.

For this choice of Σ, we consider the diagonal sequence of multiple orthogonal polynomials $(P_{n,n})$ in Definition 4.2.12. As before, such polynomials can be alternatively characterized by (4.195). Furthermore, assuming n even as before, $P_{n,n}$ is alternatively described by the Riemann-Hilbert problem Y given in Section 4.7.2.

As in the three-cut situation, the contour L defined above splits the complex plane into three regions G_0, G_1, G_2, where G_j contains the point $\hat{z}_j$, $j = 0, 1, 2$. The first transformation $Y \mapsto X$ is exactly the same as in Section 4.7.3, see Figure 4.33 for a display of the jump contours.

The second transformation $X \mapsto T$ is also similar as for the three-cut case. The only difference is concerned the starting points of integration in the definition of the g-functions.

More precisely, we define

$$\begin{aligned} g_1(z) &= \int_{z_0}^{z} \xi_1(s)ds + c_1, \qquad z \in \mathbb{C} \setminus (-\infty, z_0), \\ g_2(z) &= \int_{z_2}^{z} \xi_2(s)ds + c_2, \qquad z \in \mathbb{C} \setminus (-\infty, z_2), \\ g_3(z) &= \int_{z_0}^{z} \xi_3(s)ds + c_3, \qquad z \in \mathbb{C} \setminus (-\infty, z_0), \end{aligned} \tag{4.220}$$

where

$$c_1 = c_3 = \int_{z_2}^{z_0} \xi_{3-}(s)ds, \quad c_2 = -\pi i t_0.$$

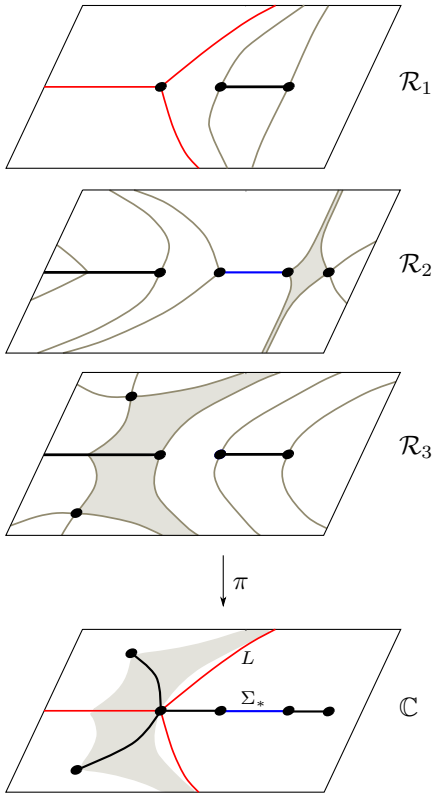

Figure 4.32: Illustration of properties (4.218) and (4.219). The trajectories highlighted on $\mathcal{R}$ in blue and red are projected onto $\mathbb{C}$ to the contours Σ_*, L, also respectively represented in blue and red. Σ_* is the interval in blue color, whereas L consists of the pieces projected from $\mathcal{R}_1$. In addition to the pieces on the real line, we extend Σ_* to Σ by constraining $\Sigma \setminus (\Sigma_* \cup \mathbb{R})$ to lie within the shaded region on $\mathbb{C}$, which consists of the projections of the gray strip domains on $\mathcal{R}$. The arcs of $\Sigma \setminus \Sigma_*$ on the complex plane are depicted in black.

As in (4.204), g_1, g_2 and g_3 admit the asymptotic expansion

$$g_1(z) = V(z) + l_1 + t_0 \log z + \mathcal{O}(z^{-1}),$$

$$g_2(z) = -\frac{2}{3}(z - t_1)^{3/2} + l_2 - \frac{t_0}{2} \log z + \mathcal{O}(z^{-1/2}), \qquad z \to \infty,$$

$$g_3(z) = \frac{2}{3}(z - t_1)^{3/2} + l_3 - \frac{t_0}{2} \log z + \mathcal{O}(z^{-1/2}),$$

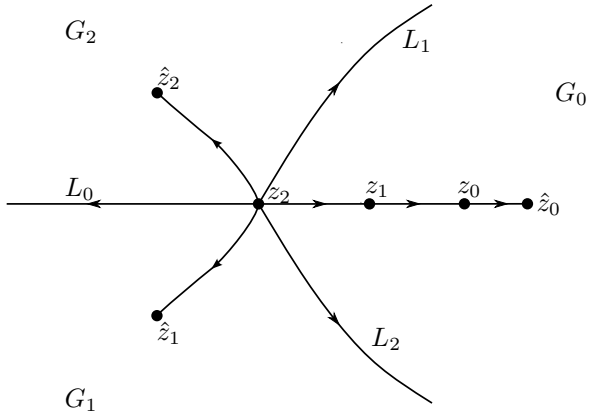

Figure 4.33: Contour $\Sigma \cup L$ for the RHP's for X and T, and the sectors G_0, G_1, G_2.

and the proof of Lemma 4.7.2 carries over without any essential modification, leading to $l_2 = l_3$ and $c_2 = i \operatorname{Im} c_3$.

For the g-functions as in (4.220), we make the transformation $X \mapsto T$ as in (4.206). The resulting RH-problem characterizing T is similar to the one presented in Section 4.7.4. The jump contour is given by $\Sigma \cup L$, see Figure 4.33 and, after simplifications, its jump matrix J_T reduces to

$$J_T = \begin{cases} \begin{pmatrix} e^{\frac{n}{t_0}(g_{1-}-g_{1+})} & 1 & 0 \\ 0 & e^{\frac{n}{t_0}(g_{3-}-g_{3+})} & 0 \\ 0 & 0 & 1 \end{pmatrix}, & \text{on } (z_1, z_0), \\ \begin{pmatrix} 1 & e^{\frac{n}{t_0}(g_{1-}-g_{3+})} & 0 \\ 0 & 1 & 0 \\ 0 & 0 & 1 \end{pmatrix}, & \text{on } (z_2, z_1) \cup (z_0, \hat{z}_0), \\ \begin{pmatrix} 1 & e^{\frac{n}{t_0}(g_1-g_2)} & 0 \\ 0 & 1 & 0 \\ 0 & 0 & 1 \end{pmatrix}, & \text{on } \Sigma_1 \cup \Sigma_2, \\ \begin{pmatrix} 1 & 0 & 0 \\ 0 & \omega^2 e^{\frac{n}{t_0}(g_{2-}-g_{2+})} & 1 \\ 0 & 0 & \omega e^{\frac{n}{t_0}(g_{3-}-g_{3+})} \end{pmatrix}, & \text{on } L_0, \\ \begin{pmatrix} 1 & 0 & 0 \\ 0 & \omega^2 e^{\frac{n}{t_0}(g_3-g_2)} & 1 \\ 0 & 0 & \omega e^{\frac{n}{t_0}(g_2-g_3)} \end{pmatrix}, & \text{on } L_1 \end{cases}$$

and

$$J_T = \begin{pmatrix} 1 & 0 & 0 \\ 0 & \omega^2 e^{\frac{n}{t_0}(g_2-g_3)} & 1 \\ 0 & 0 & \omega e^{\frac{n}{t_0}(g_3-g_2)} \end{pmatrix}, \quad \text{on } L_2.$$

Analogously to (4.207), (4.208), we now consider

$$\begin{aligned} \Phi_0(z) &= \frac{1}{t_0}\int_{z_0}^{z}(\xi_1(s)-\xi_3(s))ds, && z \in \mathbb{C}\setminus(-\infty, z_0), \\ \Phi_1(z) &= \frac{1}{t_0}\int_{z_1}^{z}(\xi_1(s)-\xi_3(s))ds, && z \in \mathbb{C}\setminus((-\infty, z_2)\cup(z_1,+\infty)), \\ \Phi_2(z) &= \frac{1}{t_0}\int_{z_2}^{z}(\xi_1(s)-\xi_2(s))ds + \Phi_1(z_2), && z \in \mathbb{C}\setminus((-\infty, z_2)\cup(z_1,+\infty)), \end{aligned} \tag{4.221}$$

and also

$$\Psi(z) = \frac{1}{t_0}\int_{z_2}^{z}(\xi_2(s)-\xi_3(s))ds, \quad z \in \mathbb{C}\setminus((-\infty, z_2)\cup(z_1,+\infty)).$$

The jump matrix J_T is then expressed in terms of these functions as

$$J_T(z) = \begin{cases} \begin{pmatrix} e^{-n\Phi_{0+}(z)} & 1 & 0 \\ 0 & e^{-n\Phi_{0-}(z)} & 0 \\ 0 & 0 & 1 \end{pmatrix}, & z \in (z_1, z_0), \\ \begin{pmatrix} 1 & e^{n\Phi_0(z)} & 0 \\ 0 & 1 & 0 \\ 0 & 0 & 1 \end{pmatrix}, & z \in (z_0, \hat{z}_0), \\ \begin{pmatrix} 1 & e^{n\Phi_1(z)} & 0 \\ 0 & 1 & 0 \\ 0 & 0 & 1 \end{pmatrix}, & z \in (z_2, z_1), \\ \begin{pmatrix} 1 & e^{n\Phi_2(z)} & 0 \\ 0 & 1 & 0 \\ 0 & 0 & 1 \end{pmatrix}, & z \in \Sigma_1 \cup \Sigma_2, \\ \begin{pmatrix} 1 & 0 & 0 \\ 0 & \omega^2 e^{-n\Psi_+(z)} & 1 \\ 0 & 0 & \omega e^{-\Psi_-(z)} \end{pmatrix}, & z \in L_0, \\ \begin{pmatrix} 1 & 0 & 0 \\ 0 & \omega^2 e^{-n\Psi(z)} & 1 \\ 0 & 0 & \omega e^{n\Psi(z)} \end{pmatrix}, & z \in L_1 \end{cases}$$

and

$$J_T(z) = \begin{pmatrix} 1 & 0 & 0 \\ 0 & \omega^2 e^{n\Psi(z)} & 1 \\ 0 & 0 & \omega e^{-n\Psi(z)} \end{pmatrix}, \quad z \in L_2.$$

The jump matrices above are in a suitable form for the opening of lenses. We open the lens $\mathscr{S}$ around (z_1, z_0) and denote by $\mathscr{S}^{\pm}$ the part of $\mathscr{S}$ on the $\pm$-side of (z_1, z_0), and by $\partial\mathscr{S}^{\pm}$ the component of the boundary of $\partial\mathscr{S}$ on the $\pm$-side of (z_1, z_0). Similarly, $\mathscr{L}_j^{\pm}$ denotes the part of $\mathscr{L}$ on the $\pm$-side of L_j, and $\partial L_j^{\pm}$ denotes the component of the boundary of $\mathscr{L}$ on the $\pm$-side of L_j. Additionally, we open the lens $\mathscr{L}$ in such a way that it does not intersect Σ, see Figure 4.34.

The functions Φ_0 and Φ_1 satisfy

$$\Phi_0(z) < 0, \quad z \in (z_0, \hat{z}_0], \qquad \Phi_1(z) < 0, \quad z \in [z_2, z_1). \tag{4.222}$$

Moreover, due to the construction of Σ_1, Σ_2 and L as in equations (4.218)–(4.219), we can be sure that (after reducing the lenses if necessary)

$$\begin{aligned} &\operatorname{Re}\Phi_0(z) > 0, \quad z \in \partial\mathscr{S}^{\pm} \setminus \{z_0, z_1\}, \\ &\operatorname{Re}\Phi_2(z) < 0, \quad z \in \Sigma_1 \cup \Sigma_2, \\ &\operatorname{Re}\Psi(z) > 0, \quad z \in \partial\mathscr{L}_0^{\pm} \setminus \{z_2\}, \\ &\pm\operatorname{Re}\Psi(z) > 0, \quad z \in \partial\mathscr{L}_1^{\pm} \setminus \{z_2\}, \\ &\mp\operatorname{Re}\Psi(z) > 0, \quad z \in \partial\mathscr{L}_2^{\pm} \setminus \{z_2\}. \end{aligned} \tag{4.223}$$

These conditions will assure the jumps for the next transformation have the right decaying properties. We stress that due to the constant $\Phi_1(z_2)$ in the definition of Φ_2 in (4.221), the strict inequality $\operatorname{Re}\Phi_2 < 0$ also holds true at the endpoint z_2 of Σ_1 and Σ_2.

We then set

$$S(z) = T(z), \quad z \text{ outside the lenses } \mathscr{S} \cup \mathscr{L},$$

and on the lenses

$$S(z) = T(z) \times \begin{cases} \begin{pmatrix} 1 & 0 & 0 \\ \mp e^{-n\Phi_0(z)} & 1 & 0 \\ 0 & 0 & 1 \end{pmatrix}, & z \in \mathscr{S}^{\pm}, \\ \begin{pmatrix} 1 & 0 & 0 \\ 0 & 1 & 0 \\ 0 & \mp\omega^{\mp} e^{-n\Psi(z)} & 1 \end{pmatrix}, & z \in \mathscr{L}_0^{\pm} \end{cases}$$

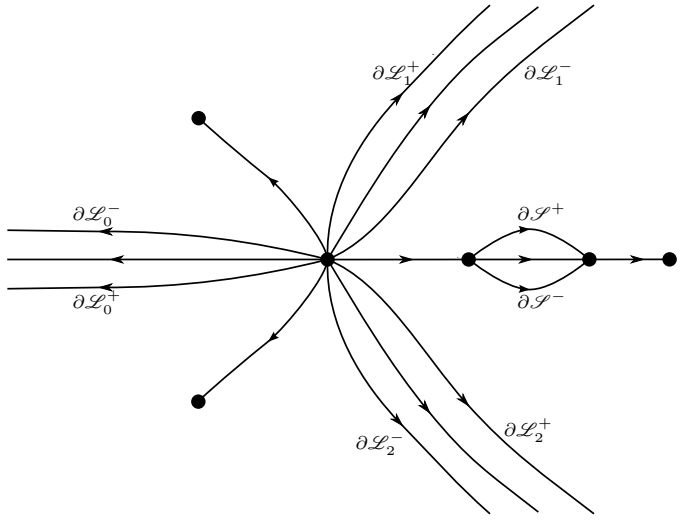

Figure 4.34: The boundary components of the lenses $\mathscr{S}$, $\mathscr{L}$ determining the contour Γ_S for S.

and

$$S(z) = T(z) \times \begin{cases} \begin{pmatrix} 1 & 0 & 0 \\ 0 & 1 & 0 \\ 0 & \mp\omega^{\mp} e^{\mp n\Psi(z)} & 1 \end{pmatrix}, & z \in \mathscr{L}_1^{\pm}, \\ \begin{pmatrix} 1 & 0 & 0 \\ 0 & 1 & 0 \\ 0 & \mp\omega^{\mp} e^{\pm n\Psi(z)} & 1 \end{pmatrix}, & z \in \mathscr{L}_2^{\pm}. \end{cases}$$

Then S satisfies a Riemann-Hilbert problem on the contour Γ_S shown in Figure 4.34. The jump matrix J_S coincides with J_T outside the lenses, and on the remaining parts of Γ_S it is given by

$$J_S(z) = \begin{cases} \begin{pmatrix} 0 & 1 & 0 \\ -1 & 0 & 0 \\ 0 & 0 & 1 \end{pmatrix}, & z \in (z_1, z_0), \\ \begin{pmatrix} 1 & 0 & 0 \\ 0 & 0 & 1 \\ 0 & -1 & 0 \end{pmatrix}, & z \in L \end{cases}$$

and

$$J_S(z) = \begin{cases} \begin{pmatrix} 1 & 0 & 0 \\ e^{-n\Phi_0(z)} & 1 & 0 \\ 0 & 0 & 1 \end{pmatrix}, & z \in \partial\mathscr{S}^{\pm}, \\ \begin{pmatrix} 1 & 0 & 0 \\ 0 & 1 & 0 \\ 0 & \omega^{\mp}e^{-n\Psi(z)} & 1 \end{pmatrix}, & z \in \partial\mathscr{L}_0^{\pm}, \\ \begin{pmatrix} 1 & 0 & 0 \\ 0 & 1 & 0 \\ 0 & \omega^{\mp}e^{\mp n\Psi(z)} & 1 \end{pmatrix}, & z \in \partial\mathscr{L}_1^{\pm}, \\ \begin{pmatrix} 1 & 0 & 0 \\ 0 & 1 & 0 \\ 0 & \omega^{\mp}e^{\pm n\Psi(z)} & 1 \end{pmatrix}, & z \in \partial\mathscr{L}_2^{\pm}. \end{cases}$$

The next step is the construction of the parametrices. In virtue of (4.222)–(4.223), the jump matrix J_S is exponentially small on the lipses of the lenses as well as in $\Sigma \setminus [z_1, z_0]$, as long as we stay away from the endpoints z_0, z_1, z_2. Near z_2, the jumps for S on Σ are still exponentially small, so for the local parametrix near z_2 we only have to take into account the jumps coming from L and $\partial\mathscr{L}$.

More concretely,

- The RHP for the global parametrix M is essentially the same as in Section 4.7.6, having in mind that $\Sigma_* = (z_1, z_0)$. We refer to Section 4.9.3 for details.
- The local parametrices near z_0, z_1 are constructed out of Airy functions in exactly the same way as in Section 4.7.7. A little more care should be taken for the parametrix near z_2. As we already observed, the jumps for S on Σ near z_2 are exponentially small, so we neglect them for the construction of the local parametrix near z_2. Hence the jump condition on $D_\delta(z_2)$ becomes

$$P_+(z) = P_-(z)J_S(z), \quad z \in D_\delta(z_2) \cap (L \cup \partial\mathscr{L}),$$

see Figure 4.35 for the jump contours of P near z_2. The remaining RHP is essentially 2×2. Although there are nine rays emanating from z_2 instead of the usual four rays, this parametrix is still constructed out of Airy functions, see for instance [95].

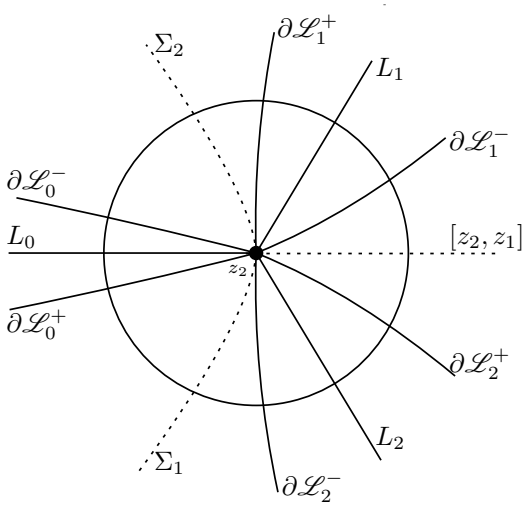

Figure 4.35: Blow up of the jump contours for S near z_2. The solid lines represent L and $\partial\mathscr{L}$, so these are contours for the jumps of the local parametrix P. The dashed lines represent Σ, and since J_S is exponentially small in these contours, they are not taken into account for the construction of P near z_2, so P is analytic across these contours.

The final transformation $S \mapsto R$ is similar as in Section 4.7.8, equation (4.216). The contour Σ_R for R is displayed in Figure 4.36.

As in the three-cut case, it turns out that the jump matrix J_R is close to the identity as $n \to \infty$: on the lipses of the lenses $\mathscr{S}$ and $\mathscr{L}$, this is true because of (4.222)–(4.223), whereas on the boundary of D_δ, this is true from the construction of the local parametrix. We only have to be careful about the jumps inside $D_\delta(z_2)$ that are not canceled by the local parametrix, which are given by

$$J_R(z) = P(z)J_S(z)P(z)^{-1} = P(z)J_T(z)P(z)^{-1}, \quad z \in \Sigma \cap D_\delta(z_2).$$

Since P is bounded near z_2, the second inequality in (4.223) together with the identity above assure us that J_R is exponentially small for $z \in \Sigma \cap D_\delta(z_2)$.

As the final outcome, we get that the jump matrix J_R satisfies

$$J_R(z) = I + \mathcal{O}(n^{-1}), \quad n \to \infty,$$

uniformly in J_R, and the analysis is concluded in a similar fashion as in Section 4.7.8.

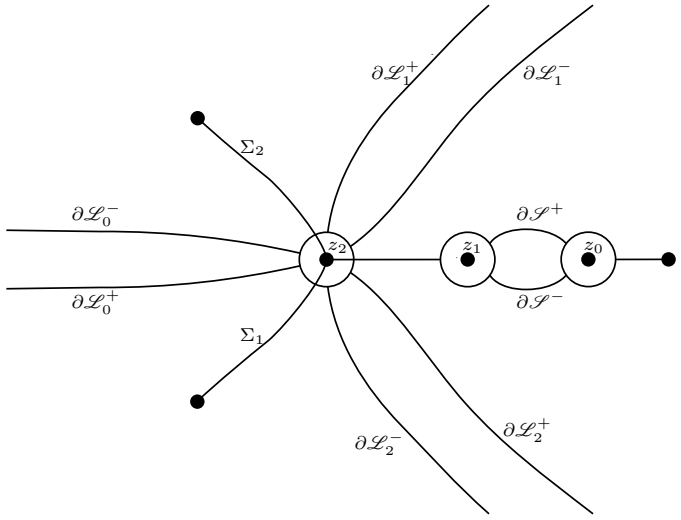

Figure 4.36: Contours for the jumps of R.

4.9 Construction of the global parametrix

In this section we prove the existence of the global parametrix in the three-cut and one-cut cases. We also construct its first row explicitly.

It is convenient to perform a regluing of the sheets forming the Riemann surface $\mathcal{R}$, in much the same spirit as used for $t_1 = 0$ in Section 4.5.1.

To do so, recall the definition of the contours L_1 and L_2 given in (4.198) and (4.219) in the three-cut and one-cut cases, respectively, which defined the sector G_0 containing the point z_0, as shown in Figures 4.29 and 4.33.

We construct a new Riemann surface

$$\widetilde{\mathcal{R}} = \widetilde{\mathcal{R}}_1 \cup \widetilde{\mathcal{R}}_2 \cup \widetilde{\mathcal{R}}_3,$$

obtained from the original surface $\mathcal{R}$ after interchanging the sectors $\pi^{-1}(G_0)\cap\mathcal{R}_2$ and $\pi^{-1}(G_0)\cap\mathcal{R}_3$. Thus the sheets $\widetilde{\mathcal{R}}_1$ and $\widetilde{\mathcal{R}}_2$ are connected crosswise along Σ_* and the sheets $\widetilde{\mathcal{R}}_2$ and $\widetilde{\mathcal{R}}_3$ are connected crosswise along L. In the three-cut case, the branch points of $\widetilde{R}$ are

$$z_j^{(1)} = z_j^{(2)},\ j = 0, 1, 2, \qquad \infty^{(2)} = \infty^{(3)},$$

whereas in the one-cut case the branch points are

$$z_j^{(1)} = z_j^{(2)},\ j = 0, 1, \qquad z_2^{(2)} = z_2^{(3)}, \qquad \infty^{(2)} = \infty^{(3)}.$$

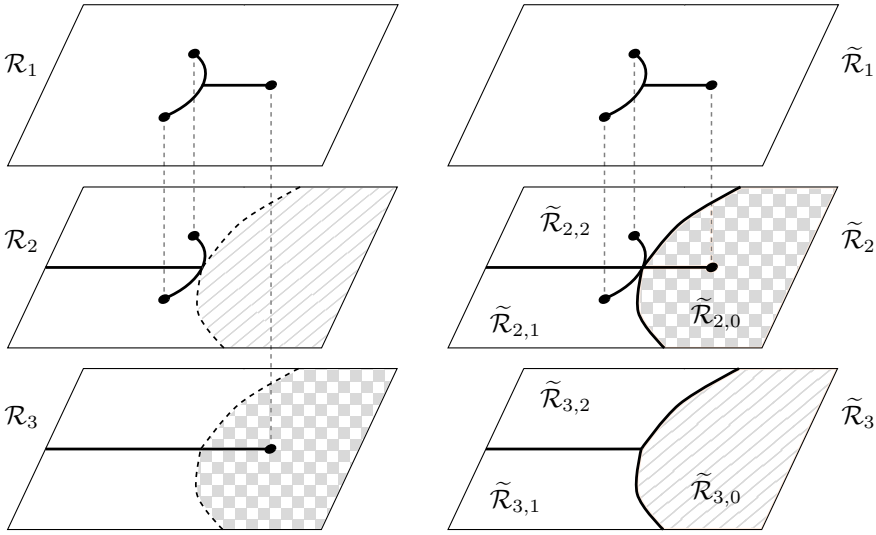

Figure 4.37: The sheet structure for $\mathcal{R}$ (left panel) and $\widetilde{\mathcal{R}}$ (right panel) in the three-cut case. The dashed lines on $\mathcal{R}_2$ and $\mathcal{R}_3$ are the (preimages through π of) the curves L_1 and L_2. They bound the shaded areas, which are interchanged between the sheets to create the new sheets $\widetilde{\mathcal{R}}_2$ and $\widetilde{\mathcal{R}}_3$. On the right panel we also distinguish the set $\widetilde{\mathcal{R}}_{j,k}$'s defined in (4.224).

We also denote

$$\widetilde{\mathcal{R}}_{j,k} = \pi^{-1}(G_k) \cap \mathcal{R}_j, \quad j = 1, 2,\ k = 0, 1, 2, \tag{4.224}$$

and refer to Figures 4.37 and 4.38 for a depiction of the regluing and the sets (4.224) in the three-cut and one-cut cases, respectively.

It is also convenient to denote by $\Sigma_{*,+}^{(k)}$ and $\Sigma_{*,-}^{(k)}$ the positive and negative sides of the cut Σ_* on the sheet $\widetilde{\mathcal{R}}_k$. Ditto for the other quantities $\Sigma_{*,j,\pm}^{(k)}$, $L_{\pm}^{(k)}$ and $L_{j,\pm}^{(k)}$. In particular, note that

$$\Sigma_{*,\pm}^{(1)} = \Sigma_{*,\mp}^{(2)}, \quad L_{\pm}^{(2)} = L_{\mp}^{(3)}.$$

We orient each arc of $\Sigma_*^{(k)}$ and $L^{(k)}$ according to the orientation induced from their projection Σ_* and L. Thus, for instance, the positive side of $\Sigma_{*,+}^{(1)}$ lies on the sheet $\widetilde{\mathcal{R}}_1$, whereas the negative side of $\Sigma_{*,+}^{(1)}$ lies on the sheet $\widetilde{\mathcal{R}}_2$.

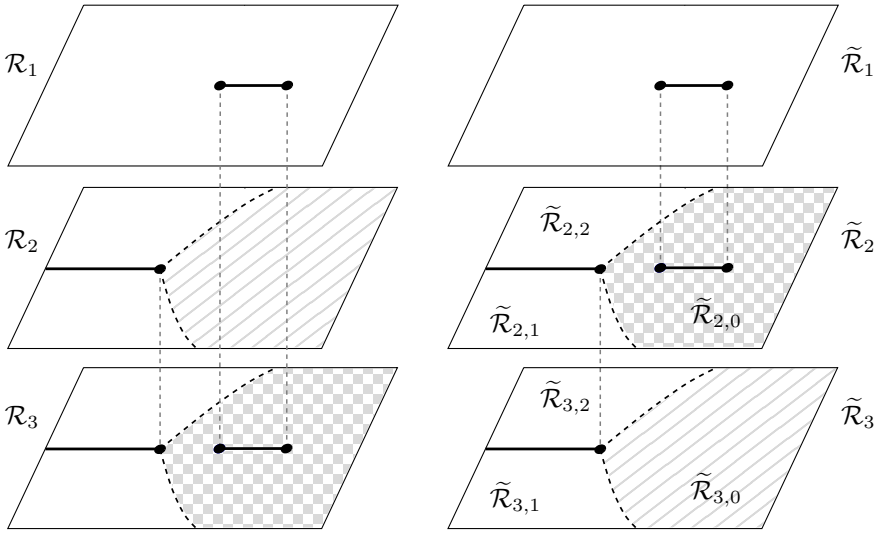

Figure 4.38: The sheet structure for $\mathcal{R}$ (left panel) and $\widetilde{\mathcal{R}}$ (right panel) in the one-cut case. The dashed lines on $\mathcal{R}_2$ and $\mathcal{R}_3$ are the (preimages through π of) the curves L_1 and L_2. They bound the shaded areas, which are interchanged between the sheets to create the new sheets $\widetilde{\mathcal{R}}_2$ and $\widetilde{\mathcal{R}}_3$. On the right panel we also distinguish the set $\widetilde{\mathcal{R}}_{j,k}$'s defined in (4.224).

4.9.1 The inverse of the rational parametrization

According to Theorem 4.2.5, the rational function h induces the bijection (4.28) between $\overline{\mathbb{C}}$ and $\mathcal{R}$, and consequently between $\overline{\mathbb{C}}$ and $\widetilde{\mathcal{R}}$. This means that there exist three meromorphic functions

$$\psi_j : \widetilde{\mathcal{R}}_j \to \overline{\mathbb{C}}, \quad j = 1, 2, 3, \tag{4.225}$$

for which

$$\psi : \widetilde{\mathcal{R}} \to \overline{\mathbb{C}}, \quad \psi\big|_{\widetilde{\mathcal{R}}_j} = \psi_j, \ j = 1, 2, 3, \tag{4.226}$$

is the inverse of h.

Set

$$\begin{aligned} \mathcal{W}_j &= \psi(\widetilde{\mathcal{R}}_j), \quad j = 1, 2, 3, \\ \mathcal{W}_{j,k} &= \psi(\widetilde{\mathcal{R}}_{j,k}), \quad j = 2, 3, \ k = 0, 1, 2, \end{aligned} \tag{4.227}$$

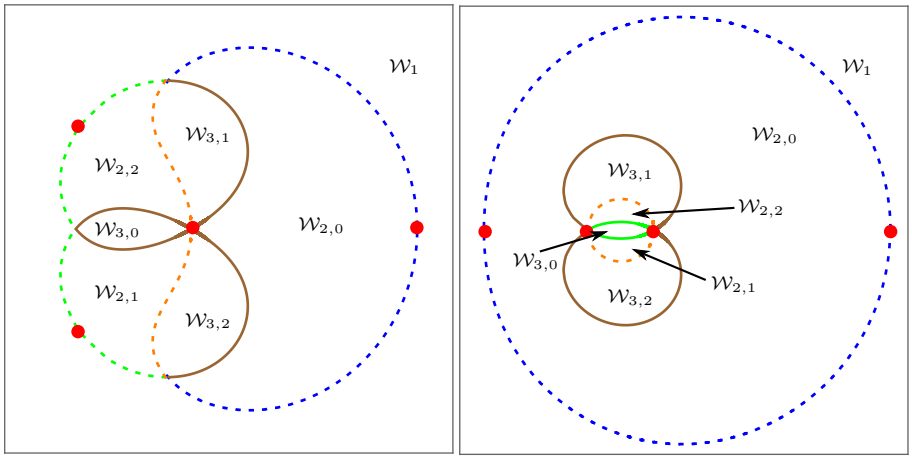

Figure 4.39: The partition of the w-plane into the sets $\mathcal{W}_{j,k}$'s in the three-cut (left panel) and one-cut (right panel) cases. The dashed lines display the inverse images of the cuts for the original Riemann surface $\mathcal{R}$ (compare with Figure 4.26), and the solid lines display the new cuts arising after the regluing that defines $\widetilde{\mathcal{R}}$. Numerical output for the choices $r = 1/20$ and $a_0 = 1/10$ (three-cut) and $a_0 = 1/4$ (one-cut).

and also

$$\begin{aligned} \Xi &= \psi(\Sigma^{(1)}_{*,+}), \\ \Lambda_j &= \psi(L^{(2)}_{j,+}), \quad j = 0, 1, 2, \\ \Lambda &= \psi(L^{(2)}_{+}) = \Lambda_0 \cup \Lambda_1 \cup \Lambda_2. \end{aligned} \tag{4.228}$$

In the three-cut case, we also define

$$\Xi_j = \psi(\Sigma^{(1)}_{*,j,+}), \ j = 0, 1, 2, \tag{4.229}$$

so that $\Xi = \Xi_1 \cup \Xi_2 \cup \Xi_3$.

Using basic properties of conformal maps, the sets (4.227)–(4.229) can be described in the w-plane. The outcome for (4.227) can be seen in Figure 4.39. The sets (4.228)–(4.229) are displayed in Figures 4.40 and 4.41 in the three-cut and one cut-cases, respectively.

Remark 4.9.1. The function ψ_1 in (4.225) is analytic in $\mathbb{C} \setminus \Sigma_*$ and maps $\mathbb{C} \setminus \Omega$ conformally to $\mathbb{C} \setminus \mathbb{D}$. Since the point $\infty^{(1)}$ on $\mathcal{R}_1$ corresponds to the point ∞ on the w-plane through ψ, we automatically get that

$$\lim_{z \to \infty} \psi_1(z) = \infty.$$

Furthermore, using the implicit function theorem,

$$\lim_{z\to\infty} \psi_1'(z) = \lim_{w\to\infty} \frac{1}{h'(w)} = \frac{1}{r}.$$

This shows that ψ_1 in (4.225) coincides with the function ψ_1 appearing in Theorem 4.2.15.

4.9.2 Construction of the global parametrix in the three-cut case

In [38], the global parametrix is constructed for $t_1 = 0$ using meromorphic differentials. In this section we reproduce their arguments to construct the parametrix in the general three-cut case.

On the Riemann surface $\widetilde{\mathcal{R}}$, consider the meromorphic differential η, defined by the condition that it has simple poles at each of the branch points $z_0^{(1)}, z_1^{(1)}, z_2^{(1)}$ and $\infty^{(2)}$, with residues

$$\operatorname{Res}(\eta, z_j^{(1)}) = -\frac{1}{2}, \quad \operatorname{Re}(\eta, \infty^{(2)}) = \frac{3}{2}, \tag{4.230}$$

and no other poles. Since the sum of residues is zero, such an η exists. It is also unique, because the genus of $\widetilde{R}$ is zero.

The set $\Sigma_{*,+}^{(1)} \cup L_+^{(2)}$ is connected and consists of a finite union of analytic arcs. Its image through the inverse ψ in (4.226) is the set $\Xi \cup \Lambda$, which can be geometrically described with standard arguments in conformal mapping, and is displayed in Figure 4.40. Since $\overline{\mathbb{C}} \setminus (\Xi \cup \Lambda)$ and $\widetilde{\mathcal{R}} \setminus (\Sigma_{*,+}^{(1)} \cup L_+^{(2)})$ are conformally equivalent, it readily follows from Figure 4.40 that the domain $\widetilde{\mathcal{R}} \setminus (\Sigma_{*,+}^{(1)} \cup L_+^{(2)}) \subset \widetilde{\mathcal{R}}$ is simply connected and does not contain poles of η. In particular, this implies that the function

$$u(p) = \int_{\infty^{(1)}}^{p} \eta, \quad p \in \widetilde{\mathcal{R}} \setminus (\Sigma_{*,+}^{(1)} \cup L_+^{(2)}),$$

where the integration goes along any path that does not cross $\Sigma_{*,+}^{(1)} \cup L_+^{(2)}$, is well defined and analytic.

From Figure 4.40 and conformal equivalence, it follows that for a given $p \in \Sigma_{*,+}^{(1)} \cup L_+^{(2)}$, we can write the difference $u_+(p) - u_-(p)$ as an integral over a closed contour going around exactly one of the branch points $z_j^{(1)}$. Consequently we learn from (4.230) and the Residues Theorem that

$$u_+(p) - u_-(p) = \pm\pi i, \quad p \in \Sigma_{*,+}^{(1)} \cup L_+^{(2)}. \tag{4.231}$$

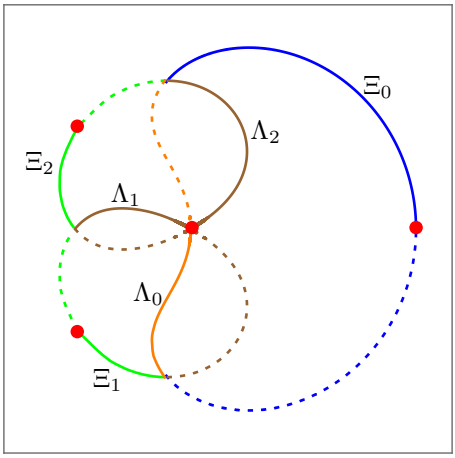

Figure 4.40: In solid lines the sets Λ_j and Ξ_j, $j = 0, 1, 2$, are displayed; these are the image through ψ of the jumps for m. In dashed lines, the remaining images through ψ of the cuts of $\widetilde{\mathcal{R}}$ are shown. The solid lines also correspond to the jump contours for f in the three-cut case. Numerical output for $r = 1/20$ and $a_0 = 1/10$.

We thus define

$$m(p) = e^{u(p)}, \quad p \in \widetilde{\mathcal{R}} \setminus \Sigma^{(1)}_{*,+} \cup L^{(2)}_{+}.$$

Note that (4.231) implies that

$$m_+(p) = -m_-(p), \quad p \in \Sigma^{(1)}_{*,+} \cup L^{(2)}_{+}. \tag{4.232}$$

Set

$$m_k = m\big|_{\widetilde{\mathcal{R}}_k}, \quad k = 1, 2, 3.$$

The functions m_1, m_2 and m_3 are analytic in $\mathbb{C} \setminus \Sigma_*$, $\mathbb{C} \setminus (\Sigma_* \cup L)$ and $\mathbb{C} \setminus L$, respectively. Combining with the condition (4.232) we immediately get that

$$\begin{aligned}(m_{1+}(z), m_{2+}(z), m_{3+}(z)) \\ = (m_{1-}(z), m_{2-}(z), m_{3-}(z)) J_M(z), \quad z \in \Sigma_* \cup L.\end{aligned} \tag{4.233}$$

In addition, (4.230) gives

$$m_k(z) = \mathcal{O}\left((z - z_j)^{-1/4}\right), \quad z \to z_j, \quad k = 1, 2, \tag{4.234}$$

and also

$$m_k(z) = \mathcal{O}(z^{-3/4}), \quad z \in \infty, \quad k = 2, 3. \tag{4.235}$$

Furthermore, since $u(\infty^{(1)}) = 0$, we also have

$$m_1(z) = 1 + \mathcal{O}(z^{-1}), \quad z \to \infty. \tag{4.236}$$

In summary, (4.233)–(4.236) tell us that the row vector (m_1, m_2, m_3) satisfies the conditions for the first row of M.

To construct the remaining rows of M, consider a basis $f_1 \equiv 1, f_2, f_3$ of the vector space of functions analytic on $\widetilde{\mathcal{R}} \setminus \{\infty^{(2)}\}$, with at most a double pole at $\infty^{(2)}$. Denote $f_{j,k} = f_j\big|_{\widetilde{\mathcal{R}}_k}$ and consider the auxiliary matrix

$$B = \begin{pmatrix} m_1 & m_2 & m_3 \\ m_1 f_{2,1} & m_2 f_{2,2} & m_3 f_{2,3} \\ m_1 f_{3,1} & m_2 f_{3,2} & m_3 f_{3,3} \end{pmatrix}. \tag{4.237}$$

Using (4.233), we learn

$$B_+(z) = B_-(z) J_M(z), \quad z \in \Sigma_* \cup L. \tag{4.238}$$

Furthermore, it follows from the analyticity of the $f_{j,k}$'s near finite points, and also the local behavior (4.234)–(4.236), that B satisfies the endpoint conditions for M.

Because $\det J_M = 1$, we also learn from (4.238) that $\det B$ is entire. Furthermore, a simple analysis of its entries shows that $B(z) = \mathcal{O}(z^{1/4})$ as $z \to \infty$. Since the functions f_1, f_2 and f_3 are linearly independent, this is enough to show that $\det B$ is equal to a non-zero constant. In particular, B is always invertible.

By inspection one can see that the function A in (4.200) satisfies $A_+ = A_- J_M$ on L, and using (4.238) we thus conclude that BA^{-1} is analytic on $\mathbb{C} \setminus \Sigma_*$. As $A(z) = \mathcal{O}(z^{1/4})$ and $B(z) = \mathcal{O}(z^{1/4})$, we see that BA^{-1} is bounded near ∞, and thus admits a series expansion of the form

$$(BA^{-1})(z) = C + \mathcal{O}(z^{-1}), \quad z \to \infty,$$

for some constant matrix C, which is non-singular because $\det A, \det B \neq 0$. We already observed that B satisfies (4.238) and also the endpoint conditions for M. It thus finally follows that

$$M(z) = C^{-1} B(z), \quad z \in \mathbb{C} \setminus (\Sigma_* \cup L)$$

is the desired global parametrix.

4.9.3 Construction of the global parametrix in the one-cut case

The Riemann-Hilbert problem for the global parametrix in the one-cut case assumes the following form.

- $M : \mathbb{C} \setminus (\Sigma_* \cup L) \to \mathbb{C}^{3\times 3}$ is analytic;
- $M_+(z) = M_-(z)J_M(z)$, $z \in \Sigma_* \cup L$, where J_M is defined as in (4.214);
- $M(z) = \mathcal{O}((z - z_j)^{-1/4})$ as $z \to z_j$, $j = 0, 1, 2$;
- $M(z) = (I + \mathcal{O}(z^{-1}))A(z)$, as $z \to \infty$.

Following the ideas carried out in Section 4.9.2, we start the construction of M from its first row.

As in Section 4.9.2, there exists a meromorphic differential η on $\widetilde{\mathcal{R}}$ uniquely defined through the conditions that it has simple poles at the branch points $z_0^{(1)}$, $z_1^{(1)}$, $z_2^{(2)}$ and $\infty^{(2)}$, with residues

$$\operatorname{Res}(\eta, z_0^{(1)}) = \operatorname{Res}(\eta, z_1^{(1)}) = \operatorname{Res}(\eta, z_2^{(2)}) = -\frac{1}{2}, \quad \operatorname{Res}(\eta, \infty^{(2)}) = \frac{3}{2}, \tag{4.239}$$

and no other poles.

We then consider the function

$$u(p) = \int_{\infty^{(1)}}^{p} \eta, \quad p \in \widetilde{\mathcal{R}} \setminus (\Sigma_{*,+}^{(1)} \cup L_{0,+}^{(2)}).$$

The image of $\Sigma_{*,+}^{(1)} \cup L_{0,+}^{(2)}$ through ψ is the set $\Xi \cup \Lambda_0$, which is shown in the left panel of Figure 4.41. From this figure and conformal equivalence, it easily follows that the set $\widetilde{\mathcal{R}} \setminus (\Sigma_{*,+}^{(1)} \cup L_{0,+}^{(2)})$ is not simply connected, and thus $u(p)$ depends on the path of integration chosen. However, in virtue of (4.239), it follows after a residue calculation that the value $u(p)$ is well defined modulo $2\pi i$. Having this in mind, it also holds true

$$u_+(p) - u_-(p) = \pi i \mod 2\pi i, \quad p \in \Sigma_{*,+}^{(1)} \cup L_{0,+}^{(2)}. \tag{4.240}$$

We then define

$$\widetilde{m}(p) = e^{u(p)}, \quad p \in \widetilde{\mathcal{R}} \setminus \Sigma_{*,+}^{(1)} \cup L_{0,+}^{(2)},$$

and also

$$m(p) = \begin{cases} -\widetilde{m}(p), & p \in \mathcal{W}_{2,2} \cup \mathcal{W}_{3,1}, \\ \widetilde{m}(p), & \text{elsewhere.} \end{cases}$$

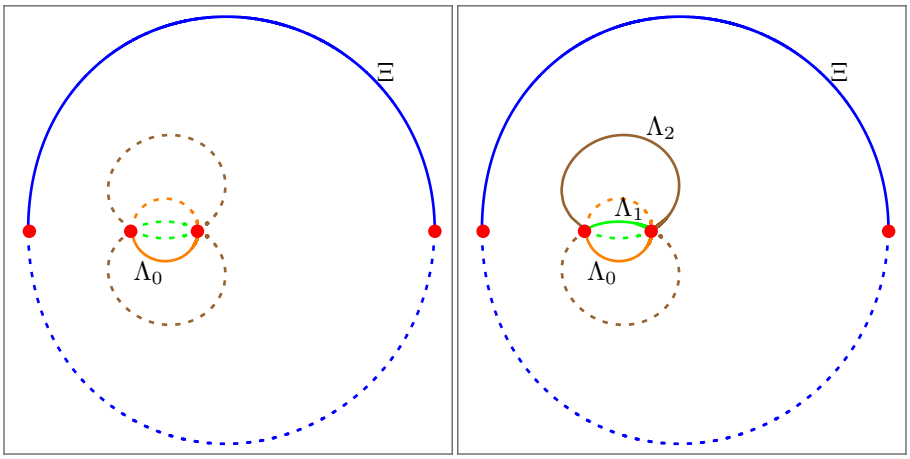

Figure 4.41: The solid lines are the images through ψ of the jumps for $\tilde{m}$ and m in the left and right panels, respectively. The dashed lines are the images of the remaining cuts. The solid lines in the right panel also correspond to the jump contours for f in the one-cut case. Numerical output for $r = 1/20$ and $a_0 = 1/4$.

The functions $\tilde{m}$ and m are analytic on $\widetilde{\mathcal{R}} \setminus (\Sigma^{(1)}_{*,+} \cup L^{(2)}_{0,+})$ and $\widetilde{\mathcal{R}} \setminus (\Sigma^{(1)}_{*,+} \cup L^{(2)}_{+})$, respectively. Furthermore, from (4.240)

$$\widetilde{m}_+(p) = -\widetilde{m}_-(p), \quad p \in \Sigma^{(1)}_{*,+} \cup L^{(2)}_{0,+},$$

and consequently, from the definition of m we get

$$m_+(p) = -m_-(p), \quad p \in \Sigma^{(1)}_{*,+} \cup L^{(2)}_{+}. \tag{4.241}$$

We refer the reader to Figure 4.41 for a display of the jump contours for $\widetilde{m}$ and m in the w-plane.

Further setting

$$m_j = m\big|_{\widetilde{\mathcal{R}}_j}, \quad j = 1, 2, 3,$$

it follows in the same way as we did in Section 4.9.2, equations (4.230)–(4.236), that the first row of the global parametrix M is (m_1, m_2, m_3). The remaining rows of M can be obtained in exactly the same way as we did in Section 4.7.6, equation (4.237) *et seq.* We skip the details.

4.9.4 Explicit construction of the first row

In Sections 4.9.2 and 4.9.3, we constructed the first row of the global parametrix in terms of the function m, which, in virtue of (4.232)–(4.236) (see also (4.241)) is unique solution to the following Riemann-Hilbert problem.

- $m : \widetilde{\mathcal{R}} \setminus (\Sigma^{(1)}_{*,+} \cup L^{(2)}_{+}) \to \mathbb{C}$ is analytic;
- $m_+(z) = -m_-(z), \ \ z \in \Sigma^{(1)}_{*,+} \cup L^{(2)}_{+}$;
- if z_j is a branch point for the sheet $\widetilde{\mathcal{R}}_k$, then

$$m_k(z) = \mathcal{O}((z - z_k)^{-1/4}), \quad z \to z_j, \tag{4.242}$$

  and as $z \to \infty$,

$$m_1(z) = 1 + \mathcal{O}(z^{-1}), \quad m_k(z) = \mathcal{O}(z^{-3/4}), \ k = 2, 3; \tag{4.243}$$

- in the three-cut case, $m_k(z)$ remains bounded as $z \to z_*$.

It turns out that the Riemann-Hilbert problem above can be solved explicitly with the help of the rational parametrization h and its inverse ψ in (4.226). If we seek for m of the form

$$f(w) = m(h(w)), \tag{4.244}$$

then it follows that f should satisfy the following scalar Riemann-Hilbert problem.

- $f : \mathbb{C} \setminus (\Xi \cup \Lambda) \to \mathbb{C}$ is analytic;
- $f_+(w) = -f_-(w)$, $w \in \Xi \cup \Lambda$;
- $f(w) \to 1$ as $w \to \infty$ and $f(w) \to 0$ as $w \to 0$.
- $f(w) = \mathcal{O}((w - w_j)^{-1/2})$ as $w \to w_j$, $j = 0, 1, 2$.

We remark that the 1/4-blow-ups for m become 1/2-blow-ups because the points z_0, z_1 and z_2 are branch points.

The jumps for f are shown in Figure 4.40 and in the right panel of Figure 4.41 for the three-cut and one-cut cases, respectively.

Thus the natural choice for f is

$$f(w) = \left(\frac{w^3}{(w - w_0)(w - w_1)(w - w_2)} \right)^{1/2}, \quad w \in \mathbb{C} \setminus (\Xi \cup \Lambda),$$

where the branch of the square root is uniquely determined by the condition that $f(w) \to 1$ as $w \to \infty$ and with branch cuts on $\Xi \cup \Lambda$.

We know that w_0, w_1 and w_2 are the zeros of h' (see Lemma 4.3.12), and consequently of the monic polynomial $\tilde{h}(w) = w^3 r^{-1} h'(w)$ as in (4.95). This means that

$$\frac{w^3}{r} h'(w) = (w - w_0)(w - w_1)(w - w_2),$$

which expresses that

$$f(w) = \left(\frac{r}{h'(w)} \right)^{1/2}. \tag{4.245}$$

From the inverse function theorem, we know that $h'(w) = 1/\psi'(z)$, where ψ is given in (4.226) and $w = \psi(z)$. Returning back to (4.245) and using (4.244), we thus get that m is given by

$$m(z) = \sqrt{r\psi'(z)}, \quad z \in \widetilde{\mathcal{R}} \setminus (\Sigma^{(1)}_{*,+} \cup L^{(2)}_{+}).$$

Recalling (4.226), we finally arrive at the expressions for the first line (m_1, m_2, m_3) of M, namely

$$m_j(z) = \sqrt{r\psi_j'(z)}, \quad j = 1, 2, 3, \tag{4.246}$$

where the branch cuts for the square root of ψ_1, ψ_2 and ψ_3 are determined from the ones in (4.245). In particular, the branch cut for m_1 is taken on Σ_*.

4.10 Proofs of Theorems 4.2.14 and 4.2.15

We now prove Theorems 4.2.14 and 4.2.15. The arguments are valid both in the three-cut and one-cut cases.

Proof of Theorem 4.2.15. Unfolding the transformations in the Riemann-Hilbert analysis, we get in particular

$$\begin{aligned} P_{n,n}(z) &= Y_{1,1}(z) \\ &= X_{1,1}(z) \\ &= T_{1,1}(z) e^{\frac{n}{t_0}(g_1(z) - V(z) - l_1)}, \quad z \in \mathbb{C} \setminus \Sigma, \end{aligned}$$

we refer to (4.196), (4.199) and (4.206) for the three-cut case, and remind that these transformations are the same in the one-cut case (with the appropriate

definition of the function g_1). For any fixed compact $K \subset \mathbb{C} \setminus \Sigma_*$, we can reduce the lens $\mathscr{S}$ and the set D_δ in such a way that

$$K \cap (\overline{\mathscr{S}} \cup \overline{D_\delta}) = \emptyset,$$

and in this case it follows further that $T_{1,1} = S_{1,1}$ on K (see for instance (4.212)–(4.213)), so

$$P_{n,n}(z) = S_{1,1}(z) e^{-\frac{n}{t_0}(g_1(z) - V(z) - l_1)}, \quad z \in K. \tag{4.247}$$

From (4.216) and the estimate (4.217), we know that as $n \to \infty$

$$\begin{aligned} S_{1,1}(z) &= R_{1,1}(z) M_{1,1}(z) + R_{1,2}(z) M_{2,1}(z) + R_{1,3}(z) M_{3,1}(z) \\ &= (1 + \mathcal{O}(n^{-1})) M_{1,1}(z), \quad z \in K. \end{aligned}$$

where for the last equality we also used that the first column of M remains bounded away from Σ_*, which is a direct consequence of the RHP satisfied by M. Also note that the implicit term above is uniform on K. Returning this last equation into (4.247), we conclude

$$P_{n,n}(z) = (1 + \mathcal{O}(n^{-1})) M_{1,1}(z) e^{\frac{n}{t_0}(g_1(z) - V(z) - l_1)} \tag{4.248}$$

uniformly on the compact $K \subset \mathbb{C} \setminus \Sigma_*$.

From (4.246) and from the definition of g_1 in (4.201) and (4.220), it immediately follows that

$$M_{1,1}(z) = \sqrt{r \psi_1'(z)}, \quad g_1(z) = G(z) + c_1,$$

where G is as in (4.56). Returning this information back to (4.248), we get (4.57) for the constant $c = c_1 - l_1$. □

Proof of Theorem 4.2.14. Since ψ_1 is the inverse of h on $\widetilde{\mathcal{R}}_1$, the derivative ψ_1' does not vanish on $\mathbb{C} \setminus \Sigma_*$, so from (4.57) we conclude that the zeros of $P_{n,n}$ accumulate on the star Σ_* in the large n limit.

Suppose now that $\mu_{n_k} \xrightarrow{*} \nu$, where (μ_{n_k}) is a subsequence of the sequence of zero counting measures (μ_n) defined in (4.55). The zeros of $P_{n,n}$ accumulate on Σ_*, so we must have

$$\operatorname{supp} \nu \subset \Sigma_*.$$

For any $z \in \mathbb{C} \setminus \Sigma_*$, it follows from (4.248) that

$$U^\nu(z) = -\int \log|s-z| d\nu(s)$$
$$= -\lim_{k\to\infty} \frac{1}{n_k} \log|P_{n_k,n_k}(z)| = -\frac{1}{t_0}\operatorname{Re}(g_1(z) - V(z) - l_1).$$

Having in mind (4.169) and (4.171), this last identity implies that

$$C^\nu(z) = -\frac{1}{t_0}(g_1'(z) - V'(z)) = -\frac{1}{t_0}(\xi_1(z) - V'(z)) = C^{\mu_*}(z), \quad z \in \mathbb{C} \setminus \Sigma_*.$$

Using the same arguments as in (4.183) *et seq.*, we thus conclude

$$U^\nu(z) = U^{\mu_*}(z), \quad z \in \mathbb{C} \setminus \Sigma_*.$$

Since Σ_* has planar Lebesgue measure zero, the above equation says that the potential of the measures ν and μ_* coincide a.e. in $\mathbb{C}$. From the Unicity Theorem [120, Theorem II.2.1] we get $\nu = \mu_*$, concluding the proof. □

4.11 Analysis of the width parameters

In this section, we analyze the parameters τ_j's that were used in Section 4.5. To do so, we need some preliminary lemmas. For the next results, we recall that w_0 and w_1 are given by Lemma 4.3.12.

Lemma 4.11.1. *For $(t_0, t_1) \in \mathcal{F}$, it is valid*

$$w_0 > r^{1/3}. \tag{4.249}$$

Additionally, for $(t_0, t_1) \in \mathcal{F}_2$,

$$|w_1| < r^{1/3}, \tag{4.250}$$

and

$$w_1 > -\frac{2a_0}{3r}, \tag{4.251}$$

and consequently,

$$|w_1| < w_0. \tag{4.252}$$

Proof. Recall that w_0 is the unique positive solution to

$$h'(w) = 0,$$

so $h'(w) < 0$ for positive w only if $w < w_0$. Simple calculations then show

$$h'(r^{1/3}) = -r - 2a_0 r^{1/3} < 0, \quad 0 < r < \frac{1}{2}.$$

giving us (4.249).

For the second inequality, we recall that w_1 is the smallest (negative) root of h' and, furthermore, $h'(w) \to r > 0$ as $w \to -\infty$, so that $h(w) > 0$ on the interval $(-\infty, w_1)$. Simple computations show that

$$h'(-r^{1/3}) = r\left(3 - \frac{2a_0}{r^{2/3}}\right).$$

For fixed a_0, the function $r \mapsto 3 - 2a_0/r^{2/3}$ is increasing, so it attains its maximum when r is chosen so that the corresponding pair (t_0, t_1) belongs to the critical curve γ_c. Using (4.34), we see that this maximum is

$$3 - \frac{3s^2}{s^2} = 0,$$

thus we get that $h'(-r^{1/3}) < 0$. Since we already observed that h' is positive on $(-\infty, w)$, this is enough to conclude that $w_1 < -r^{1/3} < 0$, which is equivalent to (4.250).

To get (4.251), we note that the function

$$a_0 \mapsto -\frac{2a_0}{3r}$$

is decreasing, so it attains its maximum value along γ_c. Recalling that $w_1 > -1$ (see Lemma 4.3.12) and using (4.60), we get

$$-\frac{2a_0}{3r} < -\frac{2(3s^2/2)}{s^3} = -\frac{1}{s} < -1 < w_1.$$

Finally, the inequality (4.252) trivially follows from (4.249)–(4.250). □

Lemma 4.11.2. *Suppose* $(t_0, t_1) \in \mathcal{F}_2$. *Then*

$$\frac{1}{w_0} + \frac{1}{w_1} > -1 \tag{4.253}$$

where w_0 *and* w_1 *are the zeros of* h' *as in Lemma 4.3.12.*

Proof. From the explicit expression of h in (4.15), we trivially have

$$h''(w) = \frac{4a_0 r}{w^3} + \frac{6r^2}{w^4} = \frac{2r}{w^4}(3rw + 2a_0). \tag{4.254}$$

Since $h'(w_j) = 0$, the chain rule gives us

$$\frac{\partial w_j}{\partial a_0} = -\frac{\frac{\partial h'}{\partial a_0}(w_j)}{h''(w_j)} = \frac{2r}{w_j^2 h''(w_j)}.$$

Using (4.254), we thus get

$$\begin{aligned}\frac{\partial}{\partial a_0}\left(\frac{1}{w_0} + \frac{1}{w_1}\right) &= -\left(\frac{1}{w_0^2}\frac{\partial w_0}{\partial a_0} + \frac{1}{w_1^2}\frac{\partial w_1}{\partial a_0}\right) \\ &= -\left(\frac{1}{3rw_0 + 2a_0} + \frac{1}{3rw_1 + 2a_0}\right). \end{aligned} \tag{4.255}$$

We know that $w_0 > 0$ and also $3rw_1 + 2a_0 > 0$, as it follows from Lemma 4.3.12 and (4.251), respectively. From (4.255) we thus conclude that the function

$$a_0 \mapsto \frac{1}{w_0} + \frac{1}{w_1}$$

is decreasing, so it attains its minimum along the critical curve Γ_c. On Γ_c, it follows from (4.33) that

$$h'(w) = \frac{s(w-1)\left(2s + w^2 + w\right)}{w^3},$$

where $s \in (0, 1/8)$, so that in this case

$$w_0 = 1, \quad w_1 = \frac{1}{2}\left(-1 - \sqrt{1 - 8s}\right),$$

and consequently for every choice of parameters in $\mathcal{F}_2$, it holds true

$$\frac{1}{w_0} + \frac{1}{w_1} > 1 - \frac{2}{1 + \sqrt{1 - 8s}} > -1,$$

as we want. □

4.11.1 Width parameters in the three-cut case

Recall that the non vanishing of the parameters τ_j, $j = 1, 2, 3, 4, 5$, introduced in (4.143)–(4.147), were used in Section 4.5.4.3 to prove that the critical graph of the quadratic differential ϖ remains unchanged in $\mathcal{F}_1$. We now verify that these quantities do not vanish.

Proposition 4.11.3. *For $(t_0, t_1) \in \mathcal{F}_1$, we have $\tau_5 < 0$.*

Proof. Follows directly from (4.126) and (4.147). □

Proposition 4.11.4. *For $(t_0, t_1) \in \mathcal{F}_1$, we have $\tau_1 > 0$.*

Proof. The rational parametrization $(\xi, z) = (h(w^{-1}), h(w))$ given by Theorem 4.2.2 induces the change of variables $s = h(w)$, $\xi_j = h(w^{-1})$, from which it follows that

$$\int_{z_2}^{z_0} \xi_1 \, ds = \int_{w_2}^{w_0} h\left(\frac{1}{w}\right) h'(w)dw, \quad \int_{z_2}^{z_0} \xi_2 \, ds = \int_{w_2}^{\tilde{w}_0} h\left(\frac{1}{w}\right) h'(w)dw,$$

where $w_2, w_0, \tilde{w}_0$ satisfy

$$z_2 = h(w_2), \qquad \xi_1(z_2) = h(w_2^{-1}) = \xi_2(z_2), \tag{4.256}$$

$$z_0 = h(w_0) = h(\tilde{w}_0), \qquad \xi_1(z_0) = h(w_0^{-1}), \qquad \xi_2(z_0) = h(\tilde{w}_0^{-1}). \tag{4.257}$$

We should remark that w_0 and w_2 are the same points given by Lemma 4.3.12.

Hence,

$$\tau_1 = \operatorname{Re} \int_{z_2}^{z_0} (\xi_1(s) - \xi_2(s))ds = \operatorname{Re} \int_{\tilde{w}_0}^{w_0} h\left(\frac{1}{w}\right) h'(w)dw. \tag{4.258}$$

We can further simplify the integral above in the following way,

$$\begin{aligned} \int_{\tilde{w}_0}^{w_0} h\left(\frac{1}{w}\right) h'(w)dw &= \int_{\tilde{w}_0}^{w_0} \left(h\left(\frac{1}{w}\right) - a_0\right) h'(w)dw + a_0 \int_{\tilde{w}_0}^{w_0} h'(w)dw \\ &= \int_{\tilde{w}_0}^{w_0} \left(h\left(\frac{1}{w}\right) - a_0\right) h'(w)dw, \end{aligned}$$

where in the last step we used the first equation in (4.257).

We use the definition of h in (4.15) to compute explicitly the last integral above, arriving at

$$\begin{aligned} \int_{\tilde{w}_0}^{w_0} h\left(\frac{1}{w}\right) h'(w)dw &= F(w_0) - F(\tilde{w}_0) \\ &\quad + r^2(1 - 4a_0^2 - 2r^2)(\log w_0 - \log \tilde{w}_0), \end{aligned} \tag{4.259}$$

where

$$F(w) = \frac{r^3}{3}w^3 + r^2 a_0 w^2 - 2r^3 a_0 w + \frac{4r^3 a_0}{w} + \frac{r^2 a_0}{w^2} + \frac{2r^3}{3w^3}$$

is determined by the condition that $F(w)+r^2(1-4a_0^2-2r^2)\log w$ is the primitive of $h(w^{-1})(h(w)-a_0)$.

The next step is to express $\tilde{w}_0$ in terms of w_0. The equation

$$h(w) - z_0 = \frac{r}{w^2}(w^3 + \frac{a_0 - z_0}{r}w^2 + 2a_0 w + r) = 0$$

has w_0 as a solution with double multiplicity and $\tilde{w}_0$ as a simple solution, that is

$$w^3 + \frac{a_0 - z_0}{r}w^2 + 2a_0 w + r = (w - w_0)^2(w - \tilde{w}_0).$$

This gives us the relation

$$\tilde{w}_0 = -\frac{r}{w_0^2}. \tag{4.260}$$

After some calculations, we are thus reduced to

$$F(w_0) - F(\tilde{w}_0) = \frac{r + w_0^3}{3w_0^6}\left(2w_0^9 - 3a_0 w_0^7 + r(r^2-2)w_0^6 + 15a_0 r^2 w_0^5 \right.$$
$$\left. +3a_0 r(1-2r^2)w_0^4 + r^2(2-r^2)w_0^3 - 3a_0 r^3 w_0^2 + r^5\right).$$

The expression $h'(w_0) = 0$ gives us additionally $w_0^3 = 2a_0 w_0 + 2r$. Replacing every multiple power of 3 in the expression under brackets above, we get

$$F(w_0) - F(\tilde{w}_0) = \frac{r + w_0^3}{3w_0^6}\left((30a_0^2 r^2 + 4a_0^3)w_0^3 + r a_0(r^2(12 - 8a_0) + 10a_0)w_0^2 \right.$$
$$\left. +6a_0 r^2(5 - r^2)w_0 + 12r^3 + 3r^5\right). \tag{4.261}$$

Recalling Lemma 4.3.8, we know that $0 < a_0, r < 1$, so the expression between parentheses above is a polynomial in w_0 with positive coefficients. Because $w_0 > 0$ (Lemma 4.3.12), we finally conclude

$$F(w_0) - F(\tilde{w}_0) > 0. \tag{4.262}$$

We now take care of the log terms in (4.259). From the definition of a_0 in (4.16),

$$0 \leq a_0 \leq \frac{1 - 4r^2}{2} < \frac{1}{2},$$

and this gives us $4a_0^2 \leq 2a_0$. Having also in mind $r < 1$,

$$1 - 4a_0^2 - 2r^2 > 1 - 2r - 2a_0 > 0, \tag{4.263}$$

where in the last step we used Lemma 4.3.8. Using also (4.260), we get

$$\operatorname{Re}\left((1 - 4a_0^2 - 2r^2)(\log w_0 - \log \tilde{w}_0)\right) = (1 - 4a_0^2 - 2r^2) \log \frac{w_0^3}{r} > 0,$$

because $w_0^3 > r$, see (4.249). Plugging this last equation and (4.262) into (4.259), and having in mind (4.258), we arrive at the desired result. □

Remark 4.11.5. Note that (4.260) and (4.261) also hold if we replace w_0 and $\tilde{w}_0$ by w_j and $\tilde{w}_j$, respectively, where w_j is a zero of $h'(w) = 0$ and $\tilde{w}_j$ is the simple zero of $h(w) - h(w_j) = 0$.

Remark 4.11.6. The keen reader might notice that a combination of (4.259)–(4.261) establishes the equivalence between (4.59) and (4.60). In fact, the mother body phase transition determined by γ_c^- corresponds to the vanishing of τ_1. Unlike for $t_1 > 0$, the transition across γ_c^- does not correspond to the coalescence of critical points of the quadratic differential ϖ (or, equivalently, of the points z_j and $\hat{z}_j$ given by Theorem 4.2.6). Instead, it corresponds to the shrinking of the domains $\mathcal{S}_1$ and $\mathcal{S}_6$ in Figure 4.23.

Proposition 4.11.7. *For $(t_0, t_1) \in \mathcal{F}_1$, we have*

$$\tau_2 > 0, \tag{4.264}$$

$$\tau_3 < 0. \tag{4.265}$$

We have not been able to verify Proposition 4.11.7 analytically, so we verified it numerically as explained next.

We start with (4.264). As in the proof of Proposition 4.11.4, we perform the change of variables $z = h(w)$, $\xi_j = h(w^{-1})$, and arrive at

$$\int_{z_0}^{z_2} \xi_1(s)ds = H(w_2) - H(w_0), \quad \int_{z_0}^{z_2} \xi_3(s)ds = H(\tilde{w}_2) - H(w_0), \tag{4.266}$$

where w_0, w_2 are as in Lemma 4.3.12, $\tilde{w}_2$ is the simple zero of $h(w) - z_2$, so alternatively given by

$$\tilde{w}_2 = -\frac{r}{w_2^2}, \tag{4.267}$$

see Remark 4.11.5, and $H(w)$ is the primitive of $h'(w)h(w^{-1})$, explicitly given by

$$H(w) = \frac{r^3}{3}w^3 + a_0 r^2 w^2 + a_0 r\left(1-2r^2\right)w + \frac{2a_0^2 r + 4a_0 r^3}{w} + \frac{2a_0 r^2}{w^2} + \frac{2r^3}{3w^3} - r^2\left(4a_0^2 + 2r^2 - 1\right)\log w. \quad (4.268)$$

In the expression above, we choose the main branch of the logarithm - actually the branch chosen is not important, because at the end we will be only interest in the real part of H. Taking the difference between the two expressions in (4.266), the integral in Equation (4.144) gets the form

$$\tau_2 = \operatorname{Re}\int_{z_0}^{z_2}(\xi_1(s)-\xi_3(s))ds = \operatorname{Re}H(w_2) - \operatorname{Re}H(\tilde{w}_2) = \operatorname{Re}H(w_2) - \operatorname{Re}H\left(-\frac{r}{w_2^2}\right). \quad (4.269)$$

Note that the right hand side of (4.269) is given only in terms of a_0, r. We then use (4.269) for numerical computation of the integral as follows.

For given r, a_0, we first solve

$$h'(w) = 0,$$

pick w_2 as the only solution with positive imaginary part (see Lemma 4.3.12), compute $\tilde{w}_2$ through (4.267) and finally get the difference $\operatorname{Re}H(w_2) - \operatorname{Re}H(\tilde{w}_2)$. By varying $r \in (0, 1/2)$ and $a_0 \in (0, \alpha)$, where

$$\alpha = \alpha(r) = \min\{3/2r^{2/3}, (1-2r)/2\} = \begin{cases} \frac{3}{2}r^{2/3}, & r \le \frac{1}{8}, \\ \frac{1-2r}{2}, & \frac{1}{8} < r < \frac{1}{2}, \end{cases}$$

we are sure to be covering every possible choice $(t_0, t_1) \in \mathcal{F}_1$ (see Proposition 4.2.7).

With this idea in mind, we evaluated τ_2 numerically with Mathematica in 300-digit precision for the range

$$r = \frac{1}{2}\frac{j}{5000}, \quad a_0 = \frac{\alpha(r)}{5000}k, \quad j,k = 1,\ldots,5000, \quad (4.270)$$

verifying that in this case $\tau_2 > 0$.

For (4.265) we proceed similarly as before to get

$$\tau_3 = \operatorname{Re}\int_{z_2}^{\hat{z}_2} (\xi_1(s) - \xi_2(s))ds = \operatorname{Re} H(\hat{w}_2) - \operatorname{Re} H(\hat{w}_2^{-1})$$

where $\hat{w}_2$ is the parameter on the w-plane for which $\xi_1(\hat{z}_2) = h(\hat{w}_2^{-1})$, $\xi_2(\hat{z}_2) = h(\hat{w}_2)$. Recalling Corollary 4.4.6, $\hat{w}_2$ is alternatively characterized as the only zero of the function f appearing in (4.116)–(4.117) that belongs to $\{w \in \mathbb{C} \mid \operatorname{Im} w > 0, |w| > 1\}$. Note that the coefficient $t_0 - 2t_1$ of f in (4.116)–(4.117) can be written only in terms of r, a_0 with the help of the system (4.31)–(4.32).

So the numerical procedure here is to find all the zeros of f, select $\hat{w}_2$ and then compute the left hand side of (4.265) through (4.260). (4.265) was again evaluated in the range (4.270) and 300-digit precision, and we verified that in this case $\tau_3 < 0$.

The outcome of the numerical evaluation of τ_2 and τ_3 for several choices of r can be seen in Figures 4.42–4.44 and Figures 4.45–4.47, respectively.

Proposition 4.11.8. *For $(t_0, t_1) \in \mathcal{F}_1$ it is valid*

$$\tau_4 > 0.$$

Proof. From (4.27) we see that the residue at infinity of ξ_1 is purely imaginary, thus

$$\operatorname{Re}\int_{z_2}^{z_*} \xi_1(s)ds + \operatorname{Re}\int_{z_*}^{z_1} \xi_1(s)ds = \operatorname{Re}\int_{z_2}^{z_1} \xi_1(s)ds, \tag{4.271}$$

where, as in (4.146), $x_* < z_*$ and on both sides of (4.271) the paths of integration are taken in $\mathbb{C} \setminus ((-\infty, z_*] \cup \Sigma_*)$.

For the remaining integral in (4.146), we deform the path of integration across Σ_* to get

$$\int_{z_2}^{z_*} \xi_2(s)ds + \int_{z_*}^{z_1} \xi_3(s)ds = \int_{z_2}^{z_0} \xi_1(s)ds + \int_{z_0}^{z_1} \xi_3(s)ds. \tag{4.272}$$

Combining (4.271) and (4.272), we obtain

$$\begin{aligned}\tau_4 &= \operatorname{Re}\int_{z_2}^{z_*} (\xi_1(s) - \xi_2(s))ds + \operatorname{Re}\int_{z_*}^{z_1} (\xi_1(s) - \xi_3(s))ds \\ &= \operatorname{Re}\int_{z_0}^{z_1} (\xi_1(s) - \xi_3(s))ds\end{aligned}$$

$$= \mathrm{Re} \int_{z_0}^{z_2} (\xi_1(s) - \xi_3(s)) ds$$

$$= \tau_2$$

where for the third equality we used the symmetry under conjugation. From (4.264) we get the desired result. □

4.11.2 Width parameters in the one-cut case

We now proceed to the analysis of the τ_j's in (4.156)–(4.161).

Proposition 4.11.9. *For $(t_0, t_1) \in \mathcal{F}_2$, the quantities τ_1, τ_2, τ_4 and τ_5, given respectively by (4.156), (4.157), (4.159) and (4.160), are never zero.*

Proof. Each of the integrals can be deformed to either one of the intervals $[z_2, z_1]$ or $[z_0, \hat{z}_0]$, where the respective integrand $\xi_j - \xi_k$ is real, continuous and never zero (see (4.130)), and hence does not change sign. □

Proposition 4.11.10. *For $(t_0, t_1) \in \mathcal{F}_2$, the quantity τ_6 given in (4.161) is strictly negative.*

Proof. Recall that w_0, w_1 and w_2 are the zeros of h' (see Lemma 4.3.12) and $\tilde{w}_j$ is the simple solution to $h(w) - h(w_j) = 0$ (see Remark 4.11.5). Proceeding in a similar manner as for Proposition 4.11.4 (see in particular (4.258)–(4.261)), we get

$$\begin{aligned}\tau_6 &= \mathrm{Re} \int_{w_0}^{w_1} h\left(\frac{1}{w}\right) h'(w) dw - \mathrm{Re} \int_{\tilde{w}_0}^{\tilde{w}_1} h\left(\frac{1}{w}\right) h'(w) dw \\ &= \frac{r + w_1^3}{3w_1^3} q(w_1) - \frac{r + w_0^3}{3w_0^3} q(w_0) + 3r^2(1 - 4a_0 r^2 - 2r^2) \log \left|\frac{w_1}{w_0}\right|, \quad (4.273)\end{aligned}$$

where here q is given by

$$q(w) = \frac{12r^3 + 3r^5}{w^3} + \frac{6a_0 r^2(5 - r^2)}{w^2} + \frac{a_0 r((12 - 8a_0)r^2 + 10a_0)}{w} + 30a_0^2 r^2 + 4a_0^3.$$

From (4.252) and (4.263),

$$3r^2(1 - 4a_0 r^2 - 2r^2) \log \left|\frac{w_1}{w_0}\right| < 0. \quad (4.274)$$

To deal with the first two terms on the right hand side of (4.273), rewrite

$$\frac{r+w_0^3}{3w_0^3}q(w_0)-\frac{r+w_1^3}{3w_1^3}q(w_1)= \\ \left(\frac{r+w_0^3}{3w_0^3}-\frac{r+w_1^3}{3w_1^3}\right)q(w_0)+\frac{r+w_1^3}{3w_1^3}(q(w_0)-q(w_1)). \quad (4.275)$$

From the rough estimate $0<a_0,r<1$ (see Lemma 4.3.8) it follows that the coefficients of q are positive, thus

$$q(w_0)>0, \quad (4.276)$$

because $w_0>0$, see Lemma 4.3.12. Furthermore, from (4.250),

$$\frac{r+w_1^3}{3w_1^3}>0. \quad (4.277)$$

Clearly,

$$\frac{r+w_0^3}{3w_0^3}-\frac{r+w_1^3}{3w_1^3}=\frac{r(w_0^3-w_1^3)}{w_0^3(-w_1)^3}>0, \quad (4.278)$$

where for the last conclusion we used $w_1<0<w_0$, see Lemma 4.3.12. Summarizing, a combination of (4.274)–(4.278) shows that the right-hand side of (4.273) is negative if we can prove that

$$q(w_0)-q(w_1)>0. \quad (4.279)$$

To see that (4.279) holds true, write

$$q(w_0)-q(w_1)=(12r^3+3r^5)\left(\frac{1}{w_0^3}-\frac{1}{w_1^3}\right)+\left(\frac{1}{w_0}-\frac{1}{w_1}\right) \\ \times\left(6a_0r^2(5-r^2)\left(\frac{1}{w_0}+\frac{1}{w_1}\right)+a_0r((12-8a_0)r^2+10a_0)\right). \quad (4.280)$$

Using again $w_1<0<w_0$,

$$\frac{1}{w_0^3}-\frac{1}{w_1^3},\frac{1}{w_0}-\frac{1}{w_1}>0. \quad (4.281)$$

In addition, using (4.253)

$$\begin{aligned} 6a_0r^2(5-r^2)\left(\frac{1}{w_0}+\frac{1}{w_1}\right)+a_0r((12-8a_0)r^2+10a_0) \\ \geq -6a_0r^2(5-r^2)+a_0r((12-8a_0)r^2+10a_0) \\ = a_0r[a_0\left(10-8r^2\right)+6r\left(r^2+2r-5\right)]. \end{aligned} \tag{4.282}$$

The term between brackets on the right-hand side above is increasing with a_0, so it attains its minimum along the critical curve γ_c. Using (4.34), we get

$$a_0\left(10-8r^2\right)+6r\left(r^2+2r-5\right)=3s^2\left(2s^7-4s^6+4s^4-10s+5\right)>0,$$

thus the left-hand side of (4.282) is positive as well. Combining this with (4.280)–(4.281), we conclude (4.279), and the proof is complete. □

Proposition 4.11.11. *The width τ_3 in (4.158) is strictly negative.*

As for the Proposition 4.11.11, we verified that $\tau_3<0$ numerically as explained next.

Proceeding as in (4.266)–(4.269) we get

$$\int_{z_2}^{\hat{z}_2}(\xi_1(s)-\xi_2(s))ds=H(\hat{w}_2)-H\left(\frac{1}{\hat{w}_2}\right)+H(w_2)-H\left(-\frac{r}{w_2}\right),$$

where w_2 and $\hat{w}_2$ are given by Lemma 4.3.12 and Corollary 4.4.6, respectively (see also Remark 4.11.5), and the function H is given in (4.268). Thus

$$\tau_3=\operatorname{Re}H(\hat{w}_2)-\operatorname{Re}H\left(\frac{1}{\hat{w}_2}\right)+H(w_2)-H\left(-\frac{r}{w_2}\right). \tag{4.283}$$

We use this last expression to verify that $\tau_3<0$ for

$$0<r<\frac{1}{8},\quad \frac{3}{2}r^{2/3}<a_0<\frac{1-2r}{2},$$

which corresponds to $(t_0,t_1)\in\mathcal{F}_2$ (see Proposition 4.2.7). We evaluated (4.283) for

$$r=\frac{1}{8}\frac{j}{5000},\quad a_0=\frac{3r^{2/3}}{2}\frac{5000-k}{5000}+\frac{1-2r}{2}\frac{k}{5000},\quad j,k=1,\dots,5000,$$

using Mathematica with 300-digit precision and verified that $\tau_3<0$. The outcome for several values of r and the whole corresponding range of a_0 can be seen in Figures 4.48–4.49.

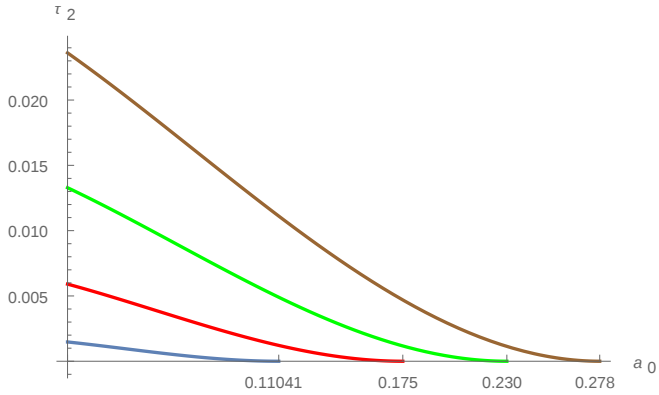

Figure 4.42: Plot of τ_2 as a function of a_0 in the three-cut case for $r = 1/50, 2/50, 3/50, 4/50$ (from bottom to top). For these choices of r, the extremal values of a_0 are attained in the critical line γ_c, so that a_0 ranges from 0 to the correspond critical value $3r^{2/3}/2$, in the present case given by $0.1105..., 0.1754..., 0.2298...$ and $0.2784...$, respectively.

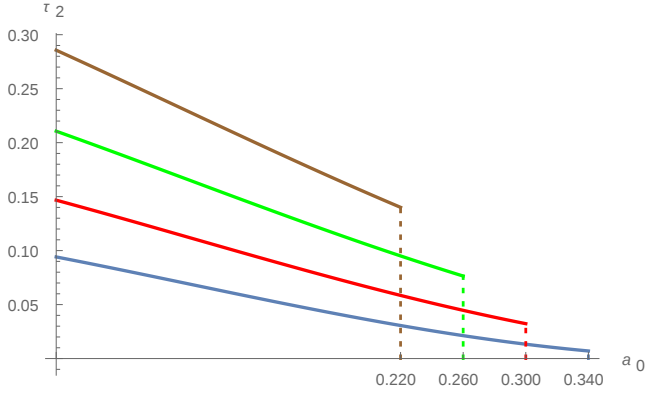

Figure 4.43: Plot of τ_2 as a function of a_0 in the three-cut case for $r = 8/50, 10/50, 12/50, 14/50$ (from bottom to top). For these choices of r, the extremal values of a_0 are attained in the critical line Γ_c, so that a_0 ranges from 0 to the correspond critical value $(1 - 2r)/2$, in the present case given by $0.34, 0.3, 0.26$ and 0.22, respectively.

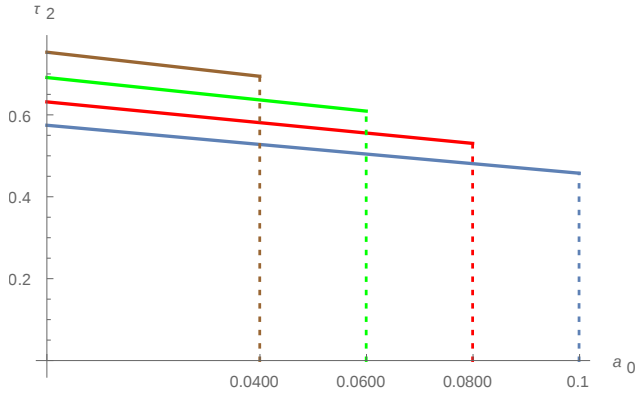

Figure 4.44: Plot of τ_2 as a function of a_0 in the three-cut case for $r = 20/50, 21/50, 22/50, 23/50$ (from bottom to top). For these choices of r, the extremal values of a_0 are attained in the critical line Γ_c, so that a_0 ranges from 0 to the correspond critical value $(1-2r)/2$, in the present case given by $0.1, 0.08, 0.06$ and 0.04, respectively.

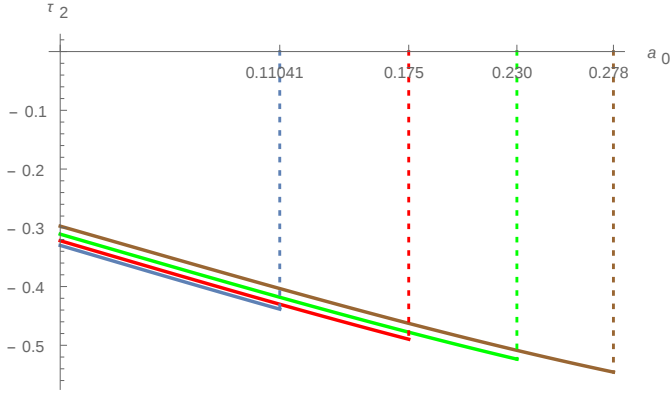

Figure 4.45: Plot of τ_3 as a function of a_0 in the three-cut case for $r = 1/50, 2/50, 3/50, 4/50$ (from bottom to top). For these choices of r, the extremal values of a_0 are attained in the critical line γ_c, so that a_0 ranges from 0 to the correspond critical value $3r^{2/3}/2$, in the present case given by $0.1105..., 0.1754..., 0.2298...$ and $0.2784...$, respectively.

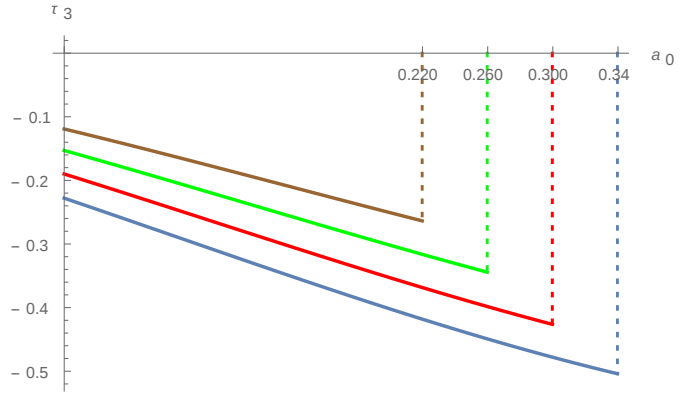

Figure 4.46: Plot of τ_3 as a function of a_0 in the three-cut case for $r = 8/50, 10/50, 12/50, 14/50$ (from bottom to top). For these choices of r, the extremal values of a_0 are attained in the critical line Γ_c, so that a_0 ranges from 0 to the correspond critical value $(1-2r)/2$, in the present case given by $0.34, 0.3, 0.26$ and 0.22, respectively.

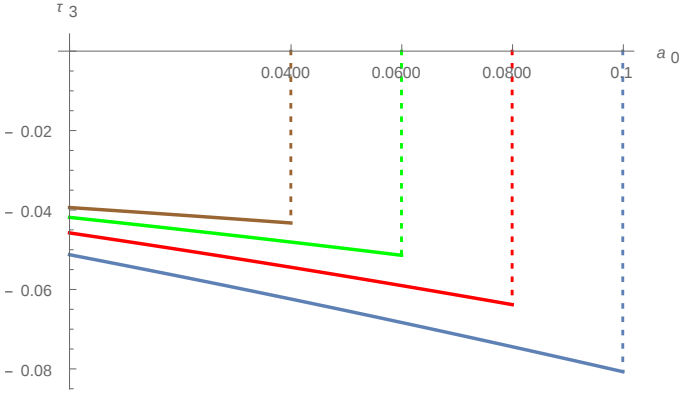

Figure 4.47: Plot of τ_3 as a function of a_0 in the three-cut case for $r = 20/50, 21/50, 22/50, 23/50$ (from bottom to top). For these choices of r, the extremal values of a_0 are attained in the critical line Γ_c, so that a_0 ranges from 0 to the correspond critical value $(1-2r)/2$, in the present case given by $0.1, 0.08, 0.06$ and 0.04, respectively.

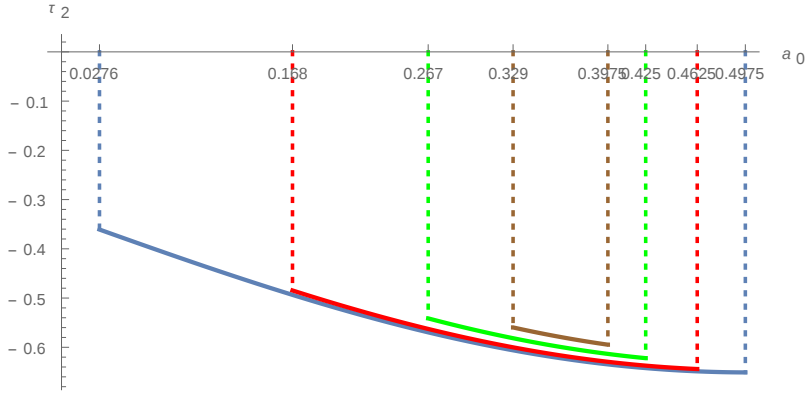

Figure 4.48: Plot of τ_3 as a function of a_0 in the one-cut case for $r = 1/400, 15/400, 30/400, 41/400$ (from bottom to top). For these choices of r, the minimal value for a_0 is along γ_c, thus given by $3r^{2/3}/3$, whereas the maximal value for a_0 is along Γ_c, hence corresponding to $(1-2r)/2$. In the present case, the minimal values are $0.0276..., 0.1680..., 0.2667...$ and $0.32852...$, respectively, whereas the maximal values are $0.4975, 0.4625, 0.425$ and 0.3975, respectively.

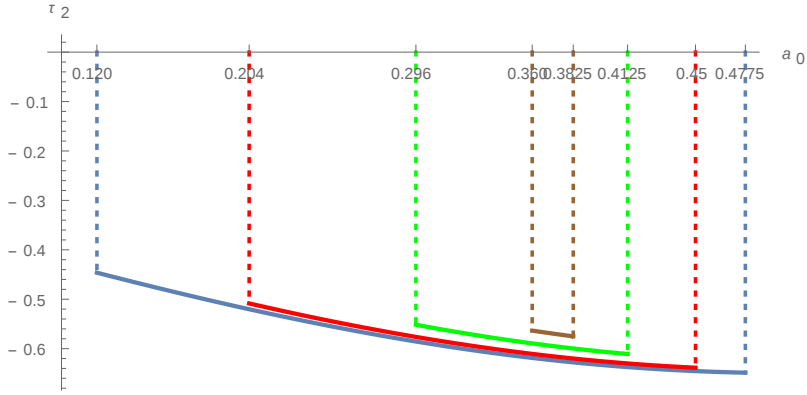

Figure 4.49: Plot of τ_3 as a function of a_0 in the one-cut case for $r = 9/400, 20/400, 35/400, 47/400$ (from bottom to top). For these choices of r, the minimal value for a_0 is along γ_c, thus given by $3r^{2/3}/3$, whereas the maximal value for a_0 is along Γ_c, hence corresponding to $(1-2r)/2$. In the present case, the minimal values are $0.1195..., 0.2035..., 0.2956...$ and $0.3598...$, respectively, whereas the maximal values are $0.4775, 0.45, 0.4125$ and 0.3825, respectively.

Conclusion and Further Research

This thesis investigated the potential-theoretic free boundary problems that arise in certain random matrix models. More precisely,

- In Chapter 2 we investigated the max-min log energy problem in polynomial external field, that arises in the description of the limiting zero distribution for the non-hermitian orthogonal polynomials, the latter being related to the hermitian matrix model with a complex potential. Using techniques from potential theory, we showed the existence of a contour solving the max-mix problem, and furthermore proved that this contour possesses the S-property in polynomial external field. In this context, quadratic differentials on the plane appeared naturally in the description of the support of the equilibrium measure of the S-contour.
- Motivated towards the analysis of the hermitian matrix model with external source, in Chapter 3 we introduced and studied in-depth the critical vector-valued measures. We obtained several structural results about them, showing their connection with algebraic equations and quadratic differentials on the associated three-sheeted Riemann surface. We explored the latter connection in order to construct a family of critical vector-valued measures for monic cubic potentials. In this construction, we employed deformation techniques in quadratic differentials that we believe are of independent interest.
- In Chapter 4 we studied the normal matrix model with a cubic plus linear algebraic potential, obtaining explicitly the associated phase diagram. We investigated the underlying mother body problem, identifying a novel phase transition. Furthermore, we carried out the Riemann-Hilbert analysis to the associated non-hermitian multiple orthogonal polynomials. One of

the key technical tools was the identification of a quadratic differential on the spectral curve which encodes the mother body measure.

There are some natural questions related to this thesis that remain open for further investigation, as we briefly explain next.

Asymptotics for non-diagonal multiple orthogonal polynomials

The asymptotic analysis of the multiple orthogonal polynomials in (3.36) was the starting point of our studies that resulted in Chapter 3. As we already mentioned in Section 3.2.3, the sequence of zero counting measures associated with the sequence $(P_{n,m})$ defined through (3.36) converges, in the limit $N = n+m \to \infty$ and $n/N \to \alpha$, to the sum of the first two components of the critical measure $\vec{\mu}_\alpha$ whose existence is assured by Theorem 3.2.12. Together with Andrei Martínez-Finkelshtein we are currently carrying out the steepest descent method to the associated 3×3 Riemann-Hilbert problem, which amongst others should ultimately lead to the mentioned result.

The hermitian matrix model with external source and max-min problems

As we mentioned in the introduction, there is an intimate connection between the critical vector-valued measures given by Definition 3.2.1 and the hermitian matrix model with external source (1.15). The investigation in Chapter 3 is one of the main steps to fully understand this connection, as critical vector-valued measures for a given potential should also satisfy the desired S-property (1.27), the latter being one of the key ingredients for the asymptotic analysis of the associated Riemann-Hilbert problem. Hence it is left to prove the existence of critical vector-valued measures for general polynomial external fields.

Although in Chapter 3 we used quadratic differentials to establish this existence for cubic potentials, this technique does not seem applicable to deal with general potentials, as the number of parameters to control become too large. The approach that seems more feasible is through the GRS theory: the vector equilibrium measure of contours with the max-min property (1.26) should also be critical. In this case, we are translating the question of existence of vector critical measures to the existence of max-min contours (which is the approach

taken in Chapter 2 for the scalar energy). This aspect will be subject of further investigation.

Planar orthogonality versus multiple orthogonality

In Chapter 3, after neglecting the boundary terms in (4.48) we traded the orthogonal polynomials $(q_{j,n})$ in (4.10) by the multiple orthogonal polynomials $(P_{j,n})$ in (4.50), establishing asymptotic limits for the latter. A natural question is whether the sequences $(q_{j,n})$ and $(P_{j,n})$ indeed have the same limiting asymptotic behavior when, say, $j = n \to \infty$. Such a question is very interesting from the viewpoint of the normal matrix model, as one could push further such limits and also study scaling limits of the correlation kernel of the model.

Appendix A

Quadratic differentials

A meromorphic quadratic differential ϖ on a Riemann surface $\mathcal{R}$ is a differential form of type $(2,0)$, given locally by an expression $f(z)dz^2$, where f is a meromorphic function of a local coordinate z. If $z = z(\zeta)$ is a conformal change of variables, then

$$\widetilde{f}(\zeta)d\zeta^2 = f(z(\zeta))(dz/d\zeta)^2 d\zeta^2$$

represents ϖ in the local coordinates ζ.

In this Appendix, we sketch the minimal background on quadratic differentials used throughout this thesis. The general references are the monographs by Strebel [133] and Jenkins [85]; some additional information can be found in [114, 126, 135].

A.1 Critical points and trajectories

The *critical* or *singular points* of $\varpi = fdz^2$ are the zeros and poles of f; recall that a zero (resp., a pole) of ϖ is a point p where in a local chart sending p to 0 we have $f(z) = z^n\psi(z)$, with $\psi(0) \neq 0$, and with the integer $n \geq 1$ (resp., $n \leq -1$). The value n is the *order* of the critical point p, and is denoted by $\eta(p)$. The rest of the points of $\mathcal{R}$ are called regular, and their order is assumed to be $\eta(p) = 0$.

Critical points of order ≤ -2 (i.e., poles of order 2 and higher) are called *infinite*, and the rest of the critical points are *finite*.

In a neighborhood of any regular point p, the primitive

$$\Upsilon(z) = \int_p^z \sqrt{-\varpi} = \int_p^z \sqrt{-f(s)}ds \tag{A.1}$$

is well defined by specifying the branch of the square root at p and continuing it analytically along the path of integration. Function $\Upsilon(z)$ provides a *distinguished* or a *natural* parameter on $\mathcal{R}$ in a neighborhood of p.

We are mostly interested in the *trajectories* of a quadratic differential ϖ. A Jordan arc $\gamma \subset \mathcal{R}$ is called an *arc of trajectory* of ϖ if it is locally mapped by Υ to a vertical line. More precisely, this means that for any point $p \in \gamma$, there exists a neighborhood U where the primitive Υ above is well defined and satisfies

$$\operatorname{Re} \Upsilon(z) = \text{const}, \quad z \in \gamma \cap U. \tag{A.2}$$

A maximal arc of trajectory is called a *trajectory* of ϖ.

Analogously, the *orthogonal trajectories* of ϖ are trajectories of $-\varpi$; they can be equivalently defined by replacing "Re" by "Im" in (A.2).

A trajectory γ extending to a finite critical point along at least one of its directions is called *critical*; in the case when it happens in both directions, we call this trajectory *bounded* (also *finite* or *short*), and *unbounded* (or *infinite*) otherwise. Notice that both ends of a short trajectory may coincide, in which case it forms a loop on $\mathcal{R}$.

A *ϖ-chain* is a connected set on $\mathcal{R}$ made of a finite union of arcs of trajectories or orthogonal trajectories of ϖ. If no curves in a ϖ-chain belong to orthogonal trajectories, we refer to it as a *path of trajectories* of ϖ (or a *ϖ-path*). In this case, in order to avoid the trivial situation, two consecutive arcs of a ϖ-path are required to intersect at a singular point of ϖ.

A.2 The local structure of trajectories

The local behavior of trajectories of a meromorphic quadratic differential ϖ is well understood.

From a point p of order $\eta(p) = n \geq -1$ emanate $n+2$ trajectories, forming equal angles $\frac{2\pi}{n+2}$ at p. This covers also regular points, meaning that through any regular point passes exactly one trajectory, which is locally an analytic arc (see Figure A.1).

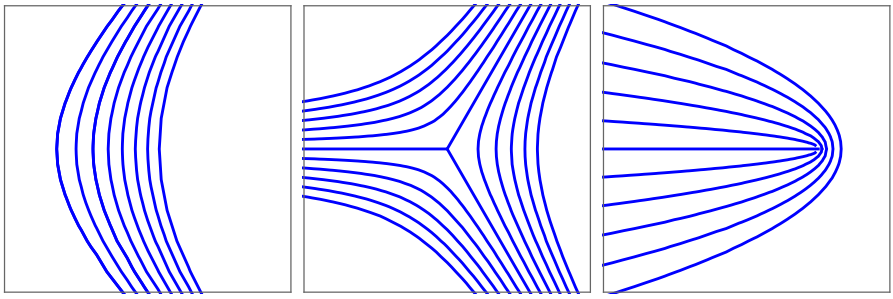

Figure A.1: Structure of trajectories in a neighborhood of a regular point (left), simple zero (middle) and simple pole (right).

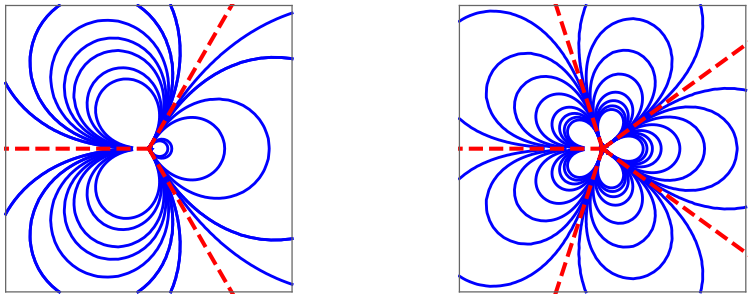

Figure A.2: Structure of trajectories (solid lines) and critical directions (dashed lines) in a neighborhood of poles of order 3 (left) and 5 (right).

An infinite critical point p or order $n \leq -3$ has a neighborhood G with the following property: there are $-(n+2)$ asymptotic directions, henceforth called *critical directions*, forming equal angles $\frac{2\pi}{-n-2}$ at p, such that each trajectory entering G stays in G and tends to p in one of the critical directions [85, Theorem 3.3]. If a trajectory is fully contained in G, then it tends to p in two consecutive critical directions (see Figure A.2).

At a double pole p there are three possibilities. For $\varpi = f(z)dz^2$, we define the *residue* c of ϖ at $z = p$ to be the residue of $\sqrt{f(z)}$ at $z = p$, which is well defined up to a sign. If $c \in \mathbb{R}$ then there are no trajectories emanating from p and the trajectories near p are closed loops. If $c \in i\mathbb{R}$, then there are trajectories emanating from c in every direction. In the rest of the cases, the trajectories near p converge to p in a spiral form (see Figure A.3).

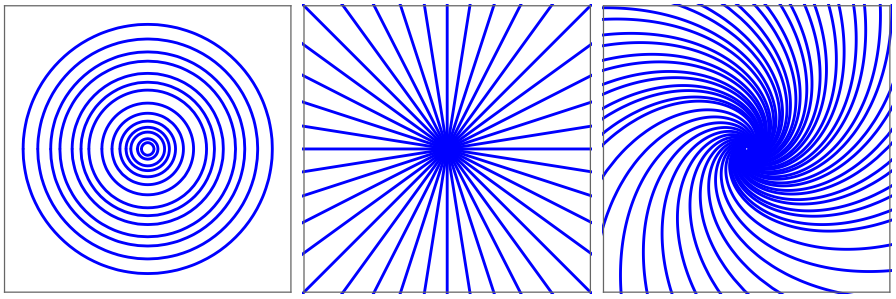

Figure A.3: Structure of trajectories in a neighborhood of a double pole for $c \in \mathbb{R}$ (left), $c \in i\mathbb{R}$ (middle) and $c \in \mathbb{C} \setminus (\mathbb{R} \cup i\mathbb{R})$ (right).

A.3 Global structure of trajectories

There are three possible behaviors for a trajectory γ in the large,

(i) γ is a closed curve containing no critical points.

(ii) γ is an arc connecting two critical points (which may coincide; in this case γ is a closed curve).

(iii) γ is an arc that has no limit along at least one of its directions.

Trajectories satisfying *(ii)* are called *short* or *finite*. Trajectories satisfying (iii) are called *recurrent*, and they are usually a major source of troubles when studying the global structure of trajectories of a given quadratic differential. Fortunately (for us) in this thesis we deal with quadratic differentials with at most 3 poles on a genus 0 compact Riemann surface, and the absence of recurrent trajectories in this case is assured by Jenkins' Three Poles Theorem [114, Thm. 8.5, page 226].

A non-recurrent trajectory γ has two limiting (extremal) values when we travel along it in both opposite directions, and these extremal values can possibly be the same, in case the trajectory is closed. For convenience, we will denote these extremal values by $p(\gamma)$ and $q(\gamma)$. For instance, for a short trajectory γ both $p(\gamma)$ and $q(\gamma)$ are finite critical points.

The set of the critical trajectories of a quadratic differential ϖ (together with their limit points, i.e. the critical points of ϖ) is the *critical graph* of ϖ, denoted by $\mathcal{G} = \mathcal{G}_\varpi$. According to [85, Theorem 3.5] (see also [133, §10]), the complement of the closure of $\mathcal{G}_\varpi$ in $\mathcal{R}$ consists of a finite number of domains called the *domain configuration* of ϖ. The knowledge of $\mathcal{G}$ (or of the domain configuration

of ϖ) is sufficient to fully understand the global structure of trajectories of ϖ, as evidenced by the following theorem:

Theorem A.3.1 (Basic Structure Theorem [85, Theorem 3.5])**.** *Let ϖ be a meromorphic quadratic differential on a compact Riemann surface $\mathcal{R}$. Suppose in addition that ϖ has no recurrent trajectories.*

Then $\mathcal{R} \setminus \mathcal{G}$ decomposes into a finite union of disjoint domains $\cup\mathcal{D}$, each of them bounded by a finite number of critical trajectories. Each domain $\mathcal{D}$ lies into one of the following four classes.

(i) **Half plane** *(or **end**) **domain**: It is swept by trajectories converging to a pole p of order ≥ 3 in its two ends, and along consecutive critical directions. Its boundary consists of a ϖ-path with two unbounded critical trajectories and a finite number of short trajectories. For some choice of the branch of the square root, the natural parameter Υ in (A.1) is a conformal map from $\mathcal{D}$ to a vertical half plane*

$$H = \{w \in \mathbb{C} \mid \operatorname{Re} w > c\},$$

for some $c \in \mathbb{R}$, and it extends continuously to the boundary of $\mathcal{D}$ with the identification $\Upsilon(p) = \infty$.

(ii) **Strip domain**: *It is swept by trajectories which both ends tend to poles p, q of order ≥ 2, possibly with $p = q$. The boundary $\partial\mathcal{D} \setminus \{p, q\}$ is a disjoint union of two ϖ-paths, each of them consisting of two unbounded critical trajectories converging to p and q, and possibly a finite number of short trajectories.*

For some real constants $c_1 < c_2$, Υ maps $\mathcal{D}$ conformally to a vertical strip

$$S = \{w \in \mathbb{C} \mid c_1 < \operatorname{Re} w < c_2\}, \tag{A.3}$$

and it extends continuously to the boundary of $\mathcal{D}$, with appropriate identification of the points p, q with the directions $\pm i\infty$.

(iii) **Ring domain**: *It is swept by closed trajectories. Its boundary consists of two connected components, where each of them is a closed ϖ-path. For a suitably chosen real constant c and some real numbers $0 < r_1 < r_2$, the function $z \mapsto e^{c\Upsilon(z)}$ maps $\mathcal{D}$ conformally to an annulus*

$$R = \{w \in \mathbb{C} \mid r_1 < |w| < r_2\}. \tag{A.4}$$

and it extends continuously to the boundary of $\mathcal{D}$.

(iv) **Circle domain**: *It is swept by closed trajectories and contains exactly one double pole, with purely real residue. Its boundary is a closed ϖ-path. For a suitably chosen real constant c and some real number $r > 0$, the function $z \mapsto e^{c\Upsilon(z)}$ is a conformal map from $\mathcal{D}$ to the circle centered at origin and radius r; it extends continuously to ∂D and sends the double pole to the origin $w = 0$.*

In case ϖ has also recurrent trajectories, a fifth class of domains has to be added to the domain configuration of ϖ; we refer the reader to [85] for further details.

For a given short trajectory γ connecting two finite critical points p, q (which coincide if γ is closed) we define its *length* by

$$\ell(\gamma) = \left| \int_\gamma \sqrt{-\varpi} \right| = \left| \operatorname{Im} \int_\gamma \sqrt{-\varpi} \right| > 0, \tag{A.5}$$

The *width of a strip domain* $\mathcal{S}$ is defined as $\sigma(\mathcal{S}) = |c_2 - c_1|$, where the constants c_1, c_2 are as in (A.3). Alternatively, it can be computed as

$$\sigma(\mathcal{S}) = \left| \int_p^q \operatorname{Re} \sqrt{-\varpi} \right|, \tag{A.6}$$

where we integrate along any path in $\mathcal{S}$ connecting two points, p and q, lying on different connected components of $\partial\mathcal{S} \setminus \{\text{poles of } \varpi\}$.

In the same spirit, the *width of a ring domain* $\mathcal{D}$ is defined as

$$\sigma(\mathcal{D}) = \frac{1}{c} \log \frac{r_2}{r_1} = \left| \operatorname{Re} \int_p^q \sqrt{-\varpi} \right|,$$

where r_1, r_2 and c are as in (A.4), and we integrate along any path in $\mathcal{D}$ connecting two points, p and q, lying on different connected components of its boundary.

For any open simply connected domain $\mathcal{D} \subset \mathcal{R}$ bounded by a ϖ-chain (that is called a *ϖ-polygon*) we define two values: the total order of the singular points of ϖ in $\mathcal{D}$ is

$$\lambda(\mathcal{D}) = \sum_{p_j \in \mathcal{D}} \eta(p_j),$$

where the summation is along all the singular points p_j of ϖ in $\mathcal{D}$, while the contribution from the singular points of ϖ on the boundary is

$$\kappa(\mathcal{D}) = \sum_{p_j \in \partial\mathcal{D}} \beta(p_j),$$

where the summation is along all the corners p_j of $\partial\mathcal{D}$,

$$\beta(p) = 1 - \theta(p_j)\,\frac{\eta(p)+2}{2\pi},$$

and $\theta(p)$ is the inner angle (in radians) at the corner p.

Both values have a simple relation, as shown by the following simple consequence of the argument principle (also known as the Teichmüller lemma, see [133, Theorem 14.1]):

Theorem A.3.2 (Teichmüller lemma)**.** *If $\mathcal{D}$ is a ϖ-polygon, then*

$$\kappa(\mathcal{D}) = 2 + \lambda(\mathcal{D}). \tag{A.7}$$

A straightforward corollary of this lemma (and also a direct consequence of the maximum principle for holomorphic functions) is the following fact:

Corollary A.3.3. *If ϖ is analytic (has no poles) in a ϖ-polygon $\mathcal{D}$, then $\partial\mathcal{D}$ must contain at least one pole of ϖ.*

This corollary is also the basis for the general principle **P.3** in Section 3.5.5.1.

Bibliography

[1] Aharonov, D., and Shapiro, H. S. Domains on which analytic functions satisfy quadrature identities. *J. Analyse Math. 30* (1976), 39–73.

[2] Álvarez, G., Martínez Alonso, L., and Medina, E. Determination of S-curves with applications to the theory of non-Hermitian orthogonal polynomials. *J. Stat. Mech. Theory Exp.*, 6 (2013), P06006, 28 pp.

[3] Álvarez, G., Martínez Alonso, L., and Medina, E. Partition functions and the continuum limit in Penner matrix models. *J. Phys. A 47*, 31 (2014), 315205, 29 pp.

[4] Ameur, Y., Hedenmalm, H., and Makarov, N. G. Fluctuations of eigenvalues of random normal matrices. *Duke Math. J. 159*, 1 (2011), 31–81.

[5] Ameur, Y., Hedenmalm, H., and Makarov, N. G. Random normal matrices and Ward identities. *Ann. Probab. 43*, 3 (2015), 1157–1201.

[6] Aptekarev, A. I. Asymptotics of Hermite-Padé approximants for a pair of functions with branch points. *Dokl. Akad. Nauk 422*, 4 (2008), 443–445.

[7] Aptekarev, A. I. ., and Arvesú, J. Asymptotics for multiple Meixner polynomials. *J. Math. Anal. Appl. 411*, 2 (2014), 485–505.

[8] Aptekarev, A. I. ., Van Assche, W., and Yattselev, M. L. Hermite-Padé approximants for a pair of Cauchy transforms with overlapping symmetric supports. *ArXiv:1505.03993*, 52 pp.

[9] Aptekarev, A. I., Bleher, P. M., and Kuijlaars, A. B. J. Large n limit of Gaussian random matrices with external source. II. *Comm. Math. Phys. 259*, 2 (2005), 367–389.

[10] Aptekarev, A. I., and Kuijlaars, A. B. J. Hermite-Padé approximations and ensembles of multiple orthogonal polynomials. *Uspekhi Mat. Nauk 66*, 6 (402) (2011), 123–190.

[11] Aptekarev, A. I., Kuijlaars, A. B. J., and Van Assche, W. Asymptotics of Hermite-Padé rational approximants for two analytic functions with separated pairs of branch points (case of genus 0). *Int. Math. Res. Pap. IMRP 2007*, 4 (2008), 128 pp.

[12] Aptekarev, A. I., Lysov, V. G., and Tulyakov, D. N. The global eigenvalue distribution regime of random matrices with an anharmonic potential and an external source. *Teoret. Mat. Fiz. 159*, 1 (2009), 34–57.

[13] Aptekarev, A. I., Lysov, V. G., and Tulyakov, D. N. Random matrices with an external source and the asymptotics of multiple orthogonal polynomials. *Mat. Sb. 202*, 2 (2011), 3–56.

[14] Aptekarev, A. I., Toulyakov, D. N., and Van Assche, W. Hyperelliptic uniformization of algebraic curves of the third order. *J. Comput. Appl. Math. 284* (2015), 38–49.

[15] Atia, M. J., Martínez-Finkelshtein, A., Martínez-González, P., and Thabet, F. Quadratic differentials and asymptotics of Laguerre polynomials with varying complex parameters. *J. Math. Anal. Appl. 416*, 1 (2014), 52–80.

[16] Baik, J., Deift, P., McLaughlin, K. T.-R., Miller, P., and Zhou, X. Optimal tail estimates for directed last passage site percolation with geometric random variables. *Adv. Theor. Math. Phys. 5*, 6 (2001), 1207–1250.

[17] Balogh, F., and Bertola, M. Regularity of a vector potential problem and its spectral curve. *J. Approx. Theory 161*, 1 (2009), 353–370.

[18] Balogh, F., Bertola, M., and Bothner, T. Hankel determinant approach to generalized Vorob'ev-Yablonski polynomials and their roots. *ArXiv:1504.00440*, 23 pp.

[19] Balogh, F., Bertola, M., Lee, S.-Y., and McLaughlin, K. D. T.-R. Strong asymptotics of the orthogonal polynomials with respect to a measure supported on the plane. *Comm. Pure Appl. Math. 68*, 1 (2015), 112–172.

[20] Balogh, F., Grava, T., and Merzi, D. Orthogonal polynomials for a class of measures with discrete rotational symmetries in the complex plane. *ArXiv:1509.05331*, 51 pp.

[21] Baratchart, L., Stahl, H., and Yattselev, M. L. Weighted extremal domains and best rational approximation. *Adv. Math. 229*, 1 (2012), 357–407.

[22] Beckermann, B., Kalyagin, V., Matos, A. C., and Wielonsky, F. Equilibrium problems for vector potentials with semidefinite interaction matrices and constrained masses. *Constr. Approx. 37*, 1 (2013), 101–134.

[23] Bergkvist, T., and Rullgård, H. On polynomial eigenfunctions for a class of differential operators. *Math. Res. Lett. 9*, 2-3 (2002), 153–171.

[24] Bertola, M. Boutroux curves with external field: equilibrium measures without a variational problem. *Anal. Math. Phys. 1*, 2-3 (2011), 167–211.

[25] Bertola, M., and Bothner, T. Zeros of large degree Vorob'ev–Yablonski polynomials via a Hankel determinant identity. *Int. Math. Res. Notices 2015*, 19 (2015), 9330–9399.

[26] Bertola, M., Gekhtman, M., and Szmigielski, J. Strong asymptotics for Cauchy biorthogonal polynomials with application to the Cauchy two-matrix model. *J. Math. Phys. 54*, 4 (2013), 043517, 25 pp.

[27] Bertola, M., and Mo, M. Y. Commuting difference operators, spinor bundles and the asymptotics of orthogonal polynomials with respect to varying complex weights. *Adv. Math. 220*, 1 (2009), 154–218.

[28] Bertola, M., and Tovbis, A. Asymptotics of orthogonal polynomials with complex varying quartic weight: global structure, critical point behavior and the first Painlevé equation. *Constr. Approx. 41*, 3 (2015), 529–587.

[29] Bessis, D., Itzykson, C., and Zuber, J. B. Quantum field theory techniques in graphical enumeration. *Adv. in Appl. Math. 1*, 2 (1980), 109–157.

[30] Björk, J.-E., Borcea, J., and Bøgvad, R. Subharmonic configurations and algebraic Cauchy transforms of probability measures. In *Notions of positivity and the geometry of polynomials* (2011), Trends Math., Birkhäuser/Springer Basel AG, Basel, pp. 39–62.

[31] Bleher, P. M., and Deaño, A. Painlevé I double scaling limit in the cubic random matrix model. *ArXiv:1310.3768*, 49 pp.

[32] Bleher, P. M., and Deaño, A. Topological expansion in the cubic random matrix model. *Int. Math. Res. Not. IMRN*, 12 (2013), 2699–2755.

[33] Bleher, P. M., Delvaux, S., and Kuijlaars, A. B. J. Random matrix model with external source and a constrained vector equilibrium problem. *Comm. Pure Appl. Math. 64*, 1 (2011), 116–160.

[34] Bleher, P. M., and Its, A. R. Semiclassical asymptotics of orthogonal polynomials, Riemann-Hilbert problem, and universality in the matrix model. *Ann. of Math. 150*, 1 (1999), 185–266.

[35] Bleher, P. M., and Kuijlaars, A. B. J. Large n limit of Gaussian random matrices with external source. I. *Comm. Math. Phys. 252*, 1-3 (2004), 43–76.

[36] Bleher, P. M., and Kuijlaars, A. B. J. Random matrices with external source and multiple orthogonal polynomials. *Int. Math. Res. Not.*, 3 (2004), 109–129.

[37] Bleher, P. M., and Kuijlaars, A. B. J. Large n limit of Gaussian random matrices with external source. III. Double scaling limit. *Comm. Math. Phys. 270*, 2 (2007), 481–517.

[38] Bleher, P. M., and Kuijlaars, A. B. J. Orthogonal polynomials in the normal matrix model with a cubic potential. *Adv. Math. 230*, 3 (2012), 1272–1321.

[39] Bleher, P. M., and Liechty, K. Exact solution of the six-vertex model with domain wall boundary conditions: antiferroelectric phase. *Comm. Pure Appl. Math. 63*, 6 (2010), 779–829.

[40] Bleher, P. M., and Liechty, K. *Random matrices and the six-vertex model*, vol. 32 of *CRM Monograph Series*. American Mathematical Society, Providence, RI, 2014.

[41] Bleher, P. M., and Liechty, K. Six-vertex model with partial domain wall boundary conditions: ferroelectric phase. *J. Math. Phys. 56*, 2 (2015), 023302, 28 pp.

[42] Bleher, P. M., and Silva, G. L. F. The mother body phase transition in the normal matrix model. *ArXiv:1601.05124* , 127 pp.

[43] Brézin, E., Itzykson, C., Parisi, G., and Zuber, J. B. Planar diagrams. *Comm. Math. Phys. 59*, 1 (1978), 35–51.

[44] Cegrell, U., Kolodziej, S., and Levenberg, N. Two problems on potential theory for unbounded sets. *Math. Scand. 83*, 2 (1998), 265–276.

[45] Chau, L.-L., and Zaboronsky, O. On the structure of correlation functions in the normal matrix model. *Comm. Math. Phys. 196*, 1 (1998), 203–247.

[46] Claeys, T., Kuijlaars, A. B. J., and Vanlessen, M. Multi-critical unitary random matrix ensembles and the general Painlevé II equation. *Ann. of Math. 168* (2008), 601–642.

[47] Claeys, T., and Wielonsky, F. On sequences of rational interpolants of the exponential function with unbounded interpolation points. *J. Approx. Theory 171* (2013), 1–32.

[48] Deaño, A. Large degree asymptotics of orthogonal polynomials with respect to an oscillatory weight on a bounded interval. *J. Approx. Theory 186* (2014), 33–63.

[49] Deaño, A., Huybrechs, D., and Kuijlaars, A. B. J. Asymptotic zero distribution of complex orthogonal polynomials associated with Gaussian quadrature. *J. Approx. Theory 162*, 12 (2010), 2202–2224.

[50] Deift, P. *Orthogonal Polynomials and Random Matrices: A Riemann-Hilbert Approach*. No. 3 in Courant Lecture Notes. American Mathematical Society, 2000.

[51] Deift, P., and Gioev, D. *Random Matrix Theory: Invariant Ensembles and Universality*. No. 18 in Courant Lecture Notes. American Mathematical Society, 2009.

[52] Deift, P., Its, A., and Krasovsky, I. Asymptotics of Toeplitz, Hankel, and Toeplitz+Hankel determinants with Fisher-Hartwig singularities. *Ann. of Math. (2) 174*, 2 (2011), 1243–1299.

[53] Deift, P., Its, A. R., and Zhou, X. A Riemann-Hilbert approach to asymptotic problems arising in the theory of random matrix models and also in the theory of integrable statistical mechanics. *Ann. of Math. 146* (1997), 149–235.

[54] Deift, P., Kriecherbauer, T., McLaughlin, K. T.-R., Venakides, S., and Zhou, X. Uniform asymptotics for polynomials orthogonal with respect to varying exponential weights and applications to universality questions in random matrix theory. *Comm. Pure Appl. Math. 52* (1999), 1335–1425.

[55] Deift, P., McLaughlin, K. T.-R., and Kriecherbauer, T. New results on the equilibrium measure for logarithmic potentials in the presence of an external field. *J. Approx. Theory 95* (1998), 388–475.

[56] Deift, P., and Zhou, X. A steepest descent method for oscillatory Riemann-Hilbert problem, Asymptotics for the MKdV equation. *Comm. Pure Appl. Math. 48* (1993), 277–337.

[57] Delvaux, S., Kuijlaars, A. B. J., and Zhang, L. Critical behavior of non-intersecting Brownian-motions at a tacnode. *Comm. Pure Appl. Math. 64* (2011), 1305–1383.

[58] Di Francesco, P., Ginsparg, P., and Zinn-Justin, J. 2D gravity and random matrices. *Phys. Rep. 254*, 1-2 (1995), 133 pp.

[59] Duits, M. Painlevé kernels in Hermitian matrix models. *Constr. Approx. 39*, 1 (2014), 173–196.

[60] Duits, M., Geudens, D., and Kuijlaars, A. B. J. A vector equilibrium problem for the two-matrix model in the quartic/quadratic case. *Nonlinearity 24*, 3 (2011), 951–993.

[61] Duits, M., and Kuijlaars, A. B. J. Painlevé I asymptotics for orthogonal polynomials with respect to a varying quartic weight. *Nonlinearity 19*, 10 (2006), 2211–2245.

[62] Duits, M., and Kuijlaars, A. B. J. Universality in the two-matrix model: a Riemann-Hilbert steepest-descent analysis. *Comm. Pure Appl. Math. 62*, 8 (2009), 1076–1153.

[63] Duits, M., Kuijlaars, A. B. J., and Mo, M. Y. The Hermitian two matrix model with an even quartic potential. *Mem. Amer. Math. Soc. 217*, 1022 (2012), v+105 pp.

[64] Elbau, P. *Random Normal Matrices and Polynomial Curves*. PhD thesis, ETH Zurich, 2006. ArXiv:0707.0425.

[65] Elbau, P., and Felder, G. Density of eigenvalues of random normal matrices. *Comm. Math. Phys. 259*, 2 (2005), 433–450.

[66] Ercolani, N. M., and McLaughlin, K. D. T.-R. Asymptotics of the partition function for random matrices via Riemann-Hilbert techniques and applications to graphical enumeration. *Int. Math. Res. Not.*, 14 (2003), 755–820.

[67] Ercolani, N. M., and McLaughlin, K. D. T.-R. A quick derivation of the loop equations for random matrices. In *Probability, geometry and integrable systems*, vol. 55 of *Math. Sci. Res. Inst. Publ.* Cambridge Univ. Press, Cambridge, 2008, pp. 185–198.

[68] Filipuk, G., Van Assche, W., and Zhang, L. Multiple orthogonal polynomials associated with an exponential cubic weight. *J. Approx. Theory 190* (2015), 1–25.

[69] Gonchar, A. A., and Rakhmanov, E. A. On the convergence of simultaneous Padé approximants for systems of functions of Markov type. *Trudy Mat. Inst. Steklov. 157* (1981), 31–48, 234. Number theory, mathematical analysis and their applications.

[70] Gonchar, A. A., and Rakhmanov, E. A. The equilibrium problem for vector potentials. *Uspekhi Mat. Nauk 40*, 4 (244) (1985), 155–156.

[71] Gonchar, A. A., and Rakhmanov, E. A. Equilibrium distributions and the rate of rational approximation of analytic functions. *Mat. Sb. (N.S.) 134 (176)*, 3 (1987), 306–352, 447.

[72] Greene, R. E., and Krantz, S. G. *Function theory of one complex variable*, third ed., vol. 40 of *Graduate Studies in Mathematics*. American Mathematical Society, Providence, RI, 2006.

[73] Gustafsson, B. On quadrature domains and an inverse problem in potential theory. *J. Analyse Math. 55* (1990), 172–216.

[74] Gustafsson, B. On mother bodies of convex polyhedra. *SIAM J. Math. Anal. 29*, 5 (1998), 1106–1117.

[75] Gustafsson, B. Lectures on balayage. In *Clifford Algebras and Potential Theory* (2002), University of Joensuu Department of Mathematics, Sirkka-Liisa Eriksson, pp. 17–63. Proceedings of the summer school held in Mekrijärvi, June 24–28, 2002.

[76] Gustafsson, B., and Lin, Y.-L. On the dynamics of roots and poles for solutions of the Polubarinova-Galin equation. *Ann. Acad. Sci. Fenn. Math. 38*, 1 (2013), 259–286.

[77] Gustafsson, B., Putinar, M., Saff, E. B., and Stylianopoulos, N. Bergman polynomials on an archipelago: estimates, zeros and shape reconstruction. *Adv. Math. 222*, 4 (2009), 1405–1460.

[78] Harary, F., and Palmer, E. M. *Graphical enumeration*. Academic Press, New York-London, 1973.

[79] Hardy, A., and Kuijlaars, A. B. J. Weakly admissible vector equilibrium problems. *J. Approx. Theory 164*, 6 (2012), 854–868.

[80] Harer, J., and Zagier, D. The Euler characteristic of the moduli space of curves. *Invent. Math. 85*, 3 (1986), 457–485.

[81] Hedenmalm, H., and Makarov, N. G. Coulomb gas ensembles and Laplacian growth. *Proc. Lond. Math. Soc. 106*, 4 (2013), 859–907.

[82] Holst, T., and Shapiro, B. On higher Heine-Stieltjes polynomials. *Israel J. Math. 183* (2011), 321–345.

[83] Hooft, G. t. A planar diagram theory for strong interactions. *Nuclear Physics B 72*, 3 (1974), 461 – 473.

[84] Huybrechs, D., Kuijlaars, A. B. J., and Lejon, N. Zero distribution of complex orthogonal polynomials with respect to exponential weights. *J. Approx. Theory 184* (2014), 28–54.

[85] Jenkins, J. A. *Univalent functions and conformal mapping.* Ergebnisse der Mathematik und ihrer Grenzgebiete. Neue Folge, Heft 18. Reihe: Moderne Funktionentheorie. Springer-Verlag, Berlin-Göttingen-Heidelberg, 1958.

[86] Kalyagin, V. A. A class of polynomials determined by two orthogonality relations. *Mat. Sb. (N.S.) 110 (152)*, 4 (1979), 609–627.

[87] Kamvissis, S., and Rakhmanov, E. A. Existence and regularity for an energy maximization problem in two dimensions. *J. Math. Phys. 46*, 8 (2005), 083505, 24 pp.

[88] Kostov, I. K., Krichever, I., Mineev-Weinstein, M., Wiegmann, P. B., and Zabrodin, A. The τ-function for analytic curves. In *Random matrix models and their applications*, vol. 40 of *Math. Sci. Res. Inst. Publ.* Cambridge Univ. Press, Cambridge, 2001, pp. 285–299.

[89] Kuijlaars, A. B. J. Multiple orthogonal polynomials in random matrix theory. In *Proceedings of the International Congress of Mathematicians. Volume III* (New Delhi, 2010), Hindustan Book Agency, pp. 1417–1432.

[90] Kuijlaars, A. B. J., and López-García, A. The normal matrix model with a monomial potential, a vector equilibrium problem, and multiple orthogonal polynomials on a star. *Nonlinearity 28*, 2 (2015), 347–406.

[91] Kuijlaars, A. B. J., Martínez-Finkelshtein, A., and Wielonsky, F. Non-intersecting squared Bessel paths and multiple orthogonal polynomials for modified Bessel weights. *Comm. Math. Phys. 286*, 1 (2009), 217–275.

[92] Kuijlaars, A. B. J., and McLaughlin, K. T.-R. Riemann-Hilbert analysis for Laguerre polynomials with large negative parameter. *Comput. Methods Funct. Theory 1*, 1 (2001), 205–233.

[93] Kuijlaars, A. B. J., and McLaughlin, K. T.-R. Asymptotic zero behavior of Laguerre polynomials with negative parameter. *Constr. Approx. 20*, 4 (2004), 497–523.

[94] Kuijlaars, A. B. J., and Silva, G. L. F. S-curves in polynomial external fields. *J. Approx. Theory 191* (2015), 1–37.

[95] Kuijlaars, A. B. J., and Tovbis, A. The supercritical regime in the normal matrix model with cubic potential. *Adv. Math. 283* (2015), 530–587.

[96] Kuijlaars, A. B. J., Van Assche, W., and Wielonsky, F. Quadratic Hermite-Padé approximation to the exponential function: a Riemann-Hilbert approach. *Constr. Approx. 21*, 3 (2005), 351–412.

[97] Landkof, N. S. *Foundations of modern potential theory*. Springer-Verlag, New York-Heidelberg, 1972. Translated from the Russian by A. P. Doohovskoy, Die Grundlehren der mathematischen Wissenschaften, Band 180.

[98] Lee, S.-Y., and Makarov, N. G. Topology of quadrature domains. *J. Amer. Math. Soc.* (2015), 37 pp. To appear.

[99] Lee, S.-Y., Teodorescu, R., and Wiegmann, P. Viscous shocks in Hele-Shaw flow and Stokes phenomena of the Painlevé I transcendent. *Phys. D 240*, 13 (2011), 1080–1091.

[100] Marchetti, D. H. U., Pereira, T., and Veneziani, A. M. Conformal deformation of equilibrium measures in normal random ensembles. *J. Phys. A 44*, 7 (2011), 075202, 21 pp.

[101] Marchetti, D. H. U., Pereira, T., and Veneziani, A. M. Asymptotic integral kernel for ensembles of random normal matrices with radial potentials. *J. Math. Phys. 53*, 2 (2012), 023303, 21 pp.

[102] Martínez-Finkelshtein, A., Martínez-González, P., and Thabet, F. Trajectories of quadratic differentials for Jacobi polynomials with complex parameters. *ArXiv:1506.03434*, 22 pp.

[103] Martínez-Finkelshtein, A., and Rakhmanov, E. A. On asymptotic behavior of Heine-Stieltjes and Van Vleck polynomials. In *Recent trends in orthogonal polynomials and approximation theory*, vol. 507 of *Contemp. Math.* Amer. Math. Soc., Providence, RI, 2010, pp. 209–232.

[104] Martínez-Finkelshtein, A., and Rakhmanov, E. A. Critical measures, quadratic differentials, and weak limits of zeros of Stieltjes polynomials. *Comm. Math. Phys. 302*, 1 (2011), 53–111.

[105] Martínez-Finkelshtein, A., Rakhmanov, E. A., and Suetin, S. P. Variation of equilibrium energy and the S-property of a stationary compact set. *Mat. Sb. 202*, 12 (2011), 113–136.

[106] Martínez-Finkelshtein, A., and Silva, G. L. F. Critical measures for vector energy: breaking the symmetry for multiple orthogonal polynomials. *In preparation*.

[107] Martínez-Finkelshtein, A., and Silva, G. L. F. Critical measures for vector energy: global structure of trajectories of quadratic differentials. *ArXiv:1509.06704*, 81 pp.

[108] Mattner, L. Strict definiteness of integrals via complete monotonicity of derivatives. *Trans. Amer. Math. Soc. 349*, 8 (1997), 3321–3342.

[109] Mhaskar, H. N., and Saff, E. B. The distribution of zeros of asymptotically extremal polynomials. *J. Approx. Theory 65*, 3 (1991), 279–300.

[110] Monakhov, V. N. *Boundary value problems with free boundaries for elliptic systems of equations*, vol. 57 of *Translations of Mathematical Monographs*. American Mathematical Society, Providence, RI, 1983. Translated from the Russian by H. H. McFaden, Translation edited by Lev J. Leifman.

[111] Nikishin, E. M., and Sorokin, V. N. *Rational approximations and orthogonality*, vol. 92 of *Translations of Mathematical Monographs*. American Mathematical Society, Providence, RI, 1991. Translated from the Russian by Ralph P. Boas.

[112] Nuttall, J. Hermite-Padé approximants to functions meromorphic on a Riemann surface. *J. Approx. Theory 32*, 3 (1981), 233–240.

[113] Perevoznikova, E., and Rakhmanov, E. A. Variations of the equilibrium energy and S-property of compacta of minimal capacity. *manuscript* (1994).

[114] Pommerenke, C. *Univalent functions*. Vandenhoeck & Ruprecht, Göttingen, 1975. With a chapter on quadratic differentials by Gerd Jensen, Studia Mathematica/Mathematische Lehrbücher, Band XXV.

[115] Rakhmanov, E. A. On the asymptotics of Hermite-Padé polynomials for two Markov functions. *Mat. Sb. 202*, 1 (2011), 133–140.

[116] Rakhmanov, E. A. Orthogonal polynomials and S-curves. In *Recent advances in orthogonal polynomials, special functions, and their applications*, vol. 578 of *Contemp. Math.* Amer. Math. Soc., Providence, RI, 2012, pp. 195–239.

[117] Rakhmanov, E. A., and Suetin, S. P. Distribution of zeros of Hermite-Padé polynomials for a pair of functions forming a Nikishin system. *Mat. Sb. 204*, 9 (2013), 115–160.

[118] Ransford, T. *Potential theory in the complex plane*, vol. 28 of *London Mathematical Society Student Texts*. Cambridge University Press, Cambridge, 1995.

[119] Riser, R. *Universality in Gaussian Random Normal Matrices*. PhD thesis, ETH Zurich, 2012. ArXiv:1312.0068.

[120] Saff, E. B., and Totik, V. *Logarithmic potentials with external fields*, vol. 316 of *Grundlehren der Mathematischen Wissenschaften [Fundamental Principles of Mathematical Sciences]*. Springer-Verlag, Berlin, 1997. Appendix B by Thomas Bloom.

[121] Savina, T. V., Sternin, B. Y., and Shatalov, V. E. On a minimal element for a family of bodies producing the same external gravitational field. *Appl. Anal. 84*, 7 (2005), 649–668.

[122] Sendra, J. R., Winkler, F., and Pérez-Díaz, S. *Rational algebraic curves - A computer algebra approach*, vol. 22 of *Algorithms and Computation in Mathematics*. Springer, Berlin, 2008.

[123] Shapiro, B., Takemura, K., and Tater, M. On spectral polynomials of the Heun equation. II. *Comm. Math. Phys. 311*, 2 (2012), 277–300.

[124] Shapiro, B., and Tater, M. On spectral polynomials of the Heun equation. I. *J. Approx. Theory 162*, 4 (2010), 766–781.

[125] Sjödin, T. Mother bodies of algebraic domains in the complex plane. *Complex Var. Elliptic Equ. 51*, 4 (2006), 357–369.

[126] Solynin, A. Y. Quadratic differentials and weighted graphs on compact surfaces. In *Analysis and mathematical physics*, Trends Math. Birkhäuser, Basel, 2009, pp. 473–505.

[127] Stahl, H. Sets of minimal capacity and extremal domains. *arXiv:1205.3811*, 112 pp.

[128] Stahl, H. Extremal domains associated with an analytic function. I, II. *Complex Variables Theory Appl. 4*, 4 (1985), 311–324, 325–338.

[129] Stahl, H. The structure of extremal domains associated with an analytic function. *Complex Variables Theory Appl. 4*, 4 (1985), 339–354.

[130] Stahl, H. Orthogonal polynomials with complex-valued weight function. I, II. *Constr. Approx. 2*, 3 (1986), 225–240, 241–251.

[131] Stahl, H. Orthogonal polynomials with respect to complex-valued measures. In *Orthogonal polynomials and their applications (Erice, 1990)*, vol. 9 of *IMACS Ann. Comput. Appl. Math.* Baltzer, Basel, 1991, pp. 139–154.

[132] Stieltjes, T. J. Sur certains polynômes. *Acta Math. 6*, 1 (1885), 321–326. Qui vérifient une équation différentielle linéaire du second ordre et sur la theorie des fonctions de Lamé.

[133] Strebel, K. *Quadratic differentials*, vol. 5 of *Ergebnisse der Mathematik und ihrer Grenzgebiete (3) [Results in Mathematics and Related Areas (3)]*. Springer-Verlag, Berlin, 1984.

[134] Van Assche, W. Padé and Hermite-Padé approximation and orthogonality. *Surv. Approx. Theory 2* (2006), 61–91.

[135] Vasil'ev, A. *Moduli of families of curves for conformal and quasiconformal mappings*, vol. 1788 of *Lecture Notes in Mathematics*. Springer-Verlag, Berlin, 2002.

[136] Zdravkovska, S. Conversation with Vladimir Igorevich Arnold. *Math. Intelligencer 9*, 4 (1987), 28–32.

[137] Zidarov, D. *Inverse Gravimetric Problem in Geoprospecting and Geodesy*. Developments in Solid Earth Geophysics. Elsevier, 1990.

[138] Zinn-Justin, P. Random Hermitian matrices in an external field. *Nuclear Phys. B 497*, 3 (1997), 725–732.

Curriculum Vitae

Guilherme Silva was born in Indaiatuba, in the state of São Paulo, Brazil, on 7th November 1989. In February 2007 he started his studies in mathematics at the Universidade Estadual Paulista - Unesp, São José do Rio Preto, Brazil, obtaining his Bachelor of Science in Mathematics in December 2010 and his Master of Science in Mathematics in March 2012. In May 2012, he moved to KU Leuven, Belgium, where he attended the Ph.D. programme in Mathematics under the supervision of Professor Arno Kuijlaars.

At KU Leuven, Guilherme Silva was a teaching assistant for the courses *Complex Analysis*, *Calculus* and *Approximation Theory*, and he supervised two bachelor theses. He was also the organizer of the classical analysis seminar from August 2013 to April 2016.

As a Ph.D. student, Guilherme Silva presented his research at the following scientific conferences.

- **May 2013.** 3rd Iberoamerican workshop on orthogonal polynomials and applications. UNESP, São José do Rio Preto, Brazil. *Speaker.*
- **May 2013.** International Conference on Approximation Theory and Applications. City University of Hong Kong. *Speaker.*
- **September 2013.** Congreso de jóvenes investigadores de la Real Sociedad Matemática Española - session on Approximation Theory (Aproximación). Universidad de Sevilla, Spain. *Speaker.*
- **September 2013.** Advanced school and workshop on random matrices and growth models. ICTP, Trieste, Italy. *Poster presentation.*
- **January 2014.** Sydney random matrix theory workshop. The University of Sydney, Australia. *Speaker.*

- **January 2014.** International symposium on orthogonality, quadrature and related topics. Tenerife, Spain. *Speaker.*
- **May 2014.** Constructive functions 2014. Vanderbilt University, Nashville, USA. *Speaker.*
- **June 2015.** SIAM Conference on Orthogonal Polynomials and Special Functions - session on Asymptotics of Orthogonal Polynomials. NIST, Gaithersburg, USA. *Speaker.*
- **June 2015.** Workshop on asymptotics in integrable systems, random matrices and random processes and universality. CRM, Montreal, Canada. *Poster presentation.*
- **March 2016.** Six-vertex models, dimers, shapes, and all that. Simons Center for Geometry and Physics, Stony Brook, USA. *Speaker.*

During his Ph.D. studies, Guilherme Silva was a visiting researcher during the months of April and October of 2014 at Indiana University - Purdue University Indianapolis, where he was invited by Professor Pavel Bleher. He also had the opportunity to give seminar talks at the following universities.

- **January 2013.** KU Leuven, Belgium.
- **September 2013.** Universidad de Almería, Spain.
- **October 2013.** UC Louvain, Louvain-la-Neuve, Belgium.
- **April 2014.** IUPUI, Indianapolis, USA.
- **August 2014.** UNESP, São José do Rio Preto, Brazil.
- **September 2014.** IMPA, Rio de Janeiro, Brazil.
- **October 2014.** IUPUI, Indianapolis, USA.
- **October 2014.** University of Michigan, Ann Arbor, USA.
- **November 2014.** Vanderbilt University, Nashville, USA.
- **May 2015.** Mathematics Ph.D. Colloquium, KU Leuven, Belgium.
- **February 2016.** KU Leuven, Belgium.
- **March 2016.** IST, Austria.
- **March 2016.** Laboratoire Paul Painlevé - Université des Sciences et Technologies de Lille, France.

List of Publications

- *S-curves in polynomial external fields*, with Arno Kuijlaars. J. Approx. Theory 191 (2015), 1–37.
- *Critical measures for vector energy: global structure of trajectories of quadratic differentials*, with Andrei Martínez-Finkelshtein. ArXiv:1509.06704, 81 pp.
- *The mother body phase transition in the normal matrix model*, with Pavel Bleher. ArXiv:1601.05124, 127 pp.

FACULTY OF SCIENCE
DEPARTMENT OF MATHEMATICS
SECTION OF ANALYSIS
Celestijnenlaan 200B
B-3001 Leuven (Belgium)